UNUSUAL MOLECULAR ARCHITECTURES IN LIQUID CRYSTAL AND POLYMER CHEMISTRY

BY

ALEXANDER JOHN PARASKOS

B.A., Environmental Science
Colby College, Waterville, ME; 1991

Submitted to the Department of Chemistry in Partial
Fulfillment of the Requirements for the Degree of

DOCTOR OF PHILOSOPHY

at the

MASSACHUSETTS INSTITUTE OF TECHNOLOGY

February, 2004

 V.1

Signature of Author: _____
Department of Chemistry
October 7, 2003

Certified by: _____
Timothy M Swager
Thesis Supervisor

Accepted by: _____
Robert W. Field
Chairman, Departmental Committee on Graduate Studies

This doctoral thesis has been examined by a Committee of the Department of Chemistry and the Department of Materials Science as follows:

Professor Daniel S. Kemp: _____
Chairman

Professor Timothy M. Swager: _____
Thesis Advisor

Professor Paula Hammond: _____
(Dept of Materials Science)

To my family and friends:
I wouldn't have made it without you.

Unusual Molecular Architectures in Liquid Crystal and Polymer Chemistry

by

ALEXANDER JOHN PARASKOS

Submitted to the Department of Chemistry, February, 2003
In partial fulfillment of the requirements for the degree of
Doctor of Philosophy in Chemistry

ABSTRACT

This dissertation details the synthesis and characterization of materials that consist of molecules with unusual shapes. We have pursued this goal into the regimes of both small molecules (liquid crystals) and polymeric materials. In both cases, the ultimate goal is the creation of materials that display unique properties that arise due to molecular organizations and/or interactions driven by the underlying shape of the molecules or subunits.

Chapter One is an introduction to the study of liquid crystals and their phases. Chapter Two and Three both describe the synthesis and characterization of bent-core tetracatenar liquid crystals. The focus in Chapter Two is on the effects that changing the bend angle and/or lateral dipole have upon the phase behavior of these compounds. We found that the thiophene-based mesogens with the largest lateral dipoles display the most stable liquid crystalline phases. We believe that this effect is due to the formation of antiparallel dimers within the phases of these compounds. Chapter Three describes the synthesis and phase behavior of thiophene-based liquid crystals with desymmetrized cores. Reduction of the symmetry had the effect of either broadening or narrowing the resulting phases, depending on the types of endgroups attached to the molecular core. Chapter Four details the synthesis and phase-behavior of triphenylene-based dione liquid crystals. These molecules are roughly half-discs in terms of molecular shape, and yet were found to form columnar mesophases typical of discotic liquid crystals. Chapter Five describes our efforts investigating a number of extended thiophene-based aromatic systems which are roughly discotic, display columnar liquid crystal phases and/or interesting structures from an electronic standpoint.

Chapter Six describes our initial steps toward establishing a new paradigm for the design of high-strength polymers through the incorporation of iptycene moieties. Our preliminary studies suggest that iptycenes can improve the properties of polymers significantly by increasing the entanglement between polymer chains. Chapter Seven describes our efforts toward using ring-opening metathesis polymerization to create liquid crystalline polymers in which the mesogenic units are tightly associated with the polymer backbones.

Thesis Supervisor: Timothy M. Swager
Title: Professor of Chemistry

Table of Contents

Chapter 1

An Introduction to Liquid Crystals

What are liquid crystals?

The two most common condensed matter phases are the crystalline solid and the isotropic liquid. Within crystalline materials the constituent molecules possess both positional order and directional order: that is, the molecules occupy specific sites within a three-dimensional lattice and the axes of the molecules point in specific directions, respectively. Within the isotropic liquid, which lies at the other extreme of the condensed phases, the molecules diffuse randomly throughout the sample freely rotating about their molecular axes, and therefore possess neither positional nor directional order.

There exist, however, a number of phases (mesophases) that possess a degree of order intermediate between that of crystalline solids and isotropic liquids. These mesophases then fall into two broad categories: plastic crystals and liquid crystals. Plastic crystals are those phases in which the molecules retain their positional order within the three-dimensional lattice, but lack directional order as they freely rotate. Conversely, there are many other phases that retain orientational order, but do not possess the positional order of a crystalline solid. These phases are typically referred to as liquid crystals, since they possess a combination of properties that are commonly associated with both liquids (fluidity) and crystals (anisotropy).[1]

As mentioned above, liquid crystal phases are fluid; that is, the molecules diffuse much like in an isotropic liquid, but as they do so they tend to retain some average orientational order. Quite often a limited degree of positional order exists as well, but the amount of order in any liquid crystalline phase is very small relative to that of crystalline solids. This fact is evidenced when considering that the transition enthalpies between crystalline phases and liquid crystalline phases are usually on the order of 50-60 kJ/mol,

which is comparable to that of a crystal to liquid transition. Transitions from liquid crystal to isotropic liquid, however, are much smaller, on the order of 1-6 kJ/mol, depending on the phase, belying the fact that the degree of order within a liquid crystal phase resembles that of an isotropic liquid more closely than that of a crystalline solid.[2]

The directional order of liquid crystal phases results in the fact that they typically exhibit anisotropic behavior. This means that various physical properties of the phases are inequivalent if measured in different directions. These properties typically include (but are not limited to) magnetic susceptibility, index of refraction, elasticity, and dielectric constant. The fact that liquid crystal phases display both fluidity and anisotropy makes them useful for device applications. By application of an electric field, for example, the liquid crystals can be reoriented, thereby reorienting the relative anisotropy of the phase.[3]

Though it is impossible to predict for certain whether or not a certain molecule will be liquid crystalline *a priori*, a number of guidelines have arisen over the years. Mesogenic (*i.e.*, mesophase-producing) compounds generally consist of fairly rigid molecules with large shape anisotropies. A large percentage of the known liquid crystals consist of a rigid aromatic core with pendant aliphatic sidechains. The formation of a liquid crystalline phase requires a delicate balance of the attractive forces (*i.e.*, dipolar forces between the aromatic cores) and the dispersive forces (*i.e.*, highly dynamic motion of the aliphatic sidechains) between neighboring molecules.

There are broad categories of liquid crystals: lyotropic liquid crystals and thermotropic liquid crystals. Lyotropics are those materials that exhibit liquid crystalline behavior only when mixed with a solvent and the phase behavior is dependent upon both

the concentration and temperature of the solution. Lyotropic liquid crystal phases are often found in amphiphilic molecules, composed of a hydrophobic group at one end and a hydrophilic group at the other end (Figure 1). Soaps, for example, often exhibit lyotropic liquid crystalline behavior at certain concentrations in water, where the hydrophobic tails assemble together presenting the hydrophilic heads to the solvent. The structure that results from soap is known as a micelle. Phospholipids can form analogous structures, which are called vesicles (Figure 2).[4] More complex structures of soaps and phospholipids can also form, such as bilayers, in which the hydrophobic chains are separated from the water by layers of hydrophobic groups. Phospholipid bilayers are in fact extremely important, as they provide the structural basis of biological membranes. The inverse situation arises if the molecules are dissolved in a non-polar solvent such as hexane; now the hydrophobic tails are presented to the solvent, while the hydrophilic heads assemble together.

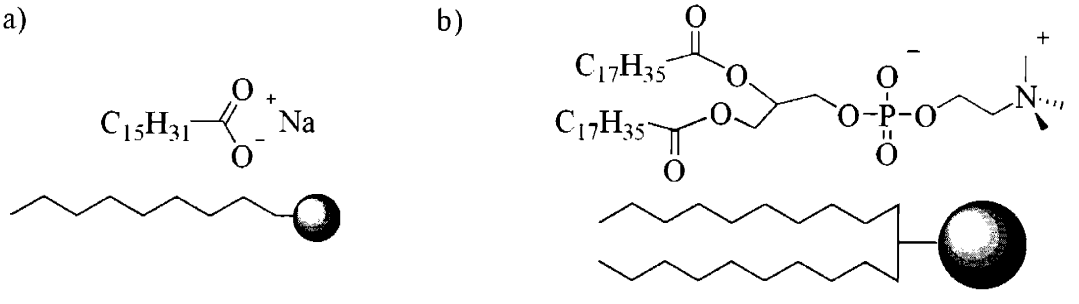

Figure 1. Lyotropic liquid crystals. (a) a soap (b) a phospholipid.

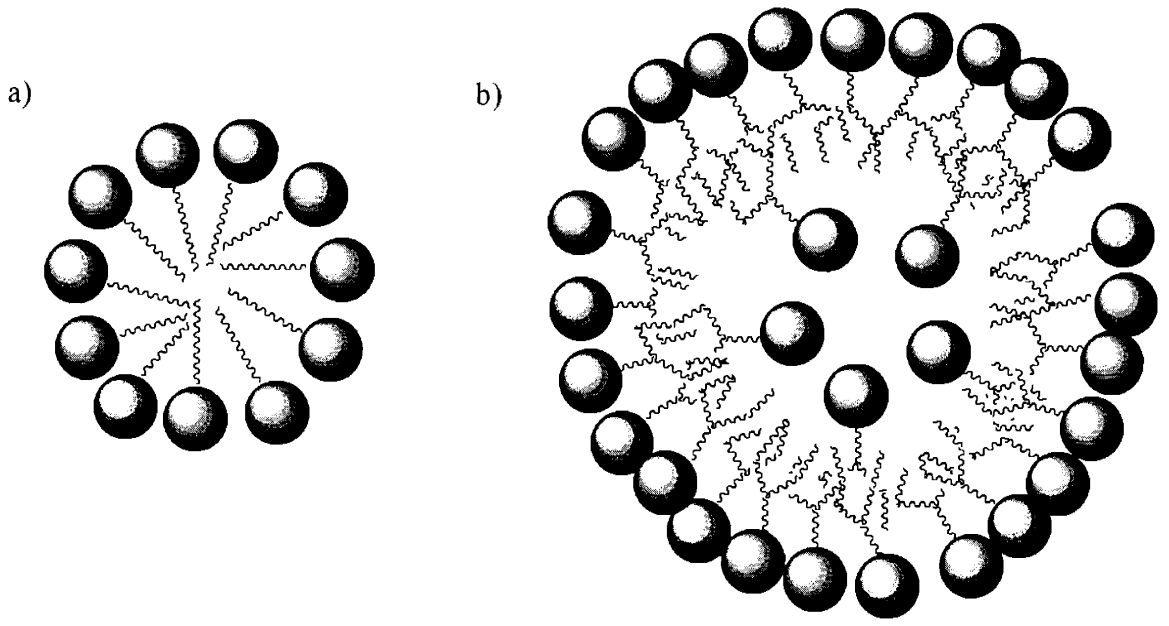

Figure 2. Structures formed by lyotropic liquid crystals. (a) a micelle (b) a vesicle.

Liquid crystals that do not require solvent and exhibit temperature-dependent phase behavior are called thermotropic liquid crystals. Mesophases observed above the melting point (from the crystal phase) upon heating are referred to as enantiotropic, and are thermodynamically stable phases. Mesophases observed only on cooling (below the melting point) are kinetically formed, thermodynamically unstable phases, and are called monotropic. Thermotropic liquid crystals are typically further classified according to their shape and composition. Metallomesogens, for example, are those thermotropic liquid crystals that incorporate a transition metal(s) into their structure. Mesogens that are roughly rod-shaped in nature are called calamitic liquid crystals, and mesogens that are roughly disc-shaped in nature are called discotic liquid crystals. Increasingly, liquid crystal research has been involved with creating mesogens that do not conveniently fit into one of the above categories, and so many new types of liquid crystals have been discovered.

Calamitic Liquid Crystals

Rod-shaped molecules often form liquid crystal phases by virtue of their large aspect ratios, and these compounds are known as calamitic liquid crystals (Figure 3). In this case, one molecular axis is much longer than the other two. Calamitic mesogens generally possess some rigidity along their long axes, as they must retain a somewhat elongated shape to produce interactions that favor alignment. This structural rigidity is often imparted by ring structures at the core of the molecule linked together either directly or by rigid linking groups, while fluidity is imparted by aliphatic sidechains at one or both end(s) of the molecule. Rod-shaped molecules form two different classes of liquid crystal phases, nematics and smectics (Figure 4).

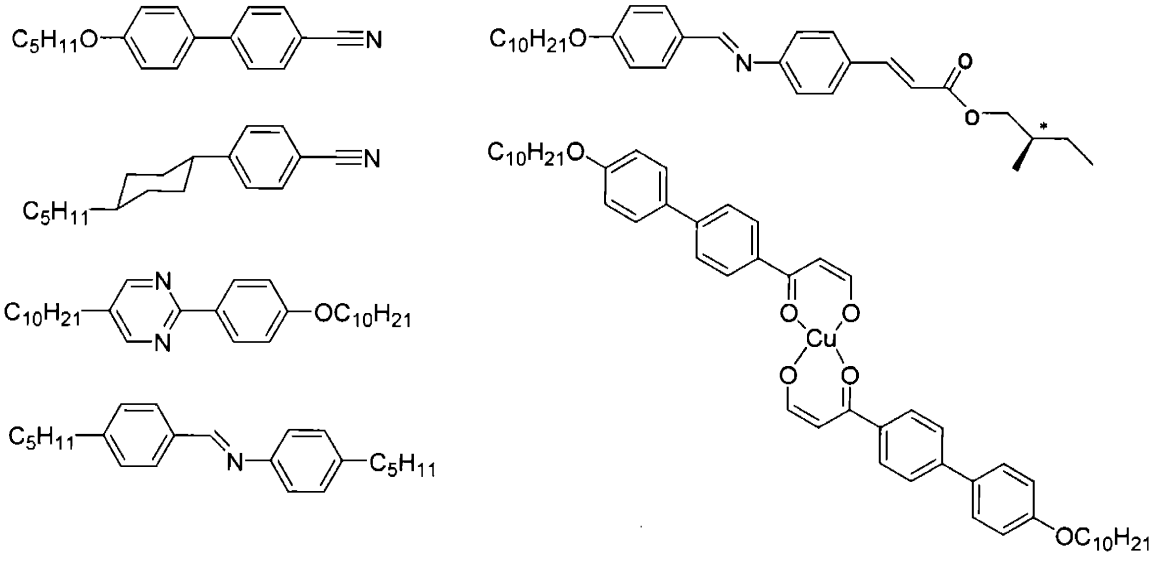

Figure 3. Examples of calamitic thermotropic liquid crystals.

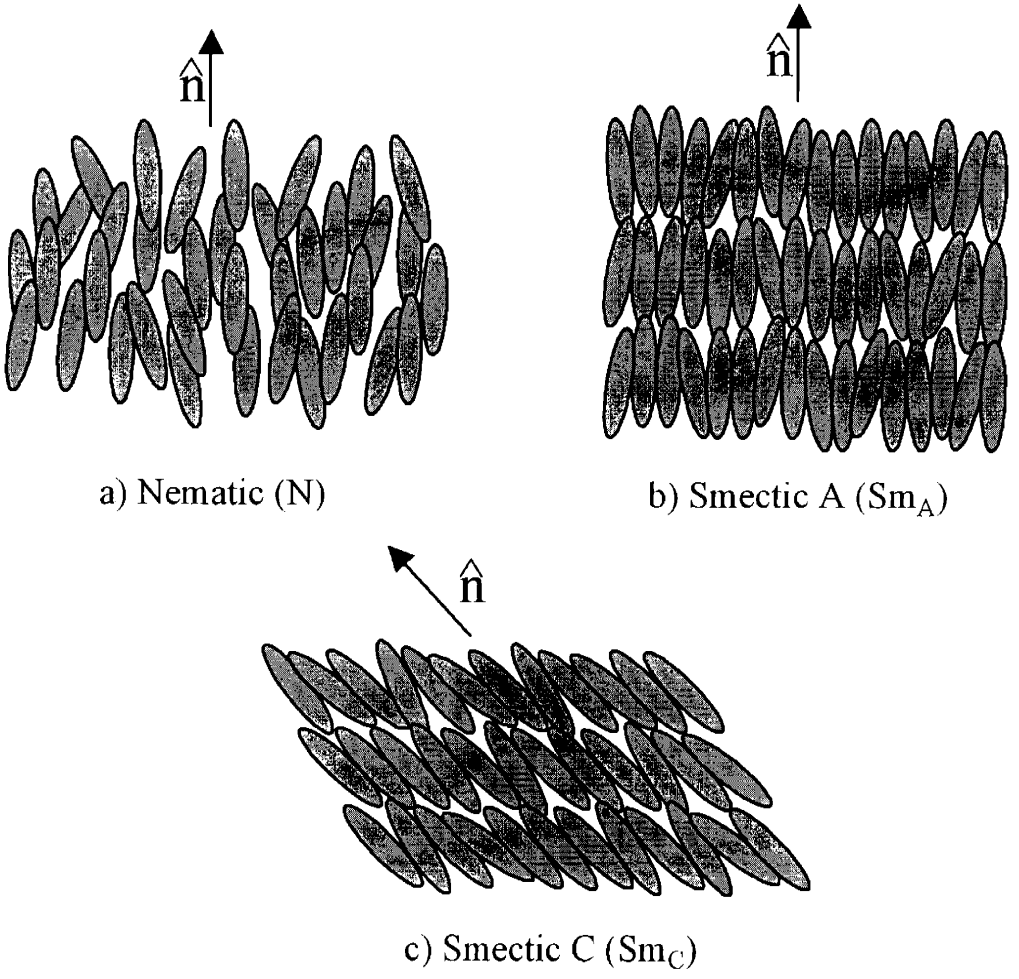

Figure 4. Phases formed by calamitic liquid crystals: (a) nematic (b) SmA (c) SmC. The letter **n** represents the director in each case.

The nematic (N) phase is the simplest (least ordered) and most fluid of all the liquid crystal phases. The molecules in this phase possess a preferred orientational direction, but otherwise they diffuse about the sample freely. In other words, they possess some degree of directional order but possess no translational order. The name nematic comes from the Greek word for thread, since these phases often show threadlike features when viewed through a polarizing microscope. Inclusion of a chiral center into a nematic mesogen breaks the inversion symmetry of the molecule and gives rise to

cholesteric (N^*) phases. These chiral nematic phases (first seen in cholesterol-containing liquid crystals) consist of nematic layers of molecules whose directors twist from layer to layer forming a helical arrangement. If the pitch of this helix is on the same order as the wavelength of light, then selective reflection of particular wavelengths can occur, giving rise to interesting optical effects.

The smectic (Sm) phases are the other phases common to calamitic liquid crystals.[5] Smectic phases are lamellar (layered) phases, in which the molecules possess positional order in addition to the orientational order of the nematics, as their centers of mass tend to be arranged in layers. These phases get their name from the Greek word for soap, as these phases reminded early researchers of lyotropic soap systems. The two most common smectic phases are the smectic A (Sm_A) and smectic C (Sm_C) phases. The smectic A phase exists when the director is perpendicular to the layer plane, while in the smectic C phase the director is tilted with respect to the layer planes. In these phases, though translational order exists between layers, no translational order exists within a given layer; in other words, each molecule may diffuse freely within its own layer, but only rarely will it "jump" from one layer to another.

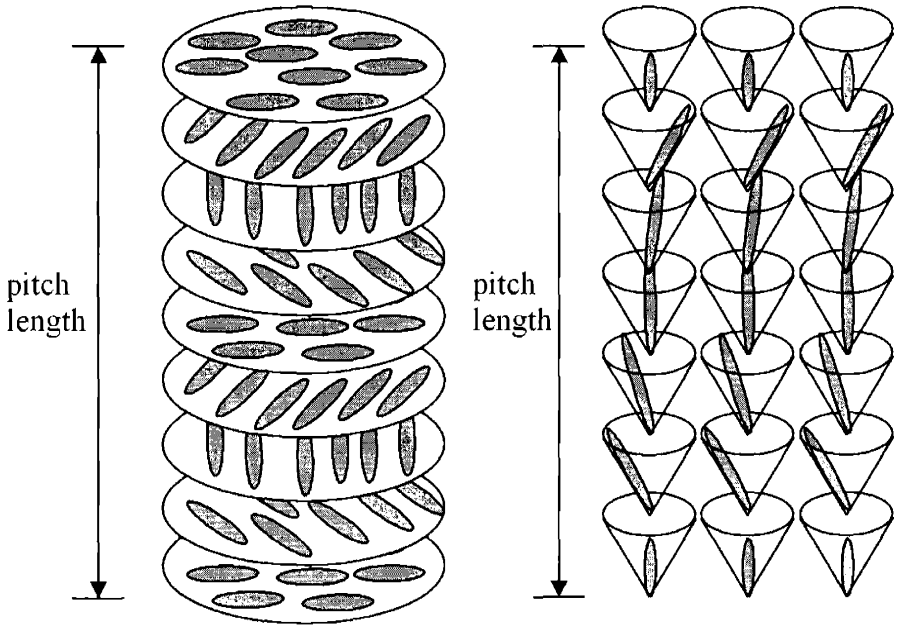

Figure 5. Structures of the: (a) chiral nematic (N^*) and (b) chiral smectic C (Sm_C^*) phases. In each case there is a 360° twist from the top layer to the bottom layer.

By introduction of a chiral center into a mesogen which displays a Sm_C phase, one may get chiral smectic C (Sm_C^*) phases analogous to the cholesteric phases of chiral nematic mesogens.[6] In these phases the director rotates around the cone generated by the tilt angle as one moves from layer to layer. Optical effects can be seen if the pitch length is on the order of the wavelength of visible light.

Discotic Liquid Crystals

For many years it was thought that only rod-like molecules (calamitics) could form liquid crystal phases. During the 1970's it was predicted and ultimately proven that disc-shaped molecules can also form liquid crystal phases. Over one thousand discotic liquid crystals have been subsequently synthesized and investigated[7] (Figure 6). The classic model for the discotic mesogen is a rigid, disc-shaped aromatic core, surrounded

by a number of aromatic sidechains. In these molecules, one molecular axis is much shorter than the other two.

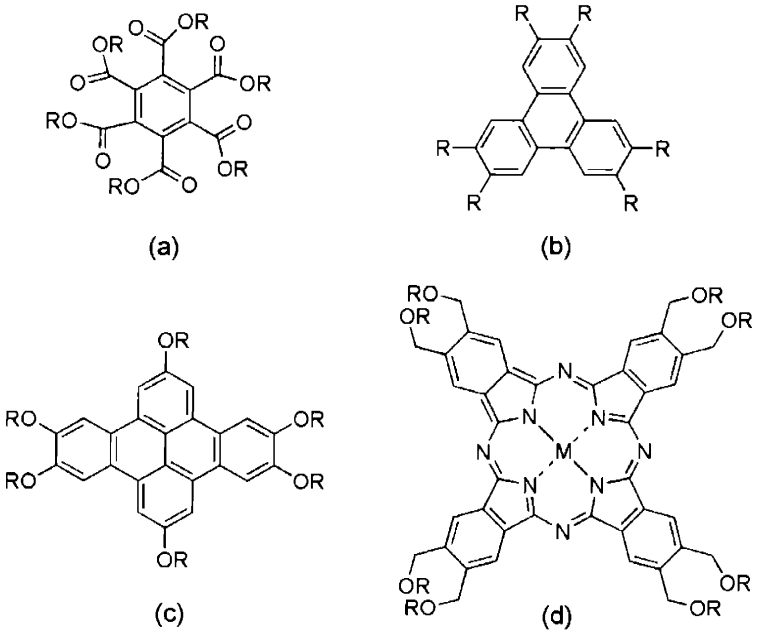

Figure 6. Discotic mesogens: (a) The first reported discotic liquid crystal was a hexasubstituted benzene (b) triphenylene-based discotic liquid crystals are extremely common in the literature (c) a dibenzopyrene discogen (d) an octosubstituted metallophthalocyanine.

The simplest type of discotic phase is the nematic phase (N_D), in which the short axes of the molecules all have a preferential average orientation along a single direction called the director. This phase is analogous to the nematic phase of calamitic molecules, as there is directional but no positional order of the mesogens. Discotic phases also exist in which the molecules possess both translational and directional order in a fashion analogous to the smectic phases of calamitic mesogens. In these phases the mesogens tend to arrange with their molecular cores stacked on upon the other in columns and so these phases are known as columnar phases. Within a column the molecules are free to

rotate around their short axis, but only rarely will a mesogen move from one column to another. These columns of molecules are often then arranged in a two-dimensional lattice, either hexagonal or rectangular, and these are known as the hexagonal columnar (D_h) or rectangular columnar (D_r) phases, respectively (Figure 7). In the hexagonal columnar phase the mesogens are arranged perpendicular to the column axis, while in the rectangular columnar phase the molecules are tilted with respect to the column axis. Varying degrees of long-range order within the columns are possible, and so the phases can be further classified as ordered or disordered columnar phases.

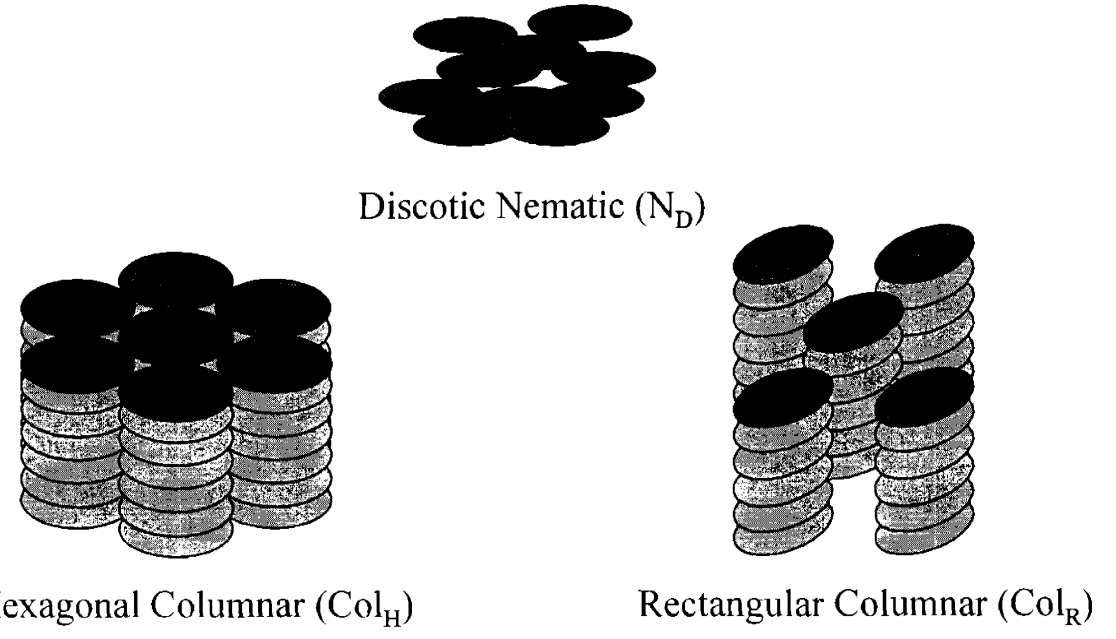

Figure 7. Liquid crystal phases formed by discotic mesogens.

Unconventionally Shaped LC's

For the first 90 years of liquid crystal research, starting with the discovery of the (N^*) phase in melts of cholesteryl acetate and cholesteryl benzoate in 1888, the prototypical mesogen consisted of a rigid-rod core substituted with terminal aliphatic sidechains.[8] The discovery in 1977 that disc-shaped mesogens could form liquid crystal phases instigated extensive efforts toward the synthesis and study of this new class of liquid crystals. Discogens were found to exhibit new phases (columnar) with organization unlike that seen for rod-shaped molecules and this suggested the possibility of creating still new classes of liquid crystals. Since then, researchers have endeavored to further liquid crystal science by creating mesogens with molecular shapes that do not follow the above formulas for liquid crystals. These mesogens have been called "unconventional" liquid crystalline compounds as they do not fit neatly into the above classifications of calamitic or discotic mesogens. The types of unconventional liquid crystals studied to date are too numerous to list, but include cyclic compounds and cyclophanes, swallow-tailed compounds, twins and oligomers, calamitic-discotic dimers, epitaxygens and bowlic liquid crystals, to name but a few (Figure 8).[9] Some unconventionally shaped mesogens with particular relevance to this thesis are described in more detail below.

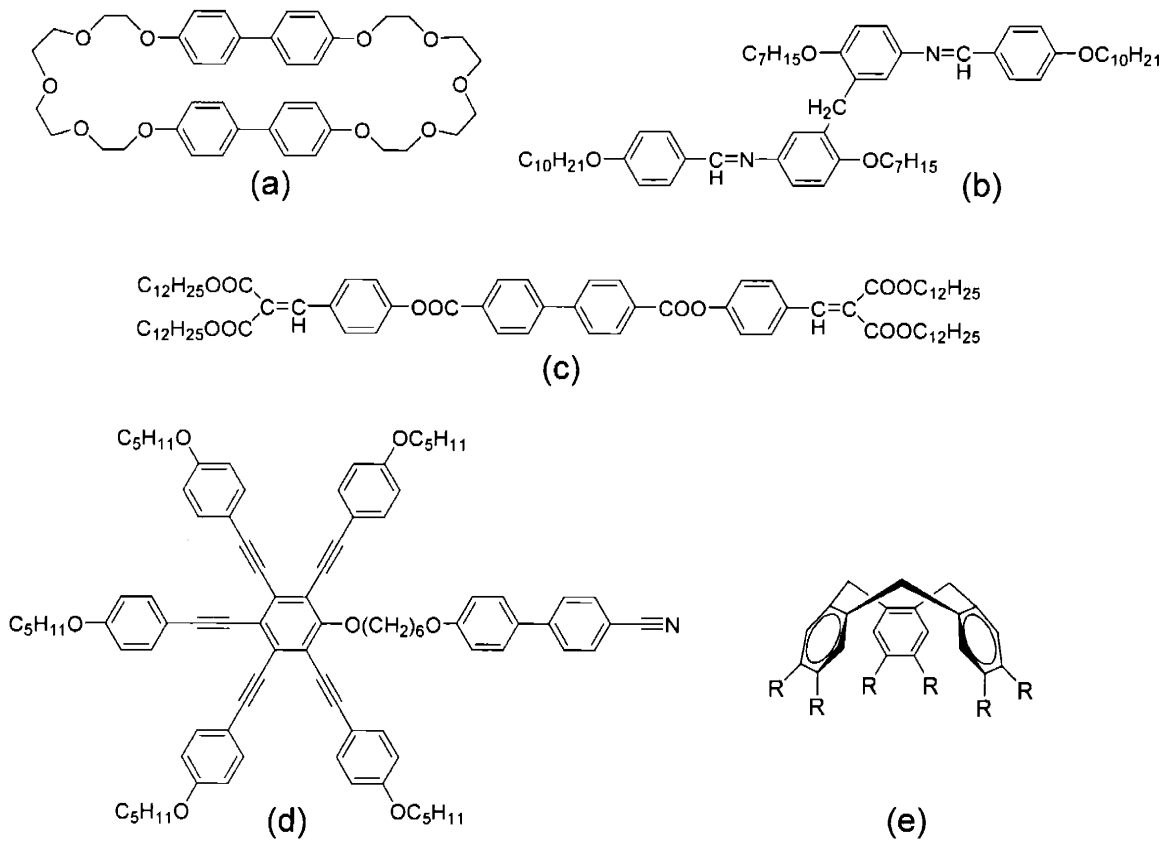

Figure 8. Examples of liquid crystals with unconventional shapes: (a) a mesogenic cyclophane (b) a ligated twin (c) a swallow-tailed mesogen (d) a calamitic-discotic dimer (e) a bowlic liquid crystal.

Polycatenars

Polycatenars are compounds with two to six aliphatic chains attached at the terminal rings of a rigid-rod mesogenic core (Figure 9). They are called bi-, tri-, tetra-, penta- and hexacatenar compounds in accordance with the number of their flexible sidechains. These compounds are known for their exceptional phase behaviors, as a single such compound may show many different mesophases upon varying the temperature.[10] Tetracatenars, for example, have been shown to exhibit not only nematic and smectic mesophases, but also columnar and cubic mesophases. Typically,

tetracatenars with shorter sidechains tend to be dominated by the influence of the molecular core and therefore are typically smectogens. Increasing the length of the sidechains leads to the predominance of columnar phases in these mesogens. Increasing the number of sidechains (for example in the case of hexacatenars) leads to the formation of predominantly columnar phases.

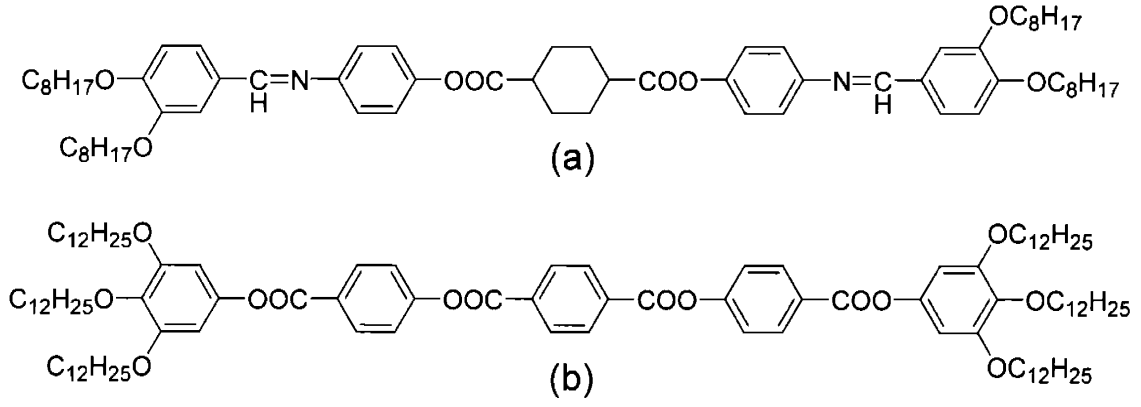

Figure 9. Examples of polycatenars: (a) a tetracatenar (b) a hexacatenar.

Bent-rods & Bananas

Mesogens with bent cores can display liquid crystal phases. Incorporation of a bent core is interesting because the decrease in molecular symmetry causes sterically induced packing between nearest neighboring molecules to become an issue, in some cases causing an additional degree of order to occur within the resulting mesophases. Many of these bent liquid crystals utilize five-membered aromatic rings to introduce the bent shape and mesogens which incorporate a 2,5-thiadiazole or 2,5-thiophene based core are particularly common. It has been demonstrated that suppression of mesomorphic behavior accompanies increasing non-linearity of the mesogenic core.[11] This is most

likely due to decreased rotational freedom about the molecular long axis caused by the increased volume required for such rotation by a bent molecule. However, it has been postulated that if such a structure could exhibit a liquid crystal phase while restricting rotation about the long axis, biaxial behavior should result, and so molecules with larger bent shapes, such as 2,5-oxadiazoles have been investigated with limited success.[12]

Undoubtedly, the most exciting result to come from the study of bent-core liquid crystals to date is the discovery of the so-called "banana" phases. These phases are unique to bent-rods and there exists no analogous counterpart to the banana phase in the field of calamitic or discotic liquid crystals. In 1996 Takezoe et. al reported strange mesophase behavior for a number of 1,3-phenylenebis[4-(4-*n*-alkyloxyphenyliminomethyl)-benzoate]s (Figure 10).[13] These compounds are unique in that they display what was ultimately identified as antiferroelectric switching behavior characteristic of a chiral Sm_C^* phase, despite the fact that these molecules possess no stereogenic centers. It had been previously thought that stereogenic centers were necessary to break the symmetry of the molecules in order to produce a phase possessing bulk chirality.[14] The macroscopic domains possessing chirality of the smectic layers were shown to arise from the cooperative molecular packing of molecules that spontaneously adopt a chiral conformation about the central ester linkages.[15] Since then many different banana phases have been discovered for a number of structurally similar molecules[16] and ferroelectric[17] as well as antiferroelectric switching behavior has been observed, but a coherent picture of the structure/property relationships governing the formation of these phases is not yet clear.

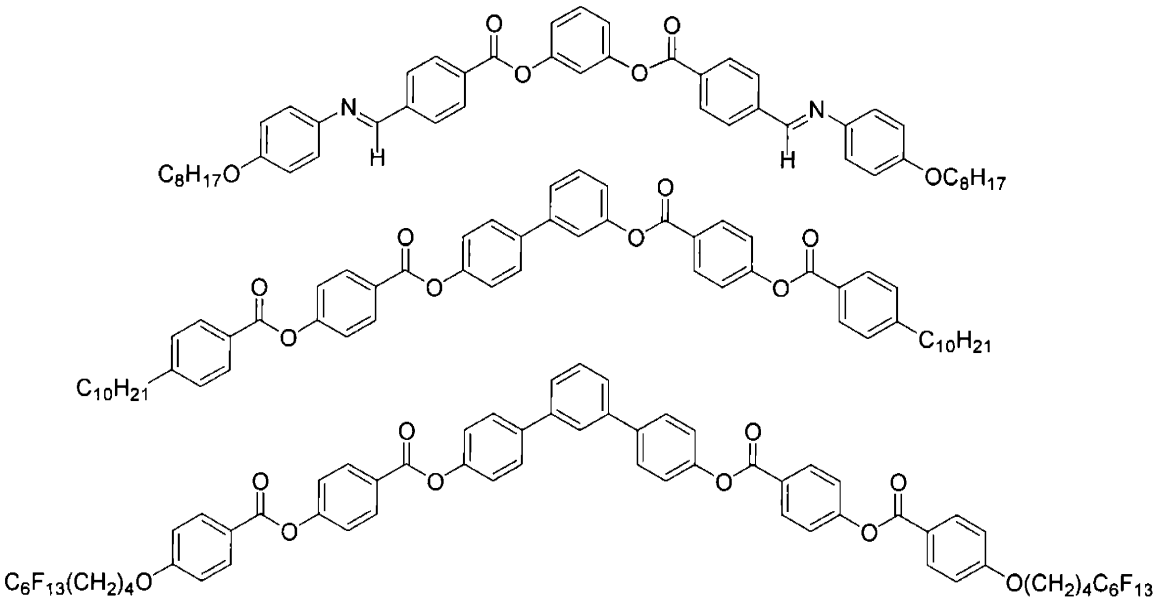

Figure 10. Three examples of bent-rods that display electrically switchable "banana" phases. Note that all examples include a benzoate linkage to the aromatic core.

Ferroelectrics/Antiferroelectrics

Ferroelectrics and antiferroelectrics are materials that possess a polar organization of molecules. These states are found in non-centrosymmetric solid-state materials as well as liquid crystals.

Ferroelectric materials possess a spontaneous polarization that can be directed by the application of an electric field (Figure 11). Ferroelectric behavior is exhibited by solid-state perovskite-type inorganic materials such as $BaTiO_3$ as well as the chiral S_C^* phases of organic liquid crystals. The ferroelectric behavior in perovskite-type materials arises due to the shift from a cubic crystal structure to a slightly deformed cubic structure below the Curie temperature (120 °C for $BaTiO_3$) of the material.[18] This results in a

displacement of the positive ions relative to the negative ions in the lattice, giving rise to a bulk polarization (Figure 12).

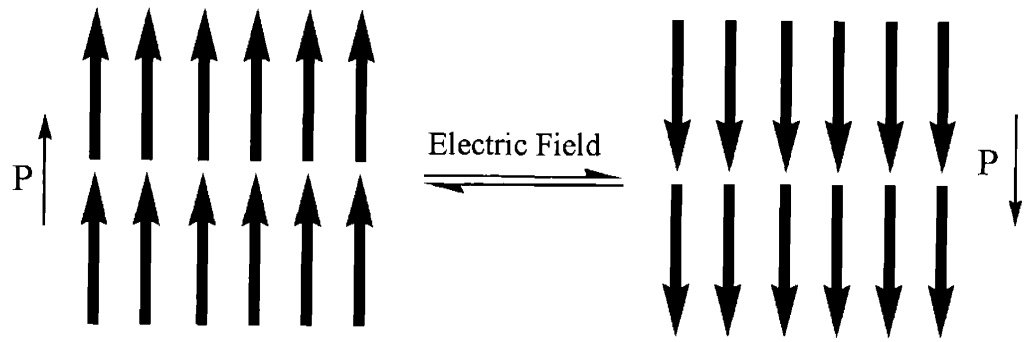

Figure 11. The bulk polarization of a ferroelectric material can be reoriented by application of an electric field.

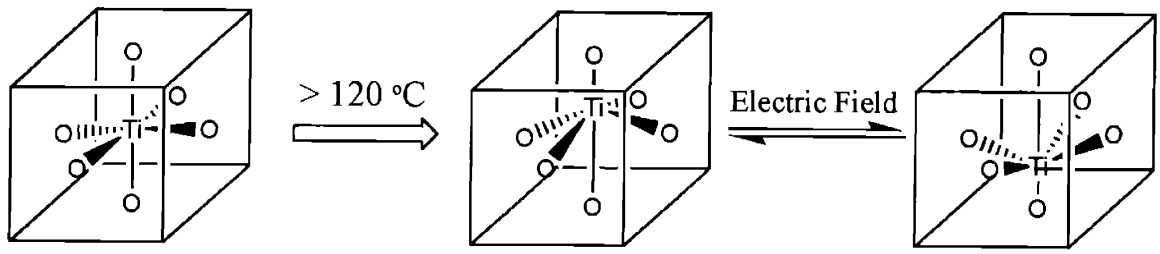

Figure 12. The origin of ferroelectric behavior in $BaTiO_3$, a perovskite-type material. Above the Curie temperature (120 °C) the cell is cubic, but below this temperature the structure is tetragonal with the Ba^{2+} and Ti^{4+} ions displaced relative to the O^{2-} ions. Ba^{2+} ions, which lie at the corners of the cubic cell, have been omitted for clarity.

Ferroelectric behavior is exhibited by liquid crystals as well. Chiral tilted smectic phases (Sm_C^*) comprised of molecules with a dipole moment perpendicular to the molecular long axis are capable of ferroelectricity (Figure 13).[19] Ferroelectric behavior

has also recently been shown for achiral "banana" type molecules, in which packing forces cause the molecules to spontaneously adopt a chiral conformation within the mesophase.[11]

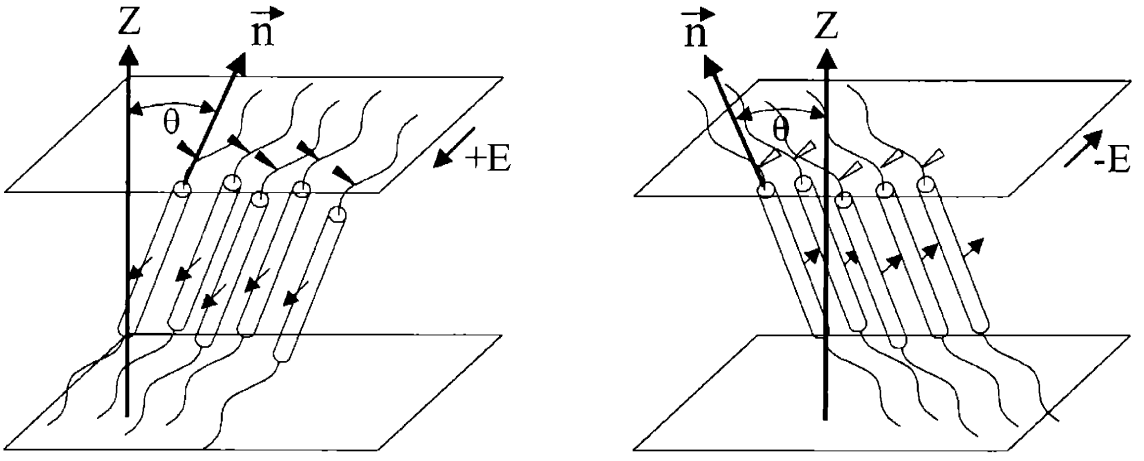

Figure 13. Ferroelectric switching of the director **n** in Sm_C^* liquid crystal phases. Switching is caused by application of an external electric field parallel to the smectic layers.

Antiferroelectric materials do not possess a bulk polarization in the ground state, but application of an external electric field can result in promotion to a higher energy state, which is polarized. Upon removal of the electric field the material relaxes back to the unpolarized ground state (Figure 14).[13]

Figure 14. Organization of an antiferroelectric phase comprised of bent-shaped molecules. The molecular dipole is perpendicular to the long axis of the molecules. The ground state (E = 0) is not polarized, since the dipoles of neighboring layers point in opposite directions, but polarized states can be induced by application of an electric field.

Polarized Microscopy of Liquid Crystals

Polarized microscopy is a powerful tool for the characterization of thermotropic liquid crystals. When liquid crystal phases are viewed through a polarizing microscope complex patterns (called textures) are observed and these textures typically provide insight into the type of organization occurring within the mesophase.[20, 21] Typically a thin film of the sample is sandwiched between glass slides, heated to the appropriate temperature and viewed between crossed polarizers under a microscope. The textures arise due to the fact that the mesophases are typically not perfectly homogeneous (although they may be made nearly homogeneous by employing surface treatments to the glass substrate) and as such defects and deformations of the phase occur. Nematic materials, for example, typically appear very fluid under the microscope due to the absence of positional order within the phase. Additionally, on untreated glass surfaces they typically give rise to schlieren textures, identified by the black bands ('schlieren brushes') representing areas of extinction occurring throughout the texture. The brushes meet at point singularities (disclinations) on the glass surface which are often caused by small pieces of dust or insoluble impurity within the sample (Figure 15). The schlieren

textures of nematics can exhibit both "two-brush" and "four-brush" disclinations, meaning that four or two brushes meet at the point singularity, respectively (Figure 16). The dark brushes occur in those areas where the director of the phase is oriented parallel to one of the polarizers. Due to the fact that the thickness of the films are often not uniform, colors are often seen caused by optical interference of the light entering the a medium with refractive index which differs to that of the glass slide. The various wavelengths of light experience differing degrees of retardation and colors are thereby produced.

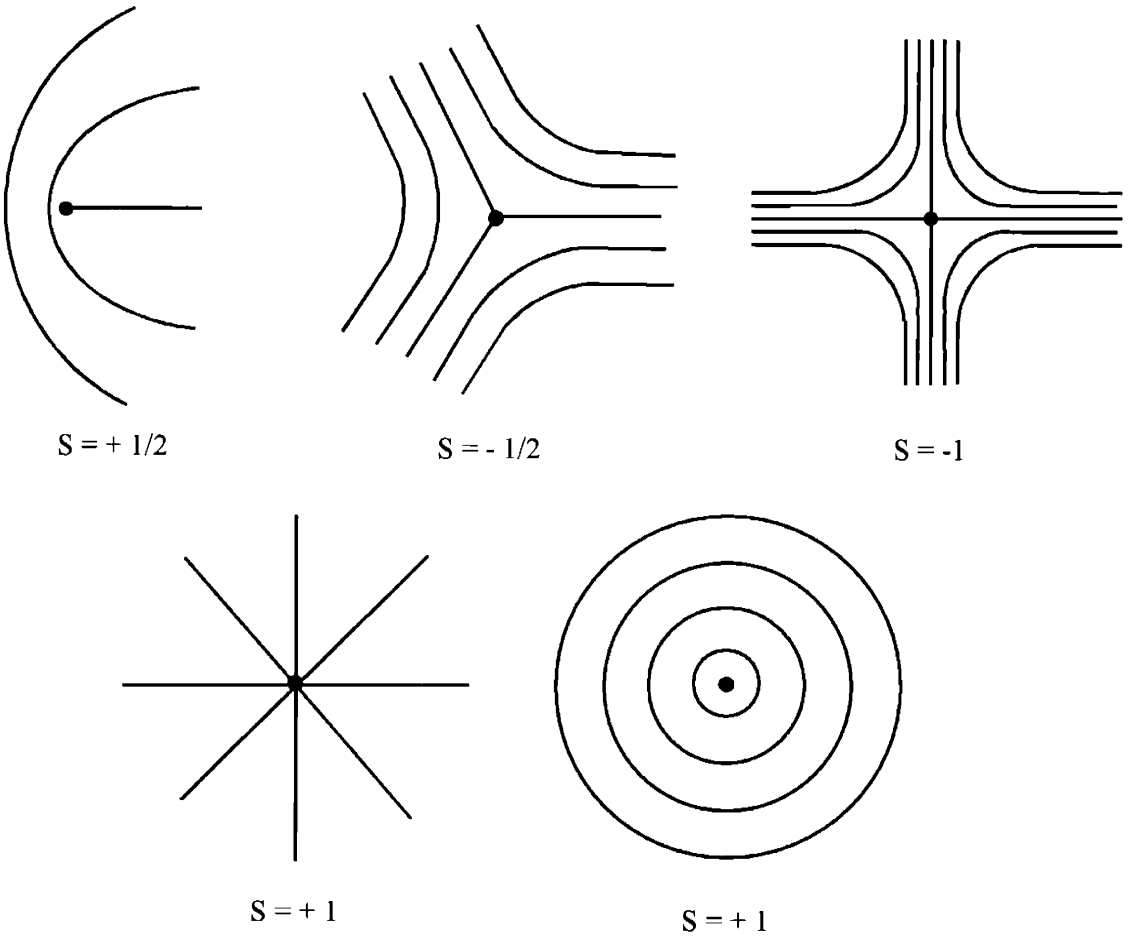

Figure 15. Some of the types of disclinations that occur in liquid crystals. The lines illustrate the orientation of the nematic director at that point in space. The strength (S) of the disclination is such that S· 2π describes the angle by which the director turns on a closed curve around the center.

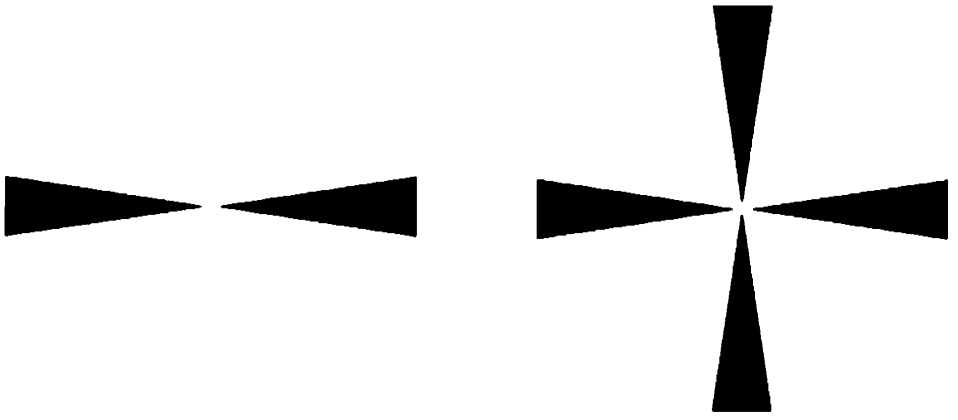

Figure 16. Schlieren textures arising from disclinations when viewed under a polarizing microscope: a 2-brush texture (left) (S = ± 1/2) and a 4-brush texture (right) (S = ± 1).

Smectic A phases exhibit either focal conic fan or homeotropic textures, while smectic C phases exhibit schlieren textures (with only 4-brush disclinations) or focal conic fan textures. Discotic textures are usually either fan-shaped or homeotropic. Clearly, while polarized microscopy is a powerful tool for the determination of liquid crystal phases it is subjective in nature and must be used in conjunction with other methods such as X-ray and DSC.

X-Ray Diffraction of Liquid Crystals

Liquid crystals are often characterized by X-ray diffraction of the mesophases. Nematic phases show only very weak diffuse scatterings, one at the molecular length and the other at approximately 4.6 Å corresponding to the average intermolecular distance and correlation of the liquid-like alkyl sidechains. Smectics display, in addition to similar broad amorphous halos in the wide angle region (~4.6 Å), sharp peaks at smaller angles corresponding to the distance between the layers of molecules.

Columnar discotic phases all display broad peaks at ~4.6 Å due to the average distances between liquid-like sidechains. Hexagonal columnar mesophases typically also display two sharp low angle peaks corresponding to the (100) and (110) Bragg peaks (Figure 15). The rectangular lattices give rise to other periodicities which can be indexed to lattices with different symmetries. Both hexagonal and rectangular columnar phases can be ordered or disordered. The ordered columnar phases are distinguished by the appearance of an additional broad peak at 3.3-3.6 Å corresponding to the distance between neighboring discotic cores within the individual columns caused dense packing of molecules within the columns.

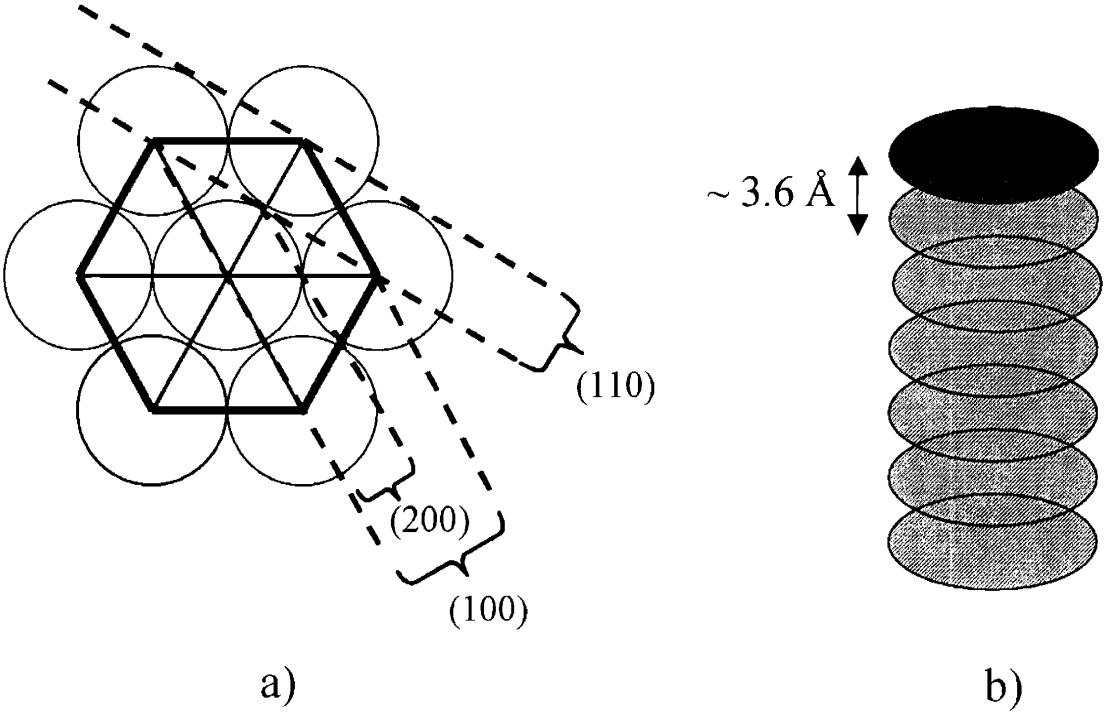

Figure 15. X-ray of columnar liquid crystals: a) Periodicities within the hexagonal lattice which give rise to low angle peaks. b) Spacing within the columns of the ordered columnar hexagonal and rectangular mesophases.

Differential Scanning Calorimetry

Differential scanning calorimetry is employed as a method to measure the enthalpy changes associated with phase transitions. The magnitude of the enthalpy change at a phase transition reveals how large a change in molecular order occurs between the two phases.[22] The transition from crystalline solid to any liquid crystal phase typically occurs with an enthalpy of 30 to 50 kJ/mol, indicating that a significant structural change is occurring between the two states. The transitions from smectic phases to isotropic liquid are much smaller, on the order of 4 to 6 kJ/mol, while smectic-to-smectic and nematic to isotropic transitions are smaller still (1 to 2 kJ/mol). While DSC does not by itself reveal the precise nature of a phase, it is a powerful tool when used in conjunction with methods such as X-ray diffraction and polarized microscopy.

References

(1) Collings, P.J. and Hird, M. *Introduction to Liquid Crystals: Chemistry and Physics*; Taylor and Francis: Philadelphia, 1997; pp 1-4.

(2) Collings, P.J. and Hird, M. *Introduction to Liquid Crystals: Chemistry and Physics*; Taylor and Francis: Philadelphia, 1997; pp 191-193.

(3) Collings, P. J. *Liquid Crystals: Nature's Delicate Phase of Matter*; Princeton University Press: Princeton, 1990; pp 35-55.

(4) Collings, P.J. and Hird, M. *Introduction to Liquid Crystals: Chemistry and Physics*; Taylor and Francis: Philadelphia, 1997; pp 133-146.

(5) Gray, G.W. and Goodby, J.W.G. *Smectic Liquid Crystals: Textures and Structures*; Leonard Hill: Glasgow and London, 1984.

(6) Gray, G.W. and Goodby, J.W.G. *Smectic Liquid Crystals: Textures and Structures*; Leonard Hill: Glasgow and London, 1984; pp 61-64.

(7) Demus, D. In *Handbook of Liquid Crystals*; Demus, D., Goodby, J., Gray, G.W., Spiess, H.-W., Vill, V. Eds.; Wiley-VCH: Weinheim, 1998; Vol 1, pp 171-175.

(8) Gray, G.W. In *Handbook of Liquid Crystals*; Demus, D., Goodby, J., Gray, G.W., Spiess, H.-W., Vill, V. Eds.; Wiley-VCH: Weinheim, 1998; Vol 1, pp 1-16.

(9) Demus, D. In *Handbook of Liquid Crystals*; Demus, D., Goodby, J., Gray, G.W., Spiess, H.-W., Vill, V. Eds.; Wiley-VCH: Weinheim, 1998; Vol 1, pp 153-170.

(10) (a) Nguyen, H.T.; Destrade, C.; Malthête, J. *Adv. Mater.* **1997**, *9*, 375-388. (b) Malthête, J.; Nguyen, H.T.; Destrade, C. *Liq. Cryst.* **1993**, *13,* 171.

(11) Dimitrowa, K.; Hauschilkd, J.; Zaschke, H.; Shubert, H. *J. Prakt. Chem.* **1980**, *322,* 933.

(12) Semmler, K. J. K.; Dingemans, T.J.; Samulski, E.T. *Liq. Cryst.* **1998**, *24*, 799-803.

(13) Niori, T.; Sekine, T.; Watanabe, J.; Furukawa, T.; Takezoe, H. *J. Mater. Chem.* **1996**, *6*, 1231-1233.

(14) Xu, Y. *Ferroelectric Materials and Their Applications*; North-Holland; 1991; pp 351-361.

(15) Link, D.R.; Natale, G.; Shao, R.; Maclennan, J.E.; Clark, N.A.; Körblova; Walba, D.M. *Science* **1997**, *278*, 1924-1927.

(16) (a) Shen, D.; Diele, S.; Wirt, I.; Tschierske, C. *Chem. Comm.* **1998**, 2573-2574. (b) Review on bananas: Pelzl, G.; Diele, S.; Weissflog, W. *Adv. Mater.* **1999**, *11*, 707-724.

(c) Heppke, G.; Parghi, D.D.; Sawade, H. *Liq. Cryst.* **2000**, *27*, 313-320. (d) Weissflog, W.; Kovalenko, S.; Wirth, I.; Diele, S.; Pelzl, G.; Schmalfuss, H.; Kresse, H. *Liq. Cryst.* **2000**, *27*, 677-681. (e) Shen, D.; Pegenau, A.; Diele, S.; Writh, I.; Tschierske, C. *J. Am.Chem. Soc.* **2000**, *122*, 1593-1601. (f) Bedel, J.P.; Rouillon, J.C.; Marcerou, J.P.; Laguerre, M.; Nguyen, H.T.; Achard, M.F. *Liq. Cryst.* **2000**, *27*, 1411-1421.

(17) Walba, D.M.; Korblova, E.; Shao, R.; Maclennan, J.E.; Link, D.R.; Glaser, M.A.; Clark, N.A. *Science* **2000**, *288*, 2181-2184.

(18) Xu, Y. *Ferroelectric Materials and Their Applications*; North-Holland; 1991; pp 1-4.

(19) Collings, P.J. and Hird, M. *Introduction to Liquid Crystals: Chemistry and Physics*; Taylor and Francis: Philadelphia, 1997; pp115-123.

(20) Demus, D.; Richter, L. *Textures of Liquid Crystals*; Verlag Chemie, Weinheim, 1978.

(21) Gray, G.W.; Goodby, J.W. *Smectic Liquid Crystals: Textures and Structures*; Leonard Hill, Glasgow, 1984.

(22) Collings, P.J. and Hird, M. *Introduction to Liquid Crystals: Chemistry and Physics*; Taylor and Francis: Philadelphia, 1997; pp.191-193.

Chapter 2

Thiophene-Based Tetracatenar Bent-Core Liquid Crystals: A Study on the Effects Bent-Angle and Lateral Dipole

Adapted from:

Eichhorn, S. H.; Paraskos, A. J.; Kishikawa, K.; Swager, T. M.
J. Am. Chem. Soc. **2002**, *124*, 12742-12751.

Introduction

The synthesis and investigation of mesogens with physical structures that deviate significantly from linearity and thereby describe an overall "bent" shape rather than a simple rigid rod has been described by numerous research groups. One interesting aspect of bent-rod mesogens is the increase in steric interaction that nearest neighboring molecules exert upon one another. In the nematic phase of ordinary calamitic mesogens, for example, the molecules freely and rapidly rotate about their long axes, thereby imparting a uniaxial nature to the material. Within a nematic phase of bent-rod molecules, however, the barrier to molecular rotation about their long axes should increase significantly as such rotation geometrically results in a larger displacement of neighboring molecules (Figure 2.1).

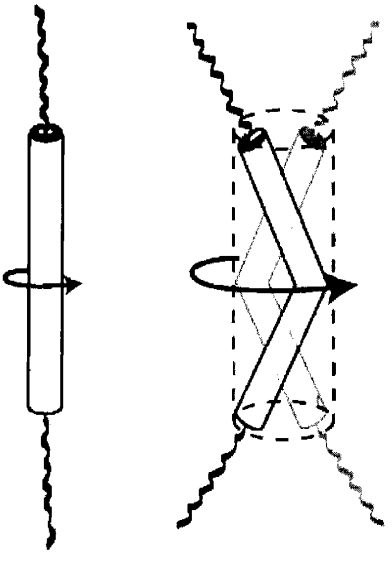

Figure 2.1. Bent-core mesogens sweep out larger areas upon rotation about their long axes than do traditional straight-rod mesogens.

Another important feature of bent-rod molecules is the decrease in molecular symmetry compared to analogous rigid rod molecules. This decrease in molecular symmetry from, for example, C_{∞} to C_{2V}, can have extremely profound implications upon the phase behavior. The most surprising result to arise from this decrease in molecular symmetry is the discovery of the so-called banana phases.[1] Novel ferroelectric and antiferroelectric mesophases were obtained from initially achiral molecules and macrophase separation of racemic mixtures into homo-chiral domains was observed.[2] However, the design principles are not understood and the majority of bent-rod (banana-shaped) mesogens do not display these new mesophases, if any mesophase at all, despite possessing similar molecular structures. The ultimate goal of being able to accurately predict the liquid crystalline properties of many molecular structures remains elusive, despite the many mesomorphic molecular structures and liquid crystalline phases that have been studied over the last hundred years.

The main thrust of this research focuses on synthesizing liquid crystals that possess bent-core shapes and additionally possess large laterally-directed dipole moments. Introduction of laterally directed dipole moments hinders rotation about the long axes of the mesogens as the interaction between the dipoles of neighboring molecules becomes increasingly significant (Figure 2.2). It was thought that this effect would add to the influence of the bent shape of the mesogens, which also inhibits rotation about the long axes, and that one of two molecular arrangements would result: either the molecules would arrange in a head-to-tail ferroelectric type organization of molecules, thereby resulting in effective packing of the bent molecules, or they would arrange in head-to-head dimers of molecules in which nearest neighboring mesogens effectively

offset each other's dipole moments (Figure 2.3).[3] Due to this inhibition of rotation, we thought that these types of molecules were reasonable candidates to display biaxial smectic or nematic phases.

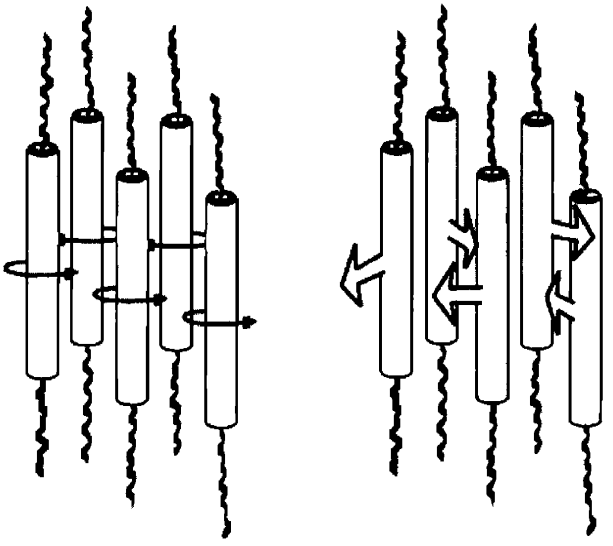

Figure 2.2. Diagram showing that the introduction of a large lateral dipole inhibits rotation as the dipoles of nearest neighboring molecules interact strongly.

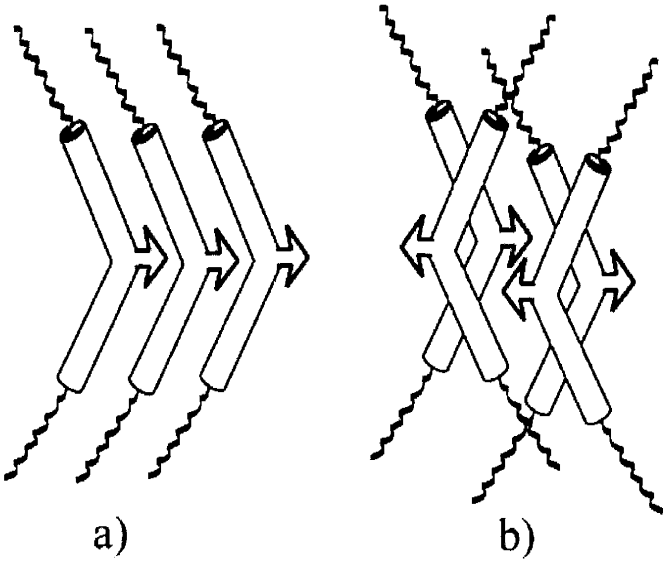

Figure 2.3. Possible packing of bent-rods with large lateral dipoles: a) head-to-tail parallel arrangement of dipoles, b) head-to-head antiparallel arrangement of dipoles.

Previous studies of bent-rod systems found that materials with severely bent molecular architectures display liquid crystalline phases with lower thermodynamic stability than analogous straight-rod derivatives.[4] We thought it crucial, therefore, that the bend angle of the mesogens be relatively modest and that the molecules deviate only slightly from linearity. Comparison with other synthetically attractive aromatic units reveals that 2,5-disubstituted thiophene describes a smaller bend angle (16.4 degrees) than 2,5-disubstituted furan or pyrrole (Figure 2.4) or the 30 degree bend angle of 1,3-disubstituted benzene.[5] Thiophene was therefore chosen as the central building block of the mesogens to be studied by our group. This route additionally enables the introduction of various lateral dipole moments by incorporation of electron-withdrawing substituents in the 3 and 4 positions of the thiophene ring.

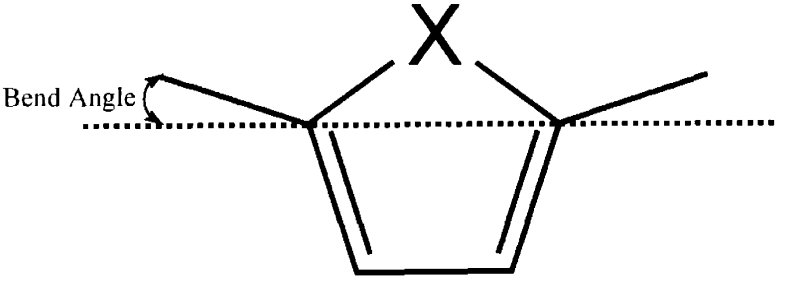

X	Bend Angle
O	29°
NH	23.7 °
S	16.4°

Figure 2.4. The relative bend angles of thiophene is much smaller than for alternative 5-membered heterocycles furan and pyrrole.

Early work on such compounds led by Keiki Kishikawa, a former Swager group postdoctoral fellow, examined a variety of 2,5-substituted thiophene-based mesogens. Though his initial studies were limited to mesogens with short aliphatic sidechains they established many of the guiding principles for subsequent investigations (Figure 2.5).[6] Compounds **I**, **II** and **III** possess the smallest molecular aspect ratios (length to width ratios) and **I** displays a nematic phase at high temperature while compounds **II** and **III** are not mesomorphic. Increasing the aspect ratio of the mesogens via incorporation of bridging alkyne groups resulted in significantly greater stability of the liquid crystalline phases of series **IV** through **VII**. The temperature ranges of the crystal phases decreased as the lateral dipole was increased from 2,5-unsubstituted series **IV** to 2,5-dibromosubstituted series **V** up through 2,5-dicyanosubstituted series **VII**, suggesting that increasing the lateral dipole results in decreased stability of the resulting mesophases. Modeling of the 2,5-dicyanosubstituted compounds suggested that these compounds possess lateral dipoles of up to 6.3 Debye, and the single crystal structures of these compounds revealed a dimer formation of neighboring molecules with an antiparallel orientation of their lateral dipoles.

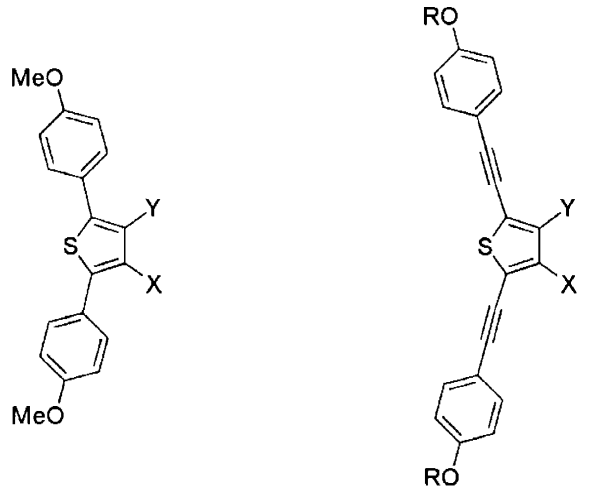

I (X = Y = H)
II (X = Y = Br)
III (X = Y = CN)

IV a (R = CH_3, X = Y = H)
IV b (R = C_4H_9, X = Y = H)
V a (R = CH_3, X = Y = Br)
V b (R = C_4H_9, X = Y = Br)
VI a (R = CH_3, X = Br, Y = CN)
VI b (R = C_4H_9, X = Br, Y = CN)
VI a (R = CH_3, X = Y = CN)
VII b (R = C_4H_9, X = Y = CN)

Figure 2.5. Initial studies by the Swager group on thiophene-based bent-core molecules focused on mesogens with short *n*-alkoxy sidechains.

We subsequently began working on the synthesis and characterization of various thiophene-based as well as benzene-based tetracatenar compounds. Tetracatenars are liquid crystals containing di(alkoxy)benzoate groups on each end of the mesogen (see Chapter 1). These types of mesogens were targeted because conventional straight-rod tetracatenars tend to give rise to a relatively wide variety of mesophases, including nematic, SmC and columnar mesophases (depending on the length of the sidechains) and so a number of mesophases are accessible from a relatively small number of compounds. A range of molecules varying in both bend angle and lateral dipole strength were

synthesized, and their phase behavior was characterized by polarizing microscopy, thermal analysis, X-ray diffraction, and electrooptical measurements.

This chapter describes research carried out by myself in collaboration with Holger Eichhorn, a former Swager-group postdoctoral fellow. In addition, a number of compounds were synthesized by Keiki Kishikawa, another former Swager-group postdoctoral fellow. The results of our collaboration were published in the Journal of the American Chemical Society within an article written by Holger and myself. Because of the close collaborative nature of the project, it is important to describe the project as a whole including results that were obtained by Holger and Keiki. Every effort has been made, however, to clarify which results are my own and which are those of my coworkers. Any compounds described in the experimental section were synthesized and characterized (including NMR, DSC, IR, X-ray and polarized microscopy) by myself.

Shorthand Nomenclature

It became apparent during discussions of the various polycatenars that a shorthand nomenclature was necessary in order to efficiently refer to the compounds. A system was adopted in which the mesogenic cores are described as catenars with DC standing for dicatenar, TrC standing for tricatenar, and TC standing for tetracatenar. The very central portion of the core is either a 2,5-thienyl (XXT), para-phenyl (pXXP), or meta-phenyl (mXXP) where the XX represents the type of catenar. The central rings of the core can be substituted with hydrogens (H), bromides (Br) or nitriles (NC). Hence, NC-TCT stands for a nitrile containing tetracatenar based on the 2,5-thienyl group. At the ends of the mesogens are benzoates containing alkyl-oxy sidechains that are para (p) or meta (m) with respect to the ester and, for example, a mpm12 designation indicates that 12 carbon

alkyl-oxy side chains are attached to both of the meta positions in addition to the para position of the benzoate. Chiral compounds are labeled (*) and the stereochemistry is given as R, S, or rac.

Results and Discussion

Synthesis. We chose a 2,5-bis(4-hydroxyphenylacetylene)thiophene **6** and its derivatives **7** and **8**, all fluorescent compounds, as central building blocks (Scheme 2.1). They were obtained in three steps from 2,5-dibromothiophene or tetrabromothiophene in analogy to previously published procedures.[7] Palladium-catalyzed cross-coupling of 4-(benzyloxy)phenylacetylene **2** with tetrabromothiophene results in selective substitution of the bromine atoms in the 2 and 5 positions to give **4,** which was subsequently treated with CuCN/CuI in 2,5-dimethylimidazlidinone at 120 °C to give the 3,4-dicyanothiophene derivative **5a**. Cleavage of the benzyl protecting groups in **4** and **5a** with bromocatecholborane afforded the diphenolic building blocks **7** and **8**, respectively, in good yields. The same synthetic approach was initially applied to obtain **6**, but the cleavage of the benzyl groups with bromocatecholborane or BBr_3 was low yielding due to the occurrence of side-reactions. Compound **6** was therefore synthesized *via* the tetrahydopyran (THP) protected precursor **3**.

An alternative synthetic approach to **8** involves cyanation of 3,4-dibromothiophene followed by the lithiation and subsequent iodination of the 2 and 5 positions (Scheme 2.1). The resulting 2,5-diiodo-3,4-dicyanothiophene was then converted to **5b** via palladium-catalyzed cross-coupling. The 42% overall yield of this pathway is similar to the yield obtained for the approach described above, but the lowest

yielding cyanation step is carried out at the beginning of the synthetic scheme, resulting in more facile purification of the following intermediates.

Esterification of the lateral hydroxy groups of **6-8** with the corresponding benzoic acid derivatives in the presence of diisopropylcarbodiimide and DMAP gave the desired symmetric di- and tetracatenars in good yields. Polycatenars possessing two different benzoic ester groups were obtained by statistical mono-esterification and subsequent chromatographic separation of the two symmetric side-products (Scheme 2.2). 1,3-bis(4-hydroxyphenylacetylene)benzene (**9a**) and 1,4-bis(4-hydroxyphenylacetylene)benzene (**10**) derivatives were synthesized for comparison purposes (Scheme 2.2). The reaction pathways were identical to the preparation of **6** and **H-TCT-mp4-14** except that 1,3-dibromobenzene and 1,2-dibromobenzene were used as central cores instead of 2,5-dibromothiophene.

Mesomorphism. The phase diagrams of all compounds were determined by temperature controlled polarizing microscopy, differential scanning calorimetry (DSC), and X-ray diffraction. All diffraction data agreed with our phase assignments and details are given for higher ordered enantiotropic mesophases. The results for the thiophene-based tetracatenars are summarized in Tables 2.1 and 2.2. Table 2.3 contains the data for bistolane-based tetracatenars.

Scheme 2.1. Synthesis of thiophene based tetracatenars.

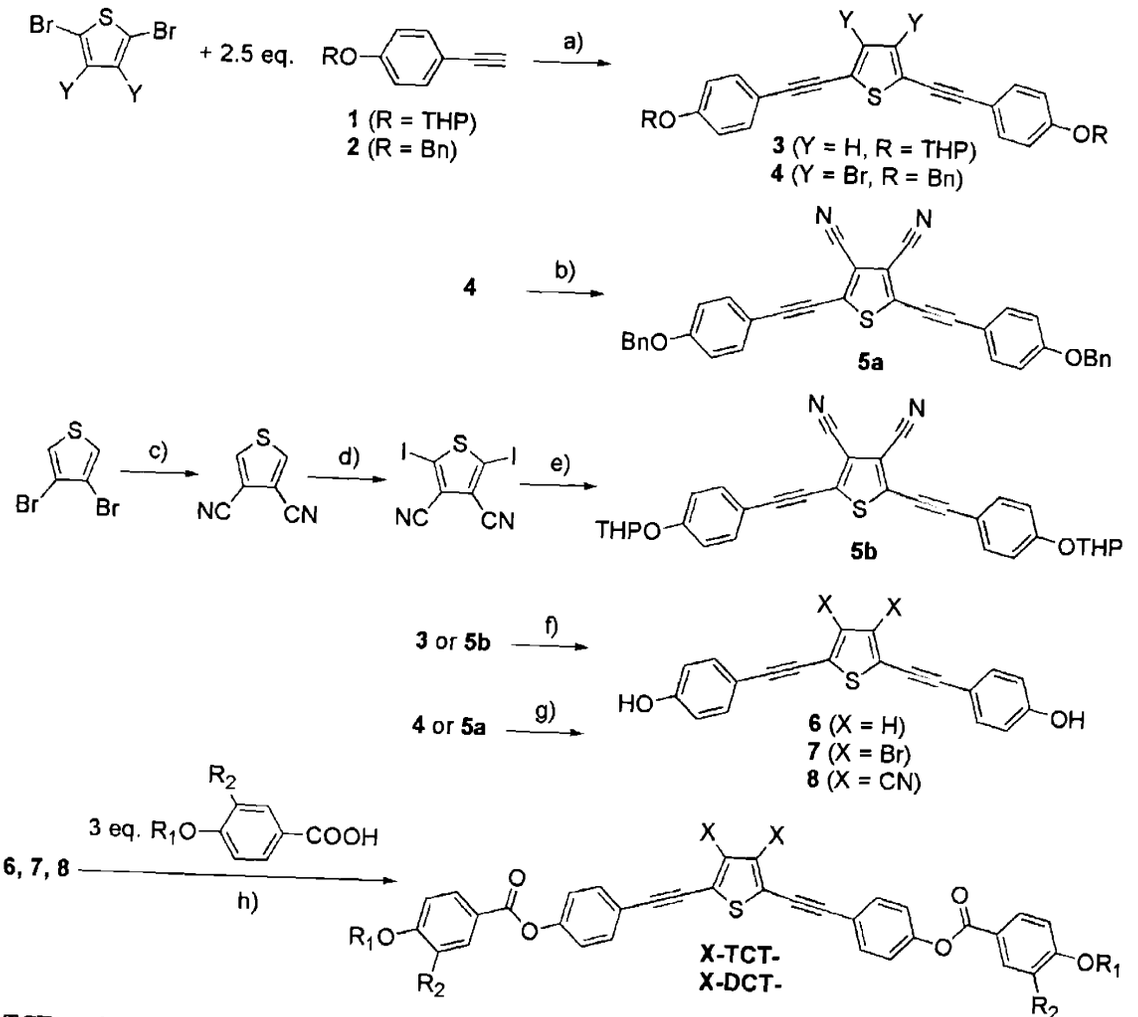

H-TCT-mp4-14: X = H; $R_1 = (C_nH_{2n+1})$, n = 4, 6, 8, 10, 12, 14; $R_2 = (OC_nH_{2n+1})$, n = 4, 6, 8, 10, 12, 14
H-TCT-mp10*(S): X = Br; $R_1 = ((S)C_2H_4C^*H(Me)C_3H_6CH(Me)_2)$; $R_2 = ((s)OC_2H_4C^*H(Me)C_3H_6CH(Me)_2)$
Br-TCT-mp4-12: X = Br; $R_1 = (C_nH_{2n+1})$, n = 4, 6, 8, 10, 12; $R_2 = (OC_nH_{2n+1})$, n = 4, 6, 8, 10, 12
Br-TCT-mp10*(S): X = Br; $R_1 = ((S)C_2H_4C^*H(Me)C_3H_6CH(Me)_2)$; $R_2 = ((s)OC_2H_4C^*H(Me)C_3H_6CH(Me)_2)$
NC-TCT-mp4-12: X = CN; $R_1 = (C_nH_{2n+1})$, n = 4, 5, 6, 7, 8, 9, 10, 11, 12;
$R_2 = (OC_nH_{2n+1})$, n = 4, 5, 6, 7, 8, 9, 10, 11, 12
NC-TCT-mp4*(S): X = CN; $R_1 = ((S)\ CH_2C^*H(Me)C_2H_6)$; $R_2 = ((S)\ OCH_2C^*H(Me)C_2H_6)$
NC-TCT-mp10*(rac);(R);(S): X = CN; $R_1 = ((S)$ or $(R)C_2H_4C^*H(Me)C_3H_6CH(Me)_2)$;
$R_2 = ((S)$ or $(R)OC_2H_4C^*H(Me)C_3H_6CH(Me)_2)$
NC-DCT-p10; 12: X = CN; $R_1 = (C_nH_{2n+1})$, n = 10, 12; $R_2 = H$
NC-DCT-p4*(S): X = CN; $R_1 = ((S)CH_2C^*H(Me)C_2H_5)$; $R_2 = H$
NC-DCT-p10*(S): X = CN; $R_1 = ((S)C_2H_4C^*H(Me)C_3H_6CH(Me)_2)$; $R_2 = H$

(a) Pd $(PPh_3)_4$, CuI, iPr_2NH, toluene, 25 °C, >90%. (b) and (c) CuCN, CuI, DMI, 120 °C, 3.5h, >60%. (d) 2.2eq. LDA, I_2, THF, -78 °C, 77%. (e) Pd $(PPh_3)_4$, CuI, iPr_2NH, toluene, 25 °C, >90%. (f) TsOH, MeOH, 25 °C, >90%. (g) BrB-catechol, DCM, 0-25 °C, >90%. (h) (iPr)N=C=N(iPr), DMAP, DCM, 0-25 °C, 70-90%.

Scheme 2.2. Synthesis of unsymmetric and benzene based polycatenars.

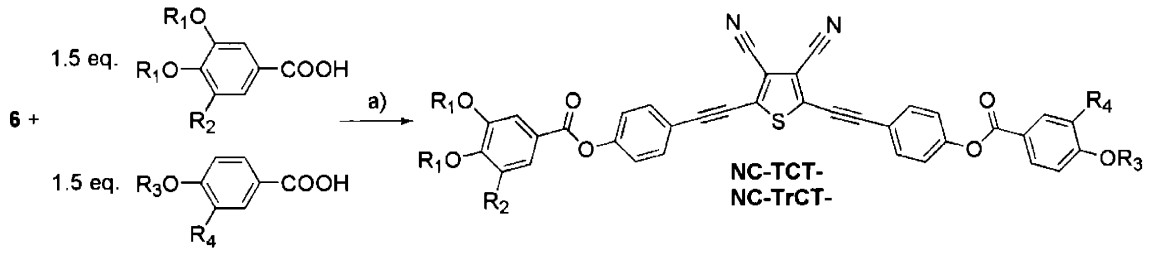

NC-TCT-mp6,mp10*(R): $R_1 = (C_6H_{13})$, $R_2 = H$, $R_3 = ((S)\ C_2H_4C^*H(Me)C_3H_6CH(Me)_2)$, $R_4 = OR_3$
side products are **NC-TCT-mp6** and **NC-TCT-p10*(R)**

NC-TrCT-mp4,p10*(S): $R_1 = (C_4H_9)$, $R_2 = H$, $R_3 = ((S)\ C_2H_4C^*H(Me)C_3H_6CH(Me)_2)$, $R_4 = H$
side products are **NC-TCT-mp4** and **NC-DCT-p10*(S)**

NC-TrCT-mp6,p10*(S): $R_1 = (C_6H_{13})$, $R_2 = H$, $R_3 = ((S)\ C_2H_4C^*H(Me)C_3H_6CH(Me)_2)$, $R_4 = H$
side products are **NC-TCT-mp6** and **NC-DCT-p10*(S)**

NC-TCT-mpm12,p8: $R_1 = (C_{12}H_{25})$, $R_2 = OR_1$, $R_3 = (C_8H_{17})$, $R_4 = H$
side products are the hexacatenar and the dicatenar

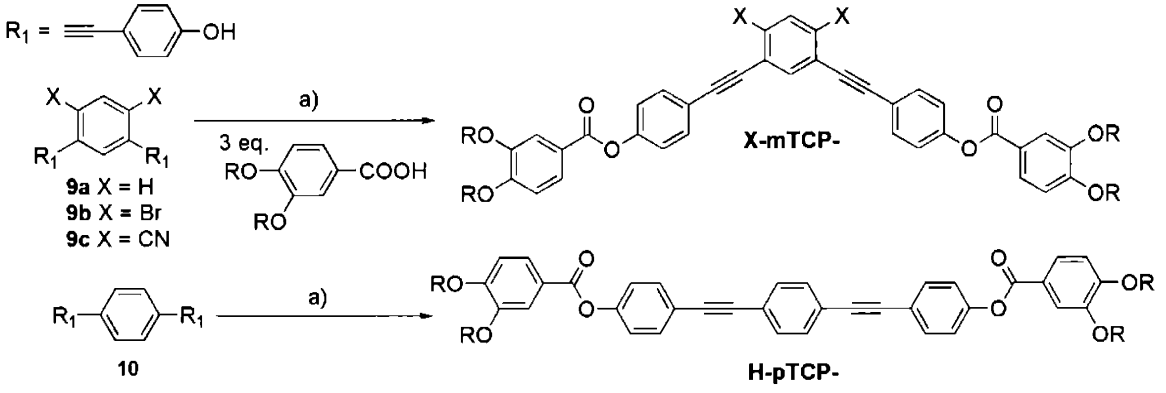

H-mTCP-mp6; 10: X = H; R = (C_nH_{2n+1}), n = 6, 10
Br-mTCP-mp6; 8; 10; 12: X = Br; R = (C_nH_{2n+1}), n = 6, 8, 10, 12
NC-mTCP-mp8; 12: X= CN; R = (C_nH_{2n+1}), n = 8, 12
H-pTCP-mp6; 10: R = (C_nH_{2n+1}), n = 6, 10

(a) (iPr)N=C=N(iPr), DMAP, DCM, 0-25 °C, 70-85%

Table 2.1. Mesomorphism of Thiophene and 3,4-Dibromothiophene-Based Tetracatenars Determined by Polarizing Microscopy, DSC and X-ray Diffraction.

Compound	Transition	*T* /°C, heating (ΔH/kJ mol^{-1})	*T* /°C, cooling (ΔH/kJ mol^{-1})
H-TCT-mp4			
H-TCT-mp6	Cr-N	137.6 (69.88)	122.9 (-67.77)
	N-I	144.1 (1.11)	142.9 (-1.14)
H-TCT-mp8	Cr-(N)[a]	138.1 (74.57)	117.6 (-73.14)
	(N)-I		133.2 (-1.22)
H-TCT-mp10	Cr-(SmC)[a]		112.0 (-62.11)
	(SmC)-(N)	127.3 (71.58)	114.8 (-6.92)
	(N)-I		125.9 (-1.09)
H-TCT-mp12	Cr-(N)[a]	133.6 (89.77)	116.9 (-87.66)
	(N)-I		120.5 (-1.26)
H-TCT-mp14	Cr-I	125.4 (91.41)	115.3 (-98.49)
H-TCT-mp10*(S)	Cr-I	99.2 (66.39)	63.2 (-44.49)
Br-TCT-mp4[†]	Cr-(N)[a]	135.2 (57.03)	87.1 (-28.31)
	(N)-I		133.9 (-1.10)
Br-TCT-mp6[†]	Cr-(N)[a]	189.6 (95.28)	127.9 (-55.14)
	(N)-I		161.1 (-1.22)
Br-TCT-mp8[†]	Cr-(N)[a]	119.5 (52.93)	84.8 (-51.14)
	(N)-I		107.6(-1.01)
Br-TCT-mp10[†]	Cr-(SmC)[a]	110.8 (47.86)	82.7 (-98.56)
	(SmC)-I		97.3 (-7.51)
Br-TCT-mp12[†]	Cr-(SmC)[a]	117.3 (67.74)	89.4 (-53.95)
	(SmC)-I		98.3 (-3.16)
Br-TCT-mp10*(S)[†]	Cr-I	103.3 (42.74)	60.9 (-47.01)

[†] Investigated by K. Kishikawa.

Table 2.2. Mesomorphism of the 3,4-dicyanothiophene based tetracatenars determined by polarizing microscopy, DSC (5 °C/min) and X-ray diffraction (2D-WAXS).

Compound	Transition	T /°C, heating (ΔH/kJ mol^{-1})	T /°C, cooling (ΔH/kJ mol^{-1})	d-values/Å (sample temp./°C)[a]	tilt angle/° SmC phase[b]
NC-TCT-mp4	Cr-N	148.4 (44.40)[1]	129.2 (-44.04)		
	N-I	162.5 (1.14)	161.4 (-1.03)		
NC-TCT-mp5	Cr-N	133.5 (40.33)[1]	116.8 (-40.87)	29.3, 3.9 (145)	
	N-I	147.6 (0.94)	146.4 (-1.67)		
NC-TCT-mp6	Cr-SmC	113.9 (32.37)	98.9 (-21.83)	28.9, 14.6, 6.3, 4.5 (118); 30.4, 4.0 (134)	38
	SmC-N	121.6 (7.08)	121.6 (-7.42)		
	N-I	144.4 (0.96)	142.8 (-0.96)		
NC-TCT-mp7	Cr-SmC	127.1 (46.46)	91.8 (-19.85)	31.5, 15.5, 6.3, 4.6 (120)	53
	SmC-I	129 (shoulder)	125.2 (-5.02)		
NC-TCT-mp8	Cr-SmC	131.2 (39.89)	109.9 (-38.48)	30.9, 15.5, 6.4, 4.7 (133)	54
	SmC-I	135.3 (6.92)	132.4 (-7.72)		
NC-TCT-mp9	Cr-SmC	119.3 (35.27)	98.9 (-30.22)	32.6, 16.4, 6.5, 4.7 (130)	56
	SmC-I	130.9 (5.50)	129.4 (-5.92)		
NC-TCT-mp10	Cr-SmC	100.5 (50.88)	86.8 (-49.88)	34.5, 17.6, 6.8, 4.7 (110); 39.0, 22.5, 19.7, 6.5, 4.6 (130)	
	SmC-Col$_h$	123.4 (2.95)	111.7 (-4.38)		
	Col$_h$-I	131.4 (3.95)	129.7 (-3.66)		
NC-TCT-mp11	Cr-Col$_h$	106.2 (59.99)[2]	94.7 (-61.61)	39.9, 23.2, 20.2, 6.8, 4.7 (120)	
	Col$_h$-I	137.5 (5.29)	136.1 (-4.19)		
NC-TCT-mp12	Cr-Col$_h$	102.8 (89.29)	87.8 (-81.35)	41.1, 23.9, 20.8, 6.3(small),4.7 (115)	
	Col$_h$-I	138.0 (2.78)	130.3 (-6.79)		
NC-TCT-mp4*(S)	Cr-I	161.0 (31.38)	107.2 (-34.33)		
NC-TCT-mp10*(rac)	Cr-(N)	101.6 (62.89)	69.4 (-37.88)		
	(N)-I		74.7 (-2.14)		
NC-TCT-mp10*(R),(S)	Cr-I	104.1 (56.57)	66.9 (-15.62)[3]		

[a] Reflections at 6-7 Å and 4-5 Å are broad halos. [b] Angle between layer and side-chain reflections of magnetically aligned samples. [1] Nematic phases were not observed at the first heating runs since the Cr-I transitions were at 189.0 (79.63) for **mp-TC-4** and at 154.8 (56.67) for **mp-TC-5**. [2] A Cr-SmC transition was observed on the first heating run, 110.6 (2.94). [3] Cold crystallization on heating run.
*All compounds in this table were synthesized and investigated by K. Kishikawa and H. Eichhorn.

Table 2.3. Mesomorphism of bistolane based tetracatenars determined by polarizing microscopy, DSC (5 °C/min) and X-ray diffraction (2D-WAXS).

Compound	Transition	T /°C, heating (ΔH/kJ mol^{-1})	T /°C, cooling (ΔH/kJ mol^{-1})	d-values/Å (sample temp./°C)[a]
H-mTCP-mp6[†]	Cr-I	122 (73.79)	98.0 (-68.56)	
H-mTCP-mp10[†]	Cr1-Cr2	95.9 (71.79)		
	Cr2-I	101.2 (13.60)	89.6 (-71.76)	
Br-mTCP-mp6	Cr-I	127.9 (56.91)[b]	82.0 (-50.81)	
Br-mTCP-mp8	Cr-I	108.9 (43.22)	88.8 (-46.43)	
Br-mTCP-mp10	Cr1-Cr2	71.5 (17.52)	68.3 (-9.59)	
	Cr2-I	109.4 (36.79)	89.8 (-44.89)	
Br-mTCP-mp12	Cr1-Cr2	83.5 (11.69)[c]	76.1 (-4.08)	
	Cr2-I	108.4 (49.16)	82.8 (71.18)	
NC-mTCP-mp8	Cr1-Cr2	66.31 (11.43)	66.2 (-7.03)	
	Cr2-I	116.5 (39.04)	95.5 (-39.03)	
NC-mTCP-mp12	Cr1-Cr2	84.2 (42.38)	83.1 (-39.31)	
	Cr2-I	110.2 (122.56)	93.7 (123.78)	
H-pTCP-mp6[†]	Cr-SmC	147.5 (28.61)	141.0 (-33.17)	27.9, 13.8, 4.5 (155 °C)
	SmC-N	164.9 (9.57)	167.5 (-8.31)	
	N-I	217.8 (1.47)	217.7 (-1.67)	
H-pTCP-mp10[†]	Cr-SmC	114.6 (58.15)	112.6 (-59.66)	31.6, 15.8, 4.5 (140 °C)
	SmC-N	159.7 (5.10)	163.3 (-5.12)	
	N-I	175.7 (0.67)	174.6 (-1.18)	

[a]Reflections at 6-7 Å and 4-5 Å are broad halos. [b]Cold crystallization on heating at 109 °C. Cold crystallization at 97 °C. [†] Investigated by H. Eichhorn.

Incorporation of a bent-core within a molecular design typically destabilizes the resulting liquid crystalline phases as the bent-rod shape of the molecules interferes with their freedom to rotate about their long axes.[8, 9, 10] In order to investigate the viability of using a 2,5-thiophene-based structural motif for the formation of stable liquid crystals, we investigated the tetracatenars **H-TCT-mp** (Table 2.1). Despite possessing moderate bend angles (154°) these compounds display exclusively monotropic mesophases (with the exception of the nematic phase of **H-TCT-mp6**). This stands in direct contrast to the corresponding straight-rod tetracatenars **H-pTCP-mp6** and **-mp10**, which exhibit SmC and N phases over wide temperature ranges, suggesting that the introduction of even

small bend-angles has dramatic consequences upon the stability of the resulting liquid crystal phases of these compounds (Table 2.3). The 3,4-dibromo substituted tetracatenars **Br-TCT-mp** also give rise to exclusively monotropic mesophases (Table 2.1). We also showed that further increasing the bend to 120° as in the **H-mTCP-mp** and **Br-mTCP-mp** derivatives exaggerates this effect and in fact results in the complete suppression of mesomorphism (Table 2.3).

We found that the introduction of a strong lateral dipole through the incorporation of cyano groups at the 3 and 4 positions of the central thiophene unit changes the mesomorphic properties of the tetracatenars. The **NC-TCT-mp** derivatives are liquid crystalline over wide temperature ranges and display a polymesomorphism typical of tetracatenars (Table 2.2). The types of mesophases progress from N, to SmC, to Col with increasing side-chain length (Figure 1). X-ray tilt angle measurements on magnetically aligned samples reveal a constant increase of tilt angle of the SmC phases from **NC-TCT-mp6** to **NC-TCT-mp9** with the SmC phase of **NC-TCT-mp10** eventually converting into a high-temperature hexagonal columnar mesophase (Col_{hex}). This behavior is typical of tetracatenars and is consistent with a model in which the increasing steric demand of the side-chains causes the phase transition from SmC to Col.[11] A cubic mesophase is displayed by **NC-TCT-mpm12,p8** which is also a reported behavior of classical tetracatenars with three terminal side-chains at one end and only one side-chain at the other end.[12]

We were quite surprised by the fact that the dicyanotetracatenars **NC-TCT-mp** display such stable liquid crystal phases. The strong lateral dipole (calculated to be 6.3 Debye) and steric hindrance introduced by the two cyano groups increases the rotational

barrier about the long axis of the mesogens and results in strong intermolecular dipole-dipole interactions. Both of these effects would be expected to promote higher melting points and decreased mesomorphism. Following this line of reasoning, tetracatenars **H-TCT-mp** (with the smallest lateral dipoles and least steric hindrance to rotation) would have been predicted to display mesophases that were significantly more stable than those of the **NC-TCT-mp** analogues, which is in direct contrast to our observations.

We have suggested that the unexpectedly broad mesomorphism of the **NC-TCT-mp** derivatives can be reasoned as the individual **NC-TCT-mp** molecules form loosely associated dimers with antiparallel dipole orientations that function as the mesomorphic unit in the liquid crystalline phase. While strict antiparallel association of nearest neighbor molecules has not been observed for calamitic liquid crystals, several classical nematic and smectic liquid crystals with strong dipoles along their molecular long axis, such as cyanobiphenyl type systems,[13] have been shown to statistically adopt antiparallel orientations. The formation of these dimers results in a mesomorphic unit in which the deleterious effects of both the bent-shape and large lateral dipoles are largely negated, as such a dimer sweeps out an approximately cylindrical volume upon rotation around its long axis (Figure 2.6). Experimental support of our hypothesis was provided by antiparallel dimer formation in single crystals of related compounds[14] and by 2-dimensional X-ray diffraction data of magnetically aligned Col_{hex} and SmC mesophases. A weak and diffuse peak centered at 0.75 nm, the expected distance between the sulfur atoms of every other thiophene unit in stacks of alternating antiparallel packing, was found in all of the diffraction patterns (Figure 2.7). A similar but sharper peak was found

in the X-ray diffraction pattern of a related hexacatenar derivative, for which antiparallel columnar packing was independently verified by photophysical methods.[15]

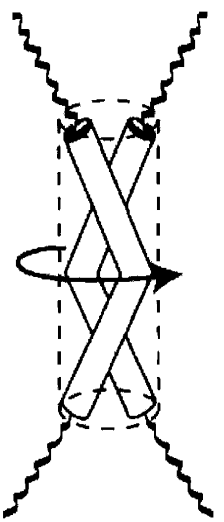

Figure 2.6. A mesogenic unit consisting of antiparallel dimers of bent-rod molecules sweeps out an approximately cylindrical volume upon rotation about the long axis.

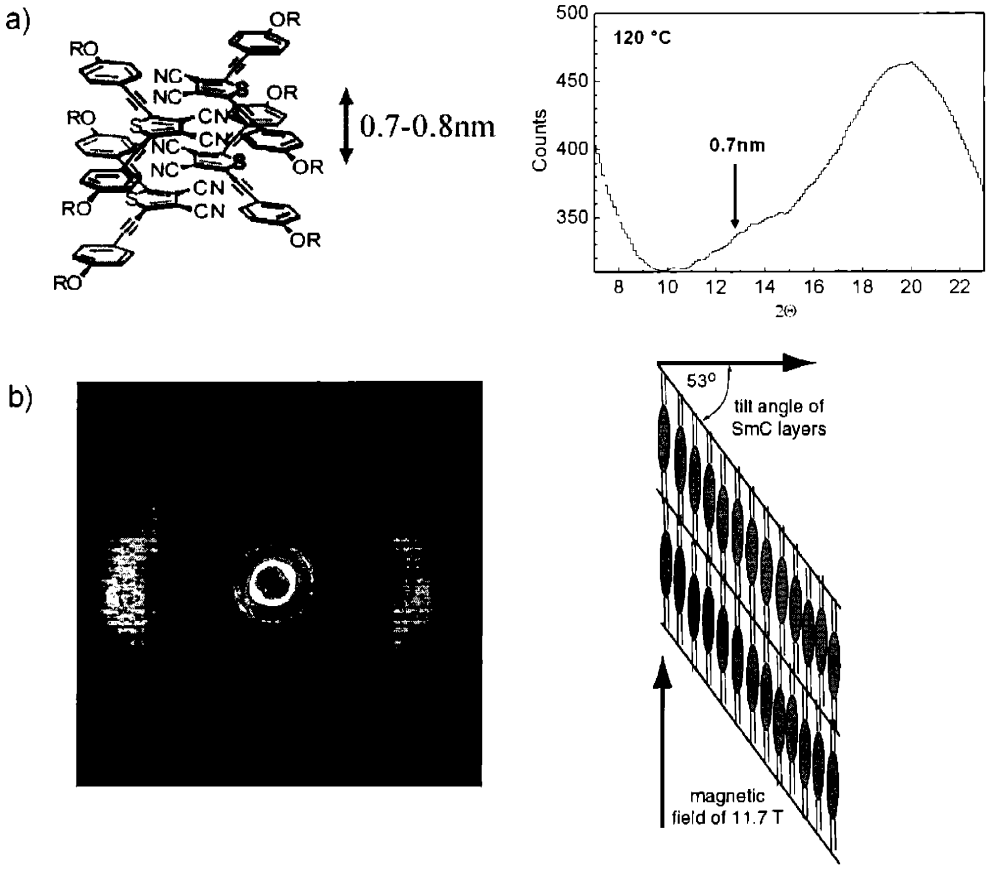

Figure 2.7. (a) 1D X-ray diffraction pattern (wide-angle region) of sample **mp-TCT-7** at 120 °C and illustrated antiparallel packing of molecules. (b) 2D X-ray diffraction pattern of a previously magnetically aligned sample of , which shows a 53° tilt angle in the SmC phase.

We were also curious to see whether this effect would extend to systems with more pronounce bend angles and so we synthesized the 1,3-dicyano **NC-mTCP-mp** bistolane derivatives, which possess a bend-angle of approximately 120° (Scheme 2.2). In this case the bend-angle proves too severe and these compounds are not liquid crystalline, despite their large lateral dipoles. It should be noted, however, that these molecules possess surprisingly low melting and crystallization temperatures between 116 °C and 93 °C (Table 2.3).

The **NC-TCT-mp** derivatives were considered candidates to display biaxial nematic phases because of the sterically and electronically hindered rotation about their molecular long axis. A tendency of mesogens to display antiparallel dimeric correlations results in mesomorphic units that may not contain lateral dipoles and a more rod-like shape. Apparently, dimers can rotate freely and no evidence for the existence of biaxiality was found by optical microscopy.[16] However, more elaborate NMR measurements would be required to provide conclusive evidence of the formation of dimers and the presence or absence of biaxiality within the phases.[17]

Summary and Conclusions

Though bent-cores and strong lateral dipoles typically disturb calamitic mesophases, we were able to demonstrate that combining both of these structural features can result in enantiotropic mesomorphism over wide temperature ranges. In fact, the phase diagram of the bent tetracatenars containing two lateral cyano groups at the central thiophene ring (**NC-TCT**) is very similar to what has been found for common straight-rod tetracatenars. We obtained nematic, smectic, columnar, and cubic mesophases by changing the length and substitution pattern of the four aliphatic side-chains. At a molecular level, however, we propose distinct differences and explain the unusual behavior of the **NC-TCT** derivatives with an antiparallel dimer formation. The antiparallel dimer formation is incompatible with the formation of chiral mesophases.

Experimental Section

^{1}H NMR spectra were recorded on a Varian Unity VXR 500, a Bruker DPX-400, and a Varian Unity 300. Chemical shifts are reported in ppm relative to residual $CHCl_3$ (δ = 7.27, ^{1}H). Multiplicities are given as s (singlet), d (doublet), t (triplet) and m (multiplet). MS investigations were run on a Finnigan MAT 8200 equipped with an Ion Tech ion source and a Bruker Daltonics Apex II 3T FT-ICR MS. Optical characterization was performed on a Leica DMRXP polarizing microscope equipped with a Wild Leitz MPS46 Photoautomat along with a Linkam LTS 350 hot stage and a Linkam TP 92 controller. Transition temperatures and heats of fusion were determined at scan rates of 5 and 10 °C/min by differential scanning calorimetry using a Perkin-Elmer DSC 7 and Pyris with a Perkin-Elmer Pyris thermal analysis data station. Variable temperature X-ray measurements were performed on an Inel system (CPS 120 detector, XRG 2000 generator, Cu K_α radiation, Minco CT 137 temperature controller (±1 °C) and a home-built heating stage) as well as a Siemens system (flat camera 2D-Xe-detector, 256×256 cells, Instec HS 400 hot stage and STC 200 controller, Rigaku RV-300 rotating anode, Ni-filtered Cu K_α-radiation). Calibration was accomplished by using mica and silicon standards (NBS) as well as silver behenate. Samples were prepared by filling each Lindemann capillary (1.5 mm) with approximately 15 mg of compound. FTIR-spectra were taken with a Nicolet Magna IR 860 and a Nicolet Impact 410. UV-Vis spectra were obtained from a Hewlett-Packard 8452A diode array spectrometer and a Varian Cary 50 spectrophotometer. Dichloromethane and THF were dried by passing through a column of activated alumina and diisopropylamine was freshly distilled from CaH_2 under an atmosphere of dry argon. All other chemicals and solvents, unless otherwise

indicated, were purchased commercially and used as obtained without further purification. Air and water sensitive reactions employed standard Schlenk techniques under argon atmosphere.

2,5-Bis(4-tetrahydropyranyloxy)phenylethynyl]thiophene (3). A 200ml Schlenk flask was charged with $Pd(PPh_3)_4$ (143mg, 0.124mmol), copper (I) iodide (24mg, 0.124mmol), and a stir bar under argon. In a separate flask, 2,5-dibromothiophene (0.28mL, 2.47mmol), THP-protected hydroxyphenylacetylene (1.00g, 4.94mmol) were dissolved in diisopropylamine (1.7mL, 12.4mmol) and toluene (100mL). The solution was purged with argon for 20 minutes and then added to the reaction (Schlenk) flask *via* a cannula. The yellow solution turned darker after about 15 minutes and was stirred at room temperature for 12 hours. The reaction mixture was washed through a silica gel pad with dichloromethane, and the obtained crude solid was recrystallized from hexane/chloroform to yield **3** as yellow crystals (960mg, 1.98mmol, 80%). ^{1}H NMR ($CDCl_3$, δ): 1.57-1.79 (m, 6H, CH_2CH_2), 1.83-1.89, (m, 4H, CH_2), 1.91-2.09 (m, 2H, CH_2), 3.58-3.63 (m, 2H, CH_2O), 3.83-3.91 (m, 2H, CH_2O), 5.43 (t, 2H, OCHO), 7.04 (d, 4H, J = 9.0 Hz, Ar-H), 7.11 (s, 2H, Ar-H), 7.45 (d, 4H, J = 9.0 Hz). ^{13}C NMR ($CHCl_3$, δ): 18.61, 25.08, 30.18, 62.03, 81.13, 93.97, 96.17, 115.46, 116.40, 124.56, 131.34, 132.86, 157.37. HRMS-EI (*m/z*): (M^+) calcd for $C_{30}H_{28}O_4S$ 484.1708, found 484.1701.

2,5-Bis[(4-benzyloxyphenyl)ethynyl]-3,4-dibromothiophene (4). Tetrabromothiophene (30.13 g, 75.4 mmol), tris(triphenylphosphine)palladium (5.4 g, 4.7 mmol), and copper iodide (1.78 g, 9.4 mmol) were dissolved in a mixture of toluene (400 mL) and diisopropylamine (27.0 mL, 19.5 g, 193 mmol) under argon. A solution of 4-benzyloxyphenylacetylene (39.12 g, 188 mmol) in toluene (100 mL) was added within 30

min *via* a cannula. The solution was stirred at room temperature for 2 d, quenched with 1 M aqueous HCl (200 mL), and the organic phase was dried over $MgSO_4$. Filtration through silica using toluene as solvent and recrystallization from THF/ethanol yielded pale yellow plates of **4** (42.49 g, 86%). ^{1}H NMR ($CDCl_3$, δ): 5.10 (s, 4H, CH_2), 6.97 (d, J = 8.8 Hz, 4H, Ar H), 7.45-7.3, (m, 5H, phenyl), 7.50 (d, J = 8.8 Hz, 4H, Ar H). ^{13}C NMR ($CHCl_3$, δ): 70.28, 80.24, 98.94, 114.44, 115.27, 118.27, 118.58, 121.51, 127.70, 128.39, 128.88, 133.55, 136.56, 159.75. HRMS-EI (*m/z*): (M^+) calcd for $C_{34}H_{22}O_2SBr_2$ 651.970724, found 651.97072.

2,5-Bis(4-hydroxyphenylethynyl)thiophene (6) A stirred suspension of **3** (521mg, 1.075 mmol) in THF (21ml), acetic acid (42ml) and water (11mL) was heated to 45 °C, at which point all solids were dissolved, and stirred for 12 hours. Ether was added (100ml) and the mixture was washed with water (5x30ml). The solvents were removed in vacuum yielding an off-white powder that was recrystallized from dichloromethane/hexanes to yield **6** as a white powder (277mg, 0.876 mmol, 82%). ^{1}H NMR ($CDCl_3$, δ): 3.52 (s, 2H, OH), 6.73 (d, J = 9.0 Hz, 4H, Ar-H), 7.01 (s, 2H, Ar-H), 7.31 (d, J = 9.0 Hz, 4H, Ar-H). ^{13}C NMR ($CDCl_3$, δ): 80.29, 93.97, 113.28, 115.30, 124.28, 130.95, 132.86, 157.29. HRMS-EI (*m/z*): (M^+) calcd for $C_{20}H_{12}O_2S$ 316.0558, found 316.0548.

Esterification of 2,5-Bis[(4-hydroxyphenyl)ethynyl]-thiophene 3 eq. of the appropriate alkoxy substituted benzoic acid were dissolved in dry dichloromethane under argon and an equal molar amount of *N,N'*-diisopropylcarbodiimide was added at 0 °C. After 2 h of stirring 1 eq. of the 2,5-bis[(4-hydroxyphenyl)ethynyl]thiophene derivative

dissolved in dry dichloromethane was added to the mixture at 0 °C. The mixtures were stirred for another 3 h at 0 °C and then allowed to warm up to room temperature. The progress of esterification was monitored by following the consumption of the diphenolic starting material and the monoester intermediate by TLC (silica, dichloromethane/ethylacetate 9:1). A complete consumption of the starting materials and intermediates was attained after 1-2 d. The solutions were concentrated in vacuum and chromatographed on silica gel using toluene/heptane mixtures as eluent to give yields of 80-95%. For analytical measurements, a further purification was achieved by filtration of a concentrated THF solution through 2 μm filters and subsequent precipitation by the addition of ethanol.

2,5-Bis[4-(3,4-dihexyloxyphenylcarbonyloxy)phenylethynyl]thiophene (H-TCT-mp6). ^{1}H NMR ($CDCl_3$): 0.87-0.91 (m, 12H, CH_3), 1.27-1.51 (m, 24H, $(CH_2)_3$), 1.84-1.90 (m, 8H, CH_2), 4.06-4.11 (m, 8H, CH_2O), 6.94 (d, 2H, J = 8.6 Hz, Ar-H), 7.18 (s, 2H, Ar-H), 7.23 (d, 4H, J = 8.7 Hz, Ar-H), 7.59 (d, 4H, J = 8.7 Hz, Ar-H), 7.66 (d, 2H, J = 2.0 Hz, Ar-H), 7.82 (dd, 2H, $J1$ = 8.6 Hz, $J2$ = 2.0 Hz, Ar-H). ^{13}C NMR ($CDCl_3$): 14.00, 22.57, 25.60, 25.64, 28.96, 29.07, 31.51, 31.53, 69.02, 69.28, 93.42, 111.83, 114.44, 120.03, 121.13, 122.07,124.42, 124.54, 131.89, 132.66, 148.62,151.25, 153.91, 164.69. HRMS-ESI (m/z): $(M+Na)^+$ calcd for $C_{58}H_{68}O_8S$ 947.4527, found 947.4560

2,5-Bis[4-(3,4-dioctyloxyphenylcarbonyloxy)phenylethynyl]thiophene (H-TCT-mp8). ^{1}H NMR ($CDCl_3$): 0.87-0.91 (m, 12H, CH_3), 1.27-1.51 (m, 40H, $(CH_2)_5$), 1.84-1.90 (m, 8H, CH_2), 4.06-4.11 (m, 8H, CH_2O), 6.94 (d, 2H, J = 8.6 Hz, Ar-H), 7.18 (s, 2H, Ar-H), 7.23 (d, 4H, J = 8.7 Hz, Ar-H), 7.59 (d, 4H, J = 8.7 Hz, Ar-H), 7.66 (d, 2H, J = 2.0 Hz, Ar-H), 7.82 (dd, 2H, J_1 = 8.6 Hz, J_2 = 2.0 Hz, Ar-H). ^{13}C NMR ($CDCl_3$): 14.09,

22.65, 25.94, 25.98, 29.01, 29.13, 29.23, 29.32, 29.34, 31.79, 69.03, 69.30, 82.31, 93.42, 111.85, 114.48, 120.04, 121.13, 122.07, 124.43, 124.55, 131.89, 132.66, 148.63, 151.26, 153.92, 164.70. IR (KBr): 2921, 2850, 2202, 1732, 1597, 1517, 1428, 1347, 1279, 1201, 1165, 1069, 1016, 867, 754. HRMS-ESI (*m/z*): $(M+Na)^+$ calcd for $C_{66}H_{84}O_8S$ 1059.5779, found 1059.5770.

2,5-Bis[4-(3,4-didecyloxyphenylcarbonyloxy)phenylethynyl]thiophene (H-TCT-mp10). ^1H NMR ($CDCl_3$): 0.87-0.91 (m, 12H, CH_3), 1.27-1.53 (m, 56H, $(CH_2)_7$), 1.84-1.91 (m, 8H, CH_2), 4.06-4.11 (m, 8H, CH_2O), 6.94 (d, J = 8.6 Hz, 2H, Ar-H), 7.18 (s, 2H, Ar-H), 7.23 (d, J = 8.7 Hz, 4H, Ar-H), 7.59 (d, 4H, J = 8.7 Hz, Ar-H), 7.66 (d, J = 2.0 Hz, 2H, Ar-H), 7.82 (dd, J_1 = 8.6 Hz, 2H, J_2 = 2.0 Hz, Ar-H). C_{13} NMR ($CDCl_3$): 14.12, 22.68, 25.95, 25.99, 29.01, 29.13, 29.34, 29.37, 29.39, 29.56, 29.59, 29.61, 31.90, 69.04, 69.30, 82.31, 93.43, 111.85, 114.48, 120.04, 121.14, 122.08, 124.43, 124.56, 131.89, 132.67, 149.64, 151.27, 153.92, 164.69. IR (KBr): 2921, 2849, 2198, 1731, 1597, 1517, 1428, 1278, 1200, 1136, 1066, 753. HRMS-ESI (*m/z*): $(M+Na)^+$ calcd for $C_{74}H_{100}O_8S$ 1171.7031, found 1171.7005.

2,5-Bis[4-(3,4-didodecyloxyphenylcarbonyloxy)phenylethynyl]thiophene (H-TCT-mp12). ^1H NMR ($CDCl_3$): 0.87-0.91 (m, 12H, CH_3), 1.27-1.51 (m, 72H, $(CH_2)_9$), 1.84-1.90 (m, 8H, CH_2), 4.06-4.11 (m, 8H, CH_2O), 6.94 (d, J = 8.6 Hz, 2H, Ar-H), 7.18 (s, 2H, Ar-H), 7.23 (d, 4H, J = 8.7 Hz, Ar-H), 7.59 (d, 4H, J = 8.7 Hz, Ar-H), 7.66 (d, 2H, J = 2.0 Hz, Ar-H), 7.82 (dd, 2H, J_1 = 8.6 Hz, J_2 = 2.0 Hz, Ar-H). ^{13}C NMR ($CHCl_3$): 14.12, 22.68, 25.95, 26.00, 29.02, 29.13, 29.36, 29.40, 29.60, 29.62, 29.66, 29.69, 31.92, 69.04, 69.31, 82.32, 93.43, 111.86, 114.49, 120.04, 121.14, 122.08, 124.43, 124.56, 131.89, 132.67, 148.64, 151.27, 153.93, 164.70. IR (KBr): 2920, 2850, 2198, 1733, 1597, 1517,

1467, 1279, 1202, 1137, 1067, 868, 753. HRMS-ESI (*m/z*): $(M+Na)^+$ calcd for $C_{82}H_{116}O_8S$ 1283.8283, found 1283.8227.

2,5-Bis[4-(3,4-ditetradecyloxyphenylcarbonyloxy)phenylethynyl]thiophene (H-TCT-mp14). ^1H NMR ($CDCl_3$): 0.87-0.91 (m, 12H, CH_3O), 1.27-1.51 (m, 88H, $(CH_2)_{11}$), 1.84-1.90 (m, 8H, CH_2), 4.06-4.11 (m, 8H, CH_2O), 6.94 (d, 2H, J = 8.6 Hz, Ar-H), 7.18 (s, 2H, Ar-H), 7.23 (d, 4H, J = 8.7 Hz, Ar-H), 7.59 (d, 4H, J= 8.7 Hz, Ar-H), 7.66 (d, 2H, J = 2.0 Hz, Ar-H), 7.82 (dd, 2H, J_1 = 8.6 Hz, J_2 = 2.0 Hz, Ar-H). C^{13} NMR ($CDCl_3$): 14.13, 22.69, 25.96, 26.00, 29.02, 29.14, 29.37, 29.41, 29.63, 29.66, 29.71, 31.93, 69.05, 69.32, 82.32, 93.43, 111.87, 114.50, 120.05, 121.15, 122.09, 124.44, 124.56, 131.89, 132.68, 148.65, 151.28, 153.94, 164.71. IR (KBr): 2916, 2848, 2190, 1732, 1597, 1518, 1470, 1431, 1277, 1200, 1135. HRMS-ESI (*m/z*): $(M+Na)^+$ cacld for $C_{90}H_{132}O_8S$ 1395.9535, found 1395.9562.

2,4-Bis(4-phenylmethoxyphenylethynyl)-1,3-dibromobenzene. 1,5-diiodo-2,4-dibromobenzene (1.50g, 7.21mmol), 4-(phenylmethoxy)phenylacetylene (1.76g, 3.61mmol), copper (I) iodide (28mg, 0.144mmol), and $Pd(PPh_3)Cl_2$ (51mg, 0.072mmol) were placed in a 250mL Schlenk flask with stir bar. The flask was evacuated, argon was introduced and dry, air-free toluene (125mL) and diisopropylamine (2.0 ml, 14.4mmol) were added sequentially *via* a syringe. The reaction was stirred at room temperature for 12 hours and quickly became orange, then brown. 25 mL of 1N HCl (aqueous) were added, the mixture was extracted with Et_2O (200ml), dried ($MgSO_4$), and filtered through a silica gel pad. The solvents were removed in vacuo and the remaining yellow solid was purified by column chromatography (silica gel, 3:2 hexane/dichloromethane eluent) and crystallized from hexane/chloroform yielding the product (1.85g, 2.85mmol, 79%) as a

white solid. ^{1}H NMR ($CDCl_3$): 5.078 (s, 4H, OCH_2Ar), 6.98 (d, 4H, J = 8.9 Hz, Ar-H), 7.32-7.44 (m, 10H, Ar-H), 7.52 (d, 4H, J = 8.9 Hz, Ar-H), 7.69 (s, 1H, Ar-H), 7.87 (s, 1H, Ar-H). ^{13}C NMR ($CDCl_3$): 70.01, 85.67, 95.37, 114.76, 114.98, 124.63, 124.99, 127.46, 128.12, 128.63, 133.27, 135.54, 136.02, 136.40, 159.29. HRMS-FAB (*m/z*): (M^+) calcd for $C_{36}H_{24}Br_2O_2$ 646.0143, found 646.0133.

2,4-Bis(4-phenylmethoxyphenylethynyl)-1,3-dicyanobenzene. 2,4-Bis(4-phenylmethoxyphenylethynyl)-1,3-dibromobenzene (1.00 g, 1.54 mmol), copper (I) cyanide (345 mg, 3.86 mmol), and a stir bar were placed in a 50ml Schlenk tube. The flask was evacuated, argon was introduced and dry DMF (20 ml) was added via a syringe. The mixture was stirred at 145 °C for 12 hours then cooled to room temperature, and 100ml of 1N NH_4Cl (aqueous) were added. The mixture was extracted with Et_2O and $CHCl_3$, the combined extracts dried over $MgSO_4$, and the solvents removed in vacuum. A small amount of brown solution of product in residual DMF was obtained, which was purified by column chromatography (silica gel, 1.5:1 DCM/hexane eluent) yielding the product (630 mg, 1.17 mmol, 76%) as a yellow crystalline solid which was used without further purification. ^{1}H NMR ($CDCl_3$): 5.12 (s, 4H, OCH_2Ar), 7.01 (d, 4 H, J = 8.4 Hz, Ar-H), 7.38-7.48 (m, 10H, Ar-H), 7.57 (d, 4H, J = 8.4 Hz, Ar-H) 7.56 (s, 1H, Ar-H), 7.85 (s, 1H, Ar-H). ^{13}C NMR ($CDCl_3$): 70.08, 83.94, 101.60, 113.13, 113.45, 115.11, 115.78, 127.39, 128.12, 128.57, 131.28, 134.00, 134.16, 136.04, 160.16. IR (KBr): 2920, 2851, 2229, 2201, 1590, 1511, 1294, 1248, 1173, 1006, 831, 699. HRMS-EI (*m/z*): (M^+) calcd for $C_{38}H_{24}N_2O_2$ 540.1838, found: 540.1825.

2,4-Bis(4-hydroxyphenylethynyl)-1,3-dibromobenzene (9b) 2,4-Bis(4-phenylmethoxyphenylethynyl)-1,3-dibromobenzene (750mg, 1.16mmol) was placed in a

100ml Schlenk flask with a stir bar which was then evacuated and filled with argon. Dry, air-free CH_2Cl_2 (50 ml) was added and the yellow solution was cooled to 0 °C after which BBr_3 (2.5 ml, 1M solution in CH_2Cl_2, 2.54mmol) was added dropwise via syringe. The solution became orange in color and was stirred at 0 °C for 30 minutes at which time 10ml of 1N HCl (aqueous) was added. The solids were extracted with $CHCl_3$, dried over $MgSO_4$ and the solvents were removed in vacuo. The remaining orange solids were purified by silica gel chromatography using 20:1/CH_2Cl_2:THF as the eluent followed by precipitation from THF/CH_2Cl_2 by the addition of hexanes yielding the product (319mg, 0.681mmol, 59%) as a yellow solid which was used without further purification. ^1H NMR ($CDCl_3$): 6.80 (d, 4H, J = 8.50 Hz, Ar-H), 7.42 (d, 4H, J = 8.50 Hz, Ar-H), 7.65 (s, 1H, Ar-H), 7.83 (s, 1H, Ar-H). ^{13}C NMR ($CDCl_3$): 85.14, 95.69, 115.53, 124.36, 125.07, 133.35, 135.46, 135.90, 149.06. HRMS-ESI (*m/z*): $[M+Na]^+$ calcd for $C_{22}H_{12}Br_2O_2$ 488.9096, found: 488.9089.

2,4-Bis(4-hydroxyphenylethynyl)-1,3-dicyanobenzene (9c). 2,4-Bis(4-phenylmethoxy-phenylethynyl)-1,3-dicyanobenzene (400 mg, 0.740 mmol) was placed in a 250 ml Schlenk flask with a stir bar. The flasks was evacuated, argon was introduced and dry, air-free dichloromethane (175 mL) was added via cannula. The mixture was cooled to –78 °C with a dry-ice/acetone bath and BBr_3 (1M in DCM, 8.9 ml, 8.9 mmol) was added drop-wise via syringe. The orange suspension was allowed to warm to room temperature. Solvents and excess BBr_3 were removed under vacuum into a cooled trap. The residue was cooled to 0 °C and first H_2O (100 ml), then EtOH (100 ml) were added. Extraction of the mixture at room temperature with Et_2O (200 mL), drying of the organic

phase over $MgSO_4$, and evaporation of the solvents in vacuum yielded an orange solid which were purified by chromatography (silica gel, 2% EtOAc in DCM) yielding **9c** (206mg, 57.2mmol, 77%) as a slightly orange solid. ^1H NMR ($CDCl_3$): 6.81 (d, 4H, J = 9.0 Hz, Ar-H), 7.48 (d, 4H, J = 9.0 Hz, Ar-H), 7.85 (s, 1H, Ar-H), 8.24 (s, 1H, Ar-H). ^{13}C NMR ($CDCl_3$): 84.57, 102.41, 104.59, 112.66, 114.62, 116.90, 132.11, 135.03, 135.07, 138.11, 161.11. HRMS-EI (*m/z*): [M^+] calcd for $C_{24}H_{12}N_2O_2$ 360.0893, found: 360.0884.

General Procedure for 1,3- and 1,4-Bis[4-(3,4-dihexyloxyphenylcarbonyloxy) phenylethynyl]benzene derivatives 9a, **9b**, or **9c** (0.167 mmol) were placed in a 25ml Schlenk flask with 3,4-(dioctyloxy)benzoic acid (0.445 mmol), DMAP (10mg, 0.083mmol), and a stir bar. Argon atmosphere was introduced and dry, air-free dichloromethane (10ml) was added *via* a syringe, followed by diiosopropylcarbodiimide (104 μl, 0.67 mmol) *via* a microsyringe. The mixture was stirred at room tempemperature for 4 days, 4ml of 1N HCl (aqueous) were added, and the mixture was extracted with $CHCl_3$. The combined organic extracts were dried over $MgSO_4$, and evaporated in vacuum. The remaining solids were purified by column chromatography (silica gel, DCM/hexane eluent) followed by recrystallization from DCM/MeOH yielding the products as a white or yellow solid in 60-70%).

2,4-Bis[4-(3,4-dihexyloxyphenylcarbonyloxy)phenylethynyl]-1,3-dibromobenzene (Br-mTCP-mp6) ^1H NMR ($CDCl_3$): 0.92 (m, 12H, CH_3), 1.36-1.38 (m, 16H, $(CH_2)_2$), 1.49-1.53 (m, 8H, CH_2), 1.85-1.88 (m, 8H, CH_2), 4.07-4.10 (m, 8H, CH_2O), 6.94 (d, 2H, J = 8.6 Hz, Ar-H), 7.25 (d, 4H, J = 8.7 Hz, Ar-H), 7.64 (d, 4H, J = 8.7 Hz, Ar-H), 7.67 (d, 2H, J = 2.0 Hz, Ar-H), 7.74 (s, 1H, Ar-H), 7.83 (dd, 2H, J_1 = 8.6 Hz, J_2 = 2.0 Hz, Ar-

H), 7.90 (s, 1H, Ar-H). ^{13}C NMR ($CDCl_3$, δ): 14.02, 22.58, 22.59, 25.62, 25.66, 28.96, 29.08, 31.53, 31.55, 69.03, 69.29, 86.61, 94.64, 111.81, 114.42, 119.88, 121.10, 122.14, 124.43, 124.70, 125.30, 132.95, 135.73, 136.43, 148.62, 151.54, 153.92, 164.68. HRMS-FAB (*m/z*): $[M+H]^+$ calcd for $C_{60}H_{68}Br_2O_8$ 1075.3359, found 1075.3332.

2,4-Bis[4-(3,4-dioctyloxyphenylcarbonyloxy)phenylethynyl]-1,3-dibromobenzene (Br-mTCP-mp8) ^1H NMR ($CDCl_3$): 0.92 (m, 12H, CH_3), 1.36-1.38 (m, 32H, $(CH_2)_4$), 1.49-1.53 (m, 8H, CH_2), 1.85-1.88 (m, 8H, CH_2), 4.07-4.10 (m, 8H, CH_2O), 6.94 (d, 2H, J = 8.6 Hz, Ar-H), 7.25 (d, 4H, J = 8.7 Hz, Ar-H), 7.64 (d, 4H, J = 8.7 Hz, Ar-H), 7.67 (d, 2H, J = 2.0 Hz, Ar-H), 7.74 (s, 1H, Ar-H), 7.83 (dd, 2H, J_1 = 8.6 Hz, J_2 = 2.0 Hz, Ar-H), 7.90 (s, 1H, Ar-H). ^{13}C NMR ($CDCl_3$, δ): 14.11, 22.67, 25.95, 25.98, 29.01, 29.13, 29.25, 29.26, 29.33, 29.35, 31.79, 31.80, 69.03, 69.30, 86.61, 94.64, 111.82, 114.45, 119.88, 121.10, 122.14, 124.44, 124.70, 125.30, 132.94, 135.73, 136.43, 148.62, 151.54, 153.92, 164.68. MS-FAB (*m/z*): $[M+H]^+$ calcd for $C_{68}H_{85}Br_2O_8$ 1188.4689, found 1188.4650.

2,4-Bis[4-(3,4-didecyloxyphenylcarbonyloxy)phenylethynyl]-1,3-dibromobenzene (Br-mTCP-mp10) ^1H NMR ($CDCl_3$): 0.92 (m, 12H, CH_3), 1.36-1.38 (m, 48H, $(CH_2)_6$), 1.49-1.53 (m, 8H, CH_2), 1.85-1.88 (m, 8H, CH_2), 4.07-4.10 (m, 8H, CH_2O), 6.94 (d, 2H, J = 8.6 Hz, Ar-H), 7.25 (d, 4H, J = 8.7 Hz, Ar-H), 7.64 (d, 4H, J = 8.7 Hz, Ar-H), 7.67 (d, 2H, J = 2.0 Hz, Ar-H), 7.74 (s, 1H, Ar-H), 7.83 (dd, 2H, J_1 = 8.6 Hz, J_2 = 2.0 Hz, J_2 = 8.6 Hz, Ar-H), 7.90 (s, 1H, Ar-H). ^{13}C NMR ($CDCl_3$, δ): 14.12, 22.68, 25.95, 25.98, 29.01, 29.13, 29.34, 29.37, 29.39, 29.56, 29.60, 29.61, 31.90, 69.03, 69.29, 86.61, 94.63, 111.82, 114.44, 119.87, 121.09, 122.14, 124.43, 124.69, 125.29, 132.94, 135.72, 136.42,

148.62, 151.53, 153.92, 164.67. HRMS-FAB (*m/z*): $[M+H]^+$ calcd for $C_{76}H_{100}Br_2O_8$ 1299.5863, found 1299.5822.

2,4-Bis[4-(3,4-didodecyloxyphenylcarbonyloxy)phenylethynyl]-1,3-dibromobenzene (Br-mTCP-mp12) ^1H NMR ($CDCl_3$): 0.92 (m, 12H, CH_3), 1.36-1.38 (m, 64H, $(CH_2)_8$), 1.49-1.53 (m, 8H, CH_2), 1.85-1.88 (m, 8H, CH_2), 4.07-4.10 (m, 8H, CH_2O), 6.94 (d, 2H, J = 8.6 Hz, Ar-H), 7.25 (d, 4H, J = 8.7 Hz, Ar-H), 7.64 (d, 4H, J = 8.7 Hz, Ar-H), 7.67 (d, 2H, J = 2.0 Hz, Ar-H), 7.74 (s, 1H, Ar-H), 7.83 (dd, 2H, J_1 = 8.6 Hz, J_2 = 2.0 Hz, Ar-H), 7.90 (s, 1H, Ar-H). ^{13}C NMR ($CDCl_3$, δ): 14.12, 22.69, 25.95, 25.99, 29.01, 29.13, 29.36, 29.40, 29.61, 29.62, 29.66, 29.69, 31.92, 69.03, 69.30, 86.61, 94.64, 111.82, 114.45, 119.87, 121.10, 122.14, 124.43, 124.69, 125.29, 132.94, 135.73, 136.42, 148.62, 151.54, 153.92, 164.67. HRMS-FAB (*m/z*): $[M+H]^+$ calcd for $C_{84}H_{116}Br_2O_8$ 1411.7115, found 1411.7067.

2,4-Bis[4-(3,4-dioctyloxyphenylcarbonyloxy)phenylethynyl]-1,3-dicyanobenzene (NC-mTCP-mp8) ^1H NMR ($CDCl_3$): 0.92 (m, 12H, CH_3), 1.36-1.38 (m, 32H, $(CH_2)_4$), 1.49-1.53 (m, 8H, CH_2), 1.85-1.88 (m, 8H, CH_2), 4.07-4.15 (m, 8H, CH_2O), 6.95 (d, 2H, J = 8.4 Hz, Ar-H), 7.29 (d, 4H, J = 8.7 Hz, Ar-H), 7.66 (d, 2H, J = 2.1 Hz, Ar-H), 7.71 (d, 4H, J = 8.7 Hz, Ar-H), 7.83 (dd, 2H, J_1 = 8.4 Hz, J_2 = 2.1 Hz, Ar-H), 7.88 (s, 1H, Ar-H) 7.96 (s, 1H, Ar-H). ^{13}C NMR ($CDCl_3$, δ): 14.07, 22.63, 25.92, 25.96, 28.98, 29.11, 29.22, 29.31, 29.30, 29.32, 31.76, 69.03, 69.31, 84.42, 100.53, 111.84, 114.41, 114.47, 115.58, 118.31, 120.90, 122.40, 124.49, 131.02, 133.66, 134.93, 136.22, 148.64, 152.56, 154.02, 164.53. HRMS-FAB (*m/z*): $[M]^+$ calcd for $C_{70}H_{84}N_2O_8$ 1081.6228, found 1081.6256.

2,4-Bis[4-(3,4-didodecyloxyphenylcarbonyloxy)phenylethynyl]-1,3-dicyanobenzene (NC-mTCP-mp12): ^{1}H NMR ($CDCl_3$): 0.87-0.91 (m, 12H, CH_3O), 1.27-1.51 (m, 72 H, $(CH_2)_9$), 1.84-1.90 (m, 8H, CH_2), 4.06-4.11 (m, 8H, CH_2O), 6.87 (d, 2H, J = 8.4 Hz, Ar-H), 7.21 (d, 4H, J = 9.0 Hz, Ar-H), 7.58 (d, 2H, J = 1.2 Hz, Ar-H), 7.63 (d, 4H, J = 9.0 Hz), 7.74 (dd, 2H, J_1 = 8.4 Hz, J_2 = 1.5 Hz, Ar-H), 7.79 (s, 1H, Ar-H), 7.87 (s, 1H, Ar-H). ^{13}C NMR ($CDCl_3$):14.07, 22.64, 25.92, 25.95, 28.97, 29.10, 29.32, 29.36, 29.57, 29.61, 29.65, 31.87, 68.98, 69.26, 84.43, 100.48, 111.80, 114.38, 114.44, 115.54, 118.26, 120.88, 122.36, 124.45, 130.93, 133.62, 134.84, 136.16, 148.63, 152.54, 154.00, 164.44.. IR (KBr): 2919, 2849, 2212, 1731, 1591, 1517, 1467, 1429, 1274, 1203, 1133, 751, 721. HRMS calcd for $C_{86}H_{116}N_2O_8$ (M+H) 1305.8810, found (FAB): 1305.8754.

References

(1) a) Niori, T.; Sekine, T.; Watanabe, J.; Furukawa, T.; Takezoe, H. *J. Mater. Chem.* **1996**, 6, 1231-1233. b) Shen, D.; Diele, S.; Wirt, I.; Tschierske, C. *Chem. Comm.* **1998**, 2573-2574. c) Pelzl, G.; Diele, S.; Weissflog, W. *Adv. Mater.* **1999**, *11*, 707-724. d) Heppke, G.; Parghi, D.D.; Sawade, H. *Liq. Cryst.* **2000**, 27, 313-320. e) Weissflog, W.; Kovalenko, L.; Wirth, I.; Diele, S.; Pelzl, G.; Schmalfuss, H.; Kresse, H. *Liq. Cryst.* **2000**, *27*, 677-681. f) Shen, D.; Pegenau, A.; Diele, S.; Writh, I.; Tschierske, C. *J. Am. Chem. Soc.* **2000**, *122*, 1593-1601. g) Bedel, J.P.; Rouillon, J.C.; Marcerou, J.P.; Laguerre, M.; Nguyen, H.T.; Achard, M.F. *Liq. Cryst.* **2000**, *27*, 1411-1421. h) Sadashiva, B.K.; Shreenivasa, H.N.; Dhara, S. *Liq. Cryst.* **2001**, *28*, 483-487.

(2) Link, D.R.; Natale, G.; Shao, R.; Maclennan, J.E.; Clark, N.A.; Korblova, E.; Walba, D.M. *Science* **1997**, *278*, 1924-1927. Heppke, G.; Moro, D. *Science* **1998**, 279, 1872-1873.

(3) Kishikawa, K.; Harris, M.C.; Swager, T.M. *Chem. Mater.* **1999,** *11*, 867-871.

(4) Cai, R; Samulski, E.T. *Liq. Cryst.* **1991**, *9*, 617.

(5) Demus, D. in *Handbook of Liquid Crystals*; Demus, D.; Goodby, J.; Gray, G.W.; Speiss, H.-W. Eds.; Wiley-VCH; Weinheim, 1998; Vol. 1, pp142-144.

(6) Kishikawa, K.; Harris, M.C.; Swager, T.M. *Chem. Mater.* **1999,** *11*, 867-871.

(7) Kishikawa, K.; Harris, M.C.; Swager, T.M. *Chem. Mater.* **1999,** *11*, 867-871.

(8) Friedman, M. R.; Toyne, K. J.; Goodby, J. W.; Hird, M. *J. Mater. Chem.* **2001**, *11*, 2759-2772.

(9) Fazio, D.; Mongin, C.; Donnio, B.; Galerne, Y.; Guillon, D.; Bruce, D. W. *J. Mater. Chem.* **2001**, *11*, 2852-2863.

(10) Dingemans, T. J.; Samulski, E. T. *Liq. Cryst.* **2000**, *27*, 131-136.

(11) a) Nguyen, H. T.; Destrade, C.; Malthête, J. *Adv. Mater.* **1997**, *9*, 375-387. b) Rais, K.; Daoud, M.; Gharbia, M.; Gharbi, A.; Nguyen, H. T. *ChemPhysChem* **2001**, *2*, 45-49.

(12) Nguyen, H. T.; Destrade, C.; Malthete, J. In *Handbook of Liquid Crystals*; Demus, D.; Goodby, J.; Gray, G. W.; Spiess, H.-W.; Vill, V., Ed.; Wiley-VCH: Weinheim, 1998; Vol. 2B, pp 865-900.

(13) Cook, M. J.; Wilson, M. R. *Liq. Cryst.* **2000**, *27*, 1573-1583.

(14) Kishikawa, K.; Harris, M.C.; Swager, T.M. *Chem. Mater.* **1999,** *11*, 867-871.

(15) Levitsky, I. A.; Kishikawa, K.; Eichhorn, S. H.; Swager, T. M. *J. Am. Chem. Soc.* **2000**, *122*, 2474-2479.

(16) Chandrasekhar, S.; Nair, G. G.; Shankar Rao, D. S.; Krishna Prasad, S.; Praefcke, K.; Blunk, D. *Liq. Cryst.* **1998**, *24*, 67-70.

(17) Hunt, J. J.; Date, R. W.; Timimi, B. A.; Luckhurst, G. R.; Bruce, D. W. *J. Am. Chem. Soc.* **2001**, *123*, 10115-10116.

Chapter 3

Thiophene-Based Bent-Core Liquid Crystals:

Effects of Endgroups and Core Symmetry

Adapted from:

Paraskos, A. J.; Swager, T. M. *Chem. Mater.* **2002**, *14*, 4523-4549.

Introduction

The search for molecules that possess rigid bent-rod shapes and are capable of forming liquid crystal phases has been an area of extensive investigation in the past decade.[1] This is largely due to the numerous reports of novel mesogenic phases (banana phases) exhibited by certain bent-rod compounds, most notably switchable antiferroelectric and ferroelectric phases.[2] These phases form domains of bulk polarization due to the spontaneous adoption of chiral structures by the inherently achiral molecules.[3] The decrease in symmetry caused by the bent shape of these molecules is central to the formation and structure of the phases themselves, as nearest-neighbor interactions and packing considerations for such mesogens become more complex than in the case of conventional calamitic molecules. However, despite the large number of molecules studied, the structure-property relationships that govern these phases still remain largely unelucidated.

One long-standing interest of the Swager group has been in utilizing the shape anisotropy of unconventional mesogens to create mesophases with polar order.[4] As discussed in the previous chapter, bent-rod mesogens which possess a large laterally-directed dipole might be expected to display polar phases due to the combination of dipolar forces and packing considerations arising from the shape anisotropy of the molecules. We have previously reported the synthesis of a number of bent-rods based on 2,5-disubstituted-3,4-dicyanothiophenes (Figure 1) (see chapter 2).[5,6] The 2,5-thienyl linkage of this design imparts a moderate bend-angle of 154° and results in mesophases with greater stability than mesogens with similar architectures and a more pronounced bend. We have also previously demonstrated that increasing the aspect ratio through the

addition of bridging ethynyl moieties promotes mesomorphism in these compounds. The incorporation of nitrile groups in the 3,4-positions of the thiophene ring imparts a very significant lateral dipole and results in a head-to-head antiparallel arrangement of molecules. This has been evidenced by the previously reported single crystal structure of a model compound **1**[4] (Figure 1) and by variable temperature 2-D X-ray diffraction and exciton coupling studies of the Col_H phase of a structurally similar hexacatenar derivative.[7] The combination of bent-shape and large lateral dipole should hinder rotation about the molecular long-axis, thereby encouraging the formation of mesophases with a biaxial component, in which there is preferential alignment perpendicular to the long-axes of the molecules. Furthermore, it has been predicted that bent-molecules with large lateral dipoles should exhibit a significant flexoelectric effect, where the physical manipulation (bending) of a thin film results in bulk polarity within the material.[8]

Our previous efforts focused on the synthesis and investigation of only a few straight-chain derivatives of type **2**, followed by numerous tetracatenars of general type **3** (Figure 1) (see Chapter 2). Compounds **3** were designed with the 3,4-dialkoxybenzoate terminal groups due to the diverse range of mesophases that tetracatenar ("four-chain") compounds exhibit in both traditional straight rod[9] and metallomesogen[10] systems. Indeed, compounds **3** were found to possess enantiotropic nematic, smectic C, and columnar hexagonal phases, depending on the length of the alkoxy sidechains.[6] The observation of SmC phases was encouraging, as this represents a step towards the realization of polar order. We were also pleased to observe nematic phases that display exclusively 2-brush disclinations by polarized microscopy, an indication that these may be thermotropic biaxial-nematic phases. [11] The conclusive demonstration of biaxiality in

thermotropic nematics has proven challenging, however, and further studies are necessary to elucidate the nature of the above mentioned nematic phases.

This chapter details our further efforts with this class of mesogens, particularly our investigation into the effects of desymmetrization of the molecular core upon mesophase behavior. We thought that by lowering the symmetry of the mesogens we could suppress crystallization by increasing the entropic cost of organization in the crystalline phase, thereby leading to lower melting temperatures and broader mesophases. Desymmetrized molecules might additionally lead to the frustration of lamellar superstructures, resulting in re-entrant nematic phases at lower temperatures and with higher order, providing further impetus for the formation of thermotropic biaxial nematic phases.

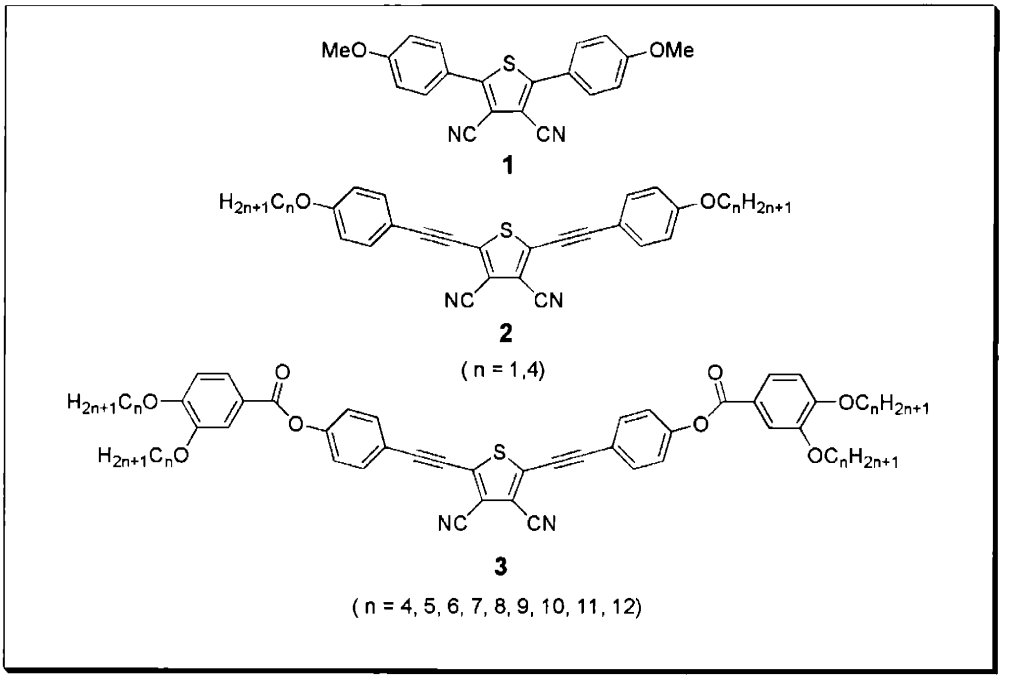

Figure 3.1. 3,4- Dicyanothiophene-based mesogens previously reported by the Swager lab.

Results and Discussion

Synthesis A number of thiophene-based mesogens were synthesized and studied (Schemes 3.1 and 3.2). The synthesis of symmetric core **12** has been previously reported.[6] Our idea of a desymmetrized core took shape as compound **7**, in which one of the acetylenic bridges has been removed. Compound **4** is prepared by palladium-catalyzed cross-coupling of 4-phenylmethoxyphenyl boronic acid with the reactive 2-position of tetrabromothiophene, [12] followed by chromatographic separation of the product of 2,5-diaddition. Chemoselective Sonogashira cross-coupling[13] at 2-position bromine of **4** with 4-phenylmethoxyphenylacetylene affords **5** in good yield, which can be converted to **6** by subsequent cyanation of the 3,4-positions of the thiophene ring with copper (I) cyanide.[14] The two benzyl protecting groups can be removed with BBr_3 in dichloromethane at low temperature, providing the desired desymmetrized core **7**. Esterification of **7** by activation of the appropriate 3,4-dialkoxyphenyl carboxylic acid with 4-dimethylaminopyridine and diisopropylcarbodiimide yields desymmetrized tetracatenar mesogens **8-11**. Etherification of unsymmetric core **7** and symmetric core **12** were carried out in the presence of PPh_3 and diethylazodicarboxylate yielding straight-chain derivatives **13-21**. Utilization of these conditions not only drives the reaction at room temperature by the formation of the exceedingly stable by-product triphenylphosphine oxide, but allows for the addition chiral alcohols with a complete inversion of stereochemistry.[15] Chiral derivative **17** is therefore accessible by the reaction of **12** with (*s*)-(+)-2-octanol. Similar synthetic strategies allow for the synthesis of 3,4-difluorothiophene derivatives **24-27** (Scheme 3.2) from starting material 2,5-dibromo-

Scheme 3.1.

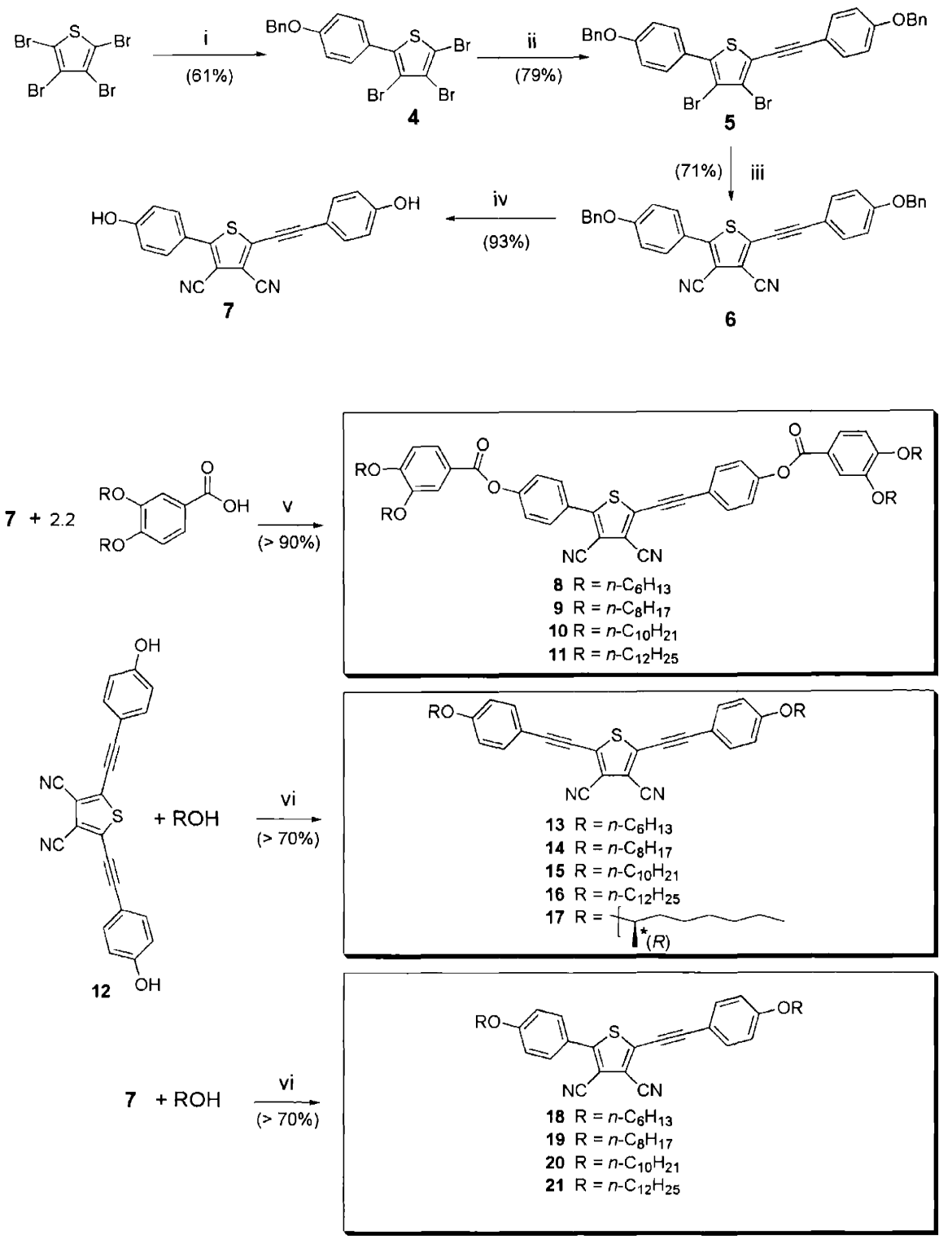

(i) *p*-BnOPhB(OH)$_2$, Pd(PPh$_3$)$_4$, Na$_2$CO$_3$, EtOH, H$_2$O, toluene, reflux. (ii) *p*-BnOPhCCH, Pd(PPh$_3$)$_2$Cl$_2$, CuI, *i*-Pr$_2$NH, toluene, r.t. (iii) CuCN (6 equiv), CuI (2 equiv), DMF, reflux. (iv) BBr$_3$, H$_2$O, DCM, -10 °C. (v) Diisopropylcarbodiimide, DMAP, DCM. (vi) PPh$_3$, DEAD, THF, r.t.

Scheme 3.2

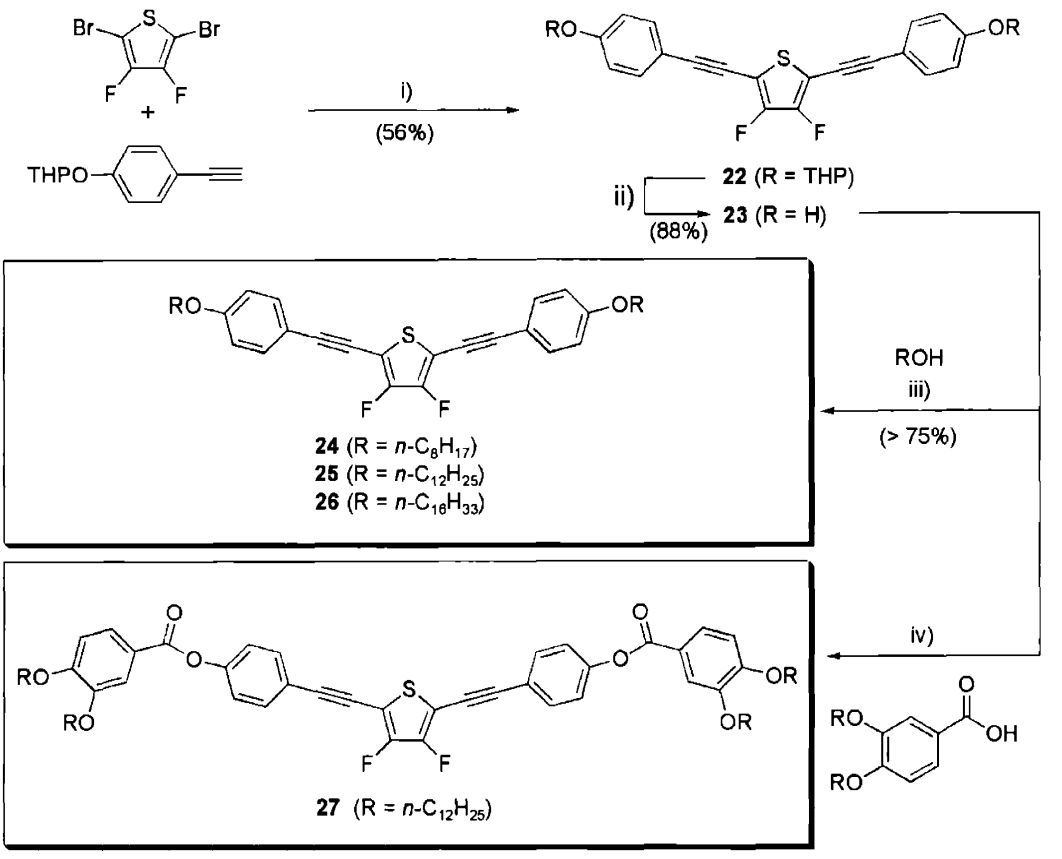

(i) $Pd(Ph_3)_2Cl_2$, CuI, *i*-Pr_2NH, toluene. (ii) AcOH, THF, H_2O, 45 °C. (iii) PPh_3, DEAD, THF. (iv) Diisopropylcarbodiimide, DMAP, CH_2Cl_2.

3,4-difluorothiophene, which is available as previously published in three steps from tetrabromothiophene.[16]

Phase Behavior. The phase behavior of the mesogens studied is listed in Table 1. Unsymmetric tetracatenar derivatives **10** and **11**, possessing long (C_{10} and C_{12}) aliphatic sidechains, exhibit Col_H phases as identified by polarized microscopy and X-ray diffraction. The shorter-chain derivatives do not exhibit any mesomorphism. This is in marked contrast to the previously studied symmetric tetracatenars **3**, in which nematic,

Table 1. Phase Behavior of Thiophene-based bent-rods.[a]

Compound	n	Behavior
8	6	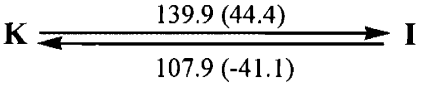
9	8	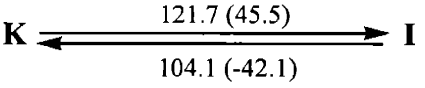
10	10	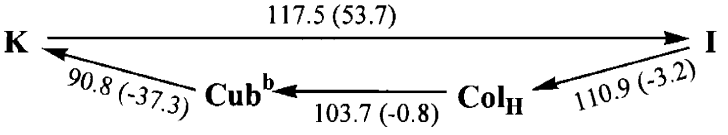
11	12	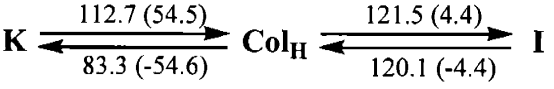
13	6	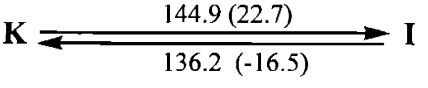
14	8	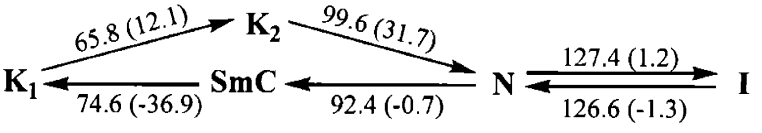
15	10	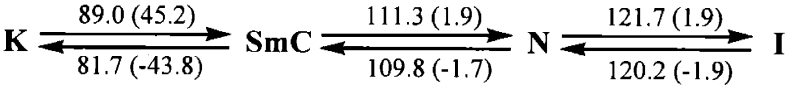
16	12	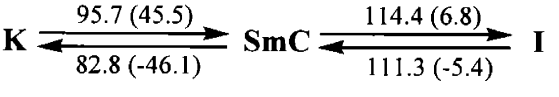

18	6	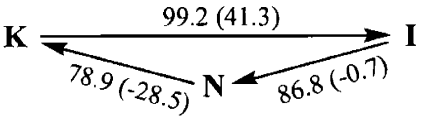
19	8	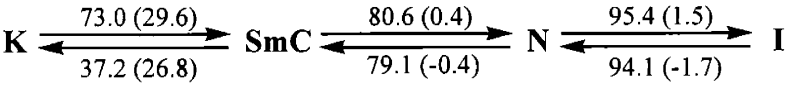
20	10	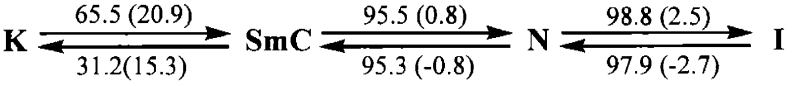
21	12	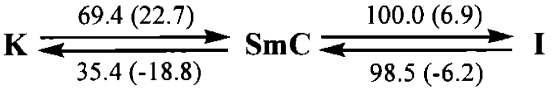
24	8	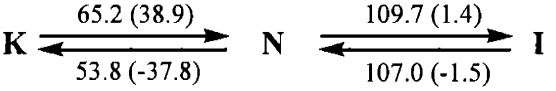
25	12	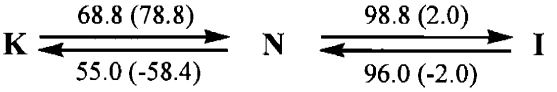
26	16	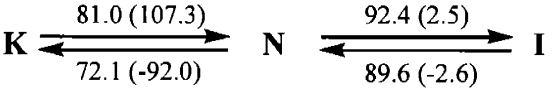
27	8	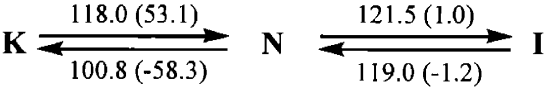

[a] The transition temperatures (°C) and enthalpies (in parentheses, kJ/mol) were determined by DSC (10 °C/min) and are given above and below the arrows. K, K_1 and K_2 indicate crystal phases, and SmC, N and I indicate smectic C, nematic and isotropic phases, respectively. [b] This phase was identified by the appearance of a pseudo-isotropic texture below the Col_H phase. We were unable to observe this thermodynamically unstable monotropic phase by X-ray diffraction due to crystallization, though the phase transition was clearly visible by DSC at the 10 °C/min scan rate.

SmC, and Col_H phases are observed depending on the length of the sidechains. In the case of these tetracatenar systems, the effect of desymmetrization is to discourage the formation of nematic and lamellar mesophases without significantly effecting the stability of the crystalline phase.

Though we had previously studied a few very short straight-chain derivatives **2** (Figure 1), the longer-chain analogues had not been explored. Our current studies of 2,5-Bis[4-(*n*-alkyloxy)phenylethynyl]-3,4-dicyanothiophenes **13-16** reveal both enantiotropic nematic and smectic C phases, depending on the length of the sidechains. Chiral analogue **17** is not liquid crystalline. The smectic C phases of **14** and **15** exhibit focal-conic textures by polarized microscopy (Figure 3.2), while the smectic C phase of compound **16** exhibits a Schlieren-type texture. Well-ordered homogeneous alignment (parallel to the slide surface) of the nematic phases of compounds **14** and **15** can be induced on slides possessing a rubbed poly-imide alignment layer, but homeotropic (perpendicular to the slide) alignment could not be achieved.

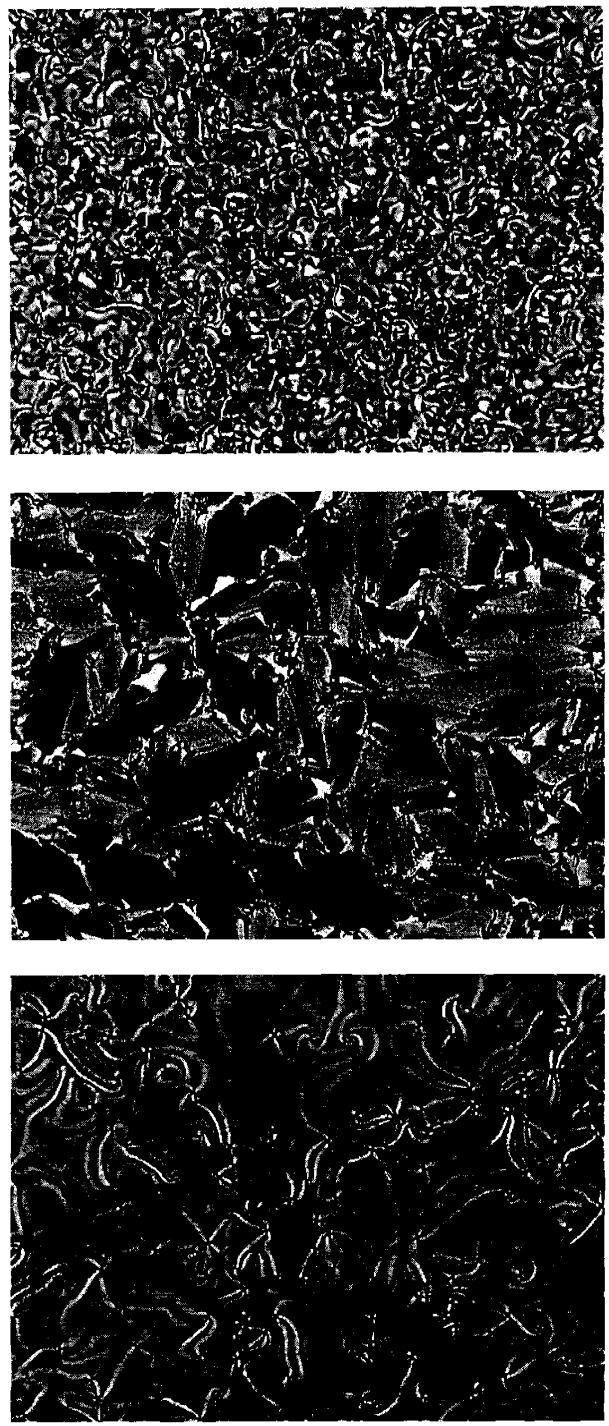

Figure 3.2. Microphotographs of the nematic Schlieren texture of 15 at 117 °C (100X) (top), the broken focal conic texture of 15 at 101 °C (200X) (middle), and the SmC schlieren texture of 21 at 98 °C (320X). Samples were sandwiched between untreated glass slides and viewed through crossed polarizers.

Desymmetrized straight-chain compounds **18-21** exhibit similar mesophases with identical alignment behavior and textural features as symmetric compounds **13-17**, but in all cases both the clearing and crystallization temperatures are significantly depressed when compared to their symmetric analogues. In such straight-chain compounds the incorporation a desymmetrized core results in broader mesophases due to destabilization of the crystal phases. It is interesting to note that this is in direct contrast to the two series of tetracatenar compounds discussed above, in which desymmetrization had a deleterious effect upon liquid crystalline behavior.

The incorporation of 3,4-difluoro substituents into the molecular core imparts a smaller lateral dipole to the resulting mesogens and resulted in the formation of enantiotropic nematic phases in both the straight-chain compounds **24-26** and the tetracatenar compound **27**. Despite the rather broad temperature ranges of the nematic phases, no lamellar phases were observed for these compounds. This is particularly striking in the case of the straight-chain derivatives, whose 3,4-dicyanothiophene analogues displayed broad, enantiotropic tilted lamellar phases.

XRD Studies Variable temperature X-ray diffraction studies were performed for the lamellar and columnar phases of each compound (Table 3.2). The Col_H phases of compounds **8-11** are characterized by the observation of sharp (100), (110) and (200) peaks in the low angle region. The SmC phases of compounds **13-21** are characterized by a large sharp (100) peak at low angle corresponding to the interlayer spacing as well as a broad reflection centered at 4.4 Å. Analysis of the higher-angle region reveals an antiparallel (dimerized) packing of the molecules in each of the smectic C and Col_H phases, as evidenced by an extra intra-core diffuse diffraction peak from 6.5-7.5 Å. We

have observed this feature extensively for half-disc mesogens in columnar phases that similarly have antiparallel dimer correlations.[17]

Table 3.2. XRD for compounds 10, 11, 14-16 and 19-21.

compd	mesophase	lattice constant (Å)	spacing obsd (Å)	Miller indices	Å (calcd)	halos obsd (Å)
10	Col_{hd}	40.5	35.1	100		7.0-7.5
	at 100 °C		20.6	110	(20.3)	3.5-7.0
			18.0	200	(17.5)	
11	Col_{hd}	42.7	37.0	100		7.0-7.5
	at 111 °C		22.9	110	(21.4)	3.5-7.0
			19.4	200	(18.5)	
14	SmC		29.7			7.0-7.5
	at 85 °C					3.5-7.0
15	SmC		32.5			7.0-7.5
	at 98 °C					3.5-7.0
16	SmC		33.1			3.5-7.0
	at 100 °C					
19	SmC		29.8			7.0-7.5
	at 65 °C					3.5-7.0
20	SmC		32.7			7.0-7.5
	at 72 °C					3.5-7.0
21	SmC		33.4			3.5-7.0
	at 60 °C					

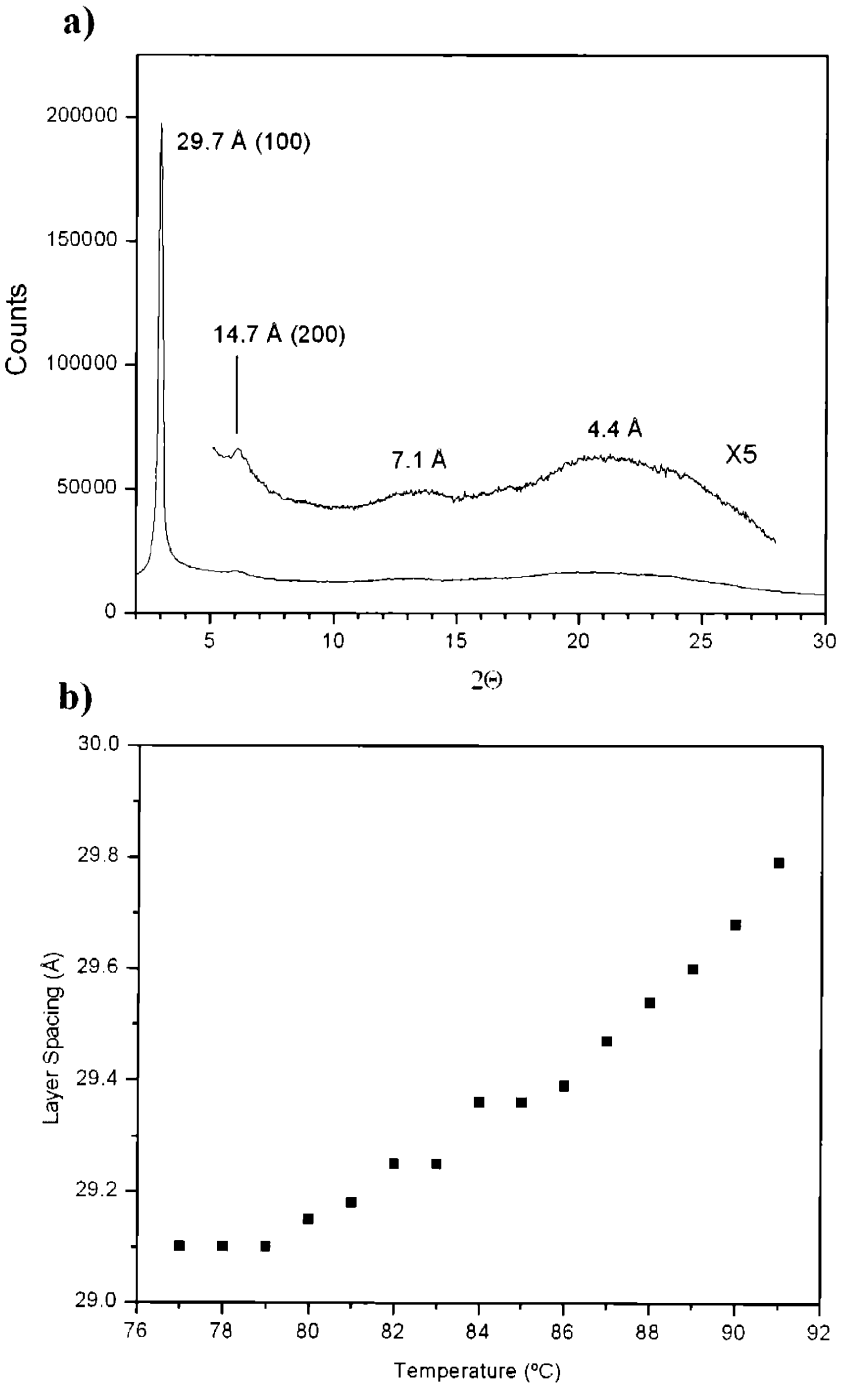

Figure 3.3. (a) Variable temperature powder diffraction X-ray of the SmC phase of compound **14** at 80 °C. A distinct halo is visible at 7.1 Å, corresponding to the distance between repeat units in an antiparallel arrangement of nearest neighbors. Also visible at higher angle (4.4Å) is the broad halo corresponding to the interaction between fluid aliphatic side chains. (b) Temperature dependence of the layer spacing (100) peak, suggesting that the tilt angle of the molecules increases with decreasing temperature.

Collecting data over several temperatures one finds that the layer spacings of the smectic C phases tend to increase with temperature (Figure 3.3). This suggests that the tilt angle decreases as the temperature increases, as is expected for tilted smectic phases.[18] Precise measurement of the tilt angles of the SmC phases of the straight-chain compounds **13-16** and **18-21** could not be achieved due to the difficulty of obtaining magnetically well-aligned samples of these compounds. 2-D variable temperature X-ray analysis of a reasonably well-aligned sample of compound **14** suggests that the tilt angle is in the range of 5-10°, measured as the deviation from orthogonality between the line described by the centers of the diffuse halos of the liquid sidechains relative to the line described by the centers of the (100) reflections of the layer spacing (Figure 3.4). This is a relatively small value when compared to previously studied SmC phases of symmetric tetracatenar compounds **3**, which have tilt angles of up to 53°. The larger tilt angles of the tetracatenars may result from the conformational mobility of the ester group combined with the tendency of these molecules to stack, which leads to the formation of columnar phases in long-chain derivatives.

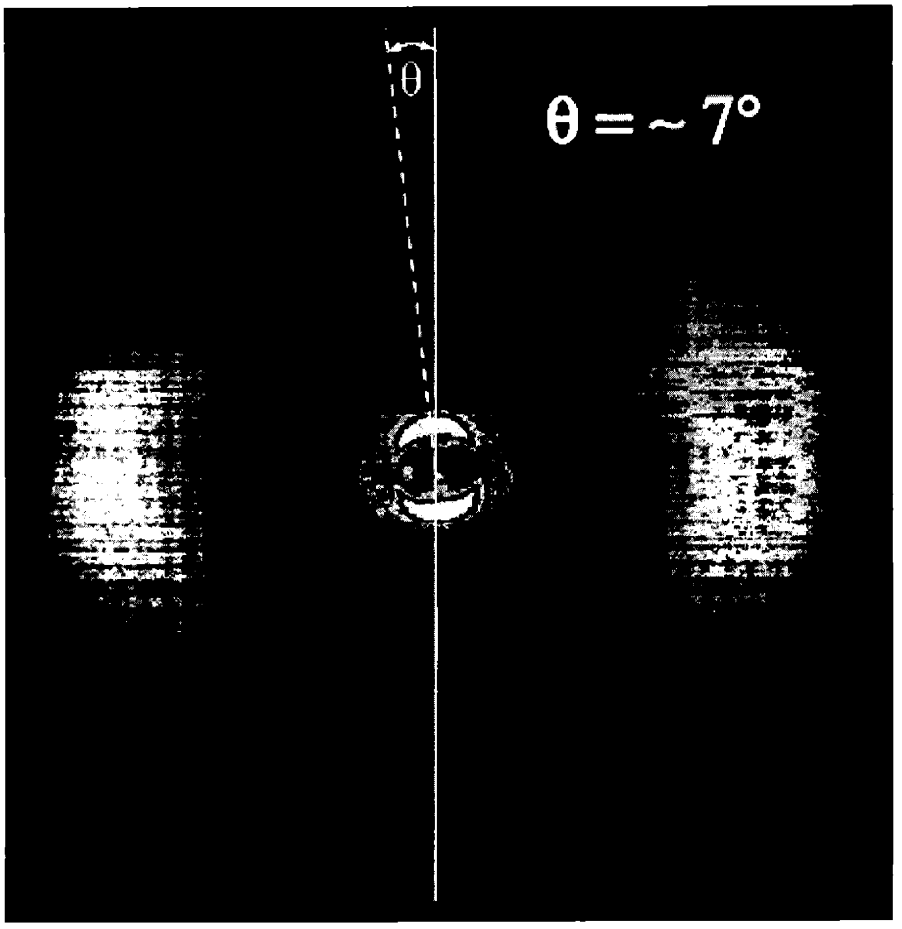

Figure 3.4. 2-D variable temperature X-ray diffraction of a magnetically aligned sample of the SmC phase of **14** at 85 °C. The inner reflections, corresponding to the layer spacing, are tilted at an angle of approximately 7° with respect to the vertically aligned outer reflections of the liquid aliphatic sidechains. This value corresponds to the tilt angle of the SmC phase.

The formation of antiparallel dimers may explain the absence of mesomorphism in the chiral analogue **17**, as efficient packing within an antiparallel arrangement of molecules is sterically disfavored by the incorporation of chiral sidechains. The addition of chiral sidechains to mesogens typically reduces the stability of the resulting mesophases[19] due to the steric interference of the chiral groups with efficient molecular

packing, but this effect is extremely exaggerated in molecules that tend to pack in an antiparallel fashion. Such an organization positions the methyl groups of neighboring molecules toward each other rather away from each other as is the case in a typical chiral mesophase (Figure 3.5). Compound **17** melts to the isotropic at 58 °C, is not mesomorphic on cooling, and crystallizes only after several minutes at room temperature. This result is consistent with previous results from our group demonstrating the incompatibility of similar compounds with chiral induction.[6]

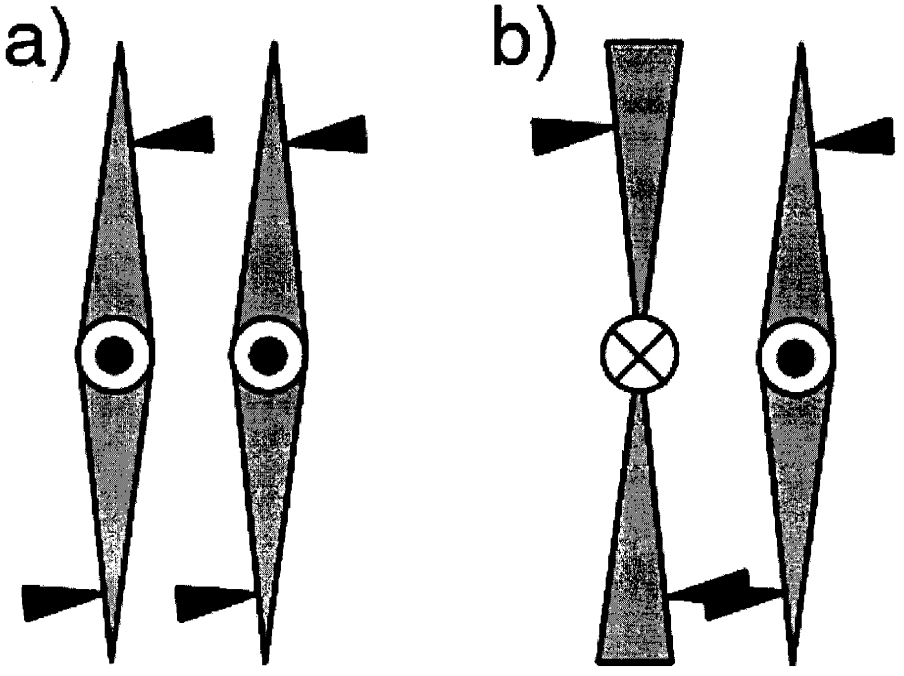

Figure 3.5. a) Parallel arrangement of chiral mesogens allows chiral groups to all face in one direction. b) Antiparallel arrangement of mesogens forces one pair of chiral groups into sterically unfavorable contact.

Summary and Conclusions

We have synthesized a number of thiophene-based bent-rod liquid crystals with large lateral dipoles. The effects of desymmetrization of the mesogenic core upon phase behavior has been probed, and it was found that the effects are dependant upon the endgroups employed. In the case of tetracatenar systems, desymmetrization does not significantly discourage crystallization, but the mesophases are clearly destabilized, leading to complete suppression of mesomorphism in compounds **8-9** and much narrower liquid crystal phases for the desymmetrized compounds **10-11**. The opposite proves to be the case for the straight-chain analogues **13-16** and **18-21**, wherein desymmetrization leads to significantly lower crystallization temperatures, resulting in much broader mesophases in the unsymmetric than in the symmetric compounds. The Col_H phases of compounds **10-11** and the smectic C phases of **14-17** and **19-21** exhibit an antiparallel arrangement of molecules, as evidenced by the appearance of a peak at 6.5-7.5 Å in the variable temperature X-ray diffraction patterns. The tilt angles of the SmC phases of straight-chain compounds **13-21** are temperature dependent and appear to be significantly lower than those previously measured for tetracatenars **3**, which may explain their compatibility with desymmetrization of the mesogenic core.

Experimental Section

General Methods Dichloromethane, THF and toluene were dried by passing through activated alumina columns. DMF was purchased from Aldrich (sure-seal) and stored over activated molecular sieves before use. (*s*)-(+)-2-Octanol was purchased from Aldrich (>99% purity). All other chemicals were of reagent grade and were used as received,

unless otherwise specified. Air and water sensitive reactions employed standard Schlenk techniques under argon atmosphere. NMR spectra were obtained on Varian Mercury-300, Bruker DPX-400 or Varian Inova-500 spectrometers. All chemical shifts are referenced to residual $CHCl_3$ (7.27 ppm for ^1H, 77.0 ppm for ^{13}C). Multiplicities are indicated as s (singlet), d (doublet), t (triplet), and m (multiplet). High resolution mass spectra were obtained at the MIT Department of Chemistry Instrumentation facility (DCIF) on a Finnigan MAT 8200 or on a Bruker Daltonics Apex II 3T FT-ICR MS. Infrared spectra were recorded on a Perkin-Elmer 1760-X FTIR in KBr pellets. DSC investigations were carried out on a Perkin-Elmer DSC-7. Optical microscopy was carried out on a Leica polarizing microscope in combination with a Linkam LTS350 hotstage. X-ray diffraction studies were carried out on samples in capillary tubes with an INEL diffractometer with a 2 kW Cu K_α X-ray source fitted with an INEL CPS-120 position-sensitive detector and an INEL FURCAP capillary furnace and with a Rigaku RV-300 rotating anode Ni-filtered Cu K_α-radiation source fitted with a Siemens flat camera 2D-Xe-detector (256 x 256 cells) and equipped with an Instec HS 400 hot stage and Instec STC2000 temperature controller. The detectors were calibrated using a silver behenate standard which was produced by Eastman Kodak, and supplied by The Gem Dugout.

2,3,4-Tribromo-5-(4-benzyloxyphenyl)thiophene (4) Tetrabromothiophene (36.78 g, 92.09 mmol) was placed in a 2-necked 2000 mL flask along with 4-benzyloxyphenyl boronic acid (20.38 g, 89.46 mmol), Na_2CO_3 (75.90 g, 716.0 mmol), trans-dichlorobis(triphenylphosphine)palladium (0.50 g, 0.43 mmol), and a stir bar. The flask was evacuated, and argon was introduced. A solvent mixture of toluene (1200 mL),

water (250 mL) and ethanol (150 mL) was sparged with argon for 20 minutes, and then added to the reaction flask via cannula. The mixture was heated to reflux with stirring for 46hours, and water was added (200 mL) followed by extraction of the organics with ether. The extracts were dried over magnesium sulfate. Column chromatography (silica gel, 2:1 hexane/chloroform eluent) yielded **4** (27.31 g, 54.3 mmol, 61%) as a white solid. ^{1}H NMR ($CDCl_3$): 5.12 (s, 2H, CH_2O), 7.05 (d, 2H, J = 8.5 Hz, Ar-H), 7.36-7.47 (m, 5H, Ar-H), 7.51 (d, 2H, J = 8.5 Hz). ^{13}C NMR ($CDCl_3$): 70.06, 109.30, 109.81, 114.98, 118.26, 124.79, 127.45, 128.12, 128.64, 130.23, 136.42, 139.86, 159.40. HRMS calcd for $C_{17}H_{11}Br_3OS$ $(M+Na)^+$: 522.7973, found (ESI): 522.7964.

3,4-Dibromo-2-(4-benzyloxyphenylethynyl)-5-(4-benzyloxyphenyl)thiophene (5)

Compound **4** (8.07 g, 16.04 mmol) was placed in a 1000 mL round-bottom flask with 4-phenylmethoxyphenylacetylene (3.337 g, 16.04 mmol), copper(I)iodide (122 mg, 0.64 mmol), trans-dichlorobis(triphenylphosphine)palladium (450 mg, 0.64 mmol) and a stir bar. The flask was evacuated and argon was introduced, followed by the addition of dry, air-free toluene (300 mL) via cannula, and cooling to 0 °C with an ice bath. Dry diisopropylamine was added via syringe and the reaction was allowed to warm to room temperature and stir overnight. The solution was filtered through silica gel pad with dichloromethane and dried ($MgSO_4$). After removal of the solvent in vacuo the remaining solids were purified by column chromatography (silica gel, gradient eluent mixture of hexanes/chloroform) followed by recrystallization from THF/MeOH yielding **5** (8.011 g, 12.71 mmol, 79%) as a yellow crystalline solid. ^{1}H NMR ($CDCl_3$): 5.11 (s, 2H, CH_2), 5.13 (s, 2H, CH_2), 6.99 (d, 2H, J = 8.7 Hz, Ar-H), 7.06 (d, 2H, J = 8.7 Hz, Ar-H), 7.34-7.50 (m, 10H, Ar-H), 7.52 (d, 2H, J = 9.0 Hz, Ar-H), 7.58 (d, 2H, J = 9.0 Hz,

Ar-H). ^{13}C NMR ($CDCl_3$): 70.03, 70.09, 80.00, 98.18, 110.42, 114.55, 114.97, 114.99, 119.62, 119.86, 125.05, 127.48, 128.14, 128.64, 128.66, 130.32, 133.20, 134.20, 134.31, 136.38, 136.50, 139.01, 159.34, 159.42. HRMS calcd for $C_{32}H_{22}Br_2O_2S$ (M^+): 627.9702, found (EI): 627.9711.

3,4-Dicyano-2-(4-benzyloxyphenylethynyl)-5-(4-benzyloxyphenyl)thiophene (6)

Compound **5** (2.303 g, 3.653 mmol) was placed in a 200 mL Schlenk flask with CuCN (1.963 g, 21.92 mmol), copper (I) iodide (1.461 g, 7.672 mmol) and stir bar. The flask was evacuated and argon was introduced, followed by the addition of dry DMF (100 mL) via cannula. The reaction was heated to 130 °C with the exclusion of light and stirred for 8 hours, at which time the reaction was cooled and dichloromethane (200 mL) was added. The solution was washed with a saturated aqueous NH_4Cl followed by water, and the organic layer was dried ($MgSO_4$). The solvent was removed in vacuo, and the resulting brown solids were purified by column chromatography on silica gel (1:1 hexane/chloroform eluent) which yielded **6** (1.36 g, 2.602 mmol, 71%) as a yellow powder. ^1H NMR ($CDCl_3$): 5.12 (s, 2H, CH_2), 5.15 (s,2H, CH_2), 7.00 (d, 2H, J = 8.7 Hz, Ar-H), 7.10 (d, 2H, J = 8.7 Hz, Ar-H), 7.33-7.48 (m, 10H, Ar-H), 7.54 (d, 2H, J = 9.0 Hz, Ar-H), 7.71 (d, 2H, J = 9.0 Hz, Ar-H). ^{13}C NMR 69.06, 69.33, 81.01, 98.05, 111.86, 114.50, 119.12, 119.32, 119.41, 121.07, 121.24, 121.32, 121.85, 122.21, 124.46, 128.97, 130.60, 132.93, 132.96, 134.87, 148.66, 151.79, 153.98, 164.63. HRMS calcd for $C_{34}H_{22}N_2O_2S$ (M+Na): 545.1294, found: (ESI) 545.1313.

3,4-Dicyano-2-(4-hydroxyphenylethynyl)-5-(4-hydroxyphenyl)thiophene (7)

Compound **6** (0.687 g, 1.09 mmol) was placed in a 200 mL Schlenk flask with stir bar. The flask was evacuated, and argon was introduced, followed by the addition of dry, air-

free dichloromethane (170 mL) via cannula, and cooling to -10 °C with a NaCl/ice bath. BBr_3 (1M in solution in dichloromethane, 5.5 mL, 5.5 mmol) was added dropwise via syringe, at which point the reaction became an orange suspension. The reaction was stirred for 1 hour at -10 °C, quenched with H_2O (20 mL), and allowed to warm to room temperature. Chloroform (100 mL) was added with a minimal amount of methanol to completely dissolve the solids. The solution was washed with water (3 X 50 mL) and dried over $MgSO_4$, and the resulting material was purified by column chromatography (silica gel, 10:1 $CDCl_3$/MeOH eluent) yielding **7** (346 mg, 1.01 mmol, 93%) a yellow solid. ^1H NMR ($CDCl_3$): 6.69 (d, 2H, J = 9.0 Hz, Ar-H), 6.78 (d, 2H, 9.0 Hz), 7.28 (d, 2H, J = 9.0 Hz, Ar-H), 7.46 (d, J = 9.0 Hz, Ar-H). ^{13}C NMR ($CDCl_3$): 76.42, 103.85, 103.95, 110.92, 111.86, 112.76, 114.21, 115.52, 116.15, 120.40, 128.98, 132.34, 133.52, 154.45, 158.97, 159.91. HRMS calcd for $C_{20}H_{10}N_2O_2S$ (M+Na): 365.0355, found: (ESI) 365.0344.

3,4-Dicyano-2-[4-(3,4-dihexyloxyphenylcarbonyloxy)phenylethynyl]-5-[4-(3,4-dihexyloxyphenylcarbonyloxy)phenyl)thiophene (8) Compound **7** (100 mg, 0.292 mmol) was placed in a 25 mL Schlenk flask with 3,4-dihexyloxybenzoic acid (207 mg, 0.643 mmol), 4-dimethylaminopyridine (18 mg, 0.146 mmol) and a stir bar. The flask was evacuated, filled with argon, and 11ml of dichloromethane was added via syringe, forming a yellow suspension. Diisopropylcarbodiimide (183 μL, 147 mg, 1.17 mmol) was added via syringe, and the solids were rapidly dissolved forming a yellow solution. The reaction was stirred at room temperature for 3 days, after which it was poured into 10 mL of 1N HCl (aqueous), extracted with chloroform, and dried over magnesium sulfate. The solvents were removed in vacuo and the resulting material was purified by column

chromatography (silica gel, 2:1 dichloromethane/hexanes) followed by repeated precipitations from THF/methanol, yielding **8** (255 mg, 0.268 mmol, 92%) as a yellow solid. ^{1}H NMR ($CDCl_3$): 0.89-0.97 (m, 12H, CH_3), 1.30-1.43 (m,16H, CH_2CH_2), 1.45-1.61 (m, 8H, CH_2), 1.84-1.92 (m, 8H, CH_2), 4.05-4.15 (m, 8H, CH_2), 6.94-6.97 (m, 2H, Ar-H), 7.30 (d, 2H, J = 8.5 Hz, Ar-H), 7.41 (d, 2H, J = 8.5 Hz, Ar-H), 7.66-7.69 (m, 4H, Ar-H), 7.83-7.84 (m, 4H, Ar-H). ^{13}C NMR ($CDCl_3$): 14.01, 22.57, 25.62, 25.66, 28.96, 29.09, 31.52, 31.55, 69.05, 69.31, 69.34, 77.98, 102.91, 106.84, 111.70, 11.85, 112.39, 114.45, 114.48, 116.30, 117.90, 120.70, 120.87, 122.47, 123.34, 124.51, 124.60, 126.71, 129.10, 132.75, 133.41, 148.67, 148.70, 152.65, 153.19, 153.43, 154.06, 154.16, 164.51. IR (KBr): 2923, 2852, 2229, 2202, 1727, 1597, 1515, 1431, 1278, 1201, 1131, 1063, 752. HRMS calcd for $C_{58}H_{66}N_2O_8S$ $(M+H)^+$: 951.4618, found (FAB): 951.4634.

3,4-Dicyano-2-[4-(3,4-dioctyloxyphenylcarbonyloxy)phenylethynyl]-5-[4-(3,4-dioctyloxyphenylcarbonyloxy)phenyl)thiophene (9) Preparation same as for **8**. ^{1}H NMR ($CDCl_3$): 0.89-0.97 (m, 12H, CH_3), 1.30-1.43 (m, 32H, $(CH_2)_4$), 1.45-1.61 (m, 8H, CH_2), 1.84-1.92 (m, 8H, CH_2), 4.05-4.15 (m, 8H, CH_2), 6.94-6.97 (m, 2H, Ar-H), 7.30 (d, 2H, J = 8.5 Hz, Ar-H), 7.41 (d, 2H, J = 8.5 Hz, Ar-H), 7.66-7.69 (m, 4H, Ar-H), 7.83-7.84 (m, 4H, Ar-H). ^{13}C NMR ($CDCl_3$): 14.09, 22.66, 25.94, 25.98, 29.00, 29.13, 29.23, 29.25, 29.32, 29.34, 31.80, 69.06, 69.31, 69.34, 77.97, 102.90, 106.82, 111.69, 111.85, 112.38, 114.46, 114.50, 116.29, 117.88, 120.69, 120.86, 122.46, 123.32, 124.51, 124.59, 126.69, 129.09, 132.74, 133.40, 148.66, 148.69, 152.65, 153.18, 153.43, 154.06, 154.16, 164.49. IR (KBr): 2921, 2851, 2229, 2198, 1726, 1597, 1516, 1432, 1278, 1200, 1131, 1062, 752. HRMS calcd for $C_{66}H_{82}N_2O_8S$ $(M+H)^+$: 1063.5870, found (FAB): 1063.5899.

3,4-Dicyano-2-[4-(3,4-didecyloxyphenylcarbonyloxy)phenylethynyl]-5-[4-(3,4-didecyloxyphenylcarbonyloxy)phenyl)thiophene (10) Preparation same as for **8**. ^{1}H NMR ($CDCl_3$): 0.85-0.94 (m, 12H, CH_3), 1.22-1.41 (m, 48H, $(CH_2)_6$), 1.43-1.58 (m, 8H, CH_2), 1.81-1.92 (m, 8H, CH_2), 4.05-4.14 (m, 8H, CH_2), 6.92-6.97 (m, 2H, Ar-H), 7.27 (d, 2H, J = 8.5 Hz, Ar-H), 7.37 (d, 2H, J = 8.5 Hz, Ar-H), 7.63-7.65 (m, 4H, Ar-H), 7.78-7.82 (m, 4H, Ar-H). ^{13}C NMR ($CDCl_3$): 14.08, 22.65, 25.91, 25.96, 28.97, 29.11, 29.31, 29.34, 29.36, 29.53, 29.56, 29.57, 31.86, 69.00, 69.27, 69.30, 77.94, 102.85, 106.75, 111.65, 111.81, 112.34, 114.43, 114.45, 116.27, 117.83, 120.66, 120.82, 122.41, 123.27, 124.46, 124.57, 126.63, 129.03, 132.65, 133.35, 148.63, 148.67, 152.61, 153.11, 153.40, 154.02, 154.12, 164.42. IR (KBr): 2919, 2849, 2233, 2194, 1727, 1596, 1516, 1278, 1200, 1131, 1063, 752. HRMS calcd for $C_{74}H_{98}N_2O_8S$ $(M+H)^+$: 1175.7122, found (FAB): 1175.7159.

3,4-Dicyano-2-[4-(3,4-didodecyloxyphenylcarbonyloxy)phenylethynyl]-5-[4-(3,4-didodecyloxyphenylcarbonyloxy)phenyl)thiophene (11) Preparation same as for **8**. ^{1}H NMR ($CDCl_3$): 0.84-0.90 (m, 12H, CH_3), 1.21-1.39 (m, 64H, $(CH_2)_8$), 1.43-1.52 (m, 8H, CH_2), 1.82-1.90 (m, 8H, CH_2), 4.04-4.12 (m, 8H, CH_2), 6.91-6.94 (m, 2H, Ar-H), 7.28 (d, 2H, J = 8.5 Hz, Ar-H), 7.38 (d, 2H, J = 8.5 Hz, Ar-H), 7.63-7.67 (m, 4H, Ar-H), 7.79-7.82 (m, 4H, Ar-H). ^{13}C NMR ($CDCl_3$): 14.12, 22.68, 25.95, 25.99, 29.00, 29.13, 29.35, 29.40, 29.61, 29.65, 29.68, 31.91, 69.04, 69.31, 69.34, 77.97, 102.90, 106.82, 111.69, 111.85, 112.38, 114.50, 114.50, 116.29, 117.88, 120.69, 120.86, 122.46, 123.33, 124.51, 124.59, 126.69, 129.09, 132.74, 133.40, 148.67, 148.70, 152.65, 153.18, 153.43, 154.06, 154.16, 164.49. IR (KBr): 2920, 2849, 2229, 2198, 1726, 1596, 1466, 1431,

1278, 1201, 1131, 1063, 752. HRMS calcd for $C_{82}H_{114}N_2O_8S$ $(M+H)^+$: 1287.8374, found (FAB): 1287.8353.

Symmetric Compounds:

3,4-Dicyano-2,5-bis[4-(hexyloxy)phenylethynyl]thiophene (13) Placed **12** (52 mg, 0.142 mmol) in a 25 mL Schlenk flask with PPh_3 (82 mg, 0.312 mmol) and a stir bar. The flask was evacuated and filled with argon several times. Dry, air-free THF (5 mL) was added via syringe. Diethylazodicarboxylate (49 μL, 0.312 mmol) was added via syringe, at which point the solution became an intense red color. After stirring for 48 hours the original yellow color had returned to the solution. Organics were washed with water, dried ($MgSO_4$) and removed in vacuo, yielding a dark yellow solid which was purified by column chromatography (silica gel, 1:1 hexane/dichloromethane eluent) followed by multiple precipitations from dichloromethane/methanol, yielding 55 mg (0.104 mmol, 73%) of **13** as a yellow solid. ^{1}H NMR ($CDCl_3$): 0.88-0.93 (t, 6H, CH_3), 1.28-1.40 (m, 8H, $(CH_2)_2$), 1.40-1.55 (m, 4H, CH_2), 1.78-1.84 (m, 4H, CH_2), 4.00 (t, 4H, J = 6.5 Hz, CH_2O), 6.91 (d, 4H, J = 8.5 Hz, Ar-H), 7.52 (d, 4H, J = 8.5 Hz, Ar-H).^{13}C NMR ($CDCl_3$): 14.03, 22.57, 25.64, 25.64, 29.04, 31.52, 68.25, 77.38, 104.44, 111.53, 111.99, 113.50, 114.87, 133.90, 161.00. HRMS cacld for $C_{34}H_{34}N_2O_2S$ $(M+Na)^+$: 557.2233, found (ESI): 557.2223.

3,4-Dicyano-2,5-bis[4-(octyloxy)phenylethynyl]thiophene (14) Preparation same as for **13**. ^{1}H NMR ($CDCl_3$): 0.88-0.93 (t, 6H, CH_3), 1.28-1.40 (m, 16H, $(CH_2)_4$), 1.40-1.55 (m, 4H, CH_2), 1.78-1.84 (m, 4H, CH_2), 4.00 (t, 4H, J = 6.5 Hz, CH_2O), 6.91 (d, 4H, J = 8.5 Hz, Ar-H), 7.52 (d, 4H, J = 8.5 Hz, Ar-H). ^{13}C NMR ($CDCl_3$):14.10, 22.65, 25.97, 29.08, 29.21, 29.31, 31.79, 68.25, 77.38, 104.44, 111.53, 111.99, 113.49, 114.87, 133.61,

133.91, 161.00. IR (KBr): 2923, 2853, 2229, 2193, 1602, 1518, 1290, 1253, 1153, 833. HRMS calcd for $C_{38}H_{42}N_2O_2S$ $(M+Na)^+$: 613.2859, found (ESI): 613.2895.

3,4-Dicyano-2,5-bis[4-(decyloxy)phenylethynyl]thiophene (15) Preparation same as for **13**. ^1H NMR ($CDCl_3$): 0.88-0.93 (t, 6H, CH_3), 1.28-1.40 (m, 24H, $(CH_2)_6$), 1.40-1.55 (m, 4H, CH_2), 1.78-1.84 (m, 4H, CH_2), 4.00 (t, 4H, J = 6.5 Hz, CH_2O), 6.91 (d, 4H, J = 8.5 Hz, Ar-H), 7.52 (d, 4H, J = 8.5 Hz, Ar-H). ^{13}C NMR ($CDCl_3$): 14.11, 22.67, 25.95, 29.06, 29.30, 29.34, 29.53, 31.87, 68.24, 77.38, 104.44, 111.52, 111.97, 113.46, 114.86, 133.59, 133.89, 160.99. HRMS calcd for $C_{42}H_{50}N_2O_2S$ $(M+Na)^+$: 669.3485, found (ESI): 669.3464.

3,4-Dicyano-2,5-bis[4-(dodecyloxy)phenylethynyl]thiophene (16) Preparation same as for **13**. ^1H NMR ($CDCl_3$): 0.88-0.93 (t, 6H, CH_3), 1.28-1.40 (m, 32H, $(CH_2)_8$), 1.40-1.55 (m, 4H, CH_2), 1.78-1.84 (m, 4H, CH_2), 4.00 (t, 4H, J = 6.5 Hz, CH_2O), 6.91 (d, 4H, J = 8.5 Hz, Ar-H), 7.52 (d, 4H, J = 8.5 Hz, Ar-H). ^{13}C NMR ($CDCl_3$): 14.12, 22.67, 25.95, 29.07, 29.34, 29.54, 29.57, 29.62, 29.64, 31.90, 68.23, 77.38, 104.43, 111.50, 111.96, 113.46, 114.86, 133.57, 133.87, 160.98. HRMS calcd for $C_{46}H_{58}N_2O_2S$ $(M+Na)^+$: 725.4111, found (ESI): 725.4103.

3,4-Dicyano-2,5-bis[4-(1-methylheptyloxy)phenylethynyl]thiophene (17) Preparation same as for **13**. ^1H NMR ($CDCl_3$): 0.88-0.93 (t, 6H, CH_3), 1.28-1.54 (m, 22H), 1.56-1.63 (m, 2H), 1.64-1.82 (m, 2H), 4.39-4.49 (m, 2H), 6.88 (d, 4H, J = 8.7 Hz, Ar-H), 7.50 (d, 4H, J = 8.5 Hz, Ar-H). ^{13}C NMR ($CDCl_3$): 14.14, 19.63, 22.63, 25.44, 29.25, 31.78, 74.06, 77.42, 104.43, 111.43, 111.58, 113.30, 115.73, 133.45, 133.80, 160.00. HRMS calcd for $C_{38}H_{42}N_2O_2S$ $(M+Na)^+$: 613.2859, found (ESI): 613.2823.

Unsymmetric Compounds:

3,4-Dicyano-2-(4-hexyloxyphenylethynyl)-5-(-4-hexyloxyphenyl)thiophene (18)

Compound **7** (50 mg, 0.146 mmol) was placed in a 25 mL Schlenk flask with PPh_3 (84 mg, 0.321 mmol) and a stir bar. The flask was evacuated and argon was introduced. THF (5 mL), *n*-Hexanol (40 μL, 0.312 mmol), and diethylazodicarboxylate (51 μL, 0.312 mmol) were added via syringe, respectively, and the reaction was stirred at room temperature for 48 hours. The solution became a deep red color upon the addition of DEAD, and faded to yellow over the course of the reaction. The poured into water and the organics were extracted with chloroform. The extracts were dried over magnesium sulfate and purified by column chromatography (silica gel, 1:1 hexane/dichlormethane eluent) followed by precipitation from dichloromethane/methanol yielding **18** (52 mg, 0.101 mmol, 71%) as a yellow solid. ^{1}H NMR ($CDCl_3$): 0.89-0.94 (m, 6 H, CH_3), 1.29-1.40 (m, 8H, $(CH_2)_2$), 1.40-1.55 (m, 4H, CH_2), 1.78-1.84 (m , 4H, CH_2), 3.99-4.03 (m, 4H, CH_2O), 6.90 (d, 2H, J = 9.0 Hz, Ar-H), 6.99 (d, 2H, J = 9.0 Hz, Ar-H), 7.51 (d., 2H, J = 9.0 Hz, Ar-H), 7.69 (d, 2H, J = 9.0 Hz, Ar-H). ^{13}C NMR ($CDCl_3$): 14.01, 22.55, 25.61, 29.00, 29.03, 31.50, 31.51, 68.20, 68.35, 76.74, 103.78, 105.01, 112.05, 112.27, 112.93, 114.79, 115.24, 115.44, 121.65, 129.15, 132.32, 133.71, 153.86, 160.76, 161.53. IR (KBr): 2927, 2855, 2221, 2191, 1602, 1519, 1461, 1302, 1252, 1187, 1171, 1020, 832. HRMS calcd for $C_{32}H_{34}N_2O_2S$ $(M+Na)^+$: 533.2233, found (ESI): 533.2218.

3,4-Dicyano-2-(4-octyloxyphenylethynyl)-5-(4-octyloxyphenyl)thiophene (19)

Preparation same as for **18**. ^{1}H NMR ($CDCl_3$): 0.89-0.94 (m, 6 H, CH_3), 1.29-1.40 (m, 16H, $(CH_2)_4$), 1.40-1.55 (m, 4H, CH_2), 1.78-1.84 (m , 4H, CH_2), 3.99-4.03 (m, 4H, CH_2O), 6.90 (d, 2H, J = 9.0 Hz, Ar-H), 6.99 (d, 2H, J = 9.0 Hz, Ar-H), 7.51 (d., 2H, J =

9.0 Hz, Ar-H), 7.69 (d, 2H, J = 9.0 Hz, Ar-H). ^{13}C NMR ($CDCl_3$): 14.09, 22.64, 25.95, 29.03, 29.08, 29.20, 29.29, 29.31, 31.78, 68.21, 68.36, 76.74, 103.78, 105.04, 109.41, 112.06, 112.28, 112.94, 114.80, 115.25, 115.45, 121.67, 129.17, 132.33, 133.72, 153.88, 160.77, 161.54. HRMS calcd for $C_{36}H_{42}N_2O_2S$ $(M+Na)^+$: 589.2859, found (ESI): 589.2856.

3,4-Dicyano-2-(4-decyloxyphenylethynyl)-5-(4-decyloxyphenyl)thiophene (20)

Preparation same as for **18**. ^{1}H NMR ($CDCl_3$): 0.89-0.94 (m, 6 H, CH_3), 1.29-1.40 (m, 24H, $(CH_2)_6$), 1.40-1.55 (m, 4H, CH_2), 1.78-1.84 (m , 4H, CH_2), 3.99-4.03 (m, 4H, CH_2O), 6.90 (d, 2H, J = 9.0 Hz, Ar-H), 6.99 (d, 2H, J = 9.0 Hz, Ar-H), 7.51 (d., 2H, J = 9.0 Hz, Ar-H), 7.69 (d, 2H, J = 9.0 Hz, Ar-H). ^{13}C NMR ($CDCl_3$): 14.12, 22.67, 25.96, 29.05, 29.09, 29.31, 29.34, 29.55, 31.88, 68.23, 68.38, 76.74, 103.80, 105.09, 112.07, 112.30, 112.95, 114.83, 115.28, 115.49, 121.70, 129.20, 132.37, 133.74, 153.92, 160.80, 161.56. IR (KBr): 2920, 2850, 2223, 2193, 1601, 1517, 1464, 1302, 1253, 1174, 1129, 1014, 829. HRMS calcd for $C_{40}H_{50}N_2O_2S$ $(M+Na)^+$: 645.3485, found (ESI): 645.3499.

3,4-Dicyano-2-(4-dodecyloxyphenylethynyl)-5-(4-dodecyloxyphenyl)thiophene (21)

Preparation same as for **18**. ^{1}H NMR ($CDCl_3$): 0.89-0.94 (m, 6 H, CH_3), 1.29-1.40 (m, 32H, $(CH_2)_6$), 1.40-1.55 (m, 4H, CH_2), 1.78-1.84 (m , 4H, CH_2), 3.99-4.03 (m, 4H, CH_2O), 6.90 (d, 2H, J = 8.9 Hz, Ar-H), 6.99 (d, 2H, J = 8.9 Hz, Ar-H), 7.51 (d., 2H, J = 8.9 Hz, Ar-H), 7.69 (d, 2H, J = 8.9 Hz, Ar-H). ^{13}C NMR ($CDCl_3$): 14.13, 22.68, 25.96, 29.04, 29.08, 29.34, 29.55, 29.58, 29.63, 29.65, 31.91, 68.22, 68.37, 103.79, 105.07, 112.07, 112.28, 112.95, 114.81, 115.47, 121.68, 129.19, 132.36, 133.73, 153.91, 160.78, 161.54. IR (KBr): 2920, 2849, 2214, 2194, 1603, 1518, 1465, 1252, 1178, 1037, 832. HRMS calcd for $C_{44}H_{58}N_2O_2S$ $(M+Na)^+$: 701.4111, found (ESI): 701.4131.

3,4-Difluoro-2,5-bis(4-tetrahydropyranyloxy)phenylethynyl]thiophene (22) 2,5-Dibromo-3,4-difluorothiophene (400 mg, 1.44 mmol) was placed in a 100 mL Schlenk flask with 4-(tetrahydropyranyloxy)phenylacetylene (591 mg, 2.92 mmol), $Pd(PPh_3)_4$ (83 mg, 0.072 mmol), copper(I)iodide (14 mg, 0.072 mmol) and a stir bar. The flask was repeatedly evacuated and filled with argon. In a separate flask a mixture of 1.0 mL DIPA (7.2 mmol) in 50 mL toluene were degassed by sparging with argon for 20 min, after which it was added to the reaction flask via cannula. The solution was stirred at room temperature for 12 hours after which the solvents were removed in vacuo, and the remaining solids were purified by silica gel chromatography (3:2 hexane:dichloromethane eluent) yielding **22** (417 mg, 0.801 mmol, 56%) as a yellow crystalline powder. ^{1}H NMR ($CDCl_3$, δ): 1.60-1.78 (m, 6H, CH_2CH_2), 1.85-1.90 (m, 4H, CH_2), 1.99-2.04 (m, 2H, CH_2), 3.61-3.65 (m, 2H, CH_2O), 3.85-3.91 (m, 2H, CH_2O), 5.47 (t, 2H, OCHO), 7.05 (d, 4H, J = 8.7 Hz, Ar-H), 7.46 (d, 4H, J = 8.7 Hz, Ar-H). ^{13}C NMR ($CHCl_3$, δ): 18.57, 25.06, 30.15, 62.02, 75.98, 96.14, 98.77, 103.42, 114.64, 116.44, 133.08, 145.71 (dd, J_1 = 268.2 Hz, J_2 = 19.6 Hz), 157.82. ^{19}F NMR ($CDCl_3$, δ vs. $CFCl_3$): 45.56 (s). MS-EI (*m/z*): (M^+) calcd for $C_{30}H_{26}F_2O_4S$: 520.1514, found: 520.1510.

3,4-Difluoro-2,5-bis(4-hydroxyphenylethynyl)thiophene (23) 3,4-Difluoro-2,5-Bis(4-tetrahydropyranyloxy)phenylethynyl]thiophene **22** (323 mg, 0.620 mmol) was placed in a 100 mL round-bottom flask to which THF (12 mL), glacial acetic acid (25 mL) and H_2O (7 mL) were added. The suspension was heated to 45 °C and stirred for 5 h, at which point the resulting yellow solution was allowed to cool to room temperature. Diethyl ether (100 mL) was added and the organics were washed with water (5 x 50 mL), dried

over $MgSO_4$ and concentrated in vacuo yielding 192 mg (0.545 mmol, 88%) of **23** as a slightly yellow powder. ^1H NMR ($CDCl_3$, δ): 3.72 (s, 2H, Ar-OH), 6.73 (d, 4H, J = 8.7 Hz, Ar-H), 7.30 (d, 4H, J = 8.7 Hz, Ar-H). ^{13}C NMR ($CHCl_3$, δ): 75.26, 98.96, 103.31 (d, J = 11.5 Hz), 112.57, 115.49, 133.21, 144.43 (dd, J_1 = 267.8 Hz, J_2 = 19.0 Hz), 157.96. ^{19}F NMR ($CDCl_3$, δ vs. $CFCl_3$): 43.42 (s). MS-EI (*m/z*): (M^+) calcd for $C_{20}H_{10}F_2O_2S$: 352.0364, found: 352.0349.

3,4-Difluoro-2,5-bis[4-(octyloxy)phenylethynyl]thiophene (24) 3,4-Difluoro-2,5-Bis(4-hydroxyphenylethynyl)thiophene **23** (40 mg, 0.114 mmol) was placed in a 25 mL Schlenk tube with PPh_3 (66 mg, 0.250 mmol) and a stir bar. The flask was evacuated and filled with argon, and 10 mL of dry, air-free THF was added via syringe. Dry *n*-octanol (40 μL, 0.250 mmol) and diethylazodicarboxylate (40 μL, 0.250 mmol) were added sequentially via microsyringe. The mixture was stirred at room temperature for 48 h, diluted with 25 mL CH_2Cl_2, washed with H_2O and dried over $MgSO_4$. The crude product was purified by silica gel chromatography (3:1 hexane/CH_2Cl_2 eluent) followed by precipitation from CH_2Cl_2 with MeOH yielding **24** (50 mg, 0.087 mmol, 76%) as a yellow powder. ^1H NMR ($CDCl_3$, δ): 0.87-0.97 (m, 6H, $-CH_3$), 1.29-1.42 (m, 16H, $(CH_2)_4$), 1.43-1.58 (m, 4H, CH_2), 1.78-1.85 (m, 4H, CH_2), 3.96-4.02 (m, 4H, OCH_2), 6.88 (d, 4H, J = 8.7 Hz, Ar-H), 7.46 (d, 4H, J = 8.7, Ar-H). ^{13}C NMR ($CDCl_3$, δ): 14.11, 22.65, 25.99, 29.13, 29.22, 29.33, 31.79, 68.12, 75.87, 98.86, 103.42, 113.58, 114.61, 133.18, 145.67 (dd, J_1 = 267.8 Hz, J_2 = 19.0 Hz), 159.94. ^{19}F NMR ($CDCl_3$, δ vs. $CFCl_3$): 46.99 (s). IR (KBr): 2920, 2851, 2202, 1604, 1580, 1505, 1464, 1286, 1246, 1170, 976, 827, 530. HRMS-EI (*m/z*): (M^+) calcd for $C_{36}H_{42}F_2O_2S$: 576.2868, found: 576.2878.

3,4-Difluoro-2,5-bis[4-(dodecyloxy)phenylethynyl]thiophene (25) Preparation same as for **24**. ^{1}H NMR ($CDCl_3$, δ): 0.87-0.97 (m, 6H, -CH_3), 1.29-1.42 (m, 32H, $(CH_2)_8$), 1.43-1.58 (m, 4H, CH_2), 1.78-1.85 (m, 4H, CH_2), 3.96-4.02 (m, 4H, OCH_2), 6.88 (d, 4H, J = 8.7 Hz, Ar-H), 7.46 (d, 4H, J = 8.7, Ar-H). ^{13}C NMR ($CDCl_3$, δ): 14.13, 22.69, 25.98, 29.12, 29.35, 29.36, 29.56, 29.58, 29.63, 29.65, 31.91, 68.11, 75.87, 98.86, 103.38 (d, J = 5.7 Hz), 113.57, 114.60, 133.18, 145.67 (dd, J_1 = 268.3 Hz, J_2 = 19.0 Hz), 159.94. ^{19}F NMR ($CDCl_3$, δ vs. $CFCl_3$): 45.43 (s). IR (KBr): 2918, 2849, 2210, 1607, 1499, 1251, 974, 836, 538. HRMS-EI (*m/z*): (M^+) calcd for $C_{44}H_{58}F_2O_2S$: 688.4120, found: 688.4140.

3,4-Difluoro-2,5-bis[4-(hexadecyloxy)phenylethynyl]thiophene (26) Preparation same as for **24**. ^{1}H NMR ($CDCl_3$, δ): 0.87-0.97 (m, 6H, -CH_3), 1.29-1.42 (m, 48H, $(CH_2)_{12}$), 1.43-1.58 (m, 4H, CH_2), 1.78-1.85 (m, 4H, CH_2), 3.96-4.02 (m, 4H, OCH_2), 6.88 (d, 4H, J = 8.7 Hz, Ar-H), 7.46 (d, 4H, J = 8.7, Ar-H). ^{13}C NMR ($CDCl_3$, δ): 14.13, 22.69, 25.98, 29.13, 29.37, 29.56, 29.58, 29.66, 29.67, 29.69, 31.92, 68.12, 75.87, 98.86, 103.41, 113.58, 114.62, 133.19, 145.68 (dd, J_1 = 267.7 Hz, J_2 = 19.0 Hz), 159.94. ^{19}F NMR ($CDCl_3$, δ vs. $CFCl_3$): 45.42 (s). IR (KBr): 2917, 2848, 2190, 1498, 1250, 976, 837. HRMS-EI (*m/z*): (M^+) calcd for $C_{52}H_{74}F_2O_2S$: 800.5372, found: 800.5358.

3,4-Difluoro-2,5-bis[(4-(3,4-dioctyloxyphenylcarbonyloxy)phenylethynyl] thiophene (27) 3,4-Difluoro-2,5-Bis(4-hydroxyphenylethynyl)thiophenene **23** (40 mg, 0.114 mmol) was placed in a 25 mL Schlenk tube with 3,4-dihexyloxybenzoic acid (95 mg, 0.250 mmol), DMAP (7 mg, 0.057 mmol) and a stir bar. The flask was evacuated and filled with argon. Dry dichloromethane (10 mL) was added via cannula and diisopropylcarbodiimide (71 μL, 0.454 mmol) was added via microsyringe. The reaction

was stirred for 48 h at room temperature after which it was diluted with 25 mL CH_2Cl_2, washed with H_2O and dried over $MgSO_4$. The crude product was then purified by column chromatography (3:2 hexane/CH_2Cl_2 eluent) and precipitated from CH_2Cl_2 with MeOH. ^1H NMR ($CDCl_3$, δ): 0.88-0.95 (m, 12H, CH_3), 1.26-1.44 (m, 32H, $(CH_2)_8$), 1.45-1.57 (m, 8H, CH_2), 1.82-1.95 (m, 8H, CH_2), 4.03-4.15 (m, 4H, CH_2), 6.95 (d, 2H, J = 8.4 Hz, Ar-H), 7.25 (d, 4H, J = 8.7 Hz, Ar-H), 7.61 (d, 4H, J = 8.7 Hz, Ar-H), 7.66 (d, 2H, J = 2.1 Hz, Ar-H), 7.82 (dd, 4H, J_1 = 8.4 Hz, J_2 = 2.1 Hz, Ar-H). ^{13}C NMR ($CDCl_3$, δ): 14.11, 22.67, 25.95, 25.99, 29.01, 29.13, 29.25, 29.26, 29.33, 29.35, 31.80, 31.81, 69.04, 69.31, 98.13, 111.84, 114.46, 119.25, 121.04, 122.19, 124.45, 126.46, 132.87, 148.64, 151.74, 153.97, 164.64. ^{19}F NMR ($CDCl_3$, δ vs. $CFCl_3$): 46.22 (s). IR (KBr): 2922, 2848, 2206, 1736, 1599, 1428, 1273, 1198, 1082, 975, 870, 750. HRMS-EI (*m/z*): (M+H) calcd for $C_{36}H_{42}F_2O_2S$: 1073.5771, found: 1073.5730.

References

(1) Fisch, M.R.; Kumar, S. in *Liquid Crystals: Experimental Study of Physical Properties and Phase Transitions*, Cambridge University Press, 2001, pp 21-22.

(2) a) Niori, T.; Sekine, T.; Watanabe, J.; Furukawa, T.; Takezoe, H. *J. Mater. Chem.* **1996**, 6, 1231-1233. b) Shen, D.; Diele, S.; Wirt, I.; Tschierske, C. *Chem. Comm.* **1998**, 2573-2574. c) Pelzl, G.; Diele, S.; Weissflog, W. *Adv. Mater.* **1999**, *11*, 707-724. d) Heppke, G.; Parghi, D.D.; Sawade, H. *Liq. Cryst.* **2000**, 27, 313-320. e) Weissflog, W.; Kovalenko, L.; Wirth, I.; Diele, S.; Pelzl, G.; Schmalfuss, H.; Kresse, H. *Liq. Cryst.* **2000**, *27*, 677-681. f) Shen, D.; Pegenau, A.; Diele, S.; Writh, I.; Tschierske, C. *J. Am.*

Chem. Soc. **2000**, *122*, 1593-1601. g) Bedel, J.P.; Rouillon, J.C.; Marcerou, J.P.; Laguerre, M.; Nguyen, H.T.; Achard, M.F. *Liq. Cryst.* **2000**, *27*, 1411-1421. h) Sadashiva, B.K.; Shreenivasa, H.N.; Dhara, S. *Liq. Cryst.* **2001**, *28*, 483-487.

(3) Link, D.R.; Natale, G.; Shao, R.; Maclennan, J.E.; Clark, N.A.; Korblova, E.; Walba, D.M. *Science* **1997**, *278*, 1924-1927. Heppke, G.; Moro, D. *Science* **1998**, 279, 1872-1873.

(4) a) Serrette, A.G.; Carroll, P.J.; Swager, T.M. *J. Am. Chem. Soc.* **1992**, *114*, 1887-1888. b) Serrette, A.G.; Swager, T.M. *J. Am. Chem. Soc.* **1993**, *115*, 8879-8880. c) Zheng, H.; Carroll, P.J.; Swager, T.M. *Liq. Cryst.* **1993**, *14*, 1421-1429. d) Serrette, A.G.; Swager, T.M. *Angew. Chem., Int. Ed. Engl.* **1994**, *33*, 2342-2345.

(5) Kishikawa, K.; Harris, M. C.; Swager, T. M. *Chem. Mater.* **1999**, *11*, 867-871.

(6) Eichhorn, S.H.; Paraskos, A. J.; Kishikawa, K.; Swager, T.M. *J. Amer. Chem. Soc.* **2002**, *124*, 12742-12751.

(7) Levitsky, I.A.; Kishikawa, K.; Eichhorn, S.H.; Swager, T.M. *J. Am.. Chem. Soc.* **2000**, *11*, 2474-2479.

(8) a) Meyer, R.B. *Phys. Rev. Lett.* **1969**, *22*, 918. b) Billeter, J.L.; Pelcovits, R.A. *Liq. Cryst.* **2000**, *27*, 1151-1160.

(9) Malthete, J.; Nguyen, H.T.; Destrade, C. *Liq. Cryst.* **1993**, *13*, 171.

(10) a) Jacq, P.; Malthête, J. *Liq. Cryst.* **1996**, *21*, 291. b) Donnio, B.; Heinrich, B.; GulikKrzuwicki, T.; Delacroix, H.; Guillon, D.; Bruce, D.W. *Chem. Mater.* **1997**, *9*,

2951. c) Elliot, J.M.; Chipperfield, J.R.; Clark, S.; Sinn, E. *Inorg. Chem. Comm.* **2002**, *5*, 99-101.

(11) Chandrasekhar, S.; Nair, G.G.; Rao, D.S.S.; Prasad, S.K.; Praefcke, K.; Blunk, D. *Liq. Cryst.* **1998**, *24*, 67.

(12) Miura, Y.; Oka, H.; Momoki, M. *Synthesis* **1995**, 1419.

(13) Sonogashira, K.; Tohda, Y.; Hagihara, N. *Tetrahedron Lett.* **1975**, 4467.

(14) Friedman, L.; Shechter, H. *J. Org. Chem.* **1961,** *26*, 2522.

(15) Mitsunobu, O. *Synthesis* **1981**, *1*, 1-28.

(16) Sakamoto, Y.; Komatsu, S.; Suzuki, T. *J. Am. Chem. Soc.* **2001**, *123*, 4643-4644.

(17) a) Levitsky, I.A.; Kishikawa, K.; Eichhorn, S.H.; Swager, T.M. *J. Am. Chem. Soc.* **2000**, *11*, 2474-2479. b) Trzaska, S.T.; Swager, T.M. *Chem. Mater.* **1998**, *10*, 438-443. c) Zheng, H.; Xu, B.; Swager, T.M. *Chem. Mater.* **1996**, *8*, 907-911. d) Zheng, H.; Lai, C.K.; Swager, T.M. *Chem. Mater.* **1994**, *6*, 101-103.

(18) a) Luckhurst, G.R.; Timini, B.A. *Phys. Lett.* **1979**, *75A*, 91-95. b) Leadbetter, A.J. in *Molecular Physics of Liquid Crystals*, Academic Press, 1979, pp304-306.

(19) Collings, P.J.; Hird, M. *Introduction to Liquid Crystals: Chemistry and Physics*, Taylor and Francis, 1997, pp 111-131.

Chapter 4

Triphenylene-Dione Half-Disc Mesogens

Adapted from:

Paraskos, A. J.; Nishiyama, Y.; Swager, T. M. *Mol. Cryst. Liq. Cryst.* (accepted).

Introduction

With the discovery that disc-shaped molecules can stack and form columnar mesophases a new paradigm was born for the rational design of unique liquid crystal assemblies.[1] This discovery highlights the importance of considering shape anisotropy and structure-property relationships when creating novel mesogens that might potentially display new mesophases.

Since then, it has been shown that many non-discoid molecules are capable of forming columnar mesophases as well. For example, polycatenar mesogens frequently display columnar mesophases arising through the formation of aggregates[2] or dimers[3] of molecules within the columns. The Swager lab has a history designing of metallomesogens in which half-disc subunits are brought together covalently through a central metal atom(s) to form either disc-shaped[4] or propeller-shaped[5] mesogenic units. The lab of Carsten Tschierske has since described butterfly-shaped[6] and rod/half-disc shaped[7] mesogenic units. The above examples demonstrate that unfavorably shaped subunits can be strategically combined to form molecules which are mesogenic. The assembly of mesogenic units through non-covalent forces such as hydrogen-bonding,[8] coordination polymers[9] and microphase segregation[10] and has also proven effective. In previous chapters of this thesis the use of dipole-dipole interactions to increase the mesogenicity of molecules with unfavorable bent-shapes (see chapters 2 and 3) is also described.[11]

Herein we describe the synthesis and phase behavior of a series of mesogens of general structure 6,7,10,11-tetrakis(alkoxy)triphenylene-1,4-dione. These deep-red

colored organic dyes have been found to display hexagonal columnar mesophases presumably due to a correlated organization of their shapes.

Results and Discussion

Synthesis A number of triphenylene-based quinones were synthesized and studied (Scheme 3). Compounds **10** and **16** were synthesized and structurally characterized by former Swager postdoctoral fellow Claus Lugmair. Compounds **6** and **7,** as well as **13** and **19** were synthesized by former Swager group visiting scientist Yutaka Nishiyama. The synthesis of compound **18** was previously described by Aimee Rose, a former graduate student in the Swager group;[12] a similar synthetic route was followed for the synthesis of compounds **14**, **15** and **17**.

Williamson ether synthesis of the appropriate alkyl bromide with catechol affords the corresponding 1,2-dialkoxybenzene, which is iodinated with periodic acid and iodine yielding the 3,4-dialkoxy-1-iodobenzene.[13] Ullman coupling of the 3,4-dialkoxybenzenes is carried out neat with copper (220 °C) yielding the corresponding 3,3',4,4'-tetraalkoxybiphenyl cleanly in 70-75% yield after precipitation from $CHCl_3$/MeOH (Scheme 1).

Scheme 1. Synthesis of 3,3'4,4'-Tetrakis(n-alkoxy)biphenyls.

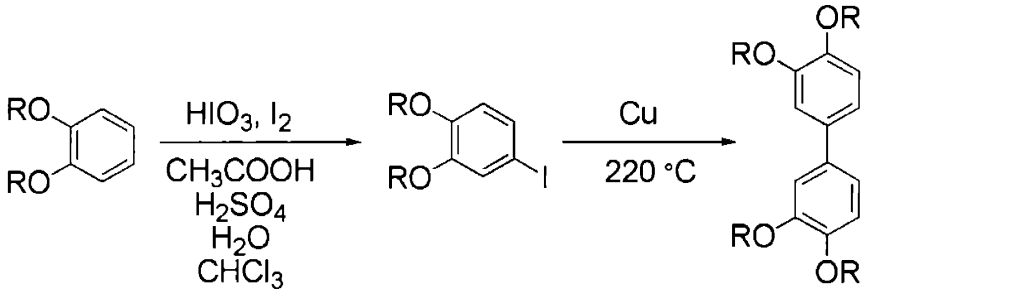

1 $R_1 = R_2 = n\text{-}C_6H_{13}$
2 $R_1 = R_2 = n\text{-}C_8H_{17}$
3 $R_1 = R_2 = n\text{-}C_{10}H_{21}$
4 $R_1 = R_2 = n\text{-}C_{12}H_{25}$
5 $R_1 = R_2 =$ 2-Ethylhexyl

Alternatively, etherification of 5-iodo-2-methoxyphenol, synthesized by the previously reported method,[14] with 1-bromo-2-ethylhexane provides 2-(2-ethylhexyloxy)-4-iodo-1-methoxybenzene in good yield after distillation. Biphenyl **7** can then be synthesized via a zinc/palladium (0) coupling in good yields (Scheme 2).

Scheme 2. Synthesis of 3,3'-Bis(2-ethylhexyloxy)-4,4-dimethoxybiphenyl.

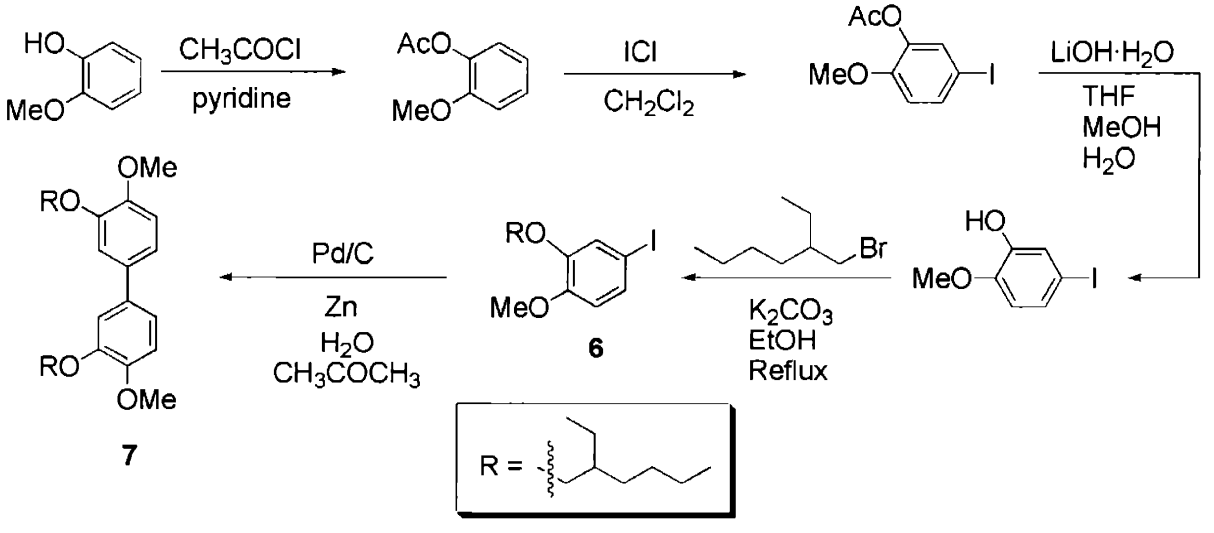

Cyclization of the resulting biphenyl compounds with *p*-dimethoxybenzene and iron (III) chloride in DCM yields the parent triphenylenes **8-13**, which are then oxidatively demethylated with cerium ammonium nitrate yielding the desired mesogenic quinones **14-19** (Scheme 3).

Scheme 3. Synthesis of mesogenic triphenylene quinones.

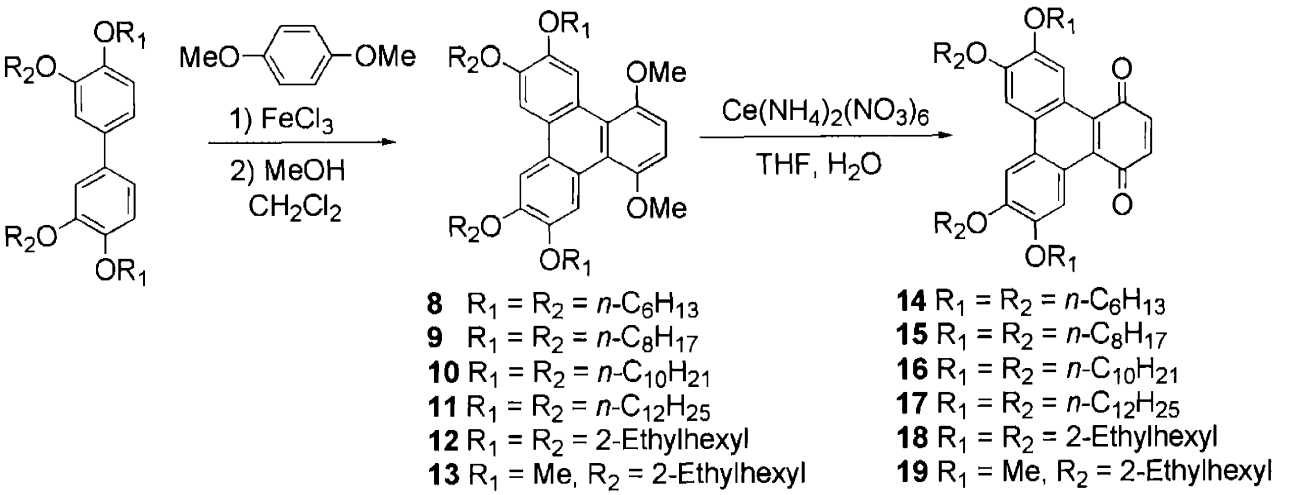

8 $R_1 = R_2 = n\text{-}C_6H_{13}$
9 $R_1 = R_2 = n\text{-}C_8H_{17}$
10 $R_1 = R_2 = n\text{-}C_{10}H_{21}$
11 $R_1 = R_2 = n\text{-}C_{12}H_{25}$
12 $R_1 = R_2$ = 2-Ethylhexyl
13 R_1 = Me, R_2 = 2-Ethylhexyl

14 $R_1 = R_2 = n\text{-}C_6H_{13}$
15 $R_1 = R_2 = n\text{-}C_8H_{17}$
16 $R_1 = R_2 = n\text{-}C_{10}H_{21}$
17 $R_1 = R_2 = n\text{-}C_{12}H_{25}$
18 $R_1 = R_2$ = 2-Ethylhexyl
19 R_1 = Me, R_2 = 2-Ethylhexyl

Dihyroquione **20** can be synthesized in near quantitative yield from parent quinone **15** via reduction with sodium hydrosulfite in a well-stirred flask of diethyl ether and distilled water.

Scheme 4. Synthesis of dihydroquinone 20.

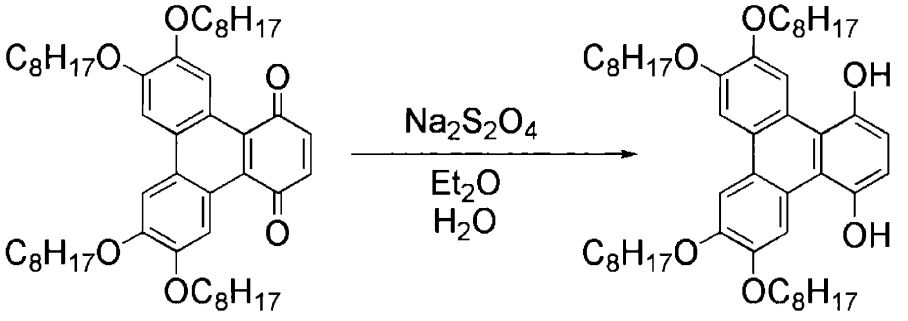

15 **20**

Phase Behaviour. The phase behaviour of the mesogens **14-19** is listed in Table 1. Despite their half-disc shapes, compounds **14, 15** and **16**, possessing *n*-hexyloxy, *n*-octyloxy and *n*-decyloxy sidechains, respectively, all exhibit enantiotropic Col_h mesophases as identified by polarized microscopy and X-ray diffraction. When viewed by polarized microscopy these compounds exhibit petal-like textures possessing features that are clearly hexagonal in nature (Figure 1). Compound **17**, with *n*-dodecyloxy sidechains, exhibits a relatively narrow monotropic Col_h mesophase, as does the bis(2-ethylhexyl)dimethyl triphenylene quinone **19**, which represents an unusual example of a columnar phase exhibited by a triphenylene-type compound possessing only two alkoxy sidechains. Quinone **18**, possessing four 2-ethylhexyl sidechains, exhibits a Col_h mesophase at room temperature. In stark contrast to the quinone compounds, none of the parent triphenylenes **8-13** are liquid-crystalline, presumably as a consequence of their half-disc shapes. In order to assure ourselves that the steric bulk of the methyl groups was not the main factor in preventing the formation of liquid crystal phases, dihydroquinone **20** was synthesized and it was found to be non-mesomorphic as well (mp

= 109 °C). This compound underwent oxidation to the parent quinone **15** after prolonged exposure to air (especially in solution) as was evident by the color changing from white to purple/red. For example, after 24 hours in $CDCl_3$ at room temperature, approximately 25% conversion had occurred (estimated by ^1H NMR).

Table 1. Phase behaviour of triphenylene quinones.

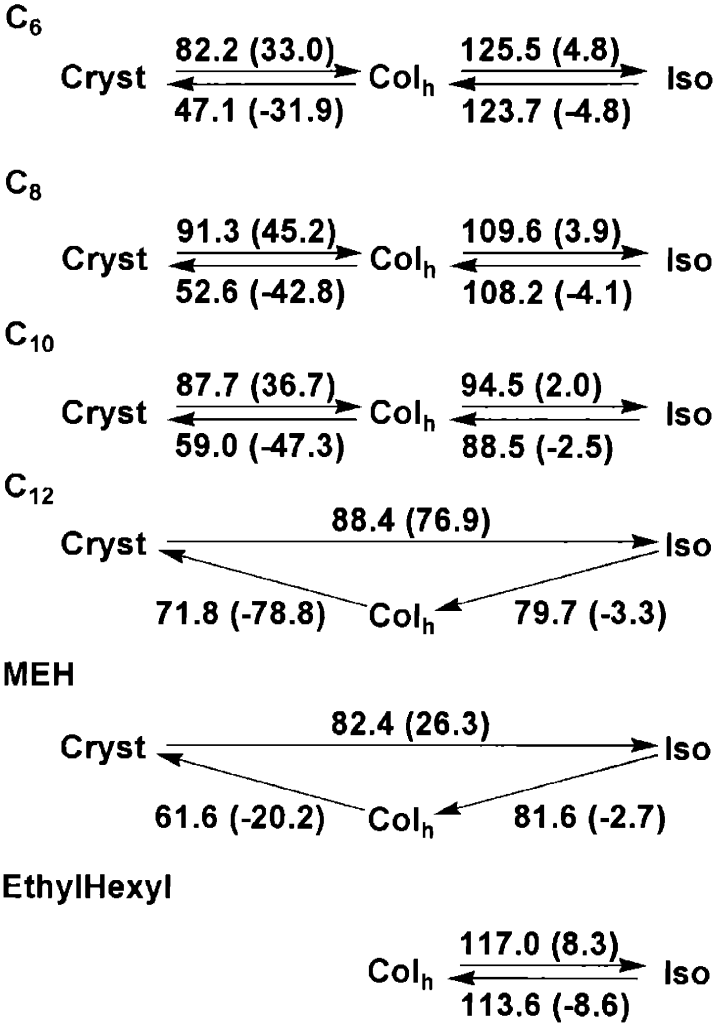

Transition temperatures (°C) and enthalpies (in parentheses, kJ/mol) were determined by DSC (10 °C/min) and are given above and below the arrows.

Figure 1. Polarized microscopy of the Colh phase of 15 at 111 °C (top) and 109 °C (bottom) (both 100x magnification).

XRD Studies. Variable temperature X-ray diffraction studies were performed for the columnar phases exhibited by each of the quinones, with the exception of compound **16** (Table 2). The Col_H phases of these compounds are all characterized by the observation of sharp (100) peaks in the low angle region. The diffraction patterns of compounds **15** and **17** also exhibit sharp (110) and (200) peaks, confirming the hexagonal nature of the phases. The wide-angle regions of the diffraction patterns all display broad halos at approximately 3.5 Å, corresponding to the distance between neighboring mesogens within individual columns. In addition, broad halos at 4.6 Å correspond to the distance between liquid-like sidechains, confirming that the phases are indeed liquid crystalline as opposed to crystal or plastic phases. Further analysis of the wide-angle region of compound **19** suggests an antiparallel (dimerized) packing of the molecules within the columns, as evidenced by the appearance of an additional diffuse scattering peak centered at approximately 6.9Å. (Figure 2) This behavior has been observed repeatedly by our group and other groups for mesogens in which packing and dipolar forces combine to cause an antiparallel dimer association of molecules within both columnar[14] and lamellar phases.[15, 11b-c] Such dimerization, most likely driven by dipole-dipole interactions (AM1 calculations on a model compound suggest a molecular dipole of 1.27D) in combination with the half-disc shape may explain the relative stability of the columnar phases of these half-disc mesogens. This would also explain the lack of mesogenicity observed for the parent triphenylenes, as these molecules lack a significant dipole and so most likely would not possess a driving force to organize in this fashion.

Table 2. XRD for compounds **14-15** and **17-19.**

compd	mesophase	lattice constant (Å)	spacing obsd	Miller indices	Å (calcd)	halos obsd
14	Col_h	19.1	16.5	100		3.5
	at 75 °C			110	9.5	4.5
				200	8.3	
15	Col_h	20.4	17.7	100		3.5
	at 92°C		10.3	110	(10.2)	4.6
			8.9	200	(8.8)	
17	Col_h	24.4	21.1	100		3.7
	at 76 °C		12.2	110	(12.2)	4.6
			10.6	200	(10.6)	
18	Col_h	20.2	17.5	100		3.7
	at 90 °C			110	(10.1)	4.6
				200	(8.8)	
19	Col_h	17.0	14.7	100		3.5
	at 100 °C			110	(8.5)	4.6
				200	(7.4)	6.9

Figure 2. Proposed antiparallel stacking of mesogenic quinones in the columnar phase.

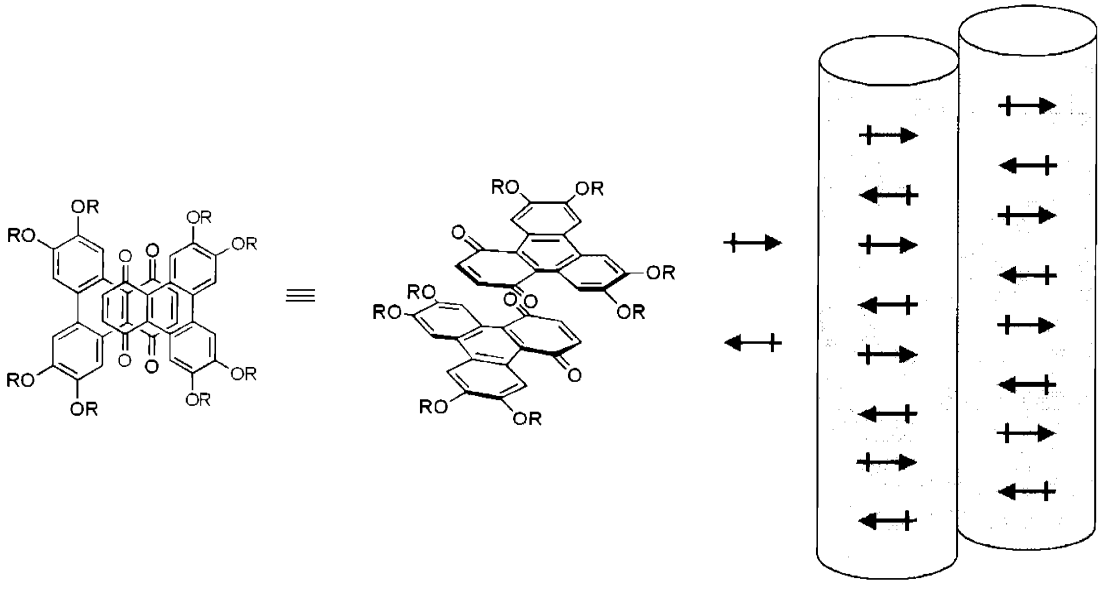

Summary and Conclusions

A variety of triphenylene quinones were prepared and shown to exhibit Col_h mesophases. Their ability to form columnar phases despite their half-disc shape may be explained by the formation of an antiparallel dimers of molecules within the liquid crystal phases, which have been observed by X-ray diffraction studies. Such a correlated organization of molecules, driven by dipole-dipole interactions, results in the formation of mesogenic units that are roughly disc-shaped. Further supporting this idea is the fact that the parent triphenylene compounds, whose dipoles are apparently not significant enough to drive an antiparallel association of molecules, are not liquid crystalline.

Experimental Section

General Dichloromethane was dried by passing through activated alumina columns. Anhydrous methanol was purchased from Aldrich (sure-seal) and stored over activated molecular sieves before use. All other chemicals were of reagent grade and were used without further purification. 1,2-Dihexyloxy-, 1,2-dioctyloxy, 1,2-didecyloxy, 1,2-didodecyloxy and 1,2-di(2-ethylhexyloxy)benzenes were prepared by the alkylation of catechol with alkyl bromide. Air and water sensitive reactions employed standard Schlenk techniques under argon atmosphere. NMR spectra were obtained on Varian Mercury-300, Bruker DPX-400 or Varian Inova-500 spectrometers. All chemical shifts are referenced to residual $CHCl_3$ (7.27 ppm for ^1H, 77.0 ppm for ^{13}C). Multiplicities are indicated as s (singlet), d (doublet), t (triplet), and m (multiplet). High resolution mass spectra were obtained at the MIT Department of Chemistry Instrumentation facility (DCIF) on a Finnigan MAT 8200 or on a Bruker Daltonics Apex II 3T FT-ICR MS.

Infrared spectra were recorded on a Nicolet Impact 410 in KBr pellets. DSC investigations were carried out on a Perkin-Elmer DSC-7. Optical microscopy was carried out on a Leica polarizing microscope in combination with a Linkam LTS350 hotstage. X-ray diffraction studies were carried out on samples in capillary tubes with an INEL diffractometer with a 2 kW CU K_α X-ray source fitted with an INEL CPS-120 position-sensitive detector. The detectors were calibrated using a silver behenate standard produced by Eastman Kodak.

2-(2-Ethylhexyloxy)-4-iodo-1-methoxybenzene (6). 5-Iodo-2-methoxyphenol (30g, 120 mmol) and K_2CO_3 (33.2 g, 240 mmol) were successively added to ethanol (150 mL) and stirred at rt. for 0.5 h, after which 1-bromo-2-ethylhexane (23.2g, 120 mmol) was added to the solution and vigorously stirred at 85 °C for 96 h. Additional K_2CO_3 (8.3 g, 60 mmol) was added to the solution after stirring for 24, 48 and 72 h. Upon cooling the reaction mixture was diluted with diethyl ether (100 mL), filtered and the remaining solids were washed with diethyl ether (50 ml). The solvent was removed under reduced pressure; the residual yellow oil was dissolved in hexane (200 mL) and washed with 1M NaOH solution (100 mL x 2) and H_2O (150 ml), respectively. After drying over $MgSO_4$, the organic layer was concentrated under reduced pressure and the residue was distilled to afford **6** as a colorless oil (37.0 g, 85 %). ^{1}H NMR ($CDCl_3$, δ): 0.91 (t, J = 6.3 Hz, 3H), 0.94 (t, J = 6.3 Hz, 3H), (m, J = 6.3 Hz, 1H), 1.80 1.58-1.30 (m, 8H), 3.83 (s, 3H), 3.84 (d, J = 6.3 Hz, 2H), 6.62 (d, J = 8.7 Hz, 1H), 7.14 (d, J = 2.1 Hz, 1H), 7.21(dd, J = 2.1, 8.7 Hz, 1H). ^{13}C NMR ($CDCl_3$, δ): 11.26, 14.40, 23.31, 24.00, 29.21, 30.60, 39.34, 56.35, 72.17, 82.64, 114.03, 122.10, 129.65, 149.75, 149.99.

3,3'-Di(2-ethylhexyloxy)-4,4'-dimethoxybiphenyl (7). 10 % Pd-C (15.7 g) and Zn dust (15.7 g, 240 mmol) were added to a mixture of acetone/ H_2O (1/1 800 mL), and the resulting suspension was stirred at room temperature for 1h after which 2-(2-ethylhexyloxy)-4-iodo-1-methoxybenzene was added dropwise and stirred at for 48 h. Hexane (150 ml) was added to the resulting solution and the solution was filtered through Celite pad. The organic layer was separated, then aqueous layer was extracted with diethyl ether (100 mL). The combined organic layers were washed with saturated brine (100 mL x 2), dried over $MgSO_4$, and then concentrated under reduced pressure leaving a light yellow oil. Purification by reduced distillation afforded **7** as a clear oil (16.2g, 86 %). ^{1}H NMR ($CDCl_3$, δ): 0.92 (t, J = 7.5 Hz, 6H), 0.96 (t, J = 7.5 Hz, 6H), 1.27-1.51 (m, 16H), 1.85 (m, J = 6.0 Hz, 2H), 3.90 (s, 6H), 3.97 (d, J = 6.0 Hz, 4H), 6.94 (d, J = 9.0 Hz, 2H), 7.08 (s, 2H), 7.09 (d, J = 9.0 Hz, 2H). ^{13}C ($CDCl_3$, δ): 11.23, 14.32, 23.29, 23.98, 29.22, 30.64, 39.43, 56.53, 72.28, 112.61, 112.73, 119.28, 134.55, 149.14, 149.34.

1,4-Dimethoxy-6, 7,10,11-tetrakis(hexyloxy)triphenylene (8). A solution of tetra(hexyloxy)biphenyl (2.50 g, 4.51 mmol) in CH_2Cl_2 (50 mL) was added dropwise to a stirred suspension of $FeCl_3$ (6.00 g, 36.99 mmol) in CH_2Cl_2 (250 mL) at 0 °C. 1,4-Dimethoxybenzene (2.50 g, 18.0 mmol) was added and the reaction was allowed to warm to room temperature and stirred for 5 h. The reaction mixture was quenched with anhydrous MeOH (70 mL) and then stirred at r.t for 0.5 h. The solvent was removed under reduced pressure and the residual solids were dissolved in diethyl ether (100 mL), washed with aqueous NH_4Cl (3 x 100 mL) and H_2O (3 x 100 mL), dried over $MgSO_4$, and concentrated under reduced pressure. The crude product was purified by column chromatography on silica gel (hexanes/CH_2Cl_2 1:1 eluent) to afford a light brown solid.

The solid was further purified by recrystallization from MeOH/$CHCl_3$ yielding **8** (3.68 g, 3.68 mmol, 82%) as white plates. ^1H NMR ($CDCl_3$, δ): 0.89-0.93 (m, 12 H), 1.32-1.43 (m, 16H), 1.32-1.51 (m, 8H), 1.82-1.99 (m, 8H), 3.91 (s, 6H), 4.12 (t, J = 6.6 Hz, 4H), 4.17 (t, J = 6.6 Hz, 4H), 7.00 (s, 2H), 7.73 (s, 2H), 9.06 (s, 2H). ^{13}C NMR ($CDCl_3$, δ): 14.39, 22.97, 26.12, 26.15, 29.53, 29.63, 31.98, 57.43, 69.17, 69.67, 106.60, 110.50, 112.97, 122.46, 123.22, 125.48, 147.68, 148.71, 152.55. HRMS-ESI (*m/z*): $(M+H)^+$ calcd for $C_{44}H_{64}O_6$ 689.4776, found 689.4760.

1,4-Dimethoxy-6,7,10,11-tetrakis(octyloxy)triphenylene (9). Preparation same as for **8**. Tetra(octyloxy)biphenyl (9.95 g, 14.92 mmol), $FeCl_3$ (19.36 g, 119.0 mmol), dimethoxybenzene (8.244 g, 59.7 mmol). Recovered **9** (8.795 g, 10.98 mmol, 74%) as a white powder. ^1H NMR ($CDCl_3$, δ):0.89-0.93 (m, 12H), 1.32-1.42 (32H), 1.56-1.59 (m, 8H), 1.94-1.96 (m, 8H), 3.99 (s, 6H), 4.21-4.25 (m, 8H), 7.09 (s, 2H), 7.82 (s, 2H), 9.16 (s, 2H). ^{13}C NMR ($CDCl_3$, δ): 14.10, 14.12, 22.68, 22.69, 26.13, 29.07, 29.15, 29.31, 29.44, 31.82, 68.72, 69.00, 103.83, 109.37, 122.17, 126.60, 128.80, 137.67, 150.58, 151.05.

1,4-Dimethoxy-6,7,10,11-tetrakis(decyloxy)triphenylene (10). Synthesis and characterization previously described. [11] ^1H NMR ($CDCl_3$, δ): 0.87-0.91 (m, 12H), 1.29-1.44 (m, 48), 1.45-1.64 (m, 8H), 1.85-2.01 (m, 8H), 4.00 (s, 6H), 4.18-4.27 (m, 8H), 7.10 (s, 2H), 7.81 (s, 2H), 9.15, (s, 2H). (^{13}C NMR ($CDCl_3$, δ):14.34, 22.92, 26.41, 29.51, 29.60, 29.77, 29.85, 29.92, 32.15, 57.34, 57.51, 69.20, 69.70, 106.66, 110.47, 113.05, 122.56, 123.31, 125.58, 147.82, 148.86, 152.70. HRMS-EI (*m/z*): $(M+H))^+$ calcd for $C_{60}H_{96}O_6$ 912.7207, found 912.7207.

1,4-Dimethoxy-6,7,10,11-tetrakis(dodecyloxy)triphenylene (11). Preparation same as for **8**. Tetra(dodecyloxy)biphenyl (0.90 g, 1.0 mmol), $FeCl_3$ (1.42 g, 8.0 mmol), dimethoxybenzene (0.56 g, 4.0 mmol). Recovered **11** (0.829 g, 81%) as a white powder. ^1H NMR ($CDCl_3$, δ): 0.89-0.93 (m, 12H), 1.28-1.56 (m, 80H), 1.94-1.96 (m, 8H), 4.00 (s, 6H), 4.21 (t, J = 6.6 Hz, 4H), 4.25 (t, J = 6.6 Hz, 4H), 7.10 (s, 2H), 7.81 (s, 2H), 9.15 (s, 2H). ^{13}C NMR ($CDCl_3$, δ): 14.45, 23.01, 26.50, 29.58, 29.69, 29.82, 29.85, 29.98, 30.04, 32.23, 57.42, 69.19, 69.69, 106.62, 110.49, 113.00, 122.47, 123.23, 125.49, 147.68, 148.73, 152.56. HRMS-ESI (*m/z*): $(M+Na)^+$ calcd for $C_{68}H_{112}O_6$ 1047.8351, found 1047.8315.

1,4-Dimethoxy-6,7,10,11-tetrakis(2-ethylhexyloxy)triphenylene (12). Synthesis and characterization previously described. [11]

1,4,6,10-Tetramethoxy-7,11-di(2-ethylhexyloxy)triphenylene (13).

Dimethoxydi(2-ethylhexyloxy)biphenyl (2.42 g, 5.0 mmol), $FeCl_3$ (6.8 g, 40.0 mmol), dimethoxybenzene (2.76 g, 20.0 mmol). Recovered **13** (2.32 g, 70%) as a white powder. ^1H NMR ($CDCl_3$, δ): 0.94 (t, J = 7.2 Hz, 6H), 1.03 (t, J = 7.2 Hz, 6H), 1.37-1.66 (m, 16H), 1.98 (m, J = 6.0 Hz, 2H), 4.02 (s, 6H), 4.05 (s, 6H), 4.17 (d, J = 6.0 Hz, 4H), 7.11 (s, 2H), 9.19 (s, 2H), 7.83 (s, 2H). ^{13}C NMR ($CDCl_3$, δ): 11.49, 14.44, 23.41, 24.13, 29.32, 30.87, 39.41, 56.17, 57.40, 72.23, 105.88, 110.43, 111.49, 122.39, 123.06, 125.45, 148.19, 148.60, 152.53. HRMS-ESI (*m/z*): $(M+H)^+$ calcd for $C_{38}H_{52}O_6$ 605.3837, found 605.3822.

6,7,10,11-Tetra(hexyloxy)triphenylene-1,4-dione (14). To a stirred THF (60 mL) solution of **8** (1.69g, 2.45mmol) an H_2O solution (15 mL) of cerium (IV) ammonium nitrate (2.82g, 5.13mmol) was added dropwise and stirred at room temperature for 2 h.

The resulting solution was poured into diethyl ether (500 mL) and washed with saturated $NaHCO_3$ solution (100 ml x 2) followed by water (100mL x 3), then dried over $MgSO_4$. The solvent was removed under the reduced pressure, and the crude product was subsequently purified by column chromatography on silica gel (1:1 hexanes/CH_2Cl_2 eluent) followed by precipitation from CH_2Cl_2/MeOH yielding **14** (11.21g, 1.83mmol, 75%) as a deep red solid. ^1H NMR ($CDCl_3$, δ): 0.89-0.93 (m, 12H), 1.38-1.43 (m, 16H), 1.49-1.60 (m, 8H), 1.95 (m, 8H), 4.22-4.26 (m, 8H), 6.84 (s, 2H), 7.72 (s, 2H), 8.93 (s, 2H). ^{13}C NMR ($CDCl_3$): 14.37, 22.95, 26.10, 29.33, 29.40, 31.93, 68.99, 69.28, 104.07, 109.58, 122.38, 126.87, 129.00, 137.87, 150.73, 151.21, 189.59. IR (KBr): 2954, 2928, 2856, 1647, 1614, 1531, 1510, 1461, 1438, 1382, 1265, 1160, 1086. HRMS-ESI (*m/z*): $(M+H)^+$ calcd for $C_{42}H_{58}O_6$ 659.4306, found 659.4331.

6,7,10,11-Tetra(octyloxy)triphenylene-1,4-dione (15). Preparation same as for **14**. Quantities: **9** (18.46 g, 23.04 mmol), cerium (IV) ammonium nitrate (26.53 g, 48.39 mmol). **15** (13.67 g, 17.73 mmol, 77%) was isolated as a deep red solid. ^1H NMR ($CDCl_3$, δ): 0.89-0.93 (m, 12H), 1.32-1.43 (m, 32H), 1.49-1.62 (8H), 1.95-1.98(8H), 4.22- 4.25 (8H), 6.82 (s, 2H), 7.68 (s, 2H), 8.91 (s, 2H). ^{13}C NMR ($CDCl_3$, δ): 14.11, 14.12, 22.68, 22.69, 26.13, 29.07, 29.15, 29.32, 29.45, 31.83, 31.84, 68.71, 68.99, 103.81, 109.35, 122.17, 126.60, 128.80, 137.67, 150.57, 151.04, 189.48. IR (KBr): 2953, 2923, 2851, 1653, 1613, 1528, 1510, 1463, 1382, 1266, 1186, 1158, 1083, 872, 823.

6,7,10,11-Tetra(decyloxy)triphenylene-1,4-dione (16). Preparation same as for **14**. ^1H NMR ($CDCl_3$, δ): 0.89-0.93 (m, 12H), 1.32-1.43 (m, 48H), 1.49-1.62 (8H), 1.95-1.98(8H), 4.22-4.25 (8H), 6.82 (s, 2H), 7.68 (s, 2H), 8.91 (s, 2H). ^{13}C NMR ($CDCl_3$, δ): 14.33, 14.34, 22.92, 26.36, 26.37, 29.31, 29.40, 29.60, 29.71, 29.73, 29.77, 29.83,

29.89, 32.15, 32.16, 69.01, 69.31, 104.22, 109.73, 122.46, 126.93, 129.09, 137.94, 150.88, 151.35, 189.72. IR (KBr): 2953, 2971, 2850, 1645, 1613, 1509, 1465, 1437, 1383, 1264, 1158, 1082, 863, 824. HRMS-EI (*m/z*): $(M+H)^+$ calcd for $C_{58}H_{90}O_6$ 882.6737, found 882.6738.

6,7,10,11-Tetra(dodecyloxy)triphenylene-1,4-dione (17). Preparation same as for **14**. Quantities: **11** (0.795 g, 0.775 mmol), cerium (IV) ammonium nitrate (0.850 g, 1.55 mmol). **15** (0.594 g, 0.597 mmol, 77%) was isolated as a deep red solid. ^{1}H NMR ($CDCl_3$, δ): 0.90 (t, J = 6.6 Hz, 12H), 1.28-1.61 (m, 80H), 1.98 (m, 8H), 4.24 (t, J = 6.6 Hz, 4H), 4.28 (t, J = 6.6 Hz, 4H), 6.87 (s, 2H), 7.76 (s, 2H), 8.96 (s, 2H). ^{13}C NMR ($CDCl_3$, δ): 14.46, 23.01, 26.46, 29.37, 29.46, 29.69, 29.79, 29.81, 29.99, 30.04, 32.23, 69.01, 69.31, 104.12, 109.62, 122.38, 126.87, 129.01, 137.88, 150.75, 151.22, 189.58. IR (KBr): 2953, 2920, 2849, 1653, 1612, 1508, 1466, 1438, 1382, 1266, 1164, 1083. HRMS-ESI (*m/z*): $(M+H)^+$ calcd for $C_{66}H_{106}O_6$ 995.8062, found 995.8104.

6,7,10,11-Tetra(2-ethylhexyl)triphenylene-1,4-dione (18). Synthesis and characterization previously described. [12]

6,10-Dimethoxy-7,11-bis(2-ethylhexaloxy)triphenylene-1,4-dione (19). Preparation same as for 14. Quantities: **13** (1.82 g, 3.0 mmol), cerium (IV) ammonium nitrate (3.29 g, 6.0 mmol). **15** (1.31 g, 76%) was isolated as a deep red solid. ^{1}H NMR ($CDCl_3$, δ): 0.92 (t, J = 7.2 Hz, 6H), 1.02 (t, J = 7.2 Hz, 6H), 1.25-1.66 (m, 16H), 1.98 (m, J = 6.0 Hz, 2H), 4.07 (s, 6H), 4.18 (d, J = 6.0 Hz, 4H), 6.87 (s, 2H), 7.75 (s, 2H), 8.97 (s, 2H). ^{13}C NMR ($CDCl_3$, δ): 11.54, 14.41, 23.36, 24.12, 29.32, 30.90, 39.27, 56.14, 71.89, 103.57, 108.59, 122.23, 126.68, 129.01, 137.80, 151.08, 151.21, 189.48. IR (KBr): 2958,

2930, 2872, 2861, 1638, 1615, 1522, 1508, 1463, 1421, 1382, 1263, 1151, 1081, 868. HRMS-ESI (*m/z*): $(M+H)^+$ calcd for $C_{36}H_{46}O_6$ 575.3367, found 575.3388.

6,7,10,11-Tetra(octyloxy)triphenylene-1,4-dihydroquinone (20). A solution of $Na_2S_2O_4$ (200mg, 1.15mmol) in 5mL H_2O was added to a solution of **15** (104 mg, 0.135mmol) in 35mL Et_2O. After one hour of vigorous stirring at room temperature, the deep red color of the ether layer had disappeared and was replaced by a pale yellow color. The solution was stirred for one additional hour and then the ether was removed in vacuo. The remaining white solid precipitate was collected by vacuum filtration, washed with water and dried under high vacuum overnight, yielding **20** (102mg, 98%). ^{1}H NMR ($CDCl_3$, δ): 0.87-0.93 (m, 12H), 1.23-1.44 (m, 32H), 1.48-1.58 (m, 8H), 1.87-1.95 (m, 8H), 4.17 (t, J = 6.8, 4H), 4.21 (t, J = 6.8, 4H), 5.42 (s, 2H), 6.82 (s, 2H), 7.79 (s, 2H), 9.11 (s, 2H). ^{13}C NMR ($CDCl_3$, δ): 14.12, 22.68, 26.15, 29.27, 29.33, 29.36, 29.45, 29.48, 31.84, 69.08, 69.49, 106.64, 112.59, 113.37, 120.40, 123.23, 125.27, 147.42, 147.68, 148.50. IR (KBr): 3288, 2952, 2923, 2850, 1611, 1519, 1466, 1419, 1386, 1268, 1238, 1191, 1168, 1093, 1065. HRMS-ESI (*m/z*): $(M+Na)^+$ calcd for $C_{50}H_{76}O_6$ 795.5534, found 795.5521.

References:

(1) (a) Chandrasekhar, S.; Sadashiva, B.K.; Suresh, K.A. *Pramana* **1977**, *9*, 471. (b) Cammidge, A.N.; Bushby, R.J. in *Handbook of Liquid Crystals* Demus, D. (c) Goodby, J; Gray, G.W.; Spiess, H.-W.; Vill, V., Ed.; Wiley-VCH: Weinheim, 1998; Vol. 2B, p693-720.

(2) Nguyen, H.; Destrade, C.; Malthête, J. *Adv. Mater.* **1997**, *9*, 375-388 and references therein.

(3) (a) Kishikawa, K.; Harris, M.C.; Swager, T.M. *Chem. Mater.* **1999**, *11*, 867-871. (b) Levitsky, I.A.; Kishikawa, K.; Eichhorn, S.H.; Swager, T.M. *J. Am. Chem. Soc.* **2000**, *122*, 2474-2479.

(4) (a) Lai. C.K; Serrette, A.G.; Swager, T.M. *J. Am. Chem. Soc.* **1992**, *114*, 7948-7949. (b) Zheng, H.; Lai, C.K.; Swager, T.M. *Chem. Mater.* **1994**, *6*, 101-103. (c) Serrette, A.G.; Lai, C.K.; Swager, T.M. *Chem. Mater.* **1994**, *6*, 2252-2268. (d) Zheng, H.; Lai, C.K.; Swager, T.M. *Chem. Mater.* **1995**, *7*, 2067-2077. (e) Zheng, H.; Xu, B.; Swager, T.M. *Chem. Mat.* **1996**, *8*, 907-911. (f) Trzaska, S.T.; Swager T.M. *Chem. Mater.* **1998**, *10*, 438-443. (g) Trzaska, S.T.; Zheng, H.; Swager, T.M. *Chem. Mater.* **1999**, *11*, 130-134.

(5) (a) Zheng, H.; Swager, T.M. *J. Am. Chem. Soc.* **1994**, *116*, 761-762. (b) Zheng, H.; Swager, T.M. *Mol. Cryst. Liq. Cryst.* **1995**, *260*, 301-306. (c) Trzaska, S.T.; Hsu, H.; Swager, T.M. *J. Am. Chem. Soc.*, **1999**, *121*, 4518-4519.

(6) Hegmann, T.; Neumann, B.; Kain, J.; Diele, S.; Tschierske, C. *J. Mater. Chem.* **2000**, *10,* 2244-2248.

(7) Hegmann, T.; Peidis, F.; Diele, S.; Tschierske, C. *Liq. Cryst.* **2000**, *27*, 1261-1265.

(8) (a) Kato, T.; Mizoshita, N.; Kanie, K. *Macromol. Rapid Commun.* **2001**, *22*, 797-814. (b) Kato, T. in *Handbook of Liquid Crystals* Demus, D.; Goodby, J; Gray, G.W.; Spiess, H.-W.; Vill, V., Ed.; Wiley-VCH: Weinheim, 1998; Vol. 2B, 969-979.

(9) (a) Serrette, A. G., Swager, T.M. *J. Am. Chem. Soc.* **1993**, *115*, 8879-8880. (b) Serrette, A.; Swager, T.M. *Angew. Chem. Int. Ed. Engl.* **1994**, *33*, 2342-2345.

(10) (a) Plehnert, R.; Schröter, J.A.; Tschierske, C. *J. Mater. Chem.* **1998**, *8*, 2611-2626. (b) Tschierske, C. *J. Mater. Chem.* **1998**, *8*, 1485-1508. (c) Pegenau, A.; Hegmann, T.; Tschierske, C.; Diele, S. *Chem. Eur. J.* **1999**, *5*, 1643-1660. (d) Tschierske, C. *J. Mater. Chem.* **2001**, *11*, 2647-2671.

(11) (a) Omenat, A.; Barberá, J.; Serrano, J.L.; Houbrechts, S.; Persoons, A. *Adv. Mater.* **1999**, *11*, 1292-1295. (b) Kishikawa, K.; Furusawa, S.; Yamaki, T.; Kohmoto, S; Tamamoto, M; Yamaguchi, K. *J. Am. Chem. Soc.* **2002**, *8*, 1597-1605. (c) Paraskos, A.J.; Swager, T.M. *Chem. Mater.* **2002**, *14*, 4523-4549. (d) Eichhorn, S.H.; Paraskos, A.J.; Swager, T.M. *J. Am. Chem. Soc.*, **2002**, *124*, 12742-12751.

(12) (a) Rose, A.; Lugmair, C.G.; Swager, T.M. *J. Am.Chem. Soc.* **2001**, *123*, 11298-11299.

(13) (a) Weck, M.; Mohr, B.; Maughon, B.R.; Grubbs, R.H. *Macromolecules* **1997**, *30*, 6430-6437. (b) Bacher, A.; Erdelen, C.H.; Paulus, W.; Ringsdorf, H.; Schmidt, H.W.; Schuhmacher, P. *Macromolecules*, **1999**, *32*, 4551.

(14) (a) Levitsky, I.A.; Kishikawa, K.; Eichhorn, S.H.; Swager, T.M. *J. Am.. Chem. Soc.* **2000**, *11*, 2474-2479. (b) Trzaska, S.T.; Swager, T.M. *Chem. Mater.* **1998**, *10*, 438-443. (c) Zheng, H.; Xu, B.; Swager, T.M. *Chem. Mater.* **1996**, *8*, 907-911. (d) Zheng, H.; Lai, C.K.; Swager, T.M. *Chem. Mater.* **1994**, *6*, 101-103.

(15) Kishikawa, K.; Furusawa, S.; Yamaki, T.; Kohmoto, S; Tamamoto, M; Yamaguchi, K. *J. Am. Chem. Soc.* **2002**, *8*, 1597-1605.

Chapter 5

Thiophene-Based Extended Aromatics

Introduction

The assembly of disc-shaped molecules into columnar liquid-crystalline structures was first observed in the late 1970's. The prototypical discotic mesogen consists of a disc-shaped aromatic core with several pendant sidechains about the periphery (see Chapter 1 and Chapter 4). The π-π interactions between neighboring molecules in combination with the repulsive effect of the dynamic aliphatic sidechains drives the stacking of the mesogens and organization into columnar structures. The parameters leading to discotic behavior are not entirely understood, however, as evidenced by recent reports of indenes and pseudoazulenes without sidechains which display columnar mesophases (Figure 1).[1]

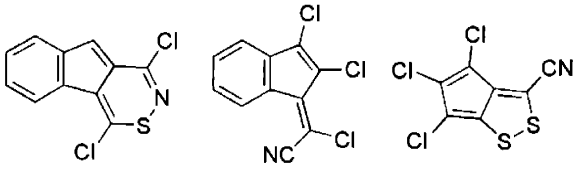

Figure 1. Columnar liquid crystalline indenes and pseudoazulenes. The molecules possess neither strict disc-shapes nor aliphatic sidechains.

Columnar liquid crystals have been shown to display high uniaxial conductivity through the stacks of aromatic cores; for example, hexahexylthiotriptycene has been shown to exhibit photoinduced conductivities (hole mobilities) of up to 0.1 $cm^2\ V^{-1}\ s^{-1}$ in the stacking direction. [2] Other discotics exhibit large conductivities upon chemical doping, for example with $AlCl_3$ and similar oxidants.[3] To achieve higher charge mobilities it appears that larger aromatic cores[4] as well as longer flexible sidechains[5] are beneficial, presumably by increasing the stacking order and overlap of adjacent molecular

π orbitals within the individual columns.[6] For this reason, extended aromatic discogens are targets for the design of electronic liquid crystals.

In the course other chemistries under development in the Swager laboratories, it became clear that we had the ability to synthesize two unique sets of extended aromatic discogens based on either a benzene or thiophene core (Figure 2). While we were working on this project the synthesis and phase-behavior of the benzene-based discogens were described by researchers at another institution; as such, they are only briefly covered here.[7] The thiophene-based molecules were not described, however, and their syntheses and phases behaviors are discussed in this chapter.

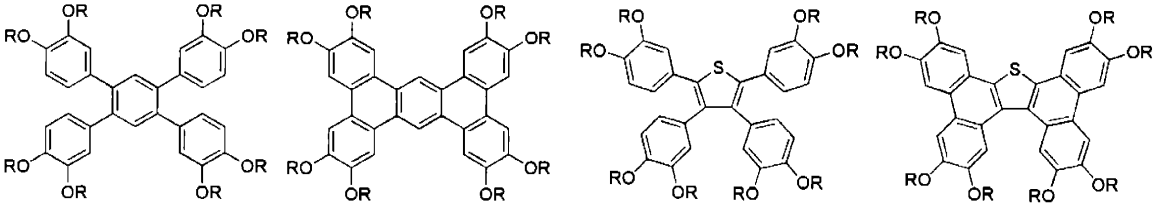

Figure 2. Architectures of the extended benzene-core (left) and thiophene-core (right) discogens described in this chapter.

While this work was in progress, former Swager group member J. D. Tovar was concurrently involved in the synthesis, oxidative cyclization and polymerization of a number of extended aromatic systems (though not liquid crystals) based on benzene and thiophene aromatic units (Figure 3).[8] J. D. found that these extended aromatics displayed interesting electronic behavior. This chapter will also detail our efforts synthesizing and studying the electrochemical behavior of a number of terthiophene derivatives that are structurally similar to those studied by J. D. (Figure 4).

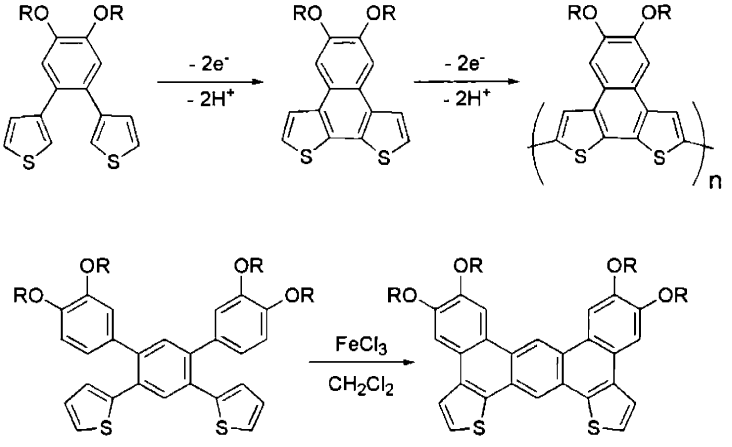

Figure 3. Some of the extended aromatic molecules and polymers investigated by former Swager graduate student J. D. Tovar.

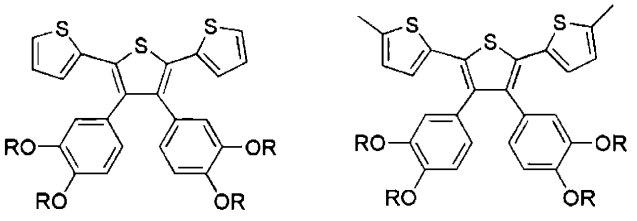

Figure 4. Terthiophene derivatives to be discussed in this chapter.

Results and Discussion

Synthesis

Our previously described investigations into thiophene-based liquid crystals (Chapters 2 and 3) focused on bent-rod type systems. This chapter describes our efforts investigating thiophene-based discotic systems. Palladium catalyzed cross-coupling (Suzuki type) of tetrabromothiophene with 4 equivalents of the appropriate 3,4-di(alkoxy)phenyl boronic acid affords the tetrakis(3,4-dialkoxybenzene)thiophenes **1** and **2** in moderate yield. The limitation of this reaction seems to be the coupling of the fourth phenyl ring to the thiophene, as a mixture of trisubstituted and tetrasubstituted compounds was always obtained, despite the investigation of many conditions for the coupling. Oxidation of compounds **1** or **2** with either $FeCl_3$, $NOSbF_6$, or $SbCl_5$ results in cyclization through a fusing of the pendant rings at the 2 and 3 positions and 4 and 5 positions of the thiophene ring, respectively (Scheme 1).

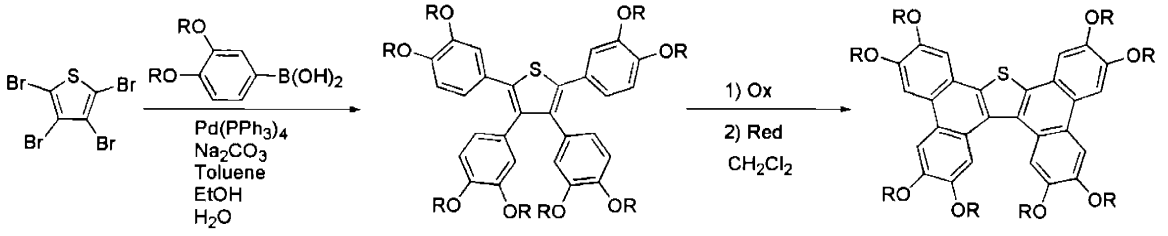

1 R = C_8H_{17} (89%)
2 R = CH_3 (56%)

3 R = C_8H_{17} (77%)
4 R = CH_3 (80%)

Scheme 1. Synthesis of thiophene-based extended aromatic discogens. In the second synthetic step, the oxidant (Ox) can be $FeCl_3$, $NOSbF_6$, or $SbCl_5$, and the reductant (Red) can be dry MeOH or hydrazine.

We were also able to synthesize entirely aromatic analogues by analogous procedures, as illustrated in Scheme 2. Suzuki coupling of phenyl boronic acid with

tetrabromothiophene yields tetraphenylthiophene **5**, which can then be cyclized with antimony (V) chloride to give the extended aromatic **6**.

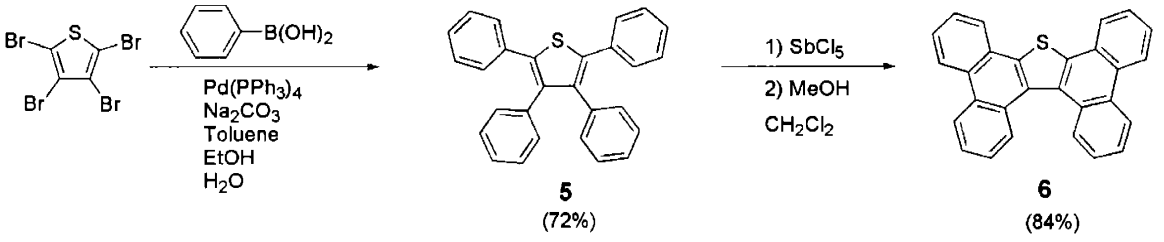

Scheme 2. Synthesis of extended aromatics **5** and **6**.

Stille-type palladium-catalyzed coupling of 2 equivalents of 2-tributylstannyl thiophene with tetrabromothiophene occurs selectively at the 2 and 5 positions of the thiophene ring, yielding the terthiophene derivative **7** in moderate yield (Scheme 3). It should be noted, however, that this step was not optimized and higher yields of **7** may be obtainable through this route. Suzuki coupling of **7** with the appropriate 3,4-dialkoxyphenyl boronic acids then affords compounds **8** and **9** in good yields. Through an analogous route starting with 5-methyl-2-tributylstannyl thiophene we were able to make the 5-methyl terthiophene derivates **10**, **11** and **12**.

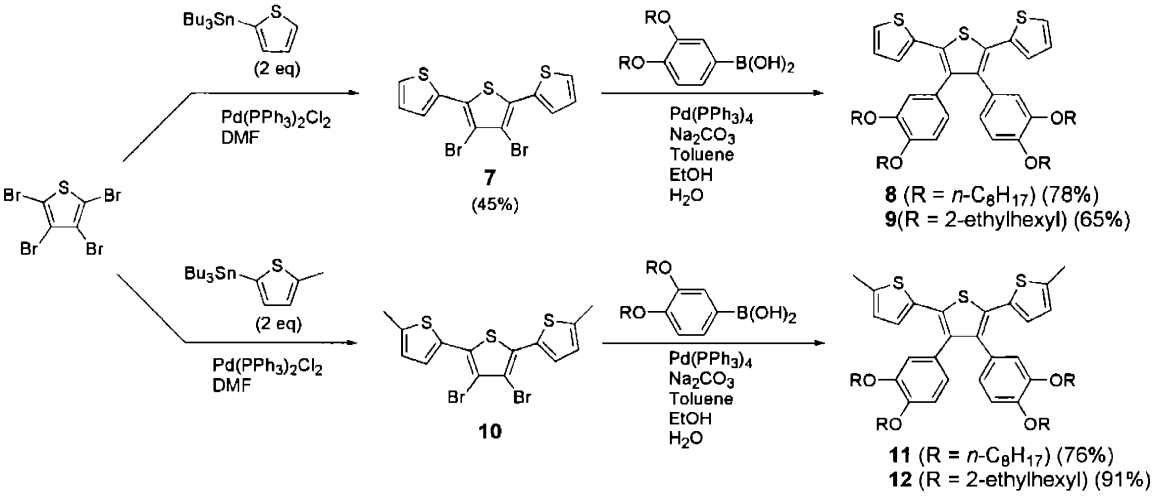

Scheme 3. Synthesis of terthiophene-derivatives **7-12**.

Phase Behavior

The phase behavior of compounds **1-6** is summarized in Table 1.

Table 1. Phase behavior of compounds **1-6**. P = plastic phase, Col_h = columnar hexagonal mesophase, K = crystal phase and I = isotropic liquid.

Compound	Phase Behavior
1	$P \underset{}{\overset{29.6\ (6.7)}{\rightleftharpoons}} Col_h \underset{30.3\ (-6.5)}{\overset{34.0\ (6.3)}{\rightleftharpoons}} I$
2	$K \underset{146.0\ (-70.4)}{\overset{209.2\ (71.6)}{\rightleftharpoons}} I$
3	$K \underset{50.4\ (-58.2)}{\overset{89.0(58.8)}{\rightleftharpoons}} Col_h \underset{116.0\ (-6.5)}{\overset{120.5\ (5.8)}{\rightleftharpoons}} I$
4	336.3 (Decomposes)
5	$K \underset{114.0\ (-22.2)}{\overset{184.5\ (27.4)}{\rightleftharpoons}} I$
6	309.9 (Decomposes)

Uncyclized tetrakis-(3,4-dioctyloxyphenyl)thiophene (compound **1**) is a waxy solid which displays a columnar hexagonal mesophase at just above room temperature. By comparision, tetrakis-(3,4-dimethyloxyphenyl)thiophene **2** melts at much higher

temperatures (209 °C) and is not liquid crystalline. This is not entirely unexpected, as the longer aliphatic sidechains of compound **1** provide the repulsive dynamic motion necessary for lower melting points as well as the organizational drive to form columns. Removal of the alkoxy groups entirely (compound **5**) results in a material with a slightly lower melting point (184 °C) than that of compound **2**, but no liquid crystalline behavior is displayed.

The cyclized compounds **3**, **4**, and **6** uniformly have higher melting points than those of their uncyclized analogues. Compound **3** displays a broad columnar hexagonal mesophase at reasonably low temperatures, though higher than that of uncyclized compound **1**. When viewed by polarized microscopy sandwiched between glass slides, compound **3** tends to display large pseudoisotropic (dark) domains, in which the columns are oriented perpendicular to the surfaces of the slides (Figure 5). Variable temperature X-ray diffraction of compound **3** is shown in Figure 6. Cyclized octa-methoxy compound **4** has an extremely high melting point (336 °C) and decomposition occurs concurrently with melting. Similarly, cyclized compound **6**, which does not possess sidechains, tends to decompose with melting (310 °C).

Figure 5. Polarized micrograph of the Col_h phase of **3** (114.9 °C, 100x). The dark (pseudoisotropic) regions are areas where the columns are oriented perpendicular to the glass slide. The long needle-like regions are areas where the columns are laying more or less parallel to the slide surfaces.

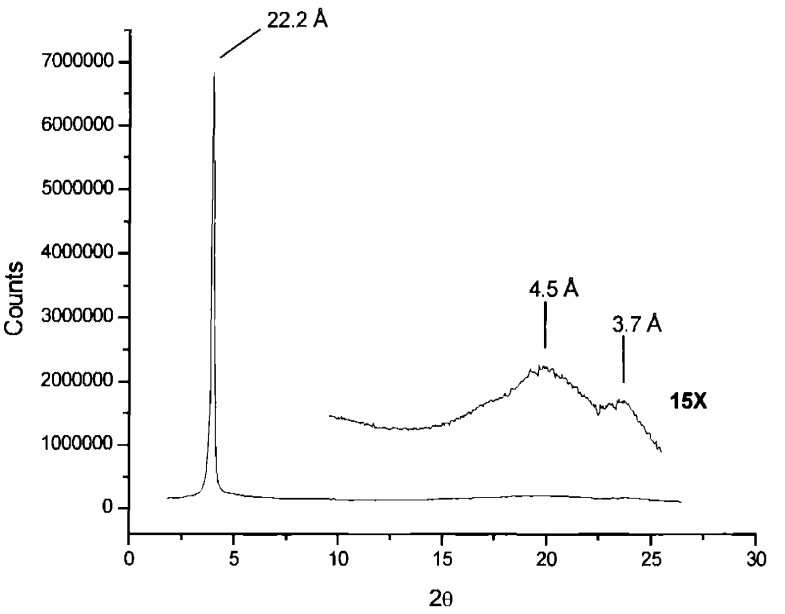

Figure 6. Powder X-ray diffraction pattern (2-D) of the Col_h phase of compound **3**.

Electrochemistry

Cyclic voltammetry (CV) provides one method for the growth and study of electronically active polymers.[9] The technique involves measuring the current of a solution while applying a changing potential over time between two electrodes (working electrode and counter electrode) relative to a reference electrode with a known redox couple. Any increase in current signals the removal of electrons from the system, indicating the oxidation of molecules near the working electrode. During the reverse scan (assuming that the material survives the oxidative event) electrons are returned to the material, and a reductive wave is observed. If an irreversible chemical event occurs during upon oxidation, however, a reductive wave may not be seen.

Thiophene-containing monomers will often undergo electrochemical polymerization. This formation of an electronically conductive polymer often occurs with polymer growth upon the electrode surface. A typical characteristic is increased electroactivity in subsequent scans, as the conducting polymer film effectively increases the surface area of the working electrode.

The electrochemistry (current vs. voltage) of uncyclized and cyclized liquid crystalline compounds **1** and **3** are shown in Figure 6. Both display two separate oxidation waves at positive potentials, revealing the potentials necessary to remove one electron (yielding the radical cation $\mathbf{1}^{\cdot+}$) and then a second electron (yielding the dication $\mathbf{1}^{++}$). Compound **1** exhibits oxidation waves at 0.81 volts and 1.01 volts, and reduction waves at 0.94 volts and 0.62 volts, but the electrochemistry clearly changes upon subsequent scans. Compound **3** exhibits oxidation waves at 0.75 volts and 1.08 volts, and reduction waves at 0.93 volts and 0.61 volts, and remains stable with subsequent cycles.

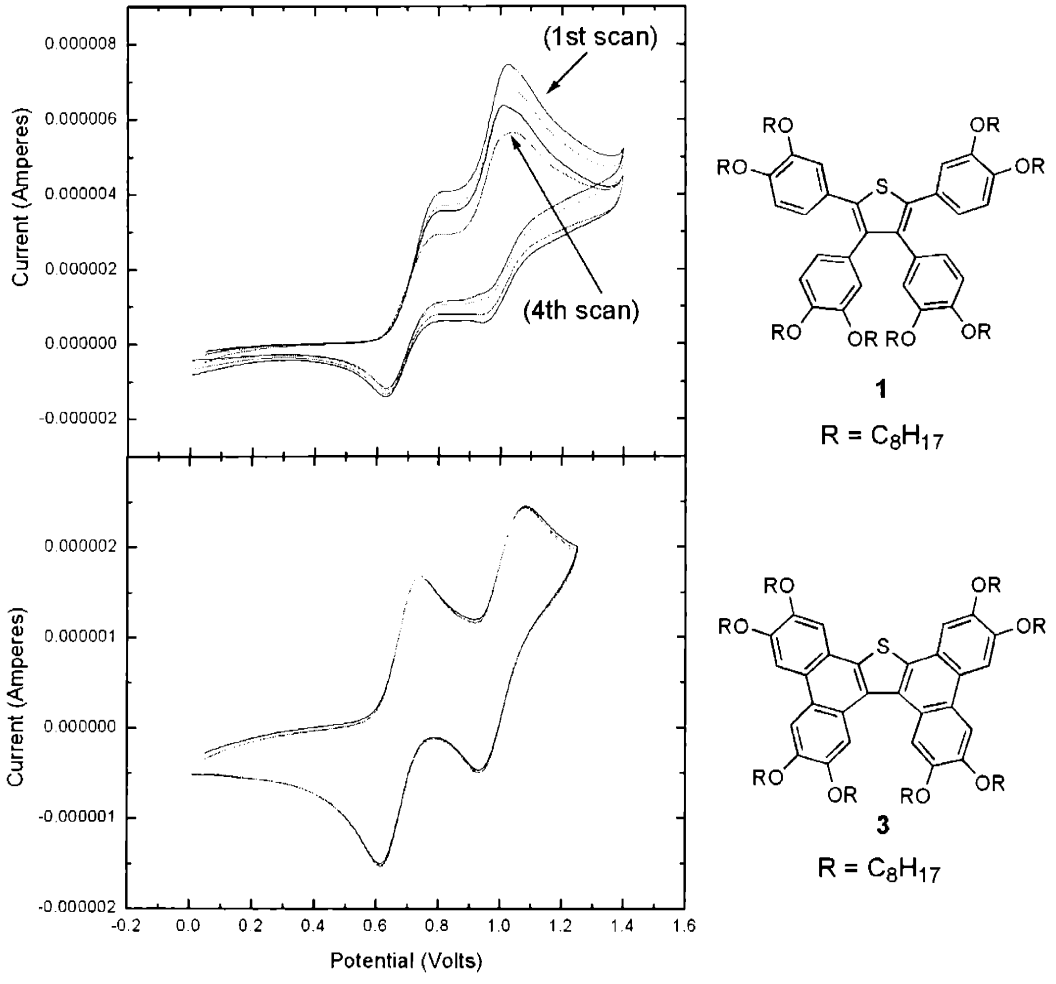

Figure 6. E-chem of uncyclized compound **1** (top) and cyclized compound **3** (bottom). Conditions: 2 mm^2 Pt button electrode in 0.1 M *n*-Bu_4NPF (CH_2Cl_2) cycled at 100mV/s. $E_{1/2}$ (Fc/Fc^+): +0.216V.

The higher voltage oxidation wave of compound **1** appears to consist of two separate peaks in the first scans, one at 1.01 volts and one at 1.05 volts. The definition between these peaks is lost as the electrochemical characteristics change with subsequent scans. This may be due to irreversible electrochemical cyclization reactions of compound **1** to form the half cyclized product as well as the fully cyclized product

compound **3**, which then begins to increase in concentration at the electrode surface (see Figure 7). Indeed, this would explain change in the CV upon multiple scans of compound **1**.

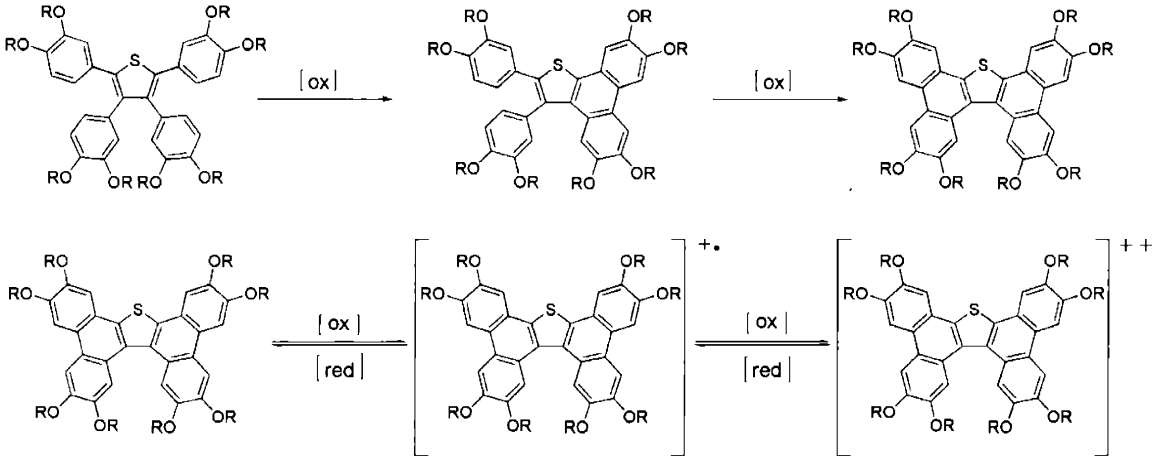

Figure 7. Electrochemical cyclization of compound **1** to compound **3** is followed by subsequent reversible oxidative and reductive events.

To investigate the chemistry of compound **1** further, CVs were run in which the scan rate was increased substantially. If the irreversible cyclization reactions are fast, then at higher scan rates we should observe an increase in the concentration of the half cyclized compound and fully cyclized compound **3** at the elecrode, as we allow less time for these species to diffuse away from the surface. If, on the other hand, the cyclization reactions are relatively slow, we may see only the elecroactivity of compound **1** because it will be reduced to its neutral state prior to cyclization. Figure 8 shows the CV of compound **1** at a scan rate of 1.0 V/s (ten times faster than in Figure 6). The oxidation

and reduction peaks do not seem to change potential with time, suggesting that the cyclization process is slow relative to the scan rate.

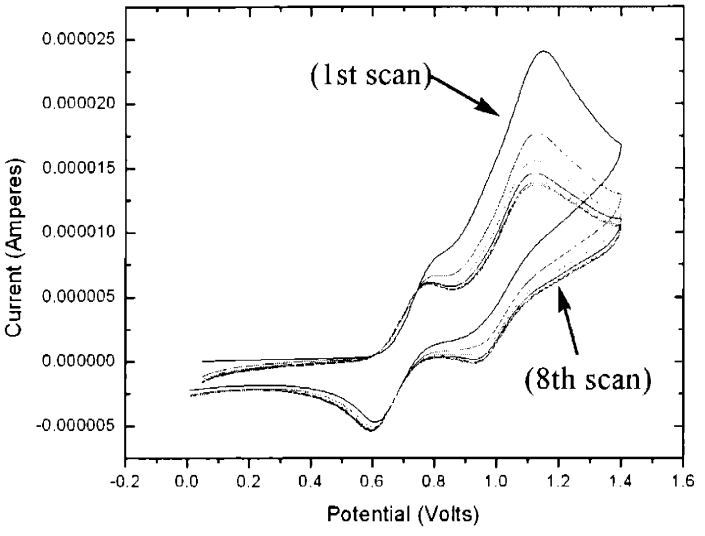

Figure 8. Fast scan e-chem of uncyclized compound **1** (1.0 V/s). The CV begins to resemble that of compound **3** after multiple cycles. Conditions: 2 mm^2 Pt button electrode in 0.1 M *n*-Bu_4NPF (CH_2Cl_2) cycled at 1.0 V/s. $E_{1/2}$ (Fc/Fc^+): +0.216V.

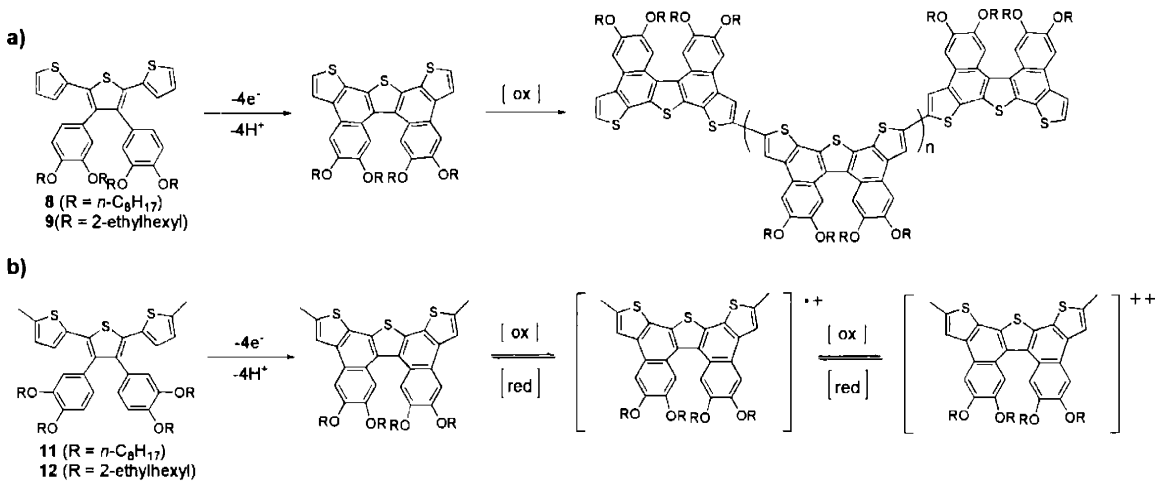

Figure 9. Possible electrochemical paths of (a) polymerizable and (b) methyl-blocked terthiophene derivatives.

The electrochemistry of terthiophene compounds **8**, **9**, **11** and **12** were interesting, but did not give well-behaved electroactive films. It was anticipated that compounds **8** and **9** would be able to undergo both cyclization and polymerization through the 2,2' positions of the pendant thiophene rings (Figure 9). However, no significant film growth was observed by cyclic voltammetry, perhaps due to the extreme delocalization and stabilization of the radical anion species that results upon oxidation (Figure 10). This may prevent polymerization by rendering the material at the electrode unreactive.

Compound **9** clearly undergoes a reaction upon oxidation, which produces new oxidation peaks at 0.61 volts and 0.86 volts and reduction peaks at 0.64 and 0.46 volts. The hysteresis between the oxidation and reduction peaks suggests that species with low conductivity is generated on the surface, partially blocking the electrode and reducing the electroactivity with subsequent cycles. Compound **12** exhibits oxidation peaks at 0.71 volts and 1.19 volts, but only one reductive peak is visible at 0.59 volts. This behavior

may be evidence of an irreversible electrochemical cyclization during the higher oxidative event at 1.19 volts. However, attempts to clarify these events by scan-rate dependence did not give conclusive results.

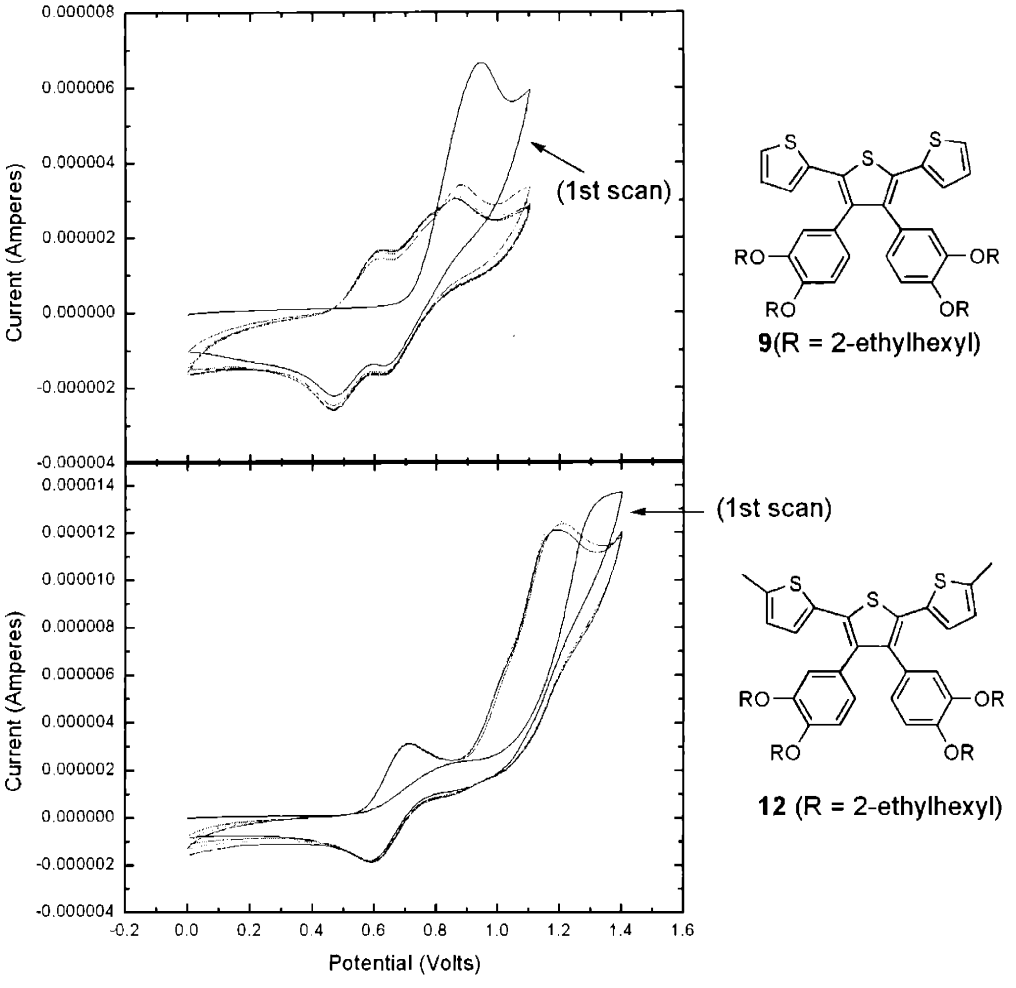

Figure 10. Electrochemistry of terthiophene compounds **9** and **12**. Conditions: 2 mm^2 Pt button electrode in 0.1 M *n*-Bu_4NPF (CH_2Cl_2) cycled at 1.0 V/s. $E_{1/2}$ (Fc/Fc^+): +0.281V.

Summary and Conclusions

A variety of thiophene-based extended aromatic systems were explored. While Tetrakis-(3,4-dioctyloxyphenyl)thiophene **1** and its chemically cyclized analogue **3** display hexagonal columnar phases, similar compounds with short sidechains, as well as those without any sidechains, were not liquid crystalline. Terthiophene compounds **8**, **9**, **11** and **12** were expected to be electrochemically polymerizable, but upon investigation no such polymerization was observed. This observation might be attributed to the extremely delocalized nature of the oxidized species, making them relatively unreactive toward polymerization.

Experimental Section

General: Dichloromethane was dried by passing through activated alumina columns. Anhydrous methanol was purchased from Aldrich (sure-seal) and stored over activated molecular sieves before use. All other chemicals were of reagent grade and were used without further purification. Air and water sensitive reactions employed standard Schlenk techniques under argon atmosphere. NMR spectra were obtained on Varian Mercury-300, Bruker DPX-400 or Varian Inova-500 spectrometers. All chemical shifts are referenced to residual $CHCl_3$ (7.27 ppm for ^1H, 77.0 ppm for ^{13}C). Multiplicities are indicated as s (singlet), d (doublet), t (triplet), and m (multiplet). High resolution mass spectra were obtained at the MIT Department of Chemistry Instrumentation facility (DCIF) on a Finnigan MAT 8200 or on a Bruker Daltonics Apex II 3T FT-ICR MS. Infrared spectra were recorded on a Nicolet Impact 410 in KBr pellets. DSC investigations were carried out on a Perkin-Elmer DSC-7. Optical microscopy was carried out on a Leica polarizing microscope in combination with a Linkam LTS350

hotstage. X-ray diffraction studies were carried out on samples in capillary tubes with an INEL diffractometer with a 2 kW CU K_α X-ray source fitted with an INEL CPS-120 position-sensitive detector. The detectors were calibrated using a silver behenate standard produced by Eastman Kodak.

Tetrakis-(3,4-dioctyloxyphenyl)thiophene (1) Tetrabromothiophene (106mg, 0.265 mmol) was placed in a 25 mL Schlenk flask with 3,4-dioctyloxyphenyl boronic acid (501mg, 1.33 mmol), $Ph(PPh_3)_4$ (15.3 mg, 0.0133mmol), Na_2CO_3 (281 mg, 2.65 mmol) and a magnetic stir bar. The flask was evacuated and backfilled with argon. Toluene (10 mL), EtOH (2 mL) and water (1.5 mL) were purged with argon for 20 minutes and then added to the reaction flask via cannula. The reaction was heated to 90 °C with stirring for 18 hours, after which it was cooled to room temperature and water (20 mL) was added. The aqueous phase was extracted with EtOAc (20 mL) and the combined organic solutions were dried over magnesium sulfate and concentrated in vacuo. The remaining dark oil was purified by silica gel chromatography with 2:1 hexanes:$CHCl_3$ eluent yielding **X** (329 mg, 89%) as a waxy solid. ^{1}H NMR ($CDCl_3$, δ): 0.86-0.91 (m, 24H, CH_3), 1.24-1.39 (m, 72H), 1.55-1.68 (m, 8H), 1.74-1.83 (m, 8H), 3.60 (t, 4H, J = 6.5 Hz, -CH_2O-), 3.66 (t, 4H, J = 6.5 Hz, -CH_2O-), 3.89 (t, 4H, J = 6.5 Hz, -CH_2O-), 3.96 (t, 4H, J = 6.5 Hz, -CH_2O-), 6.50-6.53 (m, 4H, Ar-H), 6.62-6.65 (m, 2H, Ar-H), 6.70-6.75 (m, 4H, Ar-H), 6.84-6.87 (m, 2H, Ar-H). ^{13}C NMR ($CDCl_3$, δ): 14.09, 22.66, 22.67, 22.68, 25.95, 25.98, 26.00, 26.05, 28.98, 29.04, 29.24, 29.26, 29.28, 29.30, 29.35, 29.36, 29.38, 29.45, 31.80, 31.83, 68.73, 68.94, 68.99, 69.03, 112.91, 113.09, 114.43, 116.55, 121.28, 123.26,

127.15, 129.46, 137.13, 138.48, 147.66, 148.14, 148.25, 148.34. HRMS-EI (*m/z*): (M^+) calcd for $C_{92}H_{148}O_8S$ 1436.0787; found 1436.0749.

Tetrakis-(3,4-dimethoxyphenyl)thiophene (2) Tetrabromothiophene (1.50 g, 3.76 mmol) was placed in a 500 mL Schlenk flask with 3,4-dimethoxyphenyl boronic acid (3.76 g, 20.7 mmol), $Ph(PPh_3)_4$ (250 mg, 0.22 mmol), Na_2CO_3 (3.18 g, 30.0 mmol) and a magnetic stir bar. The flask was evacuated and backfilled with argon. Toluene (250 mL), EtOH (50 mL) and water (30 mL) were purged with argon for 20 minutes and then added to the reaction flask via cannula. The reaction was heated to 80 °C with stirring for 72 hours and then was cooled to room temperature, diluted with Et_2O (150 mL), washed with water (150 mL) and dried over magnesium sulfate. The solvents were removed in vacuo and the remaining solids were purified silica gel chromatography with 100:1 CH_2Cl_2/MeOH eluent. The purer fractions were then recrystallized from MeOH with a minimal amount of CH_2Cl_2, yielding **X** (1.329 g, 2.11 mmol, 56%) as a slightly off-white crystalline powder. ^1H NMR ($CDCl_3$, δ): 3.53 (s, 6H, CH_3O), 3.60 (s, 6H, CH_3O), 3.83 (s, 6H, CH_3O), 3.87 (s, 6H, CH_3O), 6.52 (d, 2H, J = 1.8 Hz, Ar-H), 6.59 (dd, 2H, J_1 = 8.4 Hz, J_2 = 1.8 Hz, Ar-H), 6.69 (d, 2H, J = 8.4 Hz, Ar-H), 6.74 (d, 2H, J = 1.8 Hz, Ar-H), 6.78 (d, 2H, J = 8.4 Hz, Ar-H), 6.92 (dd, 2H, J_1 = 8.4 Hz, J_2 = 1.8 Hz, Ar-H).

^{13}C NMR ($CDCl_3$, δ): 55.50, 55.67, 55.74, 55.79, 110.65, 110.88, 112.26, 114.14, 121.37, 123.25, 127.02, 129.31, 137.31, 138.42, 147.61, 148.20, 148.27, 148.32. HRMS-ESI (*m/z*): (M^+) calcd for $C_{36}H_{36}O_8S$ 628.2125; found 628.2155.

Octakis(octyloxy)tetraphenyldibenzothiophene (3) Tetrakis-(3,4-dioctyloxyphenyl)thiophene **(1)** (561 mg, 0.397 mmol) was placed in a flask, which was then evacuated and backfilled with argon. Dry CH_2Cl_2 (20 mL) was added via syringe.

In a separate 100 mL Schlenk flask placed $FeCl_3$ (643 mg, 3.97 mmol) and evacuted, backfilling with argon. Dry CH_2Cl_2 (50 mL) was added to the flask with $FeCl_3$ via syringe, and the flask was cooled with a water/ice bath. The solution of **1** was added to the suspension of $FeCl_3$ via cannula with vigorous stirring and cooling. The mixture became a deep purple color, and as soon as the addition was complete, argon was bubbled through the reaction mixture as it was allowed to warm to room temperature. The reaction stirred for 30 minutes and dry MeOH (30 mL) was added via syringe, the color disappeared and a yellowish precipitate formed. The precipitate was collected and precipitated repeatedly from CH_2Cl_2 by adding MeOH yielding **3** (432 mg, 0.306 mmol, 77%) as a slightly off-white solid. ^{1}H NMR ($CDCl_3$, δ): 0.86-0.94 (m, 24H, CH_3O), 1.21-1.49 (m, 68H), 1.56-1.64 (m, 12H), 1.75-1.80 (m, 4H), 1.94- 2.02 (m, 12H), 3.84 (br, 4H), 4.06 (br, 4H), 4.24-4.34 (m, 12H), 7.54 (s, 2H, Ar-H), 7.95 (s, 2H, Ar-H), 8.13 (s, 2H, Ar-H). ^{13}C NMR ($CDCl_3$, δ): 14.09, 22.68, 26.09, 26.13, 26.16, 29.25, 29.31, 29.34, 29.41, 29.48, 31.79, 31.84, 68.96, 69.03, 69.85, 69.96, 106.45, 106.92, 107.62, 110.58, 122.49, 123.51, 123.57, 124.24, 129.92, 134.33, 147.32, 148.14, 149.15, 149.51. HRMS-ESI (*m/z*): $(M+Na)^+$ calcd for $C_{92}H_{144}O_8S$ 1432.0474; found 1432.0444.

Octakis(methoxy)tetraphenyldibenzothiophene (4) Tetrakis-(3,4-dimethoxyphenyl)thiophene **(2)** (188 mg, 0.299 mmol) was placed in a 100 mL Schlenk flask with a magnetic stir bar. The flask was evacuated, backfilled with argon, and 50 mL of dry CH_2Cl_2 was added via syringe. The flask was cooled with a dry-ice/acetone bath and $SbCl_5$ (1.8 mL, 1.0 M in DCM, 1.8 mmol) was added dropwise via syringe, resulting in a deep purple color with the first drops followed by a green color with subsequent drops. The reaction was stirred at –78 °C for 2.5 hours and then dry, air-free

MeOH (30 mL) was added slowly via syringe. The cooling bath was removed and the reaction became much lighter in color with white precipitate. The stirring was continued at room temperature for 18 hours. Dichloromethane (50 mL) was added and the organics were washed with water (5 x 50 mL) and dried over magnesium sulfate. The solvents were removed in vacuo and the remaining solids were recrystallized from MeOH with a minimum volume of CH_2Cl_2 yielding **4** (150 mg, 239 mmol, 80%) as a slightly off-white crystalline solid. . ^{1}H NMR ($CDCl_3$, δ): 3.79 (s, 6H, CH_3O), 4.11 (s, 6H, , CH_3O), 4.18 (s, 12H, CH_3O), 7.38 (s, 2H, Ar-H), 7.82 (s, 2H, Ar-H), 7.83 (s, 2H, Ar-H), 8.01 (s, 2H, Ar-H). ^{13}C NMR ($CDCl_3$, δ): 55.80, 55.99, 56.01, 56.19, 103.82, 104.03, 104.74, 108.61, 122.18, 122.89, 123.37, 124.14, 129.57, 134.33, 146.56, 148.06, 149.20. HRMS-ESI (*m/z*): $(M+Na)^+$ calcd for $C_{36}H_{32}O_8S$ 647,1710; found 647.1690.

Tetraphenylthiophene (5) Tetrabromothiophene (1.79 g, 4.47 mmol) was placed in a 500 mL Schlenk flask with phenyl boronic acid (3.00 g, 24.6 mmol), $Ph(PPh_3)_4$ (258 mg, 0.22 mmol), Na_2CO_3 (3.8 g, 36 mmol) and a magnetic stir bar. The flask was evacuated and backfilled with argon. Toluene (250 mL), EtOH (50 mL) and water (30 mL) were degassed with purging argon for 20 minutes and then added to the reaction flask via cannula. The reaction was heated to reflux with stirring for 72 hours and then was cooled to room temperature, diluted with Et_2O (150 mL), washed with water (150 mL) and dried over magnesium sulfate. The solvents were removed in vacuo and the remaining solids were purified by silica gel chromatography with 2:1 hexanes/CH_2Cl_2 eluent and then recrystallized from hexanes with a minimal amount of CH_2Cl_2, yielding **X** (1.248 g, 3.218 mmol, 72%) as a slightly off-white crystalline powder. ^{1}H NMR ($CDCl_3$, δ): 6.97-6.99 (m, 4H), 7.11-7.15 (m, 6H), 7.21-7.26 (m, 10H). ^{13}C NMR ($CDCl_3$, δ): 126.58,

127.18, 127.81, 128.28, 129.19, 130.83, 134.22, 136.41, 138.53, 139.45. HRMS-ESI (*m/z*): $(M+H)^+$ calcd for $C_{36}H_{36}O_8S$ 389.1358; found 389.1345.

Cyclized Phenyl (6) Tetraphenylthiophene **5** (50 mg, 0.129 mmol) was placed in a 25 mL Schlenk tube with a magnetic stir bar. The flask was evacuated and backfilled with argon. Dry CH_2Cl_2 (10 mL) was added via syringe, the reaction was cooled with an acetone/dry-ice bath, and $SbCl_5$ (1M in CH_2Cl_2, 0.90 mL, 0.90 mmol) was added dropwise via syringe. The color became purple and then dark green with time as the reaction was allowed to warm to room temperature and stir for 24 hours. Dry MeOH (25 mL) was added via syringe and a white precipitate formed immediately. Stirred for 12 hours at room temperature, then diluted with $CHCl_3$ (100 mL), washed with water and dried the organic layer over $MgSO_4$. The solvents were removed and the remaining solid was precipitated from CH_2Cl_2/MeOH, yielding **6** (42 mg, 0.108 mmol, 84%) as a white solid. HRMS-ESI (*m/z*): $(M+H)^+$ calcd for $C_{28}H_{16}S$ 384.0967; found 384.0953.

2,5-Bis(2-thienyl)-3,4-dibromothiophene (7) 5-Methyl-2-tributylstannyl thiophene (4.205 g, 10.86 mmol) was placed in a 100 mL Schlenk with DMF (45 mL) and was degassed by sparging with argon for 30 minutes. Tetrabromothiophene (1.886 g, 4.72 mmol), $Pd(PPh_3)_2Cl_2$ (100 mg, 0.142 mmol) and a magnetic stir bar were placed in a separate 100 mL Schlenk which was then evacuated and backfilled with argon. The degassed DMF solution of 5-methyl-2-tributylstannyl thiophene was then added via cannula to the flask containing the catalyst. The reaction was stirred at 100 °C for 72 hours, then cooled to room temperature, diluted with 200 mL hexanes and washed with H_2O (3 x 50 mL). The organic layer was dried over $MgSO_4$, filtered, and the solvents were removed in vacuo. The remaining solids were recrystallized from hexanes, yielding

7 (926 mg, 2.13 mmol, 45%) as a yellow crystalline solid. ^{1}H NMR ($CDCl_3$, δ): 2.53 (s, 6H, CH_3), 6.76 (dd, 2H, J_1 = 6.5 Hz, J_2 =1.5 Hz), 7.25 (d, 2H, J = 6.0 Hz). ^{13}C NMR ($CDCl_3$, δ): 15.34, 111.43, 125.62, 127.01, 130.85, 131.66, 141.63.

2,5-Bis(2-thienyl)-3,4-bis(3,4-octyloxyphenyl)thiophene (8) 2,5-Bis(2-thienyl)-3,4-dibromothiophene (159 mg, 0.391mmol) was placed in a 50 mL Schlenk with 3,4-dioctyloxyphenyl boronic acid (444 mg, 1.174 mmol), $Pd(PPh_3)_4$ (45 mg, 0.039 mmol), Na_2CO_3 (332 mg, 3.13 mmol) and a magnetic stir bar. The flask was evacuated and backfilled with argon. A mixture of toluene (30 mL), EtOH (5 mL) and H_2O (3 mL) which had been degassed by purging with argon for 20 minutes was added via cannula and the reaction was then heated to 80 °C with stirring for 72 hours, cooled to room temperature, and poured into H_2O (50 mL). Et_2O (50 mL) was added and the organic layer was washed with H_2O (2 x 50 mL) and dried over $MgSO_4$. The solution was filtered and the solvents were removed in vacuo. The remaining oil was purified by silica gel chromatography with 5:1 hexane/CH_2Cl_2 eluent, yielding **7** (278 mg, 0.304 mmol, 78%) as a yellow oil. ^{1}H NMR ($CDCl_3$, δ): 0.88-0.93 (m, 12H, CH_3), 1.28-1.42 (m, 36H), 1.43-1.52 (m, 4H), 1.65-1.72 (m, 4H), 1.78-1.87 (m, 4H), 3.75 (t, 4H, J = 6.5 Hz, CH_2O-), 3.95 (m, 4H, J = 6.5 Hz, CH_2O-), 6.62-6.65 (m, 4H), 6.72 (d, 2H, J = 8.0 Hz), 6.90 (dd, 2H, J_1 = 5.0 Hz, J_2 = 3.5 Hz), 7.01 (dd, 2H, J_1 = 3.5 Hz, J_2 = 1.0 Hz), 7.12 (dd, 2H, J_1 = 5.0 Hz, J_2 = 1.0 Hz). ^{13}C NMR ($CDCl_3$, δ): 14.09, 22.67, 25.98, 26.04, 29.08, 29.25, 29.29, 29.32, 29.38, 29.43, 31.81, 31.82, 68.88, 69.02, 112.89, 116.30, 123.22, 125.37, 125.63, 126.74, 128.29, 130.64, 136.35, 139.95, 148.37, 148.44. HRMS-EI (*m/z*): (M^+) calcd for $C_{56}H_{80}O_4S_3$ 935.5111; found 935.5142.

2,5-Bis(2-thienyl)-3,4-bis(3,4-(2-ethyl)hexyloxyphenyl)thiophene (9) 2,5-Bis(2-thienyl)-3,4-dibromothiophene (200 mg, 0.492 mmol) was placed in a 50 mL Schlenk flask with 3,4-di(2-ethyl)hexyloxyphenyl boronic acid (745 mg, 1.97 mmol), $Pd(PPh_3)_4$ (57 mg, 0.049 mmol), Na_2CO_3 (418 mg, 3.94 mmol) and a magnetic stir bar. The flask was evacuated and backfilled with argon. A mixture of toluene (30 mL), EtOH (5 mL) and H_2O (3 mL) which had been degassed by purging with argon for 20 minutes was added via cannula and the reaction was then heated to 80 °C with stirring for 72 hours, cooled to room temperature, and poured into H_2O (50 mL). Et_2O (100 mL) was added and the organic layer was washed with H_2O (2 x 50 mL) and dried over $MgSO_4$. The solution was filtered and the solvents were removed in vacuo. The remaining oil was purified by silica gel chromatography with 6:1 hexane/CH_2Cl_2 eluent, yielding **8** (290 mg, 0.317 mmol, 65%) as a yellow oil. ^1H NMR ($CDCl_3$, δ): 0.87-0.98 (m, 24H), 1.26-1.59 (m, 32H), 1.62-1.68 (m, 2H), 1.73-1.79 (m, 2H), 3.59-3.64 (m, 4H), 3.80-3.87 (m, 4H), 6.64 (d, 2H, J = 1.8), 6.67 (dd, 2H, J_1 = 8.0 Hz, J_2 = 1.8 Hz), 6.74 (d, 2H, J = 8.5 Hz), 6.91-6.93 (m, 2H), 7.02-7.04 (m, 2H), 7.13-7.15 (m, 2H). ^{13}C NMR ($CDCl_3$, δ): 11.11, 11.23, 23.05, 23.79, 23.92, 29.07, 29.19, 30.54, 30.63, 39.34, 39.63, 71.48, 71.65, 112.93, 116.45, 123.20, 125.36, 125.69, 126.74, 128.22, 130.62, 136.42, 140.06, 148.85. HRMS-EI (*m/z*): (M^+) calcd for $C_{56}H_{80}O_4S_3$ 935.5111; found 935.5082.

2,5-Bis(5-methyl-2-thienyl)-3,4-dibromothiophene (10) Tetrabromothiophene (5 g, 12.5 mmol) and $Pd(PPh_3)_2Cl_2$ (263 mg, 0.375 mmol) and a magnetic stir bar were placed in a 100 mL Schlenk flask which was then evacuated and backfilled with argon. 2-Tributylstannyl thiophene (8.8 mL, 27.5 mmol) and DMF (50 mL) were placed in a separate 100 mL Schlenk, degassed with sparging argon for 30 minutes. This solution

was added via cannula to the flask containing the catalyst and the reaction was then heated to 110 °C for 18 hours with stirring. The solution was cooled to room temperature and diluted with hexanes (100 mL), washed with H_2O (3 x 50 mL), dried over $MgSO_4$ and filtered. The solvents were removed in vacuo and the remaining solids were recrystallized from hexanes, yielding **10** (1.372 g, 3.38 mmol, 27%) as a yellow crystalline solid. ^1H NMR ($CDCl_3$, δ): 7.12 (dd, 2H, J_1 = 5.1 Hz, J_2 = 3.6 Hz), 7.42 (dd, J_1 = 5.1 Hz, J_2 = 1.2 Hz), 7.48 (J_1 = 3.6 Hz, J_2 = 1.2 Hz). ^{13}C NMR ($CDCl_3$, δ): 113.10, 127.52, 127.81, 128.10, 131.73, 134.71. HRMS-EI (*m/z*): (M^+) calcd for $C_{14}H_{10}Br_2S_3$ 431.8306; found 431.8311.

2,5-Bis(5-methyl-2-thienyl)-3,4-bis(3,4-octyloxyphenyl)thiophene (11) 2,5-Bis(5-methyl-2-thienyl)-3,4-dibromothiophene (147 mg, 0.339mmol) was placed in a 50 mL Schlenk with 3,4-dioctyloxyphenyl boronic acid (384 mg, 1.016 mmol), $Pd(PPh_3)_4$ (40 mg, 0.034 mmol), Na_2CO_3 (287 mg, 2.71 mmol) and a magnetic stir bar. The flask was evacuated and backfilled with argon. A mixture of toluene (30 mL), EtOH (5 mL) and H_2O (3 mL) which had been degassed by purging with argon for 20 minutes was added via cannula and the reaction was then heated to 80 °C with stirring for 72 hours, cooled to room temperature, and poured into H_2O (50 mL). Et_2O (50 mL) was added and the organic layer was washed with H_2O (2 x 50 mL) and dried over $MgSO_4$. The solution was filtered and the solvents were removed in vacuo. The remaining oil was purified by silica gel chromatography with 6:1 hexane/CH_2Cl_2 eluent, yielding **9** (244 mg, 0.259 mmol, 76%) as a yellow oil. ^1H NMR ($CDCl_3$, δ): 0.86-0.93 (m, 12H), 1.24-1.42 (m, 36H), 1.42-1.51 (m, 4H), 1.65-1.73 (m, 4H), 1.80-1.85 (m, 4H), 2.36 (s, 6H, CH_3), 3.76 (t, 4H, J = 6.5 Hz, -CH_2O-), 3.96 (t, 4H, J = 6.5 Hz, -CH_2O-), 6.53-6.55 (m, 2H), 6.60-

6.63 (m, 2H), 6.71 (d, 2H, J = 8.0 Hz), 6.79 (d, 2H, J = 3.5 Hz). ^{13}C NMR ($CDCl_3$, δ): 14.09, 15.22, 22.65, 22.67, 25.98, 26.04, 29.07, 29.25, 29.30, 29.39, 29.43, 31.80, 31.82, 68.82, 68.93, 112.75, 116.19, 123.16, 124.96, 125.43, 128.52, 130.57, 134.08, 139.15, 139.91, 148.21. HRMS-EI (*m/z*): (M^+) calcd for $C_{58}H_{84}O_4S_3$ 963.5424; found 963.5398.

2,5-Bis(5-methyl-2-thienyl)-3,4-bis(-(2-ethyl)hexyloxyphenyl)thiophene (12) 2,5-Bis(5-methyl-2-thienyl)-3,4-dibromothiophene (200 mg, 0.461mmol) was placed in a 50 mL Schlenk with 3,4-(2-ethyl)hexyloxyphenyl boronic acid (697 mg, 1.84 mmol), $Pd(PPh_3)_4$ (53 mg, 0.046 mmol), Na_2CO_3 (390 mg, 3.68 mmol) and a magnetic stir bar. The flask was evacuated and backfilled with argon. A mixture of toluene (30 mL), EtOH (5 mL) and H_2O (3 mL) which had been degassed by purging with argon for 20 minutes was added via cannula and the reaction was then heated to 80 °C with stirring for 72 hours, cooled to room temperature, and poured into H_2O (50 mL). Et_2O (100 mL) was added and the organic layer was washed with H_2O (2 x 50 mL) and dried over $MgSO_4$. The solution was filtered and the solvents were removed in vacuo. The remaining oil was purified by silica gel chromatography with 6:1 hexane/CH_2Cl_2 eluent, yielding **10** (394 mg, 0.418 mmol, 91%) as a yellow oil. ^{1}H NMR ($CDCl_3$, δ): 0.82-0.98 (m, 24H), 1.22-1.59 (m, 32H), 1.59-1.64 (m, 2H), 1.65-1.81 (m, 2H), 2.38 (s, 6H, CH_3), 3.62 (d, 4H, J = 6.0, -$CHCH_2O$-), 3.84 (d, 4H, J = 6.0 Hz, -$CHCH_2O$-), 6.56 (dd, 2H, J_1 = 3.6 Hz, J_2 = 1.2 Hz), 6.61-6.68 (m, 4H), 6.71-6.76 (m, 2H), 6.81 (d, 2H, J = 3.6 Hz) ^{13}C NMR ($CDCl_3$, δ): 11.08, 11.22, 14.08, 15.22, 23.04, 23.76, 23.89, 29.05, 29.17, 30.53, 30.60, 39.28, 39.59, 71.45, 71.54, 112.85, 116.39, 123.15, 124.99, 125.52, 128.44, 130.56, 134.13, 139.26, 139.89, 148.63, 148.74.

References

(1) Barberá, J.; Rakitin, O. A.; Ros, M. B.; Torroba, T. *Angew. Chem. Int. Ed.* **1998**, *37*, 296-299.

(2) Adam, D.; Schuhmacher, P.; Simmerer, J.; Häussling, L.; Siemensmeyer, K.; Etzbach, K. H.; Ringsdorf, H.; Haarer, D. *Nature* **1994**, *371*, 141-143.

(3) Boden, N.; Borner, R. C.; Bushby, R. J.; Clements, J. *J. Am. Chem. Soc.* **1994**, *116*, 10807-10808.

(4) van de Craats, A. M.; Warman, J. M.; *Adv. Mater.* **2001**, *13*, 130-133.

(5) Arikainen, E. O.; Boden, H.; Bushby, R. J.; Clements, J.; Movaghar, B.; Wood, A. *J. Mater. Chem.* **1995**, *5*, 2161-2165.

(6) van de Craats, A. M.; Siebbeles, L. D. A.; Bleyl, I.; Haarer, D.; Berlin,, A. M.; Siebbeles, L. D. A.; Bleyl, I.; Haarer, D.; Berlin, Y. A.; Zharikov, A. A.; Warman, J. M. *J. Phys. Chem B* **1998**, *102*, 9625-9634.

(7) Artal, M. C.; Toyne, K. J.; Goodby, J. W.; Barberá, J.; Photinos, D. J. *J. Mater. Chem.* **2001**, *11*, 2801-2807.

(8) (a) Tovar, J. D.; Swager, T. M. *Adv. Mater.* **2001**, *13*, 1775-1780. (b) Tovar, J. D.; Rose, A.; Swager, T. M. *J. Am. Chem. Soc.* **2002**, *124*, 7762-7769.

(9) Bard, A. J.; Faulkner, L. R. *Electrochemical Methods*. 2nd ed. Wiley: New York, 2001.

Chapter 6

Iptycene-Containing Polymers:

Towards a New Paradigm for High-Strength Fiber-Forming Polymers

Introduction

This chapter will detail efforts toward establishing a new design principle for the creation of high-strength polymers through the incorporation of iptycene moieties into polymer backbones. Iptycenes are a class of rigid, bridged aromatic compounds whose most common members include triptycene and pentiptycene (Figure 1). Triptycene was first described by Bartlett et al in 1942 in order to compare the stability of the bridgehead radical of triptycene to that of triphenylmethane.[1] Subsequent efforts detailing the synthesis of iptycenes were described by Hart the 1980's.[2]

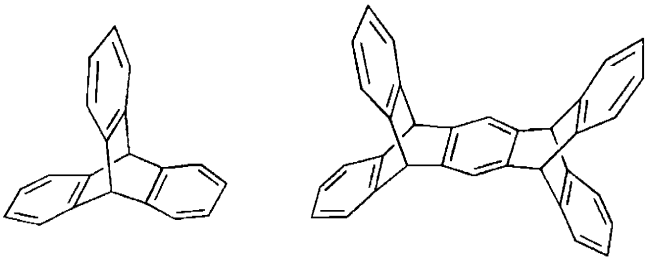

Figure 1. Two common iptycenes: triptycene (left) and pentiptycene (right).

The Swager lab first began using iptycenes within the context of fluorescent poly(phenylethynylene) (PPE) chemosensors in order to detect minute amounts of small electron-deficient analytes. In this case, a pentiptycene-containing monomer was incorporated into the PPE backbone and served as a structural scaffold (a molecular truss) to physically hold the polymer chains apart. By holding the chains apart, the iptycenes effectively prevent the self-quenching of fluorescence common to most PPE's in the solid state.[3] It was further postulated that the void space introduced by the iptycenes also creates a more porous environment in the solid state, allowing small nitroaromatics such

as TNT and DNT to more effiently intercalate, bind and quench the UV-excited polymer fluorescence through electron and energy transfer.

Structually, iptycenes inherently possess an unusually large amount of free volume due to the rigidly held aromatic faces of the molecules (Figure 2). Former Swager-group graduate student Tim Long repeatedly demonstrated in his doctoral research that the free volume of iptycenes can be exploited in order to impart unusual properties to materials. In two separate experiments, Tim dissolved extended an iptycene (trisanthracene) into: 1) an aligned nematic liquid crystalline host and 2) a polymer blend which was subsequently stretch aligned. He was able to probe the orientation of the anthracene subunits via polarized UV-vis spectroscopy and demostrate that trisanthracene tends to orient with its long axis perpendicular to the 1) director of the liquid crystal molecules or 2) stretching direction of the polymer blend.[4] Most materials tend to align with their long axes perpendicular to the director of an LC host or stretching direction of polymer host as this minimizes the disruption of the LC/polymer alignment. The unusual behavior of the iptycene molecules is attributed to the threading of the LC molecules/polymer chains through the void spaces of the trisanthracene, as this efficiently fills those spaces while minimally disrupting the host alignment (Figure 3).

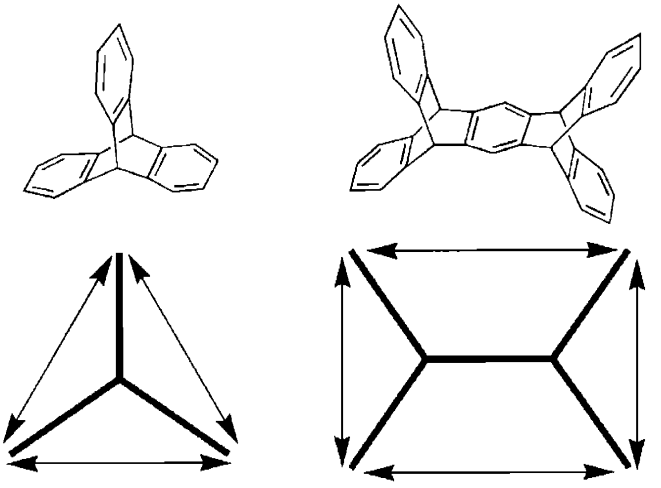

Figure 2. Triptycene and pentiptycene have unusually large free volumes (area inside of arrows) which can be filled by guest molecules.

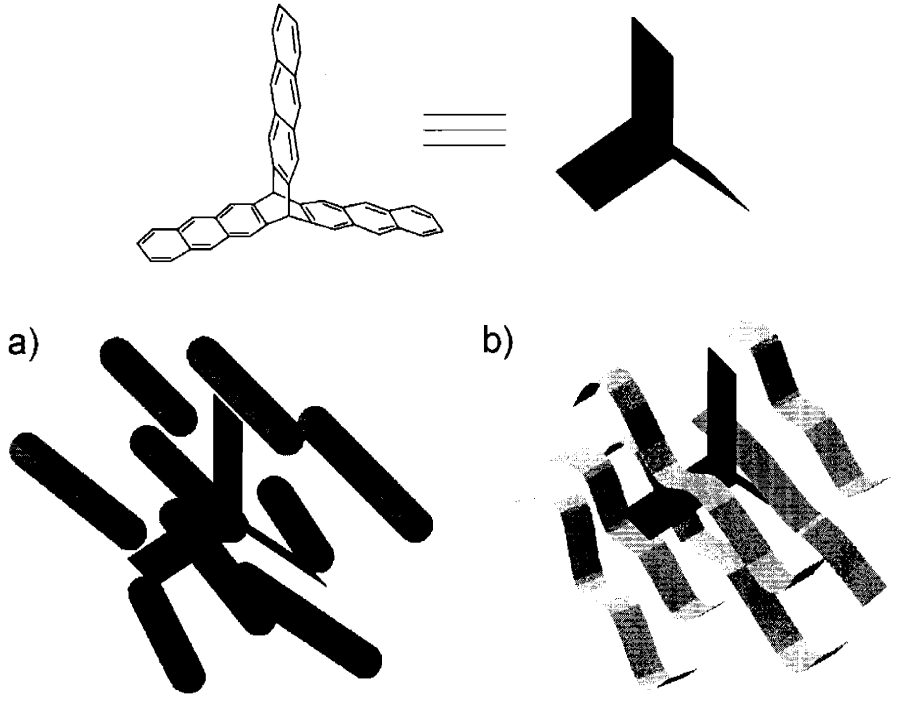

Figure 3. Alignment of trisanthracene (an iptycene) within a) a nematic liquid crystal host, and b) a stretch-aligned polymeric host. Unlike most materials, the iptycene molecules tend to align with their long-axes perpendicular to the a) nematic director of the LC molecules and b) stretching direction of the polymeric chains.

Tim Long extended this concept of iptycene free-volume induced alignment and demonstrated that the alignment of common dichroic and fluorescent dyes in LC hosts can be enhanced by up to 23% through the incorporation of one or more triptycene moieties into the molecular scaffolds of the dyes (Figure 4).[5] Building on this theme, Swager-group postdoc Zhengguo Zhu subsequently showed that iptycene-containing poly(phenylenevinylene)s (PPVs) aligned efficiently with liquid crystalline hosts and that the PPV orientation tracks with that of the LC upon application of an electric field.[6] Long also demonstrated that the free volume of iptycenes was useful for the creation of low-K dielectric materials, as the incorporation of larger iptycenes into a polymer backbone results in materials with large degrees of free volume (low density).[7]

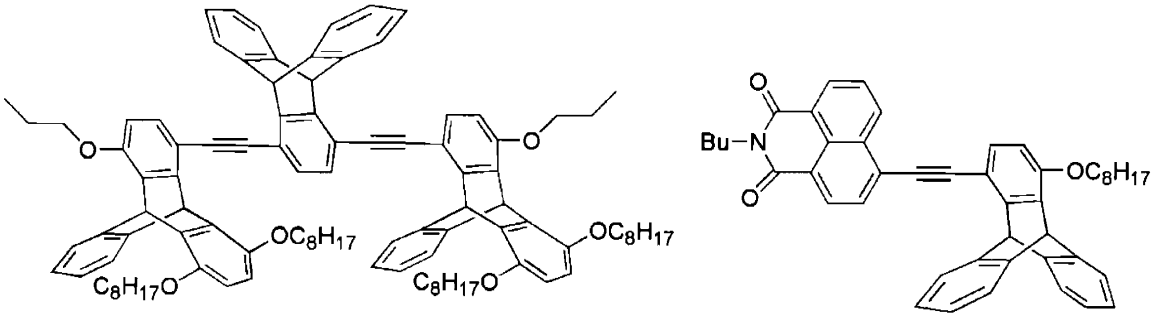

Figure 4. Iptycene-containing dyes synthesized by Long.

The work described in this chapter represents our efforts toward using iptycenes for an entirely new purpose: the creation of new high-strength polymeric materials.

High-Strength Synthetic Fibers

The groundbreaking synthesis of nylon by Carothers (DuPont) in 1935, followed by the rapid commercial development of nylon 6-6, heralded the birth of the synthetic fiber industry.[8] New polymeric formulations quickly emerged and fibers were formed of polyacrylics (1949), polyesters (1953) and polypropylene (1957).[9] These polymers were incorporated into clothes, furniture, carpets and countless other consumer products in the following decades, largely replacing natural fibers such as cotton and wool. Since then, the synthesis and characterizations of a seemingly countless number of synthetic fibers have been investigated.

The formulation, synthesis and processing of polymers to yield ultra high-strength synthetic fibers is a demanding scientific endeavor. The guiding principles toward the creation of high-strength polymers thus far are rather simple in theory, but rarely in practice. The guiding principles to date have been: 1) incorporate a high degree of aromatic content in the polymers, this will increase the stiffness of the polymer chains and lead to efficient inter-chain packing, 2) incorporate functional groups that will result in attractive forces between chains, such as hydrogen-bonding, and 3) pull and process fibers of the material, as the act of drawing the fiber from either a melt or liquid-crystalline solution often increases the order of polymer chains relative to one another, thereby increasing the inter-chain attractive forces mentioned above.[10]

One of the most successful high-strength synthetic fibers is Kevlar, discovered and manufactured by DuPont starting in the early 1970's.[11] Kevlar is the polycondensation product of *p*-phenylene diamine (PPD) and terephthaloyl chloride (TCl) (Scheme 1). The strength of Kevlar stems from the fact that it can be spun into

fibers of highly crystalline, tightly packed and highly-ordered polymer strands. Each polymer strand forms numerous hydrogen bonds with neighboring strands, resulting in an extremely rigid material of high strength (Figure 5).[12] Kevlar is also extremely fire-resistant due to its poly(aramide) structure, though its stiffness makes it unsuitable for use in clothing except in extreme cases such as space suits and jackets for fire-fighters and rescue teams.*

The example of Kevlar further serves to illustrate just how technically demanding this field of research can be; DuPont spent almost fifteen years and approximately $500 million to develop the material from its discovery to the final commercial product.[13] It has been estimated that 40 man-years of research was invested just in order to find a suitable, relatively non-toxic solvent in which to conduct the polymerization on a commercial scale.[14]**

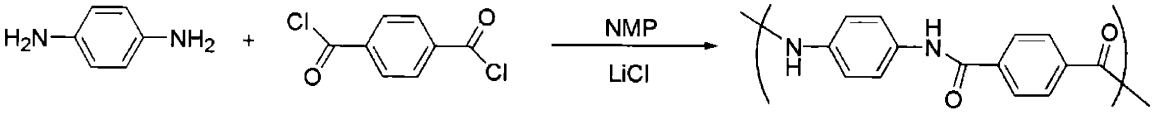

Scheme 1. Synthesis of Kevlar.

* Nomex, the isomeric polycondensation product of *m*-phenylene diamine (MPD) and isophthaloyl chloride, does not have the ability to form as many hydrogen bonds as Kevlar due to angular connectivity of the repeat units; this results in lower strength, but provides a much less stiff (and thereby more comfortable) fiber for use in fire-retardant clothing, though it lacks the physical strength of Kevlar. Blended weaves of Kevlar/Nomex are therefore commonly used in fire-retardent clothing in order to impart a balance of strength and tactile feel to the resulting garment.

** The final system was (*N*-methyl pyrrolidinone (NMP) and $CaCl_2$; the initial small-scale synthesis of Kevlar was run in the highly carcinogenic solvent hexamethylphosphoramide (HMPA).

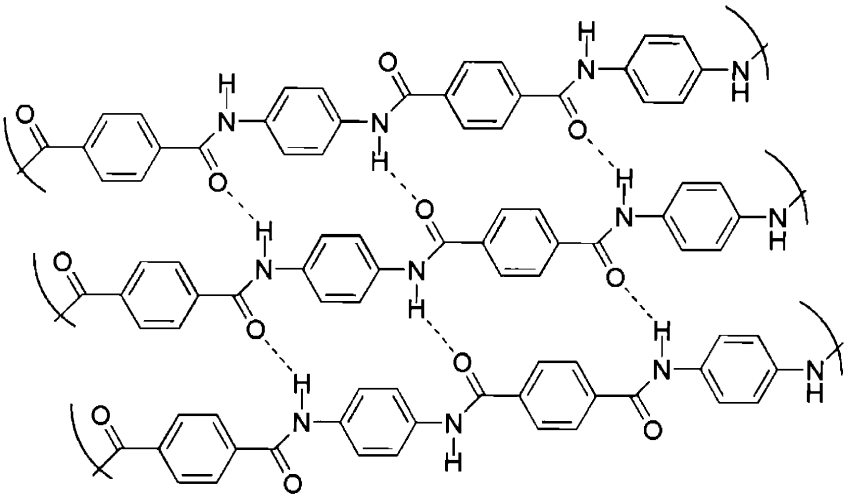

Figure 5. The strength of Kevlar results largely from the many hydrogen bonds formed between polymer strands during the spinning process.

Most other promising high-strength polymers have been designed to try to expand upon Kevlar's formula for success; they are almost without exception polymers with a high degree of aromatic content and the ability to form multiple hydrogen bonds between polymer strands. These polymers include liquid crystalline polyesters such as Vectra and the highly intra- as well as inter-strand hydrogen-bonded polymers polypyridobisimidazole (M5) and poly(*p*-phenylene benzobisoxazole) (PBO) (Figure 6).[15] The nearest exception to this rule is Spectra, which is polyethylene; however, Spectra is ultra-high molecular weight material which is then gel-spun to give extremely oriented fibers.[16] Kevlar is not the strongest of these polymers (Spectra is of approximately equal strength and PBO is slightly stronger), but its commercial dominance persists largely due to the simplicity of its structure and subsequent relative affordability. Kevlar is not without its disadvantages, however; for example, it is completely insoluble in common solvents. Therefore, Kevlar must be spun from a

lyotropic liquid crystalline solution in hot, concentrated sulfuric acid. This is a technically challenging process which requires a tremendous initial investment (as well as significant upkeep) to order to realize a production facility.

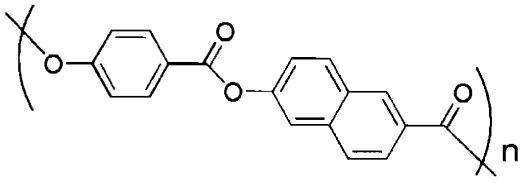

Vectra (Celanese)

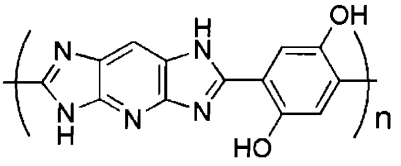

M5

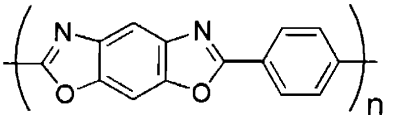

PBO

Figure 6. High-strength polymers need not be polyaramides.

The initial aim of this research was to establish whether iptycenes are capable of increasing the strength of polymers. The long-term goal would then be to utilize iptycenes in order to synthesize ultra high-strength polymers that take advantage of certain unique design principles. Incorporation of iptycenes into a polymer backbone should result in gearing and interlocking of the polymer chains and thereby increase the barrier to movement of neighboring polymer chains past one another. Assuming that the

polymer chains have been previously aligned (by the drawing of fibers, for example) then as the polymer is stretched along alignment direction the chains will slide parallel to one another until the laterally directed iptycene units begin to run into one another, resulting in elasticity followed by resistance (Figure 7). It was hoped that a combination of these effects would cause polymers which incorporate iptycenes to be stronger and more energy-absorbing materials then their non-iptycene counterparts. We decided to first look at triptycene-containing poly(ester)s, as these are easily accessible synthetically through stepwise condensation polymerizations.

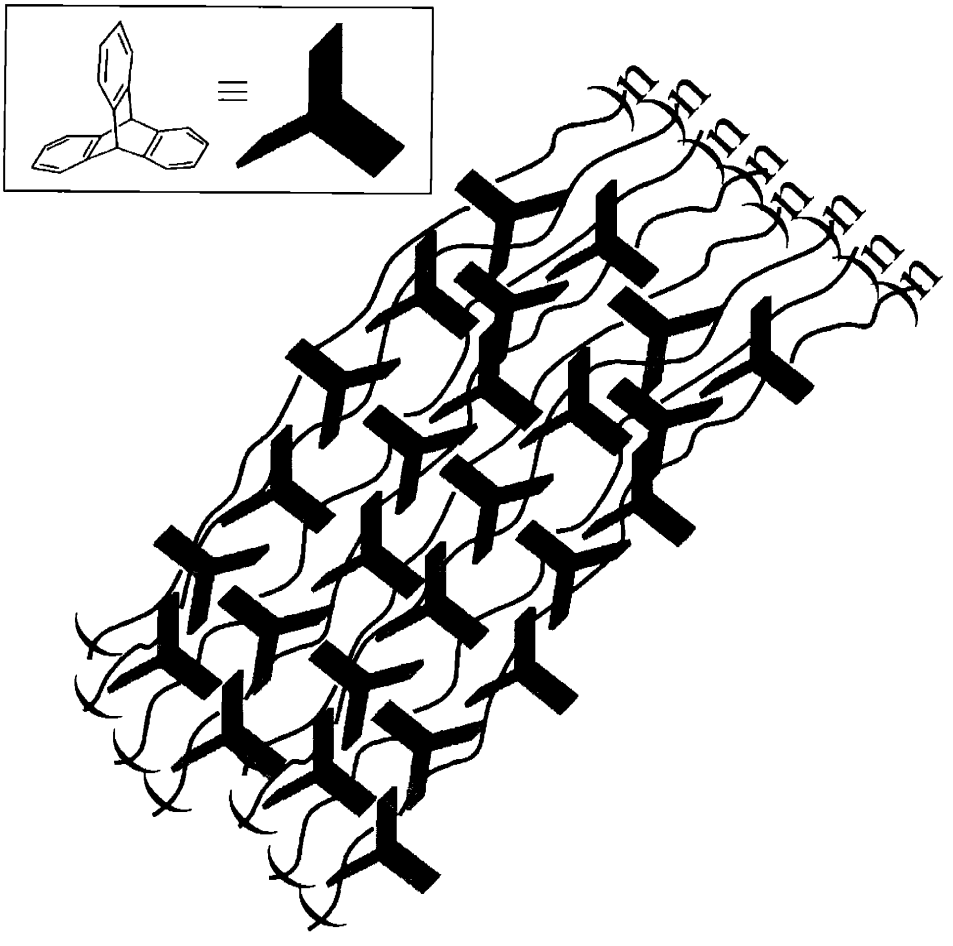

Figure 7. Incorporation of iptycenes into aligned polymers may result in increased entanglement relative to other non-iptycene polymers.

Condensation Polymerization

Condensation polymerizations are stepwise reactions in which monomers come together and react, with the elimination of a small molecule (such as water or methanol) forming a dimer. The dimer can then react with another monomer and form a trimer, or with another dimer and form a tetramer, or with an existing polymer chain making a slightly longer polymer, each time releasing another small molecule.[17] Because condensation polymerizations occur in a stepwise manner, polymer growth tends to occur relatively slowly compared to chain polymerizations, in which the monomers rapidly add to the ends of the polymer chain.

The molecular weights of condensation polymers increase slowly even at high levels of monomer conversion, as was first described mathematically by Carothers in 1929.[18] He assumed that there are N_0 molecules of monomer initially and at some arbitrary point later in the reaction there are N molecules. After this reaction time, therefore, the amount of reacted molecules is $N_0 - N$. The conversion of the reaction, p, is simply:

$$p = (N_0 - N) / N_0$$

This can also be written as:

$$N = N_0 (1 - p)$$

The average degree of polymerization (P_n) is equal to N_0 / N. Substituting this into the above equation gives:

$$P_n = 1 / (1 - p)$$

Using this equation, one can see that at 95% monomer conversion, $P_n = 1 / (1 - 0.95) = 20$. In other words, when 95% of the monomer has reacted, the average degree of

polymerization is only 20; this emphasizes the fact that very high conversions (typically greater than 99%), and therefore extremely pure monomers, are necessary conditions in order to acheive reasonably high molecular weights.

Linear condensation polymers are most commonly synthesized either by a single monomer of the AB type (where A and B represent functional groups that can react with one another), or by combining two separate AA and BB type difunctional comonomers.[19] Polymerizations of AB-type monomers is desireable in that the stoichiometry of the reaction is assured as long as the monomer is pure; however, it is not always synthetically practical to prepare monomers with the dual functionality required in this case.

Polymerizations of AA- and BB-type comonomers are often more attractive from the standpoint of monomer preparation, but precise stoichometric control of the two monomers then becomes a crucial factor (along with purity). The imbalance in the stiochiometry is represented by r; if the number of A and B groups at the beginning of polymerization are N^0_A and N^0_B respectively, then:

$$r = N^0_A / N^0_B$$

The reaction conversion p is the same as the fraction of A groups that have reacted. Each time an A group reacts a B group reacts as well, so the fraction of reacted B groups at conversion p can be represented as pN^0_A or prN^0_B. The number of unreacted groups, N_A N_B, is then:

$$N_A = (1 - p)N^0_A \quad \text{and} \quad N_B = (1 - pr)N^0_B = (1 - pr)N^0_A / r$$

There are two end groups per molecule, and the number of end groups is equal to $N_A + N_B$. The number of polymer chains, N, is therefore:

$$N = \tfrac{1}{2} (N_A + N_B)$$

By substitution:

$$N = \tfrac{1}{2}\,[(1 - p)\,N^0_A + (1 - pr)\,N^0_A / r]$$

which, with some rearranging, reduces to:

$$N = (N_A / 2)\,[1 + (1 / r) - 2p] \qquad \text{(eq 1)}$$

Since one repeating unit forms each time an A and B group react, the total number of repeating units, N_r, is:

$N_r = \tfrac{1}{2}\,(N^0_A + N^0_B)$

Recalling that $r = N^0_A / N^0_B$, then:

$$N_r = \tfrac{1}{2}\,(N^0_A + N^0_A/r) = (N^0_A / 2)\,[(r + 1) / r] \qquad \text{(eq 2)}$$

The average degree of polymerization equals the number of repeating units divided by the number of chains:

$$P_n = N_r / N, = \text{(eq 1)} / \text{(eq 2)}$$

and reduces to:

$$P_n = (1 + r) / (r + 1 - 2rp)$$

Using this equation one can figure out the maximum possible degree of polymerization P_n as dependent on the ratio of the two monomers (Table 1).[20] For example, if one has only 1 mol % excess of one component, whether due to impurity or error in weighing, then the maximum degree of polymerization achievable is 199 repeat units.

The physical properties of a given polymer can vary greatly depending on the molecular weight of the material. What constitutes a "high molecular weight" polymer, above which the properties will not change appreciably, depends largely on the chemical

structure of the polymer and the particular end use of the product. For example, commercial vinyl-based polymers typically have molecular weights of 10^5 to 10^6, while extremely stiff, polar polymers such as polyaramides may be commercially useful with molecular weights of only 15,000-20,000.[21]

Table 1. Degree of polymerization P_n as a function of the ratio of reacting functional groups A and B in a condensation polymerization,assuming 100% conversion with respect to A.

Excess of component B (mol %)	$r = N^0_A / N^0_B$	P_n
10	0.09	19
1	0.99	199
0.1	0.999	1999
0.01	0.9999	19,999

Determination of Molecular Weights

Different methods of molecular weight determination give rise to different values with varying degrees of accuracy. Methods such as osmometry and freezing-point depression give rise to the number average molecular weight, M_n,:

$$M_n = (\Sigma N_i M_i)/ (\Sigma N_i)$$

where N_i is the number of molecules with molecular weight M_i. Methods that determine molecular weights based on mass or polarizability, such as light scattering or ultracentrifugation, result in a measurement in which the species with higher masses have

a larger contribution to the measurement than the lower mass species.[22] This is the weight average molecular weight, M_w:

$$M_w = (\Sigma N_i M_i^2)/ (\Sigma N_i M_i)$$

The polydipersity index (PDI) is simply the weight average molecular weight divided by the number average molecular weight; this value indicates the how broad the distribution of molecular weights is within a given sample. A sample with a PDI = 1 is said to be *monodisperse* (all chains must be of the nearly identical molecular weights, since both methods of determination yield identical values), while a sample with PDI greater than 1 is *polydisperse*.

$$PDI = M_w / M_n$$

Flory used statistical methods to relate the molecular weight distribution of step polymerizations to the reaction conversion.[23] Though the derivation is beyond the scope of this thesis, Flory was able to show that the most probable polydispersity indices of condensation polymers are:

$$PDI = (M_w / M_n) = 1 + p$$

where p is the reaction conversion. Notice that at very high conversion levels (as p nears 1) the polydispersity approaches 2, revealing an inherent limitation in the uniformity of condensation polymerizations.

Gel-permeation chromatography (GPC), also known as size-exclusion chromatography (SEC), is an extremely convenient method for determining the appoximate molecular weight based on comparision of the polymer's effective molecular length versus a standard of known molecular weight (polystyrene, for example). A solution of the polymer is passed under pressure through a packed column of a cross-

linked organic gel such as polystyrene or of small inorganic particles such as silica. The column material contains pores of a particular average size (>30 μm); smaller molecules enter the pores and experience retention, while larger molecules cannot enter the pores and therefore pass through the column more quickly. The molecular weights determined by GPC are approximate values, especially if the polymers under comparision are structurally different than the standard to which they are compared.[24] The molecular weights of structurally rigid polymers such as conjugated polyaromatics are often artificially inflated when determined by GPC due to their higher persistence lengths relative to a common standard such as polystyrene, which is conformationally flexible.[25]

Stress-Strain and Modulus Measurements

One of the most basic tests of polymer performance is the stress/strain test. This is an experiment in which the sample is stretched until it breaks. The tensile stress (σ) is defined as the force applied on the material per unit cross section and the tensile strain (ε) is defined as the elongation of the material with respect to the initial length. The experiment is then represented graphically as a plot of stress vs. strain. There are three main types of stress/strain curves that are observed (Figure 8).

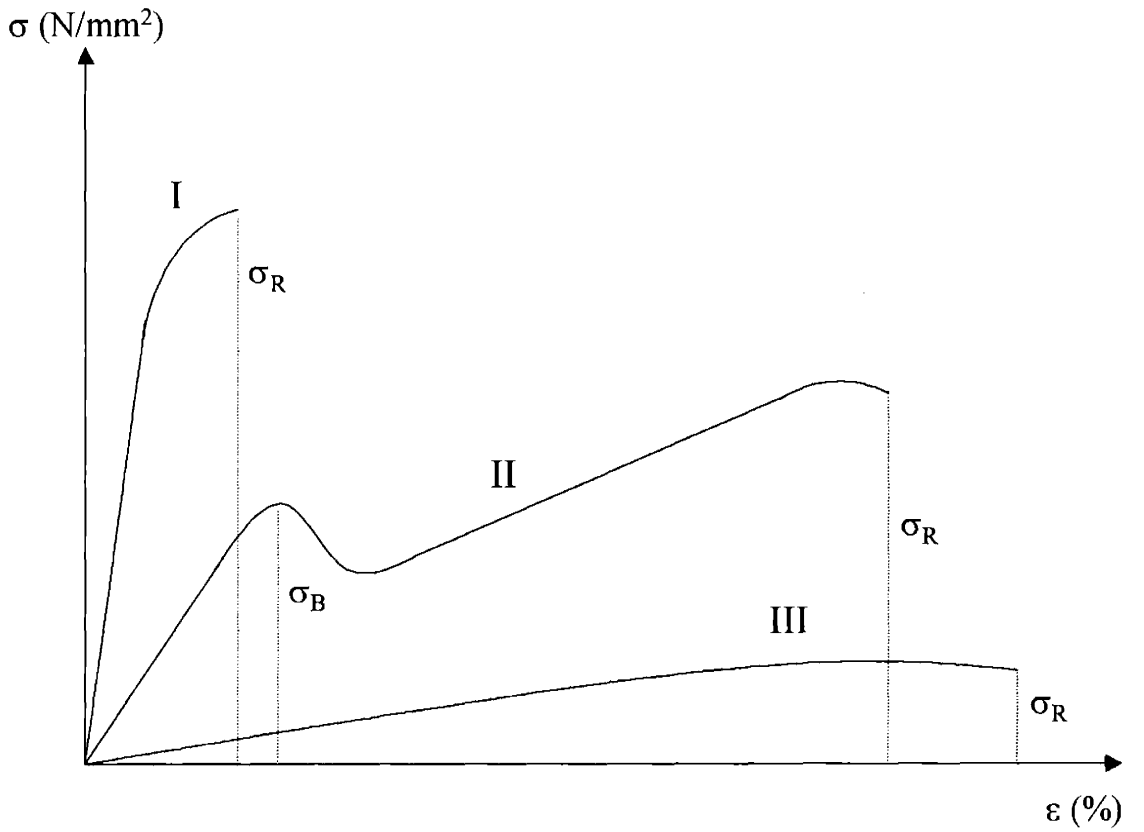

Figure 8. The three types of stress/strain curves seen for polymeric materials. The value σ_R = tensile strength at break and σ_B = yield strength. Figure adapted from Ref 10.

Polymers with steep and nearly linear stress-strain curves (curve 1) deform very little, even at high stresses. Most high-strength fibers fall into this category, as do thermosets and other materials that are inelastic and brittle. Polymers of type 2 are drawable: they deform little at low stresses, but at some stress value (the yield strength) a large deformation occurs as the material begins to extend. Once reorientation of the molecules is complete, the flow ceases and the material ultimately breaks. Drawable thermoplastic fibers and films (nylons, polyesters) fall into this category. The third group consists of materials which deform even at small stress values. These materials are plasticized thermoplastics and rubbers.

The modulus (Young's modulus) (E) is then defined as the stress divided by the strain at the breaking point. This is a measure of the stiffness, or rigidity, of a polymer.

Results and Discussion

Synthesis

The bulk of our research into the effects of iptycenes on polymer strength focused on poly(ester)s due to their relative ease of synthesis, reasonable solubilities in common organic solvents, and wealth of available comonomers. Our early attempts at polyester synthesis used triptycene hydroquinone as a monomer, as it is readily available in good yield from inexpensive starting materials (anthracene and benzoquinone).[1]

Melt Polymerizations

Attempts to synthesize **poly-1** by melt polymerization with terephthalic acid or dimethyl terephthalate were both ineffective, probably due to the high melting point of triptycene hydroquinone (melts/decomposes at 338-340 °C) (Scheme 2). In an effort to reduce the melting point of the triptycene monomer, compound **1** was synthesized in 95% yield by acetylation of triptycene hydroquinone with excess acetic anhydride in the presence of pyridine. However, the melting point of **1** is still relatively high (270 °C), and attempts to melt polymerize in the presence of either terephthalic acid or adipic acid did not proceed.

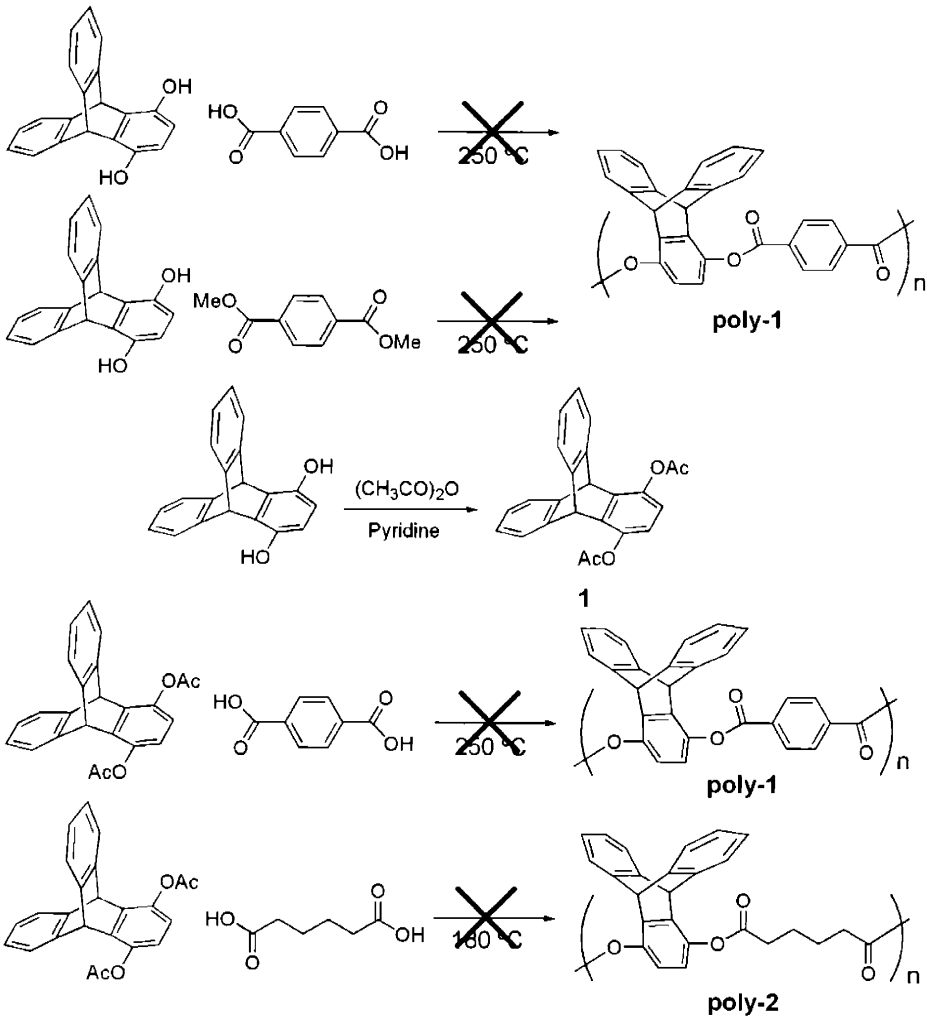

Scheme 2. Initial (unsuccessful) attempts at melt polymerizations.

Through the preparation and use of monomers with sufficiently low melting points, we were eventually able to carry out melt polymerizations successfully. One such effective route to the preparation of iptycene-based polyesters utilizes a scheme in which the melting point of the iptycene hydroquionone is lowered by the addition of trimethylsilyl groups. For example, trimethylsilyl-protected compound **2** can prepared from triptycene hydroquinone and chlorotrimethylsilane in THF using imidazole as a base (Scheme 3). This monomer has a relatively low melting point (134 °C) and once in

the molten state can be deprotected *in situ* by the addition of pyridine hydrochloride.[26] Polymers **poly-1** and **poly-2** were prepared from compound **2** and terephthaloyl chloride or adipoyl chloride, respectively, via this method. However, the extremely low solubilities and high melting points of the products **poly-1** and **poly-2** made them difficult to work with.

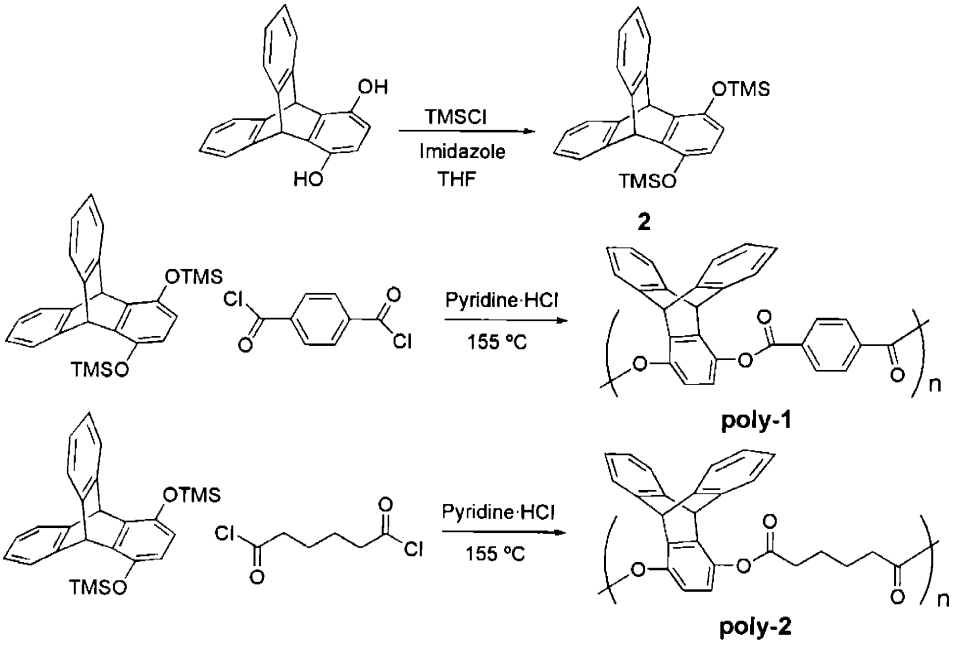

Scheme 3. Synthesis of **2**, **poly-1** and **poly-2**.

In order to create iptycene-containing polyesters with increased solubilities and lower melting points, a number of polymers incorporating flexible segments were synthesized. Random polymerizations of **2** with terephthaloyl chloride and 1,10-bis(trimethylsiloxy)decane in various ratios allows for a study of the effect of relative triptycene content to polymer properties (Scheme 4). We were interested in comparing the properties of analogous polymers in which the iptycene moieties have substituted by

simple phenyl rings; **poly-8**, **poly-9,** and **poly-10**, which contain no triptycene units, were therefore synthesized by similar procedures (Scheme 5).

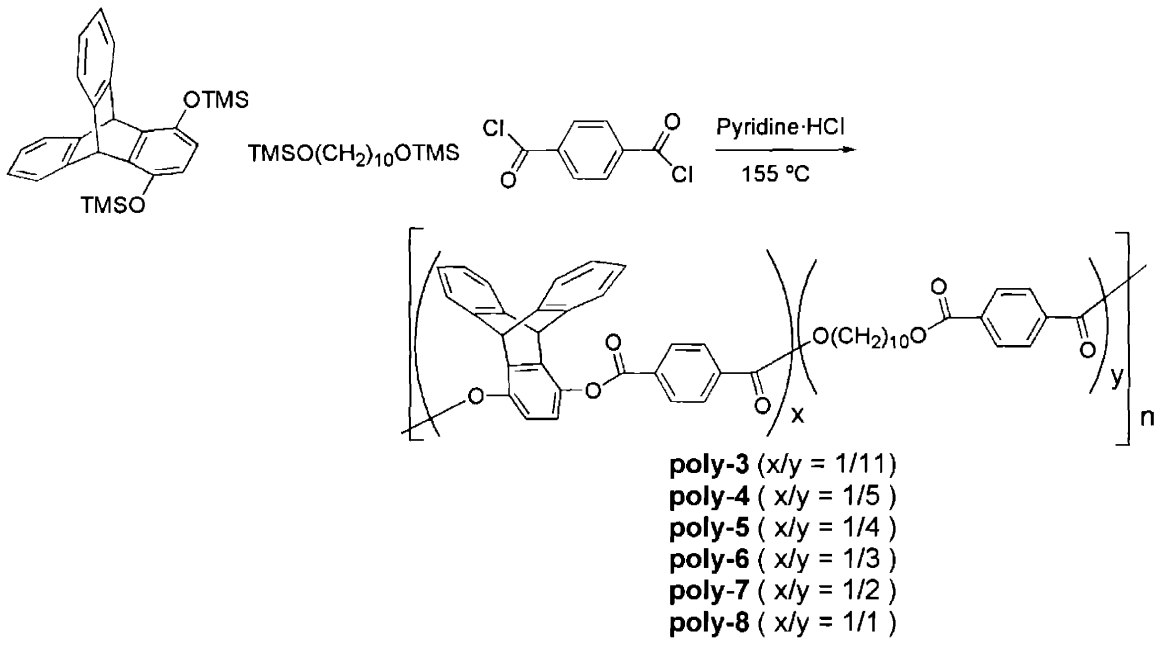

Scheme 4. The synthesis of random copolymers with varying ratios of flexible component.

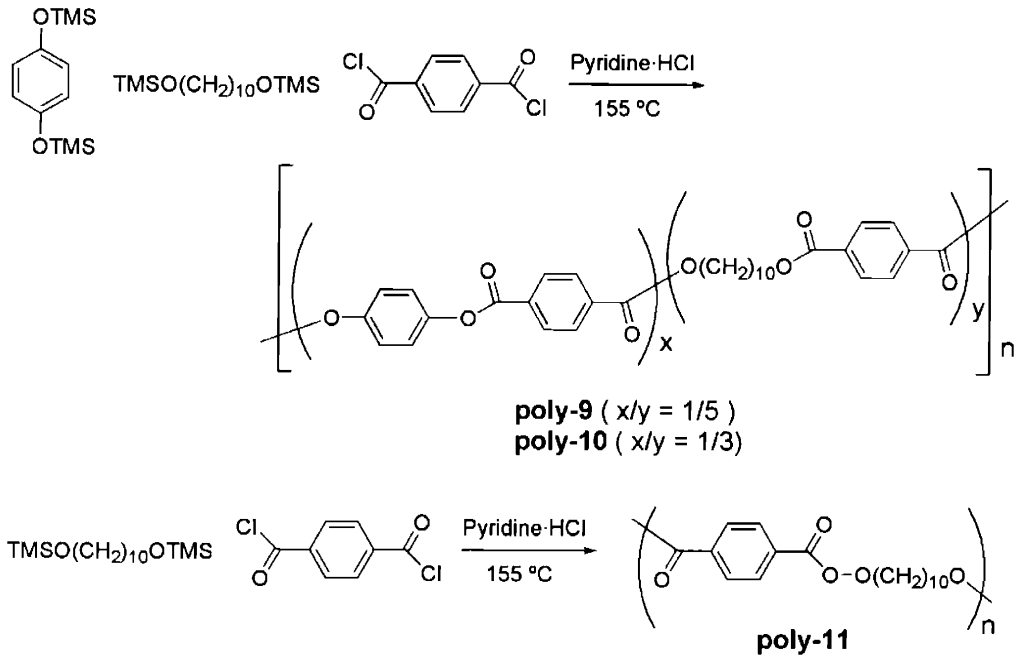

Scheme 5. Synthesis of non-iptycene polyesters **poly-9**, **poly-10**, and **poly-11**.

We investigated the possibility of incorporating iptycenes other than triptycene into polyesters to see how changing the structure affected the properties of the resulting polymers. Refluxing the [4+2] cycloadduct of naphthaquinone and anthracene[27] in glacial acetic acid with a few drops of HBr yields the extended triptycene hydroquinone **3** in good yield (Scheme 6). This can be protected subsequently with TMS groups yielding **4** in almost quantitative yield. Compound **4** was then polymerized with terephthaloyl chloride and 1,10-bis(trimethylsiloxy)decane at 155 °C via in situ deprotection with pyridine hydrochloride affording **poly-11**. In a similar fashion pentiptycene-containing **poly-12** was synthesized from the TMS-protected pentiptycene hydroquinone **5** (Scheme 7).

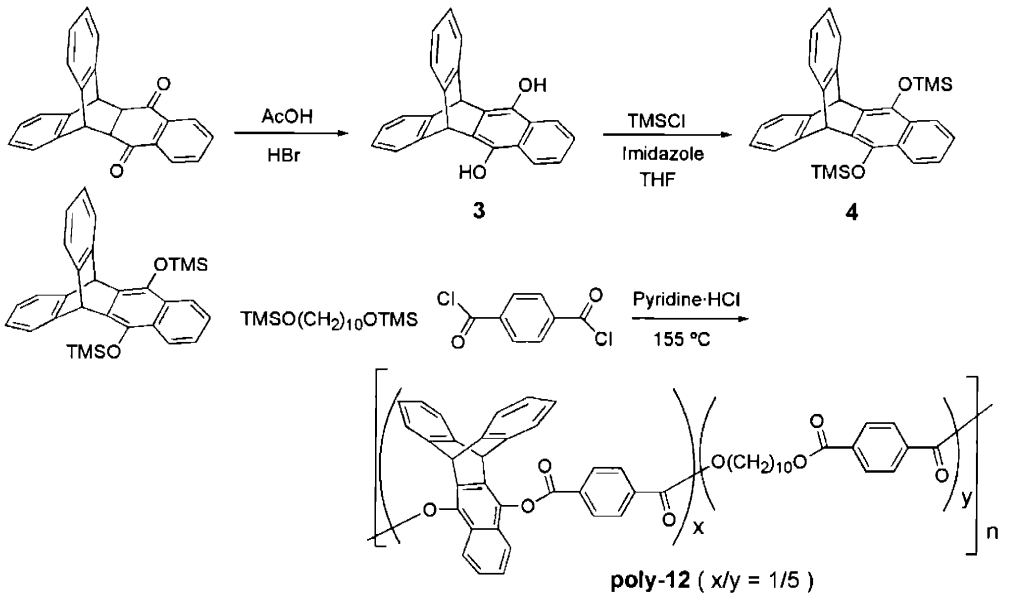

Scheme 6. Synthesis of extended trypticene polymer **poly-12**.

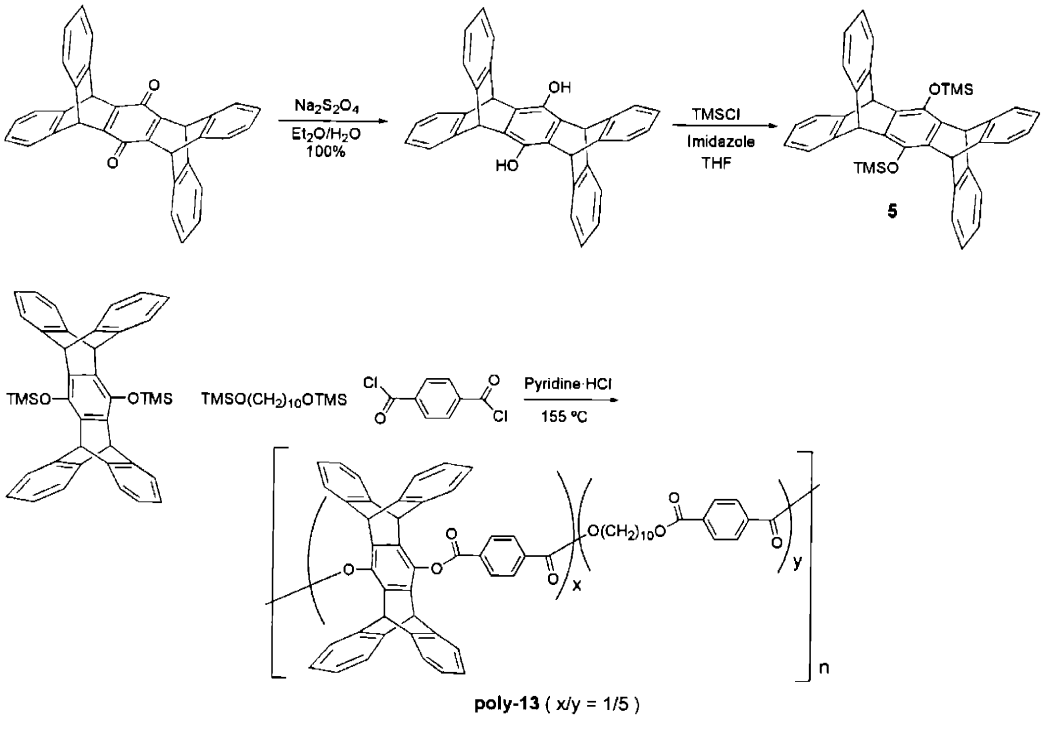

Scheme 7. Synthesis of pentiptycene-containing polymer **poly-13**.

Solution Polymerizations

We were eventually able to synthesize iptycene-containing polyesters via polymerization in solution as well (Scheme 8). Polycondensation in dichloromethane with triethylamine proceeds smoothly; interestingly, identical conditions in dichloromethane using pyridine rather than triethylamine as the base did not result in polymerization. It would seem that triethylamine helps to solubilize the iptycene hydroquinones more efficiently than pyridine, enabling the polymerization to proceed. Many different polyesters were synthesized by this route (not all described below), as we were screening for polymers with desirable properties.

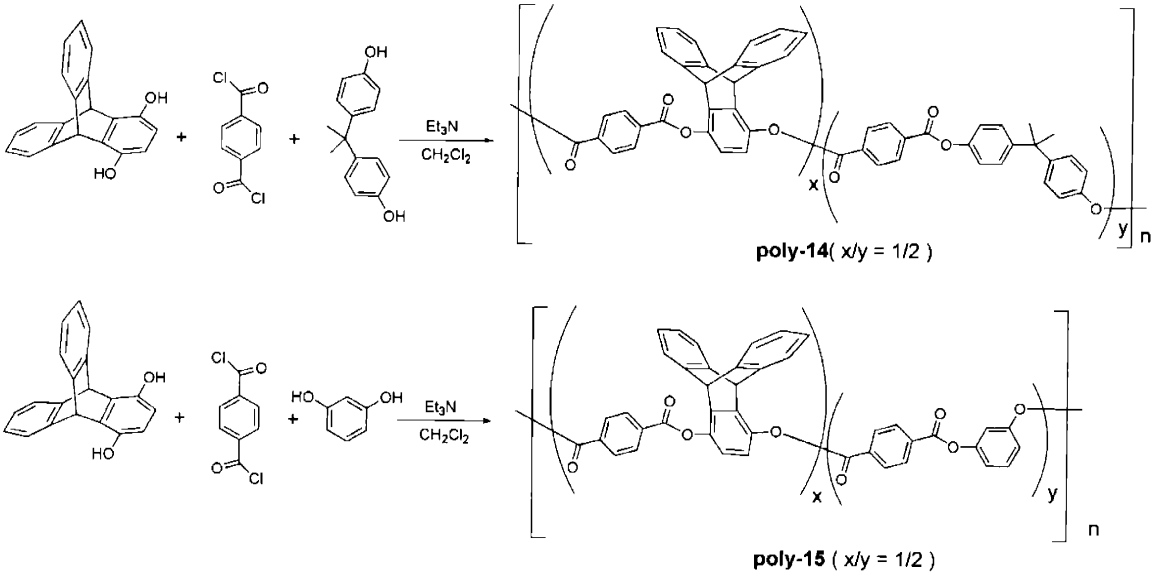

Scheme 8. Solution-phase synthesis of triptycene-containing polyesters.

The molecular weights and thermal behavior (as determined by GPC) for polymers **poly-1** through **poly-15** are compiled in Table 1.

As was mentioned previously, polymers **poly-1** and **poly-2** are extremely high melting and insoluble in common organic solvents. Incorporation of a flexible decanediol moiety changes the properties considerably. Polymers **poly-3** through **poly-8** (Scheme 4) are soluble in both THF and methylene chloride, though there is a definite trend; as we move from **poly-3** (with the greatest aliphatic content) to **poly-8** (with the least aliphatic content) the relative solubilities decrease in both solvents. Moving from **poly-3** through **poly-6** (increasing iptycene content) we see a fairly consistent decrease in the melting temperatures of the polymers, though the effect is not large. All of these polymers can be melt drawn in to fibers by heating just above the melting point and a bit of material out of the melt. These fibers were then used for the tensile tests described below. However, polymers with high triptcene content, such as **poly-7** and **poly-8** do not melt (aka- are not crystalline), but instead become rubbery above a visible glass transition, much like a cross-linked polymer. This may mean that these polymers have sufficiently high iptycene content to cause the polymer chains to be extremely amorphous and entangled.

Polymers **poly-9** and **poly-10**, which contain phenyl rings rather than triptycene units, have considerably higher melting points than tripycene-containing analogues **poly-4** and **poly-6** of similar molecular weights. Fibers of this material can also be pulled from the molten state. **Poly-11**, the copolymer of terephthaloyl chloride and 1,10-decanediol, has a higher melting point than any of the triptycene polymers of equivalent molecular weight. Polymer **poly-12** and pentiptycene containing polymer **poly-13**

become rubbery above their glass transition temperatures, indicating that they may be highly interlocked and amorphous; unfortunately, fibers of these materials have not yet been realized. Aromatic bisphenol-A polymer **poly-14** and catechol polymer **poly-15** exhibit extremely high melting points, despite possessing bent monomeric units in their chemical structures. However, they are quite soluble in solvents such as dichloromethane, THF and DMF.

Table 1. Molecular weights and thermal behavior of polymers **poly-1** through **poly-15**.

Polymer	M_n	M_w	PDI	T_g (°C)	T_m (°C)	T_{xtal} (°C)
Poly-1	n/a	n/a	n/a	-	> 350	-
Poly-2	5567	11055	1.99	130	> 350	-
Poly-3	15,080	31,172	2.07	-	113	79
Poly-4*	27,546	53,081	1.93	-	103	46
Poly-4*	61,505	133,310	2.17	-	128	106
Poly-5†	22,913	38,610	1.69	-	107	36
Poly-6*†	18,064	32,486	1.80	-	100	40
Poly-6*	40,325	75,531	1.87	-	96	44
Poly-7†	22,115	35,590	1.61	45	-	-
Poly-8†	21,195	43,035	2.03	58	-	-
Poly-9	32,010	61,929	1.93	-	121	103
Poly-10	31,850	61,968	1.94	-	139	110
Poly-11†	18,223	32,205	1.77	-	126	98
Poly-12	13,691	29,144	2.13	-	104	-
Poly-13	17,218	42,437	2.46	-	101	-
Poly-14	11,190	23,911	2.14	104	> 400	-
Poly-15	5,879	12,307	2.09	154	> 400	-

Molecular weights and polydispersities determined by GPC in THF eluent; **poly-2** was determined in DMF eluent. Thermal properties determined by DSC at 10 °C/min.
* Multiple batches of same chemical composition.
† DSC Measured by Neal Vannachi (Materials Science/ISN).

Stress-Strain and Modulus Measurements

The stress-strain measurements described in this section were measured by Nicholas Tsui in the laboratory of Ned Thomas (MIT Materials Science Dept and Institute for Soldier Nanotechnology) at the ISN facilities. These measurements were conducted on fibers that were drawn by hand from melts of the polymers. The conditions for fiber-formation were clearly not optimized; they were also not carefully controlled regarding draw-rate or temperature. Therefore, the results described in this section should be viewed as preliminary in nature, suggesting trends in behavior rather than describing absolute values of properties for the materials in question.

The most comprehesive testing was conducted comparing the triptycene polymer **poly-4** to the non-iptycene polymer **poly-9**. The two polymers are structurally identical with the exception that the triptycene unit in **poly-4** has been substituted with a phenyl ring in **poly-9**. This allows us to directly compare the polymers and determine the effect of iptycene incorporation upon the polymer properties. The two samples studied had nearly identical molecular weights and polydispersities, so that the effects can not be attributed to these causes. A comparison of the stress-strain curves of the two polymers is shown in Figure 9.

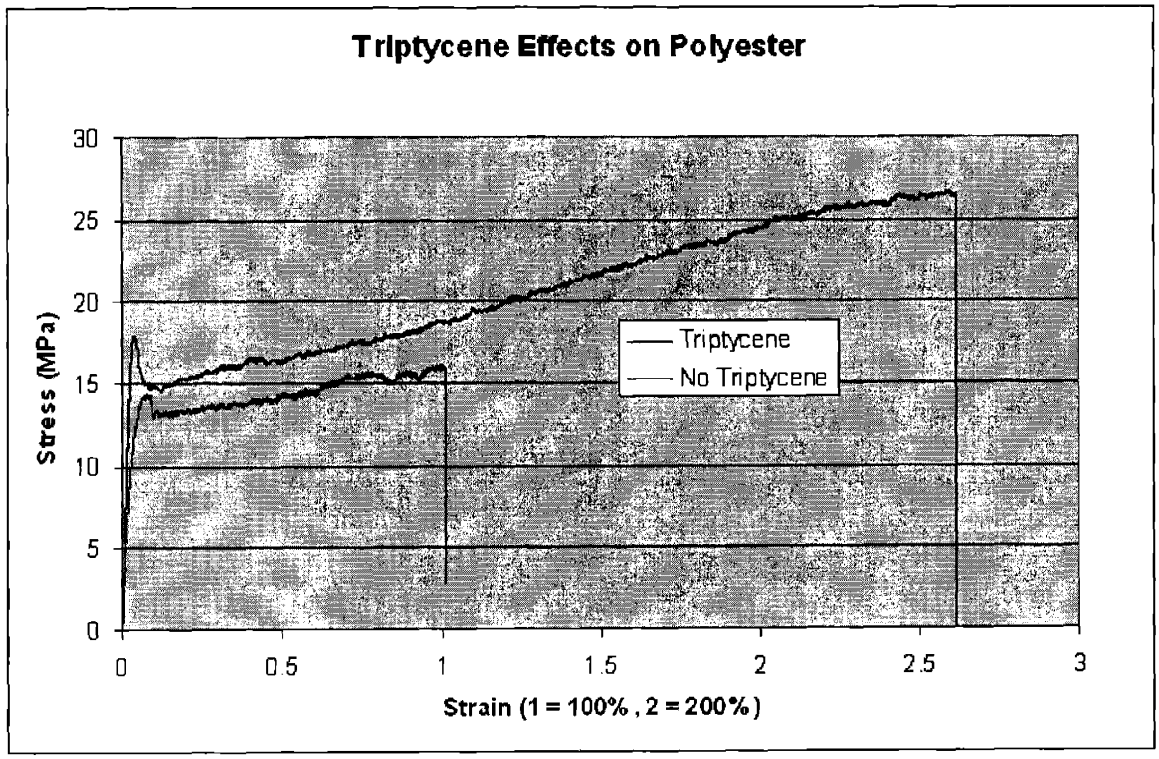

Figure 9. Stress strain curves of fibers of **poly-4** (triptycene) and **poly-9** (no triptycene). These values are the best values obtained for each polymer out of twenty fibers.

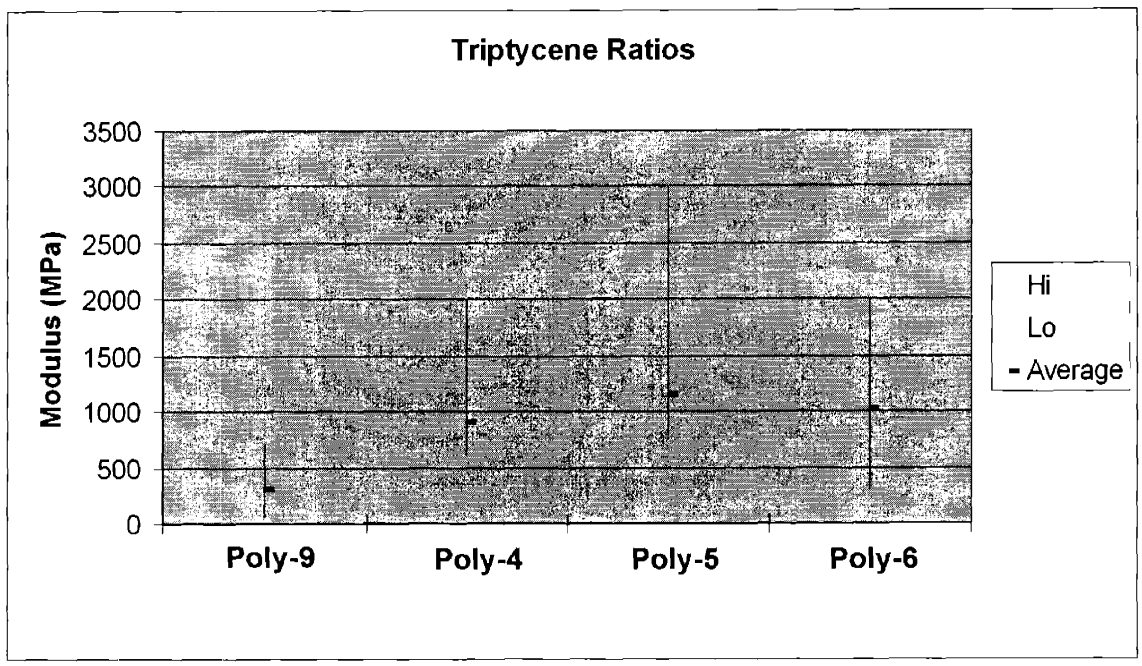

Figure 10. Distribution of Young's modulus values (high, low and average values) for poly(ester)s with varying ratios of triptycene (twenty fibers each).

The stress-strain studies show that all of the polymers are above their T_g's since they clearly exhibit steep linear behavior to start, followed by a yield point, after which the polymer stretches until it ultimately breaks. It would appear that there is some optimal amount of iptycene (in this case **poly-5** performs best) above or below which the properties decline (Figure 10). However, the iptycene polymers consistently outperform the non-iptycene polymers in several categories: 1) the yield strength, 2) the tensile strength, 3) the elongation, and 4) the Young's modulus (Figure 11). Triptycene polymer **poly-4** also demonstrated greater plastic strain recovery (12%) when stretched and then heated to 83 °C than non-triptycene polymer **poly-9** (7%). These results all suggest that triptycenes tend to increase the entanglement of polymer chains with each other.

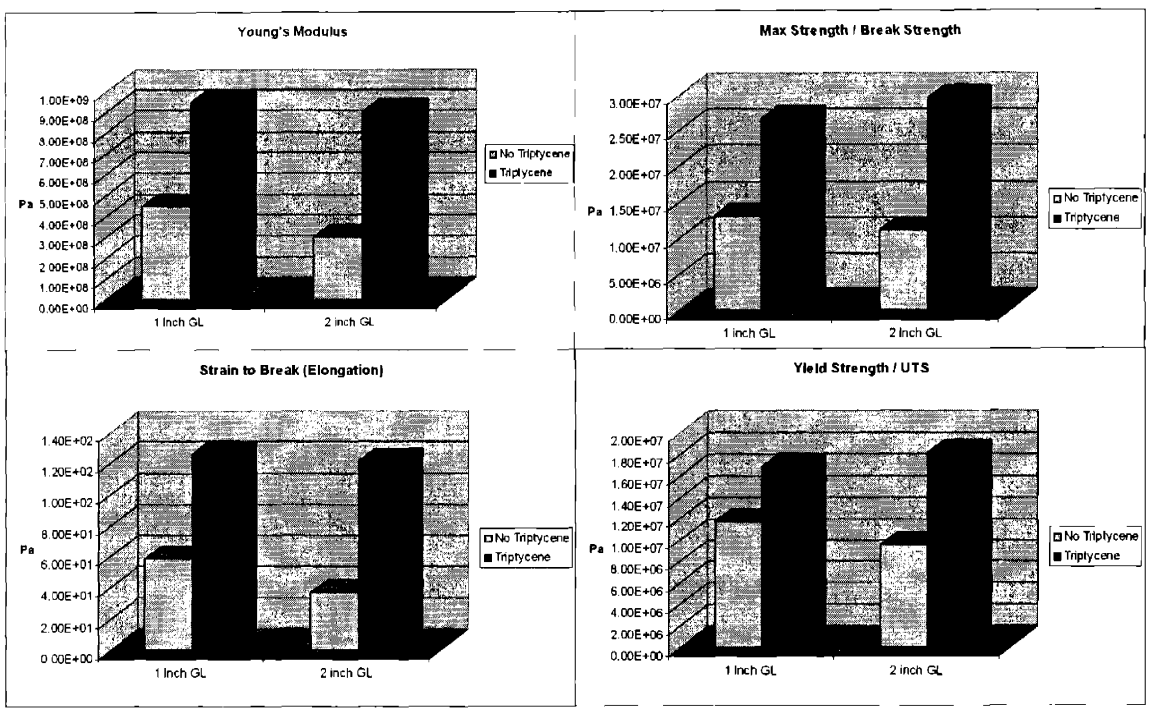

Figure 11. Comparisons of properties between triptycene-containing **poly-4** and non-iptycene **poly-9** for both 1-inch fibers and two-inch fibers. The values are averages of the tests of twenty fibers each. Iptycenes appear to enhance properties significantly.

It is also important to compare our polymers with commercial polymers such as Kevlar, nylon, PET, etc. to see how our polymers are performing. In general, we have not yet approached the realm of high-strength polymers. Kevlar, for example, exhibits a modulus of 115 GPa (elongation of 2.0%), while M-5 has a modulus of 330 GPa (elongation of 1.5%). The iptycene polymers are, however, in the same range with regard to tensile properties of some common commercial polymers (Figure 12).

It should be stressed that the tensile values of these poly(iptycene)s were obtained from samples that were only crudely processed by a rather uncontrolled and unoptimized melt-drawing process. Optimization of processing is an essential feature of most high-strength polymers, and so it is hoped that improvements in this area will result in much improved performance of these materials. We have recently found, for example, that it is possible to form drop-case films of these polymers from chlorinated hydrocarbons solvents, such as DCM and chloroform (Figure 13). Furthermore, it is entirely possible that the best way to form fibers of these materials is not by melt-drawing, but instead by wet-spinning, dry-spinning or one of the many other techniques for the formation of ordered fibers. From a chemical standpoint, future work will most likely focus on the exploration of other chemical structures with the hopes of improving the tensile characteristics of iptycene-based polymers. Ultimately, the strongest iptycene-containing polymers will very likely not be poly(ester)s, but instead more chemically robust polymers such as poly(amide)s or poly(carbonate)s.

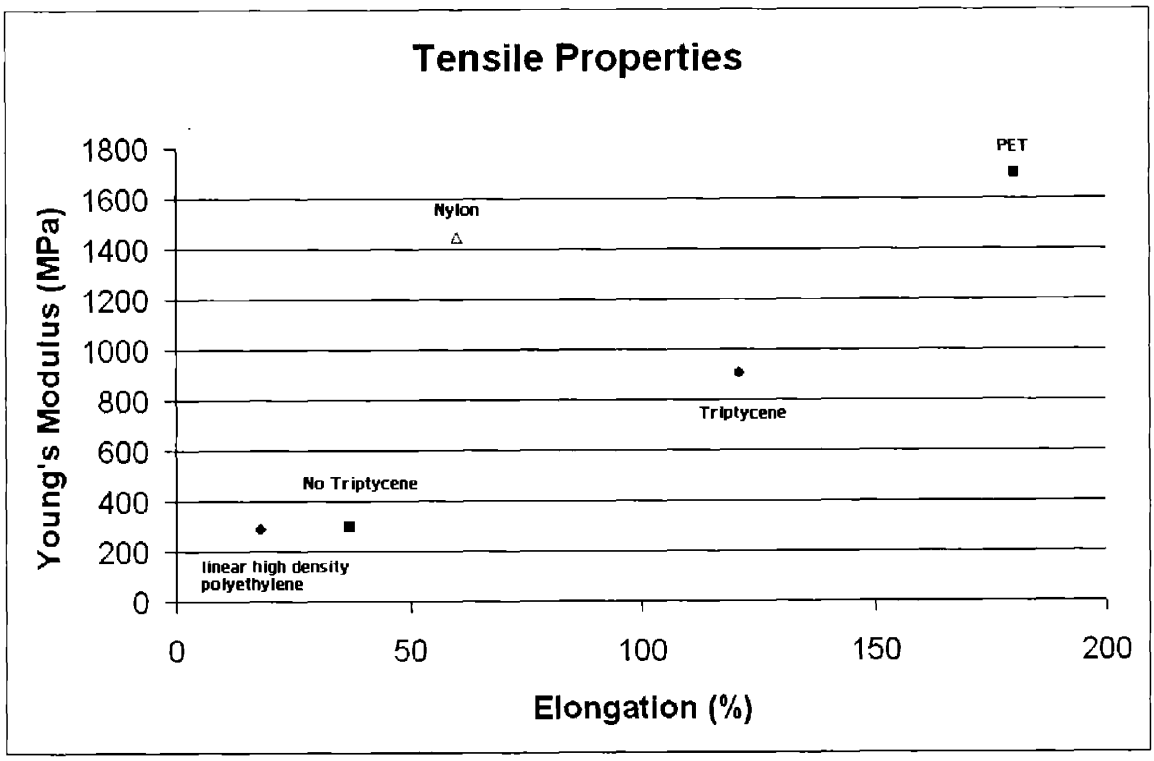

Figure 12. Comparison of the tensile properties of **poly-4** ("triptycene") and **poly-9** ("no triptycene") with LHDPE, Nylon 6, and PET.[28]

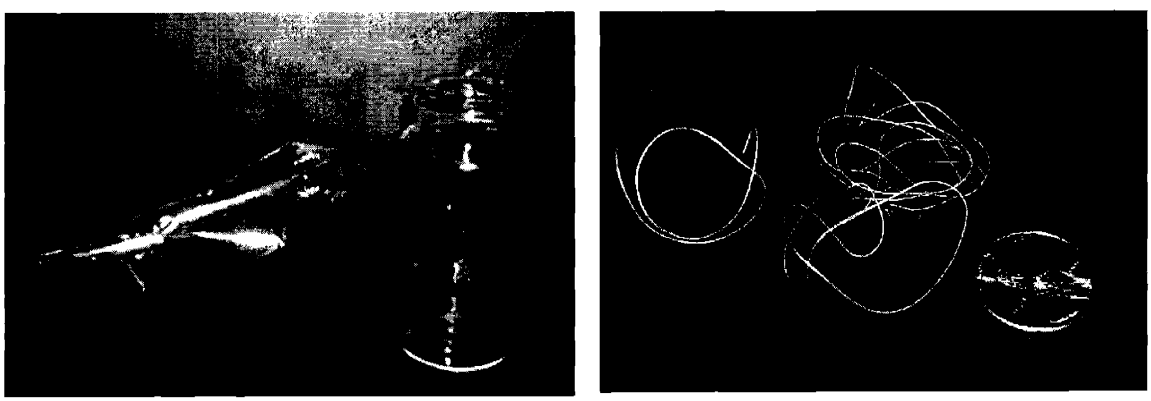

Figure 13. Iptycene polyester **poly-4** as a drop-cast film (left) and melt-drawn fibers (right). The film was drop-cast from a concentrated solution in dichloromethane.

Summary and Conclusions

The incorporation of triptycene units into poly(ester) frameworks can be accomplished by either melt polymerization or solution polymerization of suitable monomers. Preliminary results suggest that triptycene-containing polymers exhibit tensile properties which are greatly improved in comparison to analogous polymers which do not contain iptycenes. It is hoped that the incorporation of iptycenes into suitable polymeric frameworks will result in new high-strength polymers.

Experimental Section

General Methods

Dichloromethane and tetrahydrofuran (THF) were dried by passing through a column of activated alumina, unless otherwise specified. AcOH (glacial) was purchased from Mallinckrodt Baker and used as received. Terephthalyol chloride was donated by DuPont and was refluxed in $SOCl_2$ then dried in vacuo before use. Pyridine hydrochloride was purchased from Aldrich, recrystallized from $CHCl_3$ / EtOAc, washed with Et_2O and dried under vacuum before use. 1,4-Bis(trimethylsiloxy)benzene was synthesized from hydroquinone in a method procedure directly analogous to that of compound **2**; ^1H and ^{13}C NMR were identical to previously published values.[29] All other chemicals were purchased from Alpha Aesar and used as received. DSC was performed on a Perkin-Elmer TGA7 under nitrogen at a rate of 10 °C per minute. Polymer molecular weights were determined with a HP Series 1100 GPC in THF at room temperature versus polystyrene standards. ^1H NMR spectra were recorded on a Varian Unity VXR 500, a Bruker DPX-400, and a Varian Unity 300. Chemical shifts are reported in ppm relative to residual $CHCl_3$ (δ = 7.27, ^1H). Multiplicities are given as s

(singlet), d (doublet), t (triplet) and m (multiplet). MS investigations were run on a Finnigan MAT 8200 equipped with an Ion Tech ion source and a Bruker Daltonics Apex II 3T FT-ICR MS.

1,4-di(acetoxy)triptycene (1) Triptycene-1,4-hydroquinone (2.00 g, 6.99 mmol) was placed in a 50 mL schlenk flask with a magnetic stir bar. The flask was evacuated and backfilled with argon. Acetic anhydride (6 mL, 0.063 mmol) and dry pyridine (3 mL) were sequentially added via syringe. The reaction was heated to 100 ° C with stirring for 4.5 hours and then was allowed to cool to room temperature. The reaction was poured onto ice. Once the ice had melted, the resulting precipitate was collected by vacuum filtration, washed with water and dried overnight in vacuo (20 mTorr) yielding 2.47 g (6.67 mmol, 95%) of **1** as a white solid. ^{1}H NMR ($CDCl_3$, δ): 2.47 (s, 6H, CH_3COO), 5.45 (s, 2H), 6.77 (s, 2H), 7.01-7.04 (m, 4H, Ar-H), 7.37-7.39 (m, 4H, Ar-H). ^{13}C NMR ($CDCl_3$, δ): 20.99, 48.60, 119.44, 124.01, 125.46, 138.89, 143.03, 144.05, 169.04. IR (KBr): 3066, 3021, 2979, 2930, 1762, 1479, 1458, 1370, 1201. HRMS-EI (*m/z*): (M^+) calcd for $C_{24}H_{18}O_4$ 370.1200; found 370.1211.

1,4-di(trimethylsilyloxy)triptycene (2) Triptycene-1,4-hydroquione (29.32 g, 102.4 mmol) and imidazole (17.43 g, 256 mmol) were placed in a 2-necked 2 L flask with a magnetic stir bar. The flask was purged with argon and then 1 L of dry THF was added via cannula. Chlorotrimethylsilane (32.5 mL, 256 mmol) was added and the reaction was heated to reflux with stirring for 19 hours, when it was cooled to room temperature and filtered. The solvents were removed in vacuo and the remaining solid was filtered through two separate silica gel pads with CH_2Cl_2. Upon removal of the solvents, 43.07 g (100 mmol, 98%) of pure **2** remained as a white solid, which was dried under vacuum (20

mTorr) at 80 ° C overnight and brought before being used for polymerizations. ^{1}H NMR ($CDCl_3$, δ): 0.30 (s, 18H, TMSO), 5.70 (s, 2H), 6.35 (s, 2H), 6.96-6.99 (m, 4H, Ar-H), 7.36-7.39 (m, 4H, Ar-H). ^{13}C NMR ($CDCl_3$, δ): 0.58, 48.08, 117.00, 123.74, 124.82, 136.57, 144.36, 145.61. IR (KBr): 3065, 3022, 2956, 1583, 1480, 1255, 1009. HRMS-EI (*m/z*): (M^+) calcd for $C_{26}H_{30}O_2$ 430.1779; found 430.1768.

Compound 3. The cycloadduct of 1,4-naphthoquinone with anthracene (5.0 g, 14.9 mmol) was placed in a 100 mL round-bottom flask with a magnetic stir bar. Glacial acetic acid (50 mL) was added and the reaction was heated to reflux with stirring. Two drops of HBr (30 wt. % solution in acetic acid) was added and refluxing continued for 3 hours. The reaction was cooled to room temperature and the precipitate was collected, washed with hot water and dried in vacuo, yielding 3.75 g (11.2mmol, 75 %) of **3** as a slightly off-white solid.

Compound 4. Compound **3** (3.494 g, 10.39 mmol) and imidazole (1.77g, 25.96 mmol) were placed in a 250 mL Schlenk flask with a magnetic stir bar. The flask was evacuated and filled with argon. Dry tetrahydrofuran (100 mL) was added via cannula and then chlorotrimethylsilane (3.3 mL, 26 mmol) was added via syringe. The reaction was heated to reflux with stirring for 18 hours and then was allowed to cool to room temperature. Diethyl ether (100 mL) was added and the solution was filtered. The solvents were removed in vacuo and the remaining dark solid was purified by column chromatography with 2:1 hexane/ CH_2Cl_2 eluent. Upon removal of the solvents in vacuo, 2.43 g (5.05 mmol, 49 %) of **4** remained as a white solid. ^{1}H NMR ($CDCl_3$, δ): 0.40 (s, 18H, TMSO), 5.85 (s, 2H), 7.00-7.03 (m, 4H, Ar-H), 7.35-7.39 (m, 2H, Ar-H), 7.41-7.44 (m, 4H, Ar-H), 7.87-7.90 (m, 2H, Ar-H). ^{13}C NMR ($CDCl_3$, δ): 1.14, 48.06, 122.57, 123.86, 124.90,

125.20, 127.41, 129.45, 140.11, 144.95. IR (KBr): 3071, 3024, 2954, 2896, 1628, 1602, 1458, 1371, 1251, 1095, 1038, 894, 839, 752, 584. HRMS-EI (*m/z*): (M^+) calcd for $C_{30}H_{32}O_2Si_2$ 480.1935; found 480.1929.

Compound 5. Pentiptycene hydroquinone (2.030 g, 4.39 mmol) and imidazole (896 mg, 13. 17 mmol) were placed in a 100 mL Schlenk flask with a magnetic stir bar. The flask was evacuated and backfilled with argon. Dry THF (50 mL) was added via cannula and then chlorotrimethylsilane (1.70 mL, 13.4 mmol) was added via syringe. The reaction was heated to reflux with stirring for 18 hours and then was cooled to room temperature. The solvents were removed in vacuo and the remaining solids were dissolved in CH_2Cl_2 and pulled through a silica gel pad. The solvent was removed in vacuo yielding 1.79 g (2.95 mmol, 67 %) of **5** as a white solid. ^{1}H NMR ($CDCl_3$, δ): 0.41 (s, 18H, TMSO), 5.58 (s, 4H), 6.88-6.92 (m, 8H, Ar-H), 7.25-7.30 (m, 8H, Ar-H). ^{13}C NMR ($CDCl_3$, δ): 1.39, 48.45, 123.50, 124.78, 133.81, 140.51, 145.62. IR (KBr): 3065, 3021, 2956, 1460, 1301, 1260, 1194, 1111, 1019, 881, 845, 753, 551. HRMS-EI (*m/z*): (M^+) calcd for $C_{40}H_{38}O_2Si_2$ 606.2405; found 606.2426.

General Procedure for Melt Polymerizations In a dry box, 1,10-bis(trimethylsiloxy)decane were massed in a 50-mL Schenk flask, after which the appropriate ratios of bis(trimethylsiloxy)iptycene and terephthaloyl chloride were added. The flask was sealed with a septum, brought out of the glovebox, and attached to a vacuum/gas line under an argon atmosphere. The flask was heated to 155 ° C with stirring until all of the solids had melted (yellow liquid). Pyridine hydrochloride (20 mg)

was quickly added and the reaction was allowed to stir at 155 ° C for ten minutes. Another 20 mg of pyridine hydrochloride were added and the stirring was continued for one hour. During this time the flask was frequently vented by placing a needle through the septum under a while the reaction was under a positive pressure of argon. Another 100 mg of pyridine hydrochloride were added and the reaction stirred at 155 ° C for one additional hour after which it was heated to 170 ° C for one half hour. By this time the reaction had typically become quite viscous, and only a very slow stir rate was possible with a magnetic stirrer. The reaction was heated to 180 ° C and placed under vacuum overnight with slow stirring, after which it was cooled to room temperature, dissolved in dichloromethane, and precipitated into either methanol or ethanol. The white solid precipitates were collected by vacuum filtration and dried at 80 ° C in vacuo overnight. Yields were typically 94-100%.

Poly-3 Compound **2** (210 mg, 0.467 mmol, 1 eq), 1,10-bis(trimethylsiloxy)decane (1.638 g, 5.14 mmol, 11 eq), terephthaloyl chloride (1.138 g, 5.61 mmol, 12 eq). ^{1}H NMR ($CDCl_3$, δ): 1.27 (m, 132H), 1.66 (m, 44H), 4.21 (m, 44H), 5.42 (m, 2H), 6.89 (m, 1.83H), 6.96 (m, 4H), 7.29 (m, 4H), 8.03 (m, 40H), 8.14 (m, 2H), 8.34 (m, 2H), 8.52 (m, 0.18H)

Poly-4 Compound **2** (2.911 g, 7.760 mmol, 1 eq), 1,10-bis(trimethylsiloxy)decane (10.770 g, 33.800 mmol, 5 eq), terephthaloyl chloride (8.234 g, 40.559 mmol, 6 eq). 12.6 g of product was recovered preciptation from EtOH (96%). ^{1}H NMR ($CDCl_3$, δ): 1.34 (m, 72H), 1.80 (m, 24H), 4.34 (m, 20H), 4.42 (m, 4H), 5.51 (m, 2H), 6.94 (m,

1.66H), 7.03 (m, 4H), 7.36 (m, 4H), 8.11 (m, 20H), 8.29 (m, 2H), 8.41 (m, 2H), 8.60 (m, 0.33H)

Poly-5 Compound **2** (2.034 g, 4.720 mmol, 1 eq), 1,10-bis(trimethylsiloxy)decane (6.020 g, 18.890 mmol, 4 eq), terephthaloyl chloride (4.794 g, 23.616 mmol, 5 eq).

Poly-6 Compound **2** (5.016 g, 11.646 mmol, 1 eq), 1,10-bis(trimethylsiloxy)decane (11.133 g, 34.940 mmol, 3 eq), terephthaloyl chloride (9.458 g, 46.585 mmol, 4 eq). 15.49 g of product was recovered after precipitation from MeOH (100%). ^{1}H NMR ($CDCl_3$, δ): 1.34 (m, 36H), 1.78 (m, 12H), 4.38 (m, 9H), 4.12 (m, 3H), 5.51 (m, 2H), 6.95 (m, 1.5H), 7.02 (m, 4H), 7.35 (m, 4H), 8.10 (m, 12H), 8.28 (m, 2H), 8.42 (m, 2H), 8.58 (m, 0.5H).

Poly-7 Compound **2** (1.6256 g, 3.774 mmol, 1 eq), 1,10-bis(trimethylsiloxy)decane (2.4054 g, 7.549 mmol, 2 eq), terephthaloyl chloride (2.2988 g, 11.323 mmol, 3 eq). 3.815 g of product was recovered after precipitation from MeOH (99%). ^{1}H NMR ($CDCl_3$, δ): 1.37 (m, 24H), 1.79 (m, 8H), 4.35 (m, 5.3H), 4.42 (m, 2.6H), 5.51 (m, 2H), 6.95 (m, 1.3H), 7.03 (m, 4H), 7.36 (m, 4H), 8.11 (m, 6H), 8.28 (m, 2H), 8.42 (m, 2H), 8.60 (m, 0.66H)

Poly-8 Compound **2** (1.2863 g, 2.987 mmol, 1 eq), 1,10-bis(trimethylsiloxy)decane (951.7 mg, 2.987 mmol, 1 eq), terephthaloyl chloride (1.2127 g, 5.973 mmol, 2 eq). 2.0729 g of product was recovered after precipitation from MeOH (96%). ^{1}H NMR ($CDCl_3$, δ): 1.37 (m, 12H), 1.79 (m, 2H), 1.85 (m, 2H), 4.35 (m, 5.3H), 4.43 (m, 2H), 5.51 (m, 2H), 6.95 (s, 1H), 7.03 (m, 4H), 7.36 (m, 4H), 8.11 (m, 4H), 8.29 (m, 2H), 8.42 (m, 2H), 8.60 (m, 1H)

Poly-9 1,4-Bis(trimethylsiloxy)benzene (1.311 g, 5.150 mmol, 1 eq), 1,10-bis(trimethylsiloxy)decane (8.2056 g, 25.752 mmol, 5 eq), terephthaloyl chloride (6.274 g, 30.902 mmol, 6 eq). 8.53 g of product was recovered after precipitation from EtOH (94%). ^{1}H NMR ($CDCl_3$, δ): 1.42 (m, 60H), 1.78 (m, 20H), 4.35 (m, 20H), 7.32 (m, 3.8H), 8.10 (s, 20H), 8.20 (m, 4H), 8.27 (m, 4H), 8.38 (s, 0.16H).

Poly-10 1,4-Bis(trimethylsiloxy)benzene (2.572 g, 10.106 mmol, 1 eq), 1,10-bis(trimethylsiloxy)decane (9.661 g, 30.320 mmol, 4 eq), terephthaloyl chloride (8.207 g, 40.423 mmol, 4 eq). 11.36 g of product was recovered after precipitation from EtOH (97%). ^{1}H NMR ($CDCl_3$, δ): 1.34 (m, 36H), 1.78 (m, 12H), 4.35 (m, 12H), 7.32 (m, 3.5H), 8.10 (s, 12H), 8.22 (m, 4H), 8.28 (m, 4H), 8.37 (s, 0.5H).

Poly-11 1,10-Bis(trimethylsiloxy)decane (2.645 g, 8.301 mmol), terephthaloyl chloride (1.685 g, 8.301 mmol). 2.541 g of product was recovered after precipitation from MeOH (100%). ^{1}H NMR ($CDCl_3$, δ): 1.34 (m, 12H), 1.78 (m, 4H), 4.33 (t, 4H, J = 7.0 Hz), 8.10 (s, 4H).

Poly-12 Compound **4** (158 mg, 0.328 mmol, 1eq), 1,10-bis(trimethylsiloxy)decane (523 mg, 1.64 mmol, 5 eq), terephthaloyl chloride (400 mg, 1.97 mmol, 6 eq). ^{1}H NMR ($CDCl_3$, δ): 1.38 (m, 60H), 1.78 (m, 20H), 4.34 (m, 20H), 4.48 (m, 4H), 5.58 (m, 2H), 7.06 (m, 4H), 7.39 (m, 4H), 7.43 (m, 2H), 7.79 (m, 2H), 8.10 (m, 20H), 8.34 (m, 4H), 8.55 (m, 4H).

Poly-13 Compound **5** (200 mg, 0.330 mmol, 1eq), 1,10-bis(trimethylsiloxy)decane (525 mg, 1.65 mmol, 5 eq), terephthaloyl chloride (401 mg, 1.98 mmol, 6 eq). ^{1}H NMR ($CDCl_3$, δ): 1.38 (m, 60H), 1.78 (m, 17.7H), 1.87 (m, 3.3H), 4.34 (m, 17.7H), 4.46 (m, 3.3H), 5.37 (m, 4H), 6.94 (8H), 7.25 (8H), 8.10 (m, 16H), 8.38 (m, 4H), 8.55 (m, 4H).

Solution Polymerizations

Poly-14 Triptycene hydroquinone (100 mg, 0.349 mmol, 1 eq), bisphenol A (159 mg, 0.698 mmol, 2 eq) and terephthaloyl chloride (213 mg, 1.048 mg, 3 eq) were placed in a 50-mL Schlenk flask with a magnetic stir bar. The flask was evacuated and backfilled with argon. Dry CH_2Cl_2 (20 mL) was added via cannula. Dry Et_3N (3 mL) was added via syringe, which caused the tripycene hydroquinone to dissolve, and the reaction was stirred at room temperature for 24 hours. The solution was poured into MeOH (150 mL) and the precipitate was collected by vacuum filtration and dried in vacuo at 80 ° C overnight, yielding **poly-14** (362 mg, 92%) as a white solid. ^{1}H NMR ($CDCl_3$, δ): 1.22 (m, 8H), 1.59 (m, 4H), 6.98 (s, 2H), 7.18 (m, 8H), 7.35 (m, 8H), 8.32 (m, 8H), 8.47 (m, 4H).

Poly-15 Triptycene hydroquinone (260 mg, 0.908 mmol, 1 eq), catechol (200 mg, 1.816 mmol, 2 eq) and terephthaloyl chloride (553 mg, 2.724 mmol, 3 eq) were placed in a 50 mL Schlenk flask with a magnetic stir bar. The flask was evacuated, backfilled with argon. Dry CH_2Cl_2 (20 mL) was added via cannula. Dry Et_3N (3 mL) was added via syringe, which caused the tripycene hydroquinone to dissolve, and the reaction was stirred at room temperature for 24 hours. The solution was poured into MeOH (150 mL) and the precipitate was collected by vacuum filtration and dried in vacuo at 80 ° C overnight, yielding **poly-15** as a white solid. ^{1}H NMR ($CDCl_3$, δ): 5.56 (m, 2H), 6.99 (m, 8H), 7.39 (m, 8H), 8.38 (m, 12H).

References

(1) Bartlett, P.D; Ryan, M. J.; Cohen, S.G. *J. Am. Chem. Soc.* **1942**, *64*, 2649-2653.

(2) (a) Hart, H.; Shamoulilian, S.; Takehira, Y. *J. Org. Chem.*, **1981**, *46*, 4427. (b) Hart, H.; Bashir-Hashemi, A.; Luo, J. ; Meador, M.A. *Tetrahedron* **1986**, *42*, 1641.

(3) (a) Yang, J.-S.; Swager, T.M. *J. Am. Chem. Soc.* **1998**, *120*, 5321. (b) Yang, J.-S.; Swager, T.M., *J. Am.Chem. Soc.* **1998**, *120*, 11864.

(4) Long, T. M.; Swager, T. M. *Adv. Mater.* **2001**, *13*, 601-604

(5) Long, T. M.; Swager, T. M. *J. Am. Chem. Soc.***2002**, *124*, 3826-3827.

(6) Zhu, Z.; Swager, T. M. *J. Am. Chem. Soc.* **2002**, *124*, 9670-9671.

(7) Long, T. M. *Triptycenes as a Molecular Building Block to Introduce Internal Free Volume in Organic Materials.* Thesis (Ph. D.) – Massachusetts Institute of Technology, Dept. of Chemistry, 2002 (Chapter 4).

(8) Stevens, M. P. *Polymer Chemistry: An Introduction* Oxford University Press: New York, 1999; pp 364-390.

(9) Yang, H. H. *Aromatic High-Strength Fibers* Wiley-Interscience, New York, 1989; pp. 1-65.

(10) Allcock, H.; Lampe, F. W. *Contemporary Polymer Chemistry* Prentice-Hall, Inc., New Jersey, 1981; pp. 507-532.

(11) Kwolek, S. L.; Memeger, W.; Van Trump, J. E. in *Polymers for Advanced Technologies: IUPAC International Symposium* Lewin, M., Ed.: VCH, New York, 1988; 421-454.

(12) Yang, H. H. *Aromatic High-Strength Fibers* Wiley-Interscience, New York, 1989; pp. 227-268.

(13) Hounshell, D. A.; Smith, J. K. Jr. *Science and Corporate Strategy: DuPont R&D, 1902-1980* Cambridge University Press: Cambridge, 1988; 432.

(14) Tanner, D.; Fitzgerald, J. A.; Phillips, B. R. *Angew. Chem.* **1989**, *101,* 665-670.

(15) Yang, H. H. *Aromatic High-Strength Fibers* Wiley-Interscience, New York, 1989; pp. 1-65.

(16) Prevorsek, D. C. in *Polymers for Advanced Technologies: IUPAC International Symposium* Lewin, M., Ed.: VCH, New York, 1988; 557-579.

(17) Carothers, W. H. *J. Am. Chem. Soc.* **1929**, *51*, 2548-2559.

(18) Stevens, M. P. *Polymer Chemistry: An Introduction* Oxford University Press: New York, 1999; pp 1-31.

(19) Stevens, M. P. *Polymer Chemistry: An Introduction* Oxford University Press: New York, 1999; pp 285-307.

(20) a) Braun, D.; Cherdron, H.; Ritter, H. *Polymer Synthesis: Theory and Practice* Springer- Verlag: Berlin, Heidelberg, 2001; pp 211-215. b) Allcock, H.; Lampe, F. W. *Contemporary Polymer Chemistry* Prentice-Hall, Inc., New Jersey, 1981; pp. 262-264.

(21) a) Stevens, M. P. *Polymer Chemistry: An Introduction* Oxford University Press: New York, 1999; pp 35-59. b) Yang, H. H. *Aromatic High-Strength Fibers* Wiley-Interscience, New York, 1989; p 227.

(22) a) Tanaka, T. *Experimental Methods in Polymer Science: Modern Methods in Polymer Research and Technology*; Academic Press, San Diego, 2000. b) Hiemenz, P. C. *Polymer Chemistry: The Basic Concepts*; Marcel Dekker, Inc., New York, 1984; pp 659-716. c) Allcock, H.; Lampe, F. W. *Contemporary Polymer Chemistry* Prentice-Hall, Inc., New Jersey, 1981; pp. 331-372.

(23) a) Flory, P. J. *Chem. Rev.* **1946**, *39*, 137-197. b) Allcock, H.; Lampe, F. W. *Contemporary Polymer Chemistry* Prentice-Hall, Inc., New Jersey, 1981; pp. 257-261.

(24) Snyder, L.R.; Kirkland, J. J. *Introduction to Modern Liquid Chromatography* John Wiley & Sons, Inc., New York, 1979;483-540.

(25) a) Ricks, H. L.; Choudry, U. H.; Marshall, A. R.; Bunz, U. H. F. *Macromol.* **2003**, *36*, 1424-1425. b) Rader, H. J.; Spickermann, J.; Kreyenschmidt, M; Müllen, K. *Macromol. Chem. Phys.* **1996,** *197*, 3285-3296.

(26) This procedure was adapted from a similar procedure for the formation of hyperbranched polyesters: Yamaguchi, N.; Wang, J.-S.; Hewitt, M.; Lenhart, W.C.; Mourey, T.H. *J. Poly.Sci.Part A: Poly. Chem.* **2002**, *40*, 2855-2867.

(27) Patney, H.K. *Synthesis* **1991**, 694-695.

(28) Values from: *Polymer Data Handbook*; Mark, J. E., Ed.; Oxford University Press: New York, 1999. Available online at: http://www.oup-usa.org/pdh/

(29) Stewart, R. F.; Miller, L. L. *J. Am. Chem. Soc.* **1980**, *102*, 4999-5003.

Chapter 7

Mesogen/Main-Chain Coupled Polymers by Ring-Opening Metathesis Polymerization (ROMP)

Introduction

Previous chapters discuss the properties of liquid-crystalline systems in general (Chapter 1) and certain thiophene-based (Chapters 2 and 3) and quinone-containing discotic (Chapter 4) liquid crystals in detail. This chapter describes our attempts to create liquid-crystalline polymer systems in which the liquid crystal moiety is intimately coupled to the main-chain of the polymer without fitting into the category of formal main-chain liquid crystalline polymers.

Liquid Crystal Polymers (LCPs)

It is well known that certain polymers display liquid-crystalline behavior. These polymers exhibit ordered fluid states that are directly analogous to the liquid crystalline states of small molecule liquid crystals discussed in Chapter 1. Liquid crystalline polymers are extremely useful as the LC state can impart various properties to the material such as high tensile strength (see Chapter 6) and decreased melt viscosity.[1]

Most rationally designed liquid crystalline polymers simply incorporate a mesogenic unit into the polymeric structure. The presence of the mesogenic group then drives the formation of the liquid crystal phases. Most liquid crystal polymers fall into one of two categories, depending on how the mesogenic moiety is linked to the polymer chain: main-chain or side-chain (Figure 1).

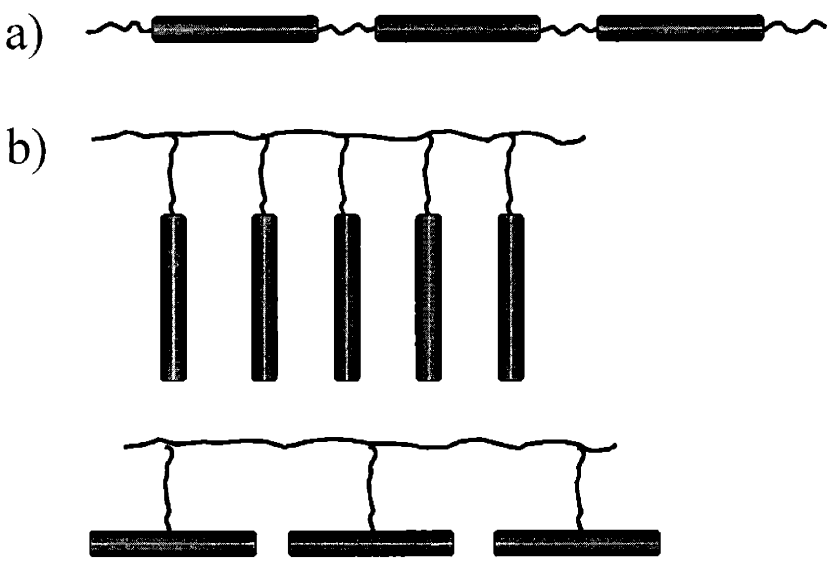

Figure 1. Liquid crystal polymers (LCPs) typically are characterized as (a) main-chain liquid crystal polymers (MCLCPs) or (b) side-chain liquid crystal polymers (SCLCPs). Mesomorphic units are represented graphically by the rigid rods.

Main-chain LC polymers (MCLCPs) are those in which the mesogenic unit is incorporated directly into the polymer chain. By definition, the polymer main chain tends to be highly ordered in the LC phases of MCLCPs. Chiral MCLCP's are additionally capable of exhibiting ferroelectric ordering (see Chapter 1).[2] Aromatic main-chain LCP's such as Kevlar (a polyaramid) and Vectra (a polyester) are discussed in Chapter 6 of this thesis; in both cases, the rigidity of the polymer backbones, combined with the high degree of order introduced by fiber drawing from the liquid crystalline states of the polymers, result in materials of extremely high strength. Chemical structures of representative main-chain liquid crystalline polymers are shown in Figure 2.

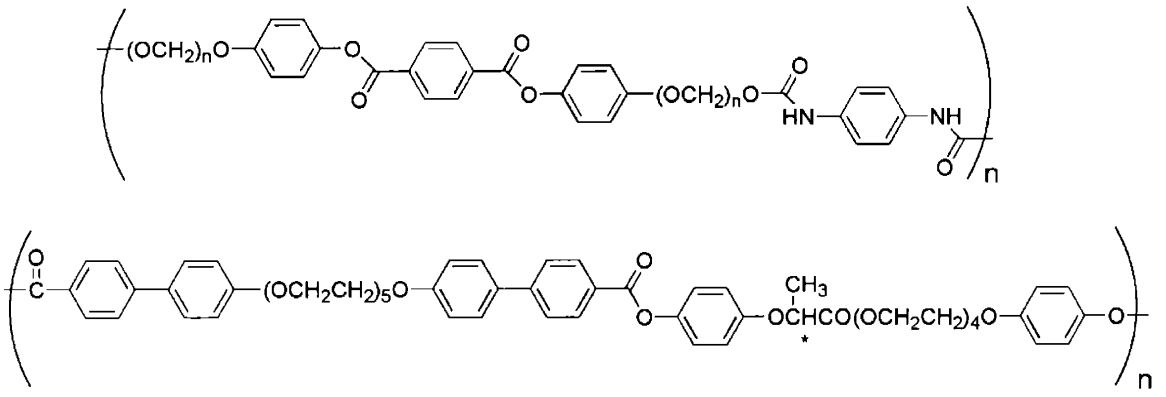

Figure 2. Main-chain LCP's which display nematic (top) and ferroelectric SmC* (bottom) mesophases.

Polymers in which the mesogenic groups are appended from the backbone by a flexible spacer unit are known as side-chain liquid crystalline polymers (SCLCPs). The size of the flexible spacer can strongly influence the liquid crystallinity of the resulting polymers and typically the use of a longer flexible spacer is preferable.[3] The main chains of SCLCPs are often disordered even within the LC phases, as the mesomorphic units are more or less free (depending on the spacer length) to orient themselves independently of the main chain. Shown in Figure 3 is a polyacrylate SCLCP synthesized by cationic polymerization[4] and a polynorbornene synthesized by ring-opening metathesis polymerization.[5] Both of these particular SCLCP's consist of rod-like (calamitic) molecules appended to the main chain through a flexible spacer. The polyacrylate organizes into lamellar (Sm_A and Sm_C) mesophases upon heating, while the ROMP polymer displays a nematic phase.

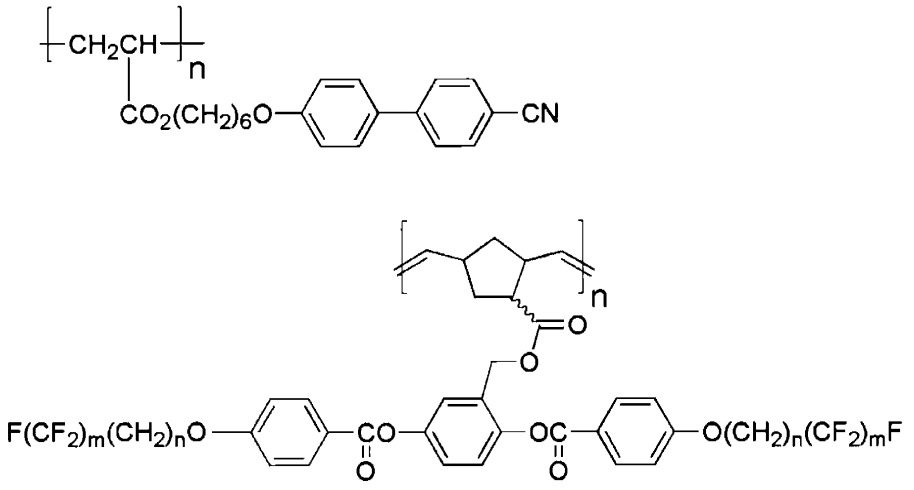

Figure 3. Side-chain LCP's which display SmA and SmC (top) and nematic (bottom) mesophases. The polymers were synthesized by cationic and ring-opening metathesis polymerizations, respectively.

Discotic liquid crystals, particularly triphenylene-based mesogens, have also been incorporated into both main-chain and side-chain LCP's. The main-chain triphenylene LCP's tend to exhibit discotic nematic or hexagonal columnar phases, depending on the specific polymeric structure and length of the spacer unit (Figure 4).[6] Side-chain triphenylene liquid crystalline polymers typically exhibit discotic hexagonal mesophases (Figure 5).[7]

Early models of SCLCP's by Finkelman et al suggested that flexible spacer moieties of sufficient lengths were necessary in order to lead to liquid crystalline order.[8] It was thought that the ability of the mesogenic groups to orient anisotropically is hindered in SCLCP's with insufficiently long spacer groups due to the tendency of the flexible main chain to orient statistically above the polymer's glass transition temperature. Ringsdorf therefore proposed the flexible spacer as a way to decouple the

order of the mesogens from the disorder of the polymer main chain, leaving them free to organize and orient themselves.[8]

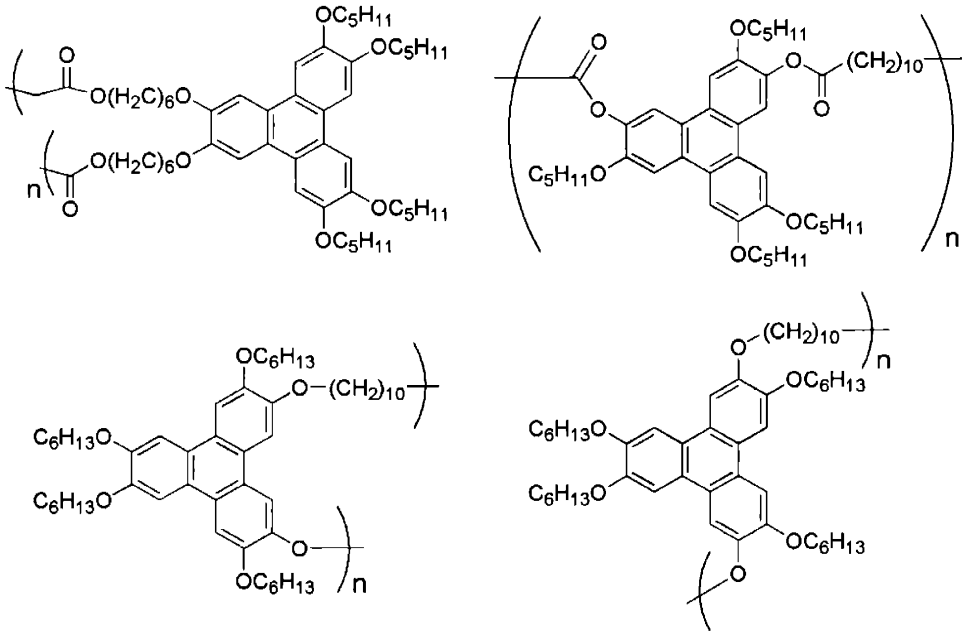

Figure 4. Previously reported triphenylene main-chain polyester and polyether LCP's.

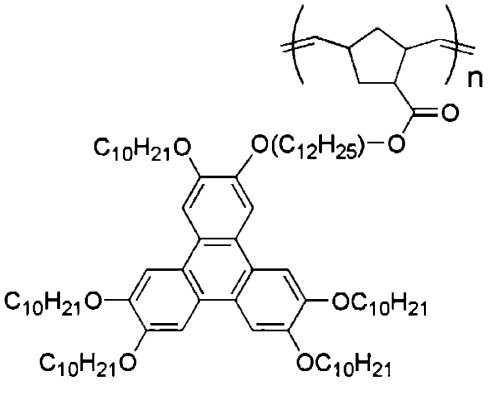

Figure 5. Previously reported triphenylene side-chain LCP synthesized by ring-opening metathesis polymerization.

SCLCP's in which the mesogens are coupled directly to the main chain do exist, however, and were known even before the proposal of the flexible spacer.[9] Since then, polymers have been described which actually blur the line between main-chain and side-chain LCP's, particularly the "mesogen-jacketed LCP's" of Zhou et al.[10] These "MJLCP's" are resemble side-chain polymers, but the mesogenic groups are attached laterally to the main chain without flexible spacers. The rigid mesogenic units form a "jacket" around the polymer backbone, forcing the main chain into an extended conformation and increasing its rigidity. Examples of the polymers studied by Zhou et al are illustrated in Figure 6. They found that these polymers exhibited extremely stable nematic phases that did not isotropize before their decomposition at above 300 °C. No smectic mesophases were found, as is often found for SCLCP's with short spacers. However, the high thermal stabilities of the MJLCP's are similar to main-chain LCP's. In addition, the chain rigidity and persistence lengths (between 11.5 and 13.5 nm in solution) of these polymers were found to be quite high, closer to those of most main-chain LCP's than side-chain LCP's.

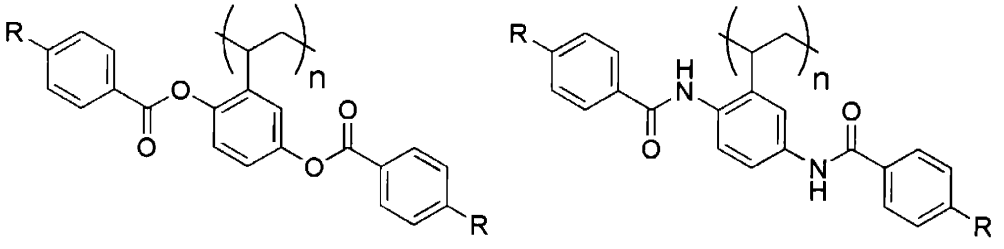

Figure 6. The general scheme of the "mesogen-jacketed" LCP's described by Zhou et al.

This chapter describes our efforts towards creating LCP's which are similar to these mesogen-jacketed LCP's, but differ in that they are coupled even more strongly to the main-chain. The general strategy is based upon a strategy which utilizes ring-opening metathesis polymerization (Figure 7). Though ROMP has been used to sythesize LCP's before, the polymers have differed structurally in that there has always been some length of flexible spacer between the polymer main-chain and the mesogenic side groups.[11] In our system the mesogen is fused to the polymer by a two-point attachment which further couples the orientation of the LC and the polymer backbone.

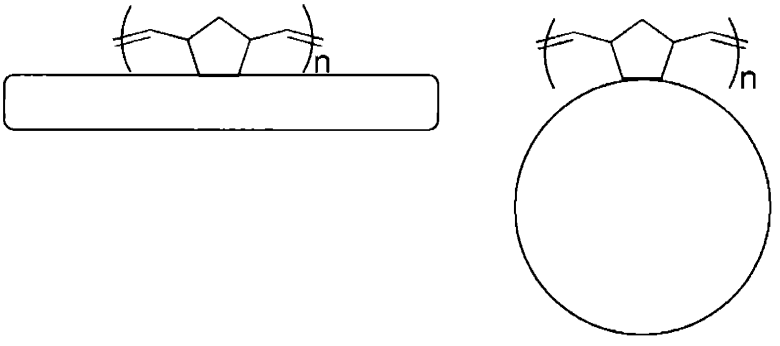

Figure 7. The general scheme of the polymers described in this chapter. Either rigid-rod (left) or disc-shaped (right) mesogens are covalently bound and tightly associated to the main chains of the polymers, which are synthesized by ring-opening methathesis polymerization.

Ring-Opening Metathesis Polymerization (ROMP)

Ring-opening metathesis polymerization is a highly efficient method for the preperation of high molecular weight polymers through a living polymerization that utilizes the ring-strain of bicyclic monomers to drive the reaction forward. The most successful catalytic systems for ROMP are the tungsten-based and molybdenum-based catalysts of Schrock and the ruthenium-based catalysts of Grubbs (Figure 8). In addition to ROMP, representatives from the tungsten, molybdenum and ruthenium catalysts have been shown to effect acyclic diene metathesis (ADMET) polymerization,[12] and the ruthenium-based systems are able to effect ring-closing metathesis as well.[13]

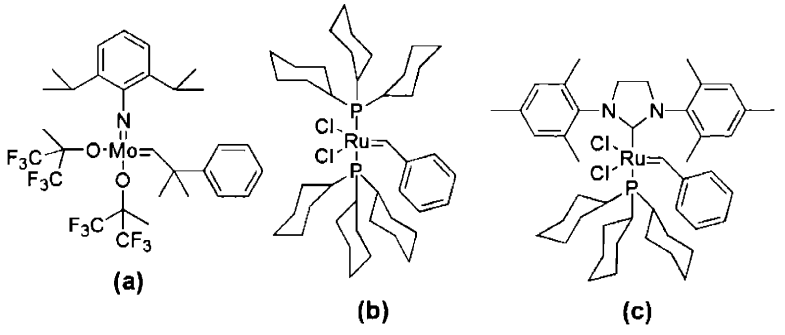

Figure 8. Popular catalysts for ROMP catalysis: (a) Schrock's molybdenum alkylidene (b) Grubb's "1st generation" and (c) "2nd generation" ruthenium benzylidine catalysts.

Each of the catalytic systems has advantages. The tungsten and molybdenum based catalysts are extremely active, but are sensitive to oxygen, moisture and certain functional groups.[14] The ruthenium catalysts are often less reactive, but are generally far more tolerant of the presence of functional groups,[15] and in our hands proved more convenient for the preparation of our polymers.

The ROMP mechanism of the ruthenium-based Grubbs' 1st generation catalyst $(PCy_3)_2PhCHRuCl_2$ begins with the dissociation of one of the phosphine ligands, which is why subsequent generations of Grubbs' catalysts include bulky electron-donating groups in place of one of the phosphine groups.[16] The phosphine typically reassociates to the reactive species after only a few cycles, attenuating the propagation rate. The dissociated complexes coordinate olefins, undergo a [2+2] cycloaddition and subsequently ring-open to generate catalytic metal-alkylidine species (Scheme 1).[17] Addition of excess phosphine is often used in order to decrease the propagation rate to the point that the polymerization becomes "living" and yields polymers of extremely narrow polydispersity indices.[18]

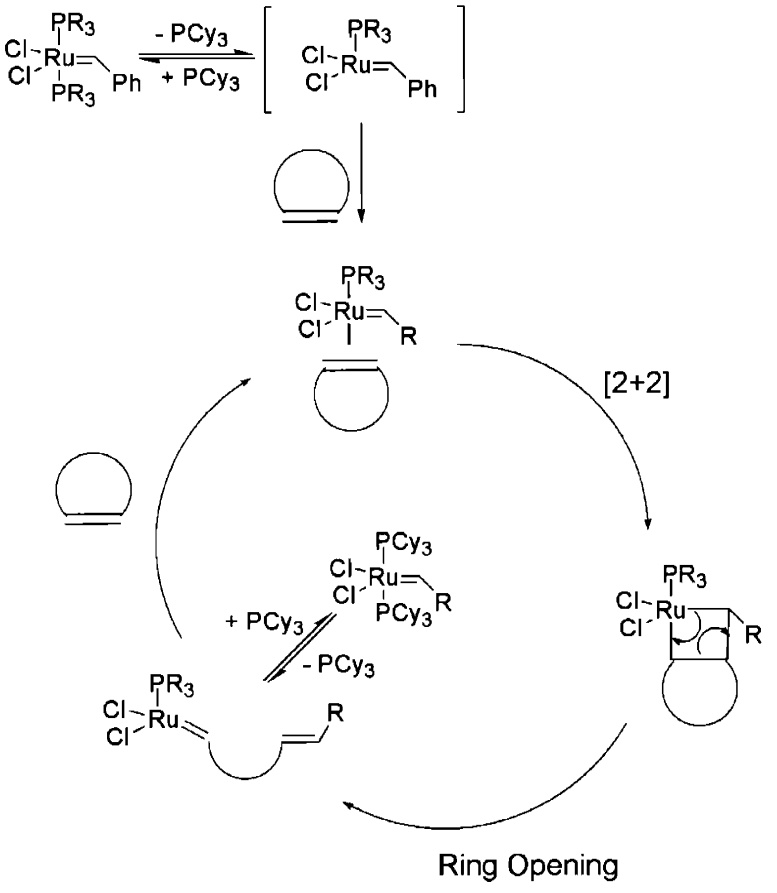

Scheme 1. Mechanism of ROMP via Grubbs' 1st generation ruthenium initiator.

Results and Discussion

Synthesis

We took two general approaches in our attempts towards synthesizing liquid-crystalline polymers with their mesogenic units intimately coupled to the main chain, both of with ultimately were designed to undergo polymerization by ring-opening metathesis, as outlined above. The first approach (Scheme 2) begins with the discotic liquid crystal compound **1**, the synthesis of which was discussed in Chapter 4 of this

thesis. Compound **1** undergoes facile [4+2] cycloaddition with cyclopentadiene to give Diels Alder adduct **2** in nearly quantitative yield. Compound **2** can be deprotonated with sodium hydride and subsequently methylated with dimethyl sulfate yielding extended triphenylene compound **3,** possessing a strained bicyclic ring. Ring-opening metathesis polymerization of this compound with Grubbs' "second generation" catalyst in dichloromethane yields polymer **poly-1**, which can subsequently be hydrogenated using *p*-tosyl hydrazide in refluxing xylenes to give **poly-2**, which possesses a slightly more flexible saturated polymer backbone.

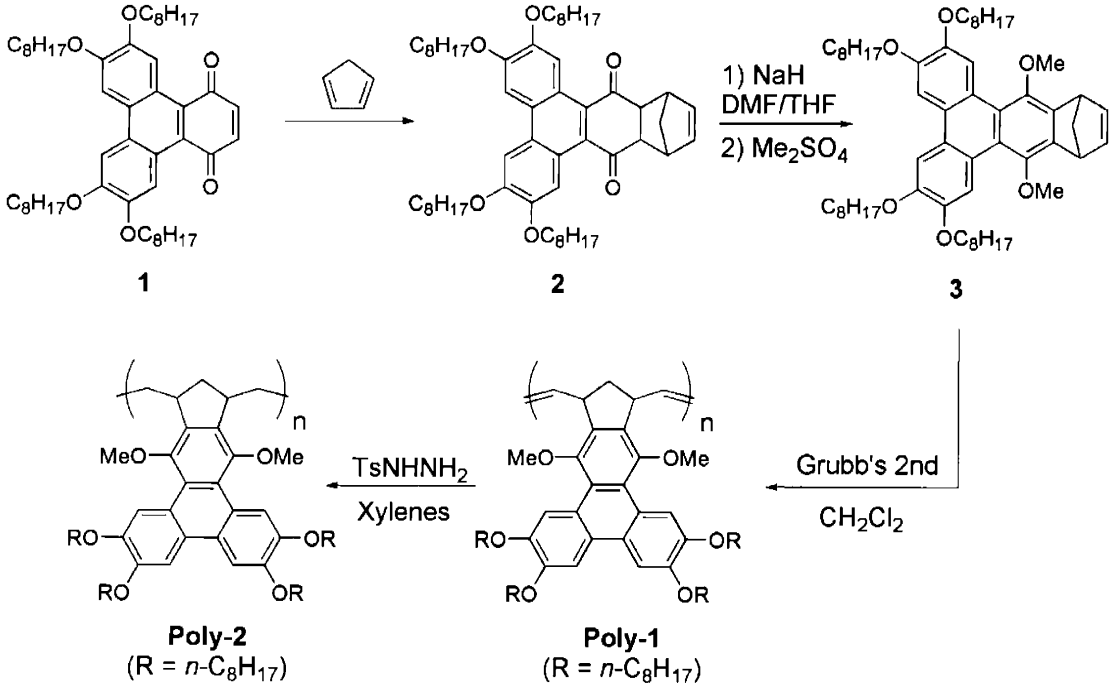

Scheme 2. Synthesis of discogen-containing ROMP polymers **poly-1** and **poly-2**.

Polymer **poly-3**, which differs from **poly-1** in that there is an oxygen atom incorporated within the polymer backbone, can be synthesized through a slightly different

route (Scheme 3). Compound **4** (synthesis described in Chapter 4 of this thesis) can be brominated selectively at the least sterically unhindered carbon atoms with 2 equivalents of elemental bromine in dichloromethane affording **5** in 82% yield after chromatography. Bromination with NBS (2 eq in dichoromethane) was also tried, but surprisingly this reaction was slightly less selective, and a mixture of mono-, di- and tribrominated products were obtained as determined by ^{1}H NMR and mass spectrometry. Addition of phenyllithium to **5** in THF results in formation of the benzyne species. If the above reaction is run in the presence of excess furan, the benzyne and furan undergo cycloaddition, yielding compound **6** in 89% yield after chromatography. Compound **6** then undergoes ring-opening polymerization with Grubb's second generation catalyst in dichloromethane, yielding **poly-3** with reasonably low polydispersities.

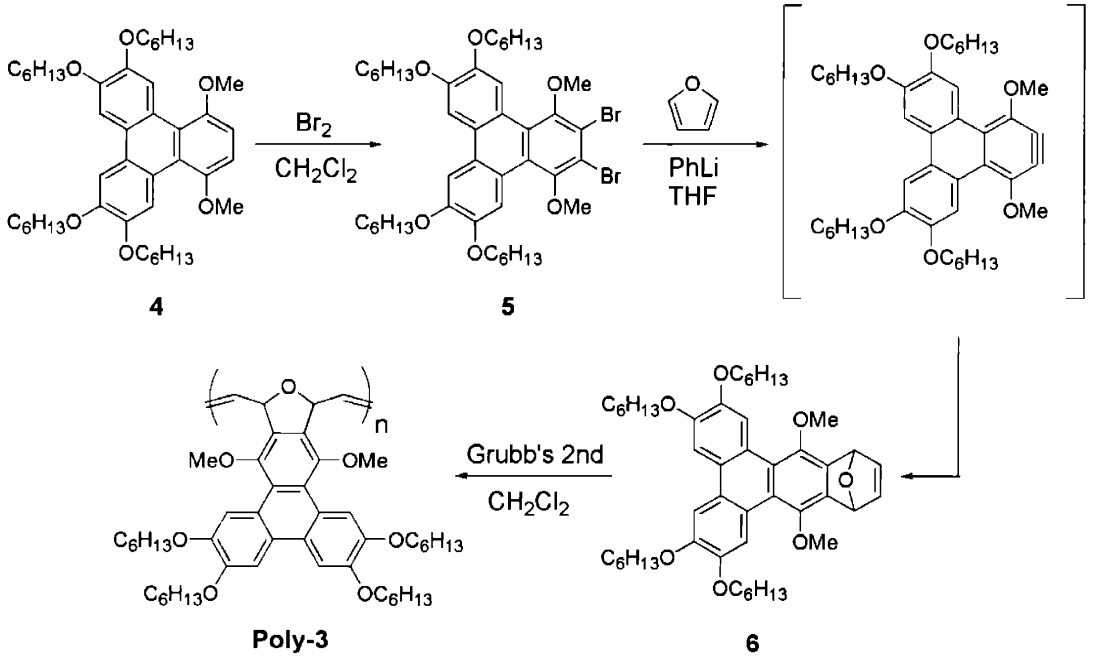

Scheme 3. Synthesis of ROMP-derived polymer **poly-3**.

Our second approach to liquid crystalline polymers focused on incorporating a classical linear (calamitic) liquid crystal into our system. In this case, we started with the Diels-Alder reaction of *p*-quinone and cyclopentadiene (Scheme 4). The cycloadduct was then tautomerized to dihydroquinone compound **7** through a method developed by Swager graduate student Hyun A. Kang. Esterification of **5** with the appropriate 4-(alkoxy)benzoate in the presence of dimethylaminopyridine and diisopropylcarbodiimide yields compounds **8** and **9** in moderate yields. These strained bicyclic compounds undergo ring-opening metathesis with Grubbs' second generation catalyst in dichloromethane to yield polymers **poly-4** and **poly-5**, which possess *n*-octyloxy and hydrogenated (*S*) citronellyl side groups, respectively.

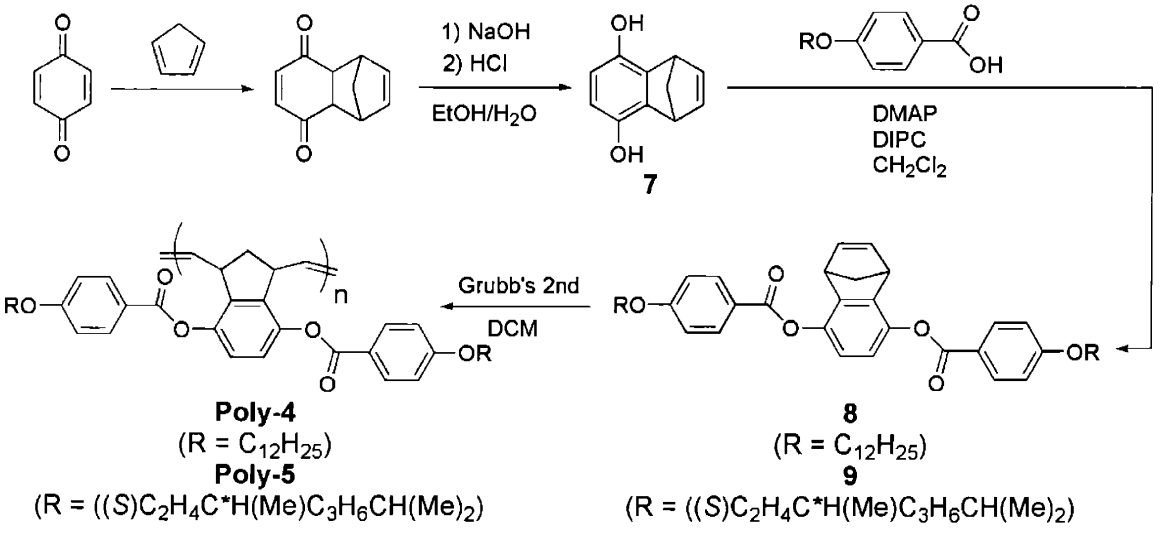

Scheme 4. Synthesis of calamitic mesogen-containing polymers **poly-4** and **poly-5**.

Table 1. Physical Characterization of Polymers Poly-1 to Poly-5.

Polymer	M_n[a]	PDI	T_g	T_m
Poly-1	**101,010**	**1.30**	**-**	**236**
Poly-2	**105,220**	**1.50**	**-**	**82**
Poly-3	**57,446**	**1.37**	**-**	**130**
Poly-4	**420,830**	**4.58**	**-**	**155**
Poly-5	**592,180**	**1.85**	**-**	**128**

[a] Molecular weights determined by gel permeation chromatography in reference to polyethylene standards.

Unfortunately, none of the polymers described above display liquid crystalline phases. It would appear that this extremely rigid two-point linkage of the mesogen to polymer backbone results in systems in which the mesogens do not possess the necessary freedom of motion to impart liquid crystallinity to the polymer as a whole. Even **poly-2**, in which the polymer backbone has been hydrogenated, does not display LC behavior, though it's melting point is significantly depressed relative to parent polymer **poly-1**. Perhaps if more powerful mesogenic groups (greatly extended aromatics or calamitics) were incorporated they could overcome the extreme rigidity of the system, resulting in liquid-crystalline polymers.

In an effort to induce liquid crystallinity in polymers **poly-1** through **-5**, contact samples were prepared with electro-deficient aromatic molecules 2,4-dinitrotoluene and 2,7-dinitro-9-fluorenone. The polymer was placed on a glass slide next to the electron deficient aromatic and melted at high temperature so that the two came in contact. TNF and DNT have been shown to induce liquid crystallinity in non-mesomorphic (both

discotic and calamitic) compounds.[19] We had hoped that these electron-deficient molecules would similarly induce liquid crystallinity within the polymers by strongly associating with the relatively electron-rich pendant moieties, thereby increasing the tendency toward stacking and order between polymer chains. However, no increase in the molecular order was detected by polarized microscopy and the polymers remained amorphous in nature.

Summary and Conclusions

A number of mesogen-containing polymers were prepared by ring-opening metathesis polymerization (ROMP). These polymers are unique in that the molecular design results in a two-point attachment of the mesogens directly to the polymer main-chain, intimately coupling them. The polymers investigated did not show liquid-crystalline behavior, probably due to the strong tendency of the polymer backbone to adopt statistical orientations. It might be possible to overcome this effect by the incorporation of mesogens with stronger tendencies to organize than those described here.

Experimental Section

Cyclopentadiene was freshly cracked and distilled from dicyclopentadiene prior to use. Dimethylformamide (DMF) was dried over 4 Å molecular sieves and stored in an air-tight pot. Dichloromethane and tetrahydrofuran (THF) were dried by passing through a column of activated alumina, unless otherwise specified. *Para*-tosyl hydrazide was purchased from Aldrich and used as received. All other chemicals were purchased from Alpha Aesar and used as received. Air and water sensitive reactions employed standard Schlenk techniques under argon atmosphere. NMR spectra were obtained on Varian

Mercury-300, Bruker DPX-400 or Varian Inova-500 spectrometers. All chemical shifts are referenced to residual $CHCl_3$ (7.27 ppm for ^1H, 77.0 ppm for ^{13}C). Multiplicities are indicated as s (singlet), d (doublet), t (triplet), and m (multiplet). High resolution mass spectra were obtained at the MIT Department of Chemistry Instrumentation facility (DCIF) on a Finnigan MAT 8200 or on a Bruker Daltonics Apex II 3T FT-ICR MS. Infrared spectra were recorded on a Perkin-Elmer 1760-X FTIR in KBr pellets. DSC was performed on a Perkin-Elmer TGA7 under nitrogen at a rate of 10 °C per minute. Polymer molecular weights were determined with a HP Series 1100 GPC in THF at room temperature versus polystyrene standards.

Compound 2. Compound **1** (11.83g, 15.34mmol) was placed in a 1L flask with a stir bar and dissolved in 600mL of undried CH_2Cl_2. Freshly cracked cylcopentadiene (8.5mL, 7.1g, 107mmol) was added over approximately 60 seconds and the reaction was stirred at room temperature with the exclusion of light for 11 hours. The solvents were removed in vacuo and the remaining yellow solids were placed on a high vacuum line (20 mTorr) for 5 hours. At this time ^1H NMR showed complete conversion to pure product. ^1H NMR ($CDCl_3$, δ): 0.88-0.93 (m, 12H, CH_3), 1.30-1.61 (m, 40H), 1.67 (s, 1H), 1.74 (s, 1H), 1.83-2.01 (m, 8H, CH_2), 3.58 (s, 2H), 3.70 (s, 2H), 4.14-4.28 (m, 8H, CH_2O), 6.18 (s, 2H), 7.75 (s, 2H), 8.31 (s, 2H). ^{13}C NMR ($CDCl_3$, δ): 14.09, 14.11, 22.65, 22.67, 26.09, 29.11, 29.16, 29.28, 29.40, 31.79, 31.81, 44.74, 47.87, 52.55, 68.70, 69.17, 104.33, 108.60, 120.87, 127.70, 133.47, 136.76, 149.82, 151.06, 200.71. IR (KBr): 2926, 2854, 1670, 1610, 1508, 1439, 1385, 1306, 1260, 1142, 1110, 1078, 1045, 994, 857, 781, 716, 568. HRMS-EI (*m/z*): (M^+) calcd for $C_{55}H_{80}O_6$ 837.6028; found 837.6053.

Compound 3. Compound **2** (1.00g, 1.19mmol) was placed in a 25mL Schlenk flask. Sodium hydride (143 mg, 60% in mineral oil, 3.58 mmol) was placed in a separate 50 mL Schlenk flask. Both flasks were evacuated and placed under argon atmosphere. Added 10 mL of dry THF via cannula to the flask with compound **2** and added 10 mL of dry DMF via cannula to the flask with the sodium hydride. The solution of compound **2** was then added dropwise via cannula to the suspension of sodium hydride in DMF. The reaction turned deep red. The solution was stirred for 40 minutes and then added dimethyl sulfate (340 μL, 3.58 mmol) via microsyringe. Stirring was continued for 16 hours under argon at room temperature, at which point the solution had turned a yellow color. The reaction was diluted with 150 mL of Et_2O, washed with water (3 x 100 mL) and dried over magnesium sulfate. The solvents were removed in vacuo yielding a yellow solid which was purified by silica gel chromatography with 1:1 hexane/dichloromethane eluent. Recovered 959 mg of solid which was further purified by recrystallization from CH_2Cl_2 / EtOH, yielding 892mg (1.03mmol, 87%) of **3** as a white solid. ^1H NMR ($CDCl_3$, δ): 0.87-0.94 (m, 12H, CH_3), 1.26-1.42 (m, 32H), 1.44-1.61 (m, 8H), 1.88-2.00 (m, 8H), 2.33-2.41 (m, 2H), 3.76 (s, 6H, CH_3O), 4.18-4.26 (m, 8H), 4.38 (s, 2H), 6.91 (s, 2H), 7.79 (s, 2H), 9.13 (s, 2H). ^{13}C NMR ($CDCl_3$, δ): 14.11, 14.12, 22.69, 26.17, 26.18, 29.32, 29.33, 29.41, 29.45, 29.49, 31.85, 47.44, 61.37, 67.68, 68.86, 69.44, 106.40, 110.85, 122.56, 123.52, 124.87, 133.11, 141.44, 142.71, 148.15, 148.37, 148.72. IR (KBr): 2923, 2854, 1612, 1538, 1513, 1264, 1121, 877, 715, 628. HRMS-EI (*m/z*): (M^+) calcd for $C_{57}H_{84}O_6$ 887.6160; found 887.6132. M.P. = 54.2 °C.

Compound 5. Compound **4** (1.486 g, 2.157 mmol) was placed in a 100 mL Schlenk flask with a stir bar. The flask was evacuated and backfilled with argon, after which 40 mL of

dry dichloromethane was added via syringe. The flask was cooled with an ice water bath and bromine (0.22 mL, 4.31mmol) was added dropwise via syringe. The ice bath was removed and the reaction was allowed to warm to room temperature for 1 hour. Et_2O (100 mL) was added and the solution was washed with saturated aqueous $Na_2S_2O_4$ (50 mL) followed by water (100 mL) and then was dried over magnesium sulfate. The solvents were removed in vacuo and the remaining dark oil was purified by column chromatography (silica gel, 2:1 hexanes/CH_2Cl_2) yielding **5** as a white crystalline solid (1.498 g, 1.77 mmol, 82%). ^{1}H NMR ($CDCl_3$, δ): 0.91-0.98 (m, 12H, CH_3), 1.35-1.48 (m, 16H), 1.52-1.63 (m, 8H), 1.84-2.02 (m, 8H), 3.74 (s, 6H, CH_3O), 4.17 (t, 4H, J = 6.6 Hz, -CH_2O), 4.26 (t, 4H, J = 6.6 Hz, -CH_2O), 7.77 (s, 2H, Ar-H), 8.99 (s, 2H, Ar-H). ^{13}C NMR ($CDCl_3$, δ): 14.04, 22.62, 22.63, 25.80, 25.82, 29.23, 29.28, 31.65, 60.53, 69.01, 69.37, 106.28, 110.72, 118.97, 121.78, 124.81, 125.34, 148.62, 149.60, 151.92.

Compound 6. Compound **5** (1.166 g, 1.38 mmol) was placed in a 25 mL Schlenk tube with a stir bar. The tube was evacuated and backfilled with argon, after which 2 mL of dry THF was added. Furan (5.0 mL, 4.7g, 69 mmol) was added via syringe and then the flask was cooled in an ice water bath. Phenyllithium (1.1 mL, 1.5 M in Et_2O, 1.65 mmol) was added slowly (1 hour) and then the reaction was stirred in the cooling bath for an additional 30 minutes. The reaction was then allowed to warm to room temperature and stirred for an additional 16 hours, at which time 25 mL of Et_2O was added and the solution was washed with water (3 x 20 mL). The solution was dried over magnesium sulfate and the solvents were removed in vacuo. The remaining solids were purified by column chromatography (2:1 CH_2Cl_2/hexanes) yielding 923 mg (1.22 mmol, 89%) of **6** as a white solid. ^{1}H NMR ($CDCl_3$, δ): 0.92-0.97 (m, 12H, CH_3), 1.36-1.50 (m, 16H),

1.52-1.63 (m, 8H), 1.90-2.01 (m, 8H), 3.81 (s, 6H, CH_3O), 4.18 (t, 4H, J = 6.6 Hz, -CH_2O), 4.25 (t, 4H, J = 6.6 Hz), 6.16 (s, 2H), 7.15 (s, 2H), 7.80 (s, 2H), 9.04 (s, 2H). ^{13}C NMR ($CDCl_3$, δ): 14.03, 14.04, 22.63, 25.80, 25.82, 29.22, 29.30, 31.65, 31.66, 61.57, 68.86, 69.36, 80.75, 106.19, 110.69, 123.24, 123.44, 125.16, 137.04, 142.43, 148.01, 148.17, 148.71. IR (KBr): 2928, 2858, 1613, 1513, 1446, 1421, 1264, 1245, 1193, 1125, 1007, 870, 835, 703, 588. HRMS-EI (*m/z*): (M^+) calcd for $C_{48}H_{66}O_7$ 755.4881; found 755.4870. M.P. = 85.6 °C.

Compound 8. Compound **7** (3.988 g, 22.92 mmol) was placed in a 500 mL Schlenk flask with 4-(dodecyloxy)benzoate (14.046 g, 45.84 mmol) , DMAP (5.62, 45.84 mmol), TsOH (856 mg, 4.5 mmol) and a stir bar. The flask was evacuated and backfilled with argon three times, after which CH_2Cl_2 (250 mL) was added via cannula. Diisopropylcarbodiimide (DIPC) (7.8 mL, 50 mmol) was added via syringe and the reaction was stirred for 3 days at room temperature. The solvents were removed in vacuo and the resulting solids were pulled through a silica gel pad (2 : 1 hexanes/dichloromethane) followed by low temperature (- 38 °C) recrystallization from acetone, yielding 8.54 g (11.3 mmol, 50%) of **8** as a white solid. ^1H NMR ($CDCl_3$, δ): 0.92 (t, 6H, J = 6.6 Hz, CH_3), 1.28-1.57 (m, 36H), 1.81-1.91 (m, 4H), 2.22-2.26 (m, 1H), 2.33-2.36 (m, 1H), 3.98 (t, J = 1.8 Hz, 2H), 4.08 (t, 4H, J = 6.6 Hz, -CH_2O), 6.82 (s, 2H), 6.87 (t, 2H, J = 1.8 Hz), 7.00 (d, 4H, J = 8.8 Hz, Ar-H), 8.18 (d, 4H, J = 8.8 Hz, Ar-H). ^{13}C NMR ($CDCl_3$, δ): 14.12, 22.68, 25.96, 29.07, 29.34, 29.35, 29.55, 29.58, 29.62, 29.64, 31.90, 48.05, 68.29, 68.44, 114.26, 119.44, 121.41, 132.29, 142.44, 142.48, 145.12, 163.48, 164. 59. IR (KBr): 2921, 2851, 1728, 1605, 1509, 1473, 1422, 1255,

1152, 1074, 1000, 844, 762, 506. HRMS-EI (*m/z*): (M^+) calcd for $C_{49}H_{66}O_6$ 773.4752; found 773.4750. M.P. = 88.7 °C.

Compound 9. Compound **7** (1.163 g, 6.685 mmol) was placed in a 250 mL Schlenk flask with 4-((S)-3,7-dimethyloctyloxy)benzoate (3.722 g, 13.370 mmol) , DMAP (1.640, 13.370 mmol), TsOH (247 mg, 1.3 mmol) and a stir bar. The flask was evacuated and backfilled with argon three times, after which CH_2Cl_2 (100 mL) was added via cannula. Diisopropylcarbodiimide (DIPC) (2.3 mL, 15 mmol) was added via syringe and the reaction was stirred for 3 days at room temperature and then poured into 50 mL of 1N HCl (aqueous). The organic layer was washed with saturated aqueous NaCl solution (50 mL) and water (2 x 50 mL), dried over magnesium sulfate, and the solvents were removed in vacuo. The resulting solids were purfied by column chromatography (2 : 1 hexanes/ CH_2Cl_2) followed by low temperature (- 38 °C) recrystallization from acetone, yielding 2.416g (3.476 mmol, 52%) of **9** as a white solid. ^{1}H NMR ($CDCl_3$, δ): ^{13}C NMR ($CDCl_3$, δ): 19.61, 22.58, 22.69, 24.63, 27.94, 29.77, 35.95, 37.21, 39.18, 48.04, 66.61, 68.44, 114.27, 119.43, 121.40, 132.28, 142.43, 142.48, 145.10, 163.45, 164.58. IR (KBr): 2953, 1728, 1603, 1604, 1509, 1480, 1254, 1211, 1152, 1067, 1006, 844, 763, 731, 649. HRMS-EI (*m/z*): (M^+) calcd for $C_{45}H_{58}O_6$ 694.4228; found 694.4246. M.P. = 50.5 °C.

Poly-1 The reaction was carried out in an air-free glovebox. Compound **3** (326 mg, 0.377mmol) was dissolved in 5 mL dry CH_2Cl_2 added quickly to Grubb's 2nd generation catalyst (1.6 mg, 0.0019 mmol) in 1mL dry CH_2Cl_2. The reaction stirred at room temperature for 21 hours and then ethyl vinyl ether (0.5 mL) was added. The reaction was brought out of the glovebox, poured into MeOH (100 mL) and the precipitated polymer was collected by centrifugation and dried in vacuo, yielding **poly-1** (306mg,

0.341mmol of repeat units, 91%) as a white solid. ^{1}H NMR ($CDCl_3$, δ): 0.71 (br, 6H), 0.85 (br, 6H), 0.98-1.60 (m, 40H), 1.59-1.99 (m, 8H), 2.63 (br, 2H), 3.70 (br, 6H), 4.07 (br, 8H), 4.40 (br, 2H), 5.88 (br, 2H), 7.68 (br, 2H), 9.00 (br, 2H).

Poly-2 Polymer **Poly-1** (75 mg, 0.087mmol) was placed into a 25 mL Schlenk tube with tosyl hydrazide (97 mg, 0.52 mmol) BHT (approx. 2 mg), 5 mL xylenes and a stir bar. The solution was freeze-pump-thawed three times to remove oxygen. The solution was heated to 110 °C with stirring. After one hour of stirring at room temperature, an additional portion of tosyl hydrazide (97 mg, 0.52 mmol) was added and the reaction stirred with heating for 16 hours. The flask was removed from the heating bath and the room temperature solution was poured into 100 mL of MeOH. The precipitate was collected by centrifugation and dried in vacuo. The polymer was redissolved in 25 mL of CH_2Cl_2, reprecipitated by pouring into MeOH, collected by centrifugation and dried in vacuo, yielding 64 mg of **poly-2**. ^{1}H NMR ($CDCl_3$, δ): 0.77 (br, 6H), 0.89 (br, 6H), 1.10 (br, 16H), 1.29 (br, 16H), 1.53 (br, 8H), 1.89 (br, 8H), 2.69 (br, 2H), 3.71 (br, 6H), 3.94 (br, 4H), 4.16 (br, 4H), 7.70 (br, 2H), 8.95 (br, 2H).

Poly-3 The reaction was carried out in an air-free glovebox. Compound **6** (49 mg, 0.065 mmol) was dissolved in 1.5 mL dry CH_2Cl_2 added quickly to via pipette to Grubb's 2nd generation catalyst (0.5 mg, 0.0006 mmol) in 1.5mL dry CH_2Cl_2. The reaction stirred at room temperature for 18 hours and then ethyl vinyl ether (0.5 mL) was added. The reaction was brought out of the glovebox, poured into MeOH (100 mL) and the precipitated polymer was collected by centrifugation and dried in vacuo, yielding **poly-3** as a white solid. ^{1}H NMR ($CDCl_3$, δ): 0.82-1.78 (br, 36H), 1.79-2.02 (br, 8H), 3.59-4.03

(br, 8H), 4.02-4.38 (br, 6H), 5.98-6.22 (br, 2H), 6.68 (br, 2H), 7.60-7.84 (br, 2H), 8.65-9.18 (br, 2H).

Poly-4 The reaction was carried out in an air-free glovebox. Compound **8** (253 mg, 0.337 mmol) was dissolved in 8 mL dry CH_2Cl_2 added quickly to via pipette to Grubb's 2nd generation catalyst (3.0 mg, 0.0035 mmol) in 1 mL dry CH_2Cl_2. The reaction stirred at room temperature for 3 hours and then ethyl vinyl ether (0.5 mL) was added. The reaction was brought out of the glovebox, poured into MeOH (100 mL) and the precipitated polymer was collected by filtration and dried in vacuo, yielding **poly-4** as a white solid. ^{1}H NMR ($CDCl_3$, δ): 0.88 (br, 6H), 1.24 (br, 36H), 1.69 (br, 4H), 3.86 (br, 4H), 5.50 (br, 2H), 6.67 (br, 4H), 6.96 (br, 2H), 7.91 (br, 4H).

Poly-5 . The reaction was carried out in an air-free glovebox. Compound **9** (209 mg, 0.301 mmol) was dissolved in 1 mL dry CH_2Cl_2 added quickly to via pipette to Grubb's 2nd generation catalyst (2.5 mg, 0.003 mmol) in 1 mL dry CH_2Cl_2. The reaction stirred at room temperature for 18 hours and then ethyl vinyl ether (0.5 mL) was added. The reaction was brought out of the glovebox, poured into MeOH (100 mL) and the precipitated polymer was collected by filtration and dried in vacuo, yielding **poly-5** as a white solid. ^{1}H NMR ($CDCl_3$, δ): 0.81 (br, 18H), 1.09 (br, 8H), 1.26 (br, 8H), 1.48 (br, 4H), 1.58 (br, 4H), 1.74 (br, 2H), 3.90 (br, 4H), 5.50 (br, 2H), 6.69 (br, 4H), 6.99 (br, 2H), 7.94 (br, 4H).

References

(1) Stevens, M. P. *Polymer Chemistry: An Introduction*; Oxford University Press: New York, Oxford, 1999; pp 83-85.

(2) Sierra, T.; Omenat, A.; Barbera, J.; Serrano, J. L. *Adv. Mater.* **1996**, *8*, 752-756.

(3) Collings, P. J.; Hird, M. *Introduction to Liquid Crystals: Chemistry and Physics*; Taylor and Francis: London, U.K., 1997; pp 93-110.

(4) Percec, V.; Lee, M. *Macromolecules* **1991**, *24*, 1017.

(5) Small, A. C.; Pugh, C. *Macromolecules* **2002**, *35*, 2105-2115.

(6) (a) Karthaus, O.; Ringsdorf, H.; Tsukruk, V. V.; Wendorff, J. H. *Lanmuir* **1992**, *8*, 2279-2283. (b) Wang, T.; Yan, D.; Zhou, E.; Karthaus, O.; Ringsdorf, H. *Polymer* **1998**, *39*, 4509-4513. (c) Boden, N.; Bushby, R. J.; Cammidge, A. N. *J. Am. Chem. Soc.* **1995**, *117*, 924-927.

(7) Weck, M; Mohr, B.; Maughon, B. R.; Grubbs, R. H. *Macromolecules* **1997**, *30*, 6430-6437.

(8) (a) Finkelman, H.; Ringsdorf, H.; Wendorff, J. H. *Macrom. Chem.* **1978**, *179*, 273-276. (b) Finkelman, H.; Happ, M.; Portugal, M.; Ringsdorf, H. *Macrom. Chem.* **1978**, *179*, 2541-2544. (c) Finkelman in *Liquid Crystals of One- and Two-Dimensional Order, Vol. 11*; Helfrich. W. and Heppke, G. Eds.; Springer-Verlag: Berlin, Heidelberg, New York, 1980; pp 238-251.

(9) (a) Perplies, E.; Ringsdorf, H.; Wendorff, J. H. *J. Poly. Sci.B, Poly. Lett. Ed.* **1975**, *13*, 243-246. (b) Blumstein, A. *Liquid Crystalline Order in Polymers*; Academic Press: New York, 1978; pp 105-140.

(10) Zhou, Q.; Wan, X.-H.; Zhang, D.; Feng, X.-D. in *Liquid-Crystalline Polymer Systems: Technological Advances*; Isayev, A. I., Kyu, T. and Cheng, S. Z. D., Eds.; ACS Symposium Series, 1996, pp 344-357.

(11) (a) Arehart, S. V.; *J. Am. Chem. Soc.* **1997,** *119*, 3027-3037. (b) Pugh, C.; Dahria, J.; Arehart, S. V.; *Macromolecules* **1997**, *30*, 4520-4532. (c) Pugh, C.; Shao, J.; Ge, J. J.; Cheng, S. Z. D. *Macromolecules* **1998**, *31*, 1779-1790. (d) Pugh, C.; Bae, J.-Y.; Dharia, J.; Ge, J. J.; Cheng, S. Z. D. *Macromolecules* **1998**, *31*, 5188-5200. (e) Kim, G.-H.; Pugh, C.; Cheng, S. Z. D. *Macromolecules* **2000**, *33*, 8983-8991. (f) Small, A. C.; Pugh, C. *Macromolecules* **2002**, *35*, 2105-2115. (h) Weck, M; Mohr, B.; Maughon, B. R.; Grubbs, R. H. *Macromolecules* **1997**, *30*, 6430-6437.

(12) Review: Schewendeman, J. E.; Church, A. C.; Wagener, K. B. *Adv. Synth. Catal.* **2002**, *344*, 597-613.

(13) Fu, G. C.; Nguyen, S. T.; Grubbs, R. H. *J. Am.Chem. Soc.* **1993**, *115*, 9856.

(14) Nomura, K.; Schrock, R. R. *Macromolecules* **1996**, *29*, 540.

(15) Review of Ru-based metathesis catalysts: Trnka, T.M.; Grubbs, R. H. *Acc. Chem. Res.* **2001**, *34*, 18.

(16) (a) Scholl, M. S.; Ding, S.; Lee, C. W.; Grubbs, R. H. *Org. Lett.* **1999**, *1*, 953. (b) Sanford, M.S.; Love, J. A.; Grubbs, R. H. *J. Am. Chem. Soc.* **2001**, *123*, 6543-6554.

(17) Benedicto, A. D.; Novak, B. M.; Grubbs, R. H. *Macromolecules* **1992**, *25*, 5893-5900.

(18) Bielawski, C. W.; Grubbs, R. H. *Macromolecules* **2001**, *34*, 8838-8840.

(19) a) Green, M. W.; Ringsdorf, H.; Juergen, W.; Wuestefeld, R. *Angew. Chem.* **1990**, *102*, 1525-1528. b) Singer, D.; Liebmann, A.; Praefcke, K.; Wendorff, J. H. *Liq. Cryst.* **1993**, *14*, 785-794. c) Letko, I.; Diele, S.; Pelzl, G.; Weissflog, W. *Liq. Cryst.* **1995**, *19*, 643-646. d) Hegmann, T.; Jens, K.; Diele, S.; Pelzl, G.; Tschierske, C. *Angew. Chem., Int. Ed.* **2001**, *40*, 887-890. e) Manickam, M.; Belloni, M.; Kumar, S.; Varshney, S. K.; Shankar Rao, D. S.; Ashton, P. R. ; Preece, J. A. Spencer, N. *J. Mat. Chem.* **2001**, *11*, 2790-2800.

Curriculum Vitae

Alexander Paraskos

ACADEMIC INTERESTS

Materials-directed organic chemistry, liquid crystals and liquid crystalline polymers, chemistry and properties of structural polymers, organic electronic materials, supramolecular chemistry.

EDUCATION

1997 – 2003 **Massachusetts Institute of Technology** *Cambridge, MA*
Candidate for Ph.D. in Organic Chemistry
Dissertation Adviser: Professor Timothy M. Swager

1994-1997 **University of Colorado, Boulder** *Boulder, CO*
Continuing Education Student, Chemistry
Cumulative GPA 3.83/4.0

1987-1991 **Colby College** *Waterville, ME*
B.A., Environmental Science, May 1991.

RESEARCH EXPERIENCE

1998-2003 **Massachusetts Institute of Technology** *Cambridge, MA*
Advisor: Professor Timothy M. Swager
Position: Research Assistant
• Synthesized, purified, and characterized numerous unconventional liquid crystalline compounds. Explored the effects of different structural variables upon liquid crystalline behavior of bent-rod mesogens. Identified liquid crystalline phase behaviors by employing a combination of techniques including 1D and 2D variable temperature X-ray diffraction, polarized microscopy and differential scanning calorimetry.
• Currently synthesizing triptycene and pentiptycene containing poly(esters) in order to study the influence of the iptycene units on the polymers' structural characteristics.

1995-1998 **University of Colorado, Boulder** *Boulder, CO*
Advisor: Professor Josef Michl.
Position: Undergraduate Research Assistant
• Assisted with the development of methodology for the symmetric coupling of bicylo[1.1.1]pentane rigid rod molecules via cuprate oxidation. Synthesized and purified numerous compounds and contributed to the writing and publication of results.

TEACHING EXPERIENCE

Spring 1999 **MIT Department of Chemistry Teaching Assistant (Organic Chemistry)**
• Led recitation classroom for undergraduate organic chemistry. Planned and organized lesson plans, wrote problem sets, and worked actively with undergraduate students.

Fall 1998 **MIT Department of Chemistry Laboratory Assistant**
• Supervised and instructed chemical laboratory techniques to undergraduate students.

TECHNICAL PROFICIENCIES

Synthetic organic chemist: small molecule purification and characterization
Materials design, synthesis, and characterization
Liquid crystal and liquid crystalline polymer design, synthesis and characterization
Structural polymer synthesis, purification and characterization
Variable temperature X-ray diffraction (1D and 2D)
Polarized microscopy and interpretation of liquid crystalline defect textures
Inert atmosphere and Schlenk techniques

ACTIVITIES Member, American Chemical Society
Member, MIT Tinytech

ORAL PRESENTATIONS

"Interaction and Effects of Bend-Angle, Lateral Dipole, Symmetry and Chirality on the Mesomorphism of Thiophene-Based Bent-Rod Liquid Crystals." A. J. Paraskos, S. H. Eichhorn, K. Kishikawa and T. M. Swager, 224th National ACS Meeting (Boston,MA) (August 18-22, 2002).

"Lateral Dipole Controlled Mesomorphism of Bent-Rod Tetracatenars Based on 2,5-Di(phenylacetylene)thiophenes (II)." A. J. Paraskos and T. M. Swager, 2000 NEDO Meeting (Kamakura, JP) (July 21-22).

"Thiophene-Based Bent-Rod Mesogens with Large Lateral Dipoles and the Effects of Desymmetrization Upon Mesophase Stability." A. J. Paraskos, S. H. Eichhorn, K. Kishikawa and T. M. Swager, MIT Reinhoudt/Swager Mini-Symposium (August 28,2000)

POSTER PRESENTATIONS

"The Interaction and Effects of Bent-Angle, Lateral Dipole, Symmetry and Chirality on Thiophene-Based Straight-Chain and Polycatenar Liquid Crystals." A. J. Paraskos, S. H. Eichhorn, K. Kishikawa and T. M. Swager, 2002 International Liquid Crystal Conference (Edinburgh, UK) (June 30-July 5).

"Synthesis and Characterization of Novel Quinone-Containing Triphenylene-Based Discotic Liquid Crystals." A. J. Paraskos, Y. Nishiyama and T. M. Swager, 2002 International Liquid Crystal Conference (Edinburgh, UK) (June 30-July 5).

"The Effects of Lateral Dipole and Symmetry on Thiophene-Based Bent-Rod Liquid Crystals." A. J. Paraskos, S. H. Eichhorn, K. Kishikawa and T. M. Swager, 2001 MIT Materials Day Conference (Cambridge, MA) (October 29).

"The Effects of Lateral Dipole and Symmetry on Thiophene-Based Bent-Rod Liquid Crystals." A. J. Paraskos, S. H. Eichhorn, K. Kishikawa and T. M. Swager, 2001 Liquid Crystal Gordon Conference (USA) (June 24-29).

"Thiophene-Based Bent-Rod Mesogens with Large Lateral Dipoles and the Effects of Desymmetrization Upon Mesophase Stability." A. J. Paraskos and T. M. Swager, 2000 International Liquid Crystal Conference (Sendai, JP) (July 24-28).

"Synthesis and Phase-Behavior of Desymmetrized Thiophene-Based Bent-Rod Liquid Crystals." A. J. Paraskos and T. M. Swager, 1999 LC Gordon Conference (USA) (June 6-11).

PUBLICATIONS

"Effects of Desymmetrization on Thiophene-Based Bent-Rod Mesogens." A. J. Paraskos and T. M. Swager, *Chemistry of Materials* **2002**, 14 (11), 4543-4549.

"The Interplay of Bent-Shape, Lateral Dipole and Chirality in Thiophene Based Di-, Tri-, and Tetracatenar Liquid Crystals." S.H. Eichhorn, A.J. Paraskos, K. Kishikawa and T.M. Swager, *J. Amer. Chem. Soc.* **2002**, 124 (43), 12742-12751.

"Synthesis and Characterization of Novel Triphenylene-Dione Half-Disc Mesogens." A. J. Paraskos, Y. Nishiyama and T. M. Swager, *Mol. Cryst. Liq. Cryst.* **(in press)**.

"Thermally Stimulated Depolarization Currents and Optical Transmission Studies on a 3,4-Dicyanothiophene-Based Bent-Rod Liquid Crystal." C. Rosu, D. Manaila-Maximean, A. J. Paraskos, *Mod. Phys. Lett. B* **2002**, 16 (13), 473-483.

C. Mazal, A. J. Paraskos and J. Michl, "Symmetric Bridgehead-to-Bridgehead Coupling of Bicyclo[1.1.1]pentanes and [n]Staffanes" *J. Org. Chem.* **1998**, 63(7), 2116-2119.

Acknowledgements

I should start by thanking Professor Timothy Swager. For five years, Tim has been an endless source of encouragement, ideas and optimism. His dedication to chemistry and science, together with his positive attitude toward all of the associated frustrations and challenges, seem to influence everyone who works with him. His willingness to take chances and think outside the box is a constant force. "We're casting after the big fish" was a phrase I heard many times at from Tim. For me, however, Tim's most impressive accomplishment has been his ability to consistently step outside his role as MIT professor and make time for family and friends.

I was lucky enough to get the chance to travel with Tim to numerous conferences and events. Most notable were the International Liquid Crystal Conferences in Sendai, Japan and Edinburgh, Scotland in 2000 and 2002, respectively. What struck me most was the way that other scientists at the conference expressed their admiration for Tim personally as well as scientifically; they almost invariably described him (no, not just when he was present) as "a great guy", revealing a level of appreciation that went beyond science. One of the distinct pleasures of the trip was watching Tim walk around Japan clad in his Tokyo Giants baseball shirt, shorts, and sneakers. You just can't buy that kind of entertainment. If only Robert Deschenaux had been successful in his attempt to get us to go to the Karaoke bar in Sendai after we were well plied with sake and beers; now *that* would have been priceless…

Professor Josef Michl at CU Boulder had an equally powerful influence on my career in chemistry. Josef taught Intro to Org Chem when I attended CU as a continuing education student. His passion for the subject was evident in his lectures, even though the immediate subject matter was certainly beyond routine for him at that stage in his career. I approached him about the possibility of working in his lab as a researcher and within a few days I was synthesizing benzvalene with visiting Czech professor Ctibor Mazal. Josef has (or at least it seemed that way to me at the time) an almost encyclopedic knowledge of photochemistry, physical chemistry and organic chemistry, and the guy can speak six or seven languages to boot (but who's counting). I'll never forget the chalk talks that he'd give at group meetings; once he gave an off-the-cuff one-hour presentation on tensors; on another occasion he rehashed an entire ACS talk from memory that he'd seen just the day before. Josef also has an infectious love for the outdoors; several times a year his lab shuts down as he, his research group, and his family head out to the Rocky Mountains to go camping, hiking, cross-country skiing, white-water rafting, rock-climbing, or whatever else is on the agenda. I would submit that you haven't really connected with your mentor until you've worked together digging down through six feet of mountain snow for no less noble a cause than to free the cabin outhouse for further use.

My first year at MIT was not an easy one in many ways; as someone who did not major in chemistry as an undergrad, I always felt that I was just one step behind in classes. As soon as I really started to internalize the information, the exam had happened a week and a half ago. Anyway, thanks to all of my classmates, especially Mike Smith (I will go to my grave saying that MIT made a big mistake letting you go with a Master's Degree), Emma Palmacci (thanks for your grandmother's meatball recipe), Dave Amos, and Jordan Wosnick. Jordan and I went on to share a bay in the Swager lab for a year,

listening to so much jazz that our section of the lab was referred to (and not always affectionately) as "jazz alley".

Once I had settled into the lab for some serious research, I had the pleasure of working among many great characters. Bruce Yu (Goofy, the Goof, Goofy B) was always a lot of fun. Despite my pleas to stop playing musicals such as "Rent" and "The Phantom of the Opera", Bruce carried on undaunted, enjoying my discomfort as he upped the ante, joining in and singing along with the cast. I will never forget Bruce's sinking seven of ten three-pointers at the Walker basketball court after a few hours at the Muddy; that particular wager cost me a pitcher. On the other side of the lab I had Aimee Rose, who at the time seemed to be listening almost exclusively to Dave Matthews. I got my revenge with healthy doses of Jimi Hendrix, Frank Zappa, and Albert King. When she started her research Aimee was the only woman graduate student in the Swager lab; by the time she left (or soon after, anyway) there were at least seven, by my count. Now that's an improvement.

Despite any differences in our musical tastes, we all got along once involved in scholarly discussion, and to this end the CPS seminar series was born. Dr. J.D. Tovar was on hand for these occasions, lending his unique views on politics, science and Jello Biafra. Other notable regulars included, of course, Aimee ("you are troublemaker") Rose, Hindy Bronstein (the only group member that Tim admits could potentially drink him under the table), Paul "P. Diddy" Byrne, Steffan Zahn (ZAHHHHN!), Prof Mark "the shark" MacLachlan, and the unforgettable Prof. Yutaka Nishiyama.

My last two years at MIT seem like a totally separate experience to me. I would like to thank some of the people who made this time particularly enjoyable. Karen Villazor...man, us LC people made out pretty good in the end. The exotic trips: Japan, Scotland, *New Hampshire*. In addition, I've not yet met another person who goes online to read a restaurant's menu so that they're ready when they get there. Serious stuff. Phoebe, I have never heard you speak Chinese, despite my pleading. Whatever you do, remember to never yell "bravo!" at a jazz performance. Paul, with the head-first dive into home plate against the Danheiser lab, your cheap shots against me in hockey practice, and our many brutal tennis matches; what a competitor! Thanks also to the Heftys, Masa, Holger, Kenichi-san, Gigi, Juan, Craig (fo' shizzle), and the rest of the Swager group.

I wouldn't have survived without Dave Lahr and Greg with our countless trips to Lynn and the Fells with the inevitable post-bike BBQs, as well as the hockey games and practices. Those Johnny's hots are damned good, even if they make your appendix burst. Thank you to Pete, Ted, Maya, Rich, Linda and the Dwight Ritcher band for making it all a bit more bearable. Special thanks to my brother Greg and my parents John and Sophia; you always believed in me and supported me no matter where I appeared to be headed. And finally, to my wife, Stacie, for all of the great times that we've shared in Colorado, Massachusetts, Japan, Portugal and Spain, and for putting up with me even when I didn't deserve it, I love you. Hopefully the best is yet to come for us.

Scientifically, I would like to thank Mark Wall for his help in the DCIF, Li Li for mass spec, Holger Eichhorn and Yutaka Nishiyama for collaboration on the LC projects and Nick Tsui and Neal Vannachi for work on the iptycene polymers. J.D. Tovar and Paul Byrne gave much needed electrochemistry assistance. This research was supported by the Office of Naval Research and the Institute for Soldier Nanotechnology.

Appendix 1:

^{1}H and ^{13}C NMR spectra for Chapter 2

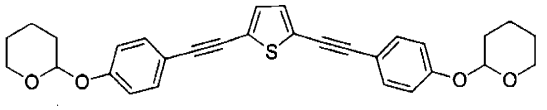

3

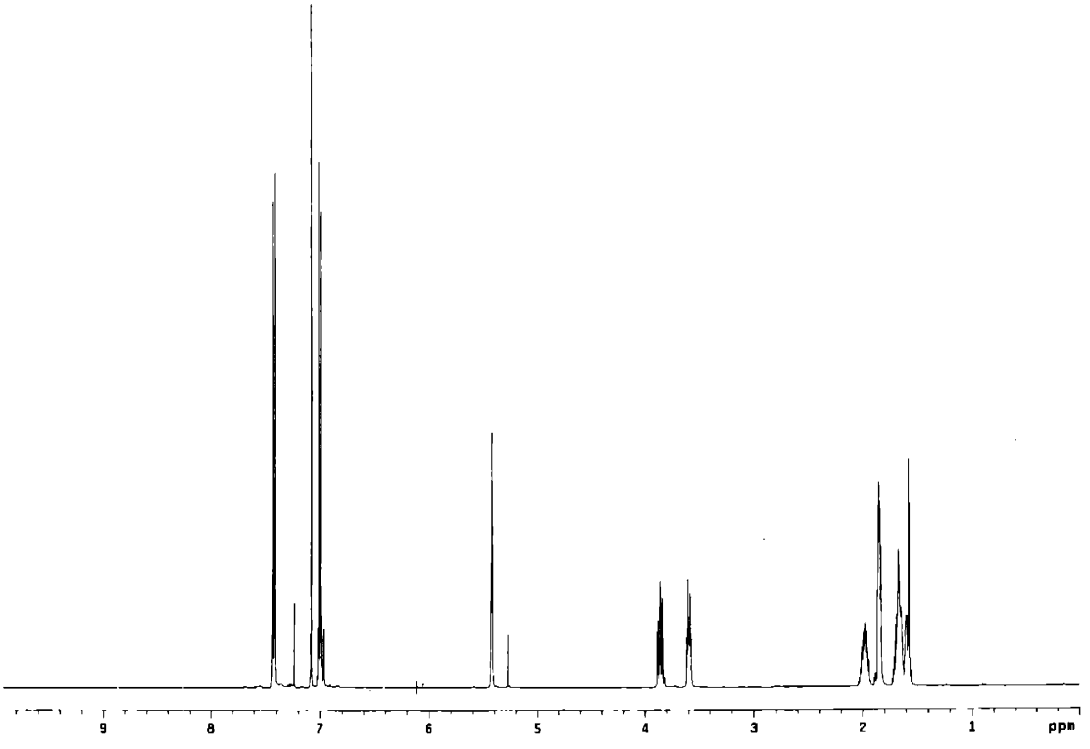

^{1}H NMR of **3** (500MHz, $CDCl_3$)

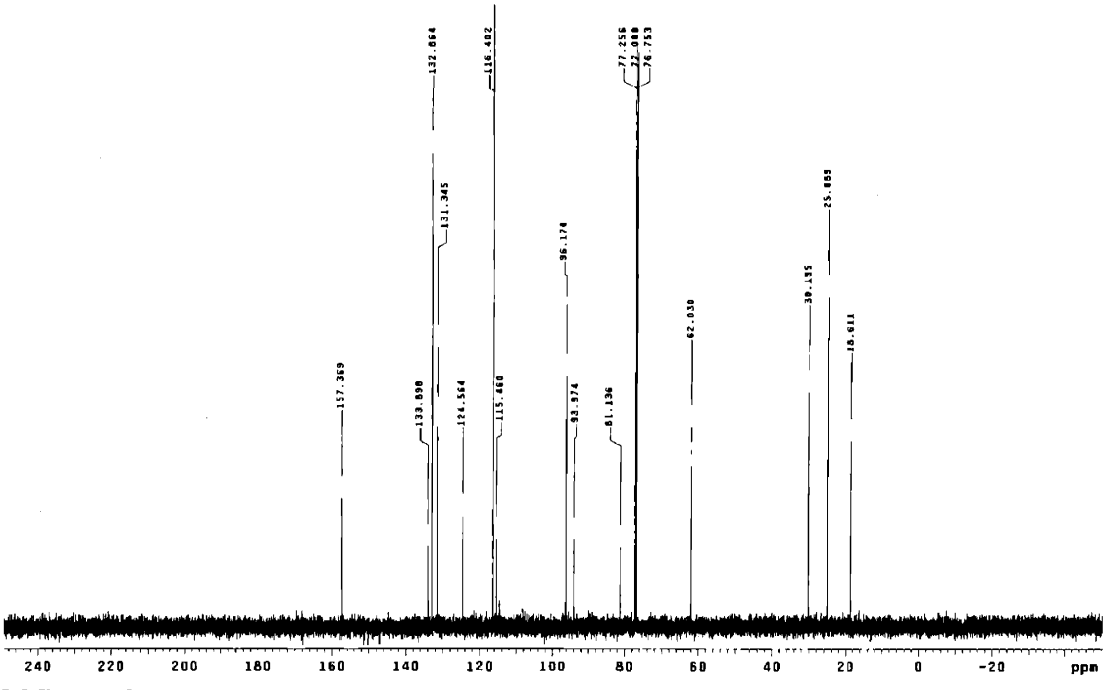

^{13}C NMR of **3** (125MHz, $CDCl_3$)

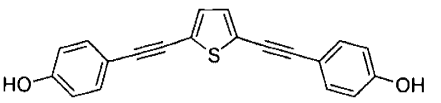

6

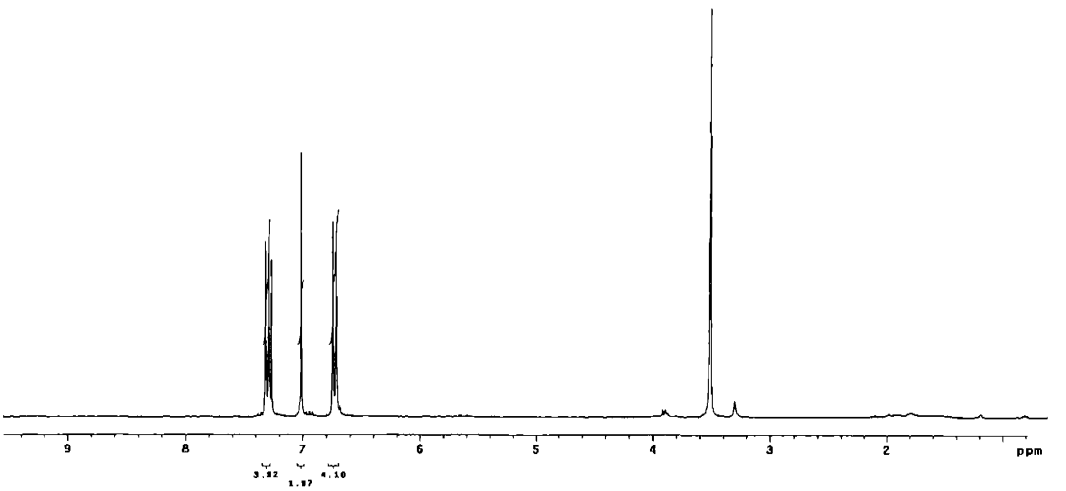

^{1}H NMR of **6** (300MHz, $CDCl_3$)

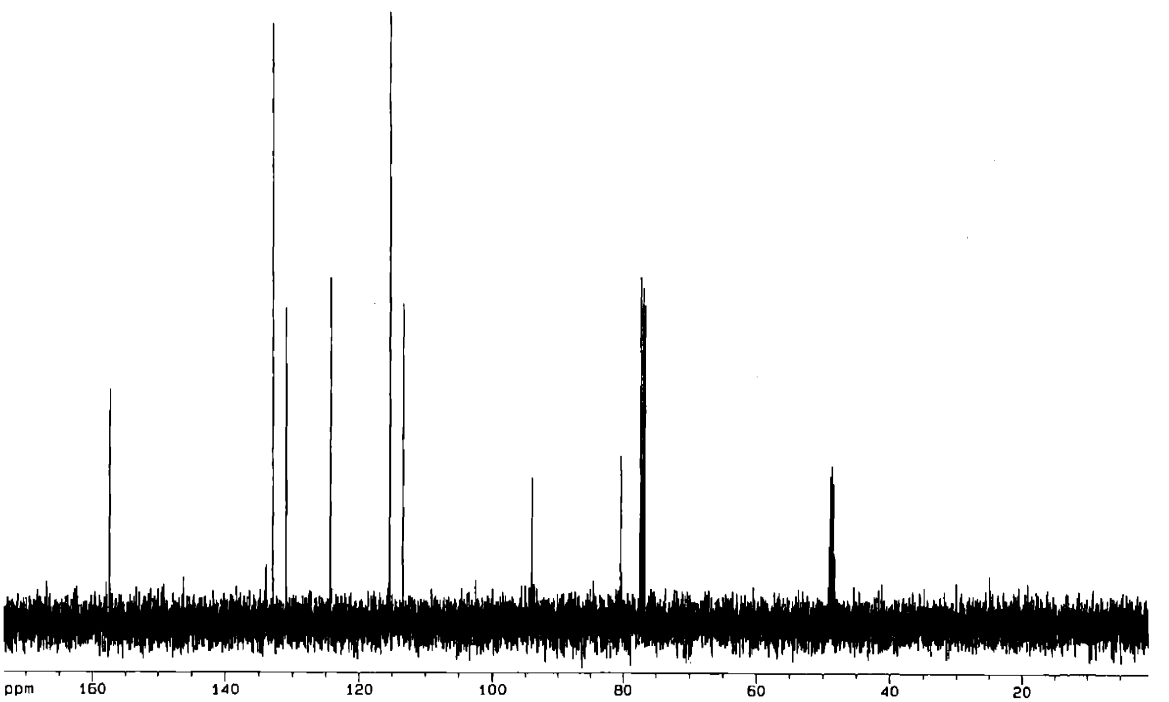

^{13}C NMR of **6** (100MHz, $CDCl_3$)

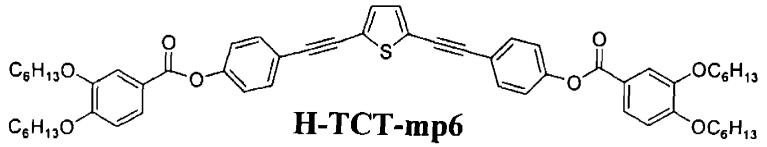

H-TCT-mp6

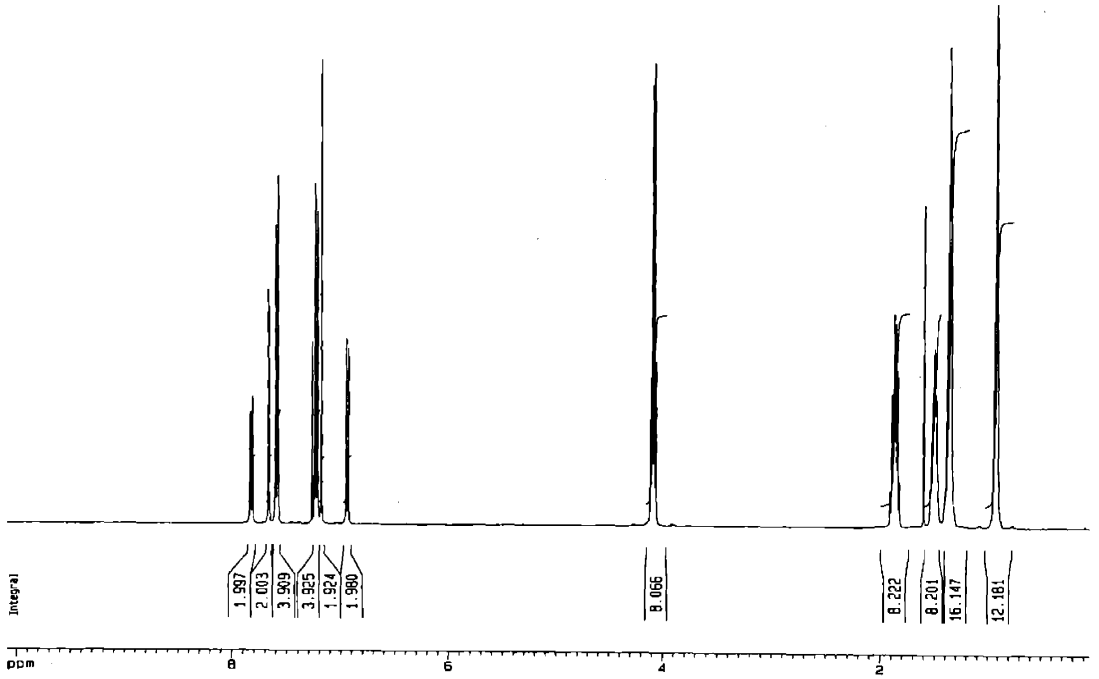

^{1}H NMR of **H-TCT-mp6** (400MHz, $CDCl_3$)

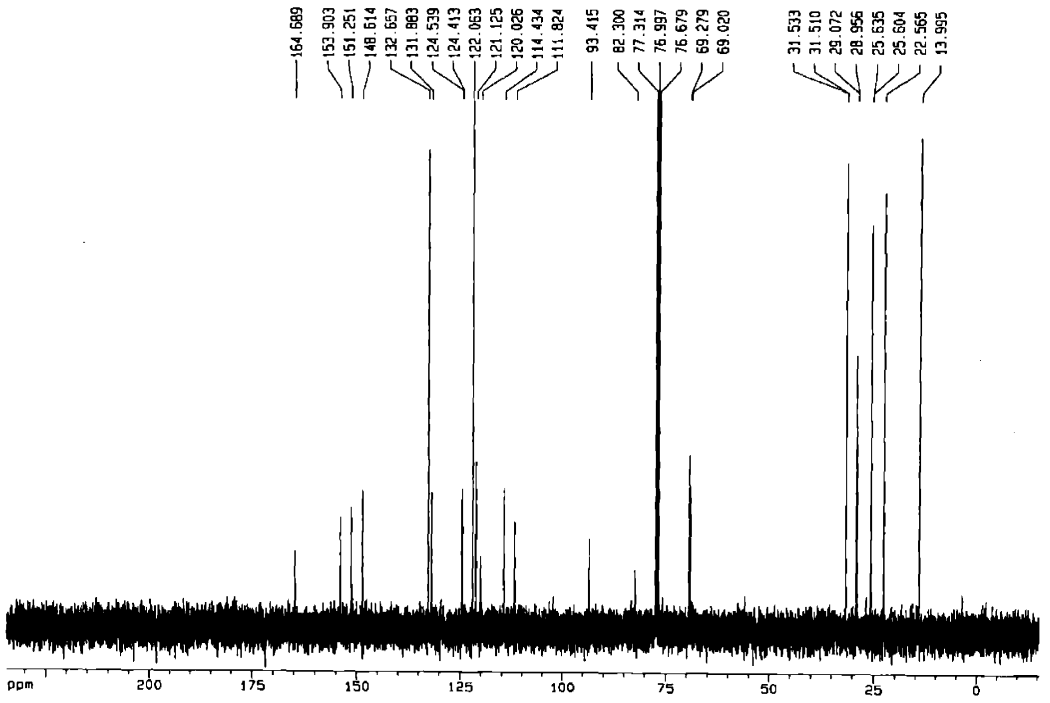

^{13}C NMR of **H-TCT-mp6** (100MHz, $CDCl_3$)

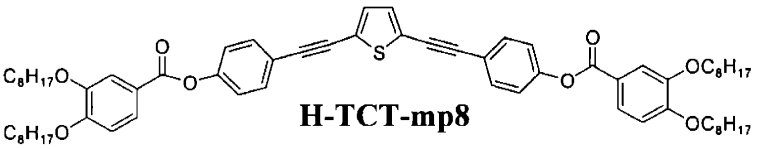

H-TCT-mp8

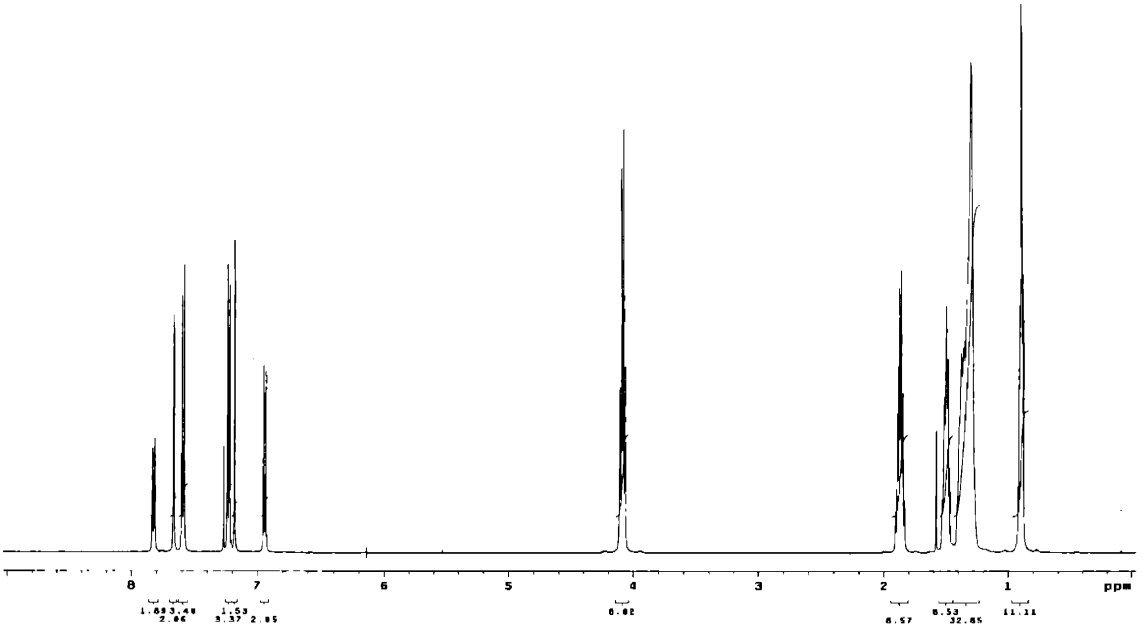

^{1}H NMR of **H-TCT-mp8** (500MHz, $CDCl_3$)

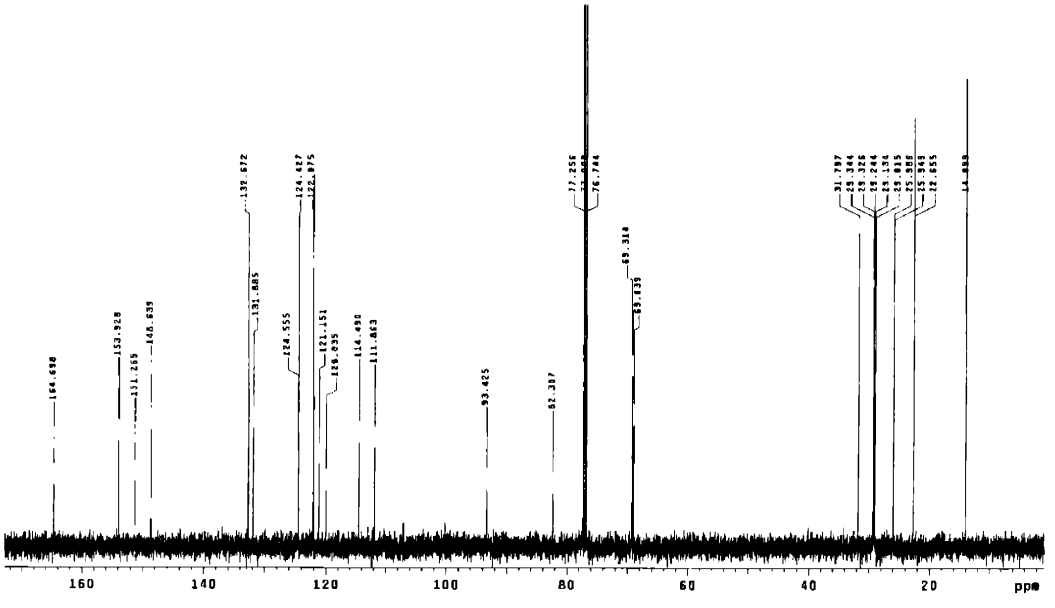

^{13}C NMR of **H-TCT-mp8** (125MHz, $CDCl_3$)

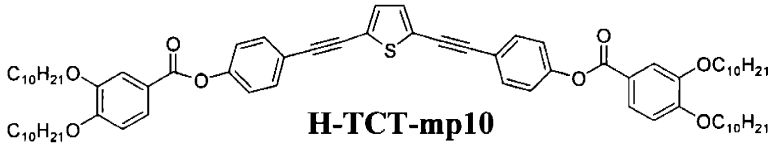

H-TCT-mp10

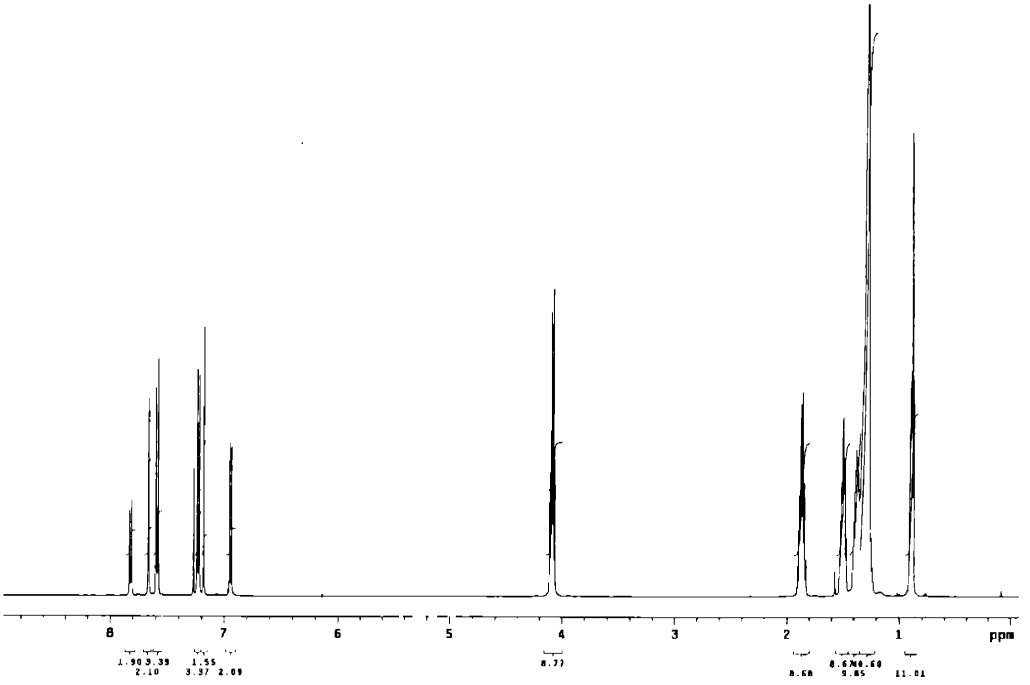

^{1}H NMR of **H-TCT-mp10** (500MHz, $CDCl_3$)

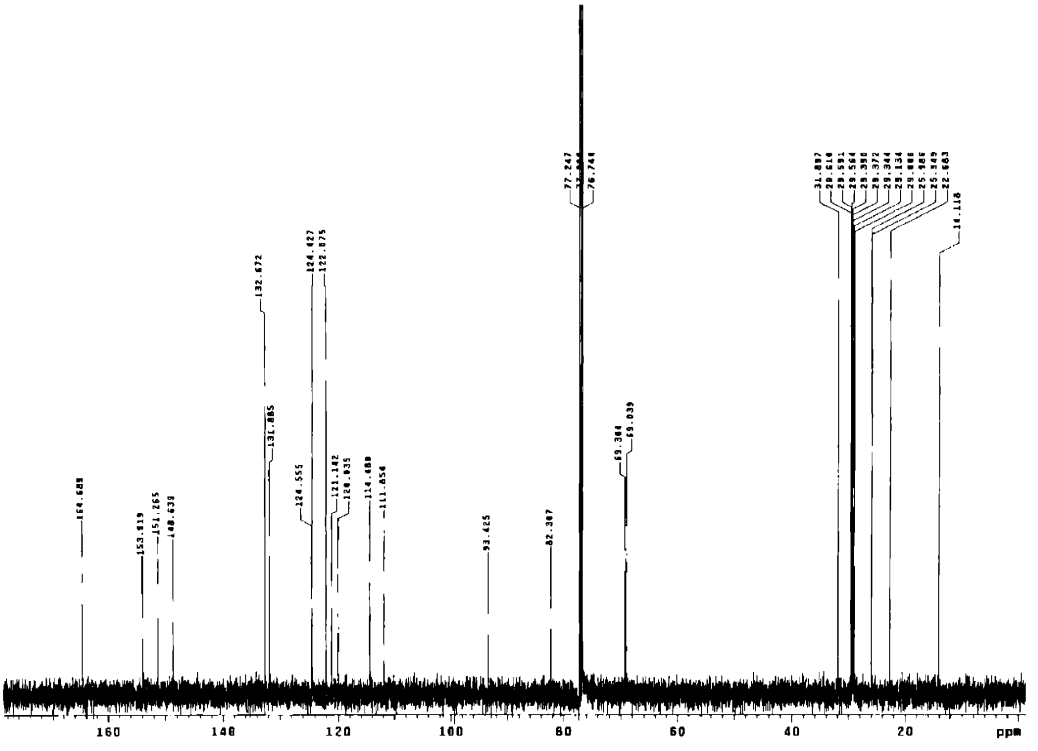

^{13}C NMR of **H-TCT-mp10** (125MHz, $CDCl_3$)

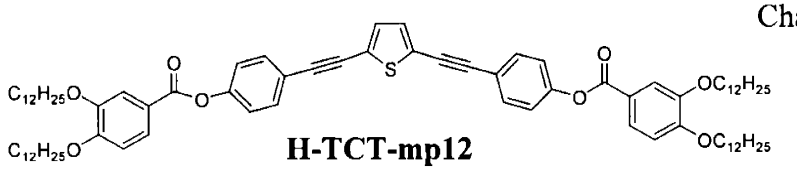

H-TCT-mp12

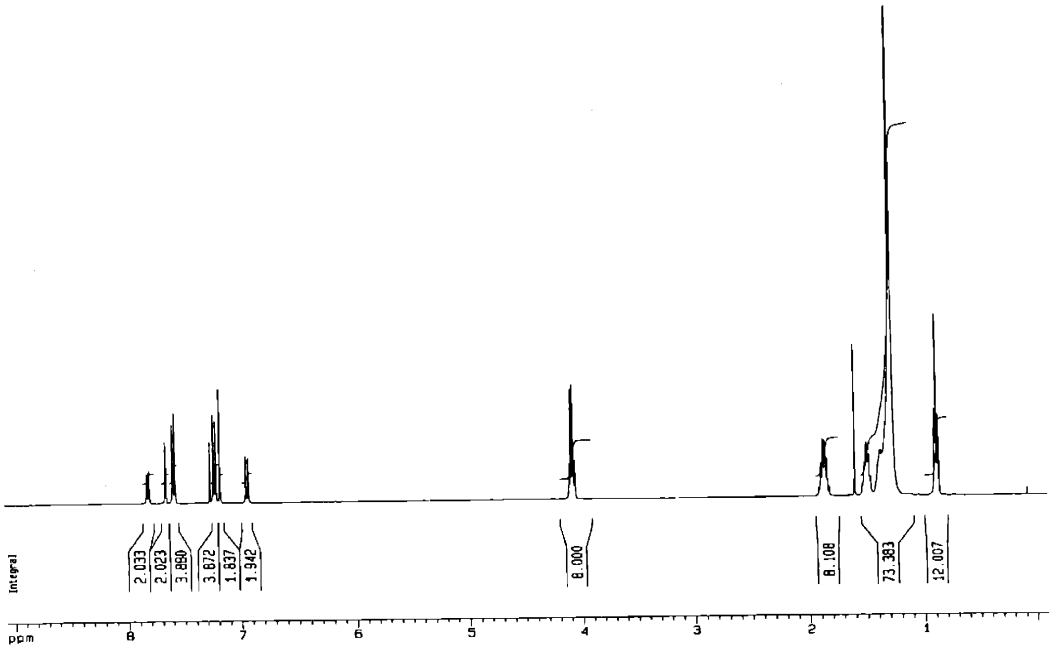

^{1}H NMR of **H-TCT-mp12** (400MHz, $CDCl_3$)

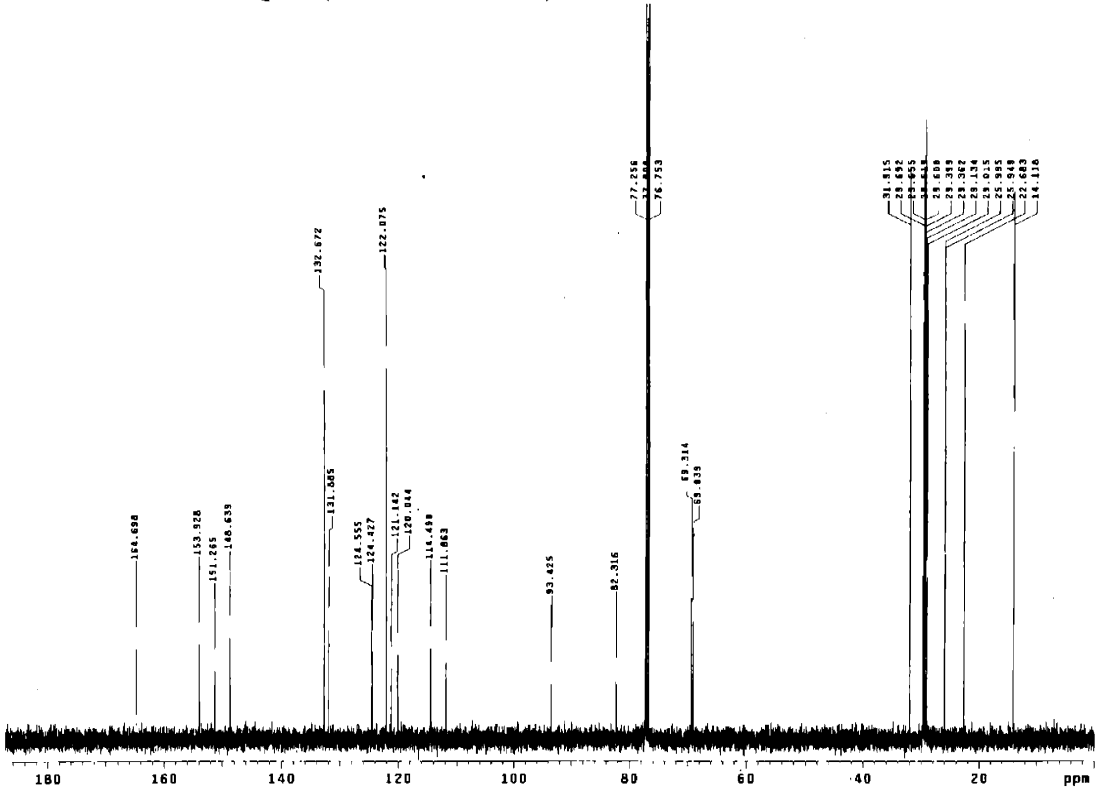

^{13}C NMR of **H-TCT-mp12** (125MHz, $CDCl_3$)

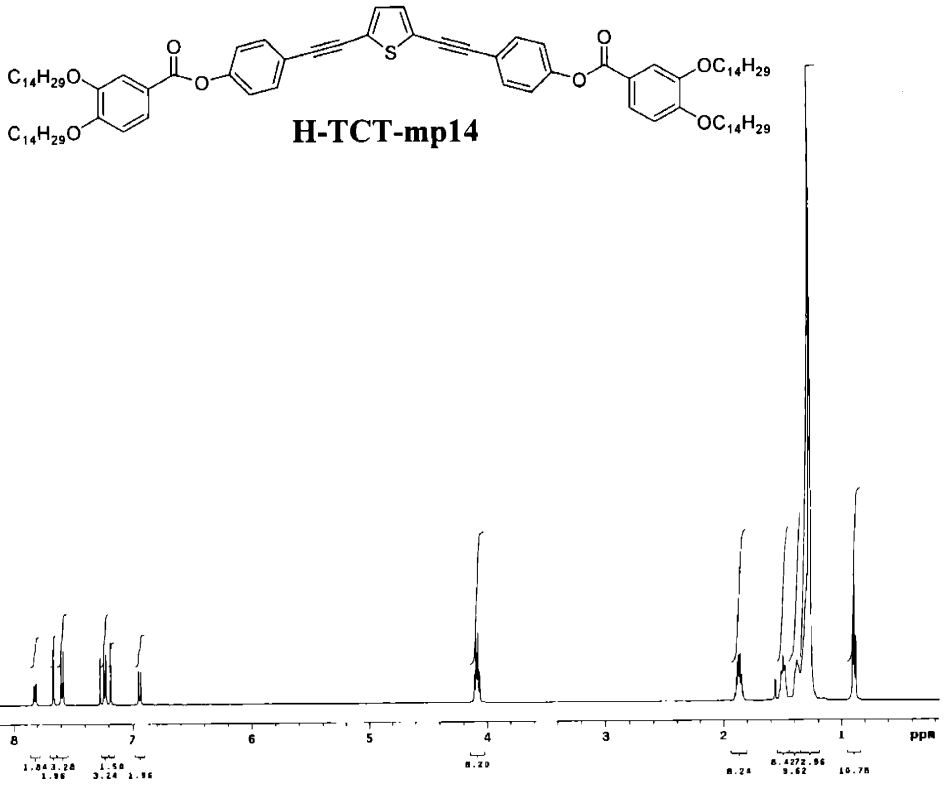

^{1}H NMR of **H-TCT-mp14** (500MHz, $CDCl_3$)

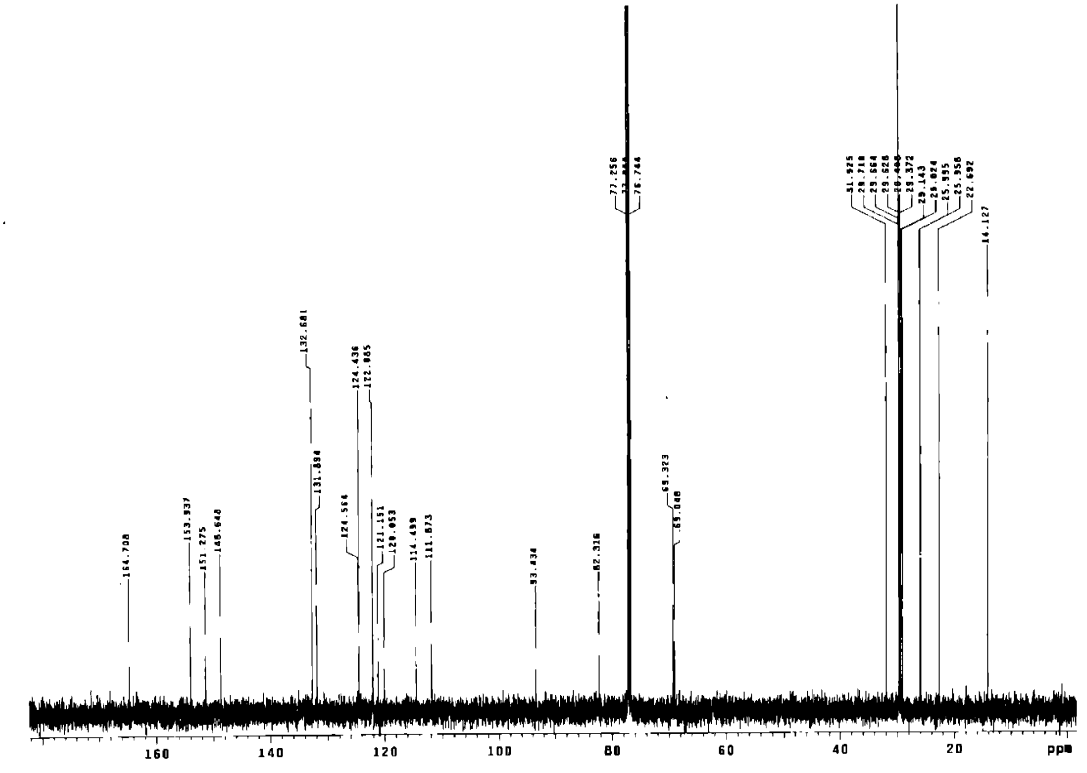

^{13}C NMR of **H-TCT-mp14** (125MHz, $CDCl_3$)

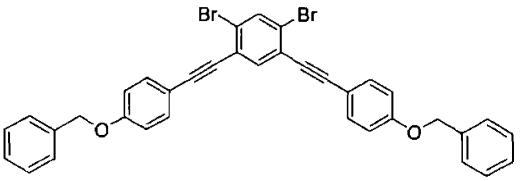

2,4-Bis(4-phenylmethoxyphenylethynyl)-1,3-dibromobenzene

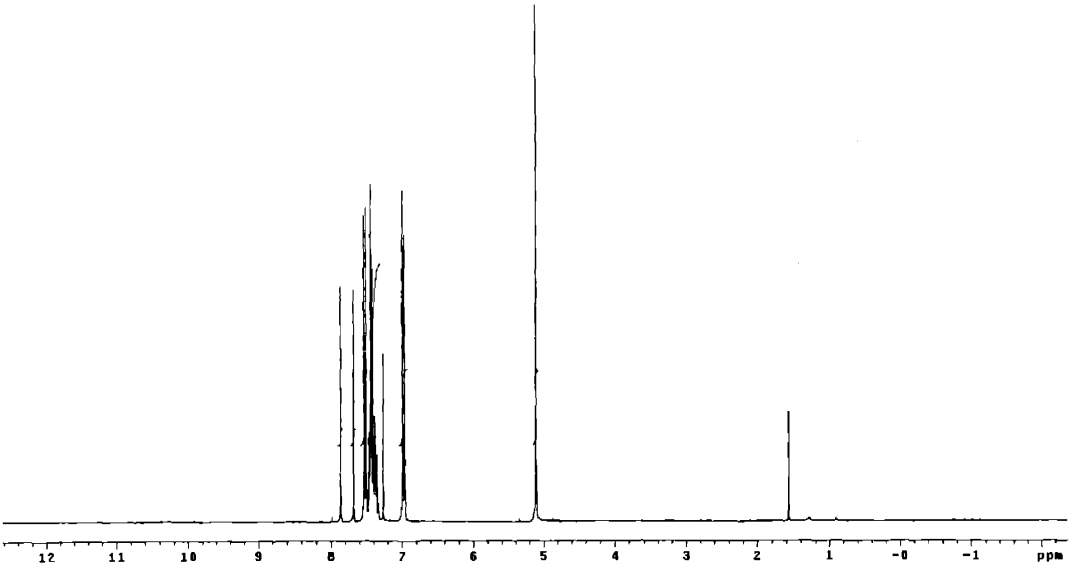

^{1}H NMR (300MHz, $CDCl_3$)

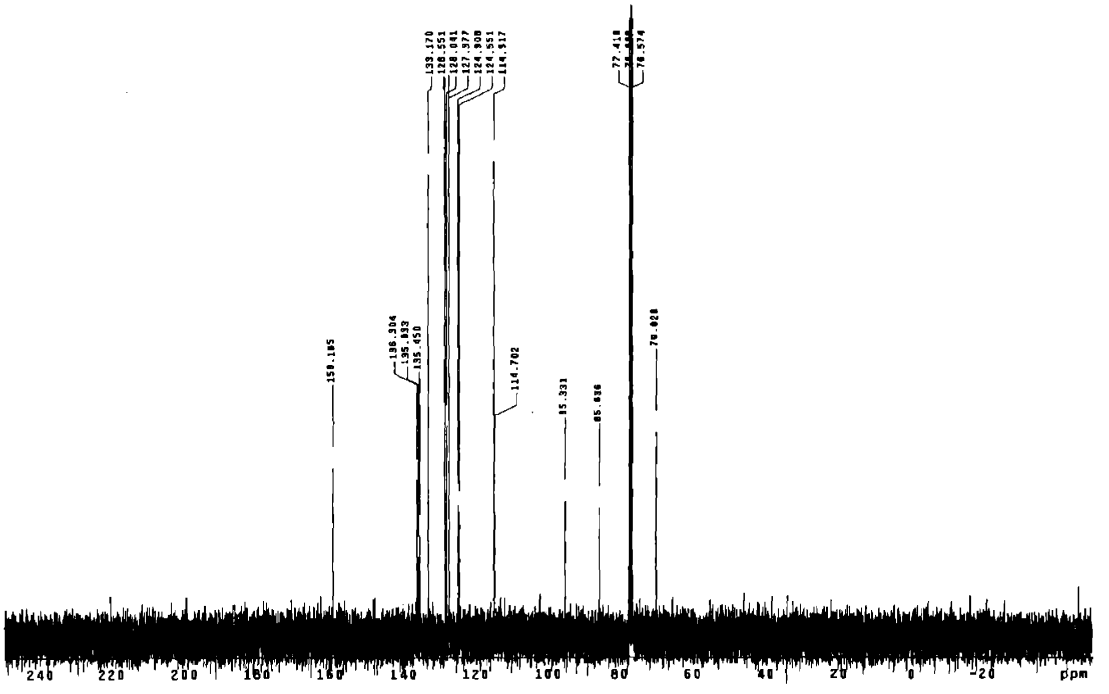

^{13}C NMR (75MHz, $CDCl_3$)

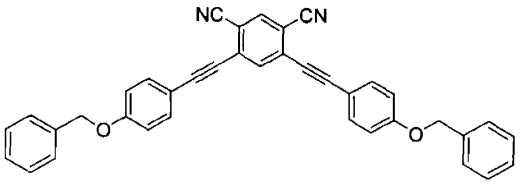

2,4-Bis(4-phenylmethoxyphenylethynyl)-1,3-dicyanobenzene

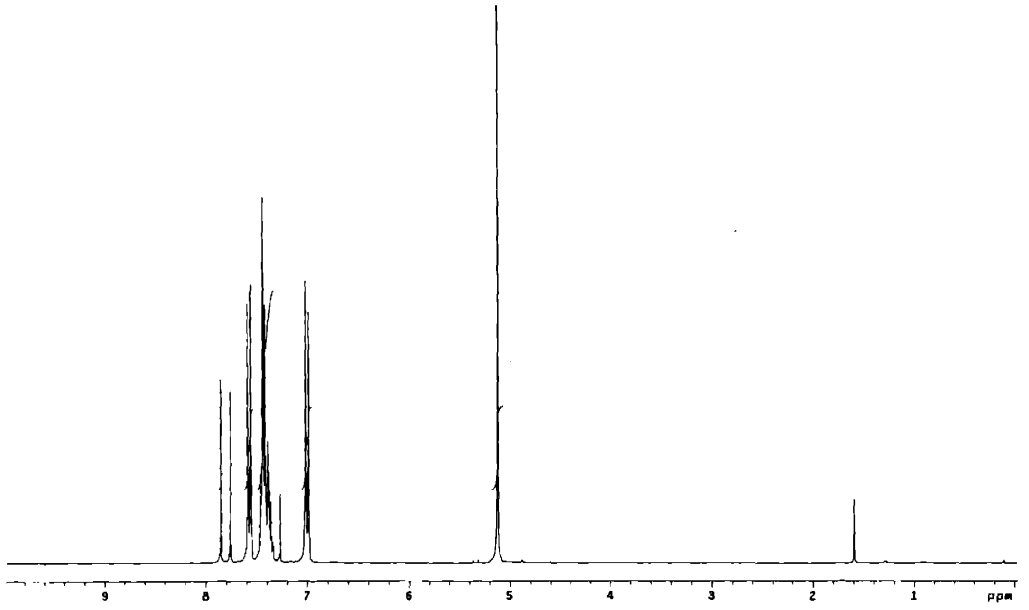

^{1}H NMR (300MHz, $CDCl_3$)

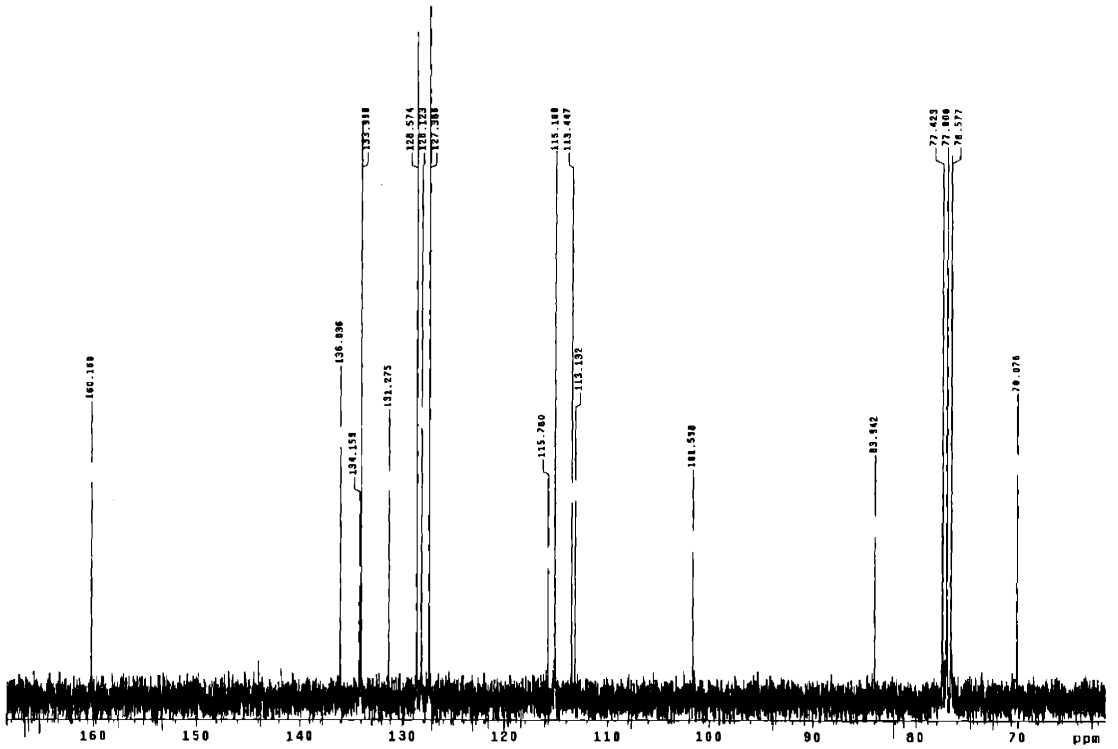

^{13}C NMR (125MHz, $CDCl_3$)

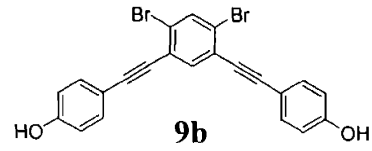

9b

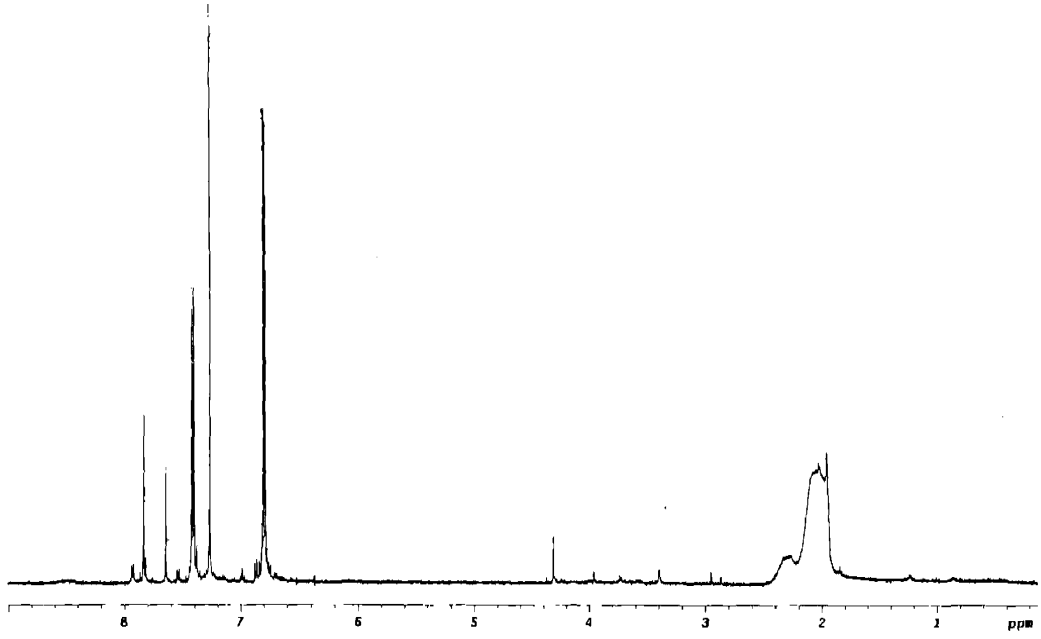

^{1}H NMR of **9b** (500MHz, $CDCl_3$)

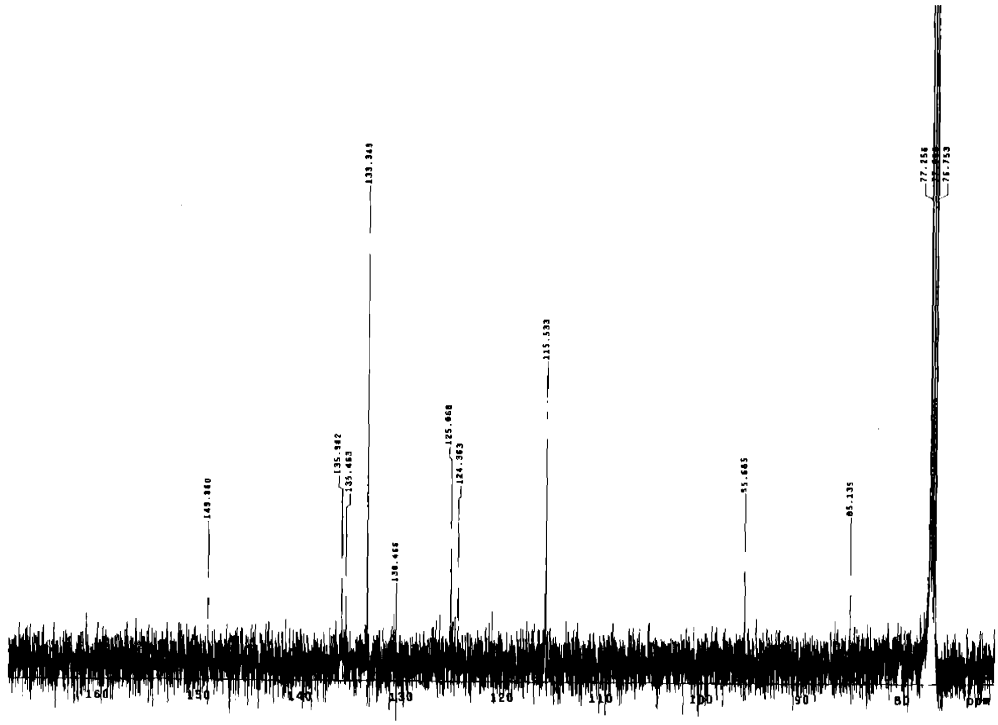

^{13}C NMR of **9b** (125MHz, $CDCl_3$)

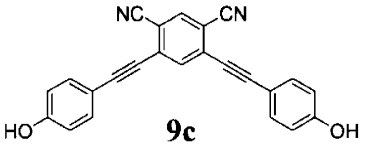

9c

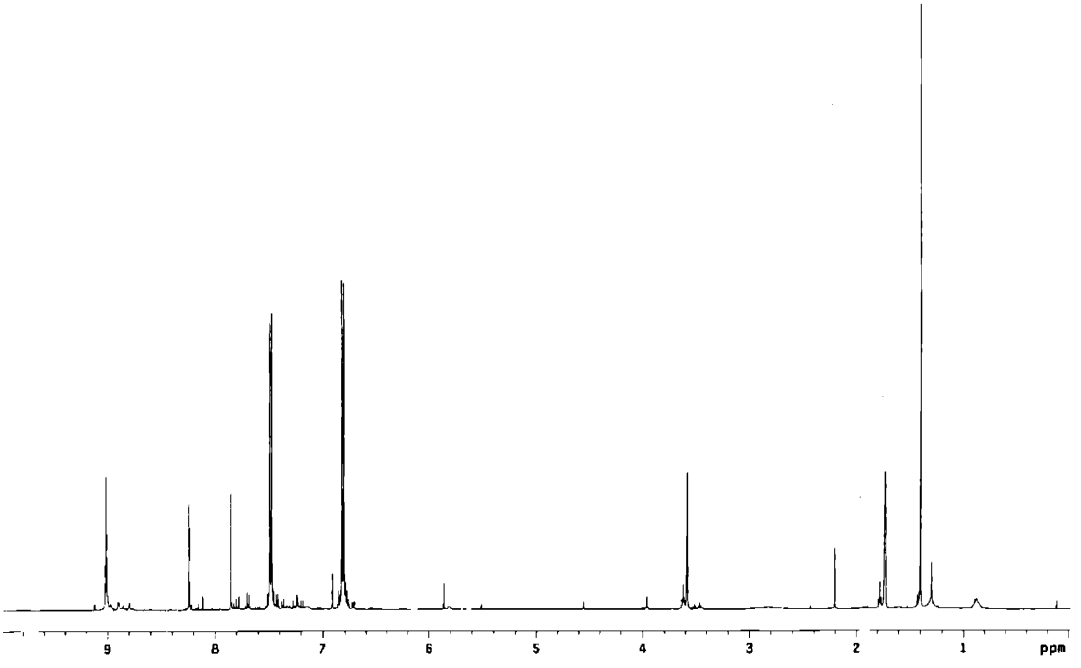

^{1}H NMR of **9c** (500MHz, $CDCl_3$)

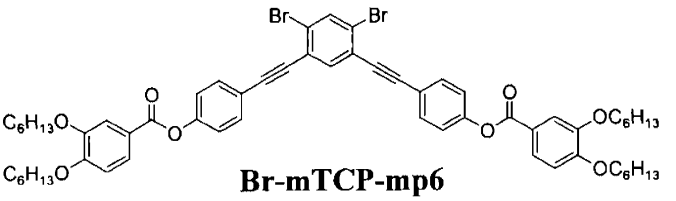

Br-mTCP-mp6

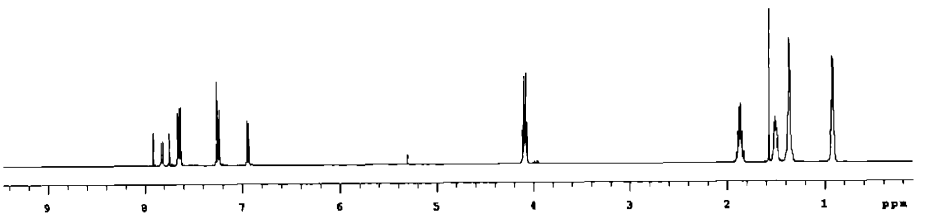

^{1}H NMR of **Br-mTCP-mp6** (500MHz, $CDCl_3$)

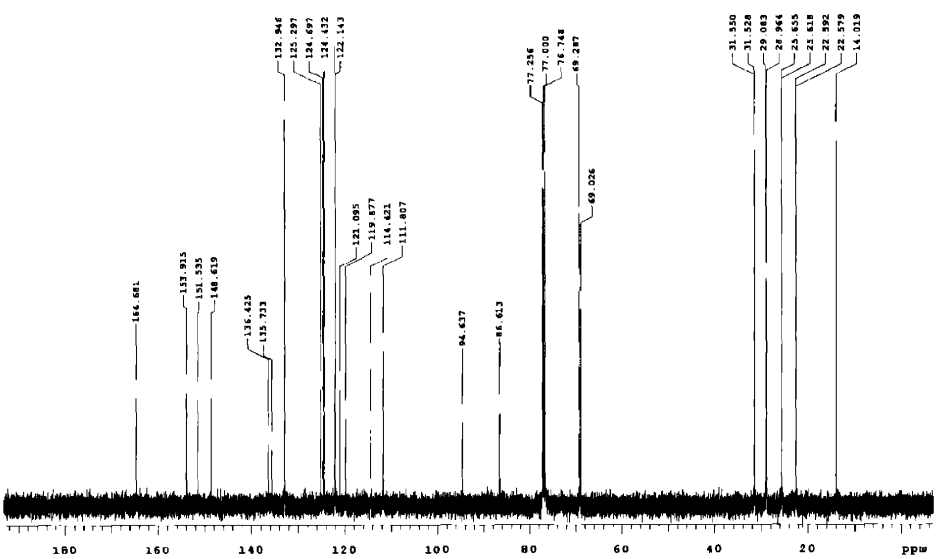

^{13}C NMR of **Br-mTCP-mp6** (125MHz, $CDCl_3$)

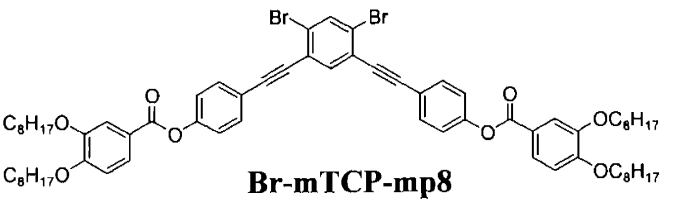

Br-mTCP-mp8

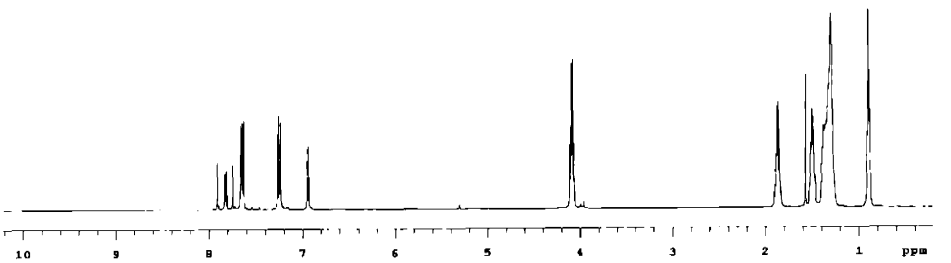

^{1}H NMR of **Br-mTCP-mp8** (500MHz, $CDCl_3$)

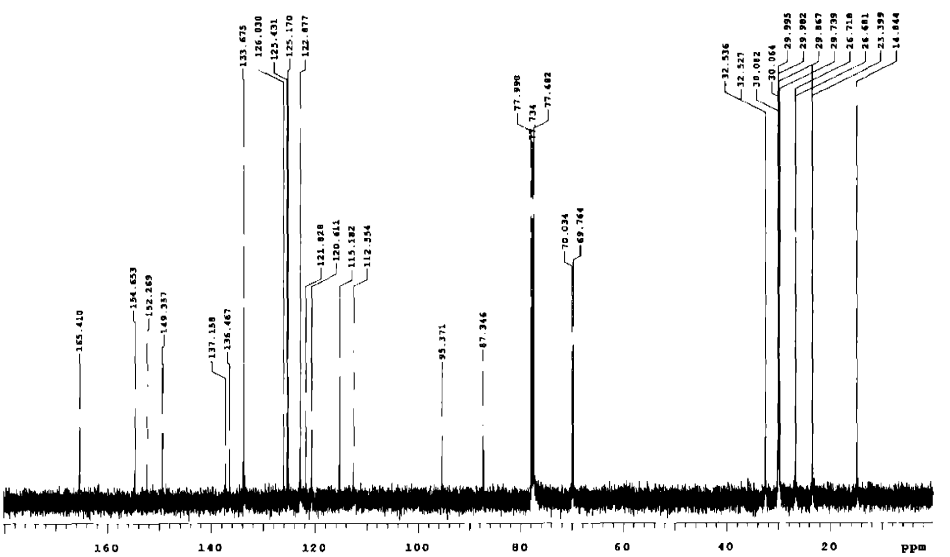

^{13}C NMR of **Br-mTCP-mp8** (125MHz, $CDCl_3$)

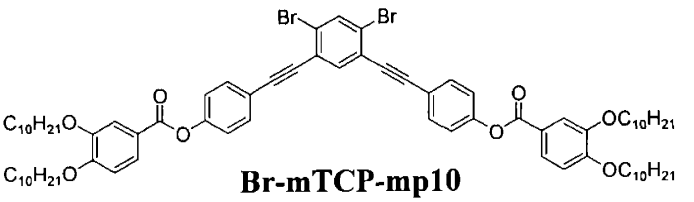

Br-mTCP-mp10

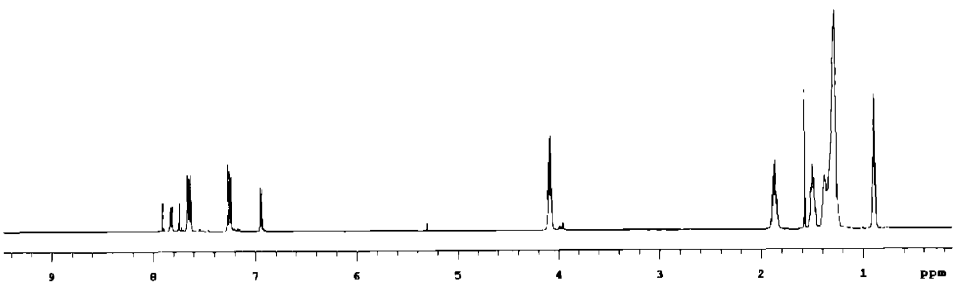

^{1}H NMR of **Br-mTCP-mp10** (500MHz, $CDCl_3$)

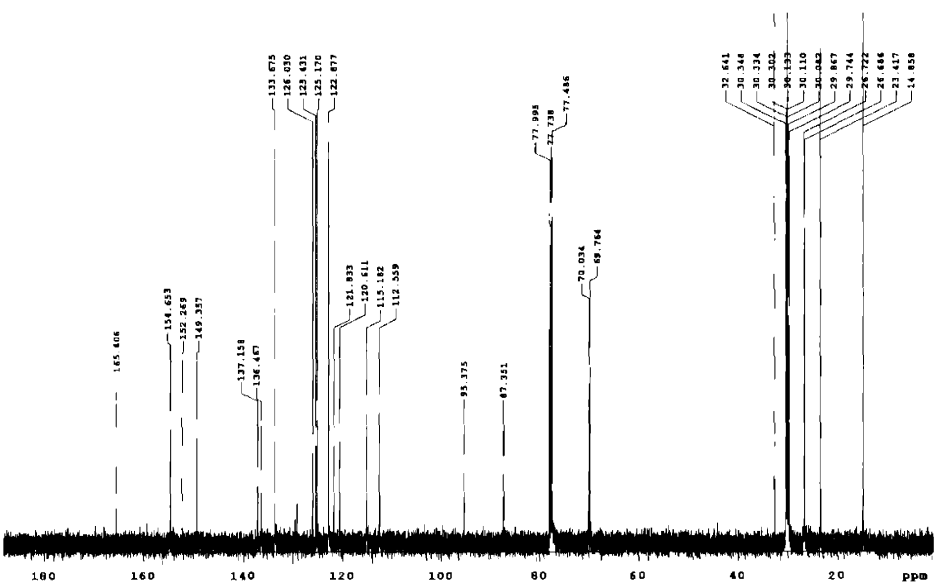

^{13}C NMR of **Br-mTCP-mp10** (125MHz, $CDCl_3$)

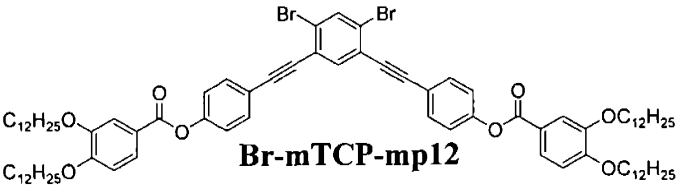

Br-mTCP-mp12

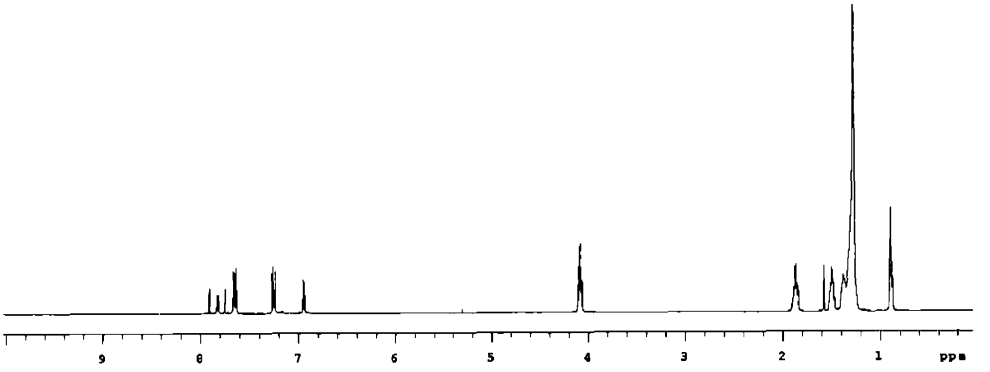

^{1}H NMR of **Br-mTCP-mp12** (500MHz, $CDCl_3$)

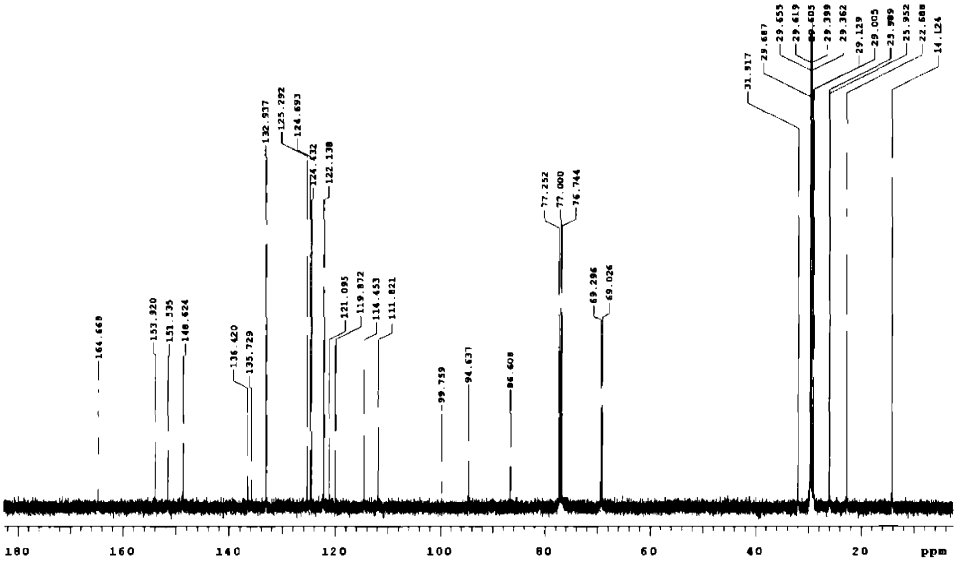

^{13}C NMR of **Br-mTCP-mp12** (125MHz, $CDCl_3$)

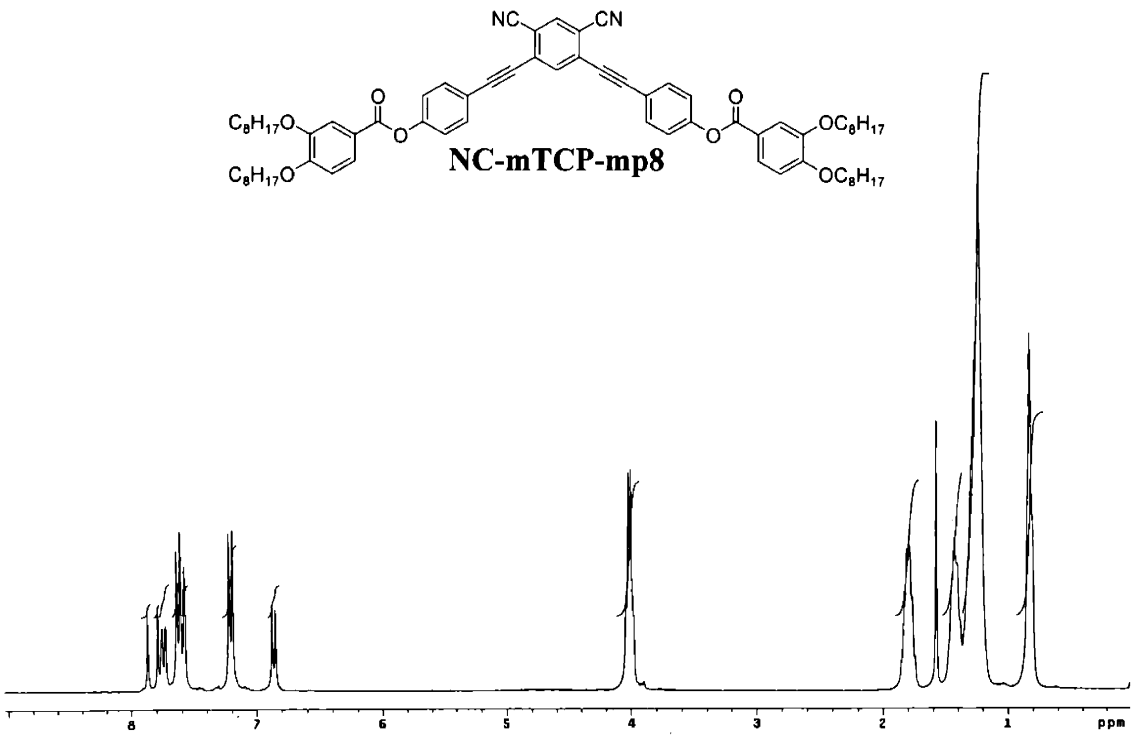

^{1}H NMR of NC-**mTCP-mp8** (500MHz, $CDCl_3$)

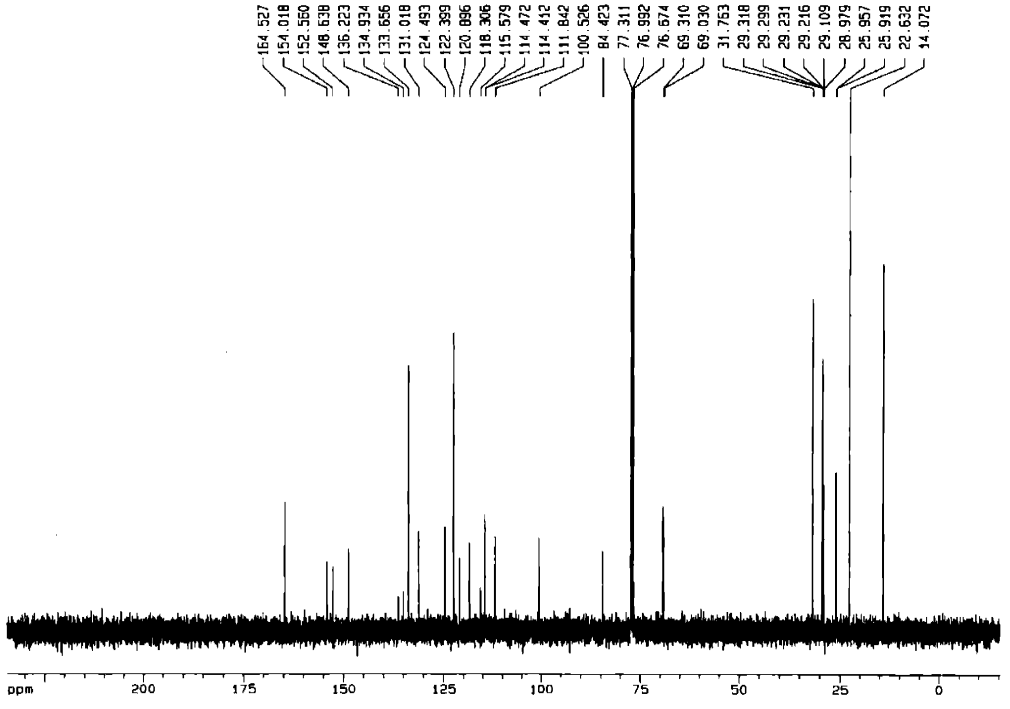

^{13}C NMR of **NC-mTCP-mp8** (125MHz, $CDCl_3$)

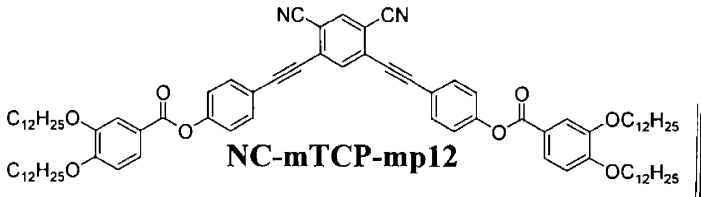
NC
CN
C12H25O
C12H25O
O
O
O
O
OC12H25
OC12H25

NC-mTCP-mp12

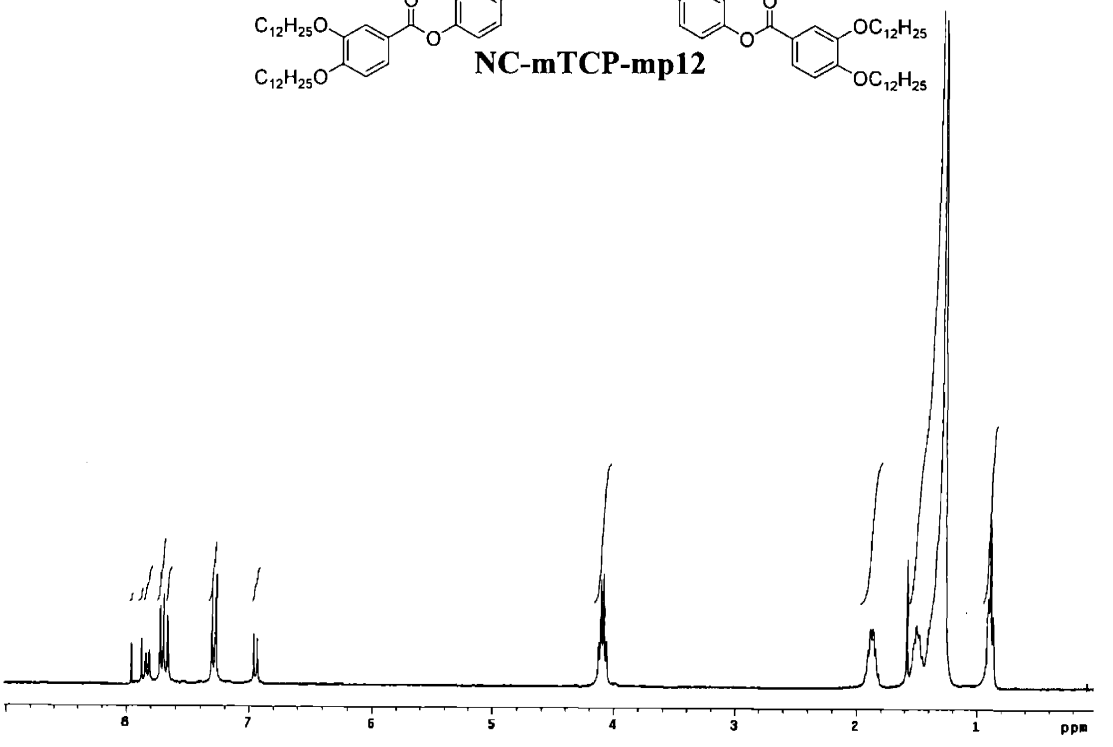
8
7
6
5
4
3
2
1
ppm

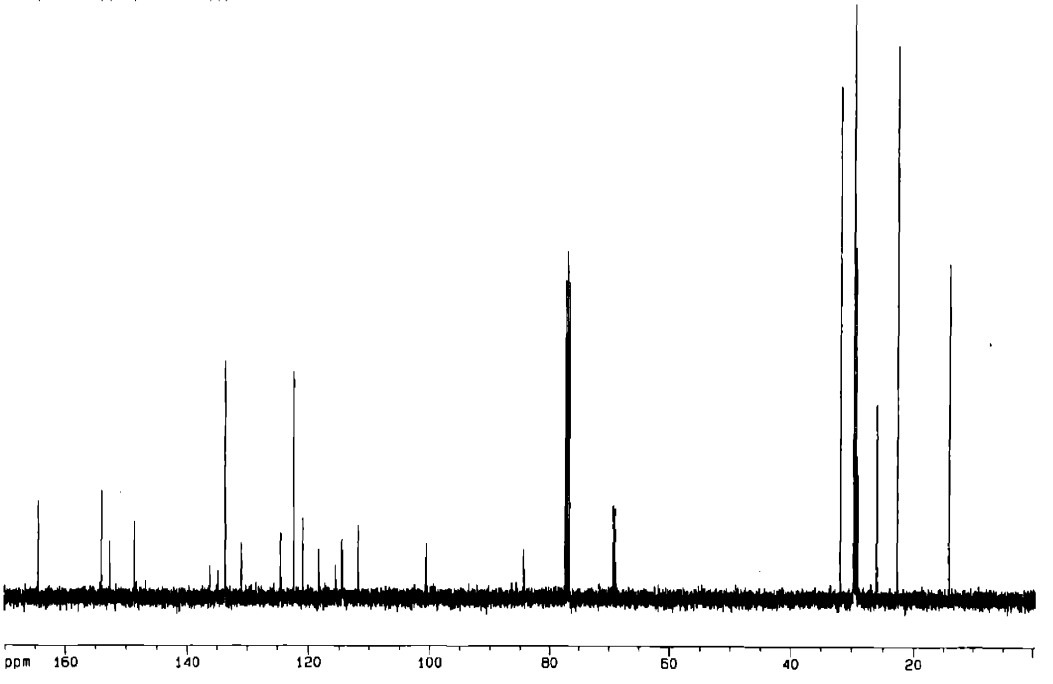
ppm
160
140
120
100
80
60
40
20

Appendix 2:

^{1}H and ^{13}C NMR spectra for Chapter 3

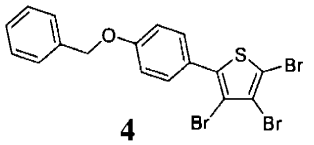

4

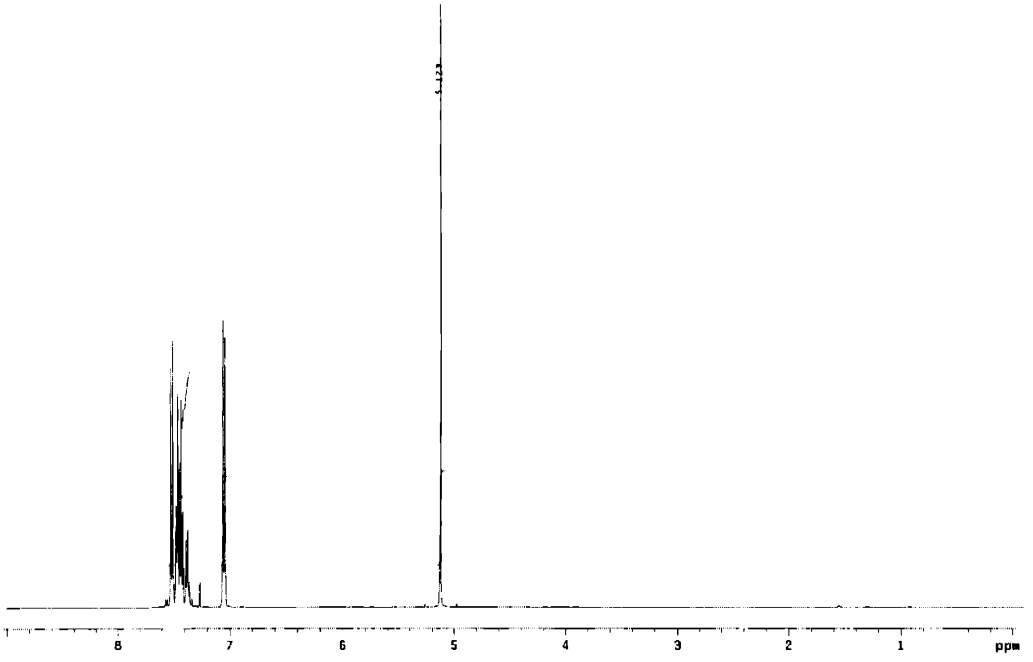

^{1}H NMR of **4** (500MHz, $CDCl_3$)

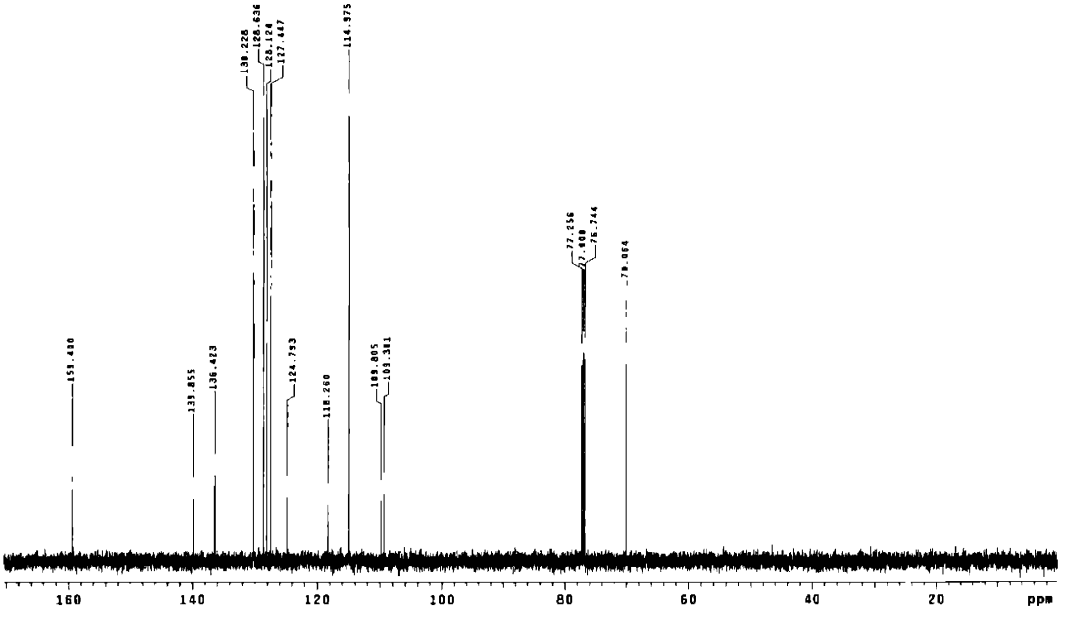

^{13}C NMR of **4** (125MHz, $CDCl_3$)

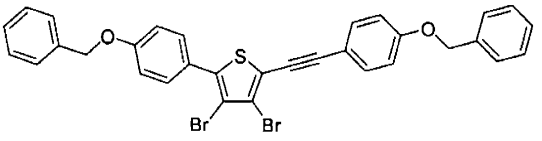

5

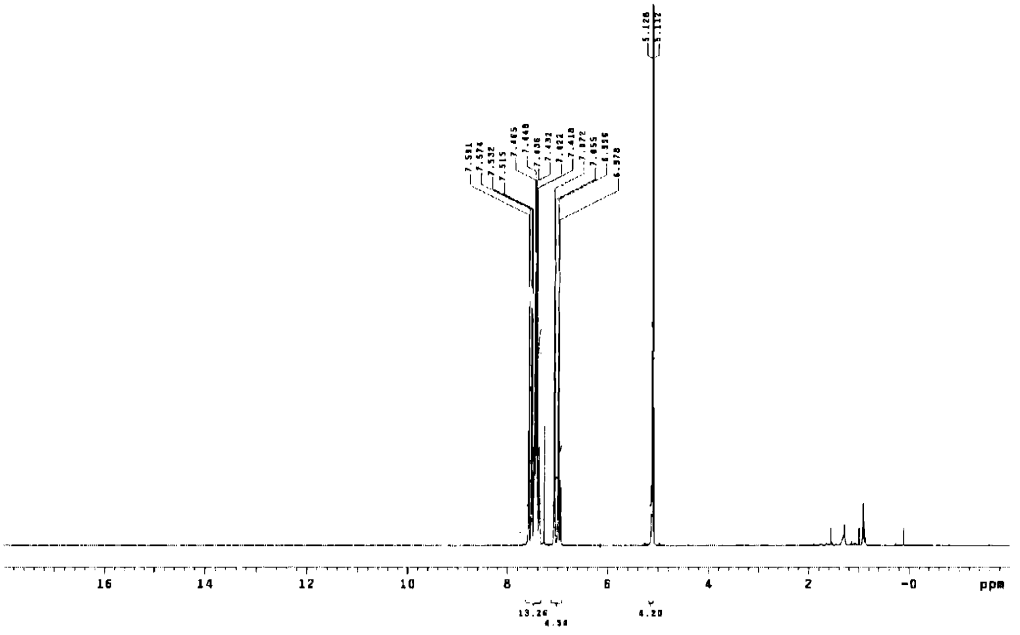

^{1}H NMR of **5** (300MHz, $CDCl_3$)

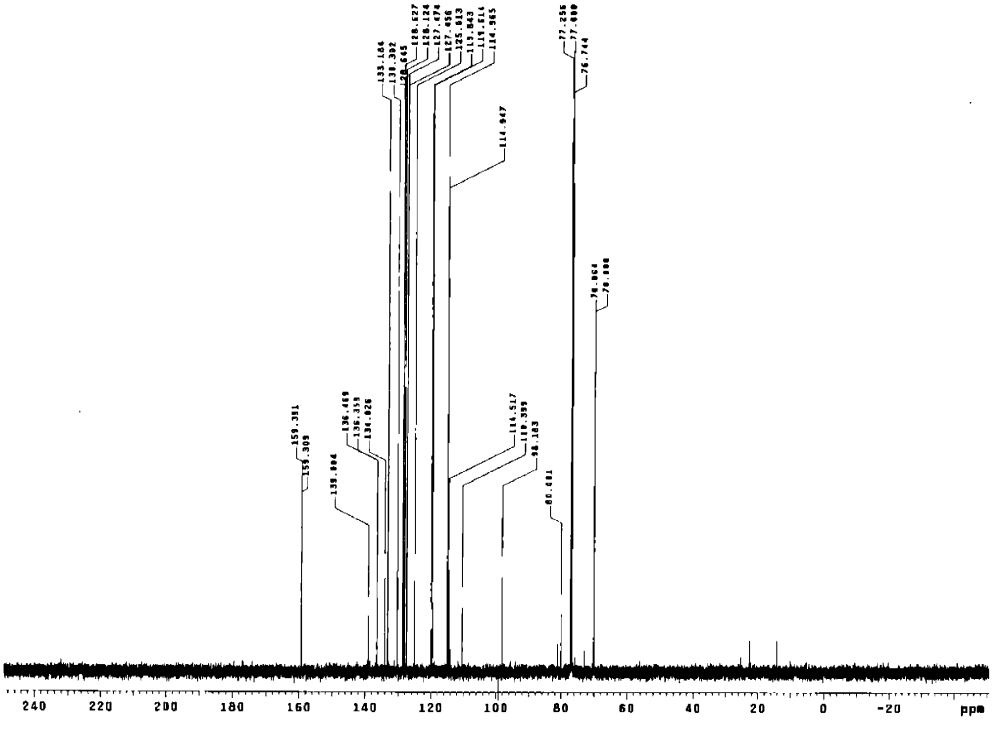

^{13}C NMR of **5** (75MHz, $CDCl_3$)

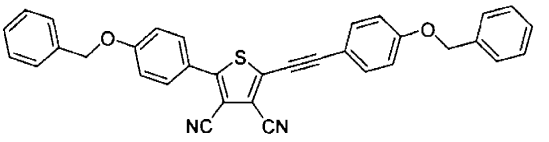

6

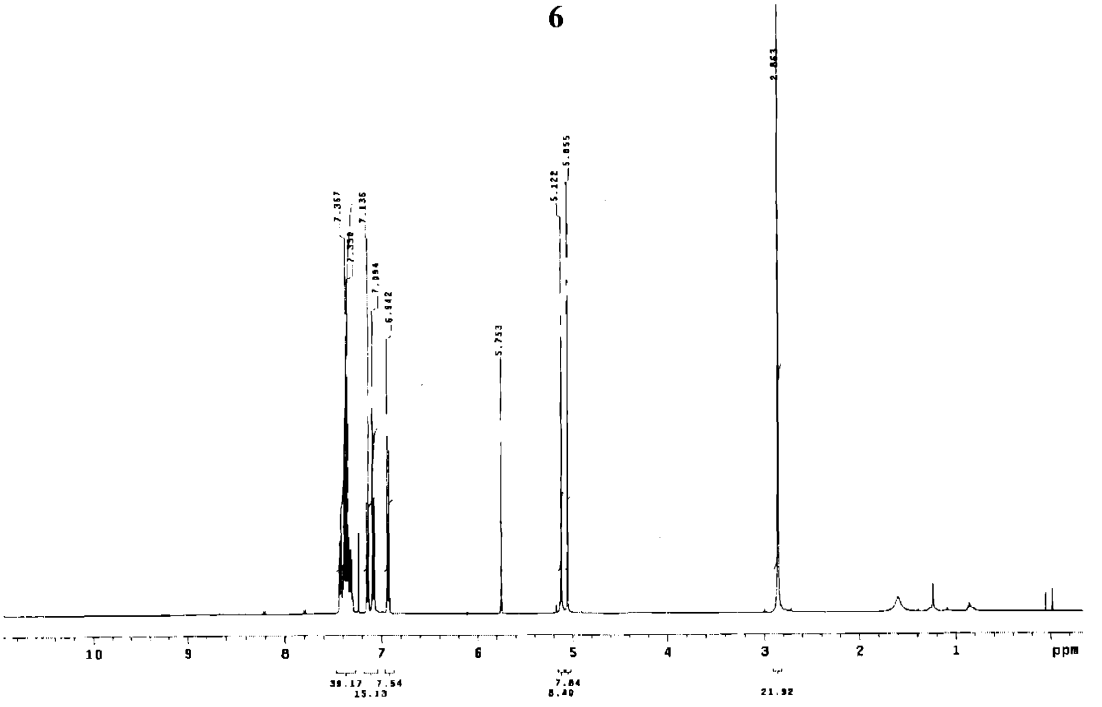

^{1}H NMR of **6** (500MHz, $CDCl_3$)

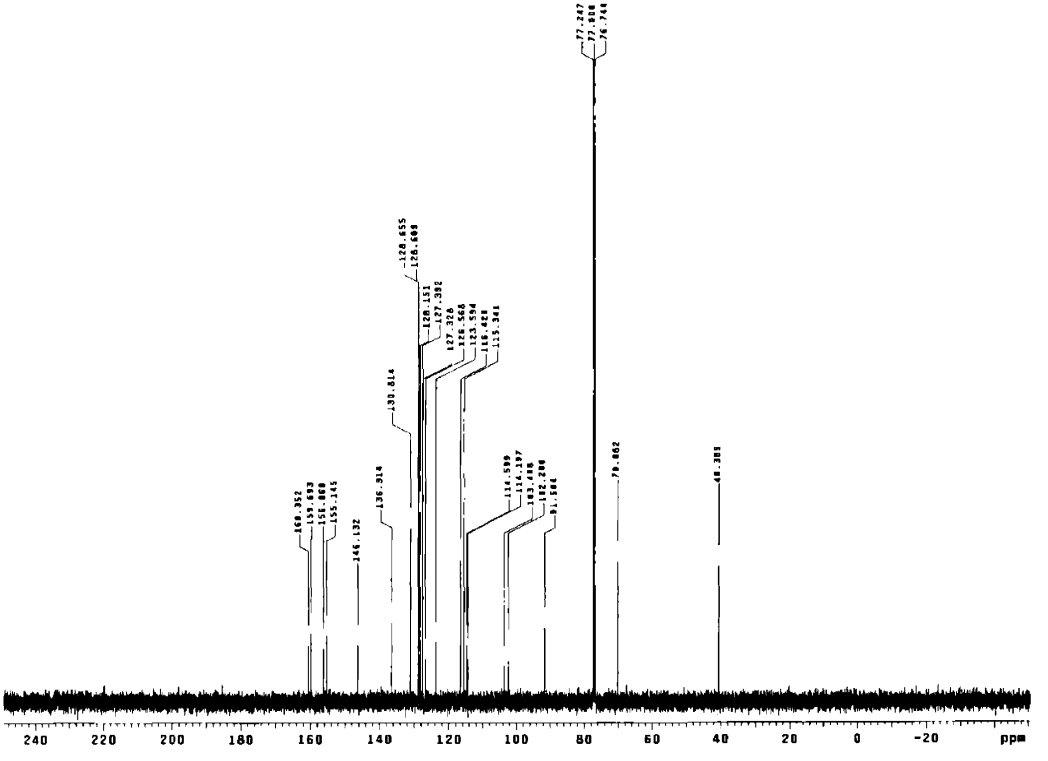

^{13}C NMR of **6** (125MHz, $CDCl_3$)

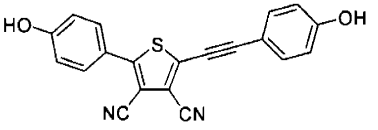

7

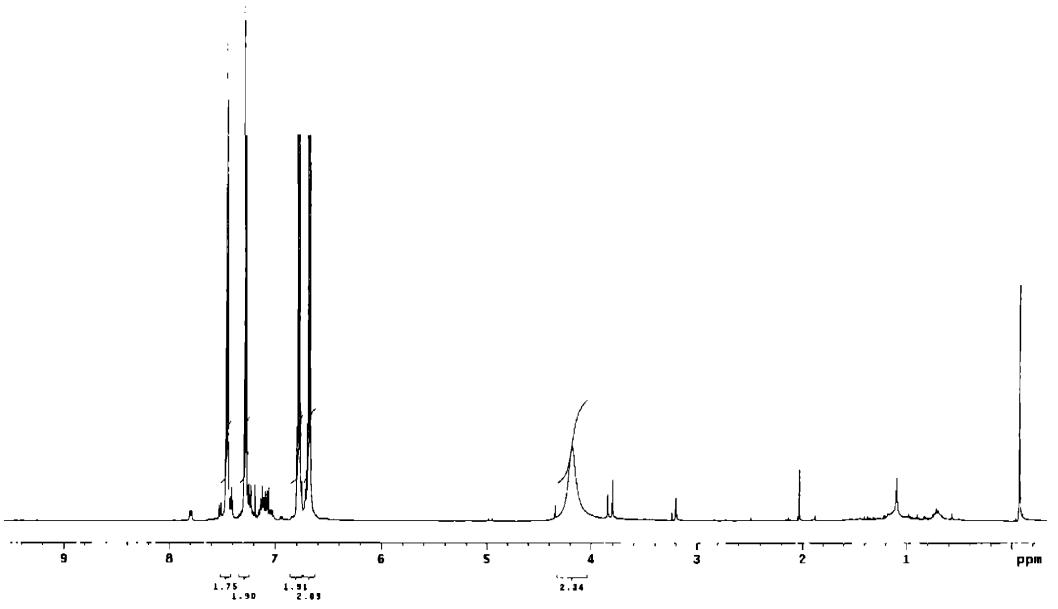

^{1}H NMR of **7** (500MHz, $CDCl_3$)

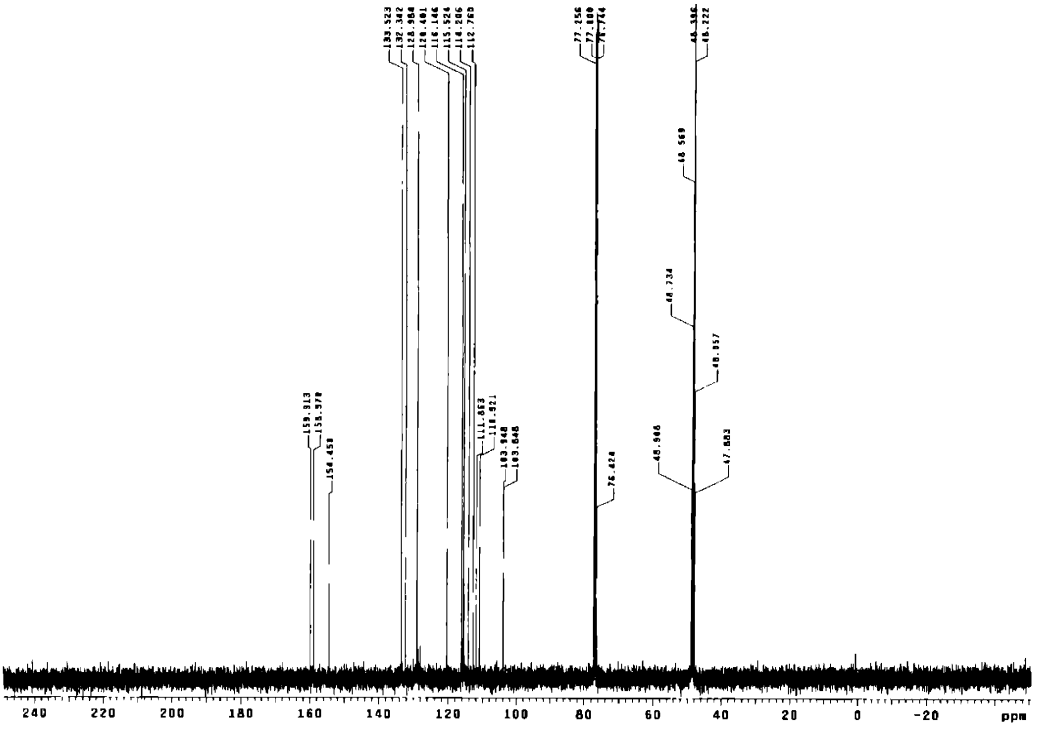

^{13}C NMR of **7** (125MHz, $CDCl_3$)

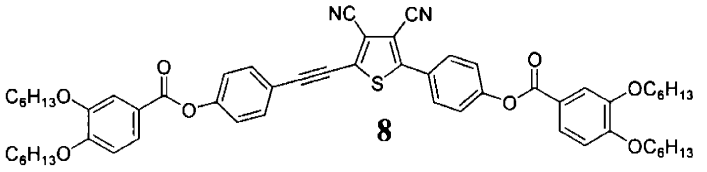

8

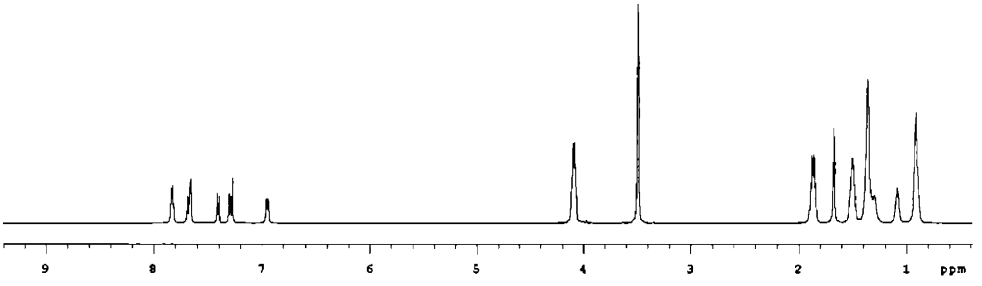

^{1}H NMR of **8** (500MHz, $CDCl_3$)

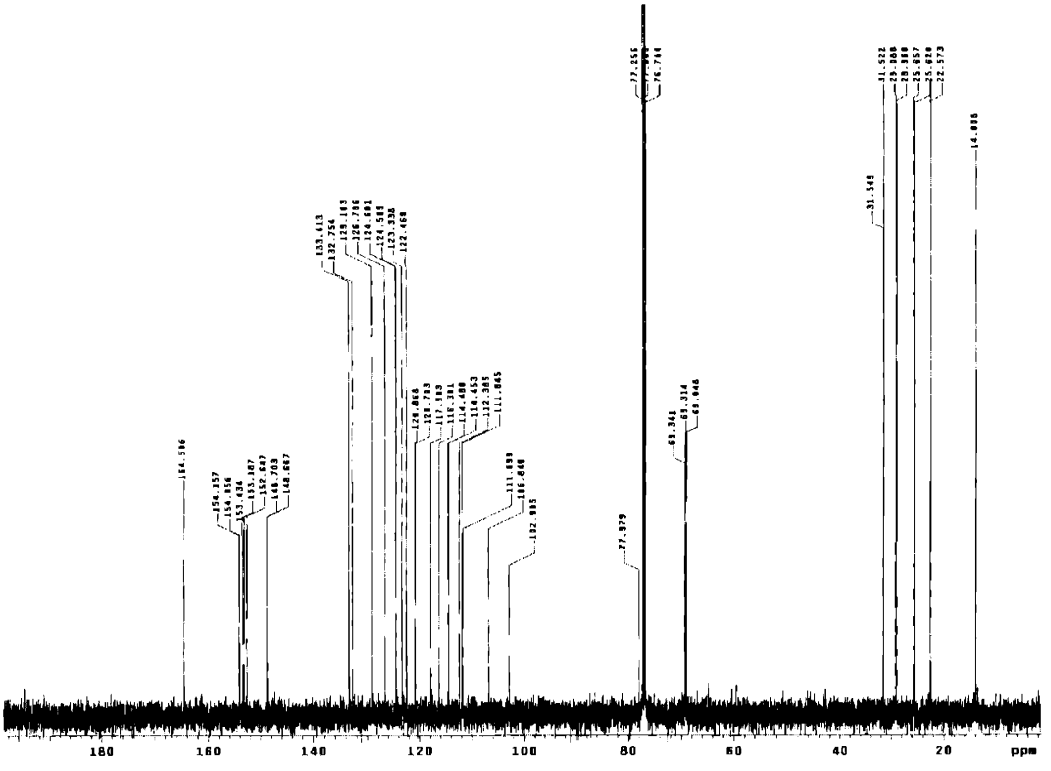

^{13}C NMR of **8** (125MHz, $CDCl_3$)

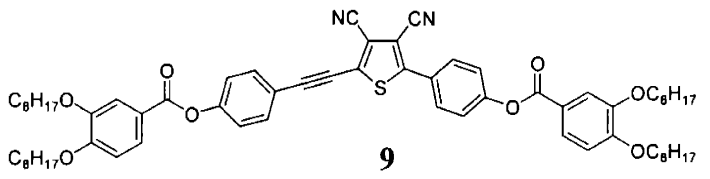

9

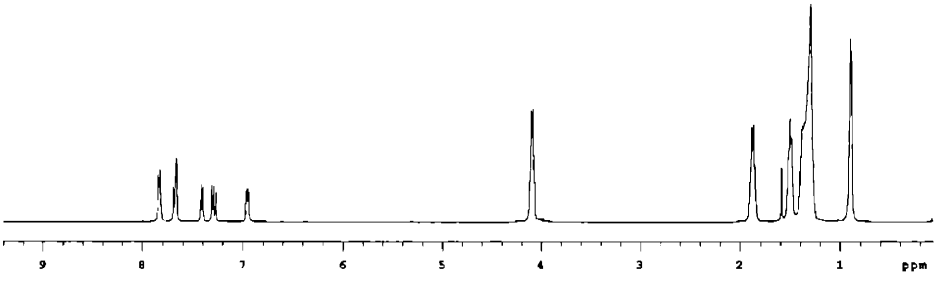

^{1}H NMR of **9** (500MHz, $CDCl_3$)

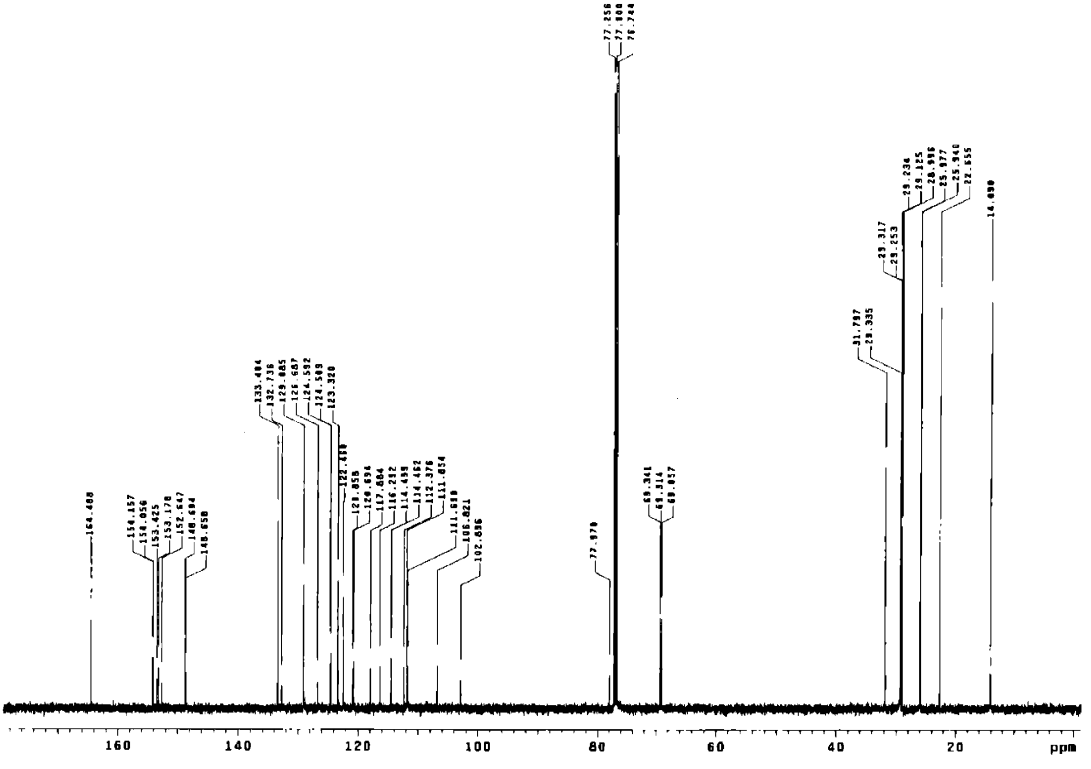

^{13}C NMR of **9** (125MHz, $CDCl_3$)

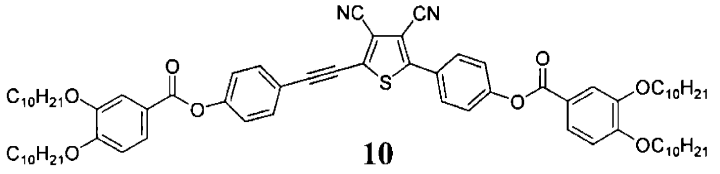

10

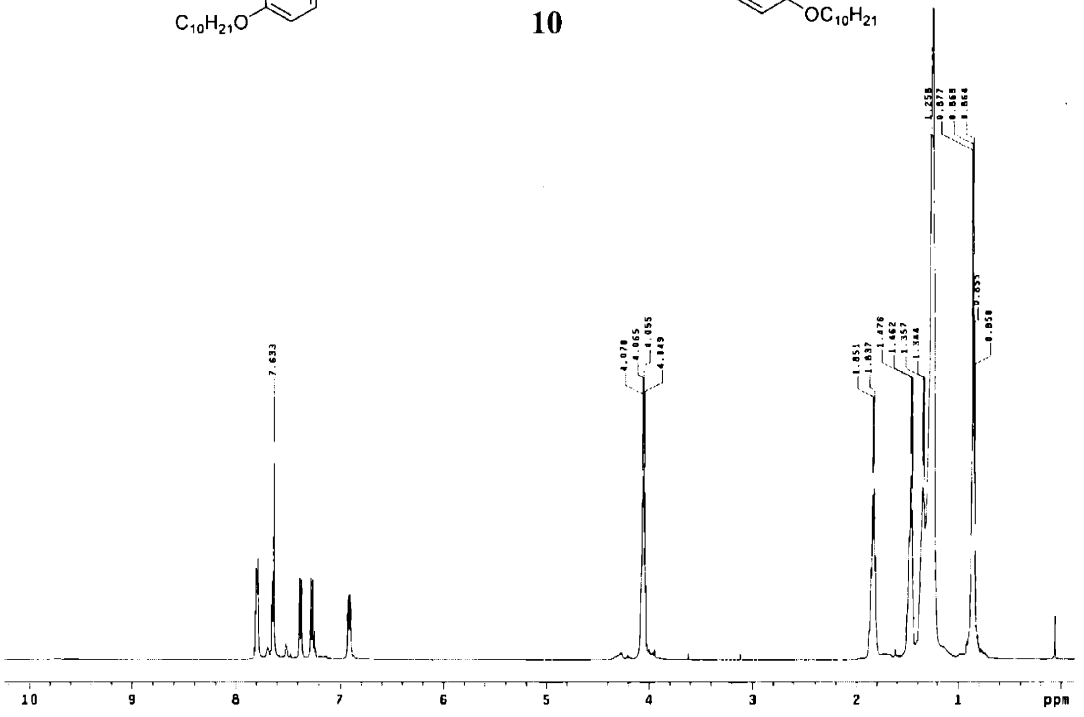

^{1}H NMR of **10** (500MHz, $CDCl_3$)

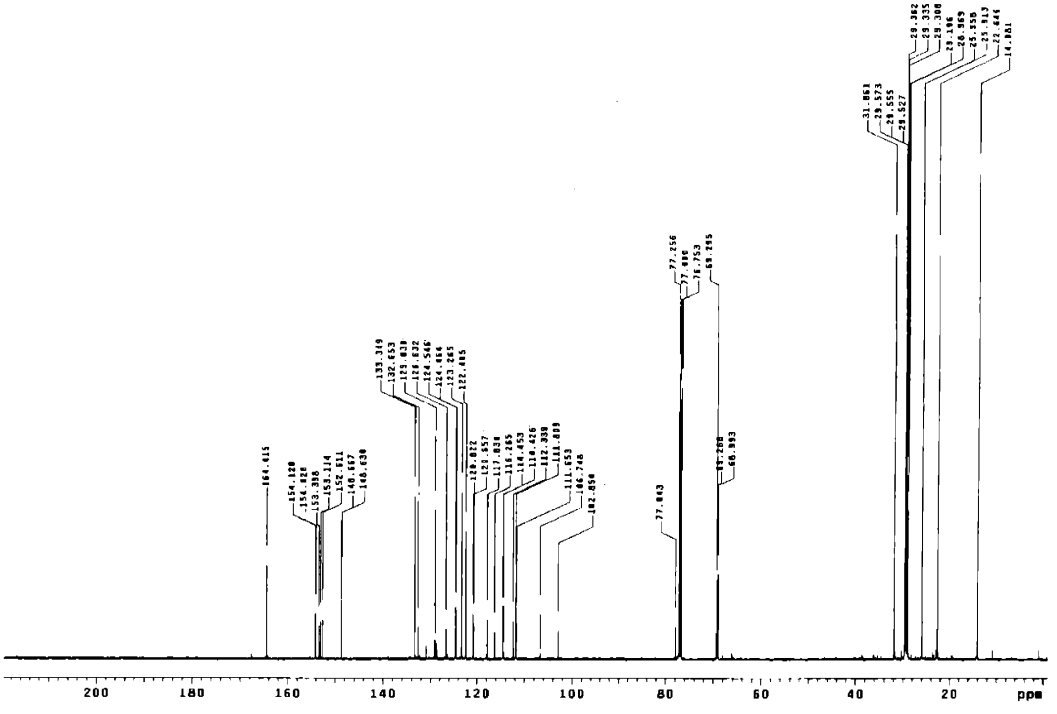

^{13}C NMR of **10** (125MHz, $CDCl_3$)

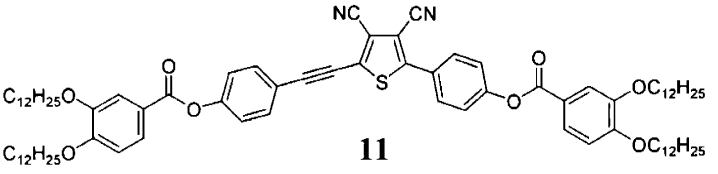

11

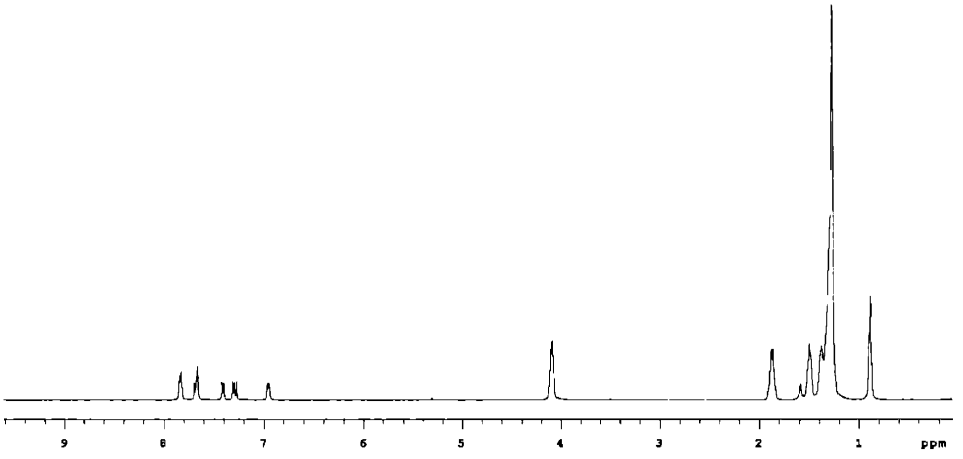

^{1}H NMR of **11** (500MHz, $CDCl_3$)

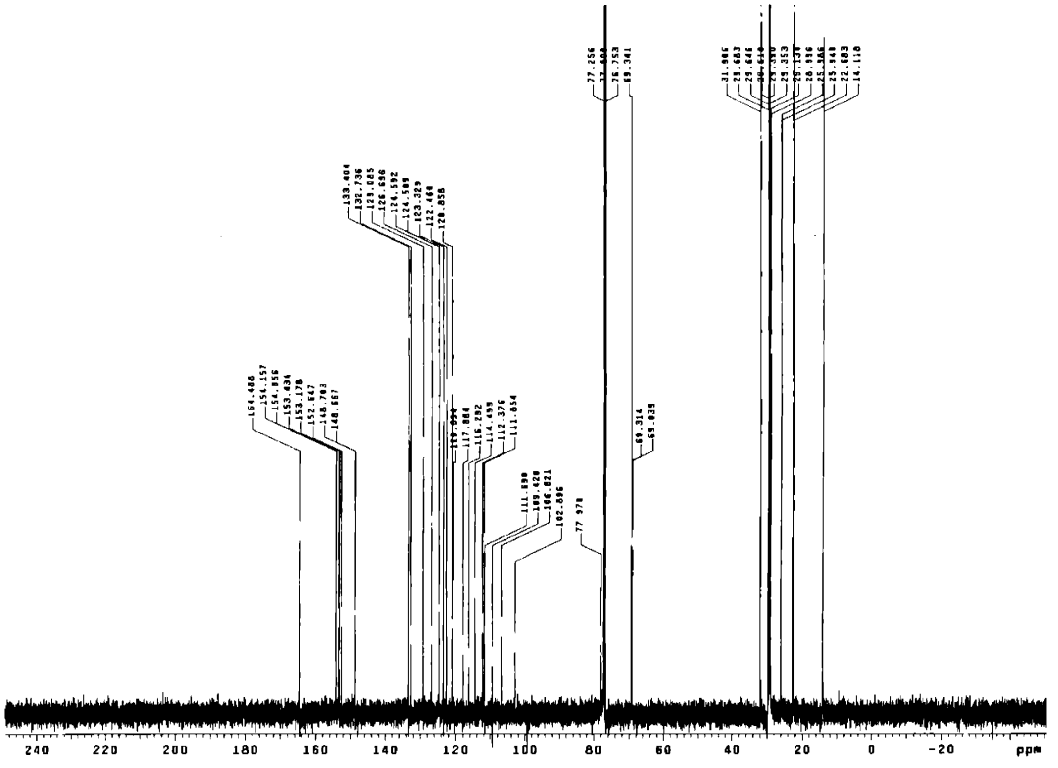

^{13}C NMR of **11** (125MHz, $CDCl_3$)

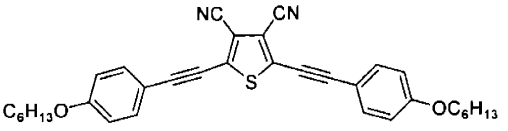

13

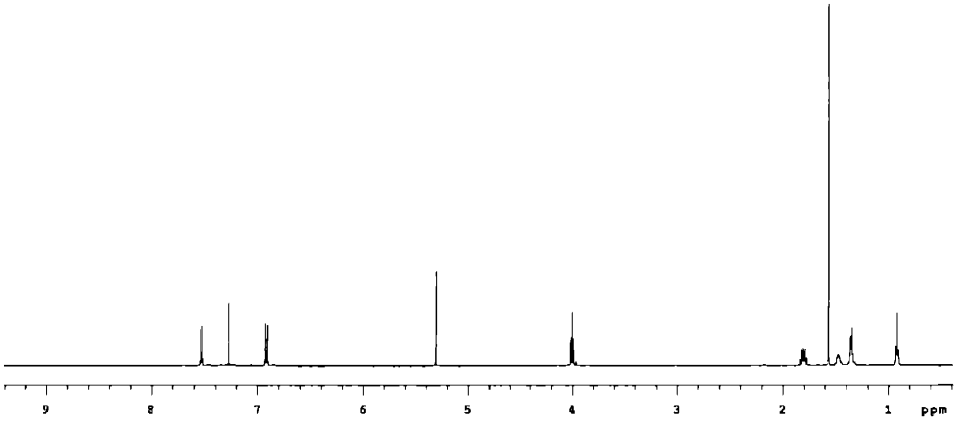

^{1}H NMR of **13** (500MHz, $CDCl_3$)

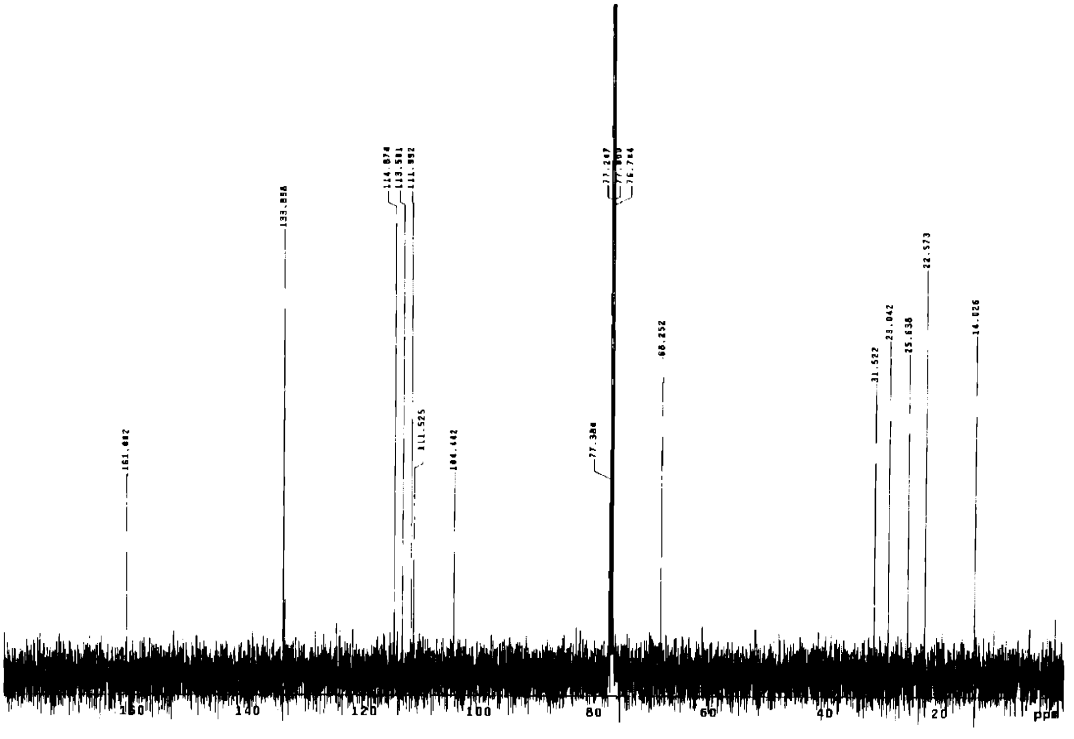

^{13}C NMR of **13** (125MHz, $CDCl_3$)

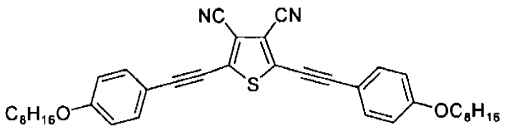

14

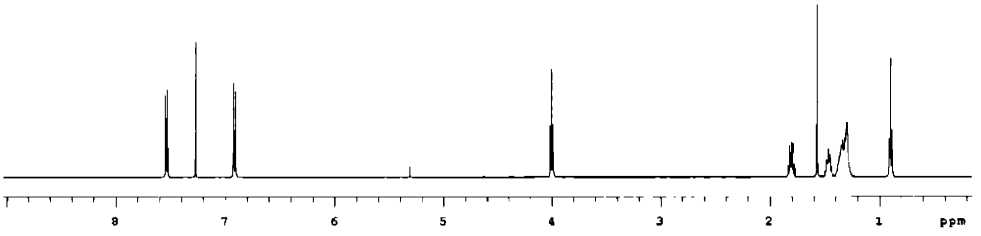

^{1}H NMR of **14** (500MHz, $CDCl_3$)

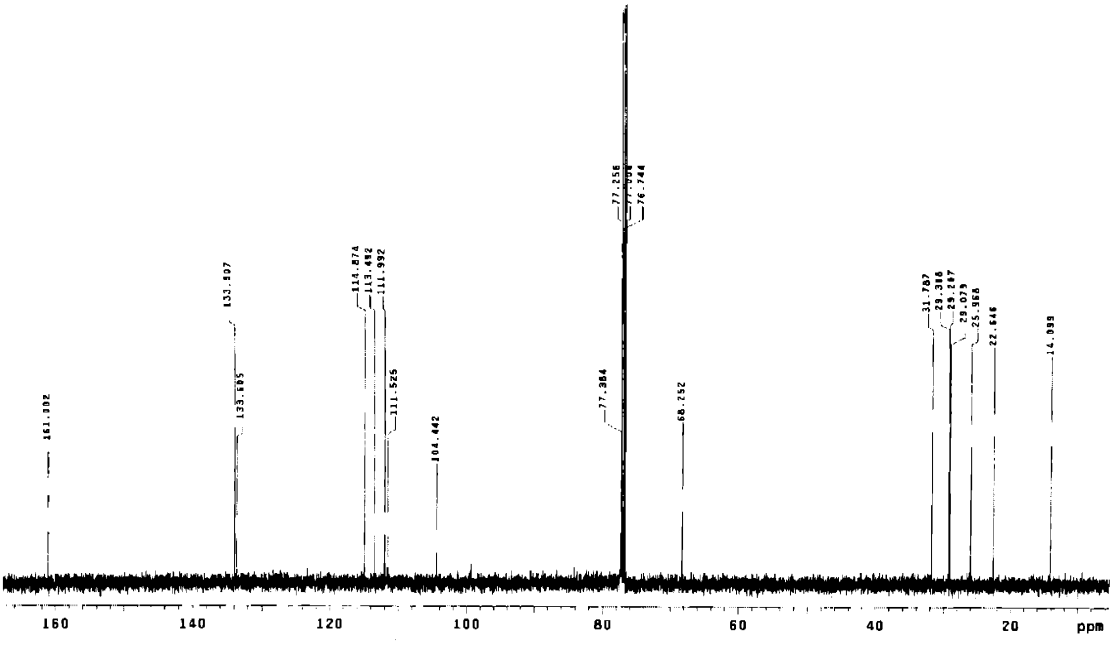

^{13}C NMR of **14** (125MHz, $CDCl_3$)

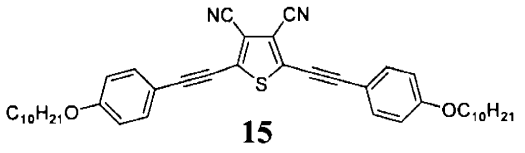

15

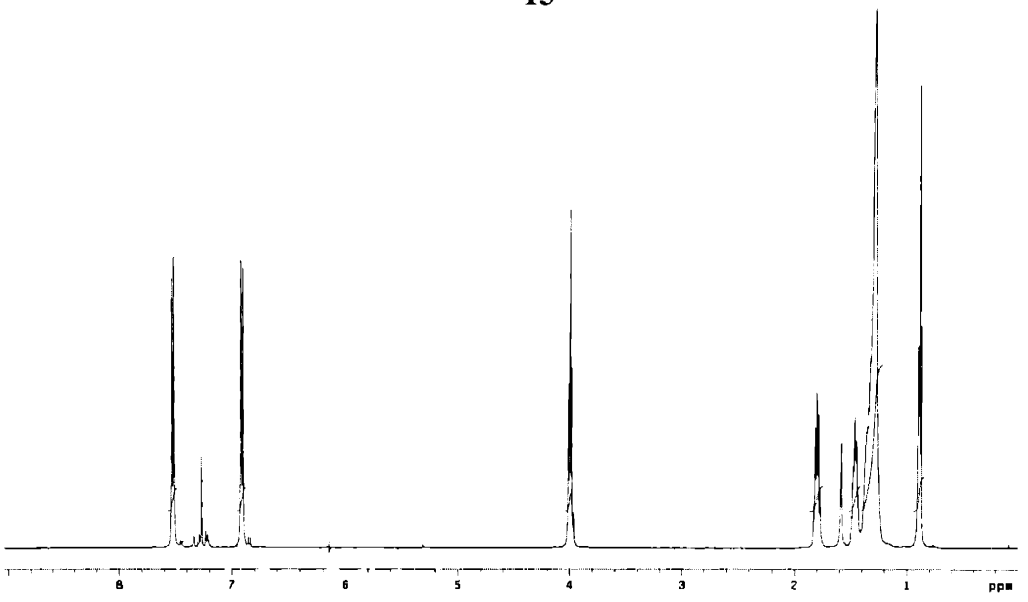

^{1}H NMR of **15** (500MHz, $CDCl_3$)

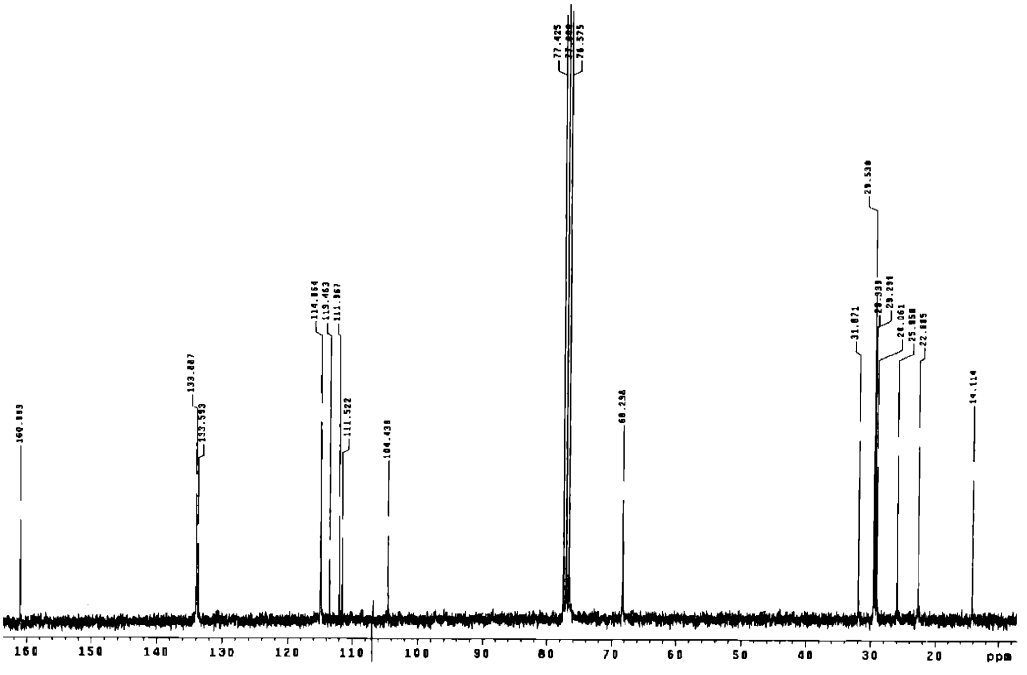

^{13}C NMR of **15** (125MHz, $CDCl_3$)

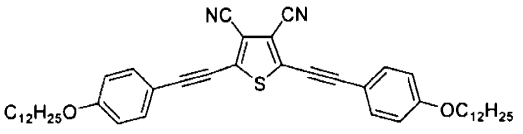

16

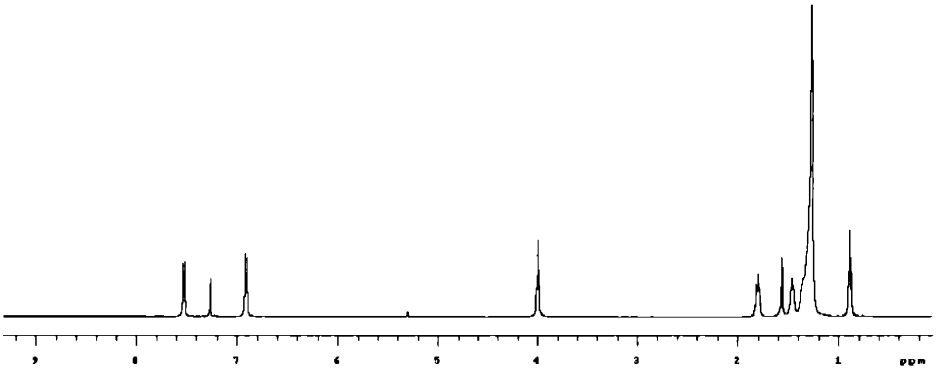

^{1}H NMR of **16** (500MHz, $CDCl_3$)

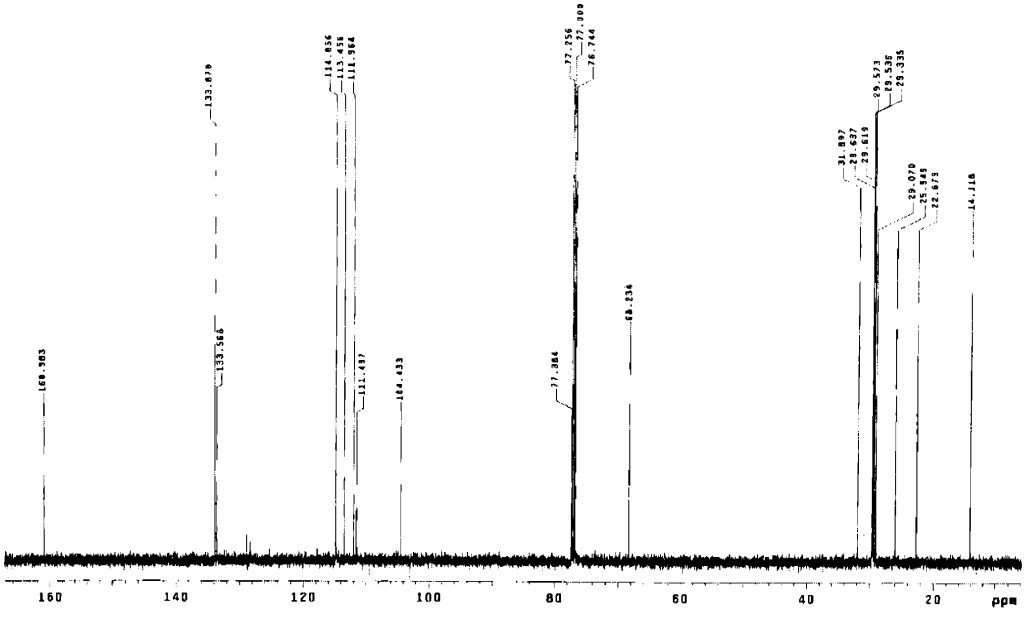

^{13}C NMR of **16** (125MHz, $CDCl_3$)

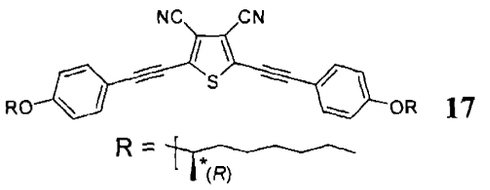

17

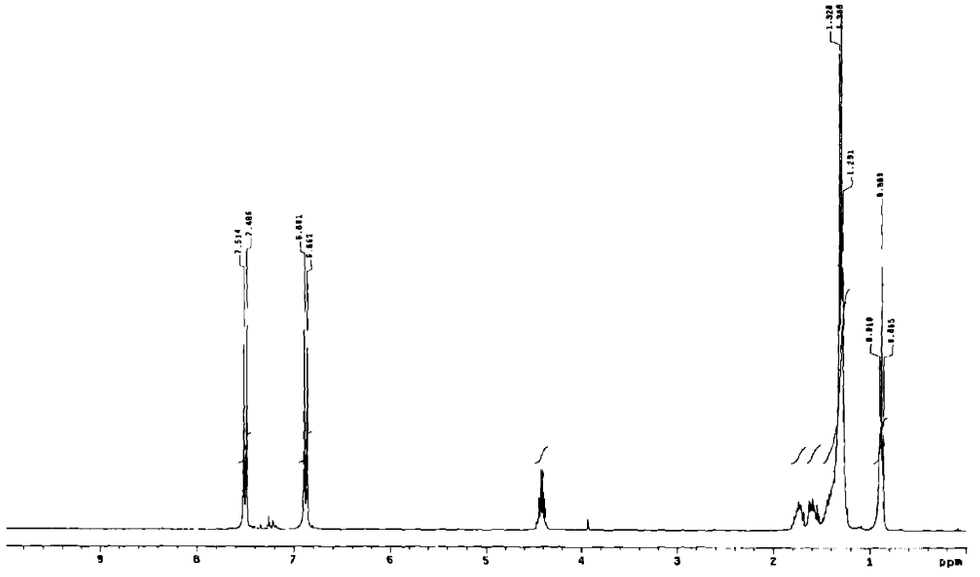

^{1}H NMR of **17** (500MHz, $CDCl_3$)

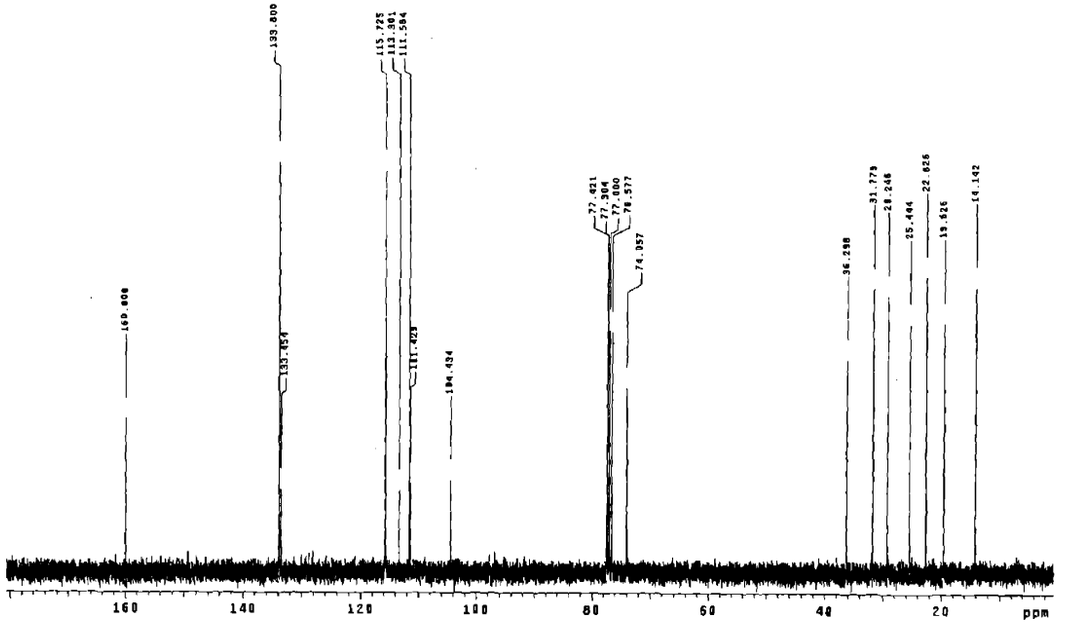

^{13}C NMR of **17** (125MHz, $CDCl_3$)

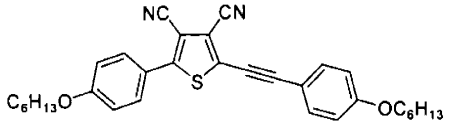

18

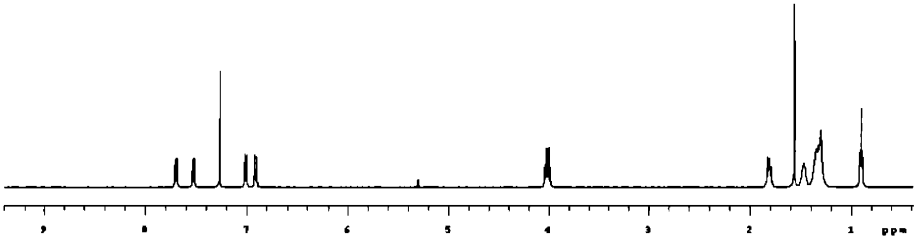

^{1}H NMR of **18** (300MHz, $CDCl_3$)

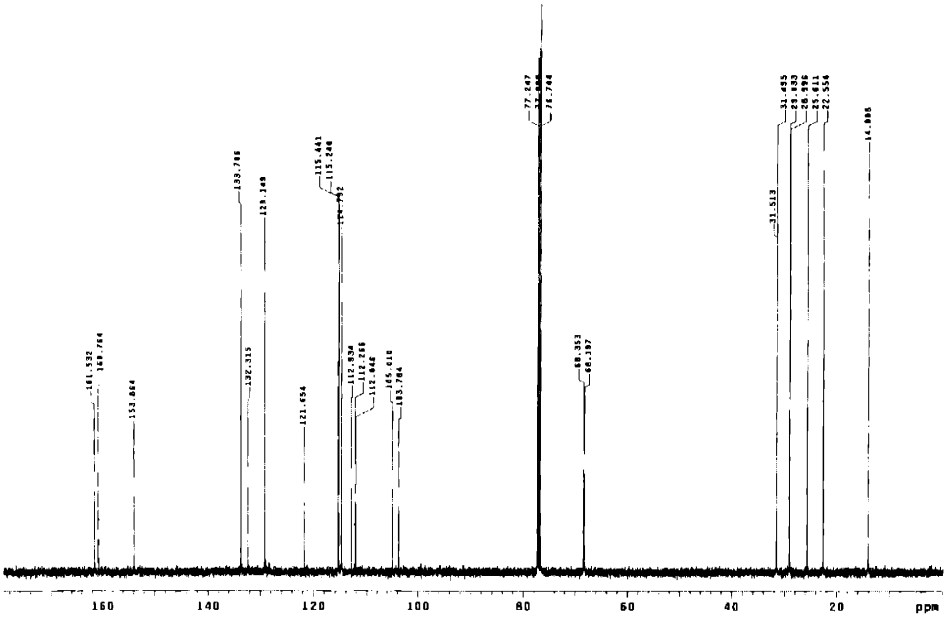

^{13}C NMR of **18** (125MHz, $CDCl_3$)

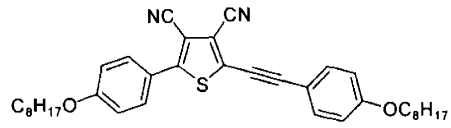

19

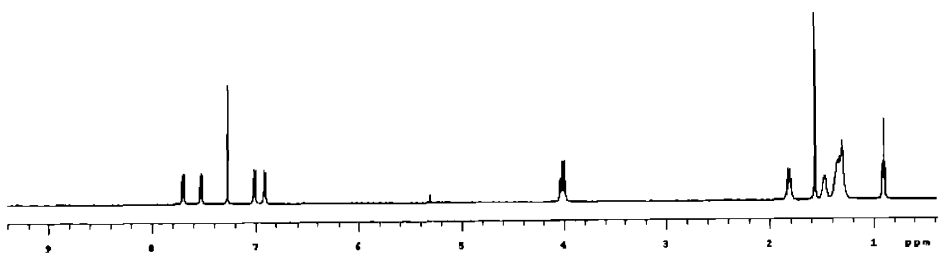

^{1}H NMR of **19** (500MHz, $CDCl_3$)

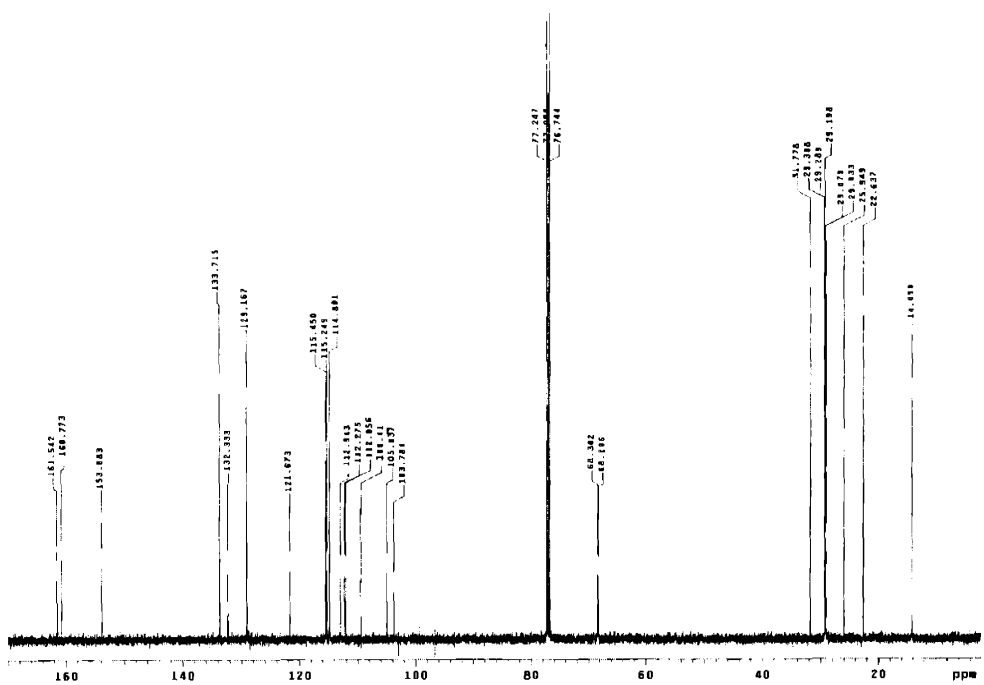

^{13}C NMR of **19** (125MHz, $CDCl_3$)

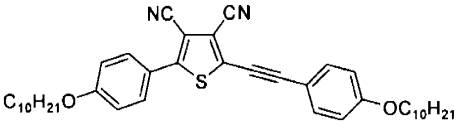

20

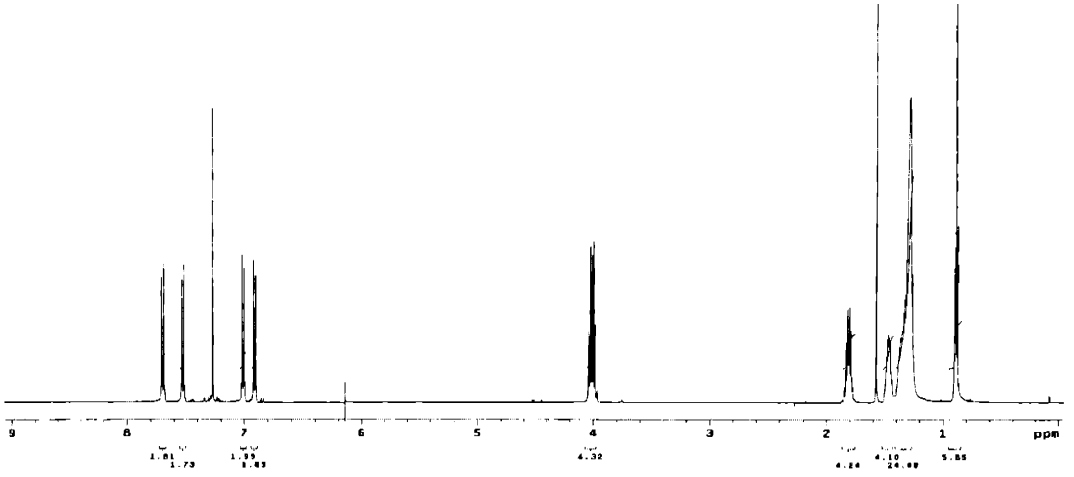

^{1}H NMR of **20** (500MHz, $CDCl_3$)

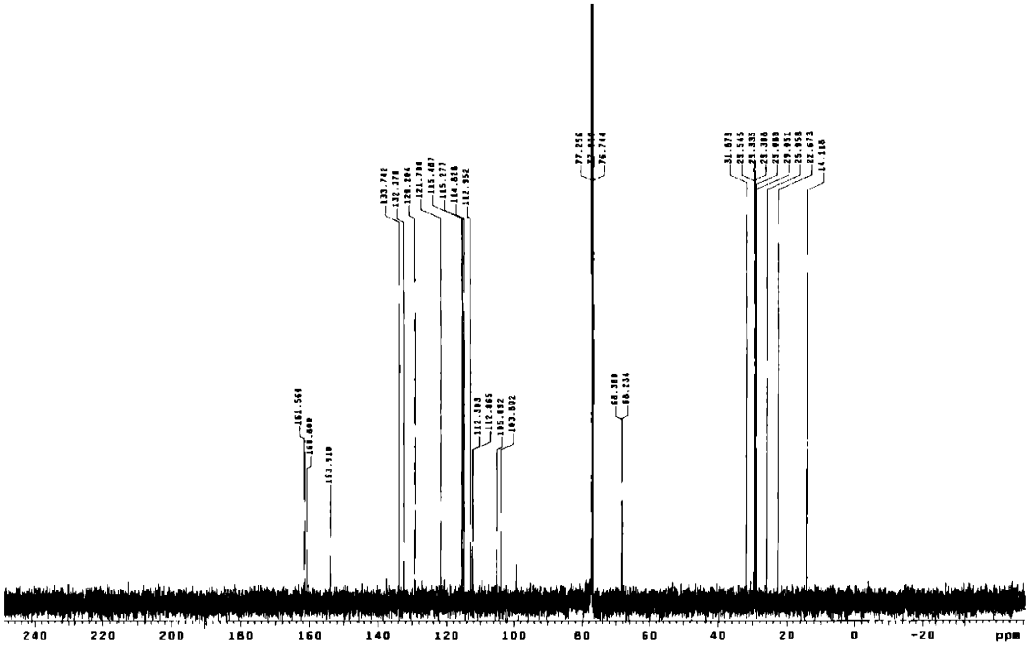

^{13}C NMR of **20** (125MHz, $CDCl_3$)

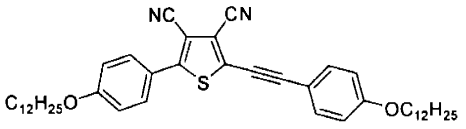

21

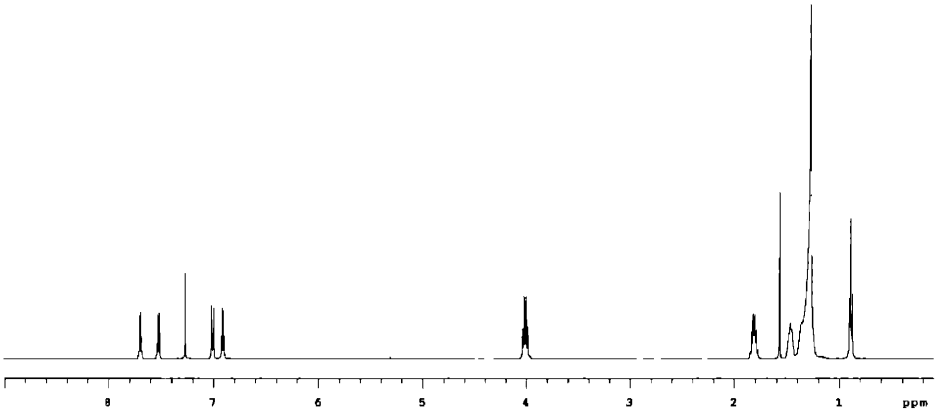

^{1}H NMR of **21** (500MHz, $CDCl_3$)

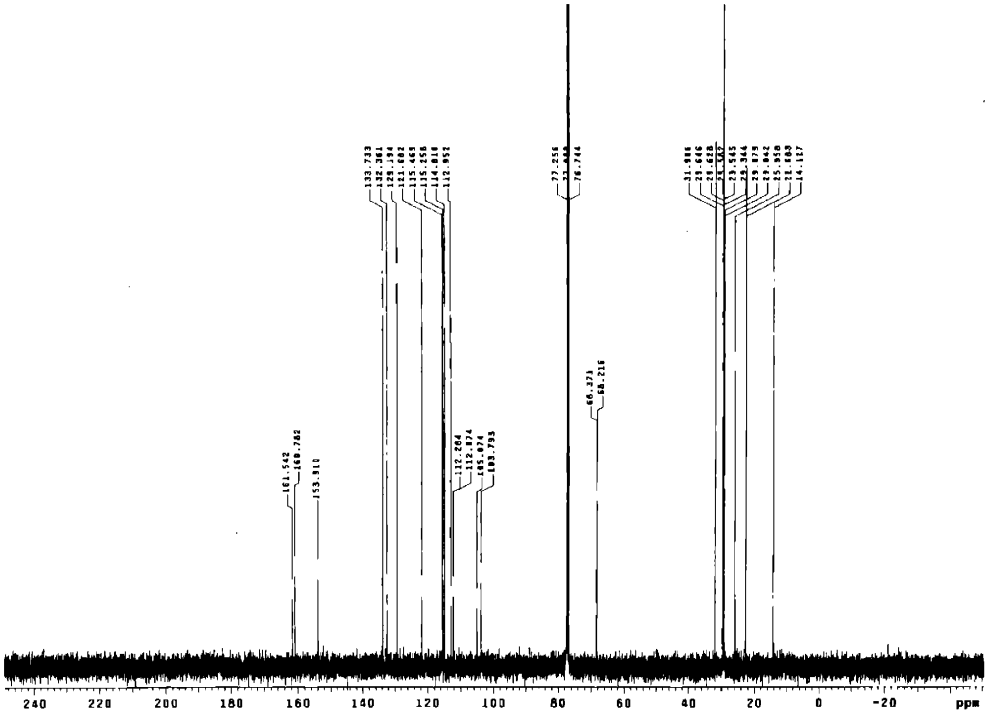

^{13}C NMR of **21** (125MHz, $CDCl_3$)

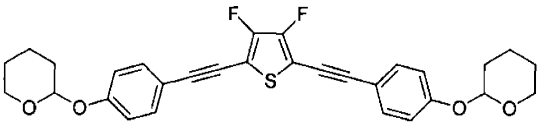

22

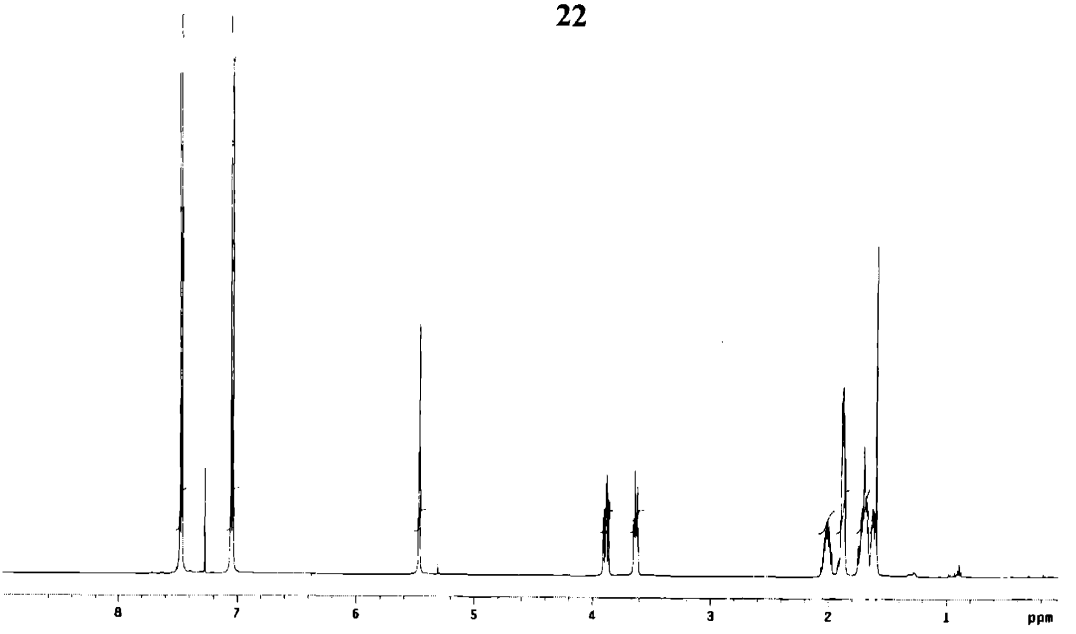

^{1}H NMR of **22** (500MHz, $CDCl_3$)

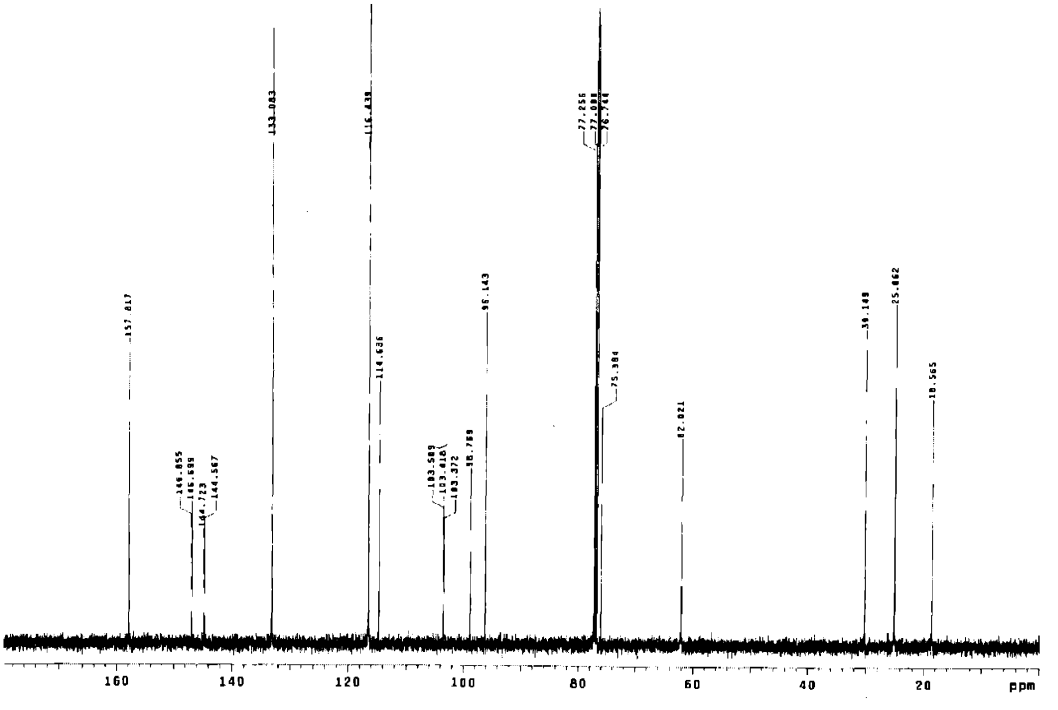

^{13}C NMR of **22** (125MHz, $CDCl_3$)

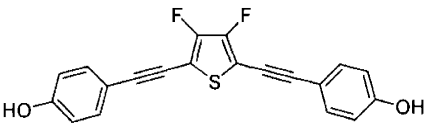

23

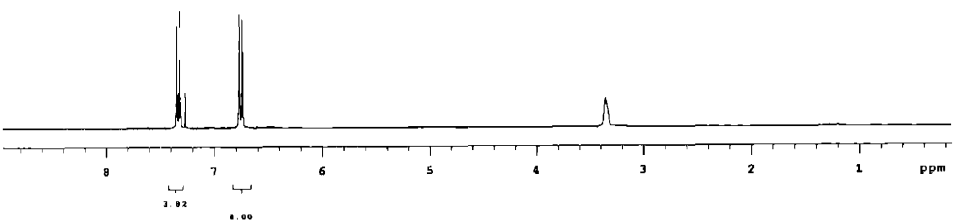

^{1}H NMR of **23** (300MHz, $CDCl_3$)

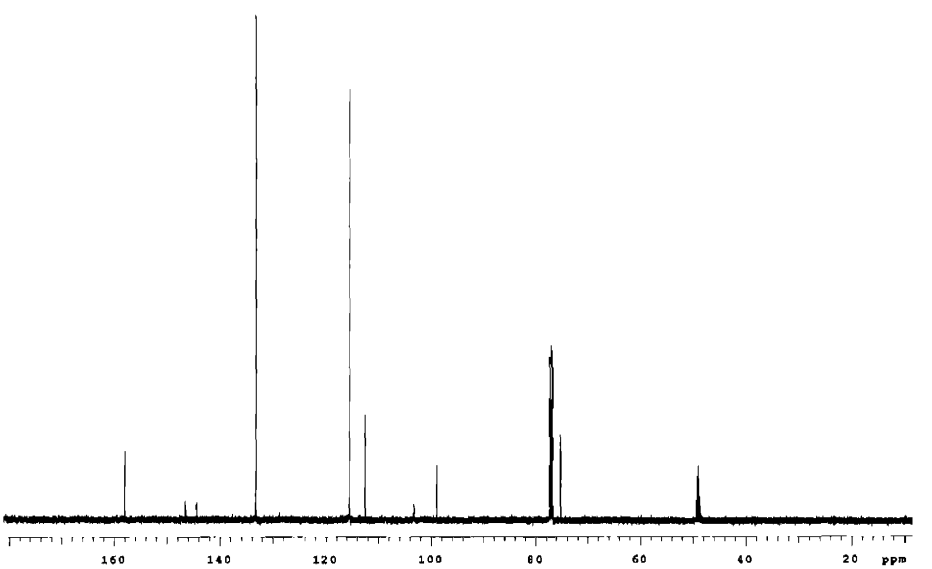

^{13}C NMR of **23** (300MHz, $CDCl_3$)

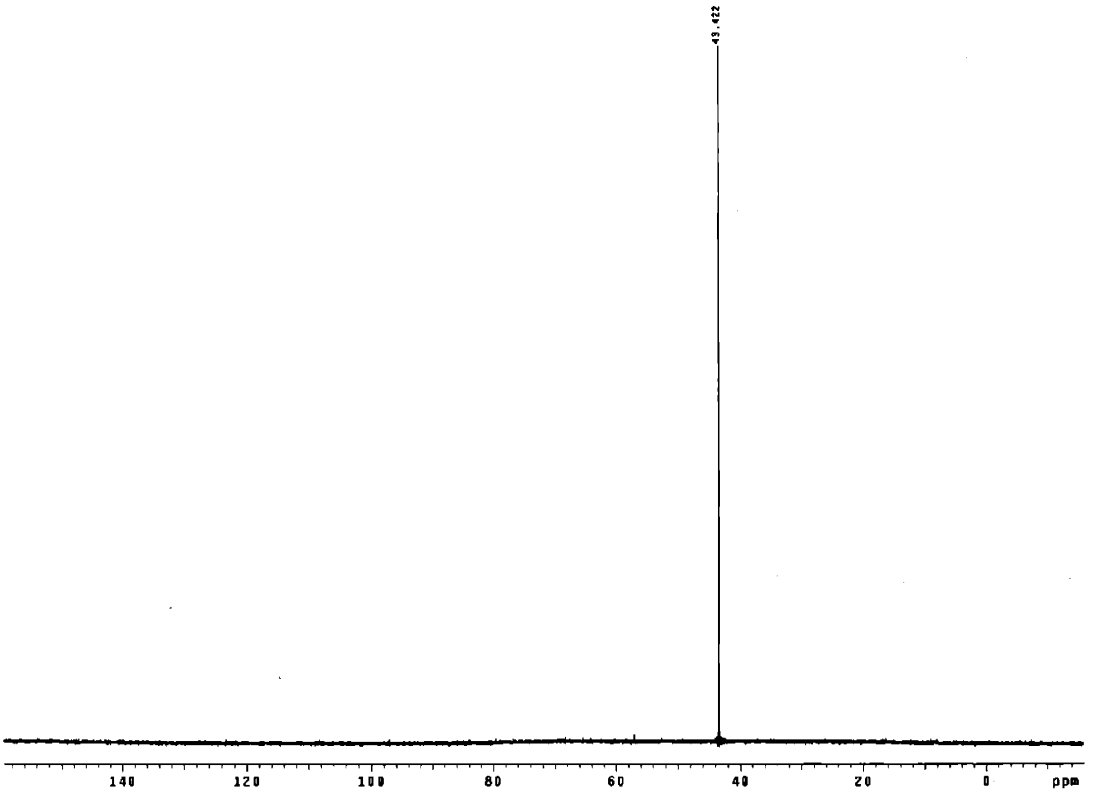

^{19}F NMR of **23** (282MHz, $CDCl_3$)

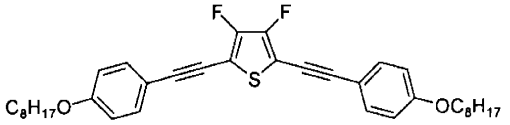

24

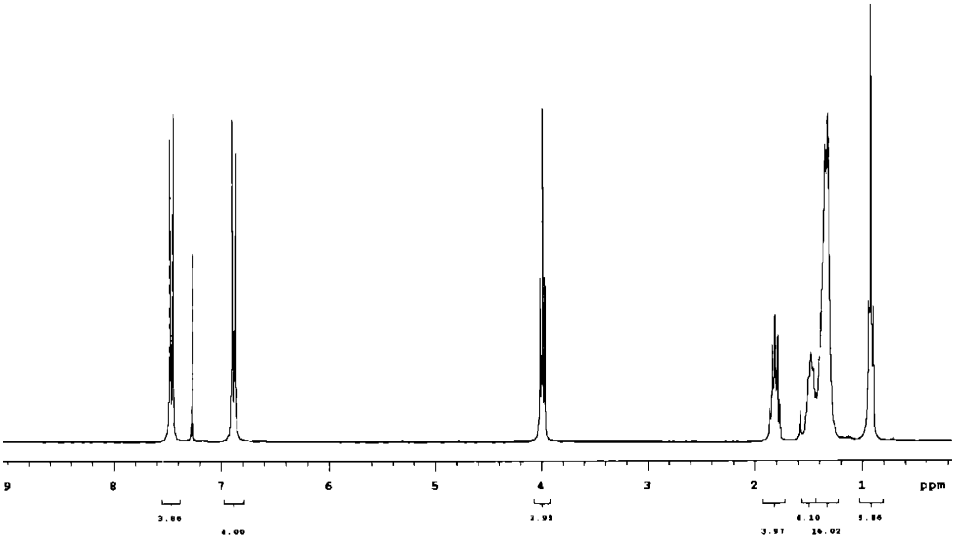

^{1}H NMR of **24** (300MHz, $CDCl_3$)

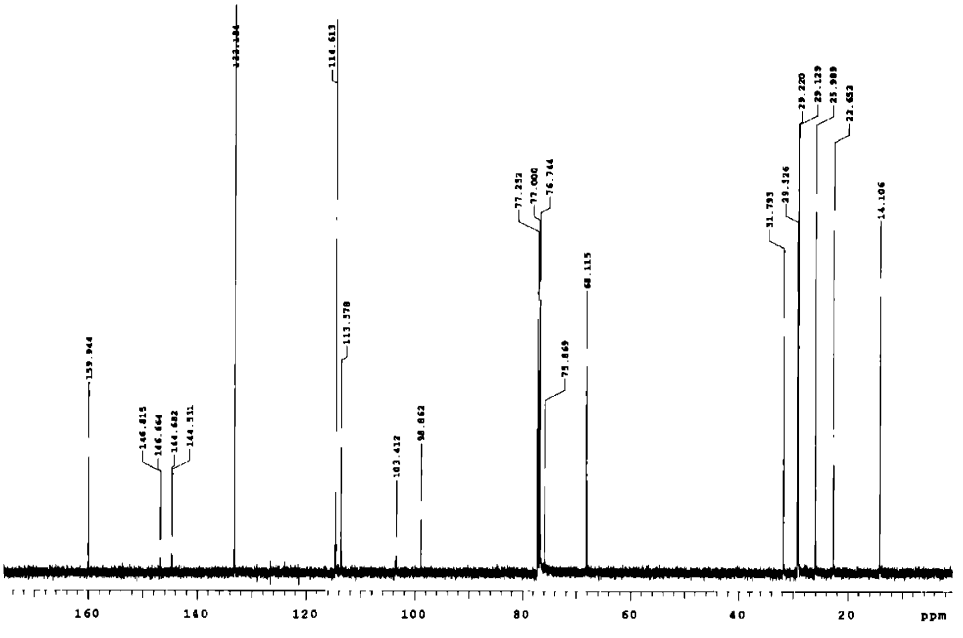

^{13}C NMR of **24** (300MHz, $CDCl_3$)

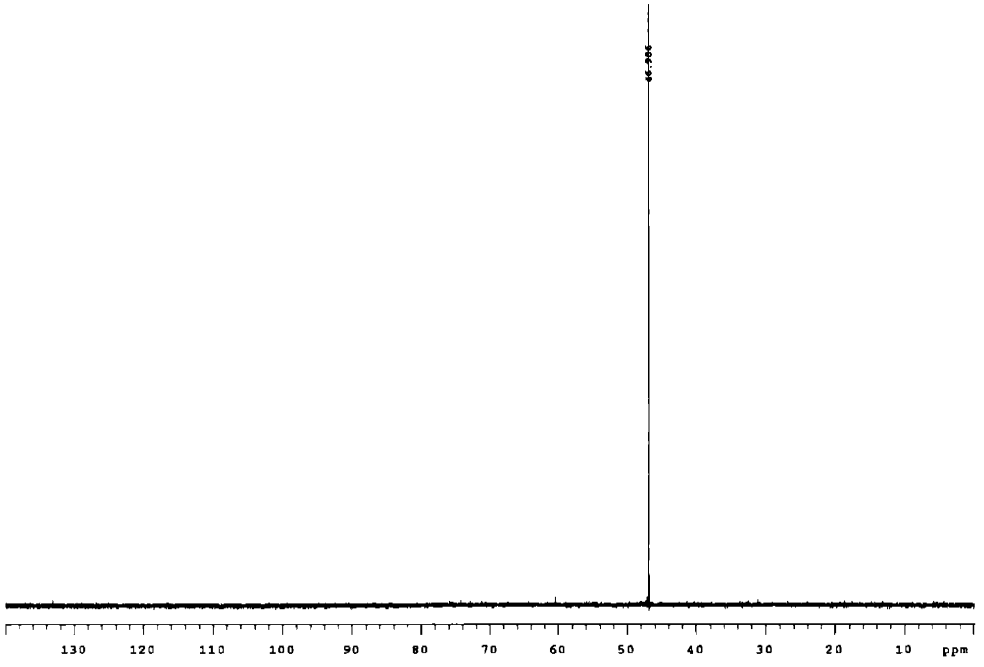

^{19}F NMR of **24** (282MHz, $CDCl_3$)

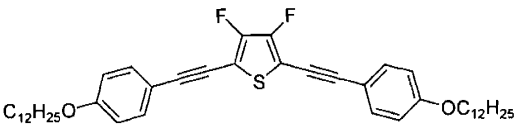

25

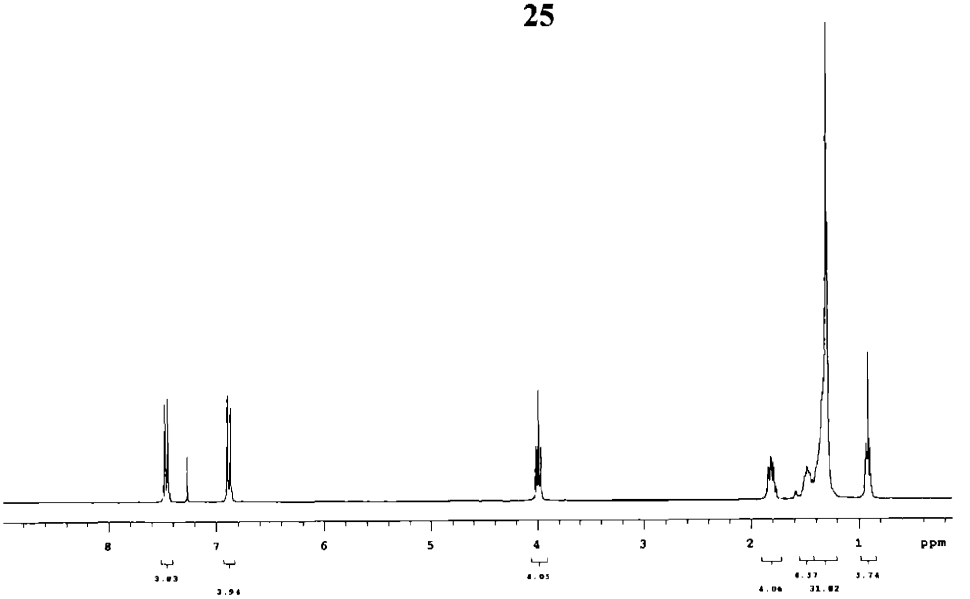

^{1}H NMR of **25** (300MHz, $CDCl_3$)

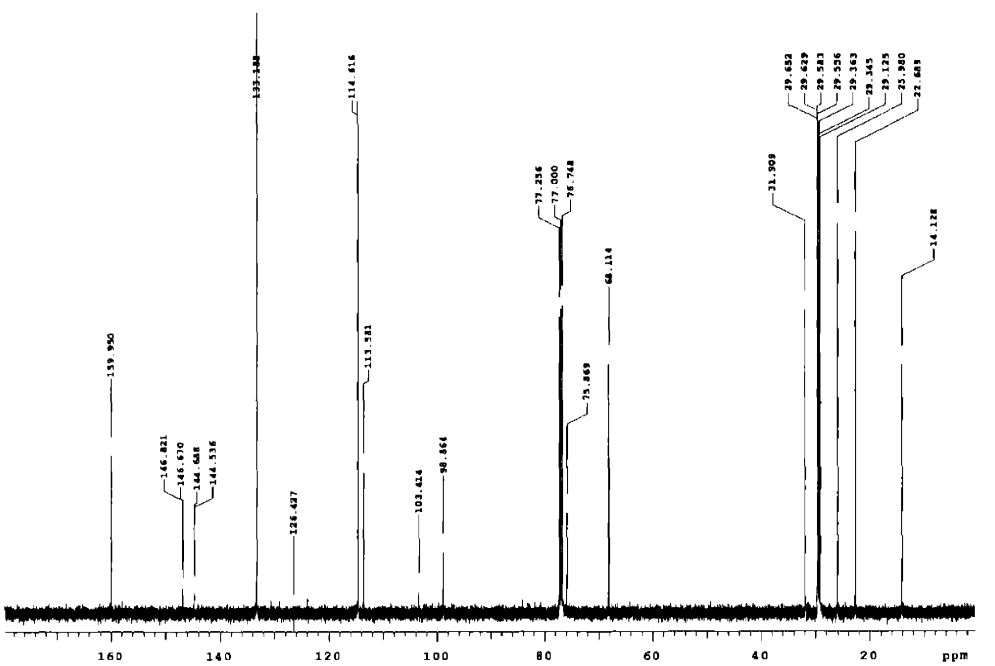

^{13}C NMR of **25** (300MHz, $CDCl_3$)

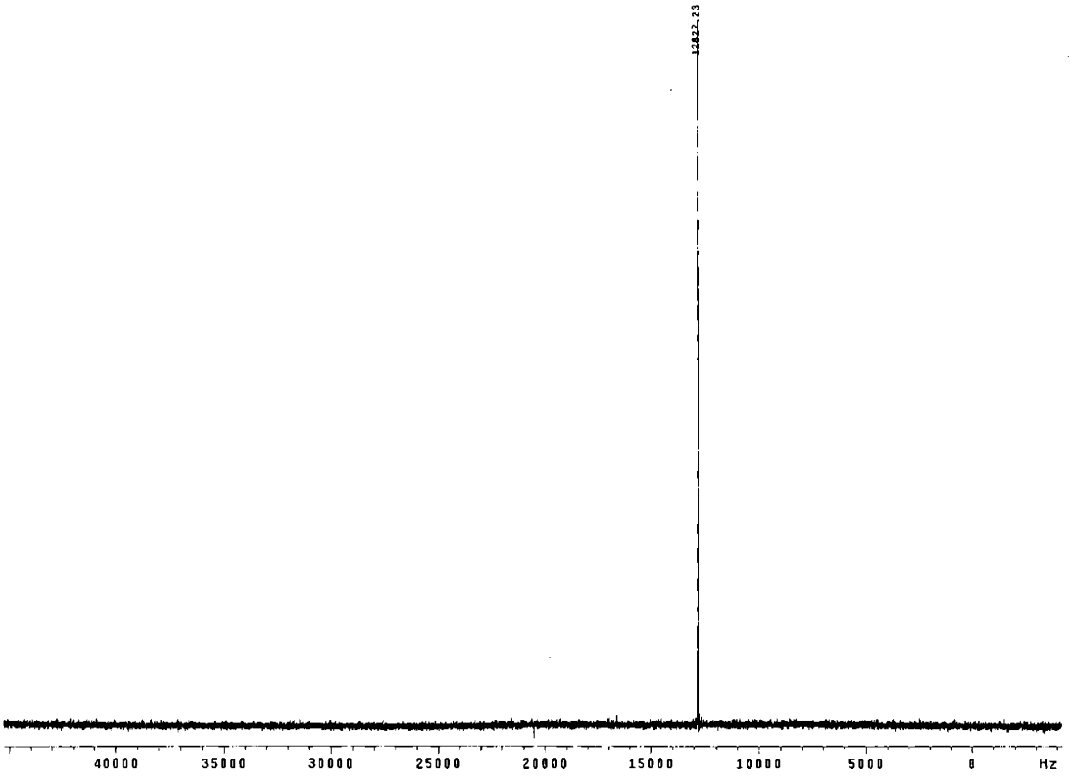

^{19}F NMR of **25** (282MHz, $CDCl_3$)

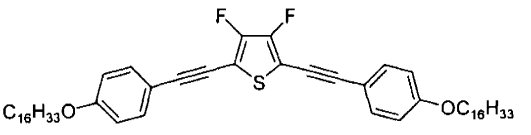

26

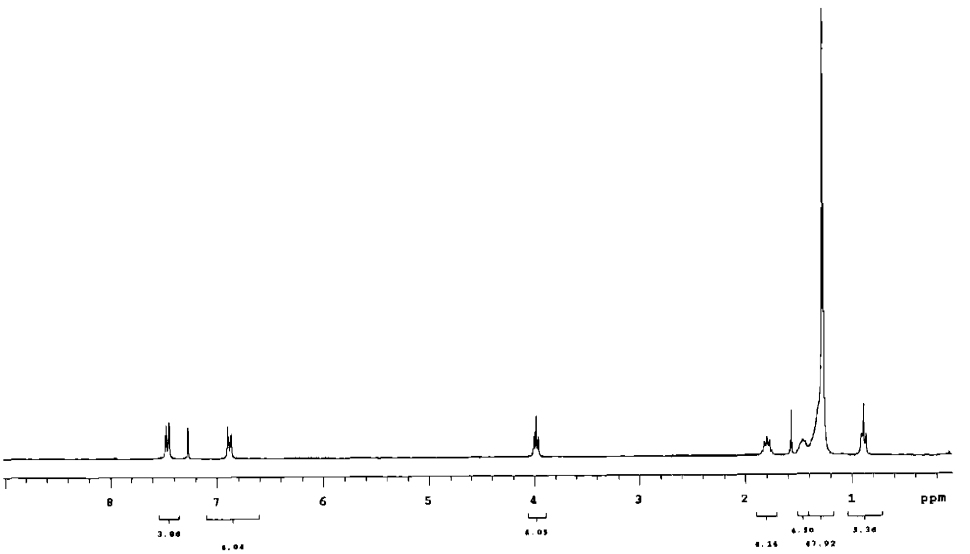

^{1}H NMR of **26** (300MHz, $CDCl_3$)

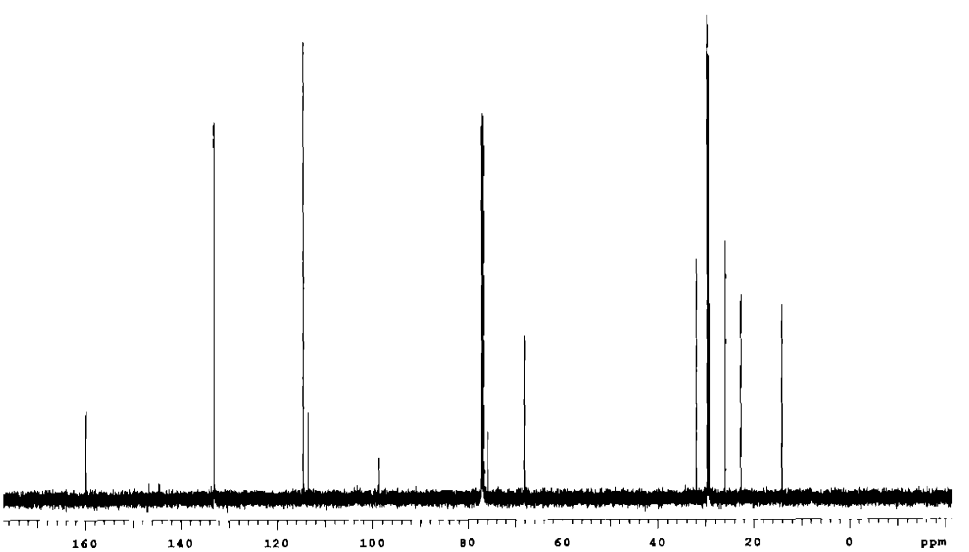

^{13}C NMR of **26** (300MHz, $CDCl_3$)

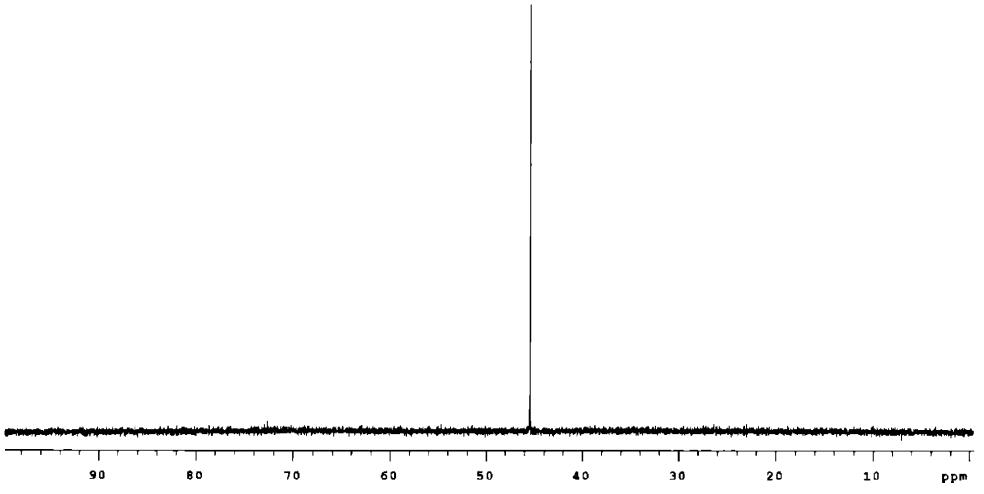

^{19}F NMR of **26** (282MHz, $CDCl_3$)

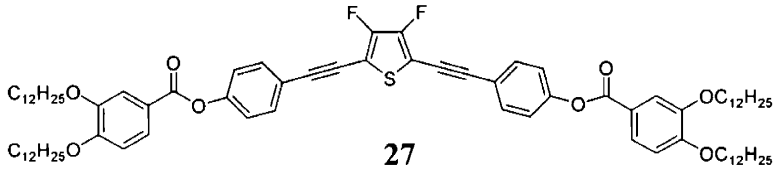

27

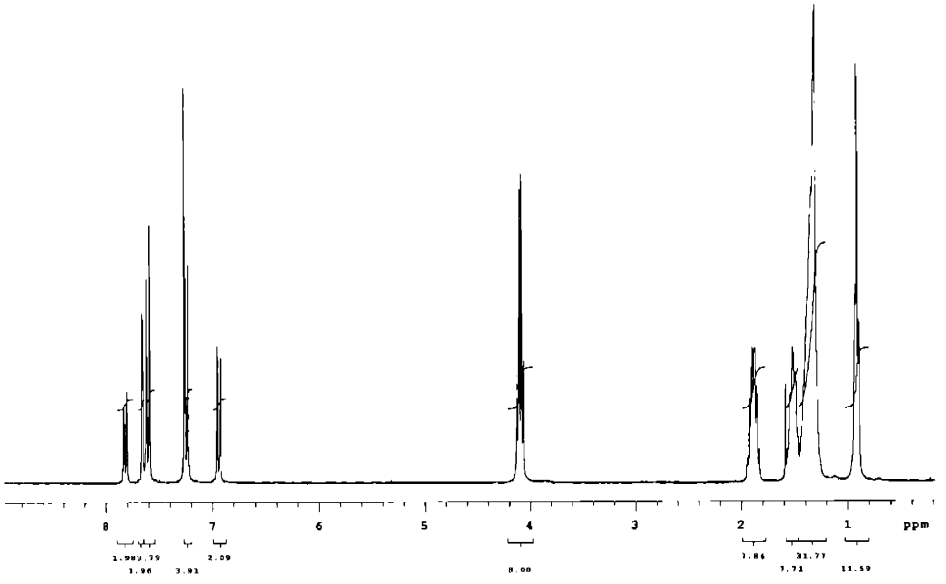

^{1}H NMR of **27** (300MHz, $CDCl_3$)

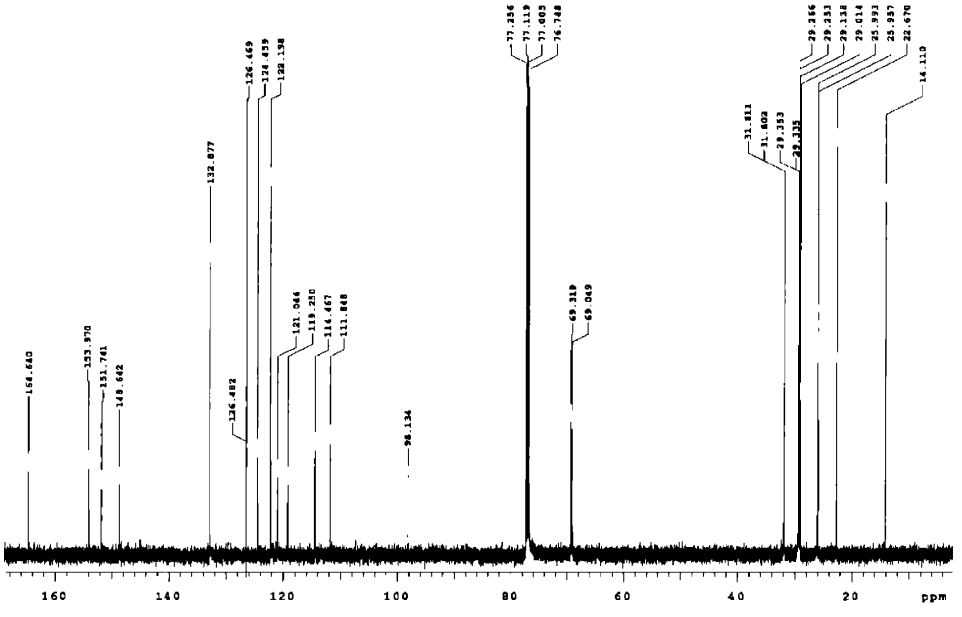

^{13}C NMR of **27** (300MHz, $CDCl_3$)

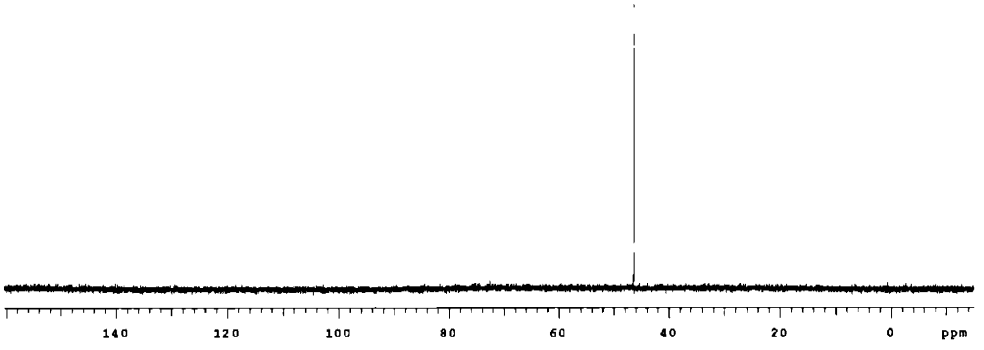

^{19}F NMR of **27** (282MHz, $CDCl_3$)

Appendix 3:

Variable Temperature X-ray Diffraction for Chapter 3

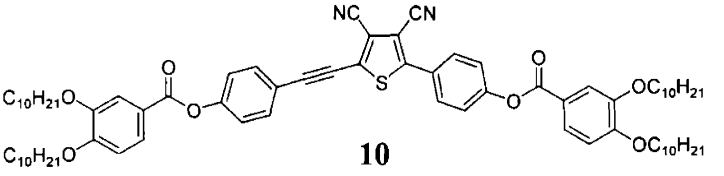

10

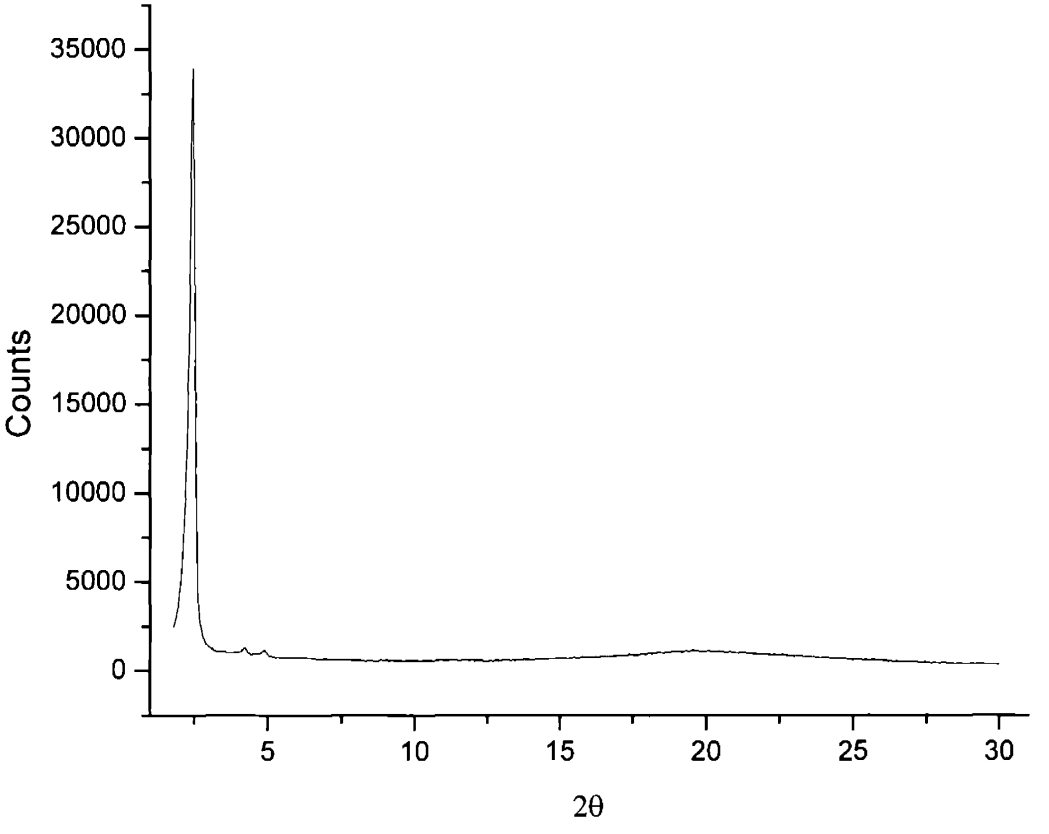

Variable temperature X-ray diffraction pattern of **10** (Col_H phase) at 108 °C.

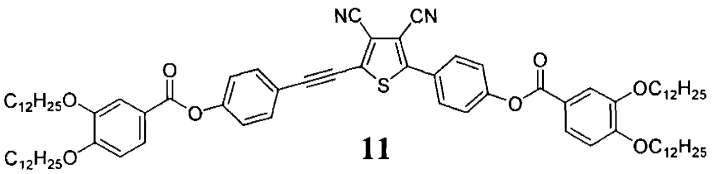

11

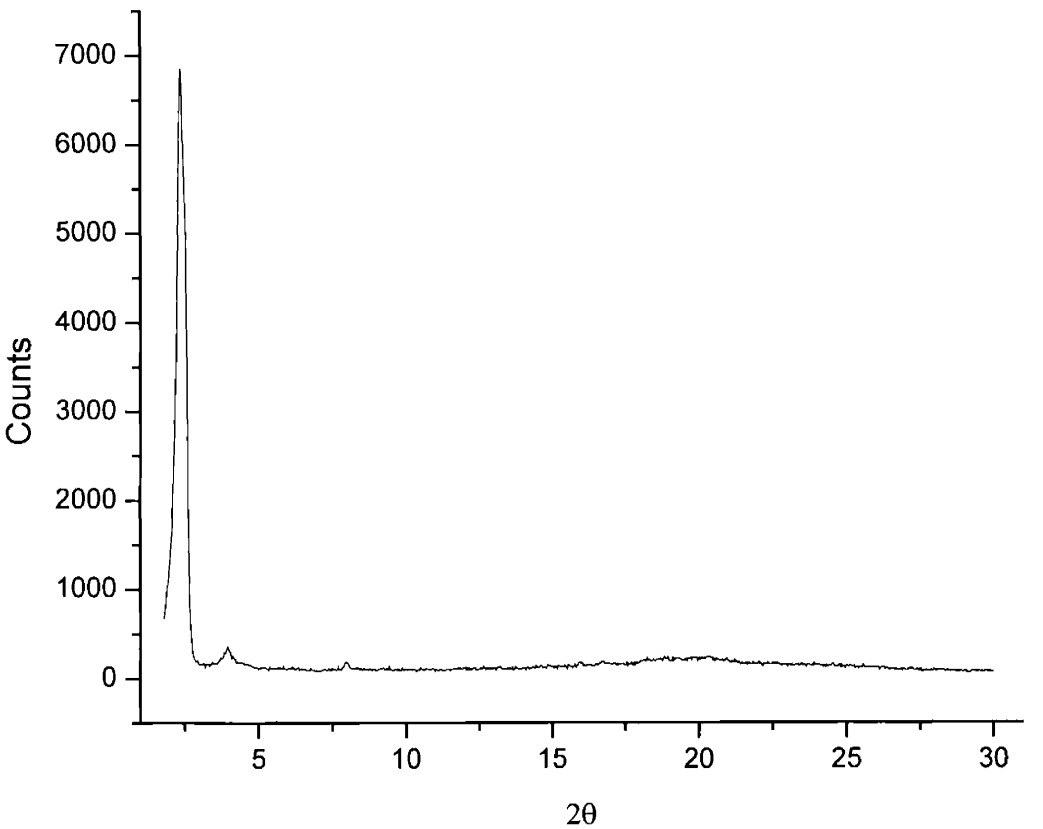

Variable temperature X-ray diffraction pattern of **11** (Col_H phase) at 115 °C.

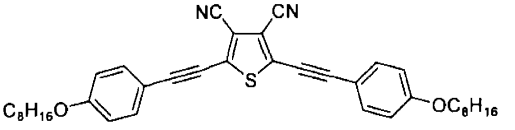

14

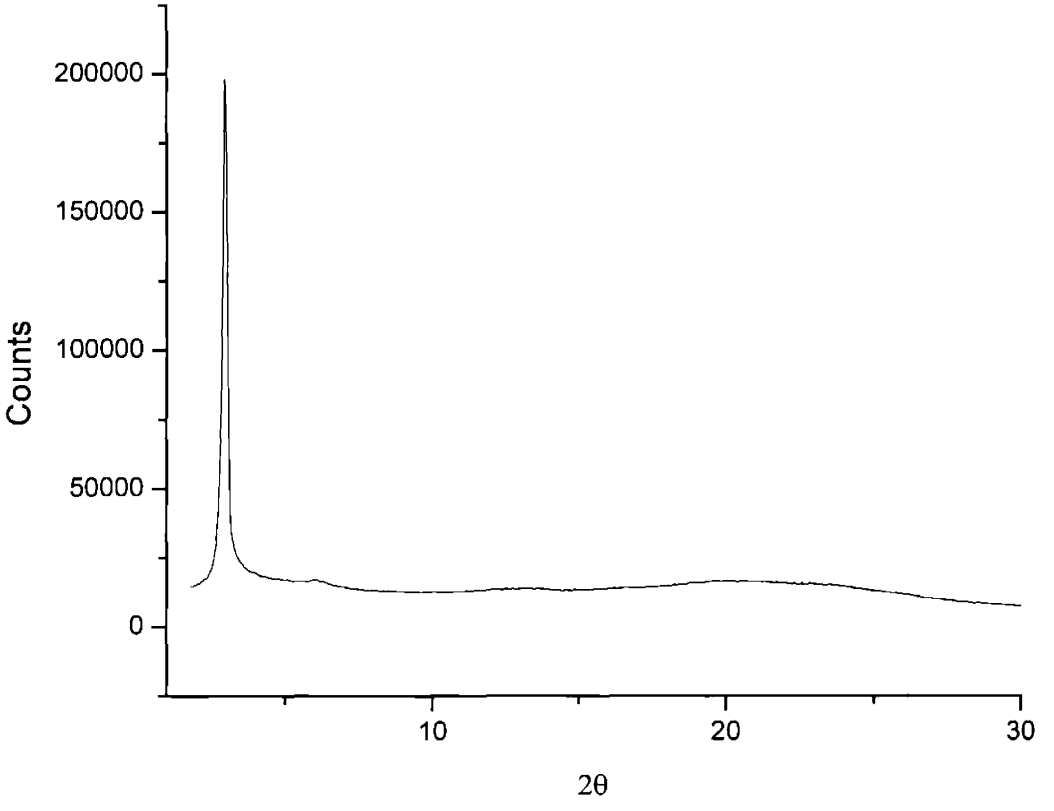

Variable temperature X-ray diffraction pattern of **14** (Sm_C phase) at 80 °C.

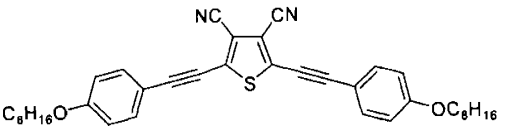

14

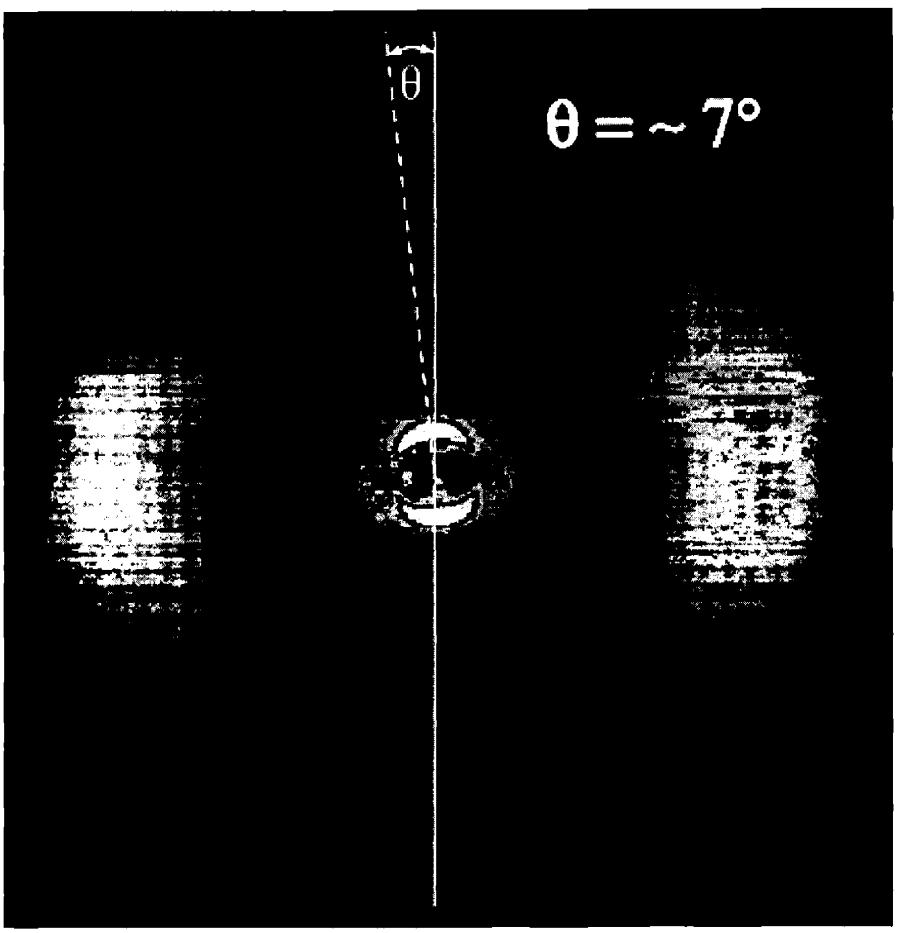

Figure X. 2-D variable temperature X-ray diffraction of a magnetically aligned sample of the SmC phase of **14** at 85 °C. The inner reflections, corresponding to the layer spacing, are tilted at an angle of approximately 7° with respect to the vertically aligned outer reflections of the liquid aliphatic sidechains. This value corresponds to the tilt angle of the SmC phase.

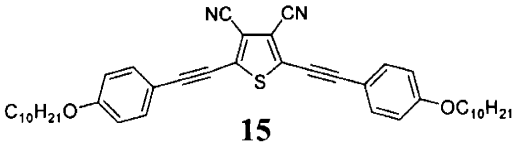

15

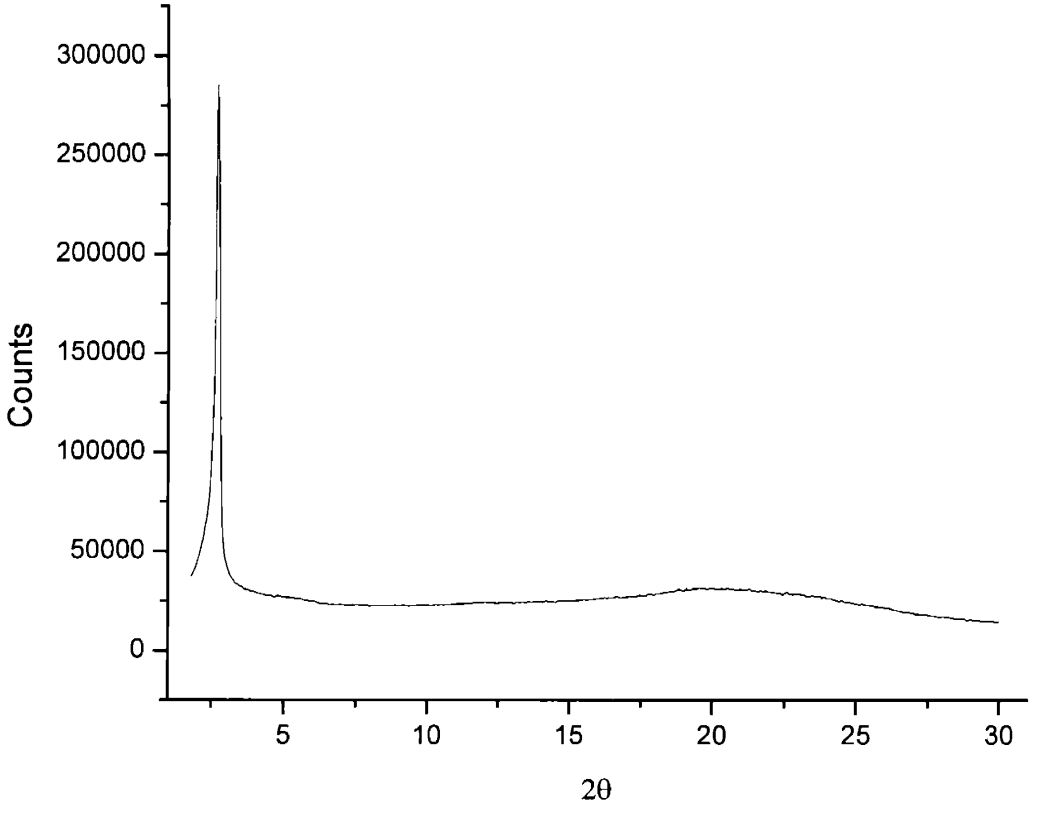

Variable temperature X-ray diffraction pattern of **15** (Sm_C phase) at 105 °C.

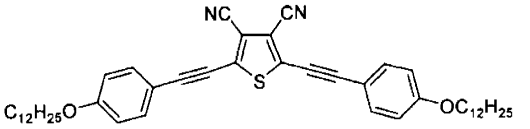

16

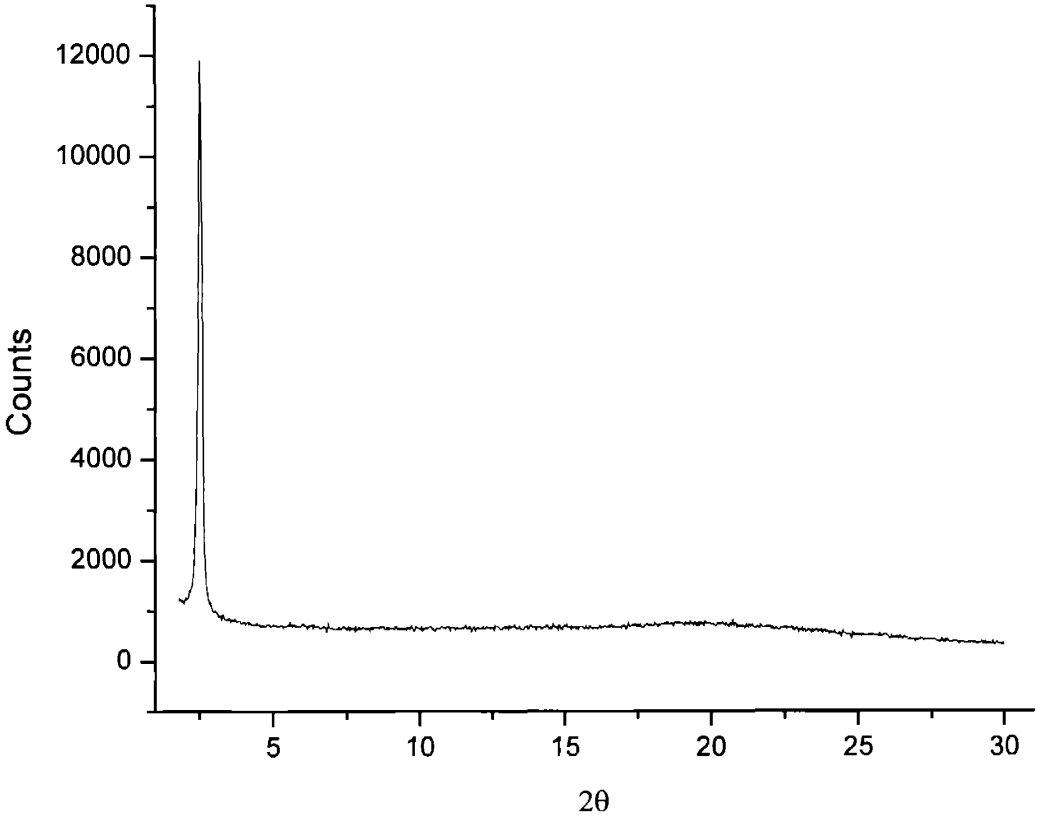

Variable temperature X-ray diffraction pattern of **16** (Sm_C phase) at 101 °C.

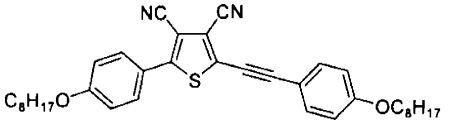

19

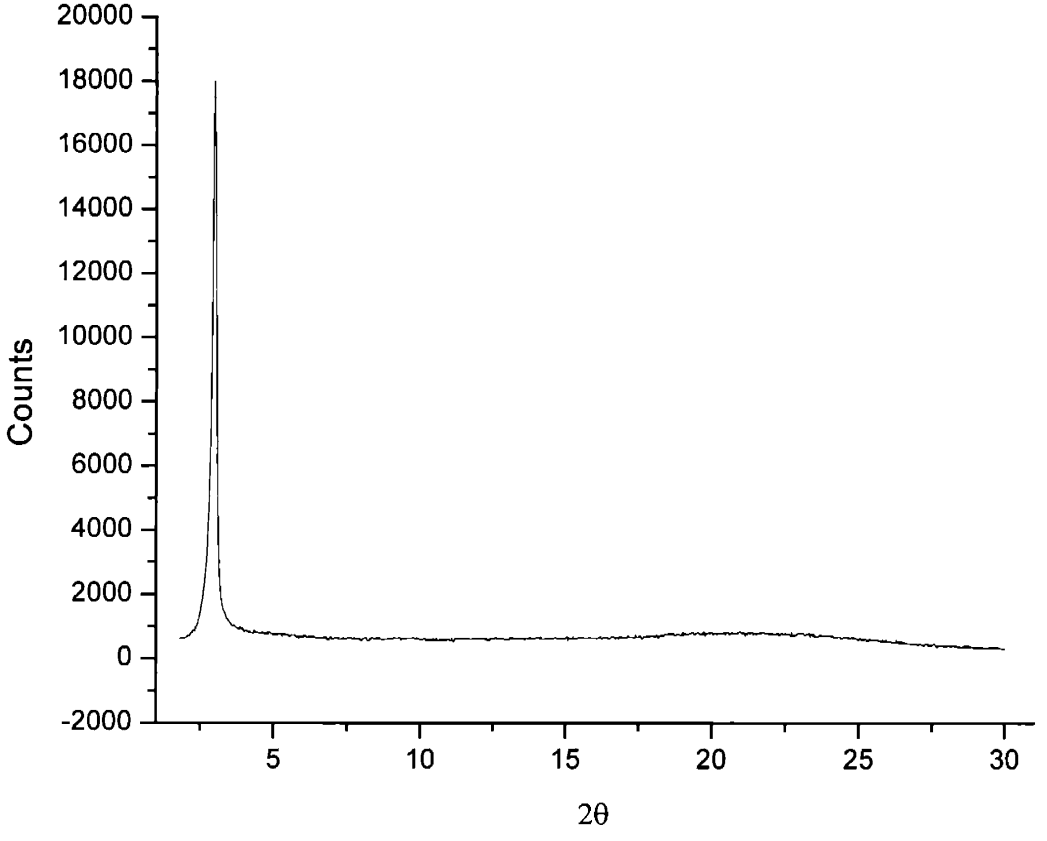

Variable temperature X-ray diffraction pattern of **19** (Sm_C phase) at 65 °C.

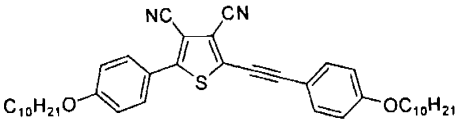

20

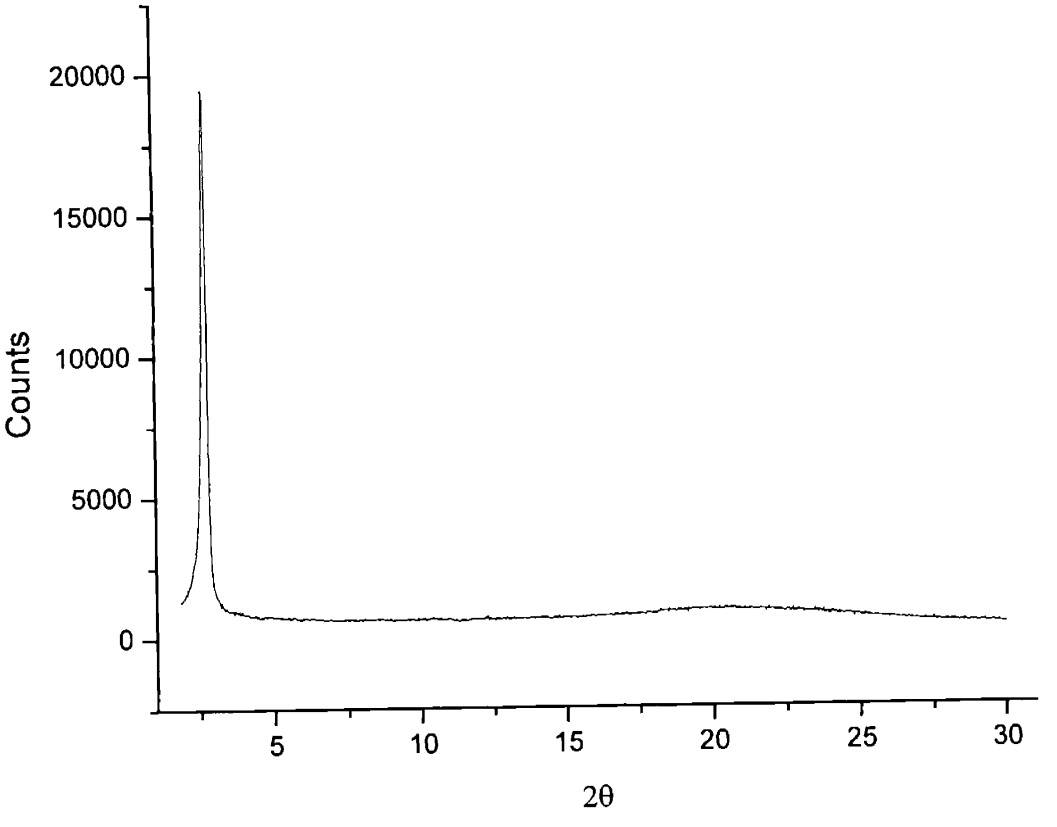

Variable temperature X-ray diffraction pattern of **20** (Sm_C phase) at 80 °C.

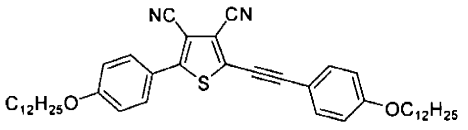

21

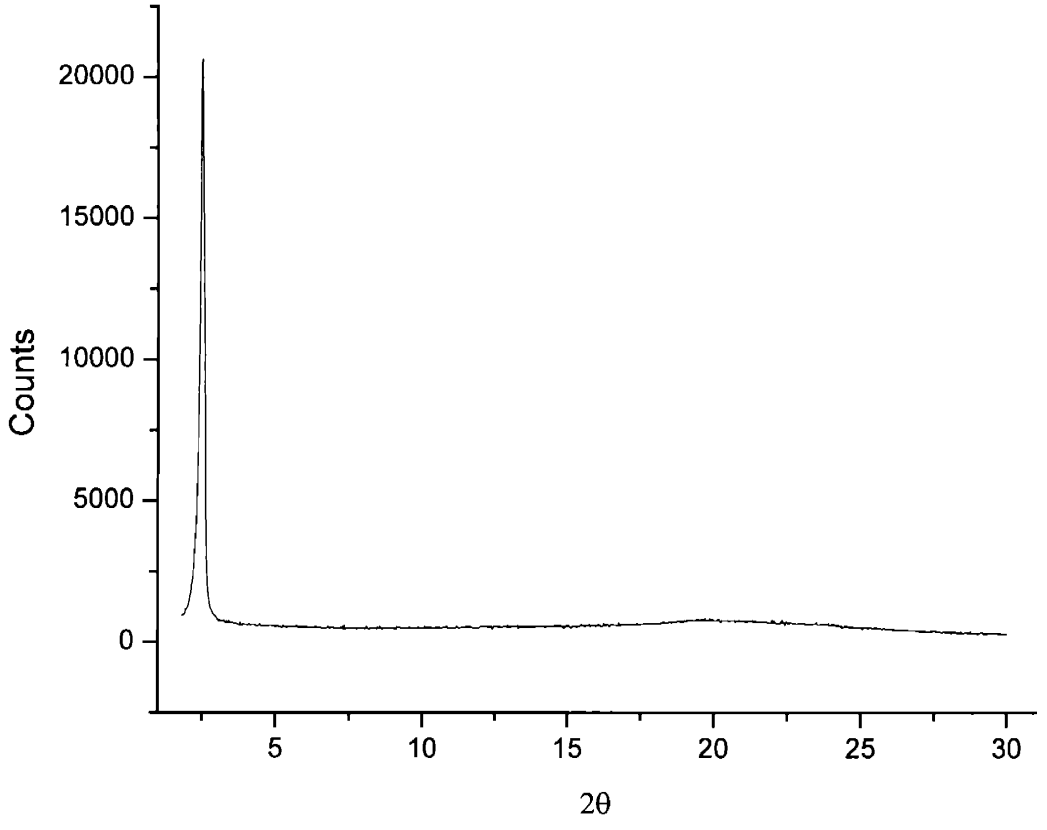

Variable temperature X-ray diffraction pattern of **21** (Sm_C phase) at 75 °C.

Appendix 4:

^{1}H and ^{13}C NMR spectra for Chapter 4

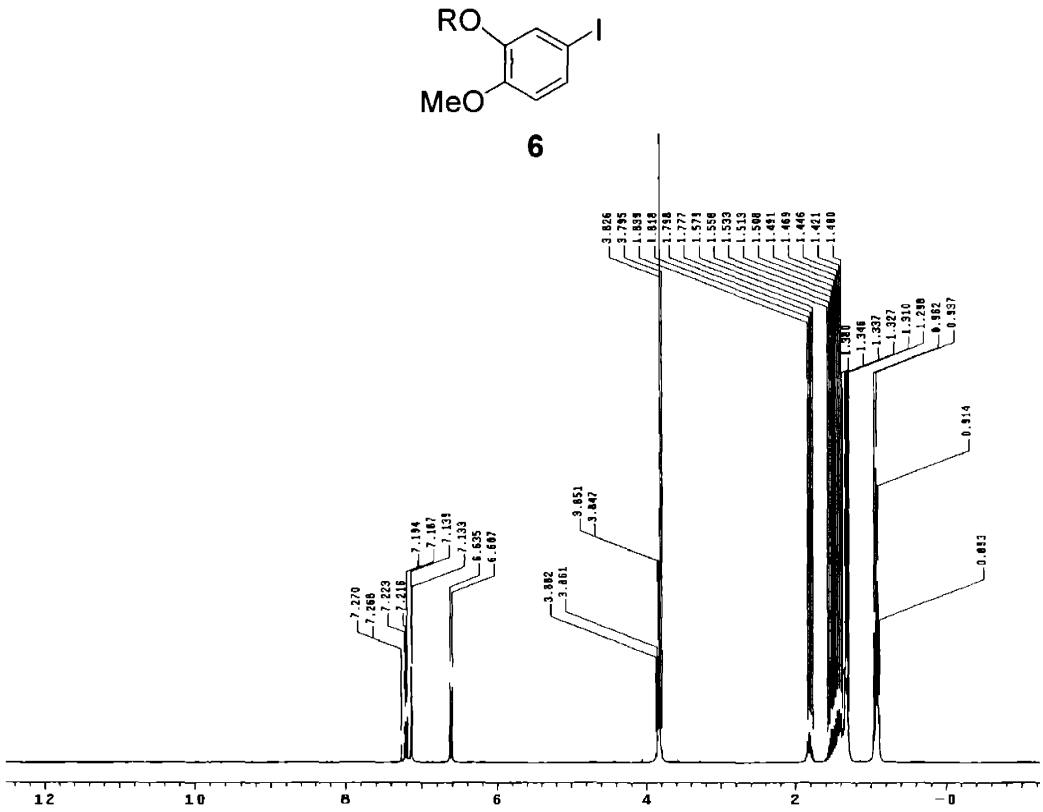

^{1}H NMR of **6** (300 MHz, $CDCl_3$)

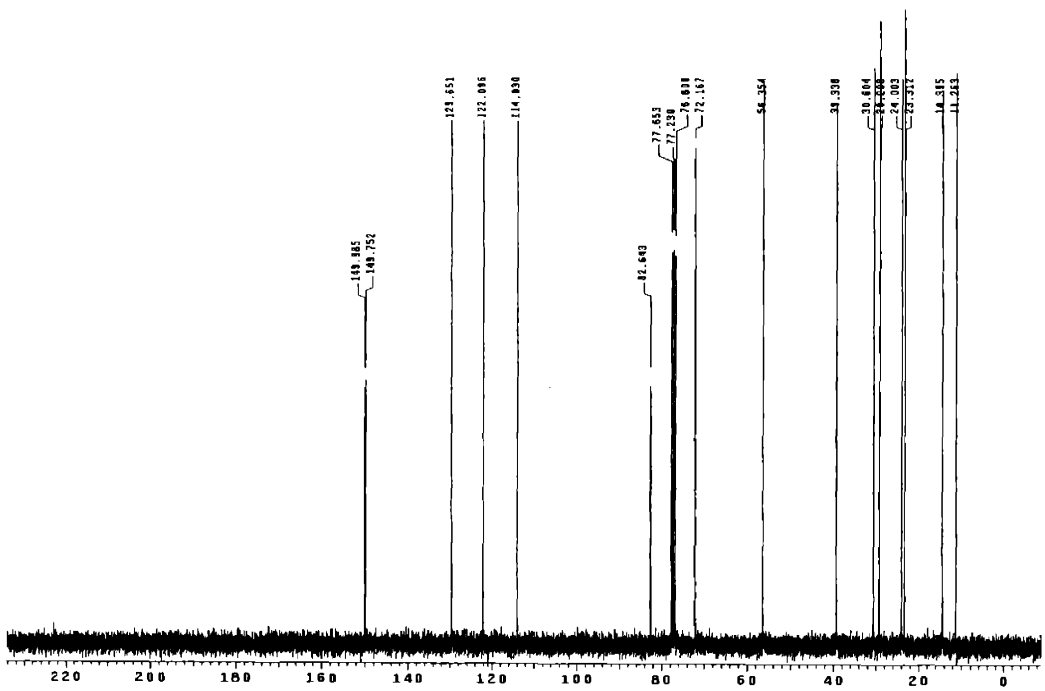

^{13}C NMR of **6** (75 MHz, $CDCl_3$)

* (Synthesis and spectroscopy of this compound by Yutaka Nishiyama)

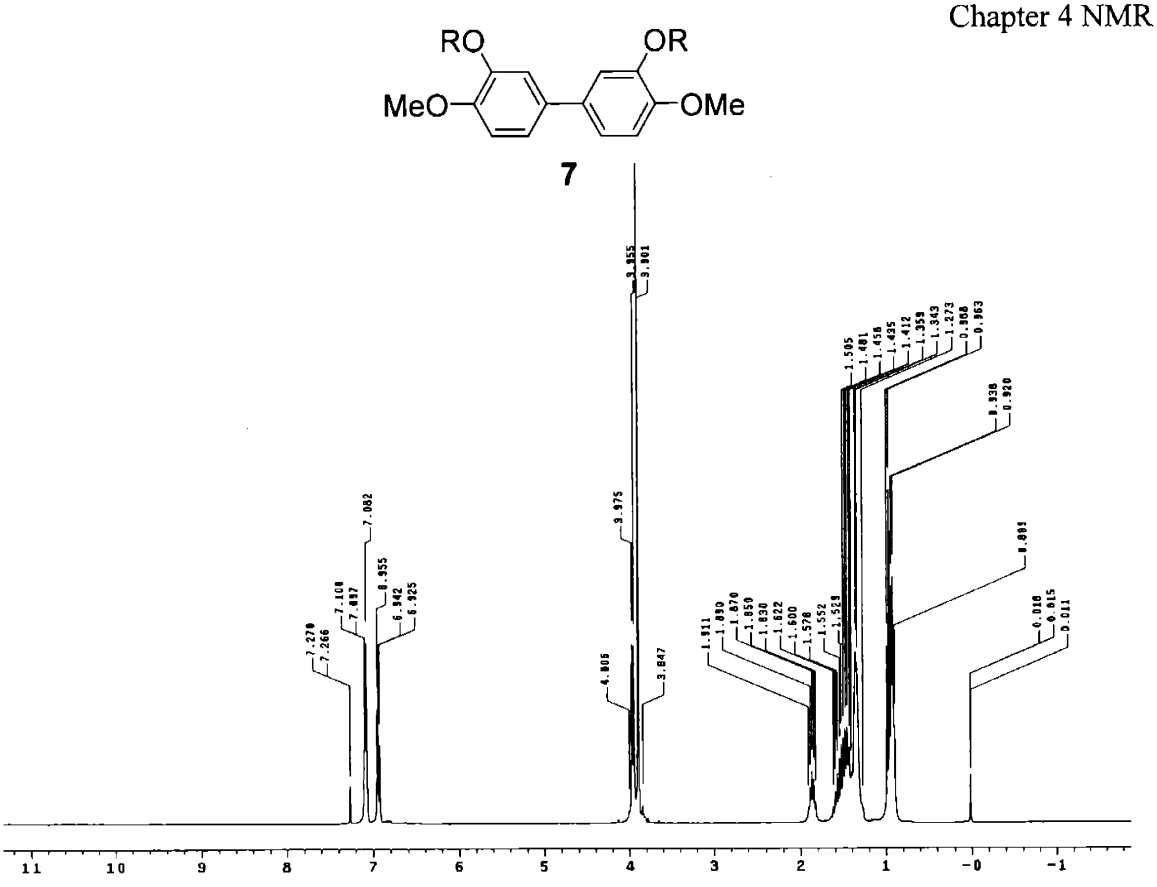

^{1}H NMR of **7** (300 MHz, $CDCl_3$)

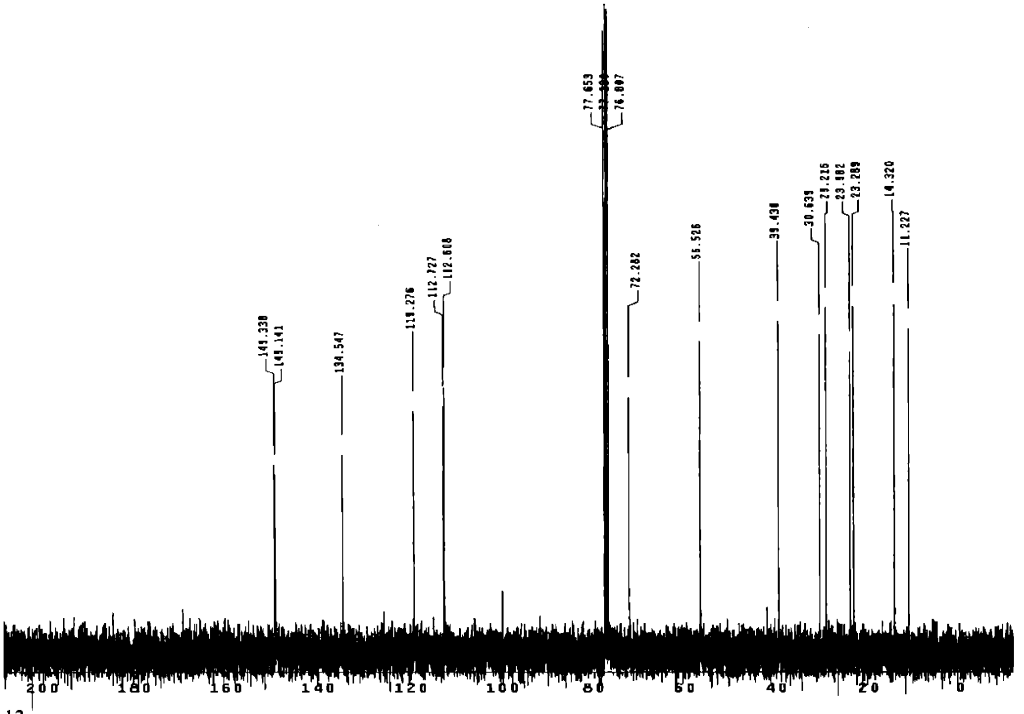

^{13}C NMR of **7** (75 MHz, $CDCl_3$)

* (Synthesis and spectroscopy of this compound by Yutaka Nishiyama)

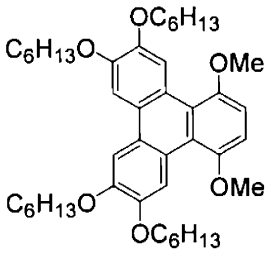

8

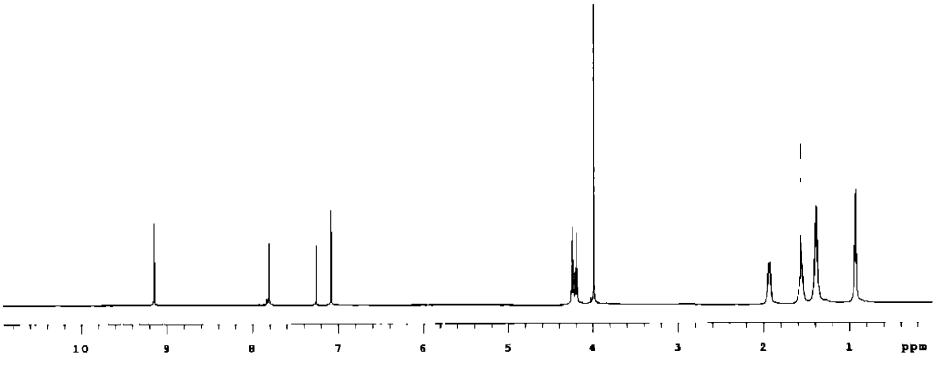

^{1}H NMR of **8** (500 MHz, $CDCl_3$)

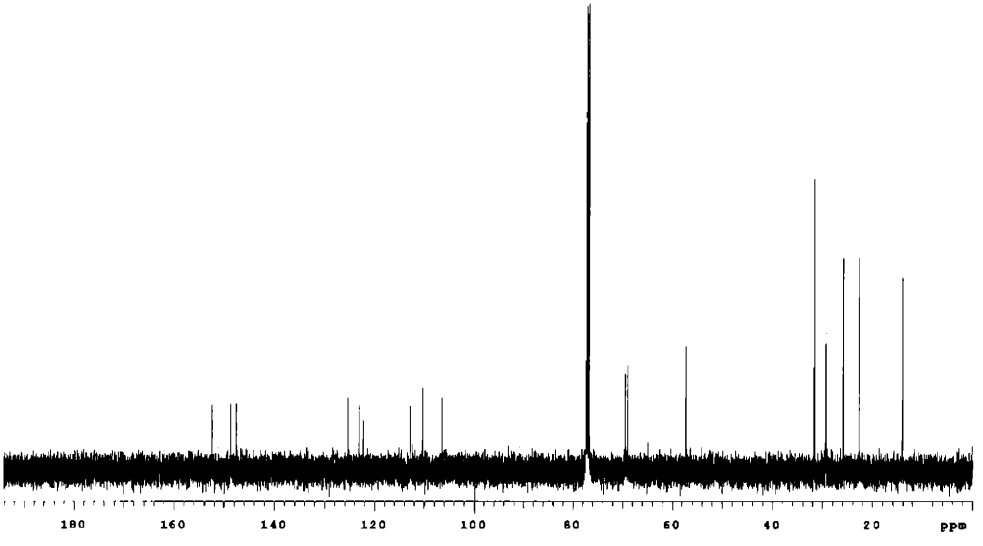

^{13}C NMR of **8** (125 MHz, $CDCl_3$)

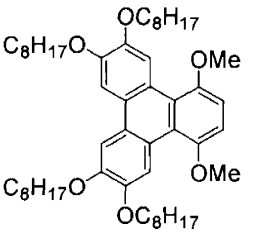

9

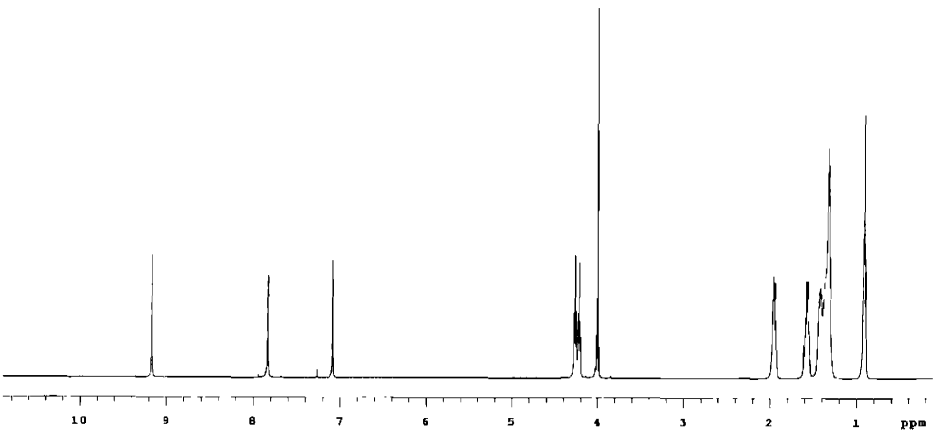

^{1}H NMR of **9** (500 MHz, $CDCl_3$)

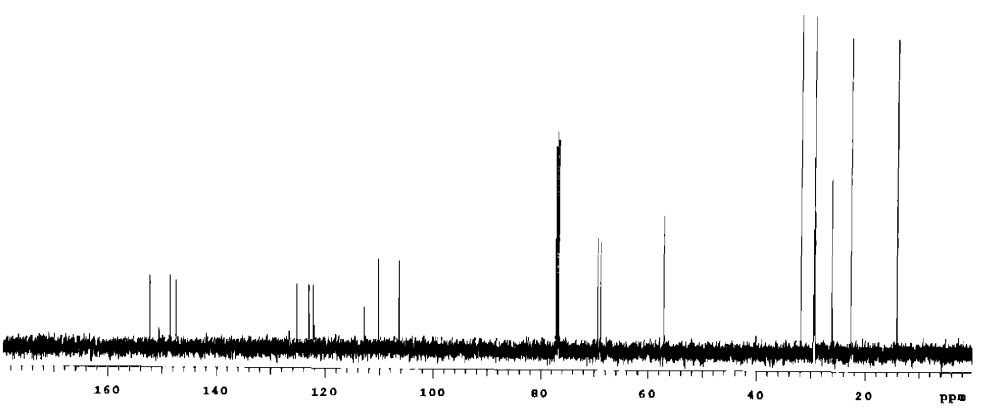

^{13}C NMR of **9** (125 MHz, $CDCl_3$)

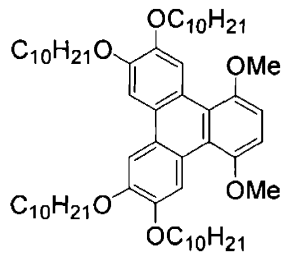

10

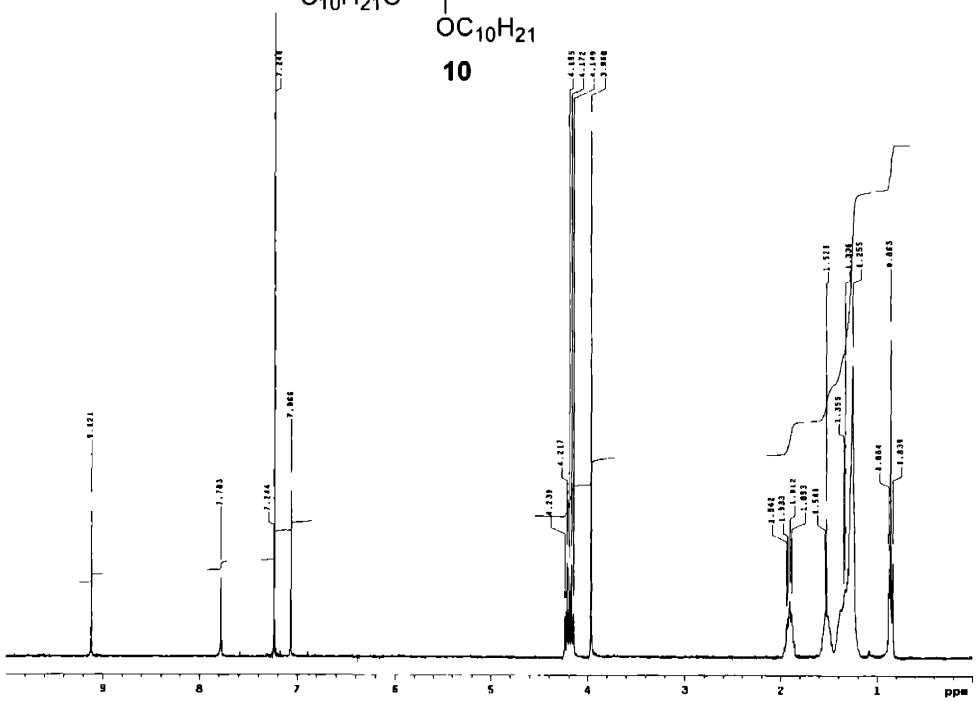

^{1}H NMR of **10** (300 MHz, $CDCl_3$)

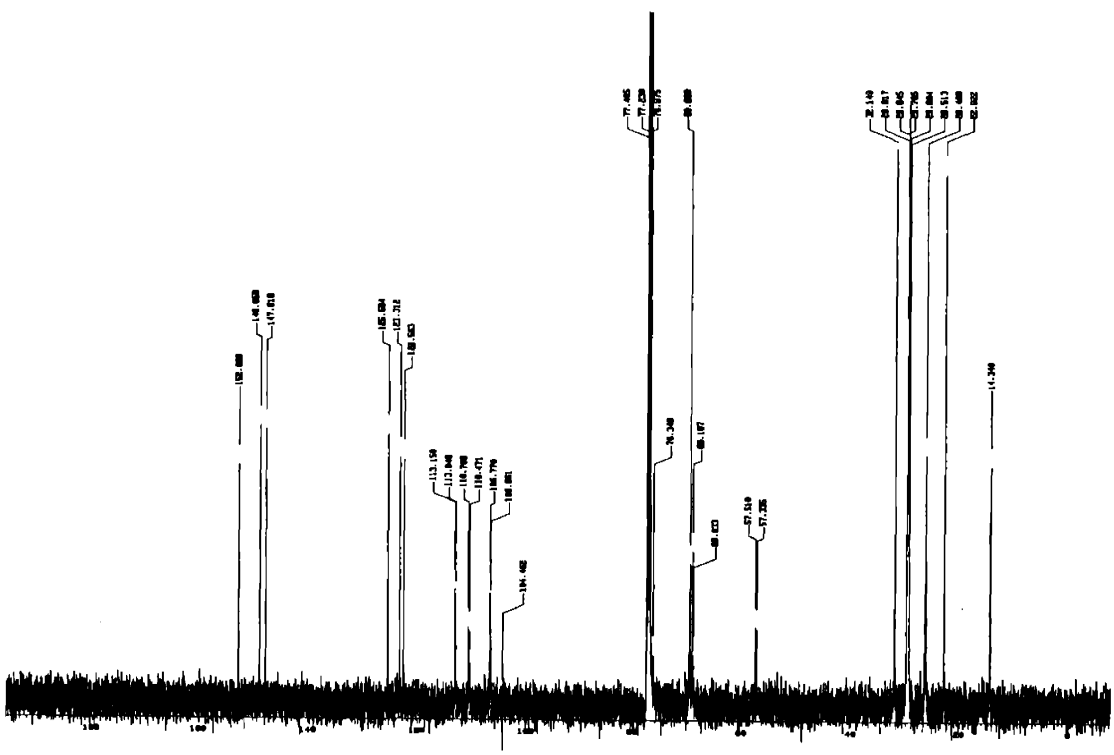

^{13}C NMR of **10** (75 MHz, $CDCl_3$)

- (Synthesis and characterization of this compound by Claus Lugmair)

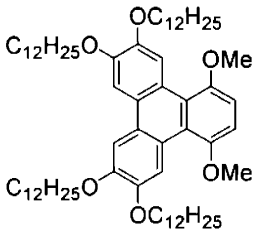

11

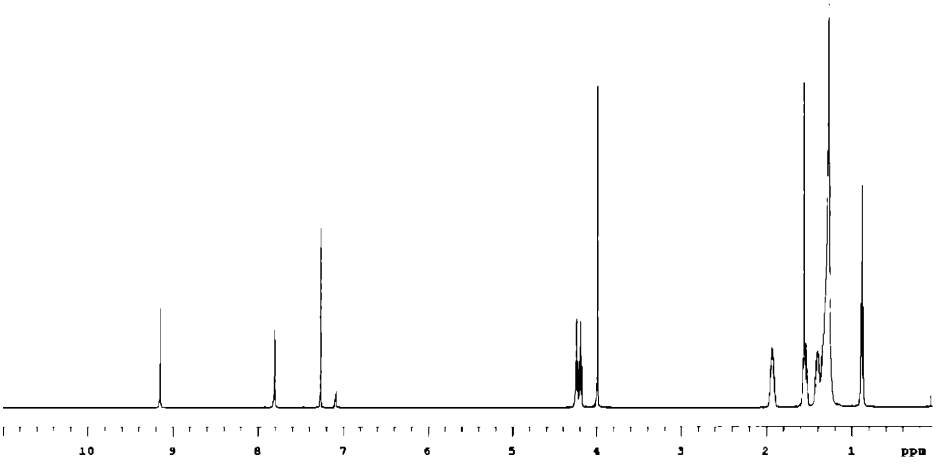

^{1}H NMR of **11** (500 MHz, $CDCl_3$)

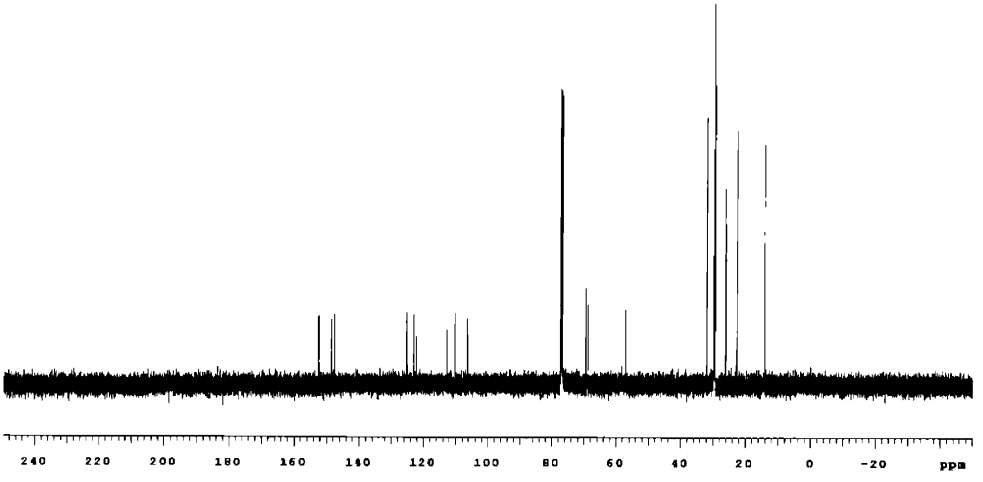

^{13}C NMR of **11** (125 MHz, $CDCl_3$)

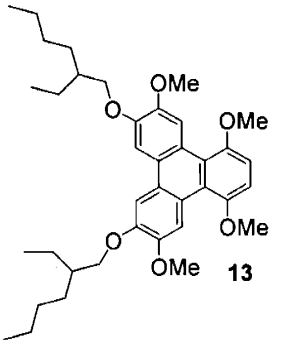

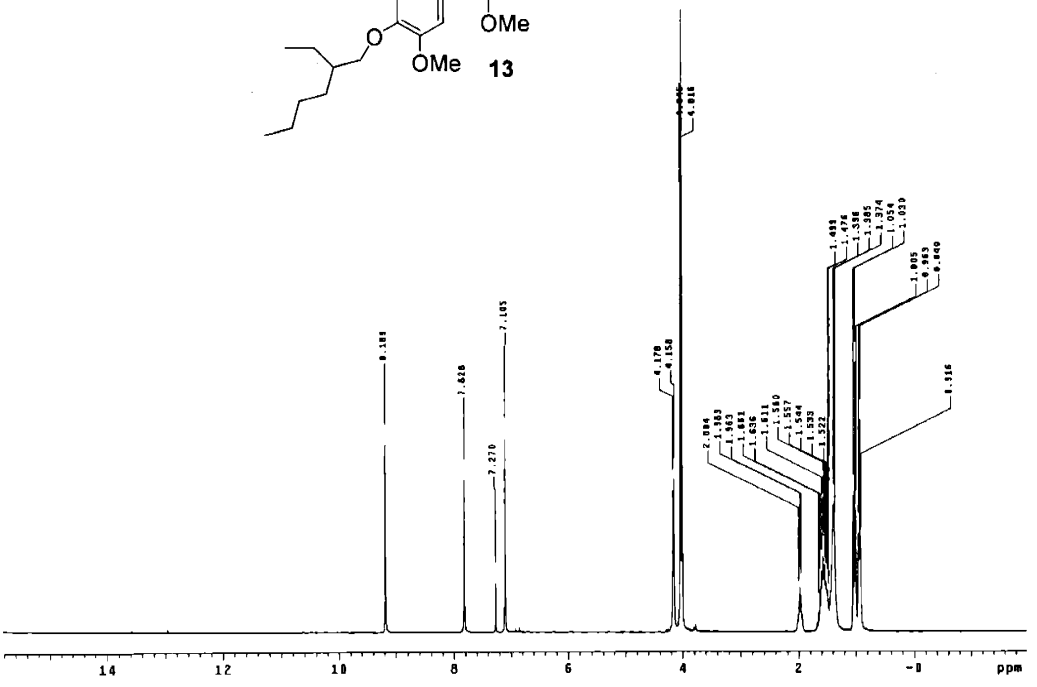

^{1}H NMR of **13** (300 MHz, $CDCl_3$)

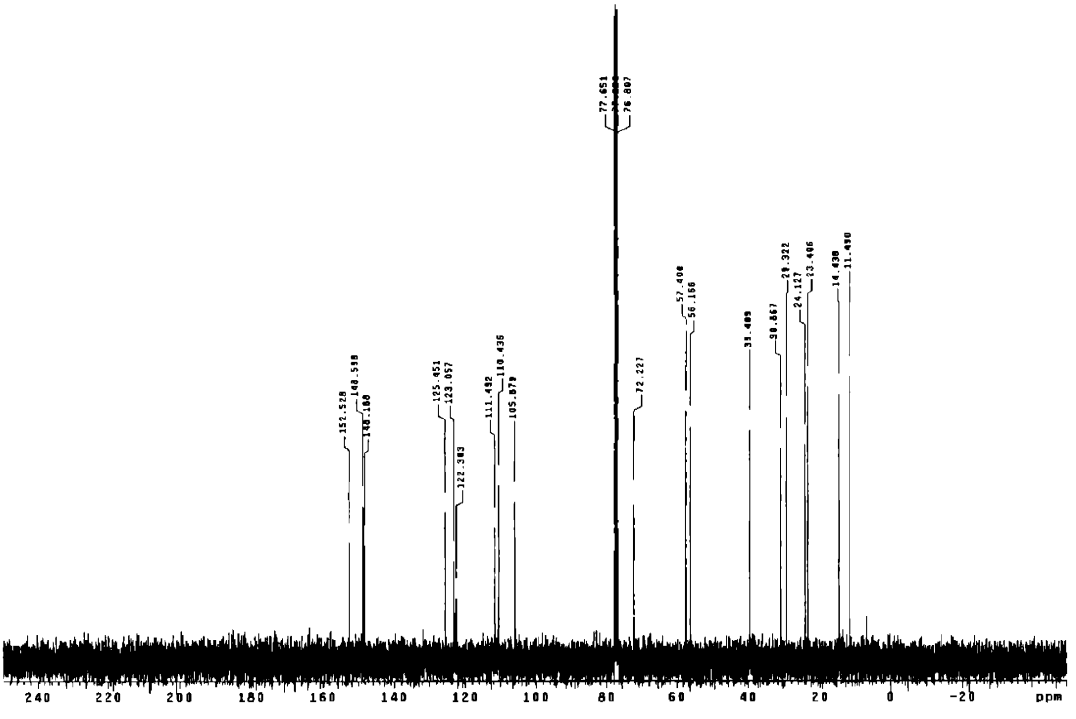

^{13}C NMR of **13** (75 MHz, $CDCl_3$)

- (Synthesis and spectroscopy of this compound by Yutaka Nishiyama)

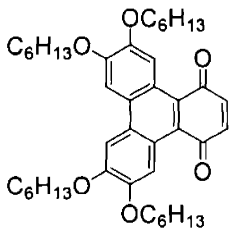

14

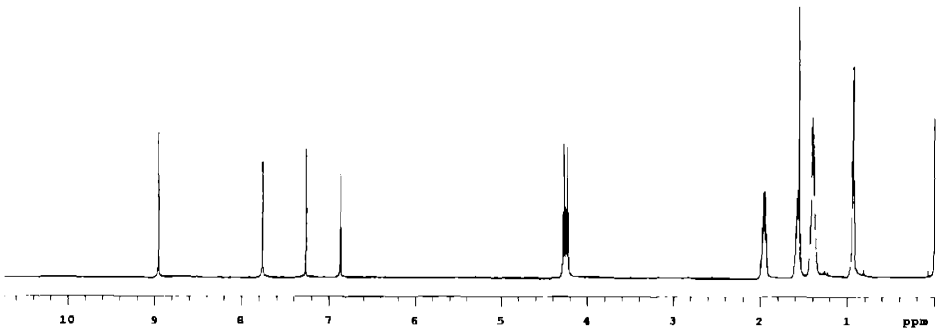

^{1}H NMR of **14** (500 MHz, $CDCl_3$)

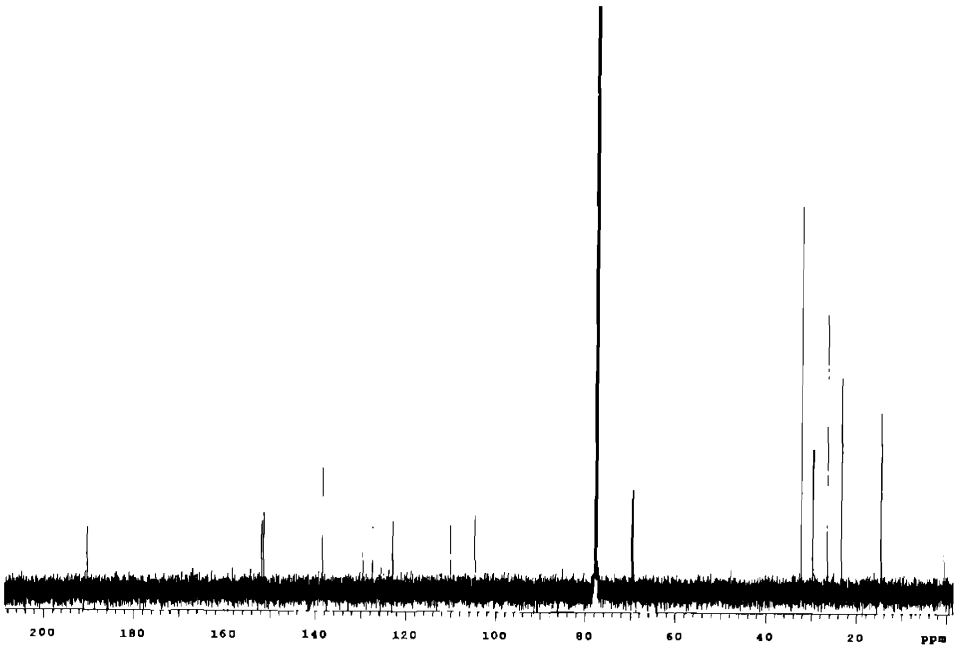

^{13}C NMR of **14** (125 MHz, $CDCl_3$)

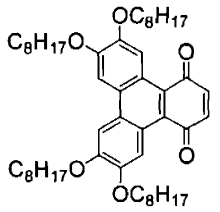

15

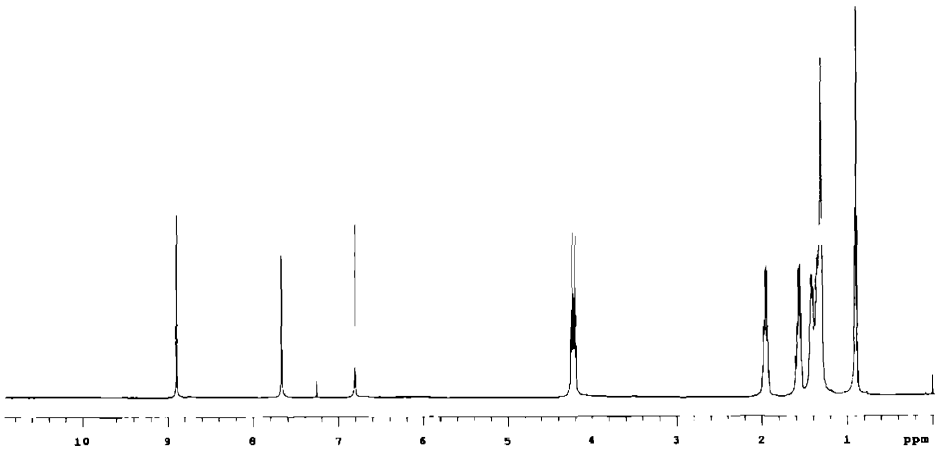

^{1}H NMR of **15** (500 MHz, $CDCl_3$)

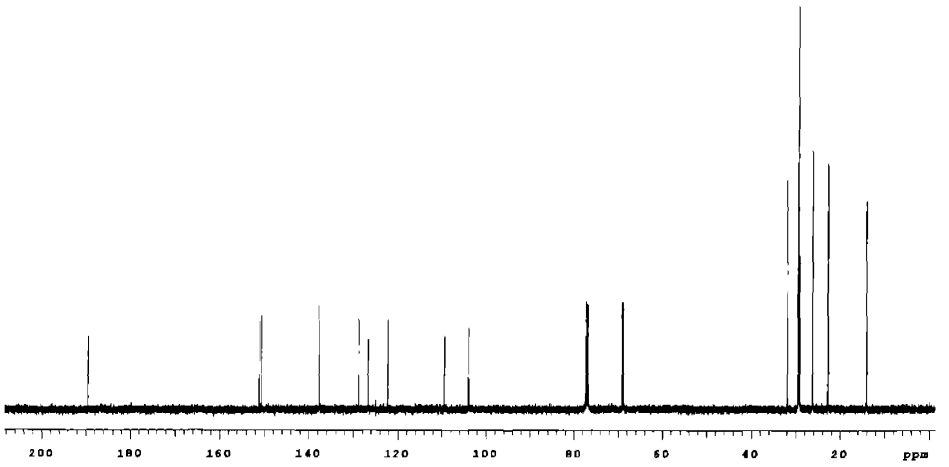

^{13} C NMR of **15** (125 MHz, $CDCl_3$)

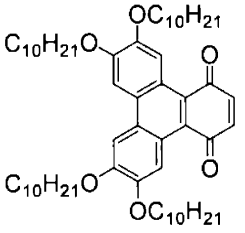

16

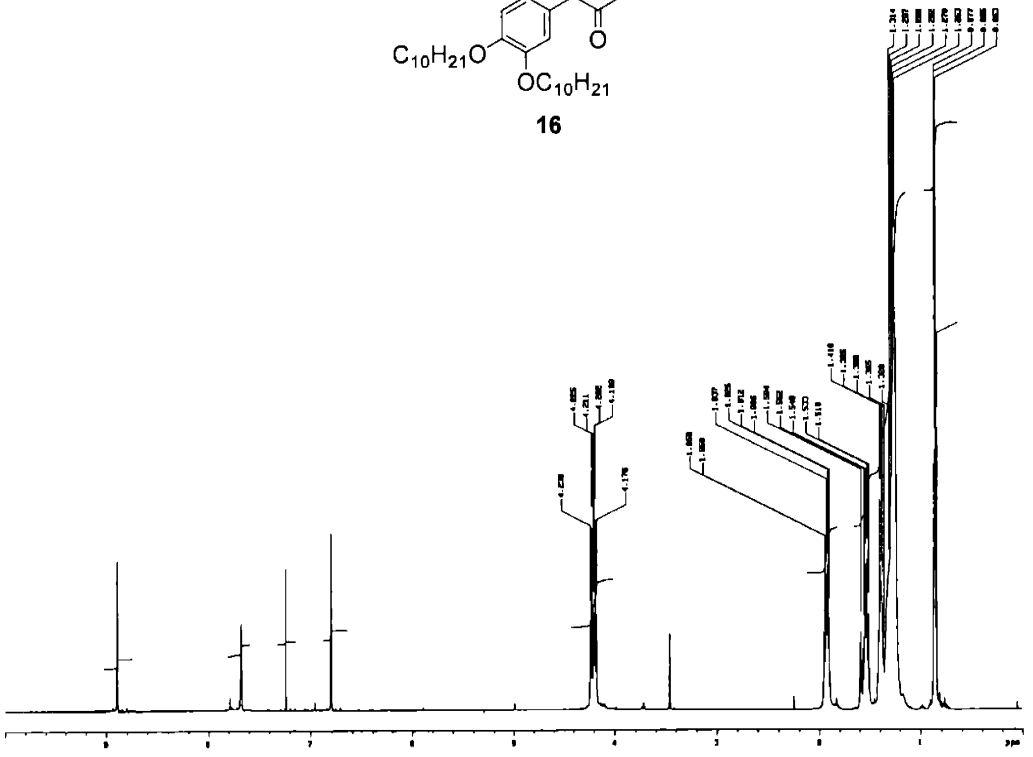

^{1}H NMR of **16** (300 MHz, $CDCl_3$)

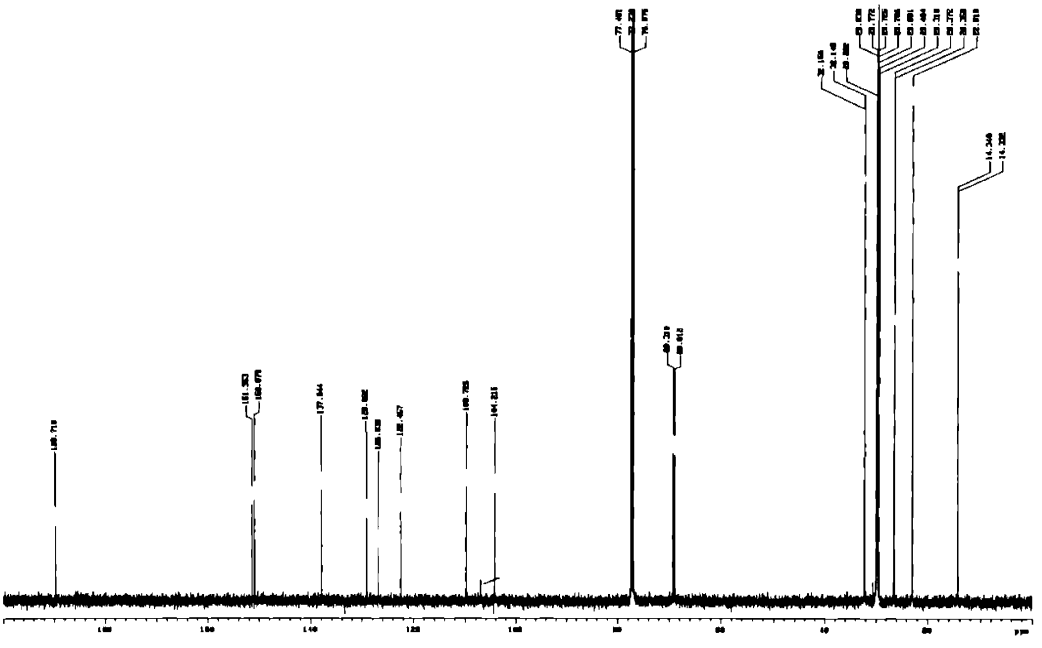

^{13} C NMR of **16** (75 MHz, $CDCl_3$)

* (Synthesis and characterization of this compound by Claus Lugmair)

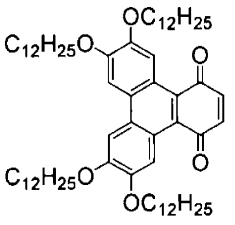

17

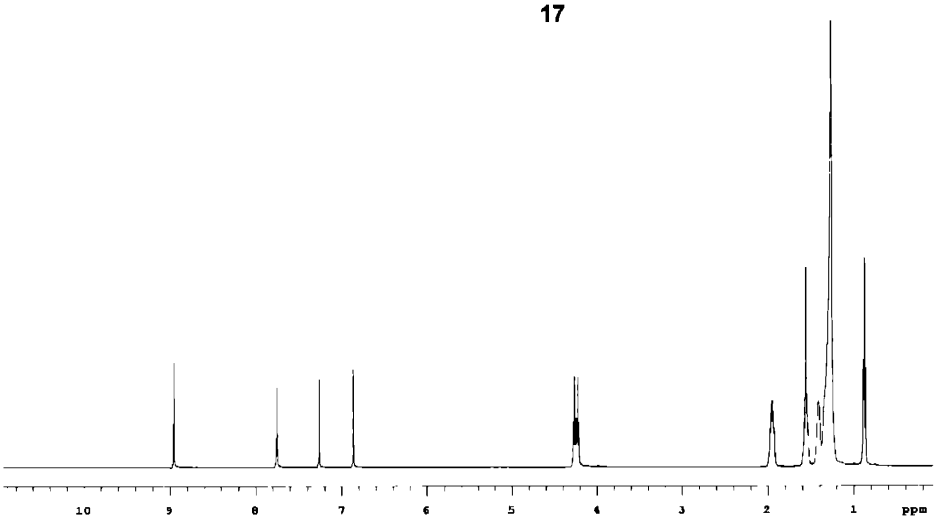

^{1}H NMR of **17** (500 MHz, $CDCl_3$)

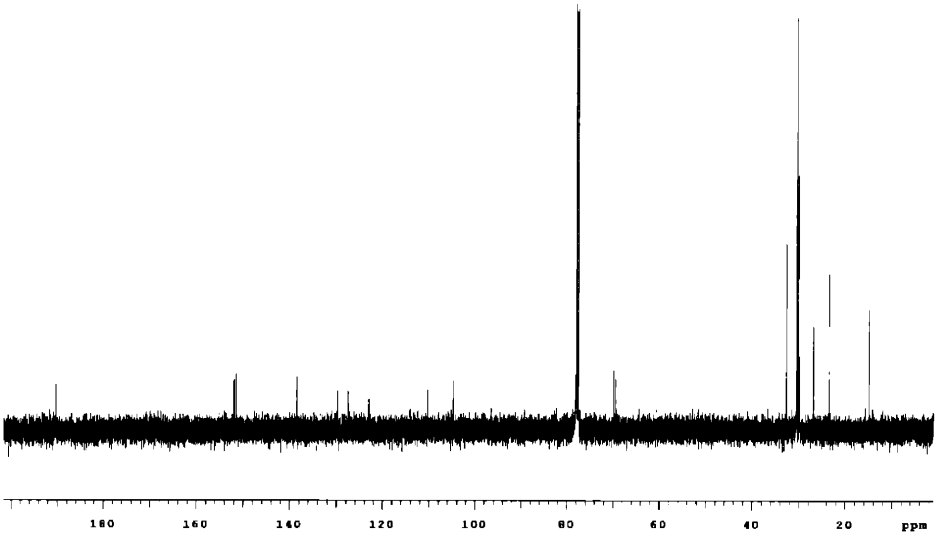

^{13}C NMR of **17** (125 MHz, $CDCl_3$)

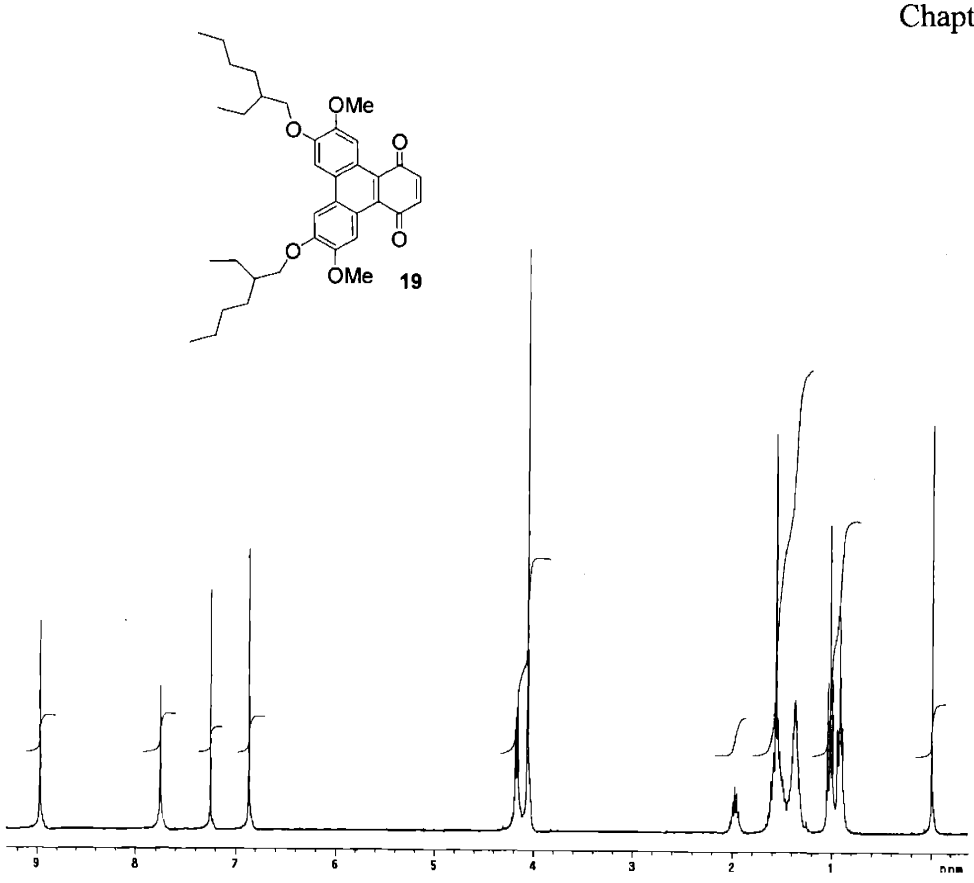

^{1}H NMR of **19** (500 MHz, $CDCl_3$)

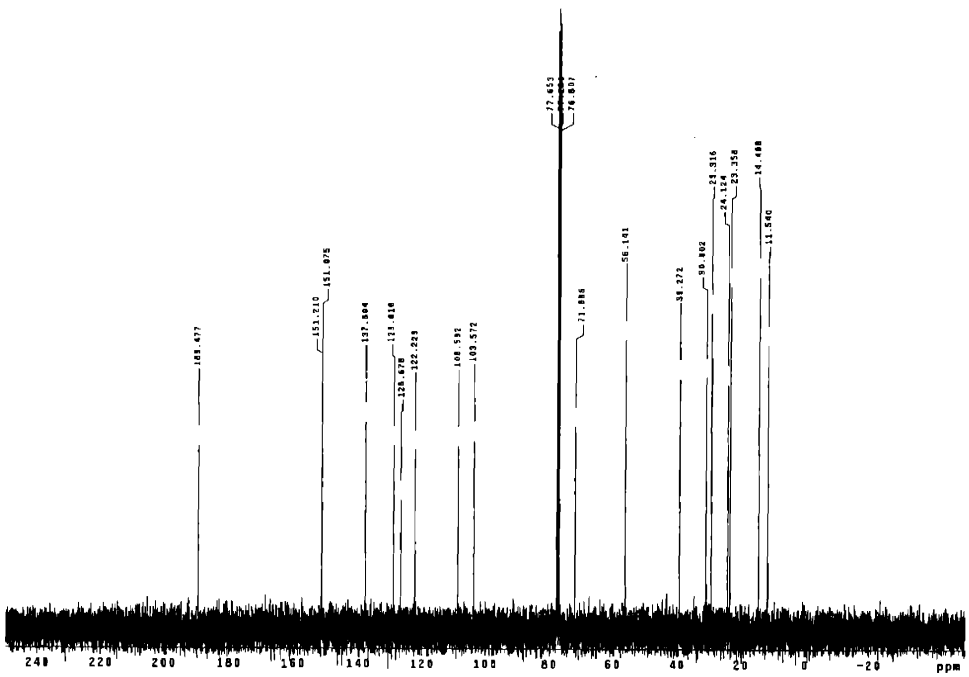

^{13} C NMR of **19** (125 MHz, $CDCl_3$)

- (Synthesis and spectroscopy of this compound by Yutaka Nishiyama)

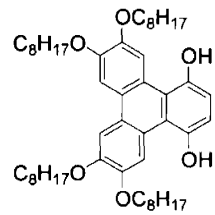

20

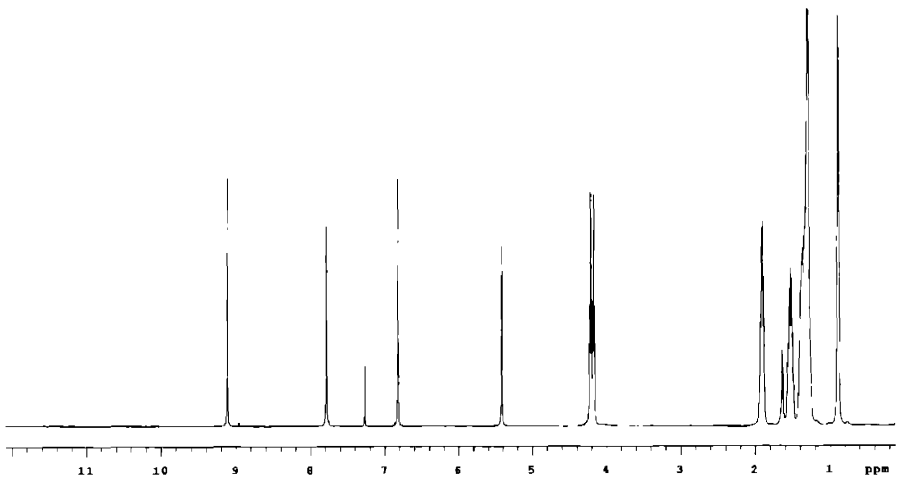

^{1}H NMR of **20** (500 MHz, $CDCl_3$)

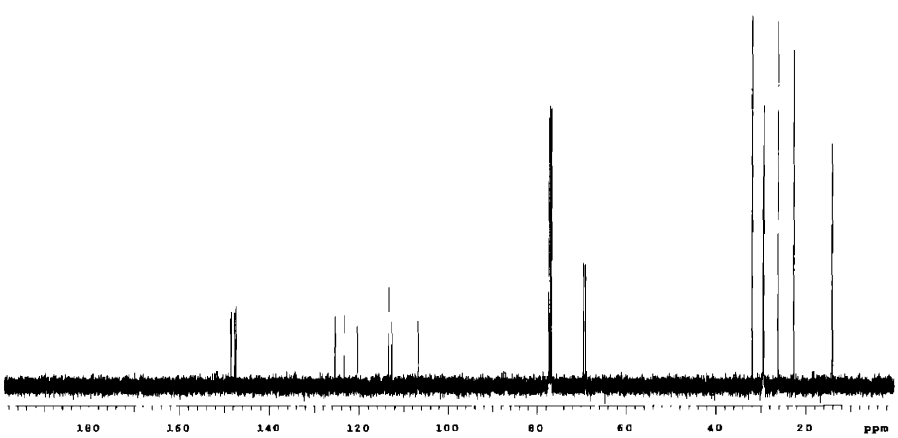

^{13}C NMR of **20** (125 MHz, $CDCl_3$)

Appendix 5:

Variable Temperature X-ray Diffraction for Chapter 4

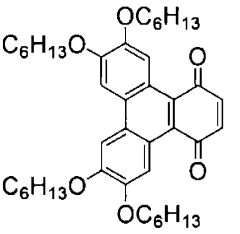

14

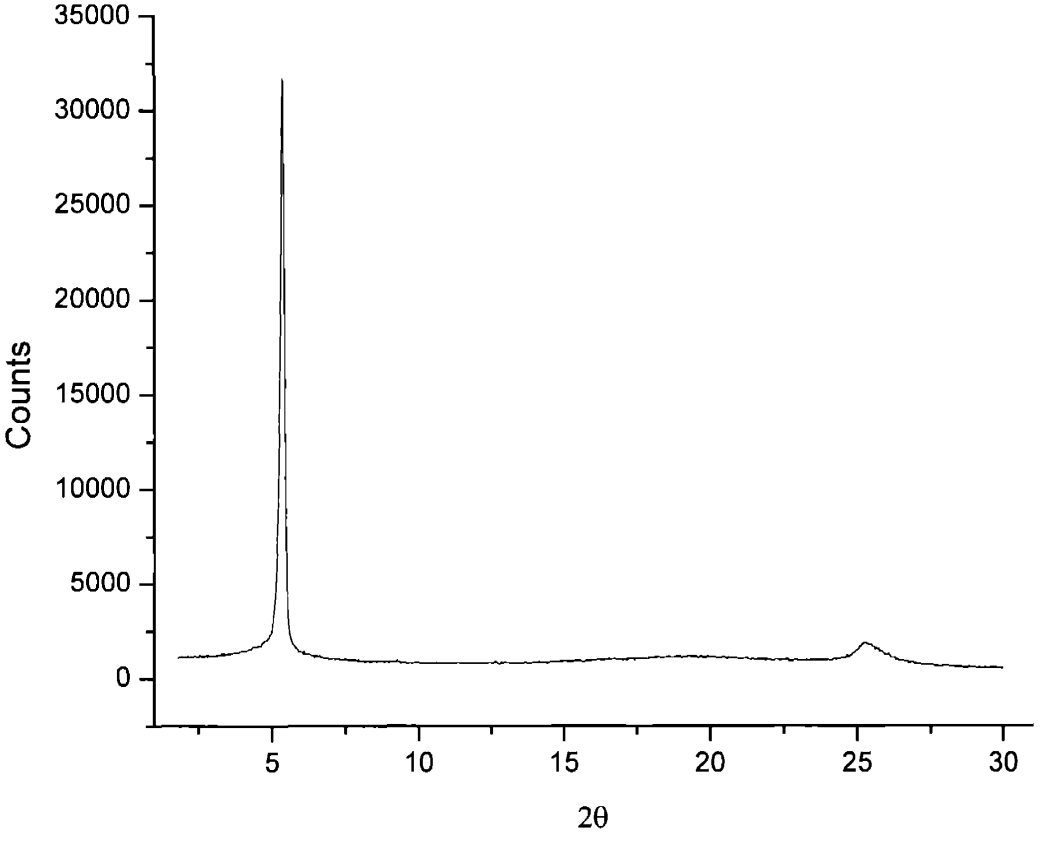

Variable temperature X-ray diffraction pattern of **14** (Col_H phase) at 75 °C.

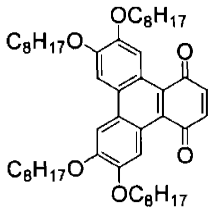

15

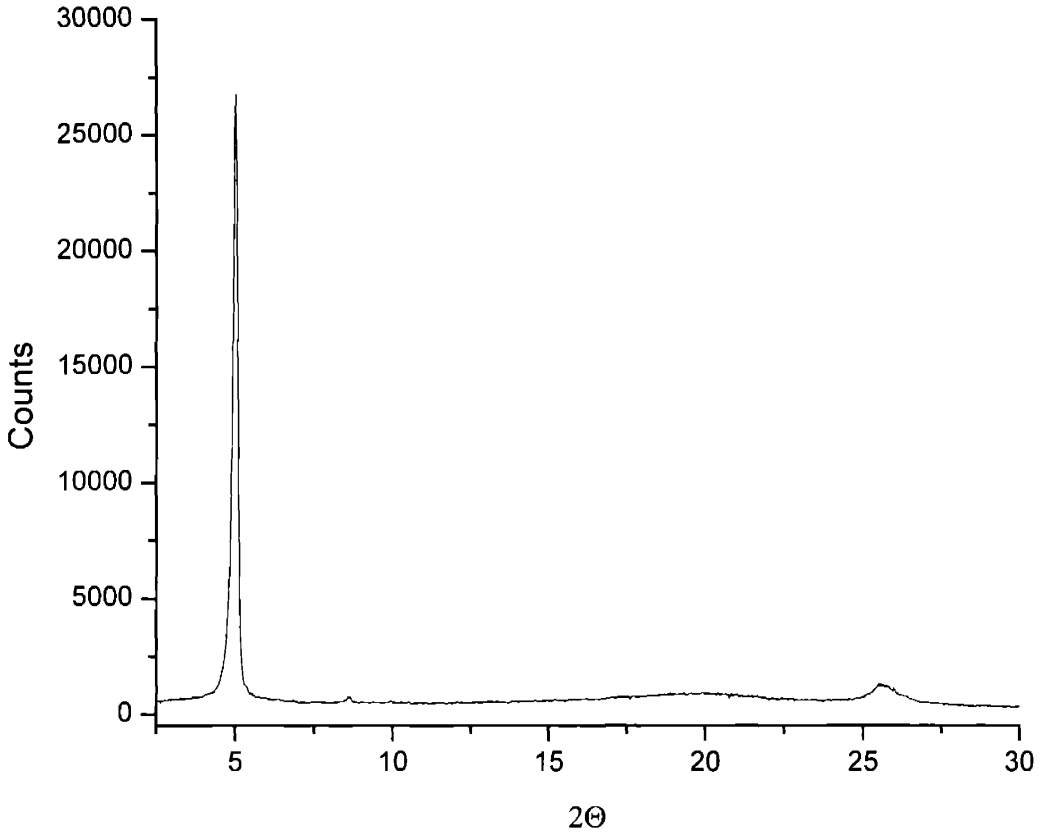

Variable temperature X-ray diffraction pattern of **15** (Col_H phase) at 92 °C.

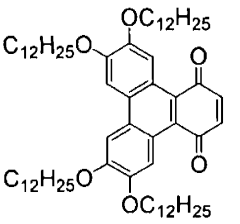

17

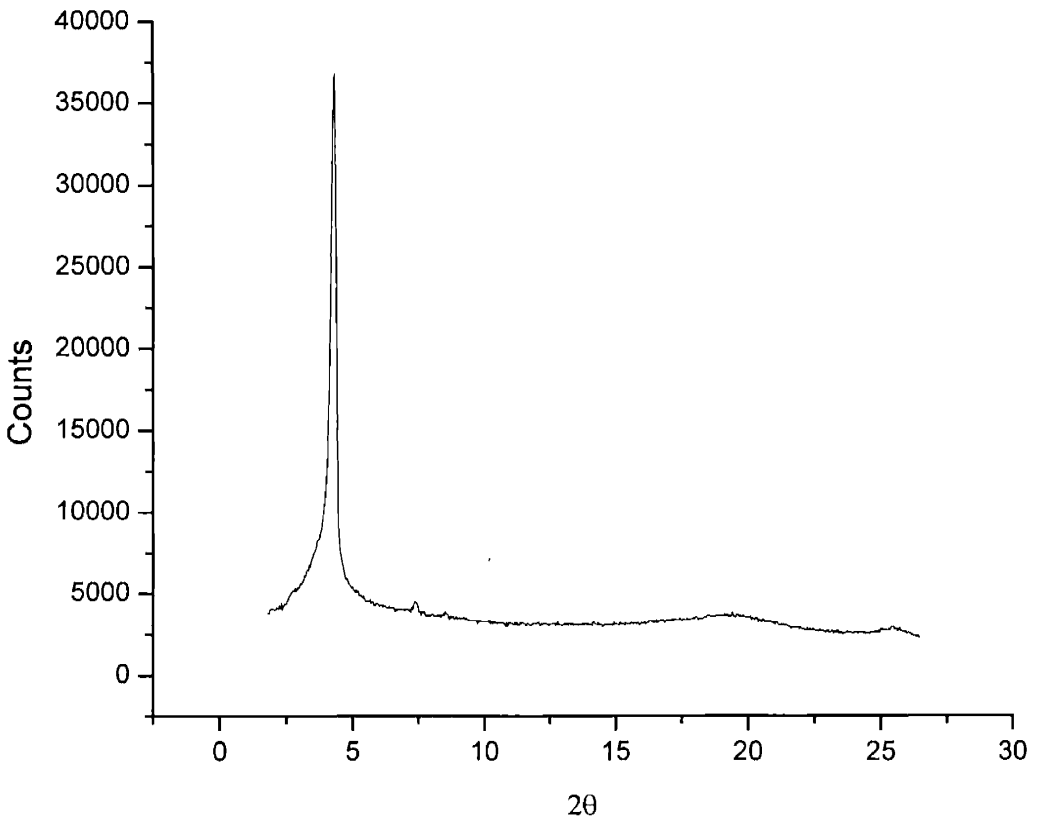

Variable temperature X-ray diffraction pattern of **17** (Col_H phase) at 76 °C.

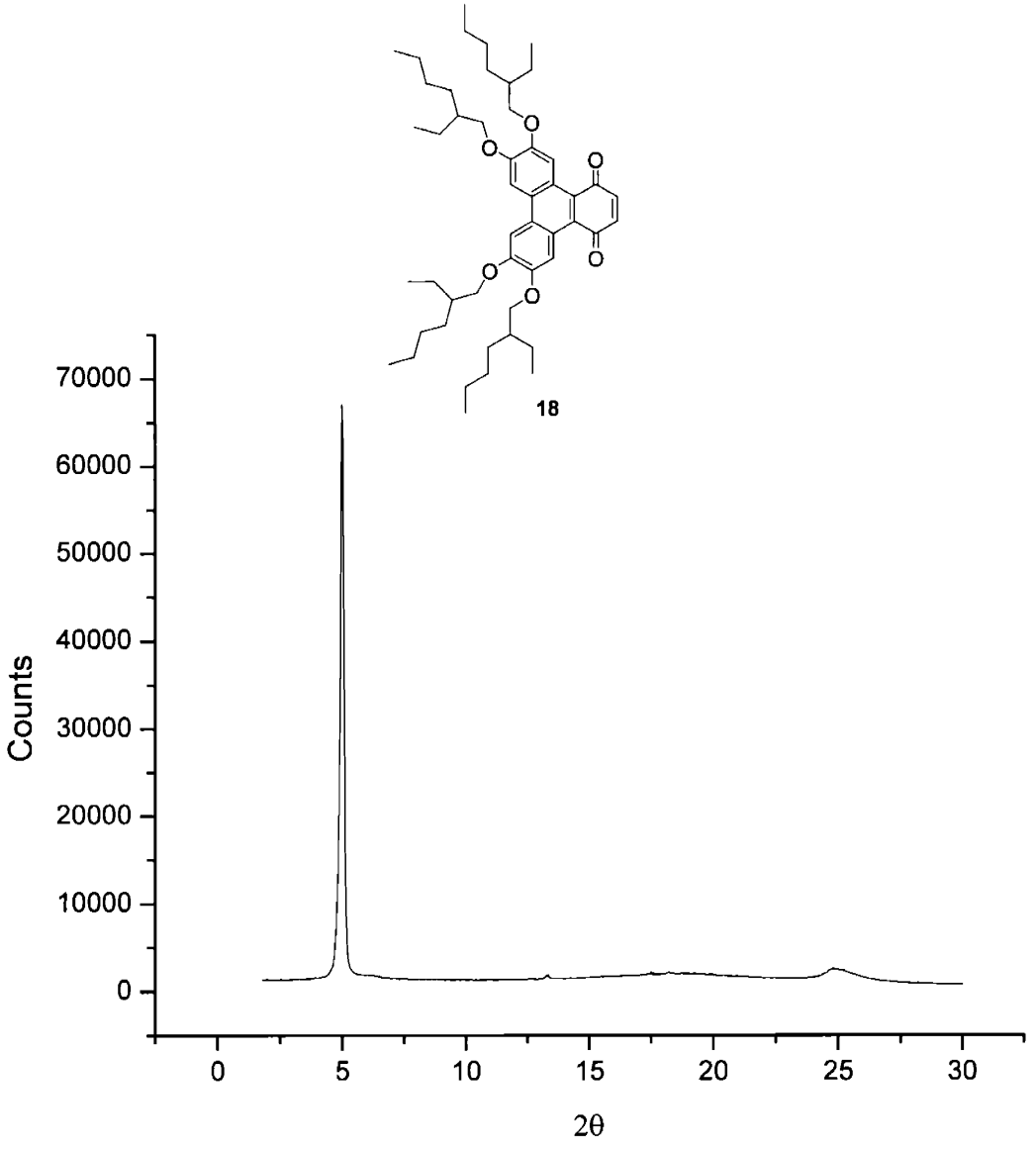

Variable temperature X-ray diffraction pattern of **18** (Col_H phase) at 90 °C.

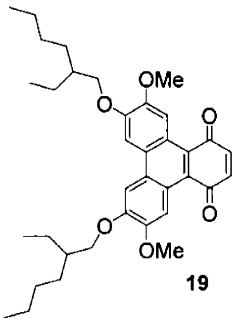

19

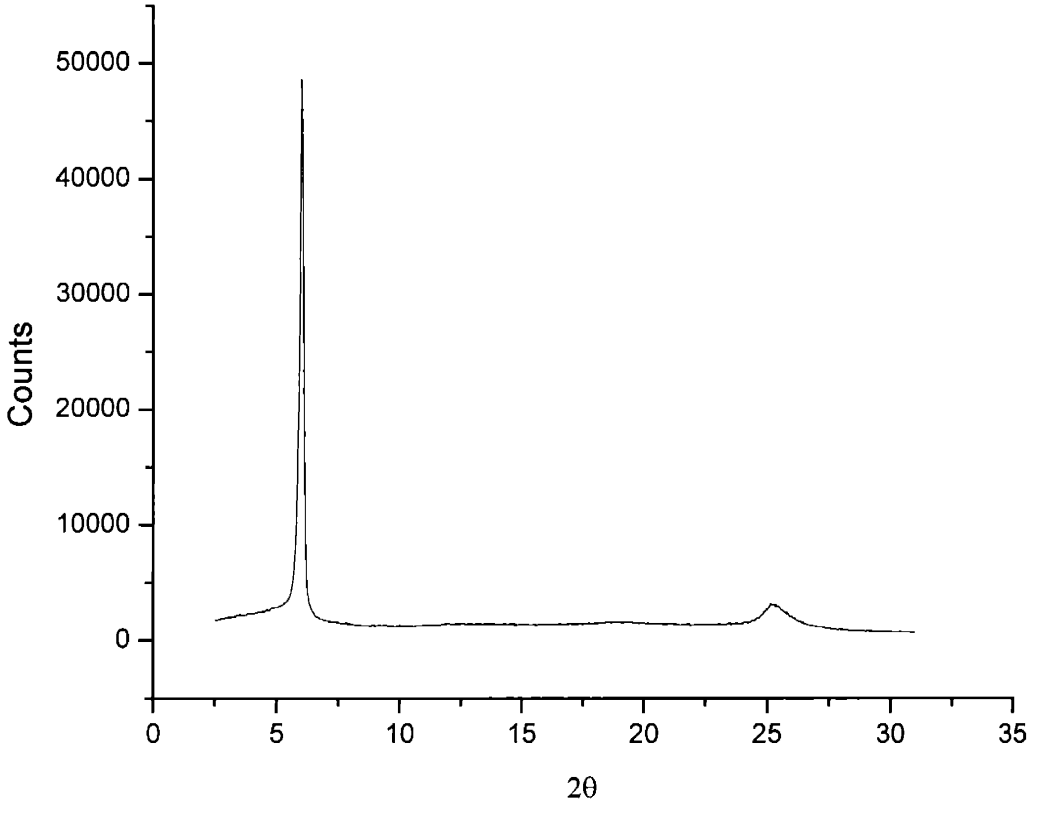

Variable temperature X-ray diffraction pattern of **19** (Col_H phase) at 82 °C.

Appendix 6:

^{1}H and ^{13}C NMR spectra for Chapter 5

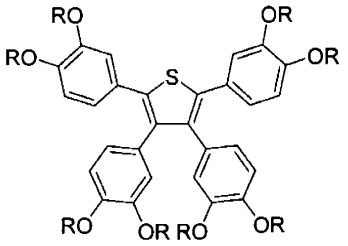

1 R = C_8H_{17}

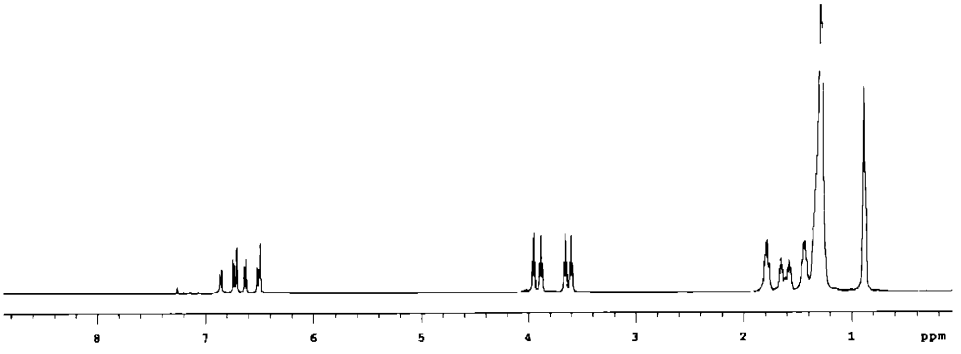

^{1}H NMR of **1** (500MHz, $CDCl_3$)

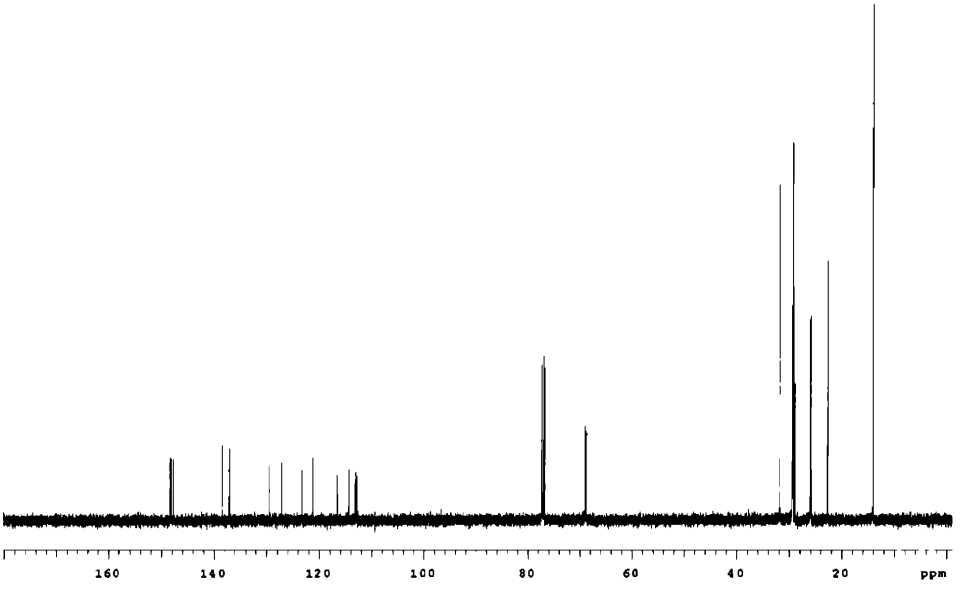

^{13}C NMR of **1** (125MHz, $CDCl_3$)

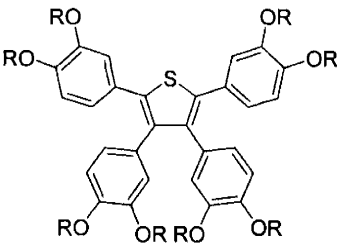

2 R = CH_3

^{1}H NMR of **2** (300MHz, $CDCl_3$)

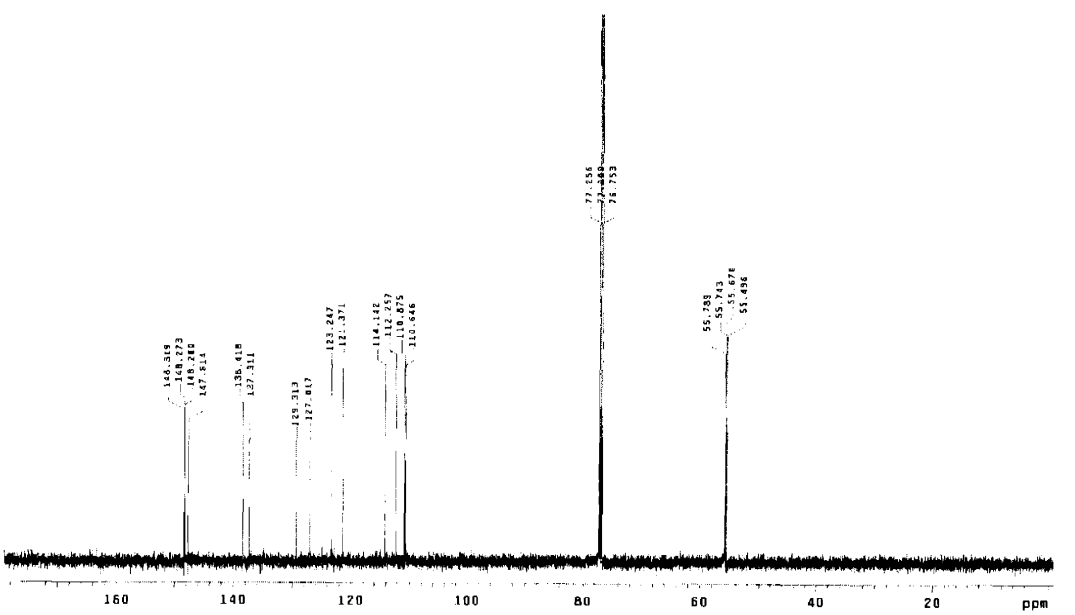

^{13}C NMR of **2** (75MHz, $CDCl_3$)

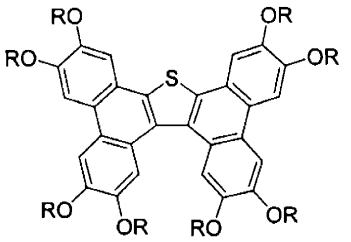

3 R = C_8H_{17}

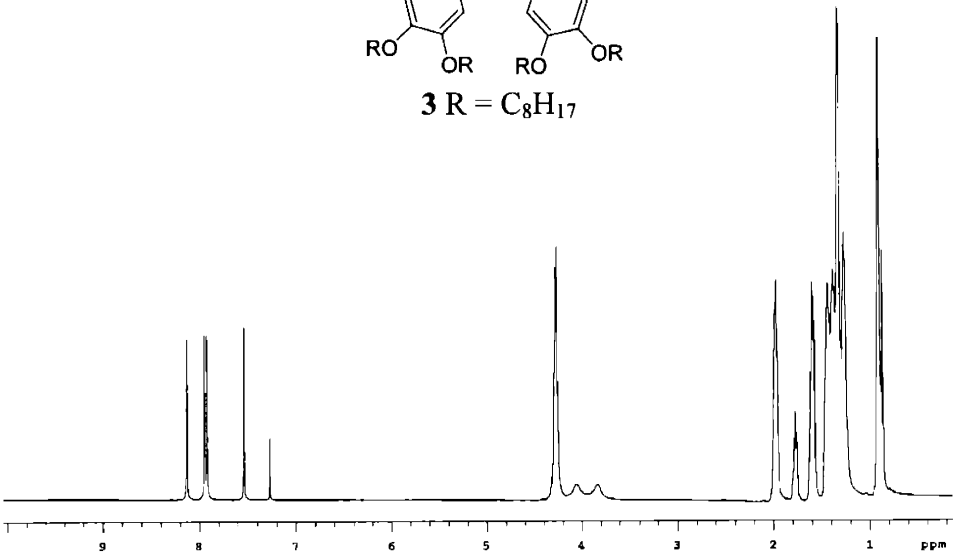

^{1}H NMR of **3** (500MHz, $CDCl_3$)

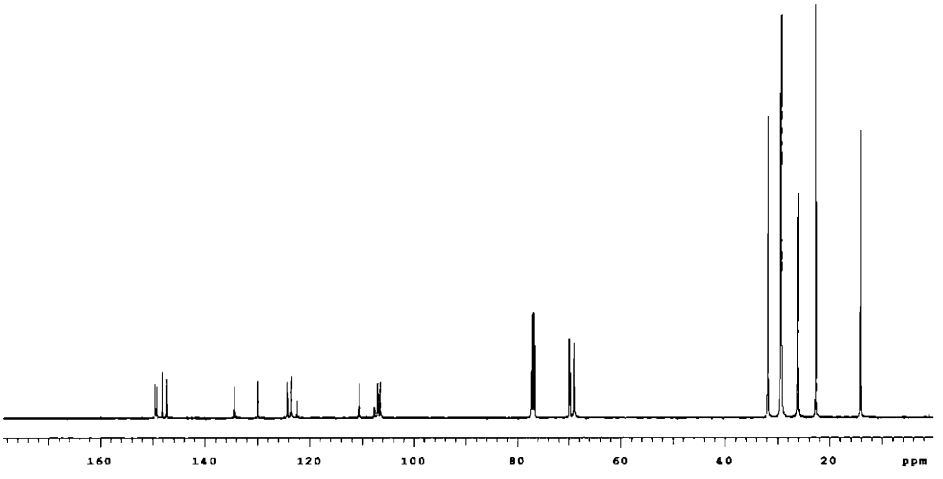

^{13}C NMR of **3** (125 MHz, $CDCl_3$)

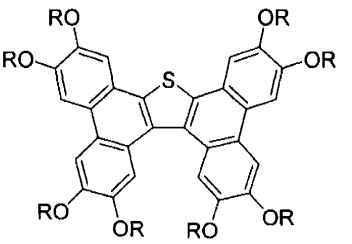

4 R = CH_3

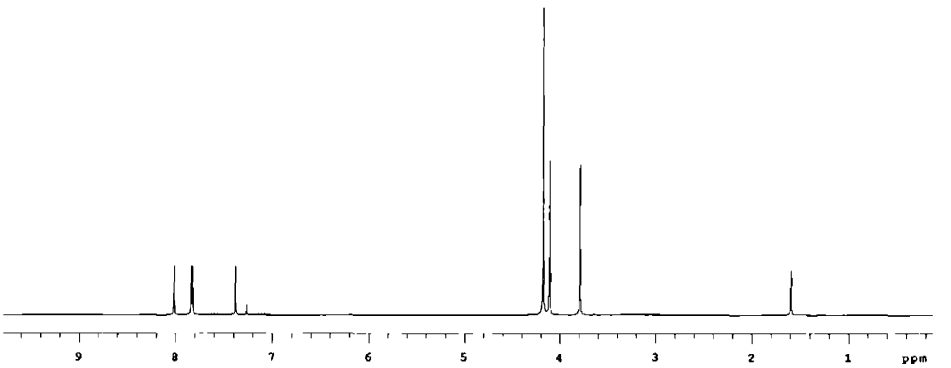

^{1}H NMR of **4** (500MHz, $CDCl_3$)

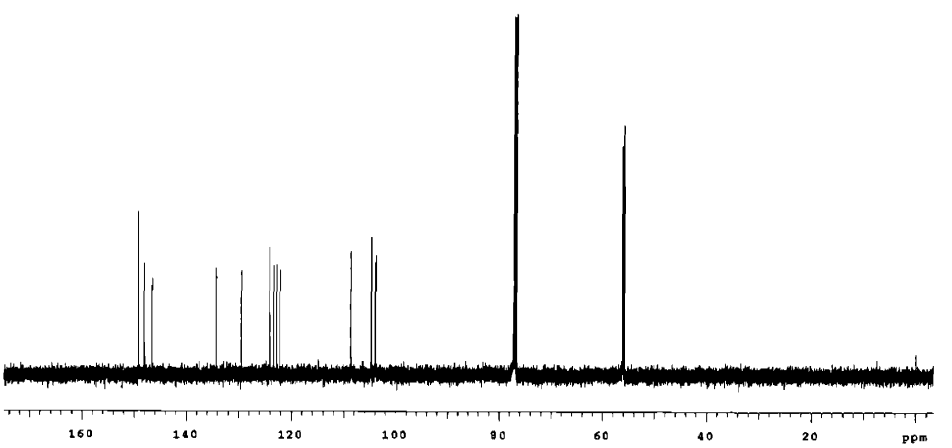

^{13}C NMR of **4** (125 MHz, $CDCl_3$)

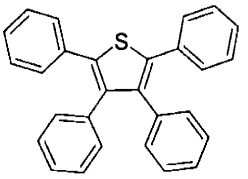

5

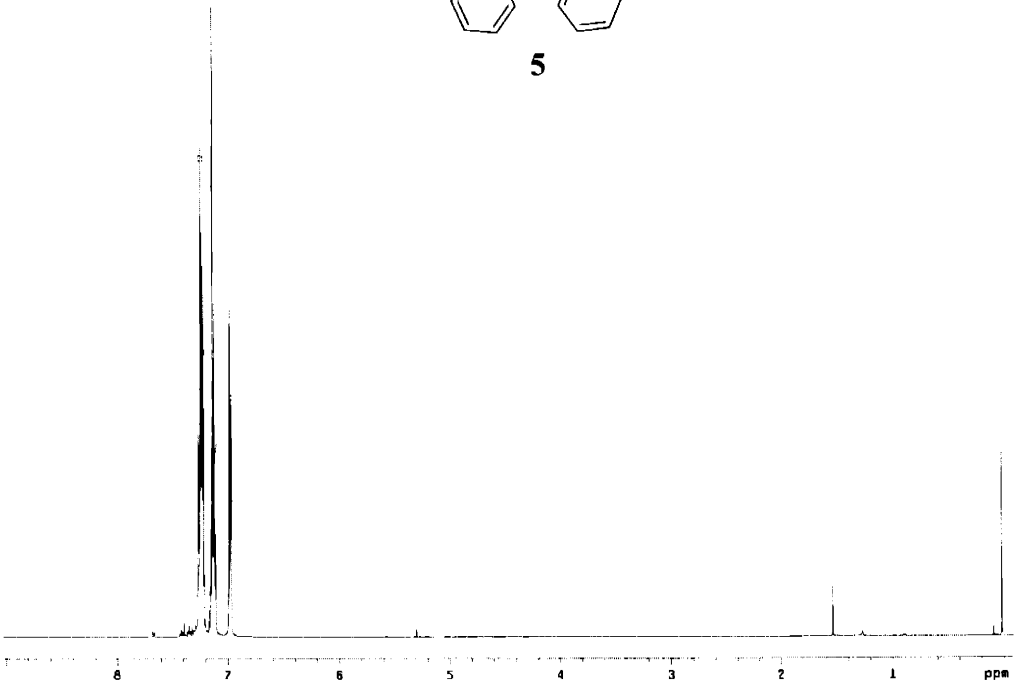

^{1}H NMR of **5** (500MHz, $CDCl_3$)

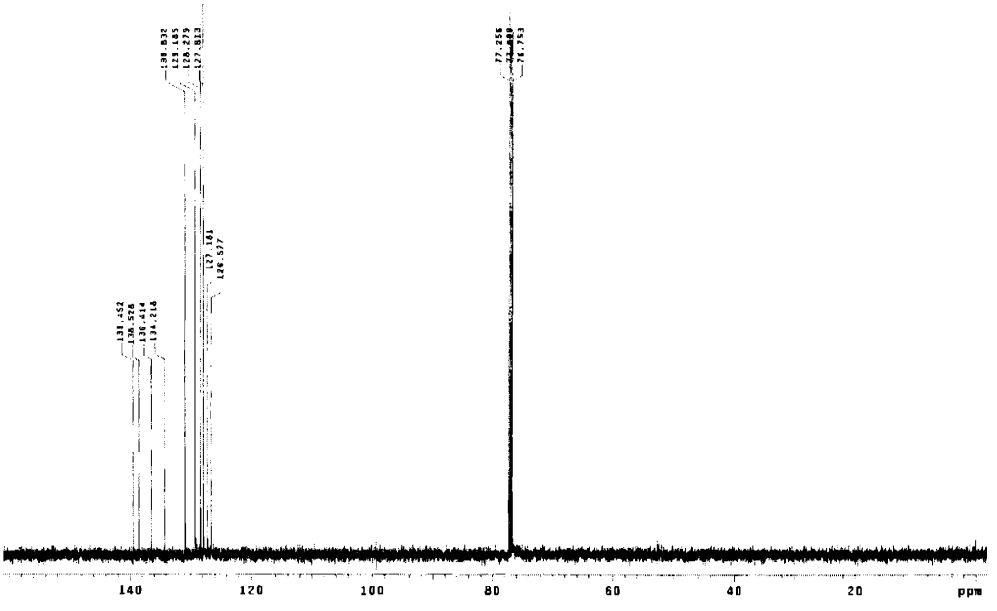

^{13}C NMR of **5** (125 MHz, $CDCl_3$)

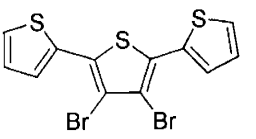

7

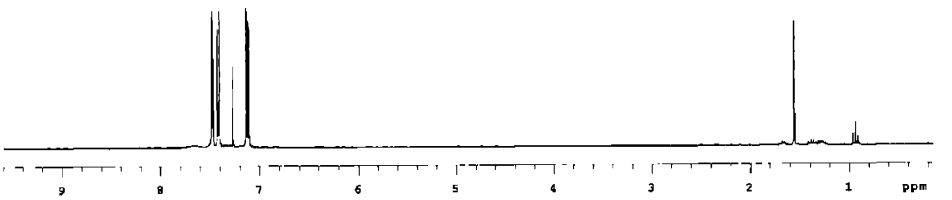

^{1}H NMR of **7** (300MHz, $CDCl_3$)

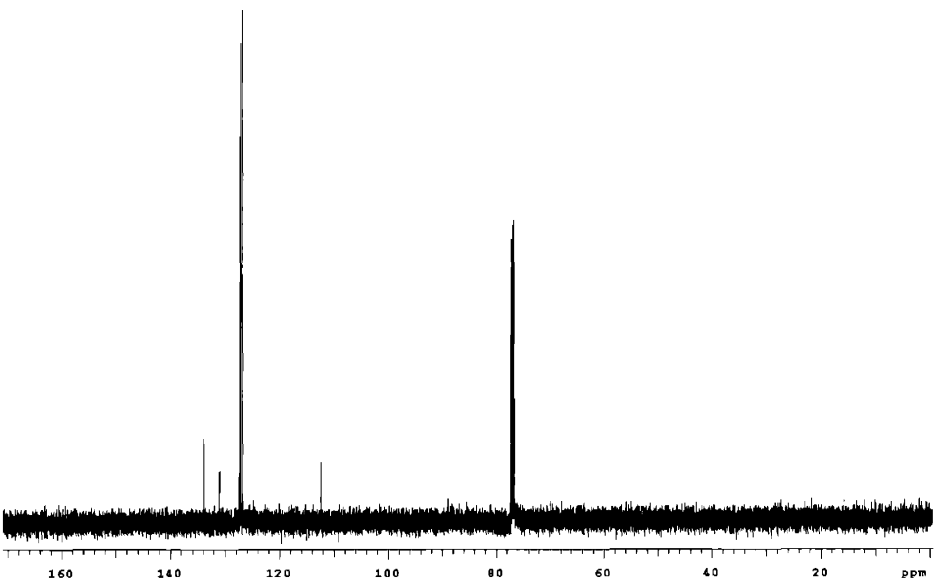

^{13}C NMR of **7** (125 MHz, $CDCl_3$)

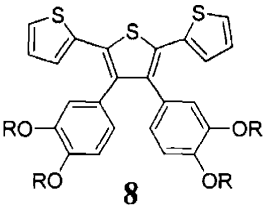

8

$R = C_8H_{17}$

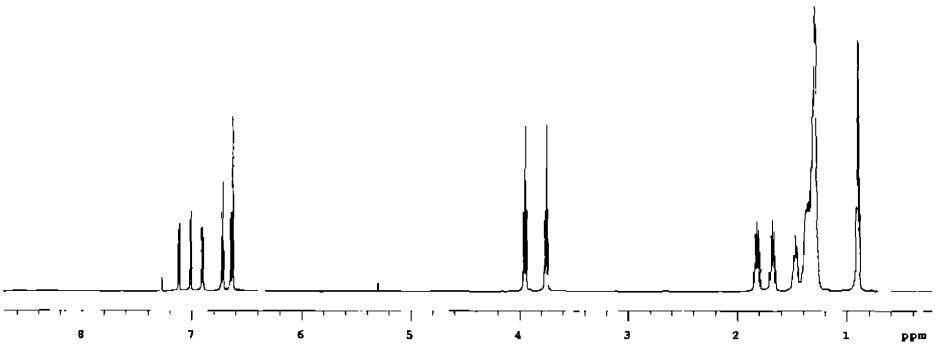

^1H NMR of **8** (500MHz, $CDCl_3$)

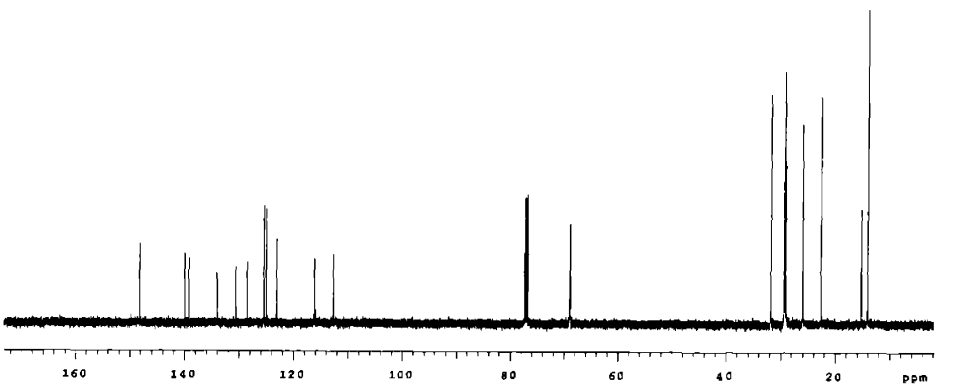

^{13}C NMR of **8** (125 MHz, $CDCl_3$)

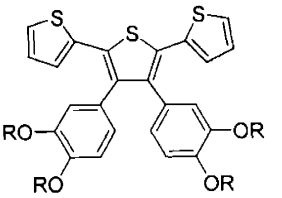

9

R = 2-Ethylhexyl

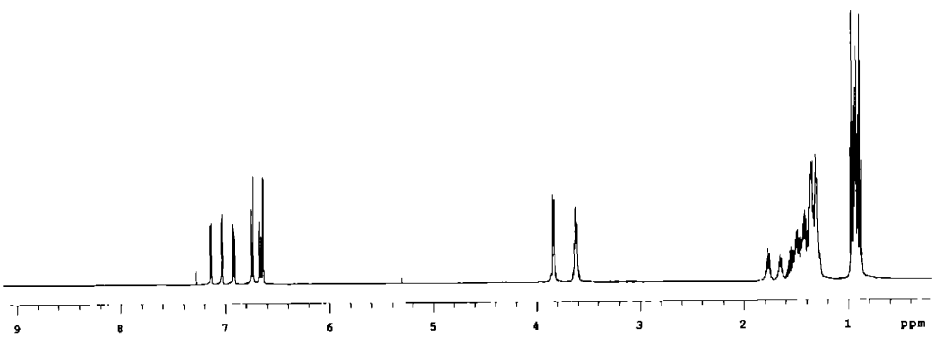

^{1}H NMR of **9** (500MHz, $CDCl_3$)

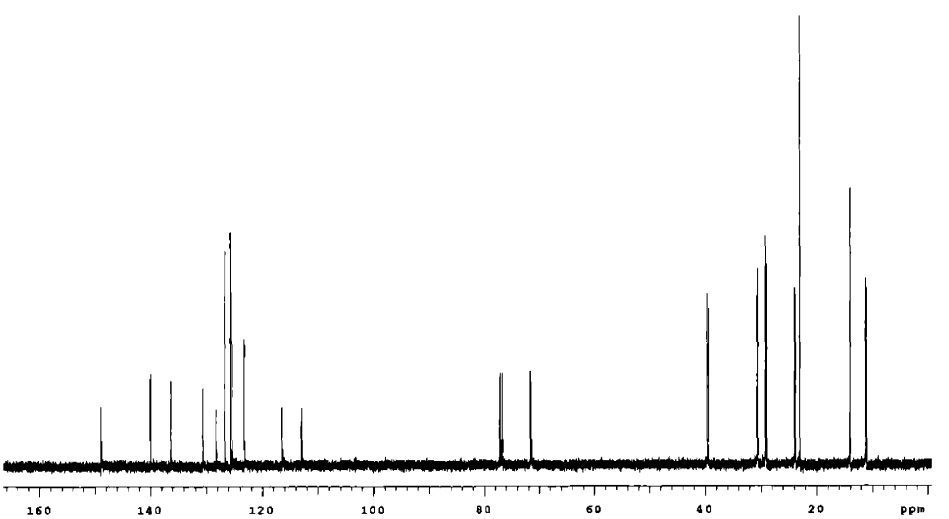

^{13}C NMR of **9** (125 MHz, $CDCl_3$)

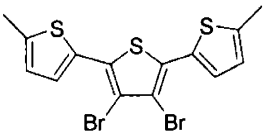

10

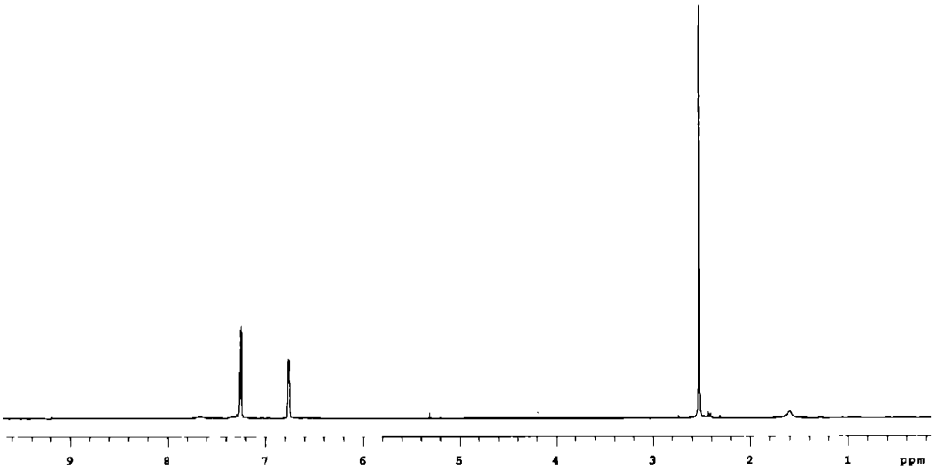

^{1}H NMR of **10** (500MHz, $CDCl_3$)

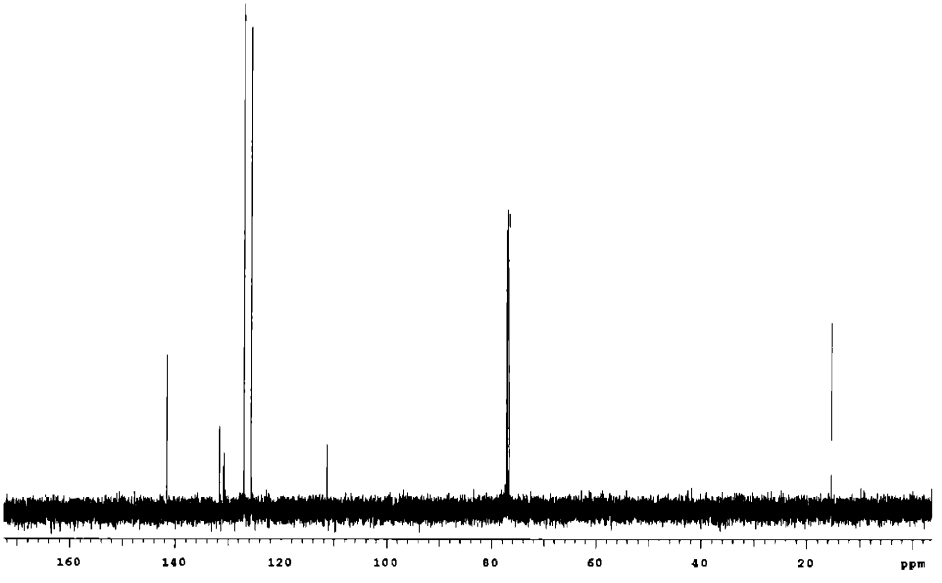

^{13}C NMR of **10** (125 MHz, $CDCl_3$)

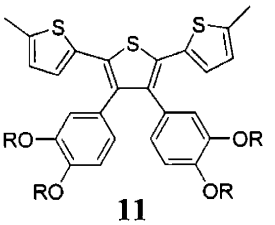

11

R = C_8H_{17}

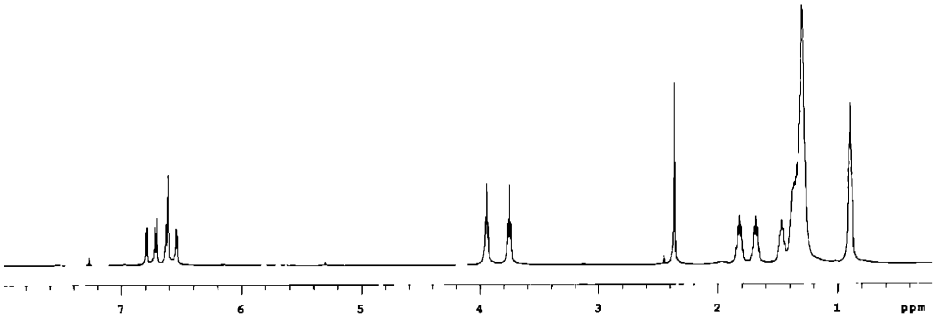

^{1}H NMR of **11** (500MHz, $CDCl_3$)

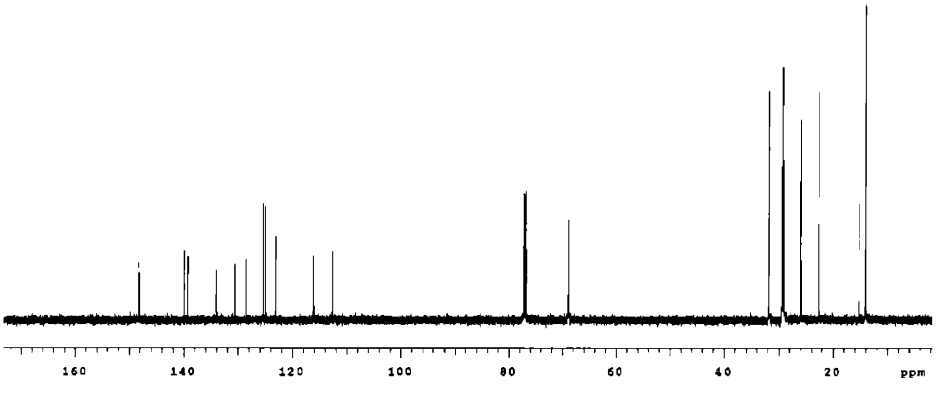

^{13}C NMR of **11** (125 MHz, $CDCl_3$)

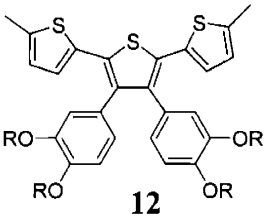

12

R = 2-Ethylhexyl

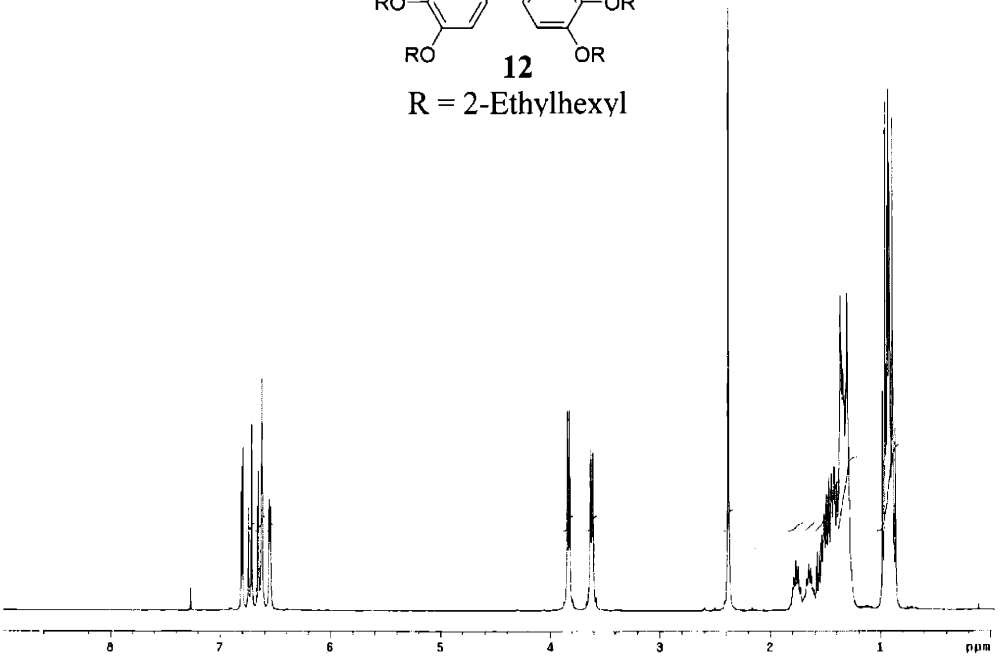

^{1}H NMR of **12** (300MHz, $CDCl_3$)

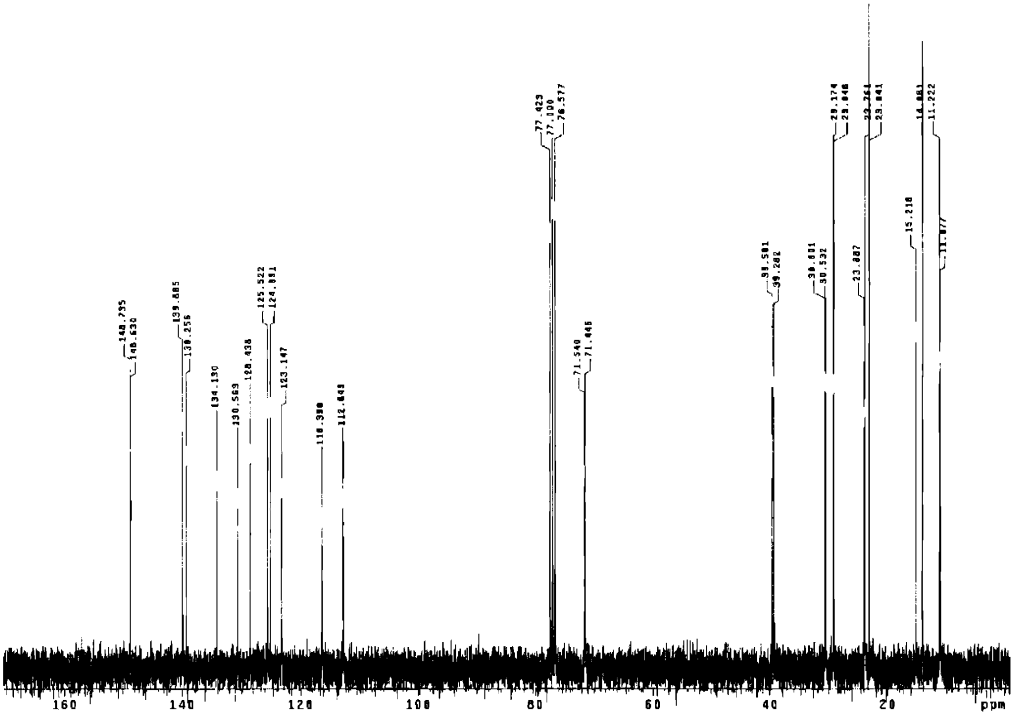

^{13}C NMR of **12** (75 MHz, $CDCl_3$)

Appendix 7

^{1}H and ^{13}C NMR spectra for Chapter 6

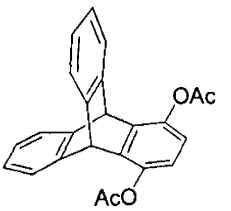

1

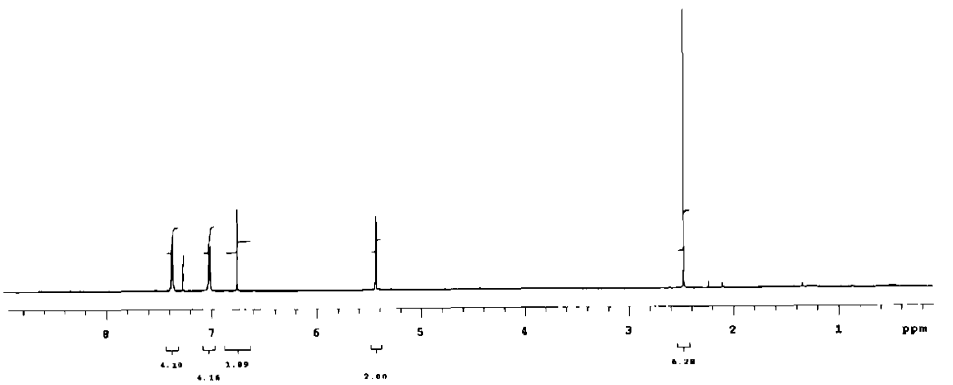

^{1}H NMR of **1** (500 MHz, $CDCl_3$)

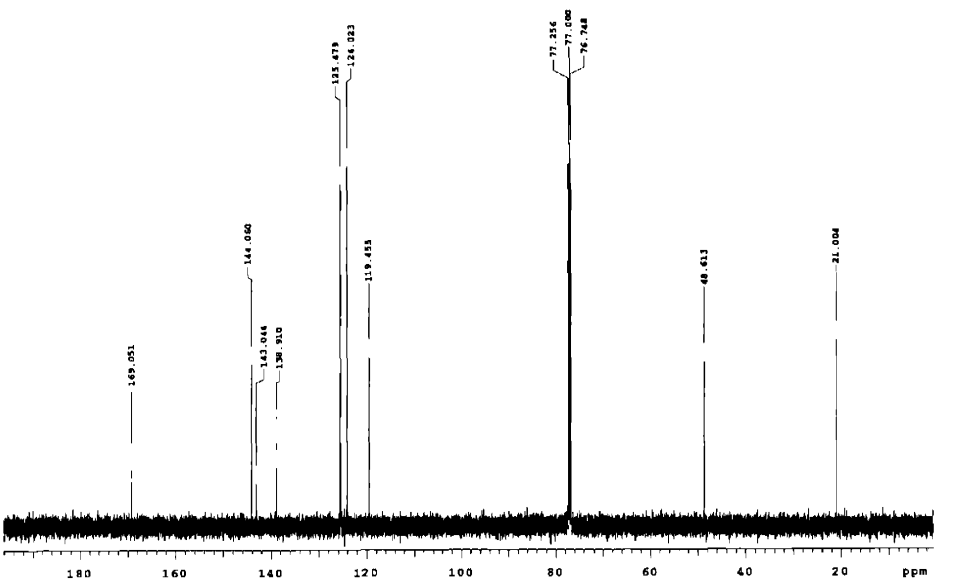

^{13} C NMR of **1** (125 MHz, $CDCl_3$)

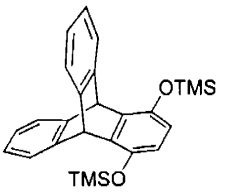

2

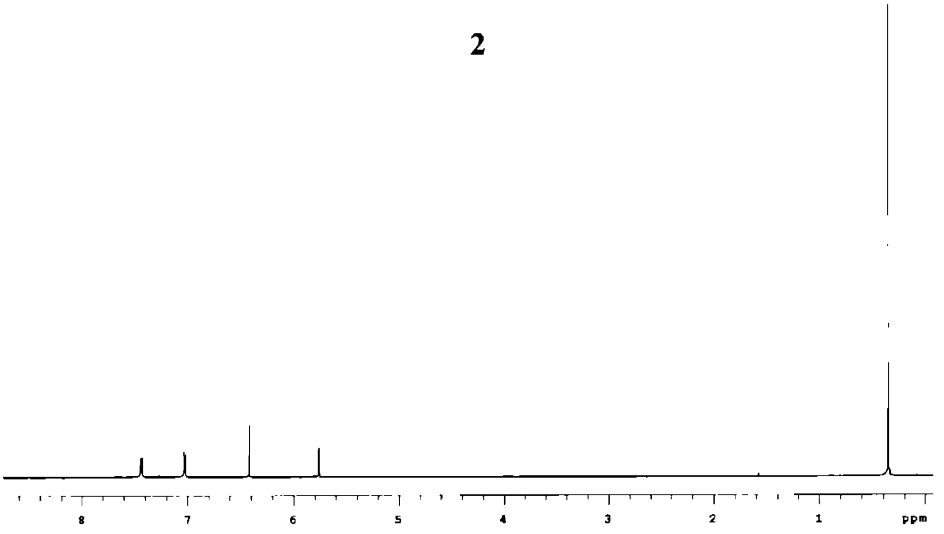

^{1}H NMR of **2** (500 MHz, $CDCl_3$)

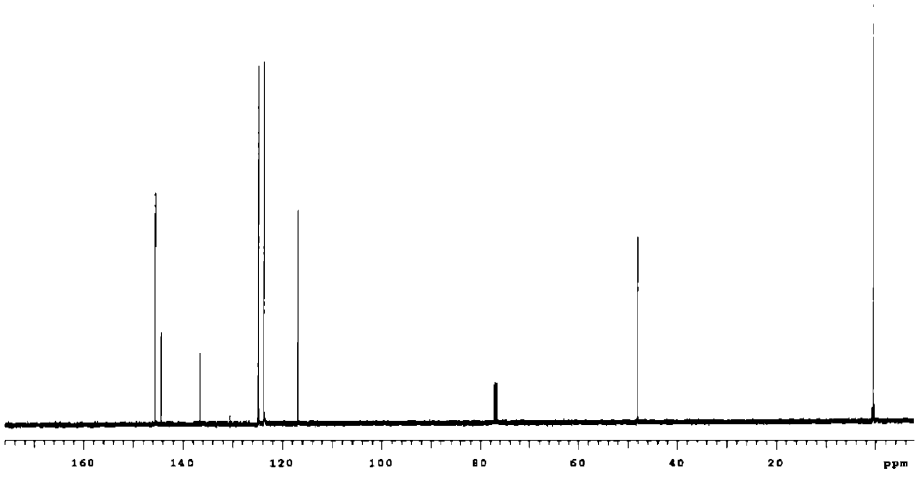

^{13}C NMR of **2** (125 MHz, $CDCl_3$)

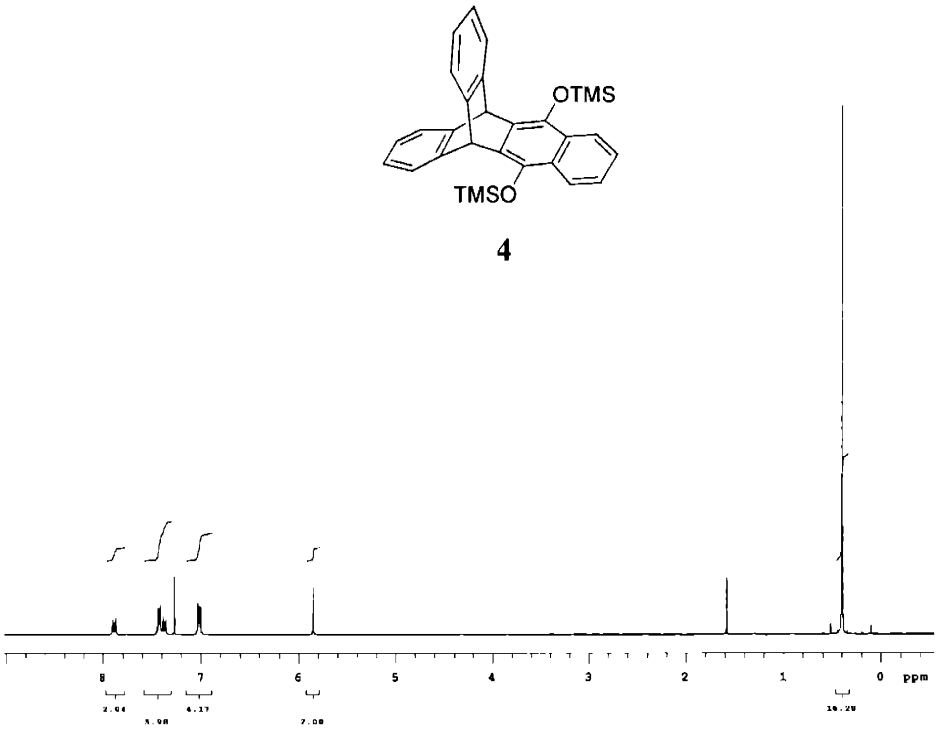

^{1}H NMR of **4** (500 MHz, $CDCl_3$)

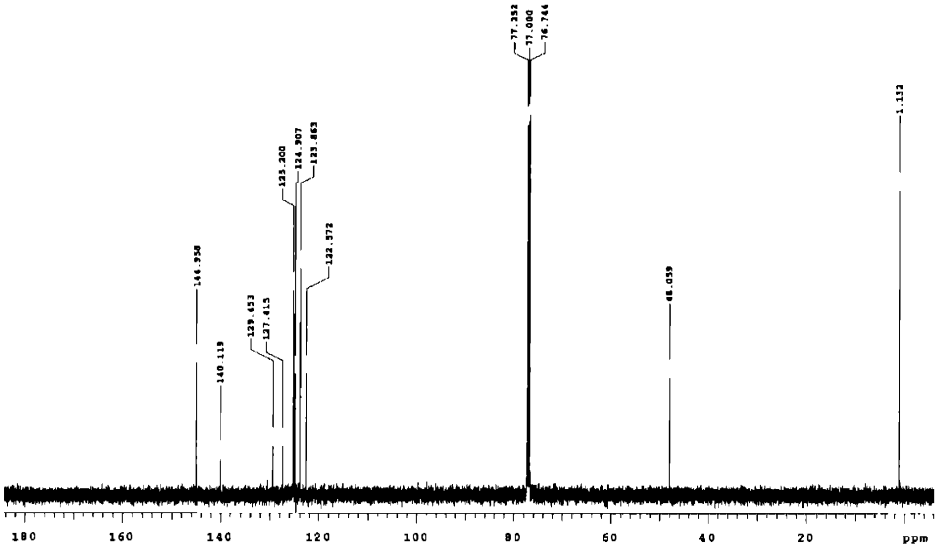

^{13} C NMR of **4** (125 MHz, $CDCl_3$)

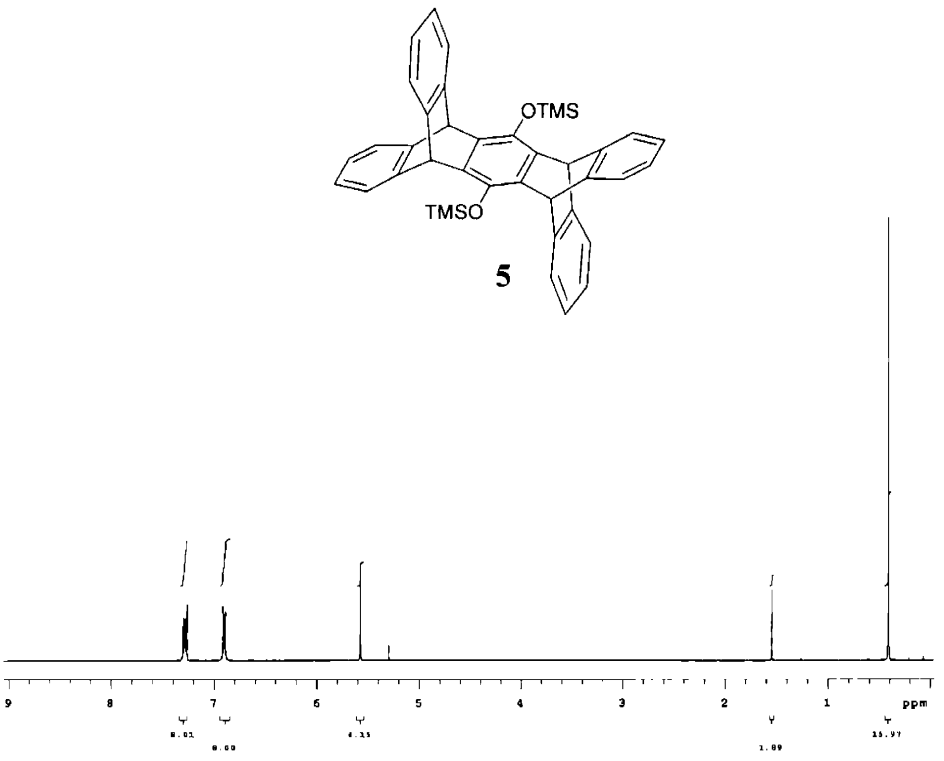

^{1}H NMR of **5** (500 MHz, $CDCl_3$)

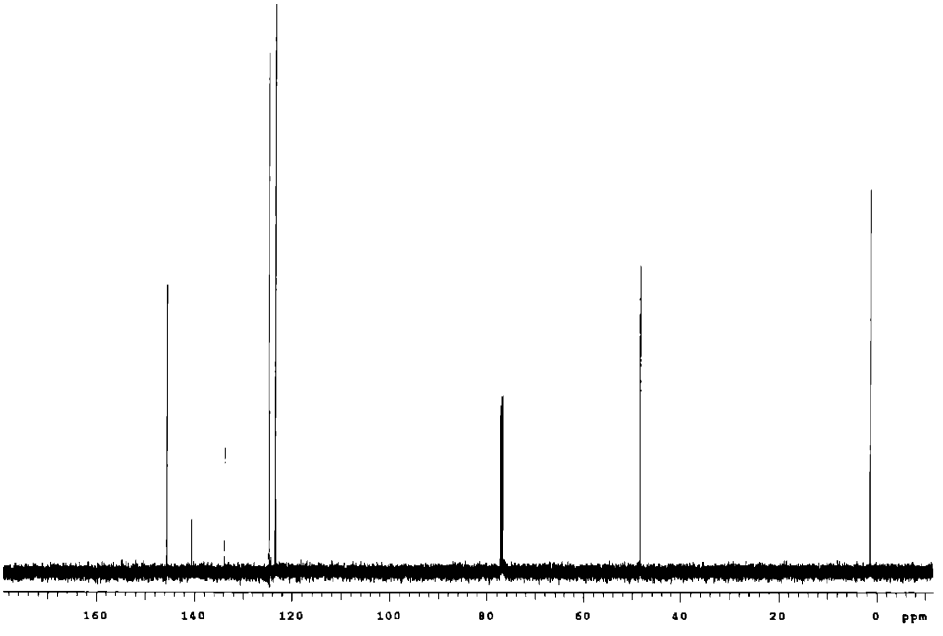

^{13}C NMR of **5** (125 MHz, $CDCl_3$)

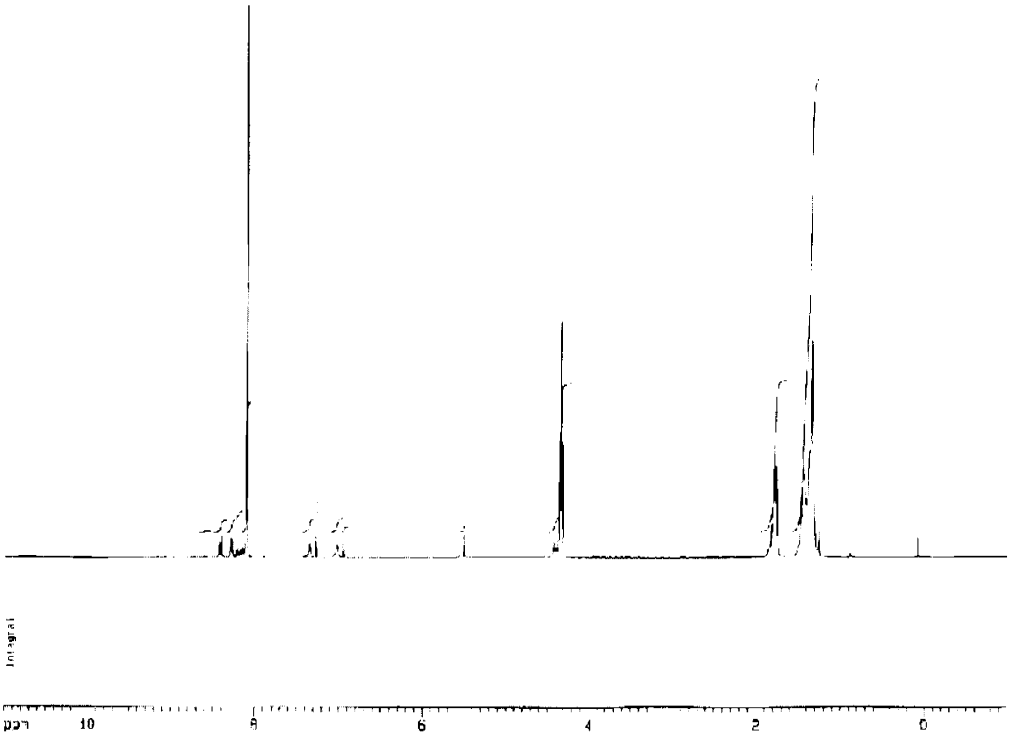

^{1}H NMR of **Poly-3** (500 MHz, $CDCl_3$)

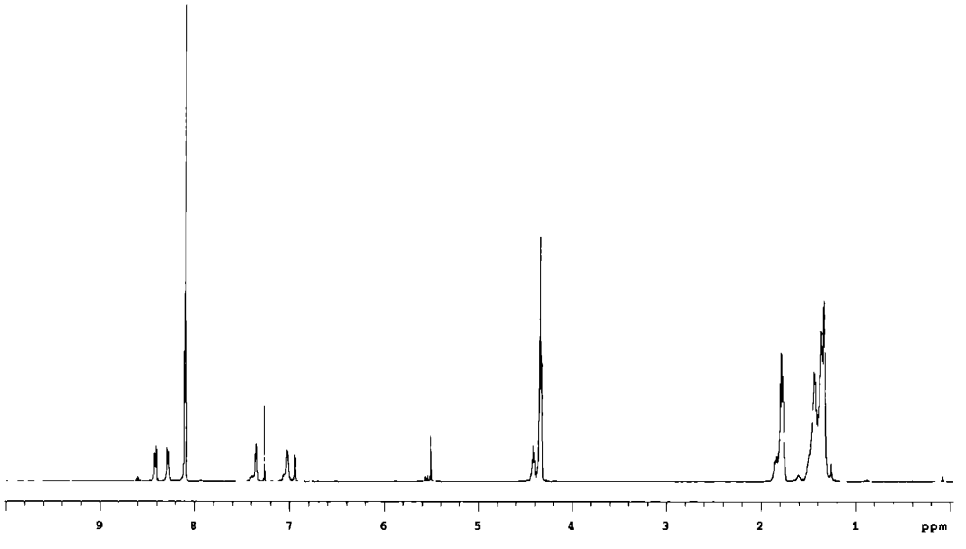

^{1}H NMR of **Poly-4** (500 MHz, $CDCl_3$)

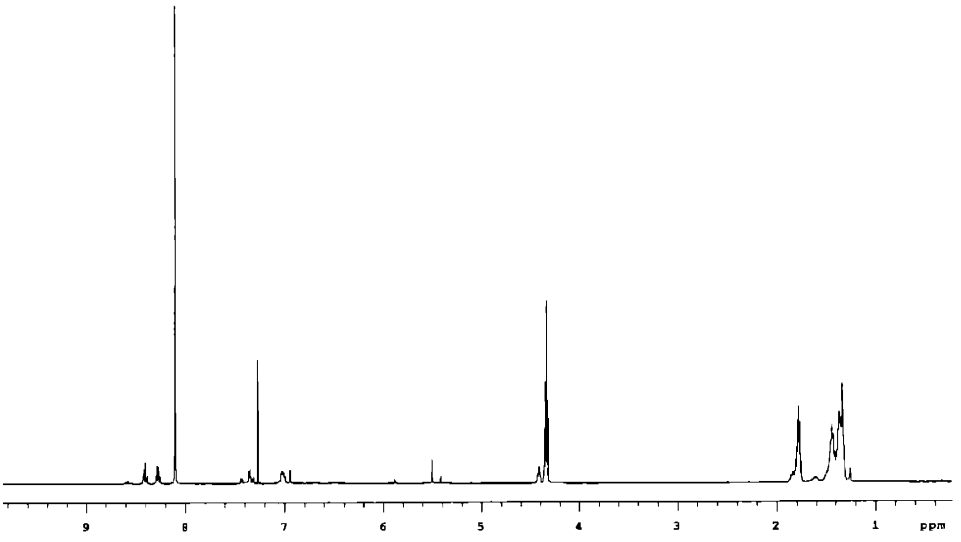

^{1}H NMR of **Poly-5** (500 MHz, $CDCl_3$)

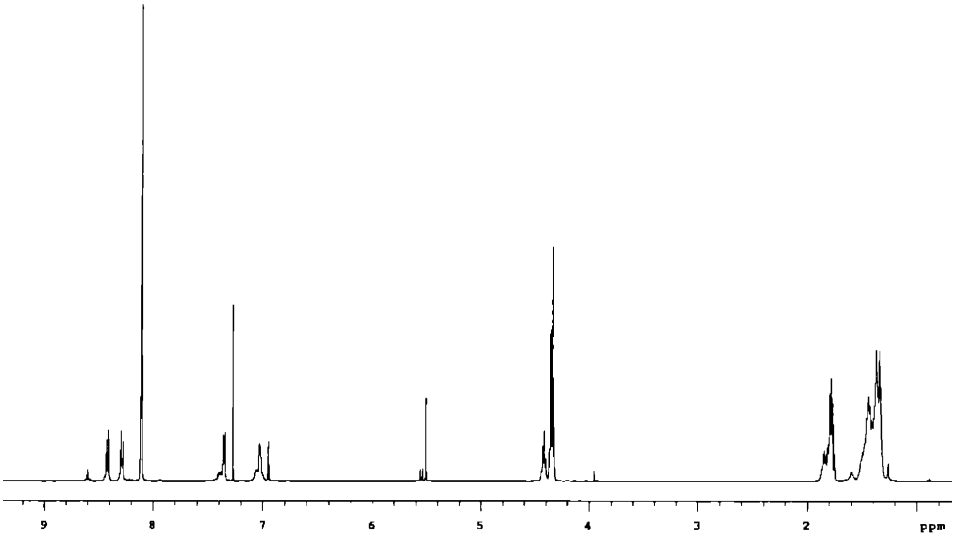

^{1}H NMR of **Poly-6** (500 MHz, $CDCl_3$)

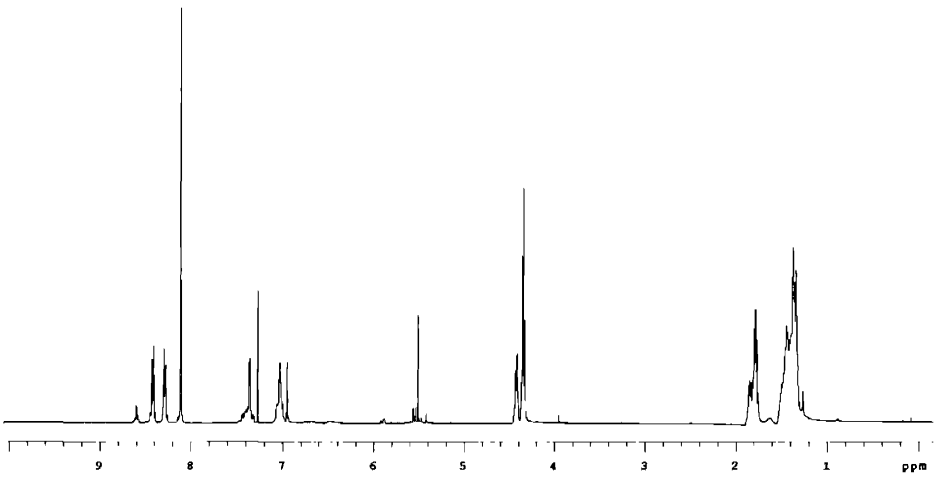

^{1}H NMR of **Poly-7** (500 MHz, $CDCl_3$)

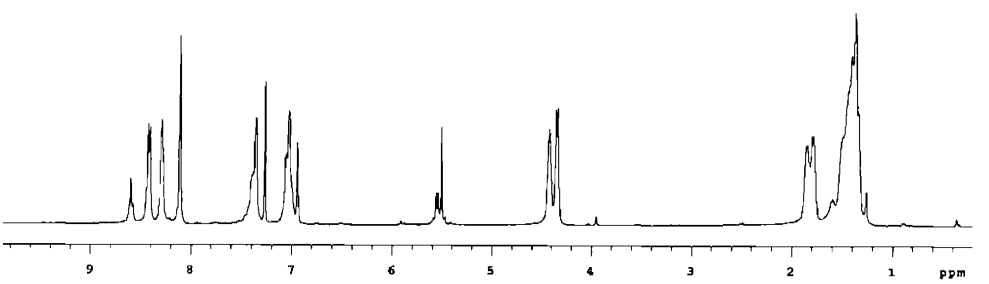

^{1}H NMR of **Poly-8** (500 MHz, $CDCl_3$)

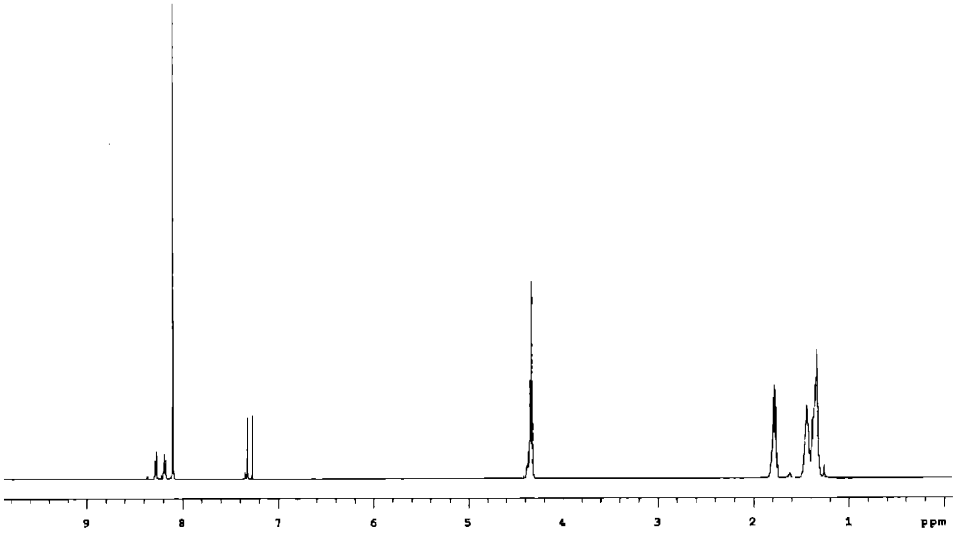

^{1}H NMR of **Poly-9** (500 MHz, $CDCl_3$)

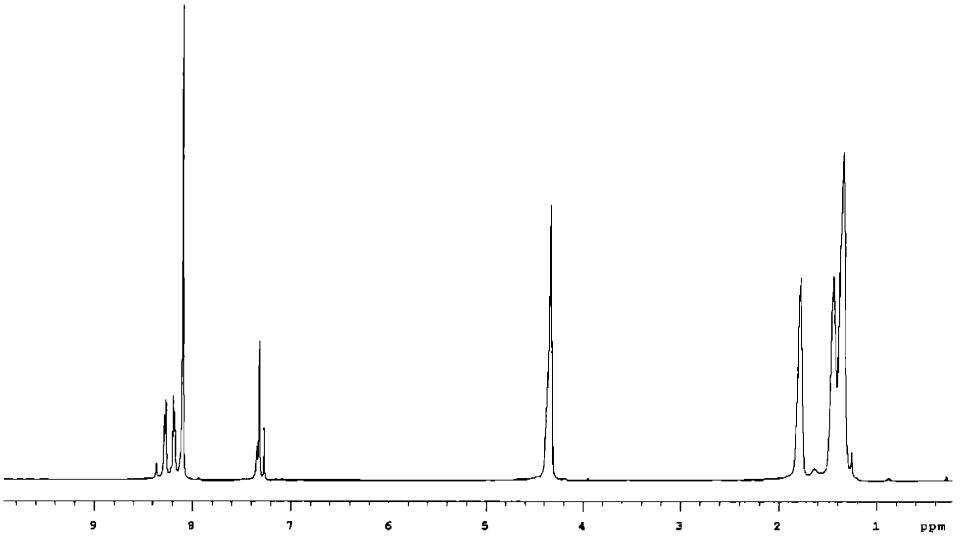

^{1}H NMR of **Poly-10** (500 MHz, $CDCl_3$)

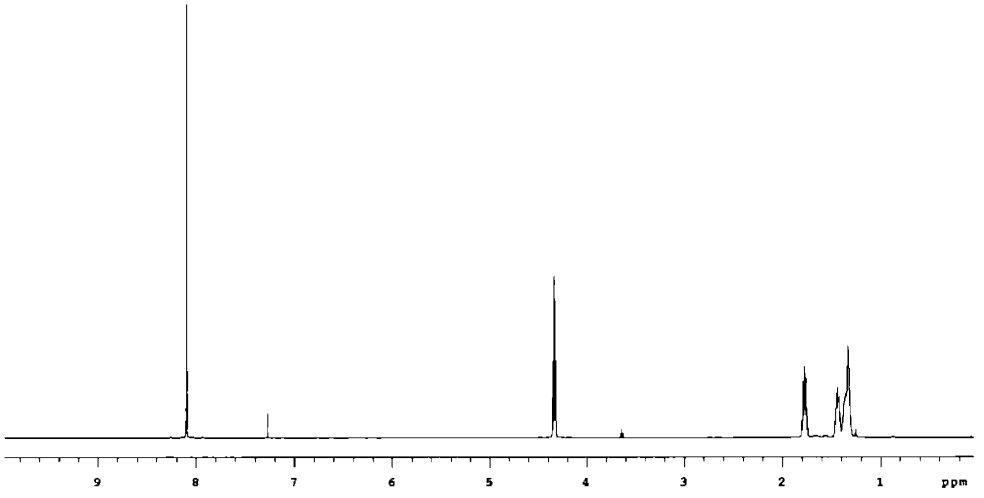

^{1}H NMR of **Poly-11** (500 MHz, $CDCl_3$)

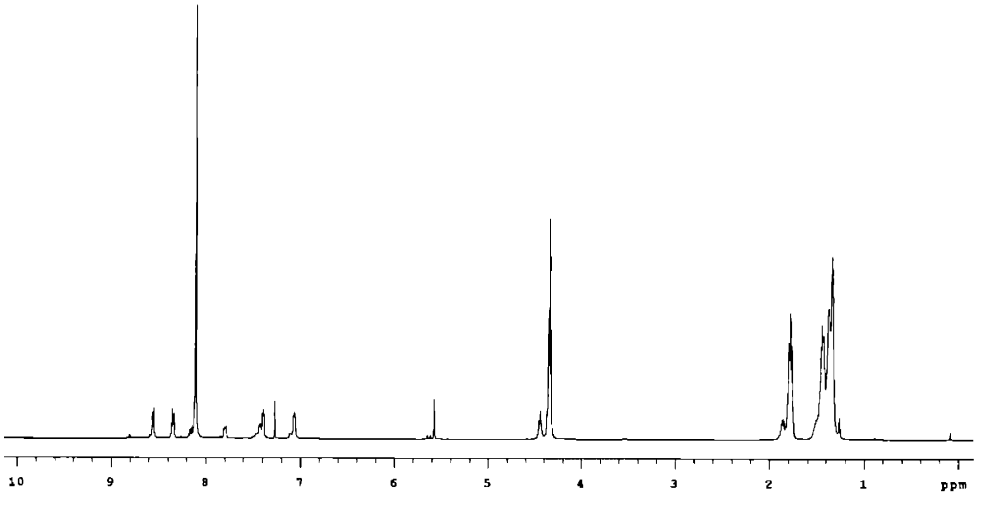

^{1}H NMR of **Poly-12** (500 MHz, $CDCl_3$)

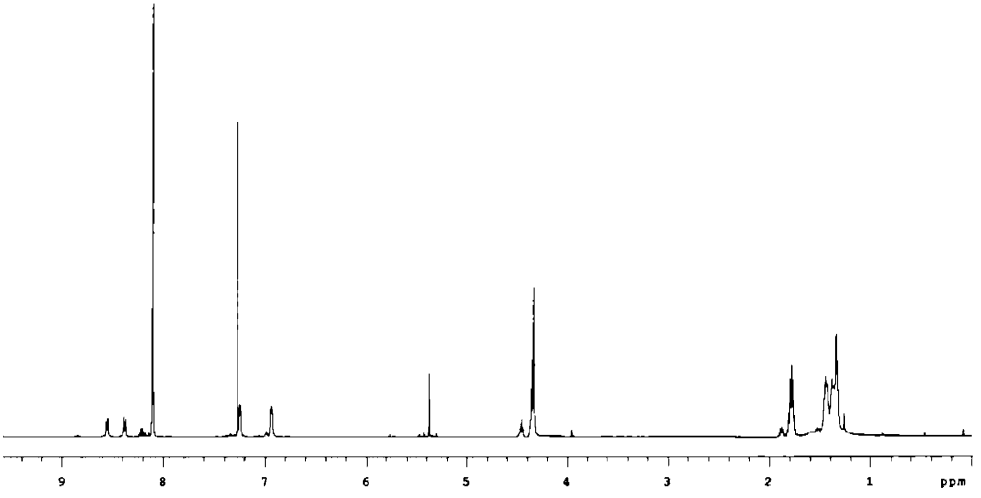

^{1}H NMR of **Poly-13** (500 MHz, $CDCl_3$)

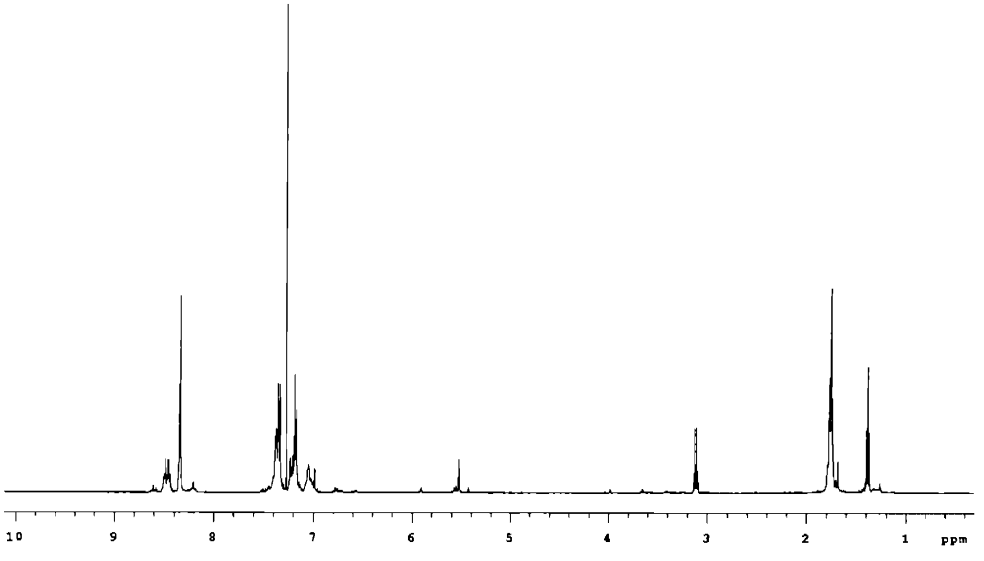

^{1}H NMR of **Poly-14** (500 MHz, $CDCl_3$)

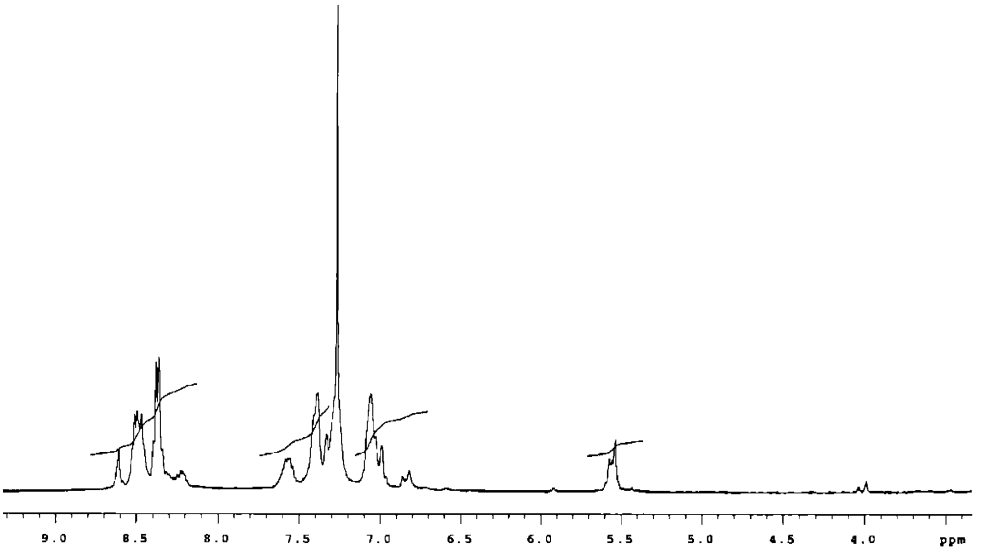

^{1}H NMR of **Poly-15** (500 MHz, $CDCl_3$)

Appendix 8:

^{1}H and ^{13}C NMR spectra for Chapter 7

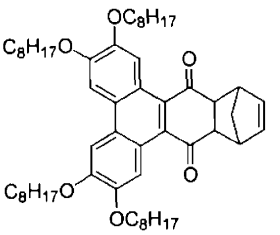

2

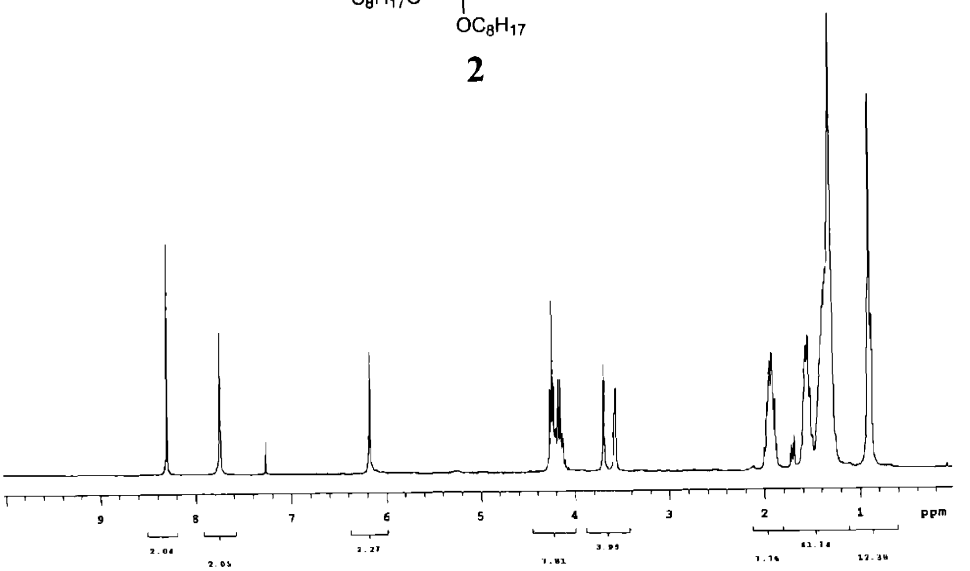

^{1}H NMR of **2** (300MHz, $CDCl_3$)

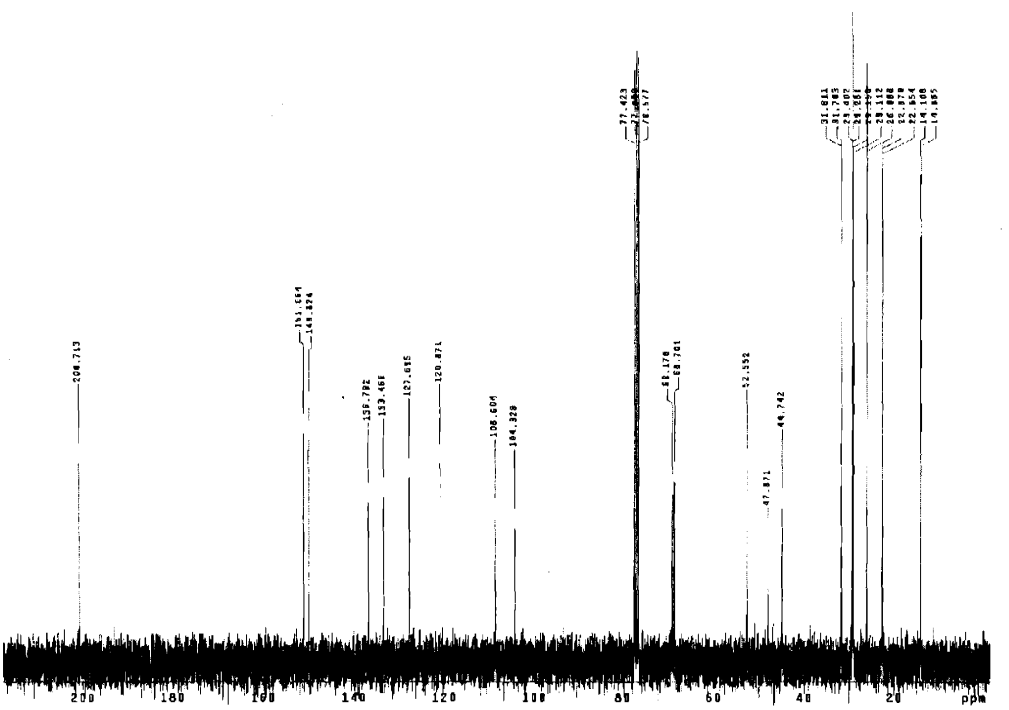

^{13}C NMR of **2** (75MHz, $CDCl_3$)

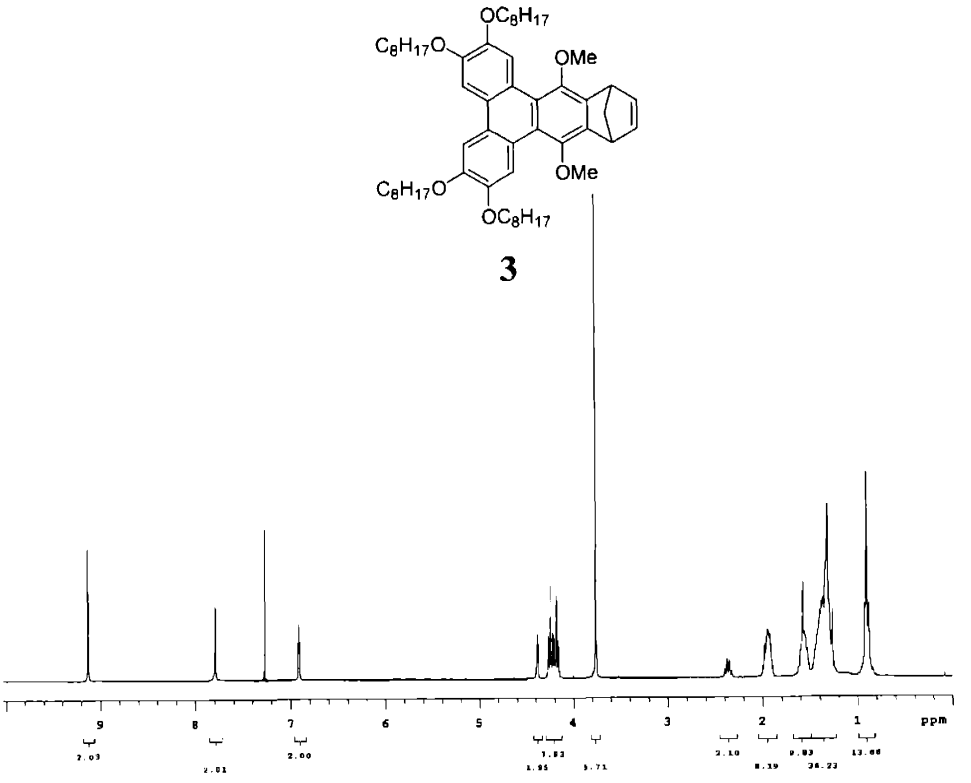

^{1}H NMR of **3** (500MHz, $CDCl_3$)

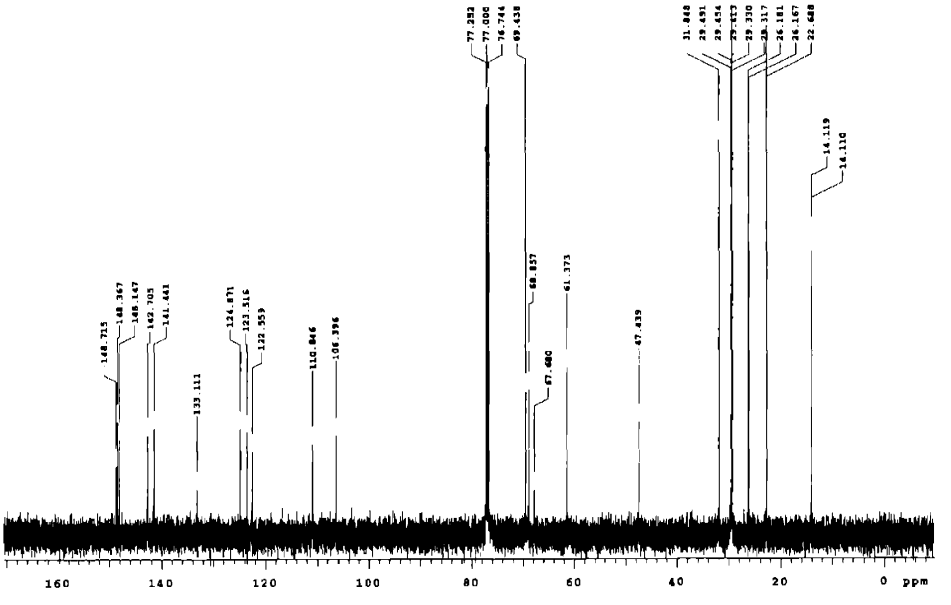

^{13}C NMR of **3** (125MHz, $CDCl_3$)

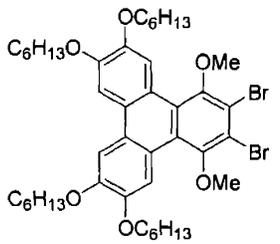

5

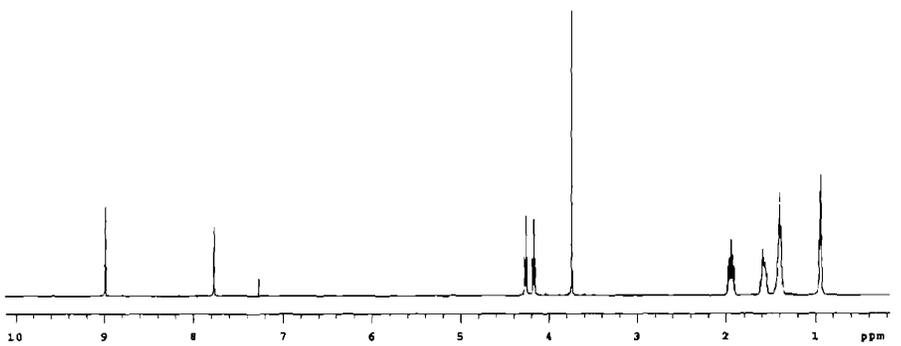

^{1}H NMR of **5** (500MHz, $CDCl_3$)

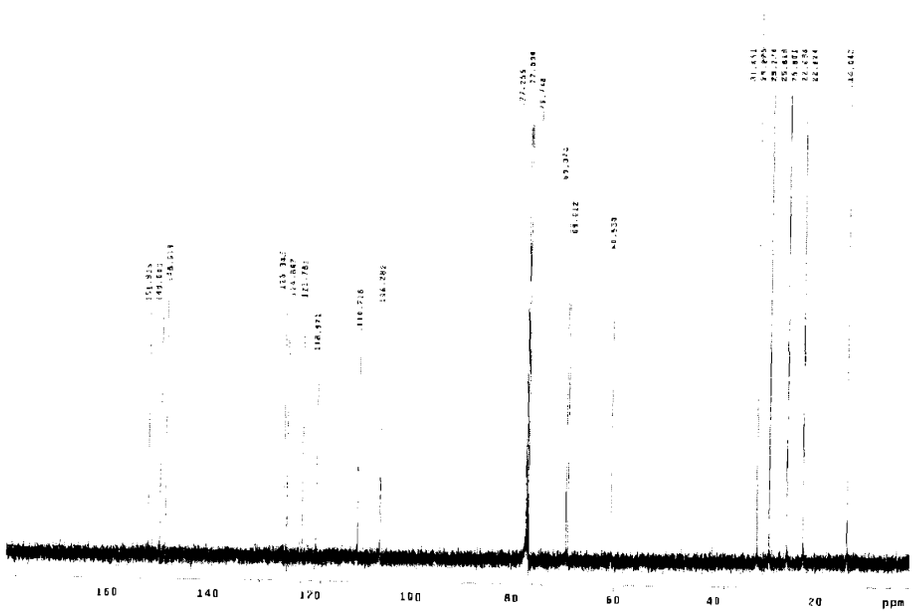

^{13}C NMR of **5** (125MHz, $CDCl_3$)

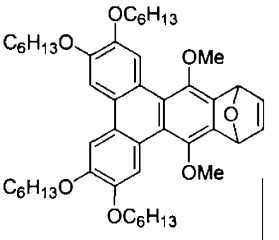

6

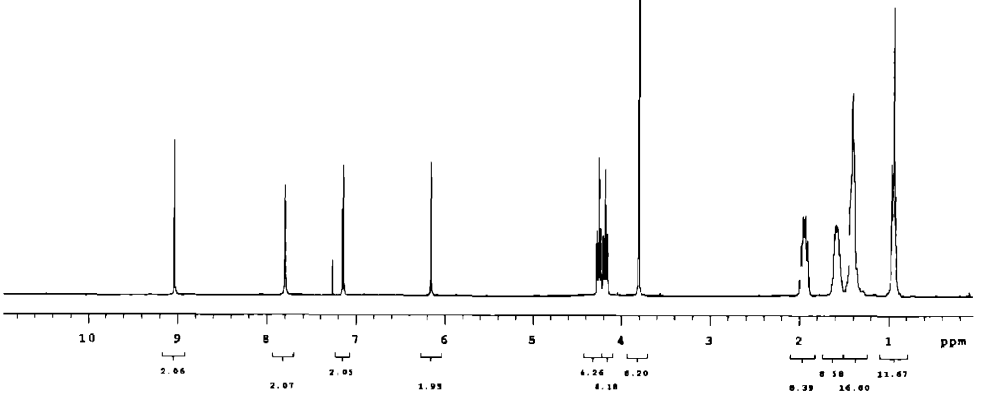

^{1}H NMR of **6** (300MHz, $CDCl_3$)

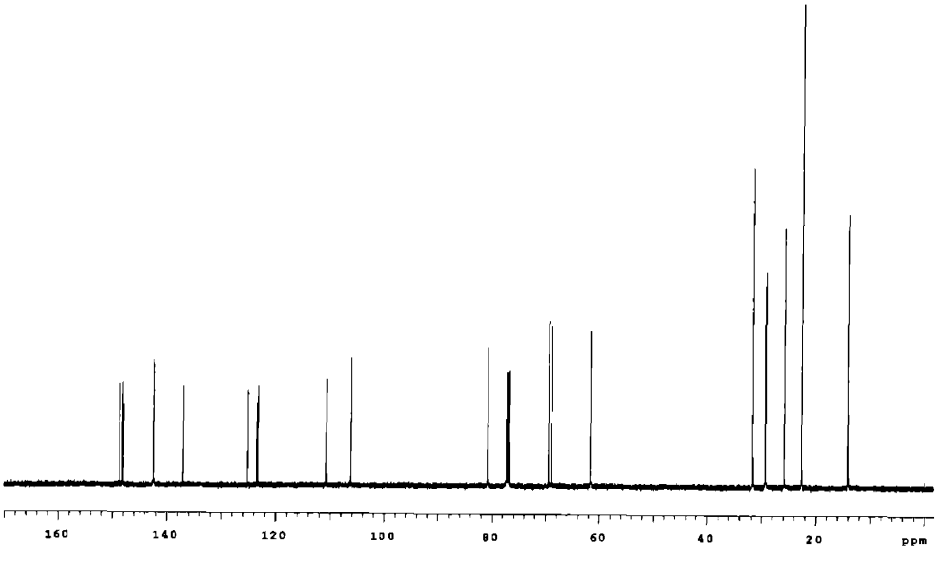

^{13}C NMR of **6** (125MHz, $CDCl_3$)

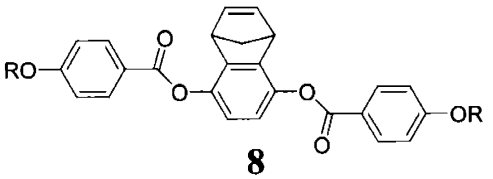

8

$R = C_{12}H_{25}$

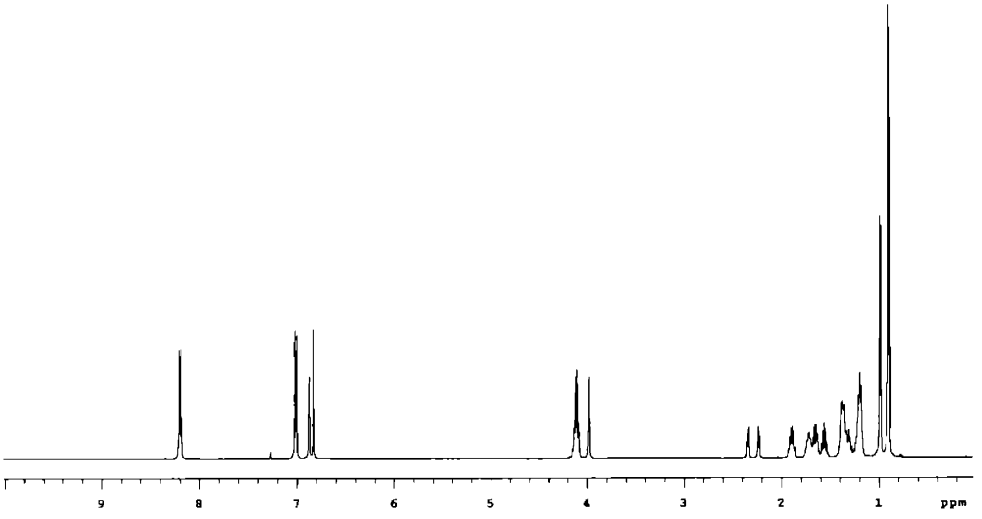

^{1}H NMR of **8** (300MHz, $CDCl_3$)

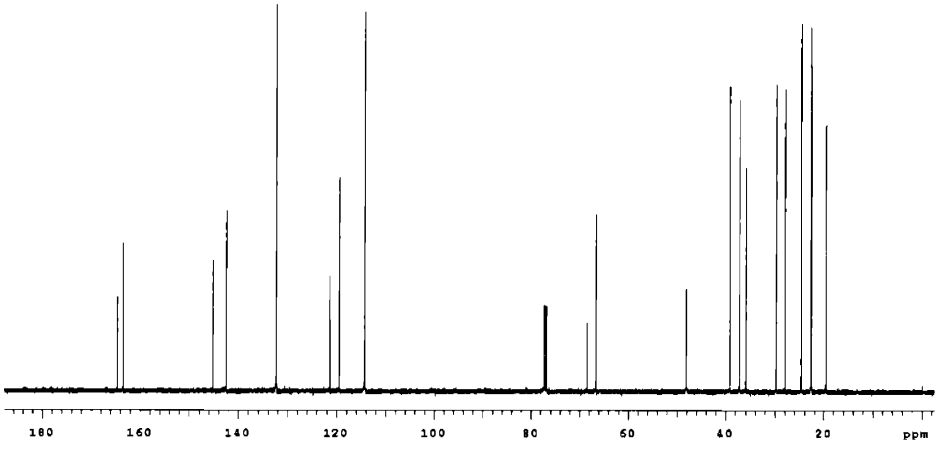

^{13}C NMR of **8** (125MHz, $CDCl_3$)

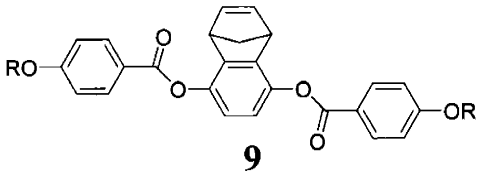

9

R = ((*S*)$C_2H_4C^*H(Me)C_3H_6CH(Me)_2$)

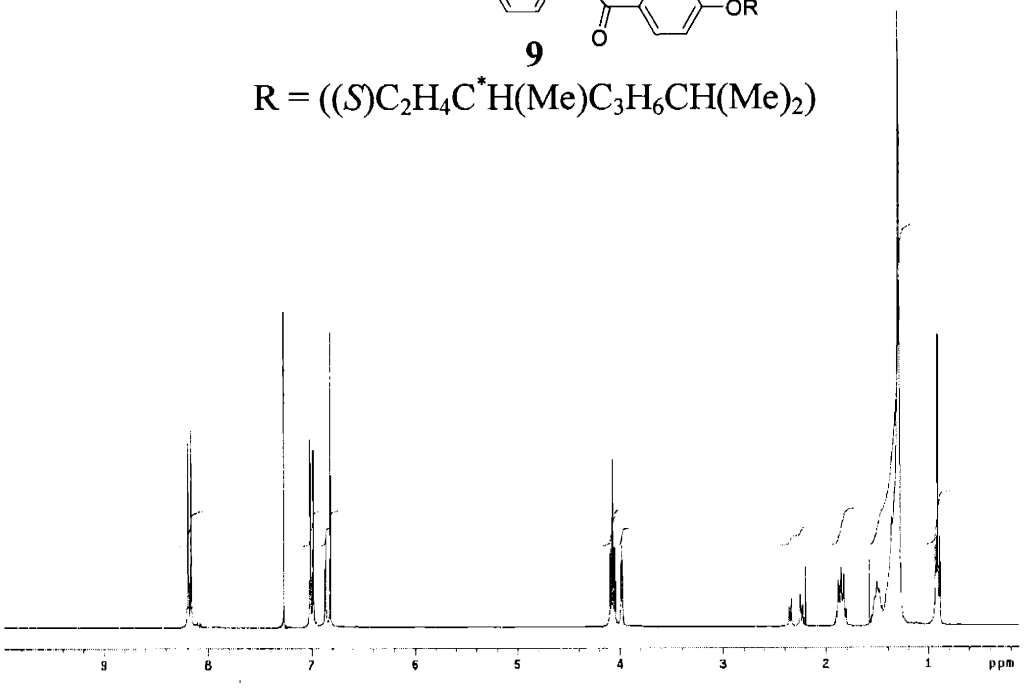

^{1}H NMR of **9** (300MHz, $CDCl_3$)

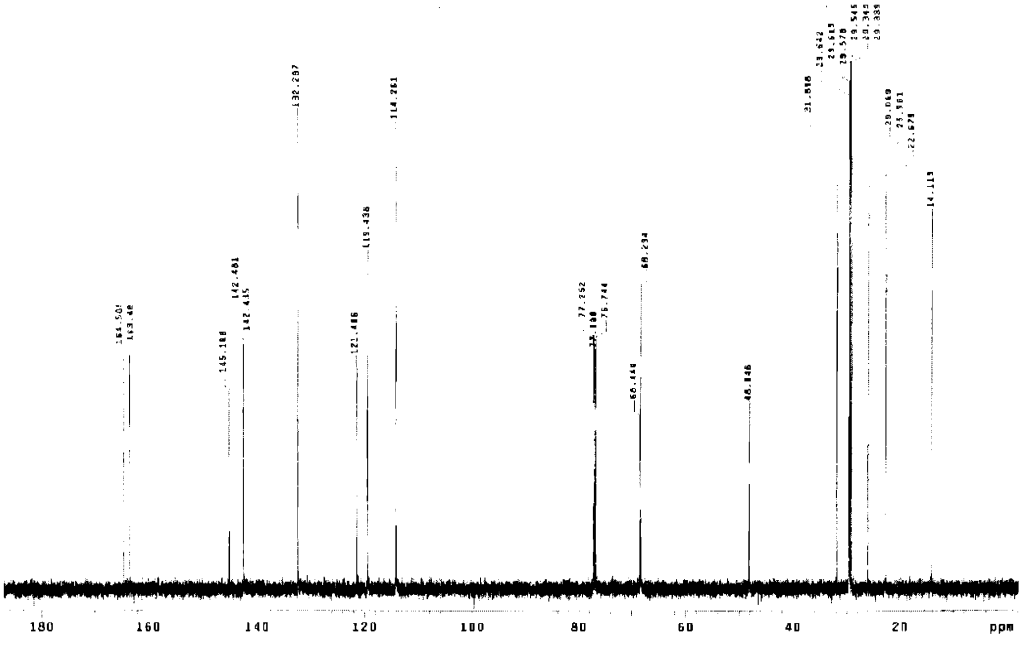

^{13}C NMR of **9** (125MHz, $CDCl_3$)

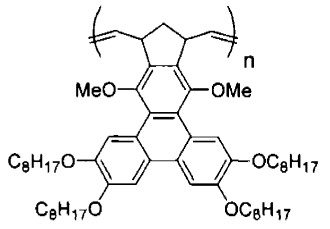

Poly-1

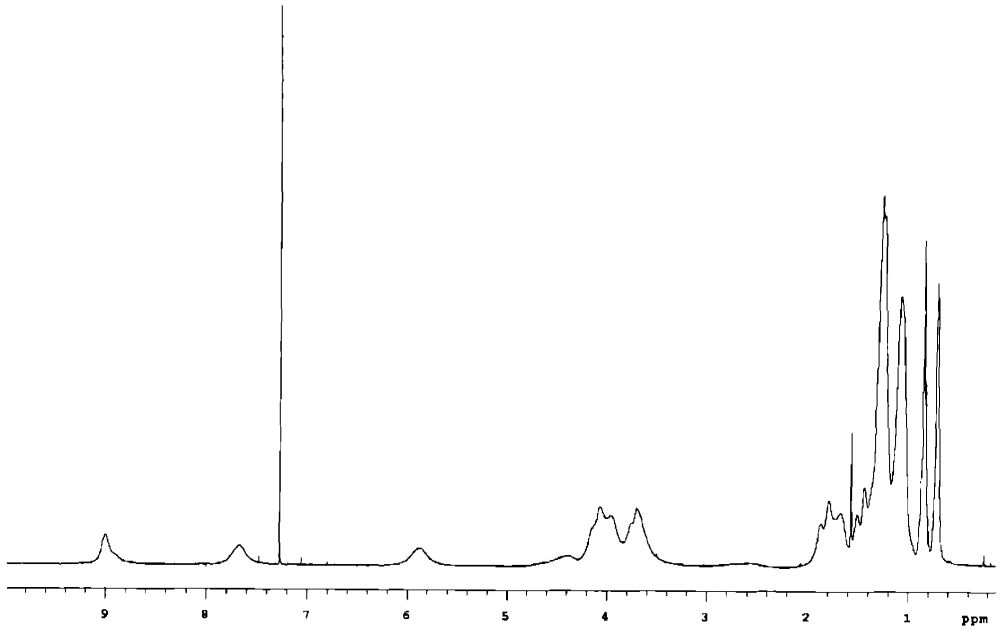

^{1}H NMR of **Poly-1** (500MHz, $CDCl_3$)

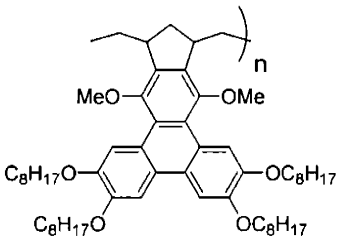

Poly-2

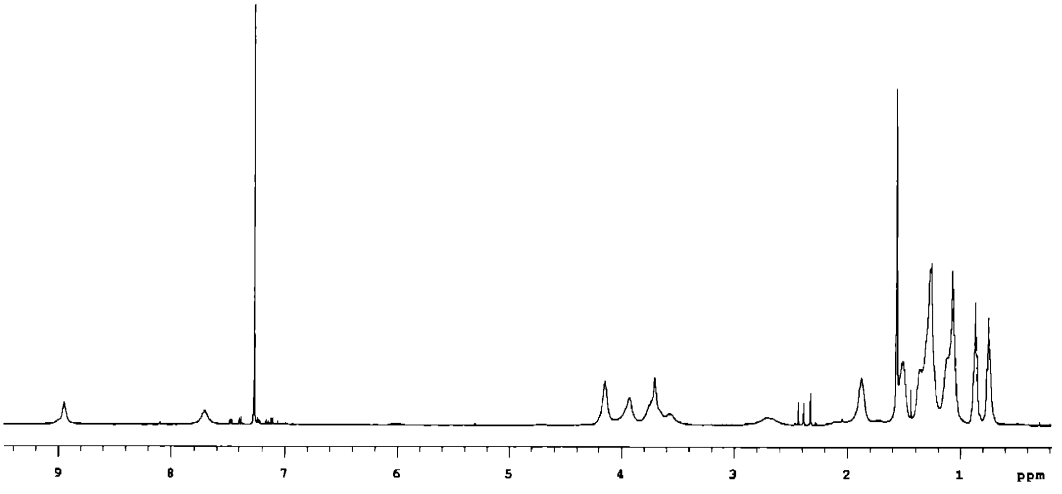

^{1}H NMR of **Poly-2** (500MHz, $CDCl_3$)

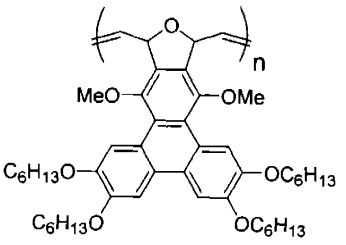

Poly-3

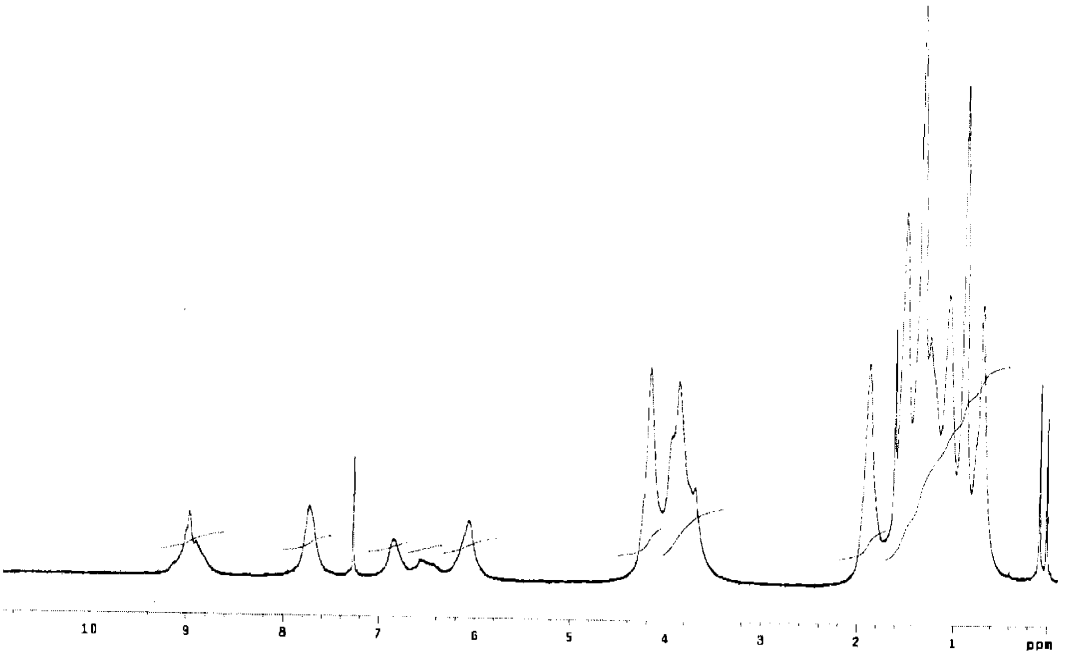

^{1}H NMR of **Poly-3** (500MHz, $CDCl_3$)

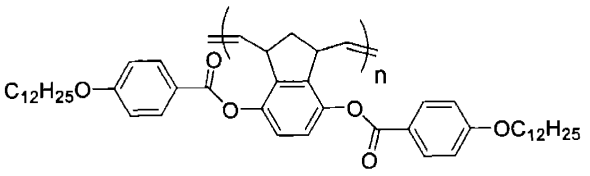

Poly-4

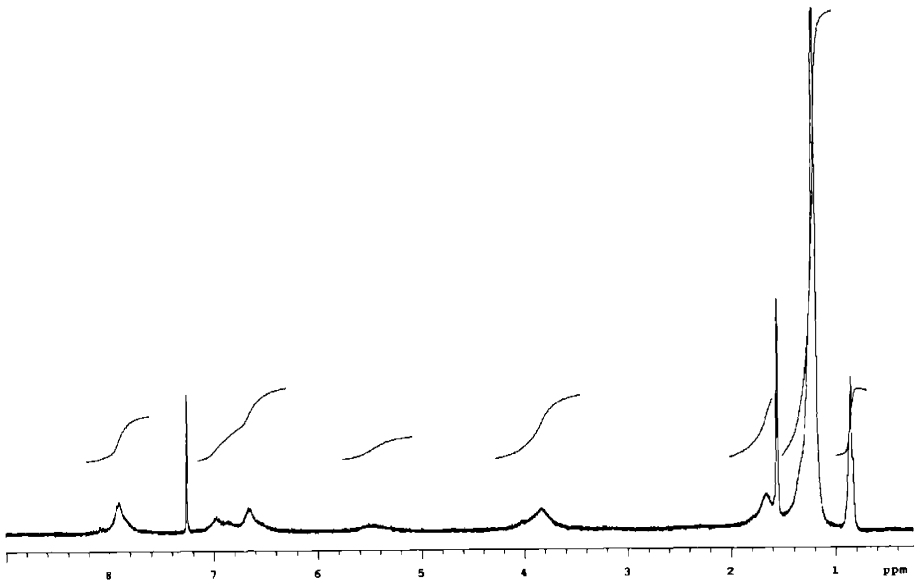

^{1}H NMR of **Poly-4** (500MHz, $CDCl_3$)

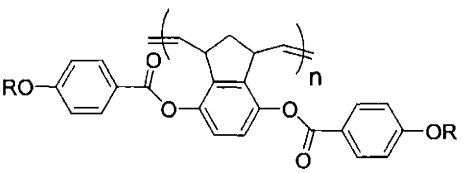

Poly-5
(R = ((S)C2H4C*H(Me)C3H6CH(Me)2)

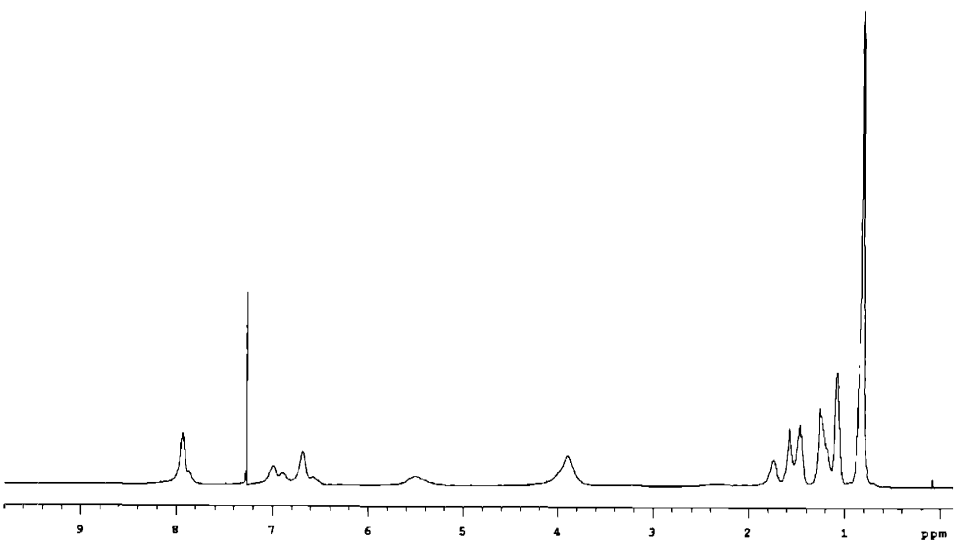

^{1}H NMR of **Poly-5** (500MHz, $CDCl_3$)